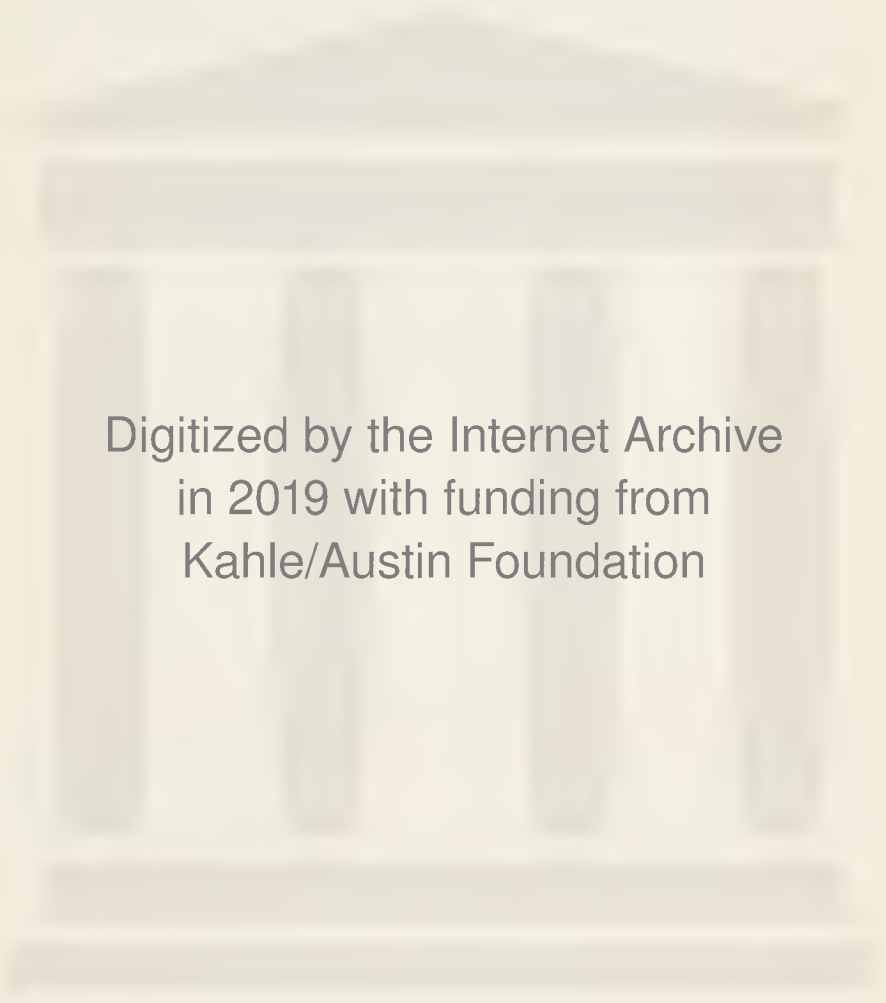


NUNC COGNOSCO EX PARTE



TRENT UNIVERSITY
LIBRARY



Digitized by the Internet Archive
in 2019 with funding from
Kahle/Austin Foundation

<https://archive.org/details/catalysis0000emme>

CATALYSIS

VOLUME IV

HYDROCARBON SYNTHESIS, HYDROGENATION AND CYCLIZATION

Edited by

PAUL H. EMMETT

W. R. Grace Professor of Chemistry

The Johns Hopkins University

Baltimore, Maryland

Contributing Authors

ROBERT B. ANDERSON

ERNST M. COHN

MURRAY GREYSON

L. J. E. HOFER

H. STEINER

S. W. WELLER

REINHOLD PUBLISHING CORPORATION

NEW YORK

CHAPMAN & HALL, LTD., LONDON

COPYRIGHT 1956 BY
REINHOLD PUBLISHING CORPORATION

All rights reserved
Second Printing 1961

Library of Congress Catalog Card Number 54-6801

Printed in the United States of America
THE GUINN CO., INC.
New York 14, N. Y.

ONULP

PREFACE

As explained in previous volumes of this series, Volumes I and II were written with a view to covering the fundamental ideas and current concepts of catalysis. The remaining volumes are intended to give the factual material as well as the interpretations that have been applied to specific fields of catalytic reactions.

Catalytic hydrogenation has sometimes been divided into those reactions in which hydrogen is simply added to unsaturated bonds and those reactions in which, in addition, bonds are broken to form products such as water vapor, hydrogen sulfide, hydro-halogens or small hydrocarbons. Today the field of catalytic hydrogenation is even broader and can hardly be covered by this classification. It includes isomerization reactions that will take place in the presence of, but not in the absence of adequate hydrogen; cyclization of paraffins and olefins to form cyclic compounds in the presence of hydrogen; and the synthesis of higher hydrocarbons, alcohols, and other compounds from hydrogen and simple molecules like carbon monoxide and carbon dioxide. Because of the complexities of any systematic classification that one might use and because of the difficulty of getting all the chapters in a given classification completed at one time, it has been found necessary to do a certain amount of mixing of these various types of hydrogenation in the three volumes (Volumes III, IV, and V) of this series devoted to various aspects of hydrogenation.

Volume III included for the most part simple hydrogenation and dehydrogenation reactions in which hydrogen is added to unsaturated bonds or is removed from saturated bonds to form unsaturated molecules. The only exception to this was a chapter on the hydrogenation of organic nitro compounds. Volume IV is devoted primarily to Fischer-Tropsch synthesis and related syntheses. Chapters 1 to 4 are given over to the Fischer-Tropsch synthesis reactions and catalysts. Chapter 5 covers the closely related field of isosynthesis, while Chapter 6 deals with the hydrogenation of carbon monoxide under such conditions as to produce methane as a principal product rather than higher hydrocarbons. Chapter 7 describes work that has been done on the destructive hydrogenation of high molecular weight compounds such as those of which coal and tar are composed. Finally, Chapter 8 recounts the development of a process for coiling straight chain hydrocarbons into rings. This necessarily entails some dehydrogenation if the starting materials are saturated hydrocarbons but could take place without dehydrogenation if the starting materials were suitable olefins. Along with cyclization is considered further dehydrogenation to form aromatics by a reaction referred to as aromatization.

Perhaps a word of explanation is needed relative to the scope of Chapter 8. The present chapter covers the field of cyclization and aromatization up to the time that it became identified with the petroleum industry as a hydro-reforming process. This latter subject will be treated in detail in a later volume.

The editor wishes to extend a special vote of thanks to the U. S. Bureau of Mines for permitting a group of its experienced research scientists to report the work on the hydrogenation of carbon monoxide and of coal. These subjects have long been under a detailed study by the Bureau and constitute good examples of some of the excellent catalytic research that has been done by research workers in laboratories sponsored by the U. S. Government. He also appreciates the willingness of Dr. H. Steiner of Manchester, England, to summarize his own and other early work in the important field of cyclization and aromatization.

As pointed out in a previous volume, each of the special fields of catalysis is being treated in the present series in such a way as to present not only a wealth of factual material but also to summarize current concepts as to the way in which the various reactions are probably taking place on catalyst surfaces. It is hoped that this blending of the practical and the theoretical will be useful to those in industry who are looking for new and profitable catalytic reactions as well as to those in and out of industry who are interested in the detailed mechanisms by which catalysts operate.

PAUL H. EMMETT

Baltimore, Md.

June 15, 1956

CONTENTS

CHAPTER	PAGE
1. THE THERMODYNAMICS OF THE HYDROGENATION OF CARBON MONOXIDE AND RELATED REACTIONS, <i>Robert B. Anderson</i>	1
Introduction.....	1
Hydrogenation of Carbon Monoxide.....	2
Hydrogenation of Carbon Dioxide.....	9
Reaction of Water with Carbon Monoxide or Carbon.....	9
Reactions of Hydrocarbons and Alcohols.....	11
General Conclusions based on Thermodynamics of Synthesis.....	14
Thermodynamics of Reactions of Iron, Cobalt, and Nickel.....	19
2. CATALYSTS FOR THE FISCHER-TROPSCH SYNTHESIS, <i>Robert B. Anderson</i>	29
Scope of the Chapter.....	29
The Development of Fischer-Tropsch Catalysts and Processes.....	29
Experimental Methods for Testing Catalysts.....	36
Cobalt and Nickel Catalysts.....	46
Iron Catalysts.....	119
Ruthenium Catalysts.....	237
Sulfur-Poisoning of Fischer-Tropsch Catalysts.....	242
3. KINETICS AND REACTION MECHANISM OF THE FISCHER-TROPSCH SYNTHESIS, <i>Robert B. Anderson</i>	257
Kinetics of the Fischer-Tropsch Synthesis.....	257
Variations of the Fischer-Tropsch Synthesis.....	298
Nature of the Catalytic Surface and Effect of Promoters.....	323
Mechanism of the Fischer-Tropsch Synthesis.....	335
4. CRYSTALLINE PHASES AND THEIR RELATION TO FISCHER-TROPSCH CATALYSTS, <i>L. J. E. Hofer</i>	373
Introduction.....	373
The Nickel System of Catalysts.....	382
The Cobalt System.....	391
The Iron System.....	406
5. THE ISOSYNTHESIS, <i>Ernst M. Cohn</i>	443
Purpose and History of the Synthesis.....	443
Description of the Synthesis.....	443
Preparation and Reactivation of Catalysts.....	444
Apparatus for Activity Tests.....	447
Synthesis Experiments.....	449
Detailed Characterization of Products.....	462
Determination of Motor Octane Number.....	467
Mechanism of Synthesis and Function of Catalyst.....	467

6. METHANATION, <i>Murray Greyson</i>	473
Introduction.....	473
Chemistry and Thermodynamics of Methanation.....	474
Catalysts.....	481
Industrial Techniques.....	506
Kinetics and Mechanisms of Reaction.....	508
7. CATALYSIS IN THE LIQUID-PHASE HYDROGENATION OF COAL AND TAR, <i>S. W. Weller</i>	513
Introduction.....	513
Wall Effects.....	514
Influence of Vehicle and Catalyst Distribution.....	515
Comparative Catalyst Tests.....	519
Stability of Catalysts.....	522
Catalysis and the Mechanism of Hydrogenation.....	523
8. CATALYTIC CYCLIZATION AND AROMATIZATION OF HYDROCARBONS, <i>H. Steiner</i>	529
Introduction.....	529
General Chemistry of the Reaction.....	530
Thermodynamic Considerations.....	535
Mechanism of the Reaction.....	535
Cyclization Catalysts.....	549
Technical Applications.....	557
Author Index.....	561
Subject Index.....	567

CHAPTER 1

THE THERMODYNAMICS OF THE HYDROGENATION OF CARBON MONOXIDE AND RELATED REACTIONS

Robert B. Anderson

*Chief, Branch of Coal-to-Oil Research, Division of Solid Fuels
Technology, Bureau of Mines, Pittsburgh, Pa.*

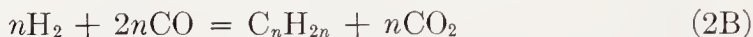
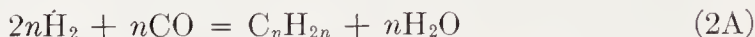
INTRODUCTION

This chapter describes the thermodynamics of many organic and inorganic reactions a number of which occur in the Fischer-Tropsch synthesis. For some of those that do not occur in the synthesis, the free energy changes are positive and sizable yields cannot be expected. However, many others are thermodynamically possible but do not occur to an appreciable extent for kinetic reasons. When two or more reactions involving the same reactants are thermodynamically possible, the yields depend upon their relative reaction rates as well as the velocities of subsequent reactions. Catalysts for the hydrogenation of carbon monoxide are quite specific or selective with respect to both the type of molecule (paraffins, olefins, alcohols, etc.) and the structure of its carbon chain.

The thermodynamics of the hydrogenation of carbon monoxide have been discussed by Smith²⁴ and Myddleton¹⁶; however, only relatively few compounds were considered by these authors. In addition, the calculations of Smith were based on older thermodynamic data that in some instances were not too reliable. Captured German documents contain two reports on the thermodynamics of synthesis reactions^{6, 22}. The thermodynamic studies of the American Petroleum Institute by Rossini and co-workers²¹ have provided excellent data for a wide variety of hydrocarbons, and these data are the basis of thermodynamic calculations involving hydrocarbons reported in this chapter as well as in other recent papers on this subject^{20, 25}. The thermodynamic data on the synthesis of alcohols, reduction of oxides, and the formation of carbides and carbonyls represent what appear to be the best available values. For reactions described in this chapter the standard state of gaseous components is 1 atm. Calculations are based on hydrocarbons and water in the vapor phase and carbon as graphite.

HYDROGENATION OF CARBON MONOXIDE

Reactions for the hydrogenation of carbon monoxide may be represented by Eqs. 1-3 for the formation of paraffins, monoolefins, and alcohols.



Equations marked A produce water and those marked B carbon dioxide. Similar equations can be written for molecules with cyclic carbon chains and diolefinic or acetylenic bonds. Equations 3A and 3B are identical for $n = 1$.

Heats of Reaction

Data on the heats of reaction are of great practical importance because removal of this heat is one of the most difficult engineering aspects in Fischer-Tropsch processes. Excessive catalyst temperatures usually lead to less desirable products, carbon deposition, and disintegration and deactivation of the catalyst. Enthalpies, calculated from the API thermodynamic tables²¹ for reactions producing hydrocarbons plus water (e.g., Eqs. 1A and 2A) are given in Figure 1, where heat of reaction per carbon atom is plotted as a function of temperature. The heats of reaction vary only slightly with temperature. For paraffins the heat of reaction per carbon atom increases (becomes less negative) with increasing carbon number, and for olefins these heats decrease with increasing carbon number. Enthalpy changes for reactions yielding hydrocarbons and carbon dioxide (Eqs. 1B and 2B), which are greater than those for the corresponding reactions producing water, may be obtained by adding the enthalpy change of the water-gas reaction, about 9.0 kcal, to the values given in Figure 1. They, too, are relatively independent of temperature and fall in the same order as heats for reactions producing water. The values in Figure 1 are, for straight-chain paraffins and 1-olefins; however, since the enthalpies for isomers with branched chains or the double bond in other positions differ by only very small amounts, these data are sufficiently accurate for most purposes.

Reactions producing elemental carbon may be represented by the following equations (the latter not involving hydrogen):

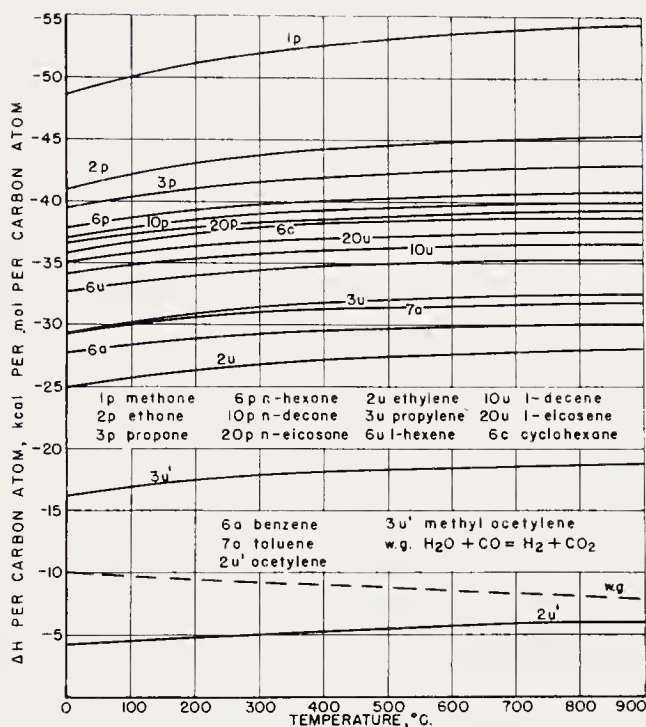
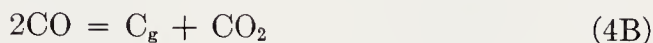


Figure 1. Heats of reaction of formation of hydrocarbons by reactions of type A (water as the oxygenated product), expressed as kcal per mol per carbon atom of the hydrocarbon. Heats of reactions of type B (carbon dioxide as the oxygenated product) are obtained by adding the heat of reaction of the water gas reaction (w.g.) to the heats for reaction of Type A.

The heats of reaction in kcal (ΔH values), calculated from API tables²¹, are

Reaction	Temperatures (°C)		
	127	227	427
4A	-31.7	-32.0	-32.3
4B	-41.4	-41.5	-41.4

Enthalpy changes in reactions producing alcohols have been calculated from heat of combustion data at 18°C summarized by Hougen and Watson¹⁰. These values approximate the heats of reaction at higher temperatures since such data are usually very nearly temperature-independent. The

data listed below are for the production of gaseous alcohol and water vapor at 18°C by Eq. 3A.

	ΔH , kcal/mole	$\Delta H/n$, kcal/mole/carbon atom
Methanol	-23.9	-23.9
Ethanol	-58.9	-29.5
Propanol-1	-98.0	-32.7

Free Energies of Reaction

Equilibrium constants for typical Fischer-Tropsch reactions according to Eqs. (1A) and (1B), respectively, are defined as

$$K_{eq} = \frac{P_{C_nH_{2n+2}} P_{H_2O}^n}{P_{H_2}^{2n+1} P_{CO}^n} \quad \text{and} \quad K_{eq} = \frac{P_{C_nH_{2n+2}} P_{CO_2}^n}{P_{H_2}^{n+1} P_{CO}^{2n}},$$

where P is the partial pressure in atmospheres. Equilibrium constants for other types of hydrocarbons are defined in a similar manner. For exact calculations fugacities rather than partial pressures should be employed; however, in the range of pressures normally used in the Fischer-Tropsch synthesis, 1 to 40 atms., calculations based on partial pressures are usually sufficiently accurate.

The synthesis reactions involve a decrease in the number of moles, hence equilibrium conversion at a given temperature increases rapidly with pressure, or at a higher pressure a given equilibrium conversion is possible at higher temperatures. This may be illustrated by writing the equilibrium constant for Eq. (1A) in terms of mole fractions, N , and total pressure, P .

$$P^{2n} K_{eq} = \frac{N_{C_nH_{2n+2}} N_{H_2O}^n}{N_{H_2}^{2n+1} N_{CO}^n}$$

It is difficult to specify a value of the equilibrium constant below which the yield is so low that the reaction may be considered to be insignificant. With Fischer-Tropsch catalysts known today, the upper limits of pressure and temperature, about 30 to 40 atms. and 400°C, are determined by changes in selectivity and rate of deterioration of the catalyst. For example, Figure 2 indicates that 80 per cent conversion of $2H_2 + 1CO$ gas to 1-decene is thermodynamically possible up to about 422, 443, or 460°C at 20, 30, or 40 atms., respectively.

The standard free energy change, ΔF° , of a chemical reaction is related to its equilibrium constant by the usual definition

$$-\Delta F^\circ = RT \ln K_{eq}$$

Equilibrium data for the hydrogenation of carbon monoxide to hydrocarbons and water (e.g., Eqs. 1A and 2A) are presented in Figures 3 to 5,

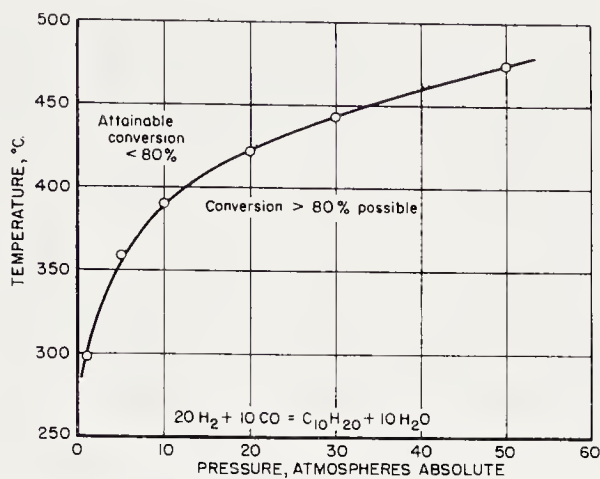


Figure 2. Influence of temperature and pressure on equilibrium conversion in a typical synthesis reaction.

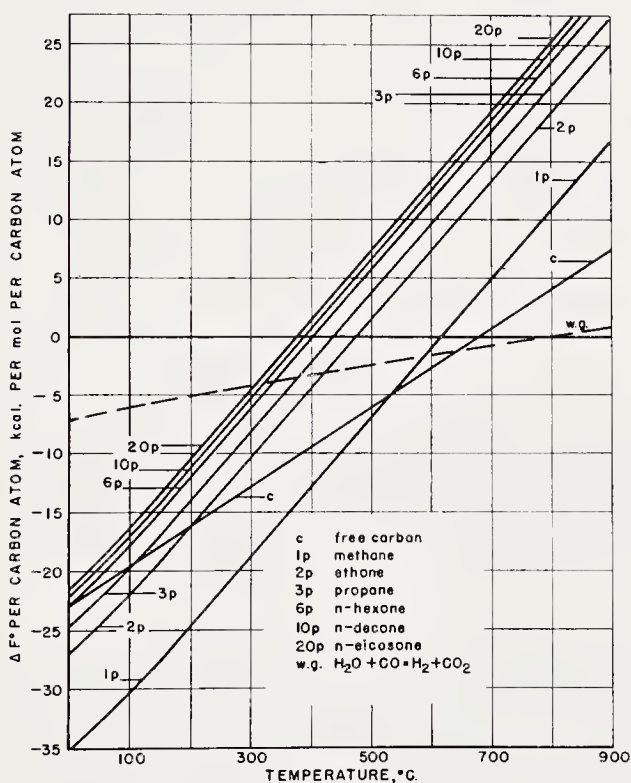


Figure 3. Standard state free energies of formation of paraffins by reactions of type A (water as the oxygenated product), expressed as kcal per mol per carbon atom of the hydrocarbon. Standard state free energies of reactions of type B (carbon dioxide as the oxygenated product) may be obtained by adding the free energy of the water gas reaction (w.g.) to the free energies of reactions of type A.

where the standard free energy change per carbon atom of the hydrocarbon, $\Delta F^\circ/n$, is plotted as a function of temperature. For reactions of type 1B and 2B, producing hydrocarbon and carbon dioxide, $\Delta F^\circ/n$ may be obtained by adding ΔF° for the water-gas reaction (w.g.) to values given in Figures 3 to 5. Figures 3 and 4 show data for *n*-paraffins and 1-olefins

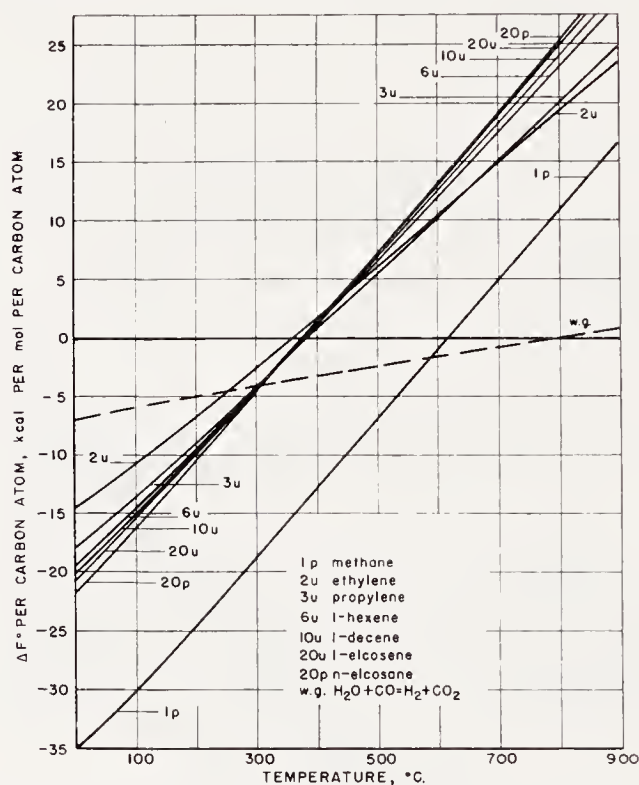


Figure 4. Standard state free energies of formation of olefins by reactions of type A (water as the oxygenated product), expressed as kcal per mol per carbon atom of the hydrocarbon. Standard state free energies of reactions of type B (carbon dioxide as the oxygenated product) may be obtained by adding the free energy of the water gas reaction (w.g.) to the free energies of reactions of type A.

only, because these values usually differ from those of branched or double-bond isomers by very small amounts.

The plots in Figures 3 to 5 closely approximate straight lines. Graphs of this type for reactions producing hydrocarbons and carbon dioxide (type B) are also linear, since the $\Delta F^\circ/n$ values are obtained by adding ΔF° for the water-gas reaction (which varies linearly with temperature) to the values for reactions of type A. $\Delta F^\circ/n$ for methane is more negative than the values for all other hydrocarbons, and below 530°C is more negative than that for the formation of graphite. For paraffins the $\Delta F^\circ/n$ curves are approximately parallel but are displaced to more positive values with in-

creasing carbon number. The magnitude of the positive displacement of these lines decreases with increasing molecular weights and the values apparently approach a limit near the line for *n*-eicosane. The slopes of curves for 1-olefins (Figure 4) change with increasing carbon number but appear to approach the same limit as the *n*-paraffin lines. Below 300°C, $\Delta F^\circ/n$

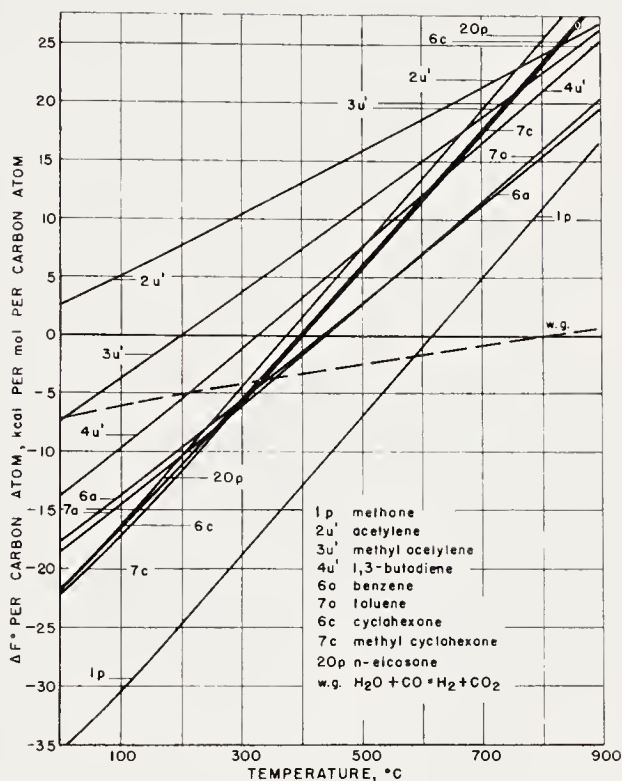


Figure 5. Standard state free energies of formation of various types of hydrocarbons by reactions of type A (water as the oxygenated product), expressed as kcal per mol per carbon atom of the hydrocarbon. Standard state free energies of reactions of type B (carbon dioxide as the oxygenated product) may be obtained by adding the free energy of the water gas reaction (w.g.) to the free energies of reactions of type A.

values for olefins become more negative with increasing carbon number, while above 500°C (except for ethylene) they become more positive with increasing carbon number. For cyclic and aromatic hydrocarbons (Figure 5), $\Delta F^\circ/n$ values are approximately the same as those for monoolefins of the same carbon number in the temperature range of the Fischer-Tropsch synthesis, 200 to 400°C. Diolefins and acetylenic hydrocarbons have more positive $\Delta F^\circ/n$ values than monoolefins.

Free energy data for production of alcohols by Eq. (3A) are given in Figure 6 which was prepared from data summarized on p. 21 of reference 25. Although, in general, these data are less exact than the API data on hy-

drocarbons²¹, they are probably sufficiently accurate for the present purposes. The standard state free energies per carbon atom, $\Delta F^\circ/n$, form a series of approximately parallel lines. As the carbon number increases, the values become more negative and possibly approach a limit somewhere near that for 20u, 1-eicosene. For reactions given by Eq. (3B) the free energy change is computed from the data in Figure 5 by multiplying $\Delta F^\circ/n$ by n and adding $(n - 1)$ times the free energy change for the water-gas

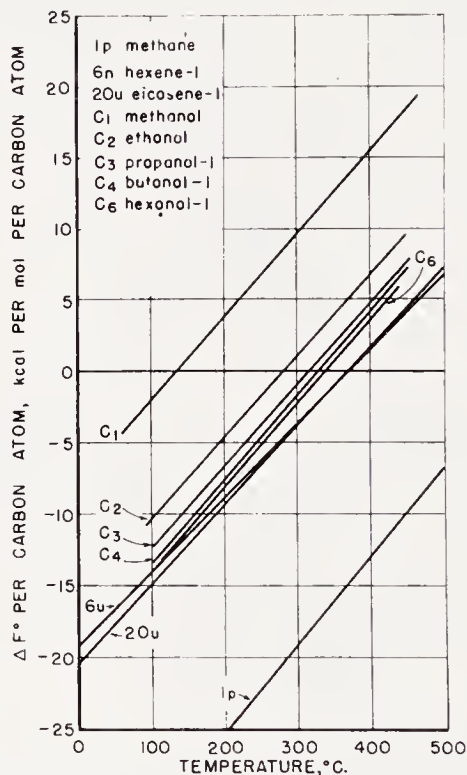


Figure 6. Standard free energy changes for reactions producing alcohols according to Equation 3A.

reaction. Thus, for ethanol formed according to Eq. (3B) at 300°C $\Delta F^\circ = n(\Delta F^\circ/n) + (n - 1)\Delta F^\circ_{w.g.}$

$$\Delta F^\circ = (2 \times 1.0) - 4.0 = -2.0 \text{ kcal/mole,}$$

$$\log_{10} K_{eq} = 2000/2.303 RT = 0.758$$

$$K_{eq} = 5.7$$

This value is higher than that for ethanol formed according to Eq. (3A), $K_{eq} = 0.18$.

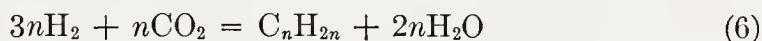
Of the primary, straight-chain alcohols considered here, large equilibrium

yields are possible except for methanol. The equilibrium conversions of $2\text{H}_2 + 1\text{CO}$ gas to methanol are

Pressure, atm. (absolute)	% Conversion to Methanol		
	225°C	250°C	300°C
1	0.3	0.1	
10	21.7	8.8	1.3
30	57.0	39.0	10.2
50		55.0	22.0

HYDROGENATION OF CARBON DIOXIDE

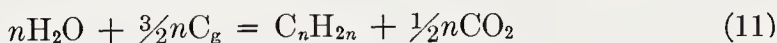
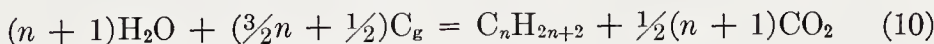
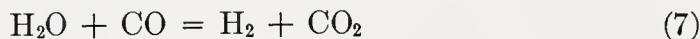
The hydrogenation of carbon dioxide to paraffins and olefins can be expressed by the following equations:



The enthalpy changes of these reactions may be obtained by subtracting the enthalpy changes of the water-gas reaction, about -9 kcal, from the value of $\Delta H/n$ given in Figure 1; i.e., the heats of reaction of Eqs. (5) and (6) are less negative by 9 kcal per mole per carbon atom than those for Eqs. (1A) and (2A). Similarly, the standard free energy per carbon atom, $\Delta F^\circ/n$, is obtained by subtracting ΔF° for the water-gas reaction from the values for $\Delta F^\circ/n$ in Figures 3 to 5. Thus, at temperatures below 800°C , ΔF° values for Eqs. (5) and (6) are less negative than those for Eqs. (1A) and (2A).

REACTIONS OF WATER WITH CARBON MONOXIDE OR CARBON

These reactions may be represented by the following equations:



In addition to reacting according to Eqs. (7), (8), and (9), water can react with carbon monoxide to produce formic acid, but, according to Pichler and Buffleb¹⁸, appreciable yields of formic acid are not produced at pressures and temperatures of the Fischer-Tropsch synthesis. Equilibrium constants and standard free energy and enthalpy changes of the water-gas

shift reaction, Eq. (7), are presented in Table 1. Standard free energy changes per carbon atom of hydrocarbons reacting according to Eqs. (8) and (9) are presented in Figure 7, and similar data for Eqs. (10) and (11) are given in Figure 8. All of these data were computed from the API tables²¹. The thermodynamics of reactions 8 and 9 have recently been discussed by Koelbel and Engelhardt¹².

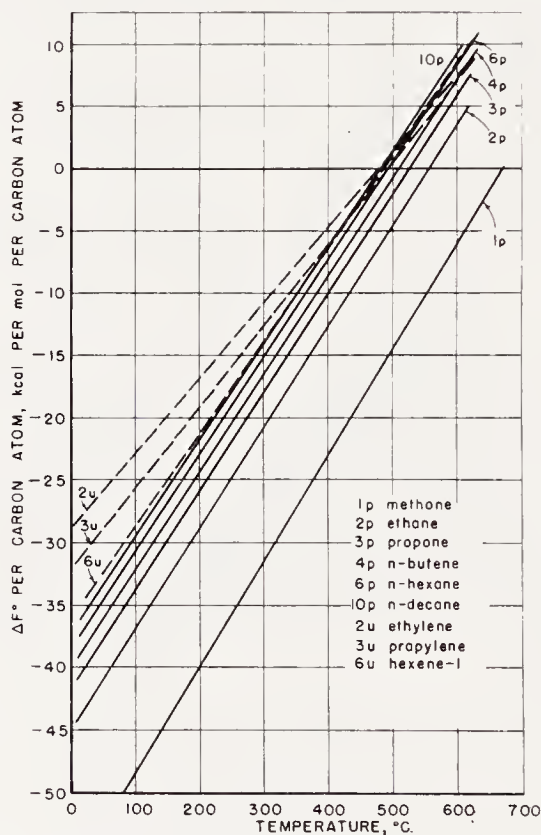


Figure 7. Standard free energy changes for the production of paraffins and olefins from water and carbon monoxide.

The equilibrium constants of the water-gas shift reaction (Eq. 7) are sufficiently large at synthesis temperatures so that at equilibrium virtually all of the water or carbon monoxide is consumed. The reaction is mildly exothermic, $\Delta H \cong -9$ kcal/mole.

Reactions of water with carbon monoxide according to Eqs. (8) and (9) are accompanied by more negative free energy changes and are more exothermic than reactions 1A and 2A by about 18 kcal per carbon atom of hydrocarbon, and by 9 kcal per carbon atom than reactions 1B and 2B.

The synthesis of hydrocarbons according to Eqs. (10) and (11), which approximate the over-all reactions involved in the production of synthetic liquid fuels from coal, is accompanied by positive $\Delta F^\circ/n$ values at all

temperatures. Since there is a decrease in the number of moles in Eqs. (10) and (11), the extent of conversion should increase with pressure; nevertheless, even at pressures as high as 1,000 atmospheres the equilibrium yield of hydrocarbons is low. However, coal is much more reactive than graphite, and with some coals these reactions may be thermodynamically possible. Reactions 10 and 11 are endothermic as shown by data in Table 2.

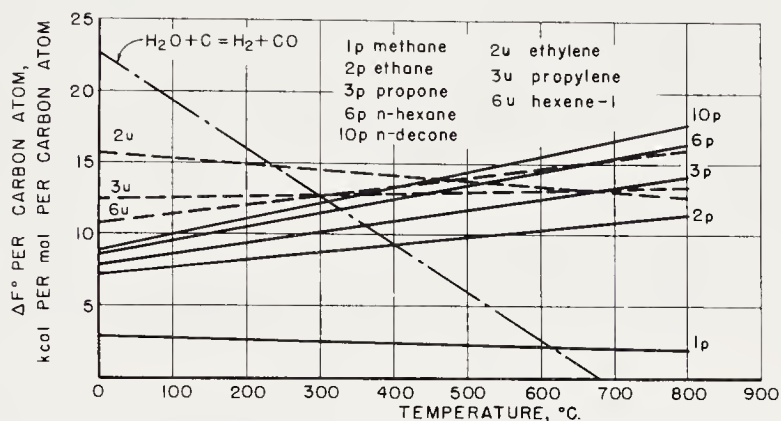


Figure 8. Standard free energy change for the production of hydrocarbons from water plus carbon.

TABLE 1. THERMODYNAMIC DATA FOR THE WATER-GAS SHIFT REACTION^a

Temp. (°C)	K_{eq}	ΔF° kcal/mole	ΔH kcal/mole
27	9.01×10^4	-6.798	-9.837
127	1.48×10^3	-5.800	-9.710
227	1.32×10^2	-4.848	-9.520
327	27.1	-3.932	-9.294
427	9.01	-3.057	-9.051
627	2.21	-1.415	-8.553
827	0.949	+0.116	-8.071
1027	0.547	+1.557	-7.621

^a From data of Ref. 21.

REACTIONS OF HYDROCARBONS AND ALCOHOLS

With the exception of methane and ethane, all hydrocarbons are thermodynamically unstable with respect to graphite and hydrogen at temperatures above 100°C, and the free energies of formation of methane and ethane become positive at about 550 and 200°C, respectively.

The equilibrium constants of isomerization reactions of paraffins or olefins usually do not differ by more than a factor of ten, but in some cases the differences may be more than 100-fold. Equilibrium composition data for pentanes, pentenes, and hexanes, computed from the API tables²¹, are given in Figures 9, 10, and 11, respectively.

Hydrogenation of olefins is thermodynamically possible under all conditions normally encountered in the Fischer-Tropsch synthesis. As the carbon number increases from 2 to 10, the equilibrium constants for the reaction, 1-olefin + H₂ = *n*-paraffin, decrease from 8×10^7 to 1.7×10^6 at 227°C and from 4.8×10^3 to 2.2×10^2 at 427°C.

Alcohols can decompose in three ways: (1) dehydrogenate to an aldehyde, (2) deformylate to an olefin or paraffin with a carbon number one less than that of the alcohol, or (3) dehydrate to the corresponding olefin. Equilibrium constants for the dehydration of alcohols are given in Table 3.

Next, thermodynamic data are presented for a variety of reactions of hydrocarbons with (a) other hydrocarbons, (b) hydrogen to yield methane and lower saturated hydrocarbons, (c) hydrogen and carbon monoxide to yield higher hydrocarbons. Equilibrium constants of a number of typical

TABLE 2. HEATS OF REACTION OF WATER AND CARBON YIELDING HYDROCARBONS ACCORDING TO EQS. 10 AND 11

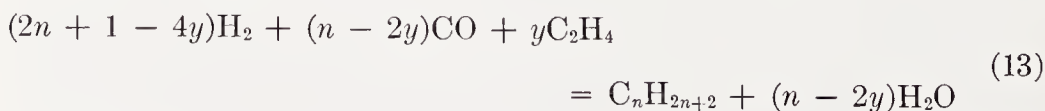
Temperature = 427°C

Carbon No.	ΔH kcal/mole	
	Paraffin	Olefin
1	+ 2.85	—
2	+10.9	+33.4
3	+17.0	+36.2
6	+34.2	+53.9
10	+57.6	+77.4

reactions between hydrocarbon molecules are given in Table 4, and similar data for the incorporation of hydrocarbons into the synthesis are given in Table 5. Free energy calculations for incorporating methane into the synthesis have been presented by Prettre²⁰. Data of this type according to the equation



are shown in Figure 12 in which the standard free energy change per mole of *n*-decane (*n* = 10) is plotted as a function of temperature for values of *x* from 0 to 10. Similar data are presented in Figure 13 for the incorporation of ethylene by the equation



to form *n*-decane with *y* varying from 0 to 5. Figure 14 gives the standard

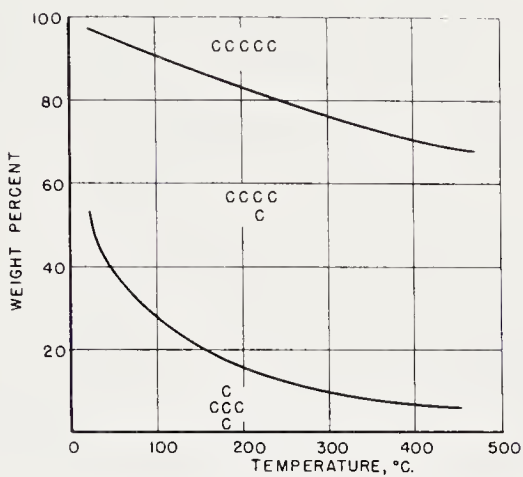


Figure 9. Equilibrium composition of pentane isomers.

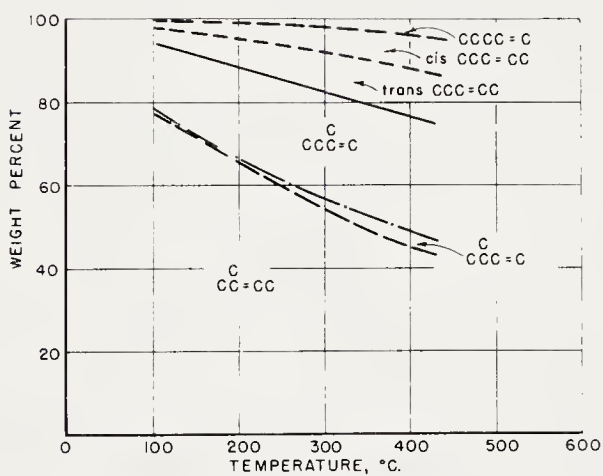


Figure 10. Equilibrium composition of pentene isomers.

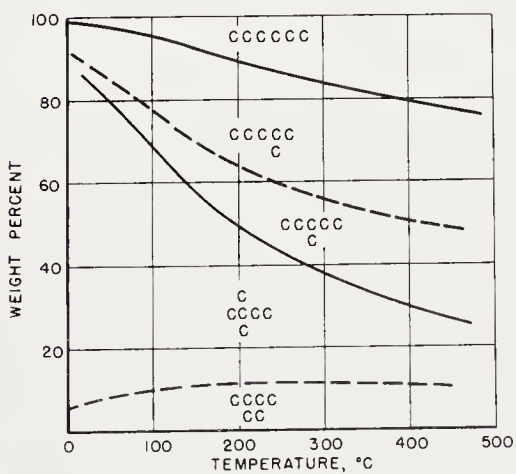
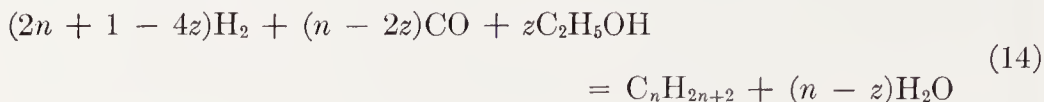


Figure 11. Equilibrium composition of hexane isomers.

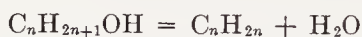
free energy changes per mole of n -decane for the incorporation of ethanol by the equation



for $n = 10$ and z varying from 1 to 5. For reactions analogous to Eqs. (12) and (14), but in which carbon dioxide is produced, the standard free energies are more negative.

By approximate thermodynamic methods, Wenner²⁷ estimated the equilibrium constants of the reactions of synthesis gas with ethylene and propylene to give propionaldehyde and isobutyraldehyde, respectively, to be

TABLE 3. EQUILIBRIUM CONSTANTS FOR THE DEHYDRATION OF ALCOHOLS^a



Alcohol	$\log_{10} K_{\text{eq}}$		
	127°C	227°C	327°C
Ethanol	0.66	1.89	2.72
Propanol-1	2.20	3.27	3.99
Butanol-1	1.76	2.96	3.78
Hexanol-1	2.31	3.66	4.60

^a Equilibrium constants calculated from approximate free-energy equations of R. R. Wenner, Ref. 27.

6×10^{12} and 2.5×10^9 at 25°C and 324 and 1.6 at 227°C. These reactions are typical of those occurring in the oxo synthesis.

GENERAL CONCLUSIONS BASED ON THERMODYNAMICS OF SYNTHESIS

Reactions

1. Reactions producing carbon dioxide (Eqs. 1B and 2B) have more negative ΔF° values (larger equilibrium constants) than corresponding reactions producing water (Eqs. 1A and 2A).

2. The standard free energy changes per carbon atom, $\Delta F^\circ/n$, for reactions producing methane are more negative than for corresponding reactions producing higher hydrocarbons. The free energy of formation of carbon is more negative than $\Delta F^\circ/n$ values for higher hydrocarbons. Hence, the production of higher hydrocarbons (rather than methane or carbon) must depend on the selectivity of the catalyst.

3. The equilibrium conversion of synthesis increases with pressure. Thus, the highest temperatures at which 80 per cent of $2\text{H}_2 + 1\text{CO}$ gas

can be converted to 1-decene and water are 298° at 1 atm., 443° at 30 atms., and 474° at 50 atms. Because of detrimental effects of high pres-

TABLE 4. EQUILIBRIUM CONSTANTS FOR REACTIONS BETWEEN HYDROCARBONS^a

Reaction ^o	log ₁₀ K _{eq}			Temperature at which K _{eq} = 1, °C
	27°C	227°C	427°C	
1. CH ₄ + C ₂ H ₆ = C ₃ H ₈ + H ₂	-10.453	-6.514	-4.709	>427
2. CH ₄ + C ₄ H ₁₀ = C ₅ H ₁₂ + H ₂	-10.155	-6.357	-4.614	>427
3. CH ₄ + C ₈ H ₁₈ = C ₉ H ₂₀ + H ₂	-10.341	-6.457	-4.684	>427
4. CH ₄ + C ₂ H ₄ = C ₃ H ₈	+7.096	+1.387	-1.032	325
5. CH ₄ + C ₄ H ₈ = C ₅ H ₁₂	+5.081	+0.008	-2.143	228
6. CH ₄ + C ₈ H ₁₆ = C ₉ H ₂₀	+4.739	+0.233	-2.343	240
7. C ₂ H ₄ + C ₂ H ₆ = C ₄ H ₁₀	+8.826	+2.424	-0.288	398
8. C ₂ H ₄ + C ₄ H ₁₀ = C ₆ H ₁₄	+9.040	+2.471	-0.300	398
9. C ₂ H ₄ + C ₈ H ₁₈ = C ₁₀ H ₂₂	+8.833	+2.353	-0.382	390
10. 2C ₂ H ₄ = C ₄ H ₈	+11.139	+3.960	+0.919	521
11. C ₂ H ₄ + C ₄ H ₈ = C ₆ H ₁₂	+9.202	+2.611	-0.172	410

^a Computed from data of Ref. 21.

^b All hydrocarbons in this table are *n*-paraffins or 1-olefins.

TABLE 5. INCORPORATION OF HYDROCARBONS INTO THE PRODUCTS OF THE SYNTHESIS^a

Reaction ^b	log ₁₀ K _{eq}			Temperature at which K _{eq} = 1, °C
	27°C	227°C	427°C	
1. CH ₄ + 4H ₂ + 2CO = C ₃ H ₈ + 2H ₂ O	26.935	6.241	-2.875	349
2. CH ₄ + 3H ₂ + 2CO = C ₃ H ₆ + 2H ₂ O	11.934	0.026	-5.268	228
3. CH ₄ + 8H ₂ + 4CO = C ₅ H ₁₂ + 4H ₂ O	55.897	13.675	-4.910	360
4. CH ₄ + 7H ₂ + 4CO = C ₅ H ₁₀ + 4H ₂ O	40.825	7.466	-7.241	312
5. CH ₄ + 16H ₂ + 8CO = C ₉ H ₂₀ + 8H ₂ O	113.270	28.106	-9.348	363
6. CH ₄ + 15H ₂ + 8CO = C ₉ H ₁₈ + 8H ₂ O	98.190	21.884	-11.689	341
7. C ₂ H ₄ + 5H ₂ + 2CO = C ₄ H ₁₀ + 2H ₂ O	46.214	15.179	+1.547	>427
8. C ₂ H ₄ + 4H ₂ + 2CO = C ₄ H ₈ + 2H ₂ O	30.977	8.814	+0.924	>427
9. C ₂ H ₄ + 17H ₂ + 8CO = C ₁₀ H ₂₂ + 8H ₂ O	132.444	36.916	-5.047	395
10. C ₂ H ₄ + 16H ₂ + 8CO = C ₁₀ H ₂₀ + 8H ₂ O	117.364	30.694	-7.388	376
11. C ₄ H ₈ + 13H ₂ + 6CO = C ₁₀ H ₂₂ + 6H ₂ O	101.467	28.103	-4.123	393
12. C ₄ H ₈ + 12H ₂ + 6CO = C ₁₀ H ₂₀ + 6H ₂ O	86.387	21.880	-6.464	368

^a Computed from data of Ref. 21.

^b All hydrocarbons in this table are *n*-paraffins or 1-olefins.

tures and temperatures on the stability, selectivity, and activity of catalysts, the upper ranges of possible temperature and pressure are not approached in usual synthesis processes, the practical upper limits for iron

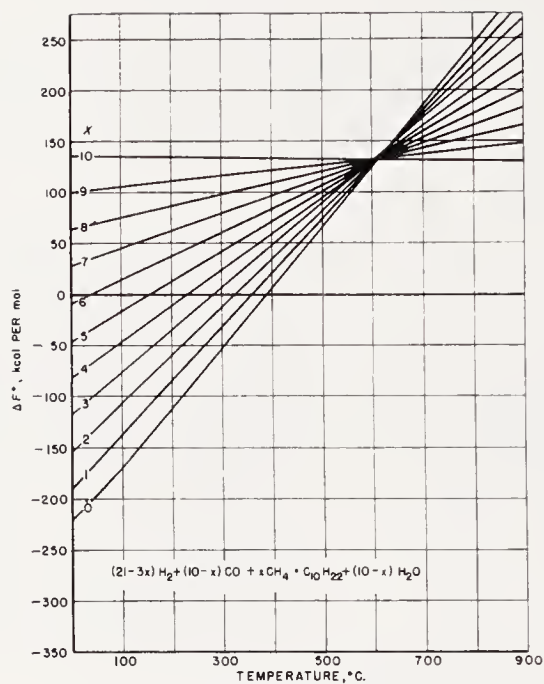


Figure 12. Standard free energy changes in the incorporation of methane.

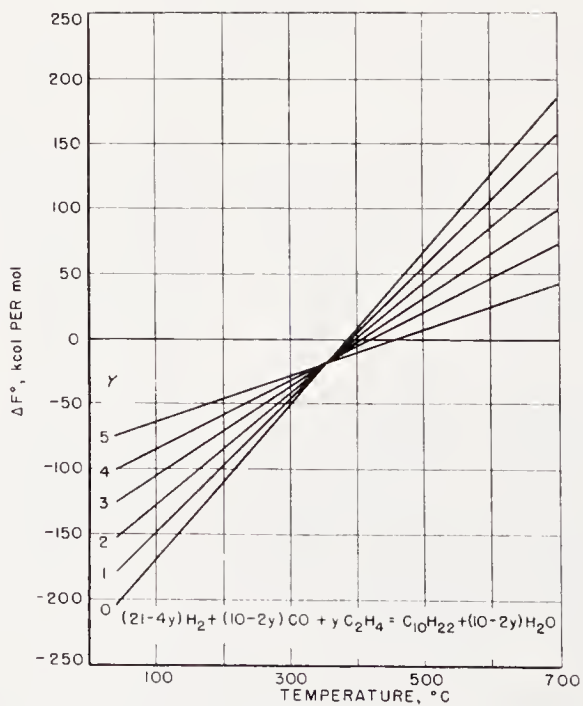


Figure 13. Standard free energy changes in the incorporation of ethylene.

catalysts being about 400°C and 30 to 40 atms. The upper limits of temperature and pressure for cobalt and nickel are considerably lower than for iron.

4. In the above ranges of temperature and pressure, sizable yields are thermodynamically possible of all types of hydrocarbons with the exception of acetylene. The equilibrium constants of cyclic and aromatic hydrocarbons, which are found in only small amounts in Fischer-Tropsch products, are about equal to those for monoolefins of the same carbon number.

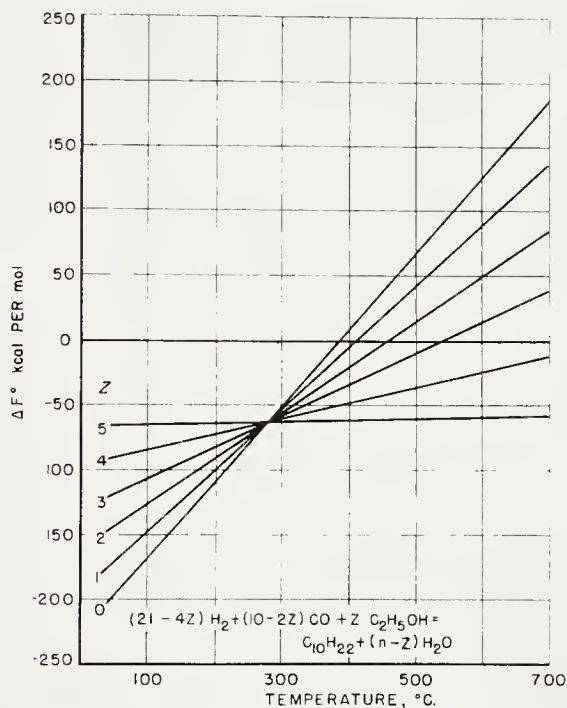


Figure 14. Standard free energy changes in the incorporation of ethanol.

5. The free energies of reactions resulting in hydrocarbons containing the same number of carbon atoms become more negative in the order: diolefins, monoolefins, paraffins.

6. Large yields of alcohols, except methanol, from the hydrogenation of carbon monoxides are thermodynamically possible under usual Fischer-Tropsch conditions. The equilibrium percentages of $2\text{H}_2 + 1\text{CO}$ gas converted to methanol at 30 atms. are 57, 39, and 10 per cent at 225, 250, and 300°C, respectively.

7. Hydrogenation of carbon dioxide to hydrocarbons or alcohols, except for acetylene and methanol, is thermodynamically possible under most synthesis conditions.

8. The equilibrium constants of the water-gas shift reaction, $\text{H}_2\text{O} + \text{CO} = \text{H}_2 + \text{CO}_2$, are large at Fischer-Tropsch temperatures. Hence, if equilibrium were attained for the water-gas reaction, almost all of the water produced by primary synthesis reactions should be converted to carbon dioxide. The fact that nearly all of the oxygen appears as water in the synthesis on nickel and cobalt, and more than 25 per cent in the synthesis on iron must be due to the relatively low rate of the water-gas reaction.

9. Reactions of water plus carbon monoxide to produce hydrocarbons are accompanied by more negative values of ΔF° and ΔH than corresponding reactions of hydrogen and carbon monoxide.

10. Reactions of water plus graphite to give hydrocarbons have positive values of ΔF° and ΔH . These reactions, which approximate the desired over-all equations for the production of synthetic fuels from coal, are thermodynamically impossible under all practical conditions and can proceed only upon gasification of coal at high temperatures ($> 700^\circ\text{C}$) followed by synthesis at temperatures below 500°C .

11. Equilibrium data for the isomerization of paraffins and olefins indicate that the concentrations of the major products of the Fischer-Tropsch synthesis, *n*-paraffins and 1-olefins, greatly exceed the equilibrium values. Hence, the isomer distribution results from the mechanism of chain growth and is not greatly affected by subsequent isomerization reactions.

12. Hydrogenation of olefins and dehydration of alcohols are thermodynamically possible under usual synthesis conditions. Thus, alcohols must be a primary product of the synthesis, while olefins and paraffins may be produced by dehydration of alcohols and hydrogenation of olefins, respectively, as well as by primary reactions.

13. Hydrocracking of paraffins (the reverse of Eqs. (1), (2) and (3) of Table 4) is thermodynamically possible at Fischer-Tropsch temperatures; but the forward reaction, combination of methane with paraffins, is not possible. Reactions involving the combination of two olefins or of an olefin with a paraffin are thermodynamically possible.

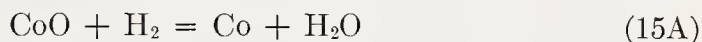
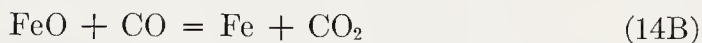
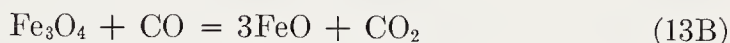
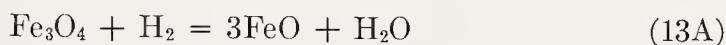
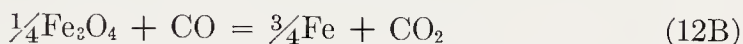
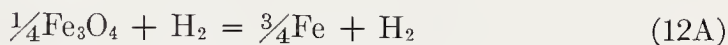
14. The standard-state free energy changes for reactions of methane, hydrogen, and carbon monoxide become more positive with increasing ratios of moles of methane to carbon atoms in the hydrocarbon. Below 300°C the reactions are thermodynamically favorable up to a ratio of 0.3.

15. Reaction of any amount of ethylene or ethanol with hydrogen-carbon monoxide mixtures is thermodynamically possible at all Fischer-Tropsch temperatures. The incorporation of methanol is thermodynamically favored over that of ethanol, while higher alcohols are less likely to be incorporated. Similarly, ethylene has a greater thermodynamic tendency to incorporate than higher olefins.

THERMODYNAMICS OF REACTIONS OF IRON, COBALT, AND NICKEL

In the remainder of this chapter the thermodynamics of reactions of iron, cobalt, and nickel are considered. Apparently, data for ruthenium are not available; however, enough information may be gathered from its known behavior to predict its possible reactions in the synthesis. First, its oxide is easily reducible; second, carbides of ruthenium have not been prepared; and third, the formation of ruthenium carbonyl requires considerably higher pressures than necessary for the iron group elements.

Thermodynamics of Oxides



For the foregoing reactions, equilibrium constants, defined as $K = p_{\text{H}_2\text{O}}/p_{\text{H}_2}$ or $K = p_{\text{CO}_2}/p_{\text{CO}}$, are plotted as functions of reciprocal temperature in Figure 15. The solid lines are taken from data of Emmett and Shultz for iron⁸ and cobalt⁷, and of Pease and Cook for nickel¹⁷. High-temperature measurements on cobalt by Kleppa¹¹ and on nickel by Fricke and Weillbrecht⁹ are shown by circles. The ease of reducibility of oxides increases in the order iron, cobalt, and nickel. At synthesis temperatures the ranges of the ratio $p_{\text{H}_2\text{O}}/p_{\text{H}_2}$ are 0.013–0.14, 79–130, and 390–1400 for iron, cobalt, and nickel, respectively. The equilibrium ratios for iron are exceeded under almost all synthesis conditions, but the ratios for cobalt and nickel are rarely attained. The values of $p_{\text{CO}_2}/p_{\text{CO}}$ required to oxidize the metals are 10 to 100 times greater than corresponding values for $p_{\text{H}_2\text{O}}/p_{\text{H}_2}$. Ferrous oxide is thermodynamically unstable below about 570°C. Ferric oxide is readily reduced to magnetite; neither ferric nor ferrous oxide occurs in used iron catalysts.

Thus, the formation of oxides of cobalt and nickel is thermodynamically improbable in the synthesis, while the formation of magnetite depends

upon the partial pressures of water and carbon dioxide: (a) at very low partial pressures oxidation does not occur; (b) at moderate partial pressures iron may be oxidized by water, while the oxide may be reduced by carbon monoxide; and (c) at higher partial pressures oxidation by both water and carbon dioxide is possible. In any case, magnetite is the iron oxide found in used iron catalysts. Surface layers of metals appear to oxidize more readily than the bulk. Thus, Almquist and Black¹ and Brunauer

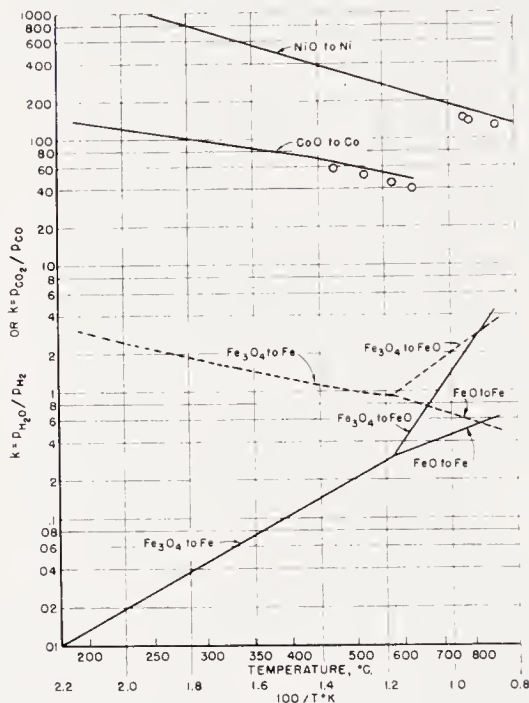
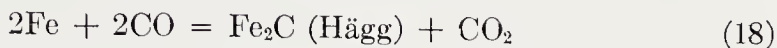


Figure 15. Equilibrium constants for the reduction of iron, cobalt, and nickel oxides. Solid curves for reduction with hydrogen, and broken curves for reduction with carbon monoxide.

and Emmett⁴ found that the surface was partially oxidized if the $p_{\text{H}_2\text{O}}/p_{\text{H}_2}$ was even one-thousandth of the equilibrium value for the bulk material.

Thermodynamics of Carbides of Iron, Cobalt, and Nickel

Thermodynamic data, chiefly from studies of Browning and Emmett^{2, 3, 13}, are available for Hägg iron carbide ($\sim\text{Fe}_2\text{C}$), cementite (Fe_3C), cobalt carbide ($\sim\text{Co}_2\text{C}$), and nickel carbide (Ni_3C). Free energies of formation of these carbides are summarized in Table 6. These data are in agreement with older work of Watase²⁶ on cementite and Schenck²³ on nickel carbide. In the Fischer-Tropsch temperature range these carbides have positive free energies of formation, i.e., they are unstable with respect to decomposition to metal and carbon. However, reactions producing carbides from carbon monoxide such as



have negative standard free energy changes. For Eq. (17), ΔF° is -16.6 and -12.9 kcal at 227 and 327°C , respectively. For Eq. (18) ΔF° is -16.2 and -12.3 kcal. No data are available for the free energy of formation of hexagonal iron carbide, but it is probably more positive than that of Hägg carbide since hexagonal carbide is known to transform to the Hägg phase at synthesis temperatures.

TABLE 6. FREE ENERGIES OF FORMATION OF CARBIDES OF IRON, COBALT, AND NICKEL

Temp. ($^\circ\text{C}$)	ΔF° , kcal/mole			
	Cementite ^a $3\text{Fe} + \text{C}_g = \text{Fe}_3\text{C}$	Hägg Carbide ^a $2\text{Fe} + \text{C}_g = \text{Fe}_2\text{C}$	Cobalt Carbide ^b $2\text{Co} + \text{C}_g = \text{Co}_2\text{C}$	Nickel Carbide ^b $3\text{Ni} + \text{C}_g = \text{Ni}_3\text{C}$
0	+4.487			
127	4.043			
177		+3.866		
227	3.461	3.821	+2.400	+7.127
327	2.82	3.458		4.653
377		3.140		
427	2.16			

^a Browning, L. C., DeWitt, T. W., and Emmett, P. H., Ref. 2.

^b Browning, L. C., and Emmett, P. H., Ref. 3.

Browning and Emmett computed equilibrium constants for the hydrogenation of Hägg iron carbide to paraffinic and olefinic hydrocarbons as shown in Table 7. The bulk-phase carbide can be hydrogenated to sizable amounts of paraffins with carbon numbers less than 5 at 227°C , while at 327°C only methane and ethane can be formed in sizable quantities. Olefins cannot be produced in appreciable quantities at any of these temperatures. Cementite is more stable than Hägg carbide, and its hydrogenation of hydrocarbons is thermodynamically less favorable. Reversing reactions A and B of Table 7 provides a possible method of preparing carbides. At 327°C it is thermodynamically possible to prepare Hägg carbide and cementite by treating iron with paraffins of carbon numbers greater than 2 or with any olefin. Carbides of iron can also be produced from methane at this temperature; however, the rate of carbide formation is low due to unfavorable thermodynamics. Carbides are produced from methane at a moderate rate at 450 to 500°C but at these temperatures only cementite

is formed. Equilibrium calculations for the hydrogenation of cobalt and nickel carbides lead to the same conclusions as those for iron carbides, i.e., olefins and higher paraffins cannot be formed in this manner.

These data preclude the hydrogenation of bulk-phase carbides as a step in the Fischer-Tropsch mechanism. However, formation of higher hydro-

TABLE 7. EQUILIBRIUM CONSTANTS FOR HYDROGENATION OF Fe_2C (HÄGG)^a

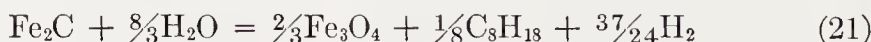


Temp. (°C)	<i>n</i>	$\log_{10} K_{\text{eq}}$	
		Paraffins, Reaction A	Olefins, Reaction B
177	2	+4.827	-5.19
	4	2.580	-5.28
	6	0.93	-6.80
	8	-0.85	
227	2	+2.829	-5.07
	4	0.184	-6.19
	6	-2.421	-8.65
	8	-5.136	
327	2	+0.339	-5.11
	4	-3.933	-8.03
	6	-8.190	-12.16
	8	-12.58	
377	2		-5.22
	4		-8.94
	6		-14.02
427	2	-0.67	
	4	-5.71	
	6	-10.52	
	8	-15.77	

^a Emmett and co-workers, Ref. 13.

carbons from one or more interstitial carbon atoms and several carbons from carbon monoxide is thermodynamically possible.

Iron carbides and metallic iron are oxidized in the Fischer-Tropsch synthesis. Typical equations for the oxidation of Hägg carbide by water are:



ΔF° values for these equations are given in Table 8. Reactions according to Eqs. (19) and (21) are thermodynamically possible under synthesis conditions; Eq. (20) may proceed depending upon the concentrations of water, hydrogen, and carbon monoxide in the gas stream. The free energy changes of corresponding reactions of cementite are more negative than those of Hägg carbide. Similar reactions for cobalt and nickel carbides have positive free energy changes because the free energies of oxidation of these metals are more positive.

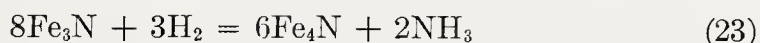
Thermodynamics of Nitrides of Iron

The thermodynamics of the nitrides of iron have been studied rather completely, but no thermal data are available for nitrides of cobalt and nickel. Carbonitrides of these metals have only recently been described, and as yet there are no thermodynamic data.

TABLE 8. FREE ENERGIES FOR REACTIONS OF WATER WITH HÄGG CARBIDE

	ΔF° , kcal/mole	
	227°C	327°C
Eq. 19	-14.38	-12.56
Eq. 20	+0.88	-0.75
Eq. 21	-9.05	-4.81

The following phases are known in the iron-nitrogen system: γ' -(Fe₄N), ϵ -(\sim Fe₃N to \sim Fe₂N), and ζ -(Fe₂N). Equilibrium data for the formation of γ' - and ϵ -iron nitride have been determined by Lehrer¹⁴ and Brunauer, Jefferson, Emmett, and Hendricks⁵. Figure 16 presents equilibrium constants for the equations



where Fe₃N in Eq. (23) represents the lower nitrogen limit of the ϵ -phase. Also included in this figure is a scale of the percentage of ammonia (in an ammonia-hydrogen mixture at 1 atm.) corresponding to the equilibrium constants. The values of the equilibrium constants and the ammonia content of the gas increase with decreasing temperatures. Thus, the ammonia contents of ammonia-hydrogen mixtures at 1 atm. are about 37 and 30 per cent for formation of Fe₄N and 77 and 70 per cent for Fe₃N at 400 and 444°C, respectively. Formation of ϵ -iron nitrides of higher nitrogen content requires higher ammonia concentrations than those cited above as,

shown in Figure 17; the concentration required to produce a nitride of a given nitrogen content is again lower at 444 than at 400°C. Although nitriding at a higher temperature is more favorable thermodynamically,

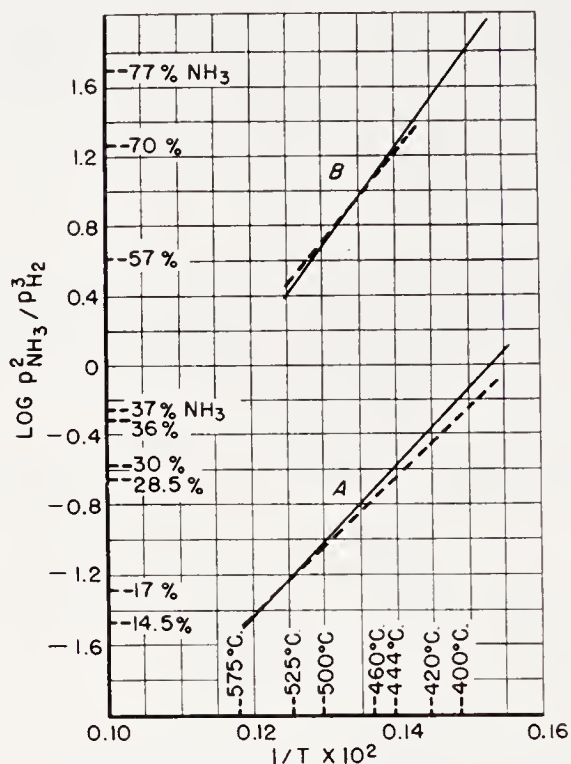


Figure 16. Equilibrium constants of the formation of iron nitrides by Equation 22 (Curve A) and Equation 23 (Curve B).

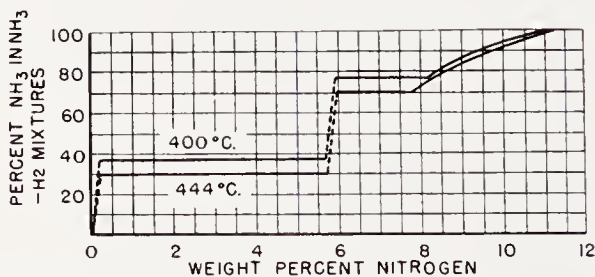


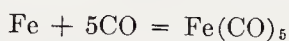
Figure 17. Equilibrium nitrogen content of iron nitrides as a function of the percentage of NH_3 in NH_3 - H_2 mixtures.

this advantage is counterbalanced by the fact that most catalytic materials decompose ammonia into nitrogen and hydrogen at an appreciable rate above 400°C.

Thermodynamics of Carbonyls

A consideration of carbonyls of the catalytically active metals is of importance in this discussion because (a) removal of the active metal by for-

mation of a volatile carbonyl is probably an important factor in limiting the Fischer-Tropsch synthesis to relatively low pressures compared with those used for the alcohol and iso-syntheses, and (b) carbonyls or carbonyl-type surface complexes may be intermediates in the reaction. The volatile carbonyls $\text{Ni}(\text{CO})_4$, $[\text{Co}(\text{CO})_4]_2$, $\text{Fe}(\text{CO})_5$, and $\text{Ru}(\text{CO})_5$ are of special interest. The thermodynamic tendency for their formation apparently decreases in the above order, although equilibrium data are available only for iron and nickel. In addition to these compounds a number of carbonyls

TABLE 9. FORMATION OF IRON PENTACARBONYL^a

Temp. (°C)	$\log_{10} K_p$	Temp. (°C)	$\log_{10} K_p$
100	-3.53	250	-11.38
150	-6.77	300	-13.06
200	-9.32	350	-14.48

^a H. Pichler and H. Walenda, Ref. 19.

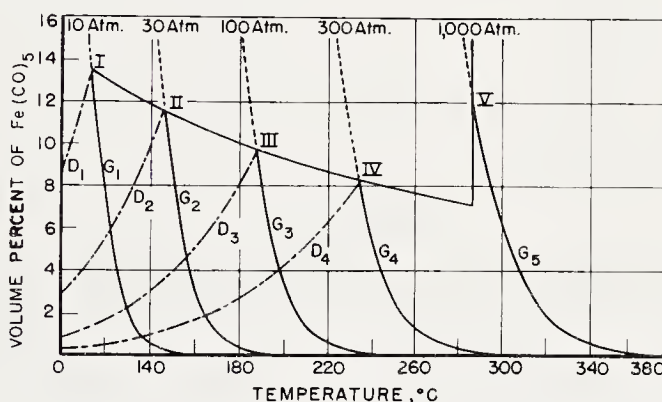


Figure 18. Equilibrium concentrations of $\text{Fe}(\text{CO})_5$ at different pressures and temperatures.

of lower volatility are known, such as $\text{Fe}_2(\text{CO})_9$, as well as hydrocarbonyls of cobalt, $\text{Co}(\text{CO})_4\text{H}$, and iron, $\text{Fe}(\text{CO})_4\text{H}_2$.

Table 9 lists equilibrium constants for the formation of iron pentacarbonyl, and Figure 18 gives equilibrium concentrations of this carbonyl as a function of temperature and pressure¹⁹. The solid curves G_1 – G_5 represent equilibrium concentrations at various temperatures and pressures, and the dotted curves D_1 – D_4 represent the percentage of carbonyl in saturated vapor. The solid line connecting the intersections of corresponding D and G curves, denoted by I–IV, represents the maximum possible concentration of carbonyl in the gas phase, because at this line the partial pressure of carbonyl equals its vapor pressure. A sharp vertical rise in this curve

occurs at the critical temperature of iron carbonyl. For iron catalysts under 10 atms. of $1\text{H}_2 + 1\text{CO}$ gas, the equilibrium concentrations of iron pentacarbonyl are 10^{-5} and 10^{-8} volume-per cent at 200 and 300°C, respectively.

The equilibrium data of Montgomery and Tomlinson¹⁵ for the formation of nickel tetracarbonyl are given in Table 10. These equilibrium constants are about 1000 greater than those for iron pentacarbonyl.

Note: The equilibrium between dicobalt octacarbonyl and cobalt tricarbonyl according to $[\text{Co}(\text{CO})_3]_4 + 4\text{CO} \rightleftharpoons 2[\text{Co}(\text{CO})_4]_2$ in the temperature range 73° to 137°C. has been described by R. Ercoli and F. Barbieri-Hermitte, *Atti accad. nazl. Lincei, Rend., Classe sci. fis., mat. e nat.* **16**, 249 (1954).

TABLE 10. FORMATION OF NICKEL CARBONYL^a
 $\text{Ni} + 4\text{CO} = \text{Ni}(\text{CO})_4$

Temp. (°C)	$\log_{10} K_p$
20	4.64
30	3.93
40	3.13
50	2.41
70	1.18
90	0.04
110	-0.95

^a See Ref. 15.

Bibliography

1. Almquist, J. A., and Black, C. A., *J. Am. Chem. Soc.*, **48**, 2814 (1926).
2. Browning, L. C., DeWitt, T. W., and Emmett, P. H., *J. Am. Chem. Soc.*, **72**, 4211 (1950).
3. Browning, L. C., and Emmett, P. H., *J. Am. Chem. Soc.*, **74**, 1680 (1952).
4. Brunauer, S., and Emmett, P. H., *J. Am. Chem. Soc.*, **52**, 2682 (1930).
5. Brunauer, S., Jefferson, M. E., Emmett, P. H., and Hendricks, S. B., *J. Am. Chem. Soc.*, **53**, 1778 (1931).
6. Dolch, P., *TOM Reel 134, Navy 5811, Item Ib-2*.
7. Emmett, P. H., and Shultz, J. F., *J. Am. Chem. Soc.*, **51**, 3249 (1929).
8. Emmett, P. H., and Shultz, J. F., *J. Am. Chem. Soc.*, **52**, 4268 (1930); **55**, 1376 (1933).
9. Fricke, R., and Weilbrecht, G., *Z. Elektrochem.*, **48**, 87 (1942).
10. Hougen, O. A., and Watson, K. M., "Chemical Process Principles. Part I," Chapt. VIII. New York, John Wiley & Sons, Inc., 1943.
11. Kleppa, O. J., *Svensk Kem. Tidskr.*, **55**, 18 (1943); *Chem. Abs.* **38**, 4855 (1944).
12. Koelbel, H., and Engelhardt, F., *Brennstoff-Chem.*, **33**, 13 (1952).
13. Kummer, J. T., Browning, L. C., and Emmett, P. H., *J. Chem. Phys.*, **16**, 740 (1948).
14. Lehrer, E., *Z. Elektrochem.*, **36**, 383 (1930).
15. Montgomery, C. W. and Tomlinson, J. R., to be published.
16. Myddleton, W. W., *J. Inst. Petroleum*, **30**, 211 (1944).

17. Pease, R. N., and Cook, R. S., *J. Am. Chem. Soc.*, **48**, 1199 (1926).
18. Pichler, H., and Bufileb, H., *Brennstoff-Chem.*, **23**, 73 (1942).
19. Pichler, H., and Walenda, H., *Brennstoff-Chem.*, **21**, 133 (1940).
20. Prettre, M., *Rev. inst. franç. pétrole et Ann. combustibles liquides*, **2**, 131 (1947).
21. Rossini, F. D., Pitzer, K. S., Taylor, W. J., Ebert, J. P., Kilpatrick, J. E., Beckett, C. W., Williams, M. G., and Werner, H. G., "Selected Values of Properties of Hydrocarbons," American Petroleum Institute, Research Project 44.
22. Schneider, *TOM Reel 134, Navy 5811, Item Ib-1*.
23. Schenk, R., *Z. anorg. Chem.*, **164**, 313 (1927).
24. Smith, D. F., *Ind. Eng. Chem.*, **19**, 801 (1927).
25. Storch, H. H., Golumbic, N., and Anderson, R. B., "The Fischer-Tropsch and Related Syntheses," Chap. I, New York, John Wiley & Sons, Inc., 1951.
26. Watase, T., *J. Chem. Soc. Japan*, **54**, 110 (1933); *Z. physik. Chem.*, **147A**, 390 (1930).
27. Wenner, R. R., *Chem. Eng. Progr.* **45**, 200 (1949).

CHAPTER 2

CATALYSTS FOR THE FISCHER-TROPSCH SYNTHESIS

Robert B. Anderson

*Chief, Branch of Coal-to-Oil Research, Division of Solid Fuels Technology,
Bureau of Mines, Pittsburgh, Pa.*

SCOPE OF THE CHAPTER

This chapter describes the development of catalysts and factors determining their behavior in the hydrogenation of carbon monoxide. A brief history of catalysts and process development, including pertinent features of the design of commercial reactors and the requirements for successful catalysts in each reactor is presented, followed by a description of typical apparatus for testing catalysts and the analytical methods employed. The available data from tests of various types of catalyst and the factors influencing their activity, selectivity, and stability are considered next. Cobalt and nickel catalysts, which are similar in many ways, are discussed first, iron catalysts next, and then ruthenium. Finally, the poisoning of catalysts by sulfur compounds is described.

A large mass of data is available for tests of catalysts of different compositions and modes of preparation, and the problem of presenting a readable and coordinated description is formidable. This difficulty arises in part from diversity of possible combinations, as well as from the fact that catalyst pretreatment and operating conditions many times produce more drastic changes in catalytic behavior than composition. Since the historical aspects are presented early in the chapter, the detailed consideration of factors influencing catalysts is presented in chronological order only where convenient, and in general the data are grouped under topics such as the effect of promoters, the effect of carriers, pretreatment methods, etc.

For bibliographical information the reader is referred to the comprehensive bibliography of the Bureau of Mines^{2a} and to reviews cited in references 93a, 104a, 181, and 198a.

THE DEVELOPMENT OF FISCHER-TROPSCH CATALYSTS AND PROCESSES

In 1902, Sabatier and Senderens¹⁶¹ reported the hydrogenation of carbon monoxide and carbon dioxide to methane on reduced nickel and cobalt

catalysts at atmospheric pressure and temperatures from 200 to 300°C. In the ensuing half century, catalysts have been developed for the hydrogenation of carbon monoxide to straight- and branched-chain olefins and paraffins, methanol and higher alcohols with both straight and branched chains, as well as other oxygenated organic molecules. To appreciate this development, the reader must realize that this period may be considered the beginning of modern catalysis. The catalytic processes for the synthesis of ammonia, hydrogenation of olefinic compounds, and the refining of petroleum were yet to be discovered. The literature of catalysts and catalytic reactions was very meager, and the theoretical aspects of catalysis were virtually unknown. Hence, the search for suitable catalysts involved exhaustive empirical testing, as will be indicated by the methods of developing the Fischer-Tropsch catalysts described in this chapter. In a sense, catalyst development still follows this course, but the chemist is guided by the immense store of experimental and theoretical knowledge collected in the intervening years.

In 1913 and 1914, patents of the Badische Anilin und Soda Fabrik¹⁸ described the hydrogenation of carbon monoxide on alkali-activated cobalt and osmium oxides supported on asbestos at 100 to 200 atmospheres and 300 to 400°C to liquid products containing alcohols, aldehydes, ketones, fatty acids, and some aliphatic hydrocarbons.

In 1923, Franz Fischer and Hans Tropsch⁶¹ of the Kaiser Wilhelm Institut für Kohlenforschung, Mulheim-Ruhr, Germany, reported the production of an oily liquid by the hydrogenation of carbon monoxide on alkalinized iron turnings at 100 to 150 atmospheres and 400 to 450°C. The process was given the name "Synthol" and the product "Synthin." The Synthin contained chiefly oxygenated molecules plus small amounts of hydrocarbons, similar to the high-pressure process described above¹⁸. However, at about 7 atmospheres, the synthol catalyst produced chiefly olefinic and paraffinic hydrocarbons plus small quantities of oxygenated organic compounds. At atmospheric pressure and low temperatures, 200 to 250°C, nickel and cobalt catalysts produced higher hydrocarbons in addition to methane. However, at these relatively low pressures and temperatures the catalysts rapidly lost activity, and a search was started for improved catalysts. These early results led to the premise that high pressures were unsuitable for the synthesis of higher hydrocarbons, and on this basis catalyst tests were usually made at atmospheric pressure. The choice of atmospheric operating pressure, although satisfactory for cobalt and nickel catalysts, was not suitable for the investigation of iron catalysts, which operate best in the range of 7 to 30 atmospheres. As a result, the development of practical iron catalysts was delayed many years.

Early catalysts of Fischer and Tropsch were made by mixing metal

oxides or thermally decomposing metal nitrates. The oxides were usually reduced in hydrogen at 350°C before use in the synthesis. The resulting catalysts were finely divided powders which were difficult to handle. A variety of methods, including pressing oxides into a cake and crushing and the addition of binders and carriers, were used to obtain granular catalysts.

The first catalyst with high activity and moderately long life was the precipitated nickel-thoria-kieselguhr catalyst reported in 1931⁵¹. The best of these was precipitated with potassium carbonate from a solution of nickel and thorium nitrates in the presence of kieselguhr and had a composition of 100 Ni:18ThO₂:100 kieselguhr. This catalyst, after reduction in hydrogen at 450°C, gave a contraction of 70 per cent at 178°C with a flow of 2H₂ + 1CO gas of 1 liter per hour per gram of nickel at atmospheric pressure. The yield of C₅+ reached 90 grams per cubic meter, corresponding to about two thirds condensed hydrocarbons and one third gaseous hydrocarbons in the total product. The catalyst remained active for at least 5 weeks. This preparation was inactive unless reduced in hydrogen prior to synthesis. The presence of copper decreased the activity of these catalysts.

A cobalt:thoria:kieselguhr (100:18:100) catalyst⁴⁹ prepared in essentially the same manner as the active nickel catalyst, proved to be even better. After reduction in hydrogen at 350°C, this catalyst produced yields of C₅+ hydrocarbons as high as 100 g/m³ of 2H₂ + 1CO at 195°C and atmospheric pressure and gave an average yield of C₅+ of 82 g/m³ for 2 months. Nevertheless, at that time this catalyst was considered to be impractical because of the scarcity of cobalt.

The development of nickel catalysts was continued in the direction of replacing the thoria with less expensive promoters. In 1932, the best nickel catalyst, Ni:MnO:Al₂O₃:kieselguhr, 100:25:10:100, was tested in an atmospheric pressure pilot plant, and yields of 70 grams of liquid hydrocarbons per cubic meter of 2H₂ + 1CO gas at 190 to 210°C were attained. In 1934, Ruhrchemie employed a catalyst of this type in a larger pilot plant of about 1,000-tons per year capacity, and in this study the deficiencies of the nickel catalyst for commercial use—poor selectivity, short life, and excessive loss of catalyst metal and promoters in the synthesis and regeneration—became readily apparent.

In 1934, cobalt catalyst development was undertaken at the Ruhrchemie laboratory under Roelen⁷². Although the cobalt catalyst of Fischer performed satisfactorily in the Ruhrchemie laboratory with yields of 120 grams of C₃+ per cubic of 2H₂ + 1CO gas for more than 60 days⁷¹, considerable research was done to produce a less expensive catalyst by changing the amount and type of kieselguhr and by decreasing the amount of thoria. For a short period, small amounts of copper were added to cobalt-thoria-kieselguhr catalysts to lower the reduction temperature so that this step

could be accomplished in the synthesis reactors; however, the presence of copper shortened the life of the catalyst considerably, and thereafter only copper-free catalysts were considered. These studies led to the $\text{Co}:\text{ThO}_2:\text{MgO}:\text{kieselguhr}$ (100:5:8:200) preparation, which became the standard catalyst in the commercial synthesis in Germany during the period 1938 to 1944.

In 1935 to 1939, laboratory and pilot plant studies on $\text{Co}:\text{ThO}_2$ -kieselguhr catalysts were made at the British Fuel Research Station, Greenwich¹⁴¹, and in general the results were comparable to those of the Germans.

In 1936, Fischer and Pichler^{56, 57, 58} reported that it was advantageous to operate precipitated, kieselguhr-supported cobalt catalysts at pressures from 5 to 15 atmospheres, this being termed the "medium pressure synthesis." These results were contrary to early experience with decomposition-type catalysts. In the medium pressure synthesis, lower yields of gaseous hydrocarbons were obtained, the catalyst life was greater than in the atmospheric synthesis, and periodic reactivation of the catalyst was unnecessary. However, the really important result of this discovery was that it directed future research into this range of pressure and led to the development of successful iron catalysts.

In the period 1930–1936, when great progress⁴⁷ was made in the development of nickel and cobalt catalysts, some research was continued on iron catalysts, chiefly because iron was inexpensive and readily available. The results, however, were not promising. The introduction of precipitated iron catalysts instead of earlier types and the use of kieselguhr as a support resulted in only slight improvements. Catalyst lives from 4 to 6 weeks and maximum yields of liquid hydrocarbon of 50 to 60 grams per cubic meter were attained. In the winter of 1936–1937, Fischer and Pichler^{59, 123, 131} increased the operating pressure on a precipitated iron catalyst from 1 to 15 atmospheres. The yields were almost doubled and the life was increased several-fold. This discovery led to intensive research on iron catalysts by several German laboratories, with the ultimate goal of developing a satisfactory iron catalyst to replace the cobalt catalysts used in the synthesis plants. The developmental programs in the various laboratories followed rather divergent paths, and in 1943 the German government arranged comparative tests at Schwarzheide, the "Reichsamtversuch," to select the most suitable iron catalyst for this purpose. The behavior of all of these catalysts was moderately good, indicating that remarkable progress had been made since the discovery of the medium pressure synthesis. Five of the six catalysts tested were precipitated iron oxide gels either with or without carriers; the sixth was a typical fused ammonia synthesis catalyst. Although a variety of promoters (copper, zinc oxide, alumina, calcium oxide) and carriers (kieselguhr, dolomite, silica gel) were used in these

preparations, the only additive essential to high activity and selectivity appeared to be alkali. Before synthesis, these catalysts were treated with hydrogen or $H_2 + CO$ mixtures to effect at least a partial reduction and, in some cases, conversion to carbides.

In 1940, Pichler and Buffleb reported the unique synthesis of very high molecular weight hydrocarbons on ruthenium catalysts with $2H_2 + 1CO$ gas at pressure up to 1,000 atmospheres. At the higher pressures, waxes of average molecular weights up to 23,000 were obtained in sizable yields.

In 1942, after a lapse of 12 years, research on the Fischer-Tropsch synthesis was resumed at the U. S. Bureau of Mines. This work and that in progress at the British Fuels Research Station were first concerned with factors influencing the production of active cobalt catalysts, principally of the Fischer or Ruhrchemie types, but by 1946 the research had shifted to iron catalysts.

In the post World War II period, principally in the United States and in England, many of the new tools of catalytic research developed in the decade 1930 to 1940 were applied to the study of Fischer-Tropsch catalysts and reaction mechanism: the determination of surface area and pore volume of catalysts; qualitative and quantitative analysis of catalytic materials by x-ray diffraction and thermomagnetic analysis; electron diffraction and microscope studies of catalysts; and the use of isotopes, C^{13} , C^{14} and deuterium, as tagged atoms in synthesis studies. In this period, kinetic studies arranged to permit simple interpretation of the variables of synthesis reactions were reported.

Removal of the heat of the reaction is the most difficult engineering problem in reactor design. The early pilot plant studies, as well as the German commercial plants from 1938 to 1944, employed fixed bed-externally cooled reactors of two types. The first reactor, used in the atmospheric pressure synthesis, consisted of a box filled with vertical parallel steel sheets spaced about 7 mm apart and traversed by horizontal cooling pipes through which water under pressure was circulated. The catalyst was placed between the steel plates. In the second, the medium pressure reactor, the catalyst was placed in a 10-mm annulus between concentric tubes which were provided with water cooling outside of the outer tube and inside the inner tube. Both of these reactors were difficult to fabricate and required large amounts of steel. Charging and removal of the catalyst was difficult. The removal of heat was rather ineffective, so that operation at low space velocities, from 80 to 100 hr^{-1} , was required to prevent overheating the catalyst. Although in the standardization of synthesis apparatus for the German war effort these reactors were selected, their inadequacy was realized and research on reactor design was continued. In the period 1938 to 1944, three processes evolved from this research: the oil-recycle process of I. G. Farben; the

oil-slurry process of Rheinpreussen, Ruhrchemie and I. G. Farben; and the hot-gas-recycle process of I. G. Farben.

Since 1940, fluidized- and entrained-catalyst techniques have been developed by American companies, especially M. W. Kellogg, Hydrocarbon Research, Standard Oil Development, and the Texas Company. In 1945, the U. S. Bureau of Mines began studies of the oil-recycle and slurry processes, and at present the oil-recycle process is well developed. Recent reports from Germany describe improved fixed-bed reactors; however, few details are available. The commercial synthesis plant of Carthage Hydrocol, Brownsville, Texas, utilizing the fluidized process, was not successful due to a variety of operating difficulties. At present, a commercial Fischer-Tropsch plant is under construction in the Union of South Africa. It will employ both fixed-bed reactors of the type recently developed in Germany and entrained-catalyst units.

In the next few pages, some of the pertinent features of reactor design will be summarized to provide the reader with a general picture of this subject. For a recent detailed description of various processes, see Storch¹⁸¹. Since the major engineering problem is the removal of the heat of reaction from the catalyst bed, the reactors that have been investigated on a pilot-plant or larger scale have been classified on this basis:

A. External cooling

1. Fixed-bed

- | | |
|----------------------------|---|
| a. Plate-type | } German commercial reactors in 1937-1944 |
| b. Double tube | |
| c. Larger tubular reactors | |

2. Fluid or entrained bed	{ Hydrocol process
	{ Kellogg process

B. Internal cooling

1. Oil as heat transfer medium

- a. Fixed-bed, oil-circulation process
b. Agitated-bed, oil-circulation process
c. Fluid-bed, slurry process

2. Gas as heat transfer medium, hot-gas-recycle process

The early German fixed-bed reactors have been described on p. 33. Fluid-fixed bed reactors consist of large tubular reactors cooled by bayonet-type heat exchangers hung from the top of the unit. With iron catalysts, the reactor is usually operated at high temperatures, 325 to 350°C, to prevent catalyst agglomeration. Pressures of 20 to 40 atmospheres are used and fresh feed space velocities of 2,000 to 2,500 hr⁻¹ with a recycle ratio of about 2:1. Patents describe cyclones and other devices for preventing carry-over of catalyst and mechanisms for removing used and introducing fresh catalyst. Although this type of reactor operated successfully in large

pilot plant units, considerable difficulty apparently related to overheating of the catalyst was experienced in the operation of the commercial reactor of the Carthage Hydrocol plant.

In the oil-circulation process, a fixed-bed catalyst is submerged in cooling oil. Synthesis gas and cooling oil are passed concurrently upward through the bed. The cooling oil flows out the top of the reactor, through a heat exchanger, and enters the bottom of the reactor. Usual operating conditions in Bureau of Mines pilot plants are: pressure, 20 atmospheres; temperature, 240 to 280°C; space velocity of fresh feed, 500 to 800 hr⁻¹; and recycle ratio, 2 or 3. The temperature increase in the bed is determined by the rate of circulation of cooling oil. With some catalysts, agglomeration of the particles led to plugging of the reactor. This difficulty was eliminated by increasing the velocity of the cooling oil sufficiently to agitate the particles. Other variations of the process involve the use of evaporative cooling by volatilization of cooling oil, and countercurrent flow of oil and gas; however, temperature control with these modifications is not as efficient and occasionally localized overheating occurs.

In the slurry process, a finely divided catalyst is suspended in cooling oil, and both catalyst and oil are circulated through an external heat exchanger. Heavy products are removed through sintered metal filters. Operating conditions are similar to those of the oil-circulation process, except that the flow of synthesis gas per unit weight of catalyst is several times larger in the slurry process.

For the slurry and oil-circulation processes, large tubular reactors should be operable, provided that the synthesis gas and cooling oil are properly distributed across the inlet portion of the reactor.

The hot-gas-recycle process employs a fixed-catalyst bed. High recirculation of end gas is required (the ratio of end gas to fresh feed being as high as 100), since the heat of reaction is dissipated by heating the gas. The gas is heated about 10°C in passing through the bed and then cooled by this amount in an external heat exchanger. Except for the high recycle ratios, operating conditions are somewhat similar to those of the fluidized synthesis: operating pressure 20 atmospheres, temperature 320 to 330°C, and space velocity of fresh gas of 270 hr⁻¹. In German studies, the cost of recirculating gas was prohibitively high, due to the large pressure drop of the catalyst bed employed. New catalysts, such as activated steel lathe turnings recently developed at the Bureau of Mines, have a large void space and a very low pressure drop; thus, by employing these catalysts, one can substantially reduce the cost of recirculation.

Figure 1 presents a simplified schematic representation of the pertinent features of Fischer-Tropsch reactors. The desired catalytic and physical characteristics of catalysts for the various reactors are summarized in

Table 1. Storch^{179, 181} has compared the various reactors with iron and cobalt catalysts in terms of space-time yield, product distribution, and steel requirement for reactors, as given in Table 2. Hall, Gall, and Smith⁷⁴ presented synthesis data comparing the fixed-bed, slurry, and fluid reactors using the same catalyst and operating conditions.

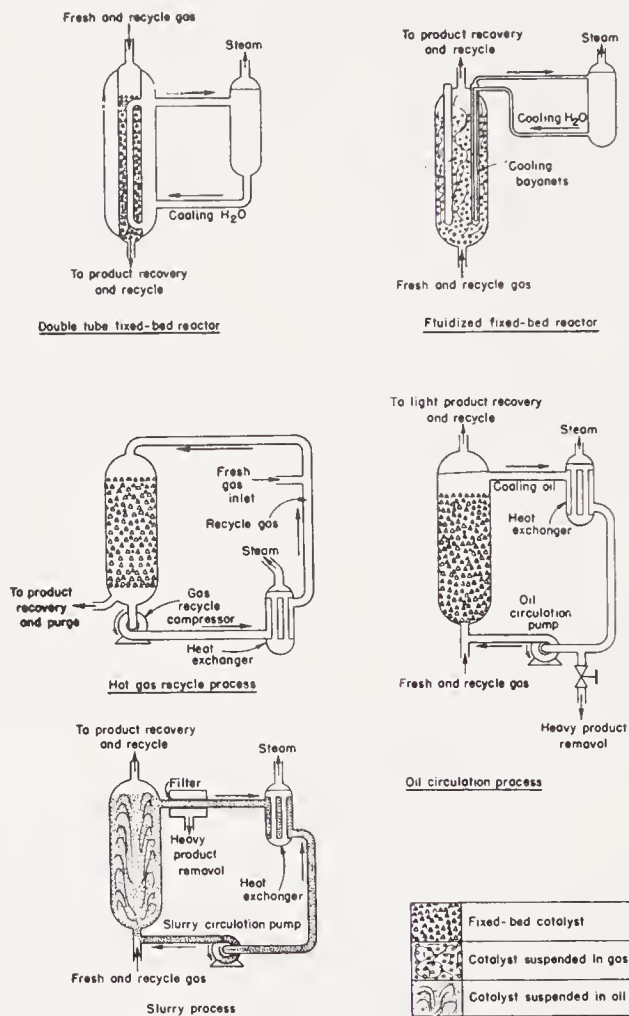


Figure 1. Schematic representation of Fischer-Tropsch reactors.

EXPERIMENTAL METHODS FOR TESTING CATALYSTS

There are no reliable methods for evaluating Fischer-Tropsch catalysts except testing them in the synthesis. Although tests of short duration, a few hours to one day, may suffice to demonstrate qualitatively whether the catalyst is active or inactive and whether the products contain chiefly gaseous or condensed hydrocarbons, experiments of one week to several months are usually required for reliable data regarding activity, selectivity,

and stability of catalysts. In some cases, marked changes in the catalytic properties occur with time; thus activity and selectivity data taken in the first day will usually not adequately represent the average values determined over a longer period of testing. Catalyst tests are usually made in small fixed dry-bed reactors, and the correlation between the results of these and other reactors varies from good to poor. In Bureau of Mines research, the fixed-bed results correlated moderately well with data from the oil-circulation process, but not with results from the slurry process. Hall and co-workers⁷⁴ found that data from fixed- and fluid-bed operation were comparable if proper corrections are made for differences in particle size of the catalyst. For fluidized-type reactors, the duration of the test can

TABLE 1. REQUIREMENT OF CATALYSTS FOR FISCHER-TROPSCH REACTORS

Type of Reactor	Desirable Characteristics of Catalysts			
	Activity	Mechanical Strength	Mechanical and Chemical Stability	Pressure Drop in Catalyst Bed
<i>Externally cooled</i>				
Fixed-bed	High	Moderate	High	Low
Fluidized-bed	Moderate	High	High	Unimportant
<i>Internally cooled, oil phase</i>				
Fixed-bed	High	Moderate	High	Low to moderate
Agitated-bed	High	High	High	
Slurry	High	Unimportant	Unimportant	
<i>Internally cooled, gas phase</i>				
Hot gas recycle	Moderate	High	High	Low

usually be shortened considerably, since flow of synthesis gas and the productivity per unit weight of catalyst usually exceed those of fixed-bed tests by a factor of 10, and a corresponding shorter catalyst life is expected. Reliable data for cobalt and nickel catalysts can be obtained at atmospheric pressure, but for iron, tests must be made at 5 to 30 atmospheres. Some typical apparatus for testing Fischer-Tropsch catalysts will be considered in the following pages.

The testing units of Fischer and Tropsch described in 1930 appear to have been adequate for the purposes for which they were employed—the assaying of a large number of catalyst preparations at atmospheric pressure. These reactors consisted of a horizontal gas-heated aluminum cylinder, outside diameter 80 mm and inside diameter 24 mm, with four glass tubes of 4 to 5 mm inside diameter.

In early experiments, the product gases were analyzed by typical volu-

metric gas analysis procedures in which hydrocarbons were burned with oxygen. This method gave only the average carbon number of the gaseous

TABLE 2. SPACE-TIME YIELD OF VARIOUS FISCHER-TROPSCH PROCESSES^a

Catalyst	Temp. (°C)	Pressure (atm.)	Space-Time Yield ^b of C ₃ +, kg/cm ³ /hr (bbl./1000 ft ³ /day)	Liquid Product Distribution				Steel in Converter (ton/bbl./day)
				Gasoline	Diesel	Wax	Alcohol	
<i>Ruhrchemie Process</i>								
Co	175-200	1	8 (45)	56	33	11	c	2.7
Co	175-200	10	10 (57)	35	35	30	c	2.4
<i>Lurgi Recycle Process</i>								
Co	190-224	10	13 (74)	50	25	25	6	1.9
Fe	230	20	14 (79)	19	19	56	6	2.1
Fe	275	20	14 (79)	68	19	8	5	2.2
<i>I.G. Liquid-Phase Process</i>								
Fe	240-250	20	8 (45)	34	28	30	8	1.2
Fe	300-310	20	16 (91)	55	33	9	3	1.0
<i>I.G. Oil Recycle Process</i>								
Fe	240-290	25	30 (170)	51	10	29	10	0.7
<i>Internally Cooled Converter Process</i>								
Co	175-225	7	20 (113)	35	35	30	c	.8
<i>I.G. Hot-Gas Recycle Process</i>								
Fe	300-320	20	32 (181)	70	17	1	12	.7
<i>Fluidized Iron Catalyst Process</i>								
Fe	300-320	20	32 (181)	75	15	1	9	.6

^a From Ref. 179.

^b Weight of total product excluding methane, ethane, and ethylene, per volume of catalyst per unit time.

^c Very small.

hydrocarbons. In later experiments, the exit gas, after removal of carbon dioxide and water, was passed through a trap at liquid nitrogen temperatures, and the gasol hydrocarbons, C₂-C₄, were separated by a simple

distillation of the condensate. Methane was estimated by combustion analysis of the scrubbed exit gas. In 1928 this condensation procedure was replaced by adsorption of light hydrocarbons in a charcoal scrubber. The hydrocarbons were stripped from the charcoal by heating and were condensed in a liquid air trap. The receiver was heated to room temperature and the amount of gasoline was determined gravimetrically.

The major criticisms that may be made of the early apparatus of Fischer are: (a) the reactor tubes were not in direct contact with a cooling medium or a material of relatively constant temperature, and overheating of the catalyst was possible. (However, the relatively low activity obtained in this period was in most cases due to poor catalysts rather than to overheating); (b) the analytical methods were crude and laborious and did not provide a sufficiently detailed characterization of synthesis products. In subsequent research, fixed-bed catalyst testing reactors have been improved. The most efficient small-scale reactor described in Fischer's papers⁵⁷ was the gas-heated, water-cooled unit (Figure 2). The apparatus shown was for two-stage operation, with two catalyst tubes in the first stage and one in the second. The temperature of the water bath surrounding the catalyst tubes was maintained by throttling the gas supply to the reactor with a temperature-sensitive element. In other laboratories, metal reactors with narrow catalyst tubes jacketed by baths of boiling liquids such as water, "Tetralin," or "Dowtherm," or narrow metal tubes surrounded by a close-fitting metal block have been successful under most fixed-bed catalyst testing conditions⁷⁶. For adequate removal of heat, the diameter of reactor tubes should be no larger than 1.5 cm. In units in which the catalyst is placed in the annulus between concentric tubes, the separation between the tubes should be less than 7 mm.

Methods for evaluating synthesis products have improved as new analytical tools became available. A method developed by Schaarschmidt¹⁶⁴ was used in some German laboratories¹⁶⁵ to estimate the extent of branching of hydrocarbons. However, this procedure, based on the separation of molecules containing tertiary carbon atoms by reaction with antimony pentachloride, has not been considered very reliable. Precision low-temperature distillation has been used to separate gaseous hydrocarbons quantitatively; however, this method is quite laborious. In the last 10 years, combinations of precision distillation, chromatographic separation, and infrared and mass spectrometric analyses have given excellent quantitative characterization of hydrocarbons up through the gasoline range as well as oxygenated molecules. The mass spectrometer has proved to be an indispensable tool in analyzing product gases, and recently developed techniques for analysis of liquid samples will further increase the usefulness of this instrument in synthesis research.

The formation of urea-adducts of straight-chain hydrocarbons and their derivatives¹³⁵ should prove a useful analytical method for determining the fraction of straight-chain molecules in higher molecular weight fractions.

The fixed-bed catalyst testing apparatus employed by the Catalyst Research and Testing Group of the U. S. Bureau of Mines at Bruceton, Pennsylvania, will be discussed in detail. Although the apparatus and procedure are not necessarily the best in every respect, they represent typical present methods for catalyst testing which yield data as precise and repro-

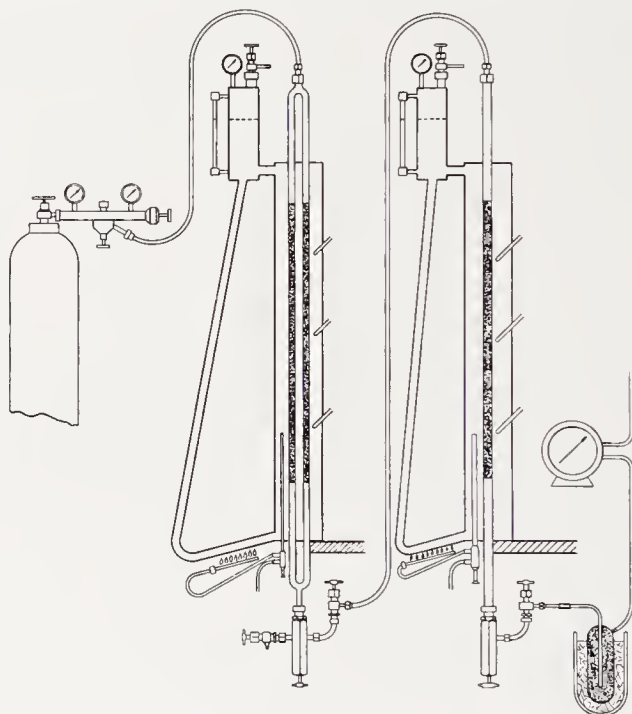


Figure 2. Two-stage laboratory-scale water-cooled reactor. (Reproduced from Ref. 57)

ducible as can be desired from small-scale apparatus. At present the laboratory (Figure 3) contains 16 testing units suitable for operation at pressures up to 21 atmospheres. A flow sheet for one of these units is shown in Figure 4. Compressed synthesis gas from commercial steel cylinders is passed through a reducing valve, adjusted to maintain a pressure about 3 atmospheres in excess of the operating pressure, and through a charcoal trap to remove sulfur compounds and iron carbonyl. Gas flow is regulated by a geared-needle valve and measured by a capillary flow meter. The pressure drop across the calibrated capillary orifices is indicated on a manometer and recorded by a ring balance instrument. For atmospheric pressure tests, an inlet wet test meter may also be used. The gas flows downward over the catalyst in the vertical converter. Liquid and solid hydrocarbons and

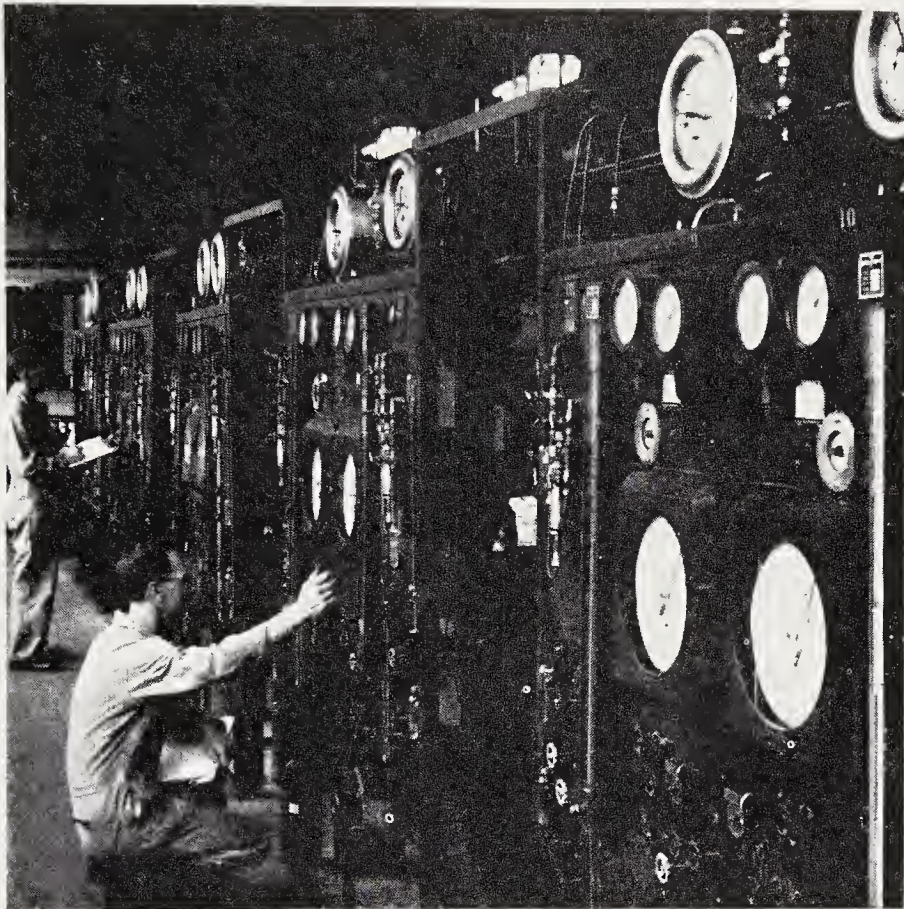


Figure 3. Catalyst testing units of the Bureau of Mines.

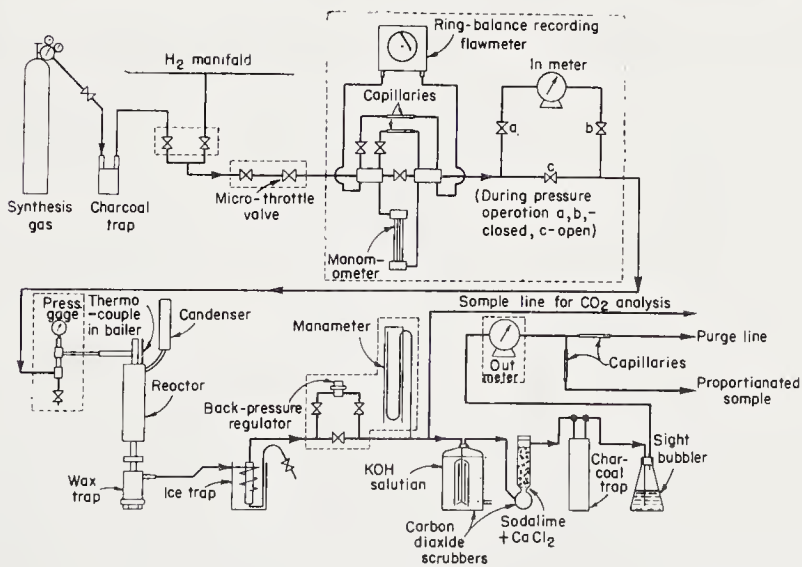


Figure 4. Flow diagram of catalyst testing apparatus. (Components within dashed lines are on front panel.)

water collect in a brass container within the wax trap, which has an easy-opening "O"-ring closure. More volatile hydrocarbons and part of the water are collected in the second trap cooled by a refrigeration system to about 1°C. The system pressure is then reduced to atmospheric with a gas-loaded back-pressure regulator. The exit gas at atmospheric pressure is passed through a wet and a dry carbon dioxide scrubber; the latter scrubber also removes most of the water vapor. The efficient, large capacity wet scrubber developed at the Bureau of Mines is described in Reference 105. In tests of cobalt and nickel catalysts, the carbon dioxide scrubbers are usually unnecessary. Gasol ($C_3 + C_4$) and volatile liquid hydrocarbons are removed by a charcoal trap. The exit gas flow is determined by an oil-filled wet test meter. Finally an exit gas sample is collected using a proportionating device consisting of two capillaries chosen so that about 1 per cent of the exit gas flows into the gas-collection bottle. The remainder of the gas goes into a purge line.

Details of the construction of a typical reactor are shown in Figure 5. The reactor is constructed of iron pipe, the catalyst tube having an internal diameter of 0.625 inch. The catalyst is supported on wire gauze soldered to the top of the retention tube. The temperature of the catalyst tube is maintained by controlling the pressure on the boiling liquid bath ("Tetralin" for 150 to 220°C, "Dowtherm A" for 200 to 400°C) in the steel jacket. For pressures from subatmospheric to 1 atmosphere gauge, the pressure controller described in Reference 180 or a Cartesian diver-type manostat is used. Higher pressures can be maintained satisfactorily by using a reducing valve to regulate cylinder nitrogen. The lower portion of the boiler is heated electrically, and the vapor is returned by the water-cooled condenser. An auxiliary electrical heater is provided to heat the lower portion of the catalyst tube to prevent the accumulation of solid hydrocarbons. The level of the boiling liquid is maintained above the top of the catalyst bed.

This reactor provides as efficient heat removal as can be expected for a tubular, fixed-bed reactor. Temperatures measured within the catalyst tube usually differed from those in the boiler by less than 1 or 2°C; however, when the boiler was operated at subatmospheric pressures a vertical temperature gradient of this magnitude, due to the hydrostatic pressure of the liquid, was observed¹¹.

In routine testing experiments^{12, 17} the space velocity and pressure are maintained constant and the temperature is varied to maintain the carbon dioxide-free contraction at about 65 per cent for iron catalysts with $1H_2 + 1CO$ gas and 70 per cent for cobalt or nickel catalysts with $2H_2 + 1CO$ gas. Testing is usually continuous, with the exception of a 2-hour period once a week when the products are removed from the reactor. At this time the products from the wax and 0°C trap are removed, the exit

gas sampled, and the charcoal trap replaced with a regenerated one. The hydrocarbons are steam-distilled from the charcoal trap¹⁸⁰. The liquid products condensed in ice are combined with liquid and solid products from

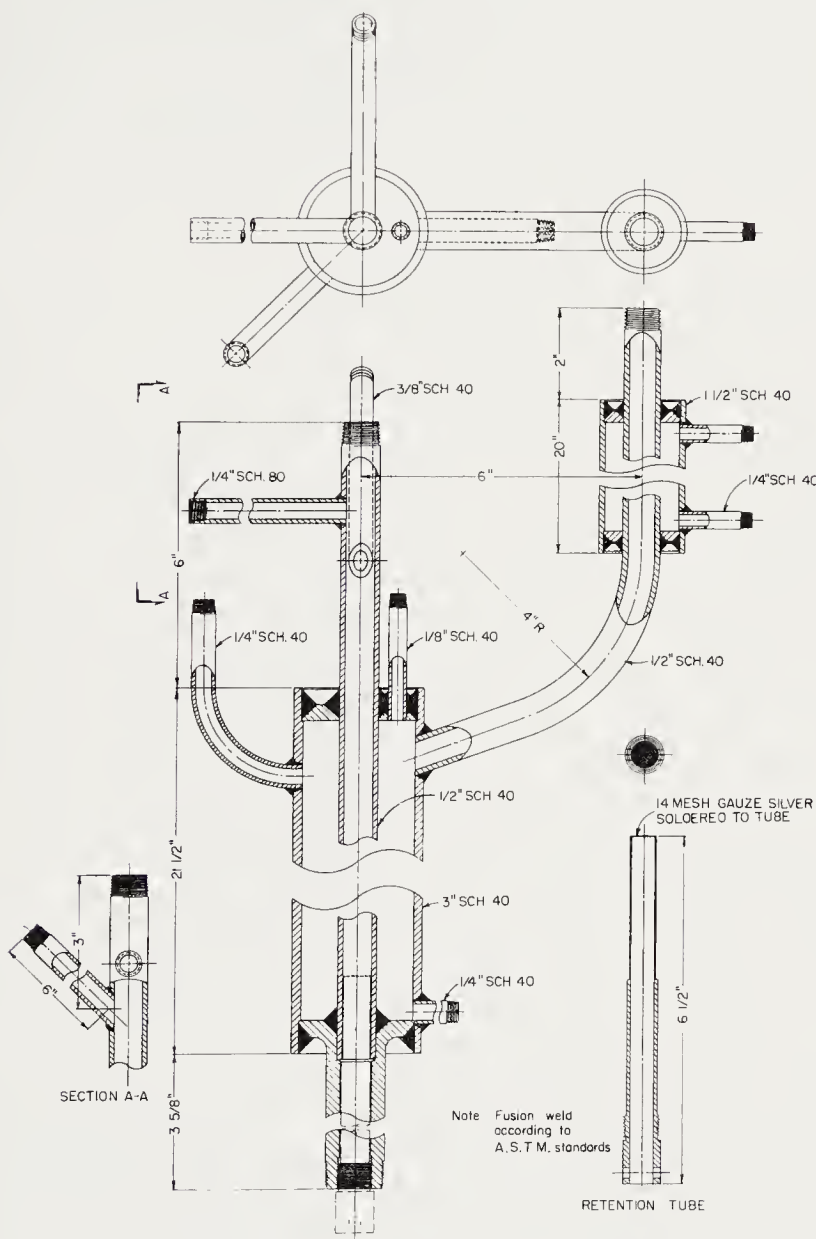


Figure 5. Single tube converter (modified Downs type)

the wax and ice traps. The charcoal trap gases are measured and a sample of this gas, as well as the exit gas sample, is analyzed by the mass spectrometer. The carbon dioxide content of the exit gas is determined twice daily by a small Haldane apparatus on spot samples.

The condensed products are analyzed by a procedure designed to give meaningful data regarding molecular weight range and types of molecules present without being excessively laborious¹⁷. The "hydrocarbon" phases are separated from the aqueous layer, and the liquid and solid "hydrocarbons" are divided into four fractions by a simple 1-plate distillation: (a) to 185°C at atmospheric pressure; (b) to 225°C at 10 mm (atmospheric equivalent of 352°C); to 225°C at 1 mm (atmospheric equivalent of 464°C). The two lower-boiling fractions (a and b) are analyzed for functional groups by the infrared method of Anderson and Seyfried³. When desired, the aqueous phase is analyzed for water and oxygenated organic molecules by mass spectrometric analysis.

Although pretreatment of catalysts at temperatures up to 400°C can be made in the testing units, these steps are usually done in a special aluminum-bronze reactor¹⁷, shown in Figure 6. The procedure used in pretreating catalysts consisted of introducing a weighed sample of catalyst into the aluminum cooling vessel (in carbon dioxide if the catalyst had been previously reduced). The block furnace, at temperature and with the desired gas flowing through it, was inverted, and the cooling vessel attached and swept free of carbon dioxide. Then the reactor was rotated to the position shown in Figure 6, causing the catalyst to fall into the heated zone. At the end of the pretreatment, the reactor was inverted and tapped with a hammer to insure that all of the catalyst would fall into the cooling vessel. The gas used in the pretreatment was passed through the reactor and cooling vessel until the sample cooled to less than 50°C. Then the gas flow was stopped and carbon dioxide was passed through the cooling vessel to protect the catalyst against accidental oxidation in transfer. With carbon dioxide flowing, the cooling vessel was detached and the sample was poured through a rubber sleeve into the glass weighing bottle, which was also being flushed with carbon dioxide. This bottle was then closed with a ground glass cap and sufficient carbon dioxide was passed through the cap to remove any air. The weight of the sample after pretreatment was obtained from the weight of the bottle plus catalyst. After weighing, the catalyst was either charged into a testing unit or returned to the block furnace for further pretreatment. In many experiments, weighed samples were removed between each step for chemical and x-ray analysis. In transferring the catalyst, the following precautions were always taken: (a) The catalyst was kept in a stream of carbon dioxide; (b) carbon dioxide was not passed over the sample until its temperature was less than 50°C; (c) all transfers were made through rubber or metal connections so that the catalyst was never exposed to air.

Since sulfur-free (less than 0.5 grains per 1000 cubic feet) synthesis gas, required for catalyst tests, is usually not available commercially, a number

of methods of gas generation are described*:

(a) Carbon monoxide may be prepared and blended with commercial electrolytic hydrogen. Carbon monoxide from the dehydration of formic acid with phosphoric acid¹⁸⁵ has a very high purity and is suitable for any use. A somewhat less pure carbon monoxide may be obtained by passing oxygen or carbon dioxide over low-sulfur carbon at elevated temperatures.

(b) Synthesis gas may be generated by gasification of carbon with water.

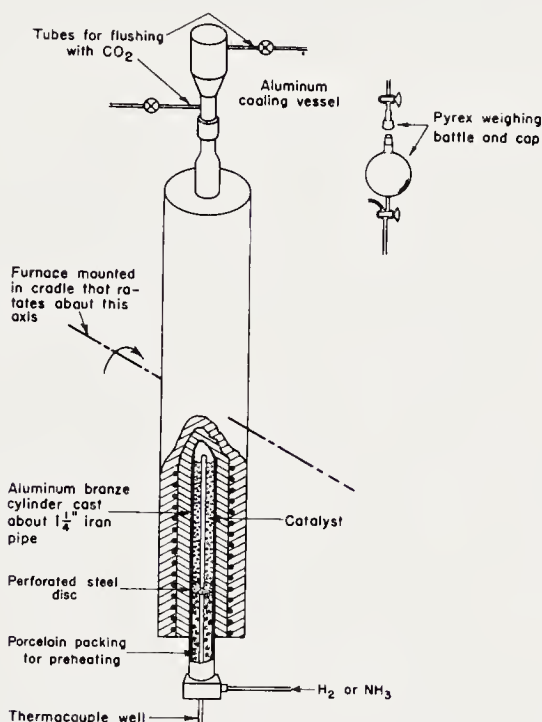


Figure 6. Reduction unit for Fischer-Tropsch catalysts. (Reproduced with permission from Ref. 17)

For small-scale preparation, an externally-heated bed of carbon is preferable¹⁷³.

(c) Methanol may be decomposed to $2\text{H}_2 + 1\text{CO}$ on a supported nickel-copper catalyst at 260 to 320°C¹⁶⁷.

(d) Gaseous or liquid hydrocarbons may be reformed with suitable amounts of steam and carbon dioxide over a nickel catalyst to give gases ranging from $1\text{H}_2 + 5\text{CO}$ to pure hydrogen¹⁴⁰. At the Bureau of Mines laboratory, Bruceton, Pennsylvania, synthesis gas is made by reforming natural gas³³. The gas for catalyst testing is passed through a charcoal scrubber at elevated pressures and then compressed into steel cylinders.

* For a general discussion of synthesis gas production, see reference 133.

COBALT AND NICKEL CATALYSTS

In the following pages the effects of the method of preparation and composition on the activity, selectivity, and life of cobalt and nickel catalysts are followed by a discussion of the pore geometry of these catalysts. Next, a discussion of the methods of pretreating catalysts, is followed by a resume of operating characteristics of catalysts and methods of regeneration. Finally, the products from cobalt and nickel catalysts are described. As the following data will show, the behavior of cobalt and nickel catalysts is, in many respects, essentially the same; therefore, they will be discussed together.

Precipitated Cobalt and Nickel Catalysts

The usual method of preparation is the addition of an alkaline hydroxide or carbonate solution to a hot aqueous solution of cobalt or nickel nitrate plus promoter nitrates. Kieselguhr or other carriers are added as an aqueous slurry at the time of precipitation. The precipitation is usually accomplished as quickly as possible by rapid addition of solutions and efficient stirring. The precipitate is separated on a suction filter or filter press and washed free of ions with distilled water. The filter cake, a soft but coherent mass, is dried in air at 100 to 120°C and then broken or cut to the desired particle size. Since this procedure results in the production of fines, numerous schemes, consisting of forming or extruding the moist cake or pelleting of the dried cake, were employed to produce particles of usable size. Details of the methods of catalyst preparation are given on pp. 139 to 143 of Reference 181.

The effect of the precipitant on the activity and selectivity of Co-ThO₂-kieselguhr catalysts as observed by Fischer and Koch⁴⁹ is given in Table 3. In these tests, potassium carbonate was the best precipitant, ammonium carbonate next best, and then sodium carbonate. The table also shows that decomposition catalysts are inferior to precipitated preparations and that precipitated catalysts, lacking either promoter or kieselguhr, had lower activities than corresponding catalysts containing both components. Subsequent work at Ruhrchemie¹⁵⁴ produced catalysts precipitated with sodium carbonate that approached in activity those precipitated with potassium carbonate.

Tsutsumi¹⁹⁰ found that active Co-Cu-U₃O₈ catalysts could be prepared from cobalt nitrate and acetate, but preparations from cobalt sulfate had low activity and those from the chloride were inactive. Although the precipitates were carefully washed, the low activity of preparations from the chloride and sulfate apparently resulted from residual ions.

Earlier, Fischer and Meyer⁵¹ studied the influence of the precipitant on nickel-thoria-kieselguhr catalysts, as shown in Table 4. For this catalyst

composition, sodium carbonate was the best precipitant, with potassium carbonate a close second. Preparations made with sodium or potassium hydroxide were virtually inactive. The differences in activity may be due

TABLE 3. EFFECT OF COMPOSITION AND MODE OF PREPARATION OF COBALT CATALYSTS^a

($2\text{H}_2 + 1\text{CO}$ gas, 1 liter per gram of Co per hour, 1 atmosphere)

Composition			Preparation	Temp. (°C)	Hours	Contraction (%)	C ₅ +, cc/m ²	C ₅ + × 100 Total Hydrocarbons
Co	ThO ₂	K ₂ g						
100	18	100	Heating of nitrate	200	72	3	—	—
100	18	—	Prec. with (NH ₄) ₂ CO ₃	205	57	12	14.5	—
100	18	100	Prec. with (NH ₄) ₂ CO ₃	200	36	66	121	56
100	18	100	Prec. with Na ₂ CO ₃	210	109	40	61.5	—
100	18	100	Prec. with K ₂ CO ₃	195	160	69	142	71
100	—	100	Prec. with K ₂ CO ₃	210	138	44.5	47.5	—

^a From Ref. 49.

TABLE 4. INFLUENCE OF PRECIPITANT ON SYNTHESIS WITH 100Ni:18ThO₂:100 KIESELGUHR CATALYSTS^a

(1 liter of $2\text{H}_2 + 1\text{CO}$ gas per hour per gram Ni at atmospheric pressure)

Precipitant	Temp. (°C)	Hours	Contraction (%)	C ₅ +, cc/m ³	C ₅ + × 100 Total Hydrocarbons
(NH ₄) ₂ CO ₃	182	90	26.5	32	—
Na ₂ CO ₃	178	40	62	103	64
NaOH	190	45	3.8	—	—
KOH	180	40	0	—	—
K ₂ CO ₃	180	65	65	112	63.5
KHCO ₃	180	117	48	66	~43

^a From Ref. 51.

to the nature of the precipitated phases, basic carbonate or oxide, with respect to (a) the ease of removal of ions from the precipitate by washing, or (b) changes in structure of the precipitate on reduction. Another possibility is interaction of the precipitant with the kieselguhr.

Influence of Promoters on Precipitated Cobalt and Nickel Cata-

lysts. Fischer and Koch⁴⁹ studied the influence of thoria, manganese oxide, copper, and other promoters on precipitated cobalt-kieselguhr catalysts. Table 5 shows that the activity and the production of higher hydrocarbons increased to a maximum at 18 ThO₂ per 100 Co. Table 6 presents data for other promoters than thoria. Catalysts containing chromium or

TABLE 5. INFLUENCE OF ThO₂ CONTENT ON SYNTHESIS WITH
Co-KIESELGUHR CATALYSTS^a

Co:kieselguhr = 100:100

(1 liter 2H₂ + 1CO gas per hour per gram Co at 1 atmosphere)

ThO ₂ per 100 Co by Weight	Temp. (°C)	Hours	Contraction (%)	C ₅ +, cc/m ³	C ₅ + × 100
					Total Hydrocarbons
0	210	138	44.5	47.5	—
12	185	64	55.5	102.5	67
18	185	64	58.5	115.5	72
24	185	64	16	17	—
48	185	64	0	0	—

^a From Ref. 49.

TABLE 6. EFFECT OF PROMOTERS OTHER THAN THORIA IN
COBALT-KIESELGUHR CATALYSTS^a

(1 liter of 2H₂ + 1CO gas per hour per gram Co at 1 atmosphere)

Promoters, parts per 100 Co	Temp. (°C)	Contraction (%)	Highest Yield C ₅ +, cc/m ³
None	210	44.5	47.5
20 Mn	215	54	68.5
20 Mg	215	48	50
20 Cu	215	17	15
20 Zn	215	53	43
20 Al	215	13	9.5

^a From Ref. 49.

aluminum oxides were less active than the preparation without promoters, while catalysts promoted with oxides of manganese, magnesium, or zinc were at least as active as the unpromoted sample. Only the manganese oxide catalyst showed an improved selectivity over the unpromoted sample. Further studies were made of manganese oxide-promoted catalysts, as shown in Table 7. For Co-Mn-kieselguhr catalysts, sodium carbonate was a better precipitant than potassium carbonate. The addition of alumina to this catalyst decreased its activity. The addition of copper to the Co-Mn-kieselguhr catalyst decreased the activity somewhat without changing the selectivity significantly. The catalysts containing copper had the advantage

that the initial reduction in hydrogen at elevated temperatures (350°C) was not necessary, since the catalyst could be reduced by synthesis gas at usual synthesis temperatures. The first satisfactory catalyst used in Ruhrchemie pilot plants, Co:ThO₂:Cu:kieselguhr = 100:18:2:200, was reduced in hydrogen at 220°C. However, the catalysts containing copper had considerably shorter lives than copper-free samples, and copper-promoted catalysts were abandoned by Ruhrchemie in about 1935¹. These studies led to Co-ThO₂-kieselguhr catalysts precipitated with sodium carbonate that closely approached the catalytic properties of those precipitated with potassium.

In 1938, Roelen^{71, 159} studied catalysts in which the thoria was partly

TABLE 7. ACTIVITY AND SELECTIVITY OF Co-Mn-KIESELGUHR CATALYSTS^a

Co:kieselguhr = 100:100

(1 liter of 2H₂ + 1CO gas per hour per gram Co at 1 atmosphere)

Catalyst Composition, per 100 Co	Precipitant	Temp. (°C)	Contraction (%)	C ₃ +, cc/m ³
18 ThO ₂	K ₂ CO ₃	190	68.5	153
15 Mn	K ₂ CO ₃	205	71.5	120
15 Mn	Na ₂ CO ₃	200	71	144.5
15 Mn + 5 Al	Na ₂ CO ₃	215	5	7
15 Mn + 1 Al	Na ₂ CO ₃	215	57	83
15 Mn + 5 Cu	Na ₂ CO ₃	205	63	118
15 Mn + 10 Cu	Na ₂ CO ₃	205	61	118
15 Mn + 20 Cu	Na ₂ CO ₃	205	59.5	106

^a From Ref. 49.

replaced by magnesia, and this work led to the Co:ThO₂:MgO:kieselguhr (100:5:8:200) used in the German commercial plants until production was terminated by the invasion of Germany in 1945. A number of catalysts of varying compositions, as shown in Table 8, were prepared and tested according to the following schedule: The first 950 hours at 185°C, 950 to 1,900 hours at 192°C, 1,900 to 2,200 hours at 193°C, and 2,200 to 2,800 hours at 194°C. The catalysts were reactivated with hydrogen at 700, 2,200, and 2,500 hours. The data are given as percentages of the total output of useful products (presumably C₃+) of the output of the best catalyst.

According to the data of Table 8, the best catalyst composition was Co:ThO₂:MgO:kieselguhr = 100:5:10:200. This catalyst had a somewhat higher mechanical strength than the Co-ThO₂-kieselguhr preparation, a desirable property for use in the German fixed-bed reactors. The Co-MgO-kieselguhr catalyst gave slightly larger yields than the Co-ThO₂-kieselguhr preparation; however, the magnesia-promoted catalysts were said to be

more temperature-sensitive and difficult to control. Roelen⁷² stated that thoria also had a special role in partially diminishing the harmful effects of impurities such as copper, calcium, and aluminum. If pure chemicals and purified kieselguhr were used, satisfactory catalysts were obtained with as little as 2ThO₂ per 100 Co; but for the commercial preparation of catalysts from less pure components, 5ThO₂ was desirable.

Similar Co-ThO₂-kieselguhr and Co-ThO₂-MgO-kieselguhr catalysts were prepared at the British Fuels Research Station and the Bureau of Mines, and the performance of the catalysts was about the same as observed by

TABLE 8. INFLUENCE OF THORIA IN CO:-ThO₂-MgO-KIESELGUHR CATALYSTS^a
Co:kieselguhr = 100:200
(2H₂ + 1CO gas at atmospheric pressure)

Parts per 100 Co		Output of products (%)
ThO ₂	MgO ^b	
5	10	100
3	10	99
2	10	99
1	10	95
0.5	10	95
—	10	92
—	15	92
15	—	90

^a From Ref. 159.

^b Based on Mg(NO₃)₂ used as starting material. MgO is incompletely precipitated and only about 80% of the magnesia was found in the catalyst.

German workers. The British workers usually added precipitated magnesia as a slurry in their preparations. The work of British and American laboratories will be considered later in this discussion.

Scheuermann¹⁶⁵, of I. G. Farbenindustrie, Oppau, demonstrated that active cobalt catalysts without promoters and carriers could be prepared. These preparations were made by dropwise addition of potassium carbonate solution to a cobalt nitrate solution over a period of 40 to 50 hours, with both solutions at room temperature. The precipitate was filtered by suction, washed, and dried at 110°C. Partial oxidation of the cobalt basic carbonate to Co₃O₄ in the drying step was desirable, since the presence of Co₃O₄ seemed to prevent excessive sintering on reduction. In any case, active catalysts were obtained only when the reduction was done at low temperatures. A partly oxidized preparation, after reduction in hydrogen

for 10 hours at 225°C, gave yields of 110 to 135 g/m³ at usual space velocities. Although the life of these catalysts was short, the studies demonstrate that neither promoters nor carriers are necessary for the production of higher hydrocarbons.

At the Oppau laboratory, the production of sizeable yields of wax was considered to be an essential feature of good catalysts, and the suitability of various preparations were judged on this basis. Many of Fischer's early tests were repeated, and essentially the same results were obtained in most instances. In atmospheric pressure tests, cobalt-kieselguhr catalysts were found to be almost as active as Fischer's standard catalyst. This unpromoted preparation remained active for at least 4 months with reactivation. Although the catalyst produced some paraffins at the start of the test, the wax yield was essentially zero after about 2 weeks. The addition of thorium to these catalysts increased the fraction of wax in the products; however, the over-all productivity of high-thorium catalysts decreased with increasing thorium content so that the total wax production (space-time-yield) decreased with increasing thorium content. Similarly, wax production was increased by adding potassium or sodium carbonate; however, the alkali content also decreased the total conversion, so that the maximum paraffin production was found with a relatively low alkali content. Oxides of magnesium, manganese, cerium, and lanthanum were tried as substitutes for thorium, but at best these preparations were only as good as Fischer's Co-ThO₂-kieselguhr catalyst. Koch and Billig⁹⁶ also studied the effect of alkali on a standard Co-ThO₂-kieselguhr catalyst in the atmospheric synthesis. As sodium carbonate increased from 0 to 2 parts per 100 Co, the percentages of the condensed product boiling above 300°C rose from 11 to 21, respectively. One part of potassium carbonate was about as effective as two of sodium carbonate. The use of increased thorium and alkali to increase the wax yield in the atmospheric pressure synthesis was not of great importance, since it was soon discovered that higher yields of wax were attainable with all standard catalysts in the medium pressure synthesis⁵⁶. At 10 atmospheres, high yields of wax were obtained from Ruhrchemie "wax-producing" catalysts¹⁶⁰, as shown in Table 9. Manganese oxide was a somewhat better promoter than thorium for wax production. The low kieselguhr content also favors wax-production, and the high wax yields from both catalysts were largely related to this factor.

Ghosh and Basak⁶⁷ tested precipitated Co-Cu-ThO₂-Ce₂O₃-kieselguhr catalysts, with and without chromic oxide as a promoter, with high flows of 1H₂ + 1CO at 5 atmospheres, as shown in Table 10. The catalysts with chromic oxide produced higher yields of C₃+ hydrocarbons and lower yields of methane than the similar preparation without this promoter.

Fischer and Meyer⁵¹ reported the effect of a number of promoters on

nickel catalysts, with and without kieselguhr, as shown in Table 11. Of the promoters described in this table, thoria was the only additive that pro-

TABLE 9. RUHRCHEMIE WAX-PRODUCING CATALYSTS^a

(Space velocity of $2\text{H}_2 + 1\text{CO}$ gas = 100 hr^{-1} ; pressure = 10 atm.)

	100 Co:15ThO ₂ : 12.5 Kieselguhr	100Co:15Mn: 12.5 Kieselguhr
Temperature, °C	175–178	165–168
CO conversion, per cent	85	65
CO conversion, to CH ₄	10	11
C ₃ ⁺ /C ₁ ⁺	0.90	0.89
Usage ratio, H ₂ :CO	2.02	2.05
Hydrocarbon yields, g/m ³		
C ₃ + C ₄	15	15
C ₅ ⁺	130	130
Distillation of C ₅ ⁺ , wt-%		
<200°C	22 (16) ^b	20 (18) ^b
200°–320°C	24 (12)	16 (12)
320°–460°C	21	22
>460°C	33	42

^a From Ref. 160.

^b Numbers in parentheses represent volume per cent olefins.

TABLE 10. CHROMIA AS A PROMOTER FOR COBALT CATALYSTS^a

$1\text{H}_2 + 1\text{CO}$ gas at 5 atm.

(100Co:12Cu:6.5ThO₂:0.7Cr₂O₃:165 kieselguhr)

Temp. °C.	With 13.5 Cr ₂ O ₃				Without Cr ₂ O ₃			
	Apparent Contraction (%)	Hydrocarbon, g/m ^{3b}		Space Velocity (hr ⁻¹)	Apparent Contraction (%)	Hydrocarbon, g/m ^{3b}		Space Velocity (hr ⁻¹)
		C ₃ ⁺	CH ₄			C ₃	CH ₄	
200					47	108	27.3	452
205	53	159	25.3	590	39	108	29.3	540
205	41	151	34.3	590	40	110	37.9	560
210					39	89	48.2	603
215	34.5	132	66.1	590				

^a From Ref. 67.

^b Yields per cubic meter of synthesis gas consumed.

duced desirable results, and the effect of the thoria content was studied in some detail, as shown in Table 12, where optimum activity and selectivity were observed for 18ThO₂ per 100Ni. A 100Ni:25MnO:10Al₂O₃:100 kiesel-

guhr⁶⁰ catalyst produced average yields of 85 grams of liquids per m³ of 2H₂ + 1CO gas at 190 to 210°C for 4 weeks.

TABLE 11. TESTS OF NICKEL CATALYSTS^a

Flow of 2H₂ + 1CO gas = 1 liter per hour per gram Ni
 Operating pressure = atmospheric
 Catalysts precipitated with Na₂CO₃

Composition	Temp. (°C)	Duration (hr)	Contraction (%)	Condensed Hydrocarbons (cc/m ³)	C ₂ + × 100
					Total Hydrocarbons
A. Preparation without kieselguhr					
Ni	230	18	1.5	—	—
100Ni:18ThO ₂	180	42	14	17	—
B. Precipitated on kieselguhr					
Ni	220	42	24	4	8
90Ni:10Ag	240	40	32	—	—
90Ni:10Bi	240	40	0	—	—
99Ni:1Co	240	40	19	—	—
100Ni:15Al ₂ O ₃	220	40	11	Trace	—
100Ni:18ThO ₂	180	42	40	63	70
90Ni:10Cu:18ThO ₂	188	93	16	8	22
100Ni:18ThO ₂ :15Al ₂ O ₃	182	90	8	6	—

^a From Ref. 51.

TABLE 12. EFFECT OF ThO₂ CONTENT ON 100Ni:100 KIESELGUHR CATALYSTS^a

Flow of 2H₂ + 1CO gas = 1 l/hr/g Ni
 Operating pressure = atmospheric. Temperature = 175°C
 Catalysts precipitated with K₂CO₃

ThO ₂ per 100 Ni	Duration (hr)	Contraction (%)	Condensed Hydrocarbons (cc/m ³)	C ₆ + × 100
				Total Hydrocarbons
12	41	52	72	55
18	41	65	113	64
24	41	58	101	64

^a From Ref. 51.

Numerous Co-Ni catalysts were tried in an effort to obtain the more desirable selectivity of cobalt catalysts with only a fraction of the cobalt normally required, but this goal was usually not achieved. Table 13 pre-

sents data from Ruhrchemie¹⁴⁸. Although the ratio of C_3+ to total hydrocarbons was higher for the 75Co-25Ni catalyst than for the corresponding Co catalyst, the largest yield of condensed hydrocarbons was obtained from the Co catalyst. The presence of nickel decreased the average molecular weight of the products, as evidenced by larger yields of gasoline and smaller quantities of wax.

Watanabe¹⁹⁸ presented data for short atmospheric pressure experiments on a variety of nickel and nickel-cobalt catalysts containing various combinations and amounts of Mn, Al_2O_3 , ThO_2 , and MgO as promoters and kaolin and kieselguhr as carriers. These data, in Table 14, show the maxi-

TABLE 13. TESTS OF Co-Ni- ThO_2 -KIESELGUHR CATALYSTS^a
(1 liter of $2H_2 + 1CO$ gas per hour per gram Co at 10 atmospheres)

Composition (parts by wt)	100Co-15 ThO_2 -200 Kieselguhr	75Co-25Ni-15 ThO_2 - 200 Kieselguhr	50Co-50Ni-15 ThO_2 - 200 Kieselguhr
Temperature, °C	185	185-195	195-200
CO converted, %	81	80	78
CH_4 , % of CO converted	11	8	15
C_3+ × 100/total hydrocarbons	83	90	60
Condensed hydrocarbons, g/m ³	125	111	97
<i>Distribution of condensed hydrocarbons, wt-%</i>			
To 195°C (gasoline)	35	57	60
195°-320°C (Diesel oil)	35	33	33
Over 320°C (wax)	30	10	7
<i>Olefins, vol. % in</i>			
Gasoline	19	12	12
Diesel oil	10	7	5

^a From Ref. 148.

mum yields attained for the catalysts. With one exception the catalysts were very active, as indicated by high real contractions. For a given Ni-Co content, the yields of liquids varied over a moderately wide range and no simple relationship between promoter and carrier composition is apparent. However, as the ratio of cobalt to nickel increased, the yields of oil per cubic meter of synthesis gas converted increased, as shown in Figure 7. Other Japanese papers^{95, 192, 193} described tests of cobalt-nickel-kieselguhr catalysts promoted with various combinations of thorium, alumina, manganese oxide, and uranium oxide.

Scheuermann¹⁶⁵ presented a brief summary of atmospheric pressure studies of precipitated cobalt-iron and nickel-iron catalysts which may be included at this point, since cobalt or nickel appeared to be the active phase, as evidenced by the fact that the principal oxygenated product was

water and not carbon dioxide. Fairly high yields were obtained with Co-Fe-kieselguhr catalysts, the yields decreasing with increasing iron content. The temperature for optimum yields of condensed hydrocarbons increased with the iron content. Ni-Fe-Al₂O₃ catalysts gave lower yields of liquid plus solid hydrocarbons, with the maximum being about 80 g/m³.

TABLE 14. SYNTHESIS TESTS WITH Ni AND Ni-Co CATALYSTS^a

(2H₂ + 1CO gas at 190°C and atmospheric pressure. Presumably constant flow per gram of Ni + Co).

Catalyst Composition							Reduction Temp. (°C)	Real Contraction (%)	Liquid + Solid Hydrocarbons ^b (cc/m ³)	Liquid + Solids (cc/m ³ Converted)
Ni	Co	Mn	ThO ₂	Kaolin	Kieselguhr	MgO				
100 ^c	—	20	—	—	100	—	450	87	121	139
100 ^c	—	20	—	—	200	—	450	74	112	151
100	—	20	—	100	200	—	450	87	120	138
100	—	20	—	100	200	—	400	77	134	174
100	—	15	3	—	200	—	450	97	129	133
100	—	15	1	100	200	—	450	74	112	151
100	—	20	1	100	200	—	450	87	129	148
70	30	15	1	100	200	—	420	89	172	194
70	30	15	3	25	200	—	420	82	164	200
70	30	20	—	100	200	—	400	34	50	147
70	30	20	1	—	200	—	410	78	123	158
70	30	20	1	100	200	—	410	62	112	181
70	30	20	3	25	200	—	410	96	151	157
70	30	—	5	—	200	5	410	96	160	167
70	30	—	5	50	200	5	410	93	157	169
50	50	15	3	—	200	—	400	74	147	198
50	50	15	3	25	200	—	400	71	147	207
50	50	—	5	—	200	8	400	93	149	160
50	50	—	5	50	200	8	400	91	162	178
30	70	—	5	—	200	8	390	89	172	193
30	70	—	5	25	200	8	390	87	167	192

^a From Ref. 198.

^b Maximum yield of several experiments.

^c Catalysts also contained 10 Al₂O₃.

Carriers in Precipitated Cobalt and Nickel Catalysts. The majority of successful cobalt and nickel catalysts employ kieselguhr as a carrier. Comparisons of cobalt and nickel catalysts, with and without kieselguhr, may be made from data in Tables 3 and 11. The optimum concentration of kieselguhr has been found between 100 to 200 parts per 100 parts of cobalt or nickel as shown in Table 15. From these data, Fischer and co-workers^{49, 51} chose 100 kieselguhr per 100 cobalt or nickel as the

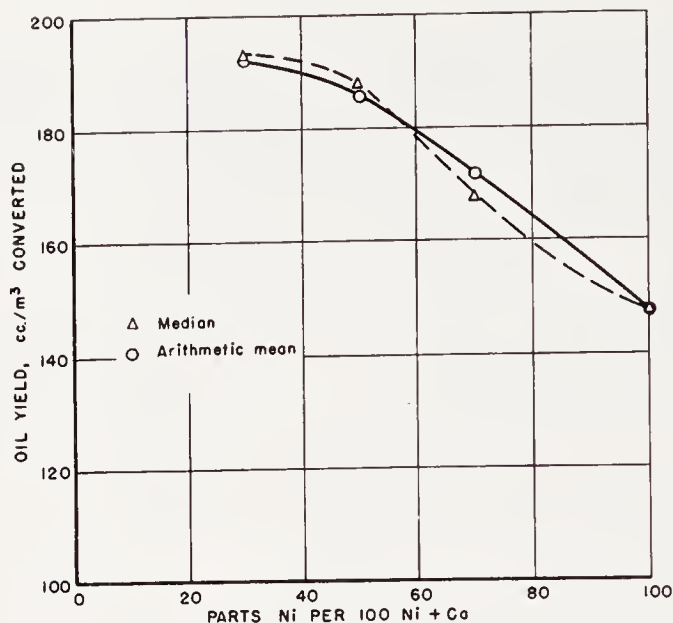


Figure 7. Average oil yields from a variety of precipitated cobalt-nickel catalysts as a function of nickel content. $2\text{H}_2 + 1\text{CO}$ gas at atm. pressure and 190°C . (From Ref. 198)

TABLE 15. INFLUENCE OF KIESELGUHR CONTENT ON Co-ThO_2 AND NiThO_2 CATALYSTS
(Constant flow of $2\text{H}_2 + 1\text{CO}$ gas per gram of metal at atmospheric pressure)

Kieselguhr per 100 Co or Ni	Temp. ($^\circ\text{C}$)	Contraction (%)	C_8^+ (cc/m ³)	$\frac{\text{C}_8^+ \times 100}{\text{Total Hydrocarbons}}$
A. $\text{Co:ThO}_2 = 100:18^a$				
20	180	41.5	79.5	62
50	180	61	118	66
100	180	53.5	91	58
150	180	54.5	113.5	70
B. $\text{Ni:ThO}_2 = 100:18^b$				
33	180	59	67	41
50	182	69	85	47
100	180	65	112	63
133	180	69	89	50
200	190	49	70	53

^a From Ref. 49. Data for first 46-88 hours of tests.

^b From Ref. 51. Data for first 45-138 hours of tests.

optimum for catalysts promoted with thoria. Ruhrchemie data¹⁵⁵ indicated that catalysts containing 200 kieselguhr per 100 cobalt were superior, as shown in Figure 8. The activity of catalysts with 200 parts of kieselguhr decreased less rapidly with time of testing than the preparation with 100 kieselguhr and the yields of liquid products remained correspondingly higher. The ratio, Co:kieselguhr = 100:200, was used in the standard Ruhrchemie Co-ThO₂-MgO-kieselguhr catalysts.

Tests of Ruhrchemie wax-producing catalysts on p. 52 suggest that wax production was favored by low kieselguhr content. This tendency was also demonstrated by data of Scheuermann¹⁶⁵ for cobalt-kieselguhr catalysts

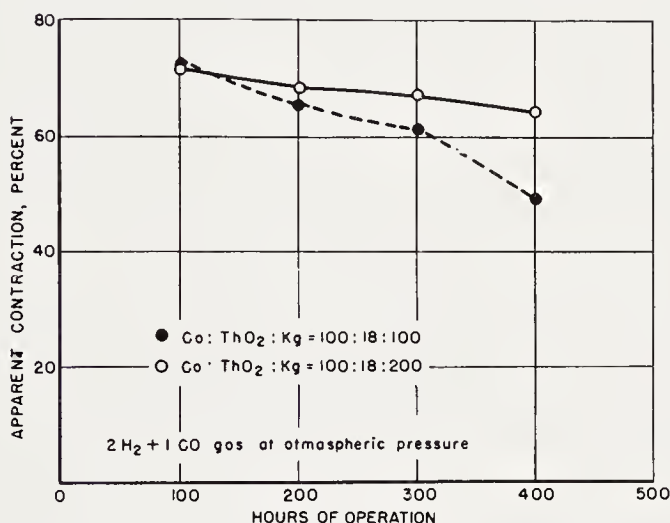


Figure 8. Effect of kieselguhr content on the variation of activity with time. (From Ref. 155)

in Table 16. Here the yield of wax decreased with increasing kieselguhr content, while the methane production remained essentially constant. In the table, only the cobalt content is given, and for comparison, the cobalt content of standard catalysts will be useful:

100Co:18ThO₂:100 kieselguhr, per cent Co = 32

100Co:6ThO₂:12MgO:200 kieselguhr, per cent Co = 24

The absence of thoria and magnesia would increase the cobalt content by only 1 or 2 per cent.

In 1933, Fischer and Meyer⁵² studied a number of the variables in the preparation of Ni:Mn:Al₂O₃:kieselguhr = 100:20:10:100 catalyst, at that time considered to be the best nickel catalyst. Synthesis tests on a series of catalysts containing three Johns Manville kieselguhrs and a num-

data were corrected to give the average catalyst activity for 4 weeks testing at 185°C. Synthesis tests of the same preparation were very reproducible, but tests of different catalyst preparations involving the same components

TABLE 18. ACTIVITY OF Co-ThO₂-MgO-KIESELGUHR CATALYSTS COMPARED WITH ANALYSIS OF EXTRACTABLE IMPURITIES AND OTHER PROPERTIES OF KIESELGUHRS^a
(2H₂ + 1CO gas at atmospheric pressure)

Kieselguhr		Kieselguhr Properties							Activity of Catalyst in Synthesis
Name	Type ^b	Extractable Impurities (%)					Bulk Density (g/l)	Surface Area (m ² /g)	
		Al ⁺⁺⁺	Fe ⁺⁺⁺	Ca ⁺⁺	PO ₄ ⁼	SO ₄ ⁼			
“Hyflo-Super-Cel”	FC	0.05	0.03	0.00	0.00	0.00	220	1.9	52
									63
									49
“Hyflo-Super-Cel” (acid-extracted) ^d	FC	.00	.00	.00	.00	.00		~1.9	45
Johns Manville II	C	.17	.04	.00	.13	.09	200	5.5	88
“Filter-Cel”	N	1.23	.75	.12	.09	.11	149	22.2	127
									124
“Filter-Cel” (acid extracted) ^d	N	.00	.00	.00	.00	.00	170	20.8	167
“Filter-Cel” (acid extracted) ^e	N	.00	.00	.00	.00	.00	170	24.1	116
“Snow Floss”	N	.80	.70	.28	.15	.12	186	19.1	87
“Dicalite 911”	N	1.41	1.14	.35	.00	.26	245	29.3	93
“Dicalite” (acid extracted) ^e	N	.00	.00	.00	.00	.00		39.2	165
Portuguese	N	1.61	.65	.00	.00	.11	345	17.5	166
									120
German	MC	.43	1.49	.02	.00	.56	137	14.9	80

^a From Ref. 13.

^b FC = flux calcined, C = calcined, N = natural, MC = mild heat treatment.

^c Activity expressed in cc (S.T.P.) of gas converted per gram of catalyst at 185°C.

^d Kieselguhr extracted with hot nitric acid for 6 hours, washed, dried, and heated at 650°C for 2 hours.

^e Kieselguhr extracted with hydrochloric and nitric acid solution for 16 hours at room temperature, washed and dried at 400°C.

sometimes varied considerably, e.g., 120 and 166 for two preparations containing Portuguese kieselguhr.

In the series of catalysts in Table 18, those prepared with flux-calcined kieselguhr ("Hyflo-Super-Cel") were the least active. The catalysts containing calcined kieselguhrs (Johns Manville II and German) were more active than those containing "Hyflo-Super-Cel," but only as active as the

least active preparations containing natural kieselguhrs. For the catalysts made with natural kieselguhrs, the activity appeared to vary inversely with the content of extractable iron, whereas no trend could be established between activity and the amount of extractable aluminum and other impurities. Catalysts containing acid-treated natural kieselguhrs usually had high activities. Since calcined and flux-calcined kieselguhrs usually had low contents of extractable iron (with the exception of German kieselguhr), their low activities must result from their small surface area or from their ordered cristobalite structure, compared with a completely amorphous structure for natural kieselguhrs¹⁴.

Electron micrographs of natural and calcined kieselguhrs, Figures 9 and 10, at magnifications of 2,000 and 20,000, respectively, reveal a variety of intricate forms. The calcined samples had less fine structure than natural kieselguhrs. For the natural kieselguhrs, no correlation was found between catalytic activity and the geometry of the carrier, such as bulk density, surface area, or size or structure of the diatoms. For example, the activities of the catalysts containing the kieselguhrs with the smallest diatoms, "Snow Floss" and Portuguese, varied as widely as the activities for catalysts containing any of the natural guhrs. It is possible that these relationships may be obscured by impurities or by difficulty in reproducing catalyst preparations. Acid-extraction of natural kieselguhrs usually increases the activity of resulting catalysts; however, with the flux-calcined guhr, this treatment did not improve the activity. Previously, Hall and co-workers of the British Fuels Research Board had observed the beneficial effect of acid extraction on catalyst activity. Teichner¹⁸⁴ found that extraction of a natural kieselguhr ("Filter-Cel") with a hot mixture of hydrochloric and nitric acids increased its area from 18.5 to 27.3 m²/g. Apparently the acid treatment converted part of the kieselguhr to a silica gel-like structure. Similar results were obtained by Craxford⁸⁴. With Ni-Mn-kaolin-kieselguhr catalysts¹⁹⁸, the yields of oil under comparable conditions were 52 and 120 cc/m³ for preparations with raw and nitric acid-washed kieselguhrs, respectively.

The principal function of the kieselguhr in precipitated cobalt and nickel catalysts is to provide a framework, resembling on a microscopic scale a brush-pile into which the catalytic components are deposited by precipitation. The bulk volume of the kieselguhr defines the volume of the catalyst, in both the raw or reduced state, as shown by a plot of Ruhrchemie data¹⁴⁸ on cobalt and nickel catalysts in Figure 11. The weight per cent of cobalt or nickel in the reduced catalyst is proportional to the weight of metal per liter of reduced catalyst. The bulk volume of unsupported catalysts usually decreases very markedly in reduction, and the resulting high density provides optimum conditions for catalyst overheating resulting in



Figure 9. Electron micrographs of kieselguhrs at a magnification of 2,000.
Natural kieselguhrs—*a*. "Snow Floss"
b. "Filter Cel"
Flux-calcined kieselguhr—*c*. "Hyflo-Super-Cel"

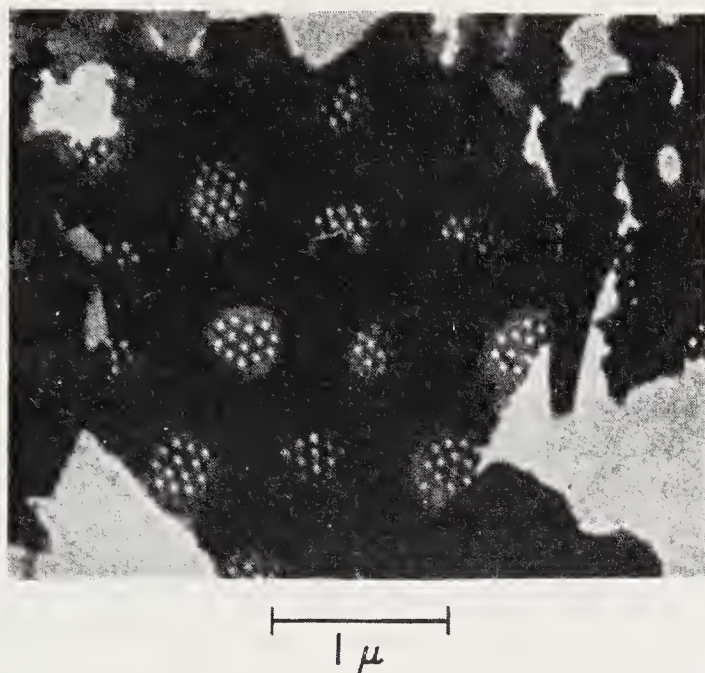


Figure 10. Electron micrograph of "Snow Floss" at a magnification of 20,000.

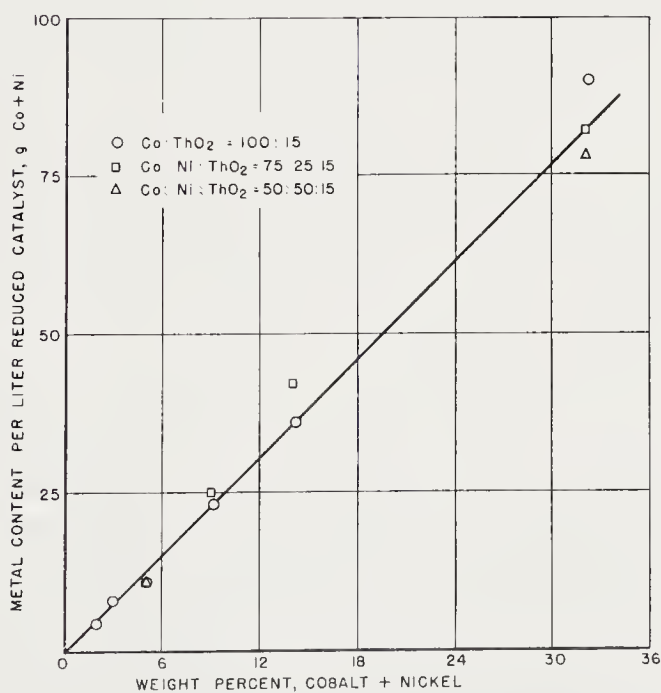


Figure 11. Comparison of the active metal content per liter with weight per cent of active metal when kieselguhr content was varied. (From data of Ref. 148)

low activity and poor selectivity. In addition, the presence of kieselguhr increases the surface areas of the catalysts in both the raw or the reduced state by a greater amount than the area of the kieselguhr. Detailed data for the influence of kieselguhr and promoters on the geometry of cobalt and nickel catalysts will be presented later in this chapter (p. 70).

Workers at I. G. Farben. at Oppau¹⁶⁵ were skeptical of the use of kieselguhr in the preparation of commercial catalysts, since the "diatomite" available in Germany was variable in both structure and chemical composition. Tests demonstrated that many kieselguhrs were improved by heating in air at 500 to 700°C. Further, the addition of small amounts of magnesium oxide (the manner was not stated) was said to make most kieselguhrs equally suitable for catalyst preparation. Tests were made with well-defined materials such as alumina, kaolin, magnesia, silica-gel, talcum, porcelain, etc., as carriers in cobalt catalysts. In general, these catalysts were poor, but with kaolin, alumina, and silica gel that had been heated to 500, 900, and 800°C, respectively, active catalysts were obtained. Wenzel²⁰² described a cobalt-zinc oxide-alumina catalyst that produced over 70 per cent hard paraffin. The alumina for this catalyst had been heated to 800°C. A cobalt-1 per cent silver catalyst, prepared by slow precipitation on a "narrow pore" silica gel, was said to be about as effective as a Co-ThO₂-kieselguhr catalyst. It had the advantage of being reducible in the synthesis reactors without the undesirable effects observed with cobalt-copper preparations and, in addition, did not require the use of thoria. Watanabe¹⁹⁸ investigated Ni and Ni-Co catalysts containing kaolin in addition to kieselguhr (Table 14); the results, however, seem to indicate that kaolin plus kieselguhr has no advantage over kieselguhr alone. In a patent, Rubin¹⁴⁶ reported that a fine mesh precipitated cobalt:magnesia: "Super Filtrol" (100:15:200) operated satisfactorily in a fluidized reactor at 200 to 210°C. The preparation containing "Super-Filtrol," an acid-treated bentonite clay, was superior in the fluidized operation to similar catalysts precipitated on kieselguhr.

Decomposition and Skeletal Cobalt and Nickel Catalysts

In general, cobalt and nickel catalysts of these types are inferior to the precipitated preparations already described, and only a brief survey of the available data will be presented. The term, "decomposition catalysts," as used here, includes preparations made by thermal decomposition to oxides of salts such as nitrates. In some cases, an easily oxidizable substance such as starch is mixed with nitrates, and on heating, this material undergoes a mild explosion, resulting in fine, fluffy oxide powder. For fixed-bed tests, these finely-divided preparations must be formed into granules. Another

variation of decomposition catalysts is prepared by mixing a finely-divided carrier such as kieselguhr with the salts or solution of salts and heating the mixture to decompose the salt. Also, porous granules of material such as silica gel may be impregnated with salt solutions and the salt decomposed thermally. "Skeletal" catalysts involve the preparation of an alloy of the active metal plus another element that can be readily leached from the alloy, leaving a skeleton of the active component. Raney nickel¹³⁴ is the best known catalyst of this type.

Decomposition catalysts of Fischer and Tropsch⁴⁶ had low activity and poor selectivity. Later, Fischer and Meyer⁵¹ studied nickel catalysts of this type, after reduction in hydrogen at 350 to 450°C. With the exception of a nickel-alumina catalyst, the samples without kieselguhr were uniformly poor. Decomposition catalysts supported on kieselguhr were somewhat more active, and alumina was again the best promoter. Thoria was not a useful promoter. Data of Table 3 show that a Co-ThO₂-kieselguhr decomposition catalyst had a very low activity compared with similar precipitated catalysts. Tsutsumi¹⁹¹ was able to prepare cobalt decomposition catalysts of approximately the same activity as precipitated catalysts; however, his best nickel catalysts were prepared by precipitation.

A Bureau of Mines catalyst, prepared by impregnation of a microsphere (1 mm diameter) silica gel with cobalt and thorium nitrates and subsequent thermal decomposition of the nitrates, showed satisfactory activity, life, and selectivity. After reduction in hydrogen at 350°C, this preparation gave high conversions of $2\text{H}_2 + 1\text{CO}$ at a space velocity of 100 hr⁻¹ at 190 to 200°C, both at 1 and 7.8 atmospheres pressure, and about the same selectivity as standard Fischer-type catalysts.

Fischer and Meyer^{53, 54} made a detailed study of nickel and cobalt skeletal catalysts. Alloys were prepared by fusing mixtures of metallic nickel or cobalt with aluminum or silicon. The alloys were crushed to "lentil-size" granules (presumably pieces of 3 to 4 mm diameter) or ground to a fine powder and then leached with an excess amount of hot aqueous sodium hydroxide solution. Aluminum was readily dissolved, and the alkali was added slowly from a dropping funnel. For the granules, about 6 hours were required. Silicon dissolved more slowly and was never completely removed. The extracted material was washed with water and stored under ethanol. The skeletal preparations had a much higher bulk density than catalysts precipitated on kieselguhr. The granules of typical precipitated catalysts contained 0.09 to 0.10 gram of cobalt or nickel per cc compared with 0.8 g/cc for extracted skeletal catalysts. The skeletal catalysts were tested in 14 mm tubes at atmospheric pressure with a flow of 4 liters of $2\text{H}_2 + 1\text{CO}$ gas per hour per 5 grams of cobalt plus nickel. These dense catalysts usually gave poor results when packed tightly in the reactor, presumably due to

low activity and poor selectivity. In addition, the presence of kieselguhr increases the surface areas of the catalysts in both the raw or the reduced state by a greater amount than the area of the kieselguhr. Detailed data for the influence of kieselguhr and promoters on the geometry of cobalt and nickel catalysts will be presented later in this chapter (p. 70).

Workers at I. G. Farben. at Oppau¹⁶⁵ were skeptical of the use of kieselguhr in the preparation of commercial catalysts, since the "diatomite" available in Germany was variable in both structure and chemical composition. Tests demonstrated that many kieselguhrs were improved by heating in air at 500 to 700°C. Further, the addition of small amounts of magnesium oxide (the manner was not stated) was said to make most kieselguhrs equally suitable for catalyst preparation. Tests were made with well-defined materials such as alumina, kaolin, magnesia, silica-gel, talcum, porcelain, etc., as carriers in cobalt catalysts. In general, these catalysts were poor, but with kaolin, alumina, and silica gel that had been heated to 500, 900, and 800°C, respectively, active catalysts were obtained. Wenzel²⁰² described a cobalt-zinc oxide-alumina catalyst that produced over 70 per cent hard paraffin. The alumina for this catalyst had been heated to 800°C. A cobalt-1 per cent silver catalyst, prepared by slow precipitation on a "narrow pore" silica gel, was said to be about as effective as a Co-ThO₂-kieselguhr catalyst. It had the advantage of being reducible in the synthesis reactors without the undesirable effects observed with cobalt-copper preparations and, in addition, did not require the use of thoria. Watanabe¹⁹⁸ investigated Ni and Ni-Co catalysts containing kaolin in addition to kieselguhr (Table 14); the results, however, seem to indicate that kaolin plus kieselguhr has no advantage over kieselguhr alone. In a patent, Rubin¹⁴⁶ reported that a fine mesh precipitated cobalt:magnesia: "Super Filtrol" (100:15:200) operated satisfactorily in a fluidized reactor at 200 to 210°C. The preparation containing "Super-Filtrol," an acid-treated bentonite clay, was superior in the fluidized operation to similar catalysts precipitated on kieselguhr.

Decomposition and Skeletal Cobalt and Nickel Catalysts

In general, cobalt and nickel catalysts of these types are inferior to the precipitated preparations already described, and only a brief survey of the available data will be presented. The term, "decomposition catalysts," as used here, includes preparations made by thermal decomposition to oxides of salts such as nitrates. In some cases, an easily oxidizable substance such as starch is mixed with nitrates, and on heating, this material undergoes a mild explosion, resulting in fine, fluffy oxide powder. For fixed-bed tests, these finely-divided preparations must be formed into granules. Another

variation of decomposition catalysts is prepared by mixing a finely-divided carrier such as kieselguhr with the salts or solution of salts and heating the mixture to decompose the salt. Also, porous granules of material such as silica gel may be impregnated with salt solutions and the salt decomposed thermally. "Skeletal" catalysts involve the preparation of an alloy of the active metal plus another element that can be readily leached from the alloy, leaving a skeleton of the active component. Raney nickel¹³⁴ is the best known catalyst of this type.

Decomposition catalysts of Fischer and Tropsch⁴⁶ had low activity and poor selectivity. Later, Fischer and Meyer⁵¹ studied nickel catalysts of this type, after reduction in hydrogen at 350 to 450°C. With the exception of a nickel-alumina catalyst, the samples without kieselguhr were uniformly poor. Decomposition catalysts supported on kieselguhr were somewhat more active, and alumina was again the best promoter. Thoria was not a useful promoter. Data of Table 3 show that a Co-ThO₂-kieselguhr decomposition catalyst had a very low activity compared with similar precipitated catalysts. Tsutsumi¹⁹¹ was able to prepare cobalt decomposition catalysts of approximately the same activity as precipitated catalysts; however, his best nickel catalysts were prepared by precipitation.

A Bureau of Mines catalyst, prepared by impregnation of a microsphere (1 mm diameter) silica gel with cobalt and thorium nitrates and subsequent thermal decomposition of the nitrates, showed satisfactory activity, life, and selectivity. After reduction in hydrogen at 350°C, this preparation gave high conversions of $2\text{H}_2 + 1\text{CO}$ at a space velocity of 100 hr⁻¹ at 190 to 200°C, both at 1 and 7.8 atmospheres pressure, and about the same selectivity as standard Fischer-type catalysts.

Fischer and Meyer^{53, 54} made a detailed study of nickel and cobalt skeletal catalysts. Alloys were prepared by fusing mixtures of metallic nickel or cobalt with aluminum or silicon. The alloys were crushed to "lentil-size" granules (presumably pieces of 3 to 4 mm diameter) or ground to a fine powder and then leached with an excess amount of hot aqueous sodium hydroxide solution. Aluminum was readily dissolved, and the alkali was added slowly from a dropping funnel. For the granules, about 6 hours were required. Silicon dissolved more slowly and was never completely removed. The extracted material was washed with water and stored under ethanol. The skeletal preparations had a much higher bulk density than catalysts precipitated on kieselguhr. The granules of typical precipitated catalysts contained 0.09 to 0.10 gram of cobalt or nickel per cc compared with 0.8 g/cc for extracted skeletal catalysts. The skeletal catalysts were tested in 14 mm tubes at atmospheric pressure with a flow of 4 liters of $2\text{H}_2 + 1\text{CO}$ gas per hour per 5 grams of cobalt plus nickel. These dense catalysts usually gave poor results when packed tightly in the reactor, presumably due to

overheating, as shown in Figure 12. In most of the tests the charge was spread in a thin layer over the bottom of the reactor tube.

With Ni-Al catalysts, it was advantageous to reduce the extracted catalyst with hydrogen before synthesis. Data in part A of Table 19 indicate that the activity and selectivity improved as the nickel content increased up to about 1Ni to 1Al by weight. The aluminum was difficult to extract from an equiatomic alloy (1Ni to 0.46Al by weight), and only partial removal of the aluminum was achieved. This sample was completely inactive at 206°C. Attempts were made to improve the catalyst by addition of promoters either to the original alloy or to the catalyst after extraction. Manganese and copper added to the original melt did not improve the catalysts,

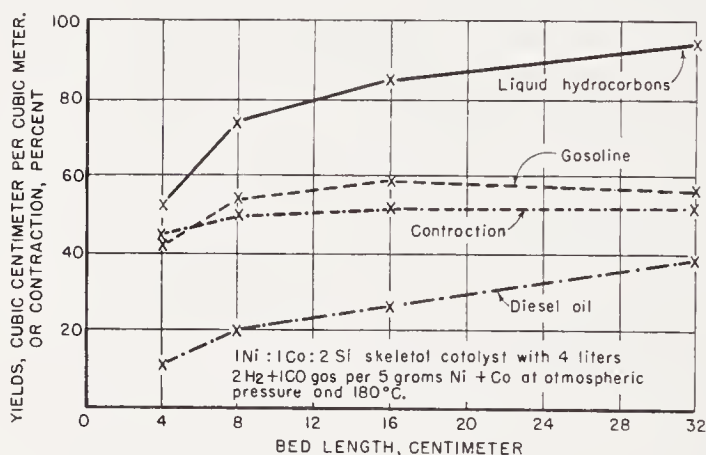


Figure 12. Effect of partially filling the catalyst tube. Catalyst containing 5 grams of Ni or Co, which would fill about 4 centimeters of catalyst tube, was spread over various lengths. (From Ref. 53)

and the activity of catalysts containing copper decreased rapidly with time. Impregnation of the extracted catalyst with thorium nitrate (part B of Table 19) improved both the activity and selectivity, whereas potassium carbonate had no activating effect.

A number of cobalt-aluminum alloys were prepared, but all of these were poor catalysts, the highest yield of condensed hydrocarbons reported being 43 cc/m³. Similar preparations containing copper were completely inactive. The inactivity of the Co-Al skeletal catalysts agreed with the observation that alumina acts as a poison for precipitated cobalt catalysts (Table 6).

Hydrogen treatment of silicon skeletal catalysts at 350°C after extraction decreased their activity appreciably, and in the tests described in Table 20, this step was omitted. Usually, alloy catalysts containing silicon had better activity and selectivity than corresponding aluminum alloys. Addition of copper to the melt produced poor catalysts. Impregnation of the

TABLE 19. TESTS OF Ni-Al SKELETAL CATALYSTS^a
(4 liters 2H₂ + 1CO gas per 5 g Ni at atmospheric pressure)

Composition		Catalyst Form ^b	Temp. (°C)	Contraction (%)	Liquid Hydrocarbons (cc/m ³)	
Ni	Al					
A. Variation of Ni to Al ratio						
1.	100	400	S	206	32	33
2.	100	200	S	206	43	43
3.	100	100	S	206	44	51
4.	100	46	S	206	0	0
B. Effect of promoters 100Ni:100Al alloy						
5.	None	G	206	46	62	
6.	+0.5% K ₂ CO ₃ ^c	G	200	38	42	
7.	+5% Th ^c	G	195	39	68	

^a All catalysts reduced in hydrogen at 350°C after extraction. Extraction procedure in tests 1 to 4 was different from that in tests 5 to 7. Data from Ref. 53.

^b S = powder; G = "lentil-size" granules.

^c Based on nickel content. Catalyst impregnated with potassium carbonate or thorium nitrate solution after extraction.

TABLE 20. TESTS OF Ni-Si, Co-Si, AND Ni-Co-Si SKELETAL CATALYSTS^a
(4 liters 2H₂ + 1CO gas per hour per 5 g Co + Ni at atmospheric pressure)

Ni : Co : Si			Catalyst Form ^b	Hours of Extraction	Temp. (°C)	Contraction (%)	Liquid Hydrocarbons (cc/m ³)
1.	100	— 100	S	5	205	32	47
2.	100	— 100	G	20	205	37	54
3.	100	— 100 ^c	G	20	205	50	68
4.	—	100 100	S	18	200	51	90
5.	—	100 100	G	42	200	20	31
6.	50	50 100	S	<i>d</i>	198	51	90
7.	50	50 100	G	<i>d</i>	198	55	96
8.	75	25 100	<i>d</i>	<i>d</i>	194	53	72
9.	67	33 100	<i>d</i>	<i>d</i>	194	53	81
10.	50	50 100	<i>d</i>	<i>d</i>	194	51	80
11.	33	67 100	<i>d</i>	<i>d</i>	194	40	70

^a From Ref. 53.

^b S = powder; G = "lentil-size" granules.

^c Impregnated with thorium nitrate solution after extraction (10Th per 100Ni).

^d Not specified.

leached alloy with thorium nitrate solution resulted in improved catalytic properties (test 3). Some of the highest activities and yields of condensed hydrocarbons were obtained with Ni-Co-Si alloys (tests 6 and 7). As illustrated by these tests and experiments 4 and 5, there was no consistent relationship between particle size and activity. Presumably, this resulted from unknown factors involved in the extraction step, since the data indicate that a prolonged extraction as well as incomplete leaching resulted in catalysts of lower activity. Tests in which the ratio of nickel to cobalt was varied indicate that catalysts with higher nickel content were the most active, while the yields of condensed hydrocarbons increased to a maximum at a ratio of 2Ni to 1Co.

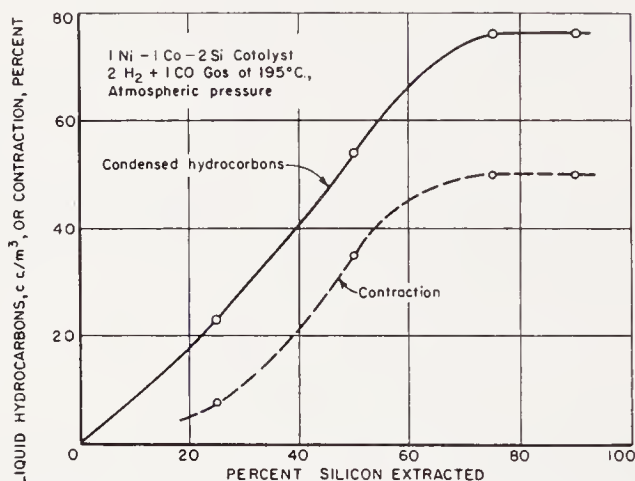


Figure 13. Effect of the extent of silicon extraction on performance of Ni-Co-Si skeletal catalyst. (From Ref. 53)

Complete leaching of silicon was usually not possible with about 90 per cent removal of the silicon being the maximum. Figure 13 presents the variation of contraction and yield of condensible hydrocarbons with the extent of extraction, of a Ni-Co-Si alloy. The activity and selectivity increased to constant values at about 75 per cent extraction of silicon. Iron was a poison for these catalysts, as shown in Figure 14. Iron skeletal catalysts containing either aluminum or silicon were inactive in the synthesis at temperatures as high as 260°C.

In the tests described, the yields from skeletal catalysts were usually considerably lower than from precipitated preparation. However, the skeletal catalyst was spread over the bottom portion of the reactor tube, the catalyst occupying roughly 10 per cent of the volume of the tube. Based on volume of catalyst, the space velocities per hour were about 600 compared with about 100 for precipitated catalysts. When five times this weight

of skeletal catalyst was spread over the same length of reactor tube and the same flow of synthesis gas (corresponding to a space velocity of 120) was used, contraction of 80 per cent and yields of condensable products of 160 cc/m³ were attained at 170°C.

Fischer and Pichler⁵⁶ state that the performance of cobalt-nickel skeletal catalyst was improved at operating pressures of 20 atmospheres and that the yield of condensed hydrocarbons was increased to about 80 g/m³ (115 cc/m³). At temperatures as low as 170°C, this catalyst produced essentially no wax.

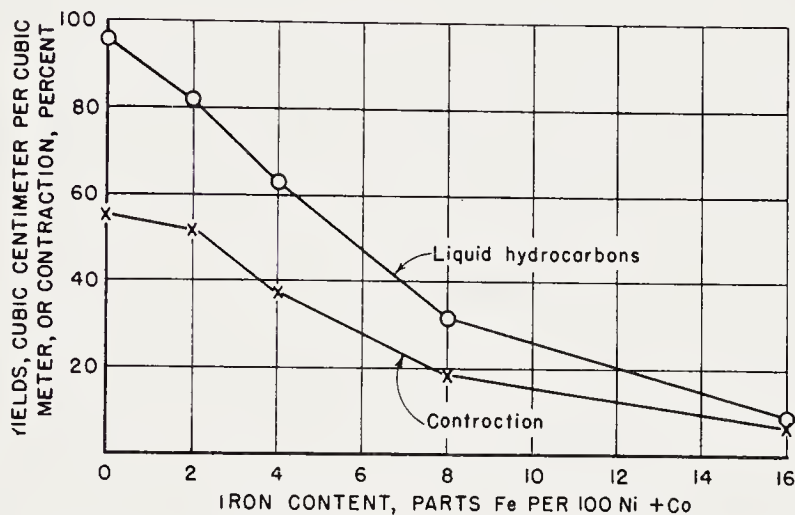


Figure 14. The influence of iron on productivity of Ni-Co-Si skeletal catalysts at 195°C and atmospheric pressure. (From Ref. 53)

Surface Areas and Pore Volumes of Cobalt and Nickel Catalysts

A knowledge of the pore geometry of catalysts is very helpful in understanding catalytic processes. These data provide basic information regarding the relationship of pore geometry to promoters and carriers, as well as the physical structure of the catalyst in the raw state, after pretreatment, after synthesis, or after reactivation. The relationship between pore geometry and catalytic activity is very complicated, and a direct proportionality between catalytic activity and surface area may be expected in only special cases. The present pages describe surface area and pore volume data for precipitated cobalt and nickel catalysts. Surface areas were determined from the physical adsorption of nitrogen⁴² at -195°C by the method of Brunauer, Emmett, and Teller²⁷. Pore volumes were determined by the helium density-mercury density method⁷.

At the Bureau of Mines, the surface areas and pore volumes of Co-ThO₂-kieselguhr and Co-ThO₂-MgO-kieselguhr preparation were determined for

the catalyst in the raw state⁷ and after reduction⁸, synthesis, regeneration⁹, and carbiding⁹. Data for raw catalysts and similar preparations lacking promoters and/or carriers⁷ are presented in Table 21. In addition to total surface areas per gram of raw catalyst, calculated areas for the cobalt basic carbonate-promoter complex, per gram of complex, i.e., everything in the catalyst except the kieselguhr, are given. In this computation, the areas of the kieselguhrs were assumed to be unchanged in the preparation of the catalyst and the areas of kieselguhr and complex were assumed to be additive. Although this calculation may not be strictly correct, because the surface of the carrier may be covered or blocked by the precipitated complex, the area of the complex represents a minimum value which may be used in comparisons with areas of unsupported catalysts.

In the raw catalyst, the area of the kieselguhr was only 10 to 20 per cent of the area of the complex. Cobalt basic carbonate (the preparation with neither kieselguhr nor promoters) had an area of 126 m²/g. The addition of promoters increased the areas of complex to 140 to 170 m²/g, but the area was not increased by addition of kieselguhr. The complex of Co-ThO₂-MgO-kieselguhr catalysts had the highest surface area. The areas of the complex of the preparations containing natural kieselguhrs were higher than corresponding areas for catalysts containing calcined kieselguhrs; however, aside from this observation, no relationship between the surface areas of catalyst and carrier was found. Pelleted catalysts had 10 to 15 per cent lower area than corresponding granules (filter-cake).

Craxford³⁴ found surface areas of raw cobalt catalysts prepared with acid washed Portuguese kieselguhr to be 129 and 130 m²/g, but with a sintered guhr (surface area = 1 m²/g) the area of the catalyst was 46 m²/g. Johnson and Ries⁹³ obtained areas varying from 200 to 300 m²/g for cobalt-kieselguhr catalysts. These high areas may have resulted from differences in method of preparation, since in their precipitation, kieselguhr was mixed with a boiling solution of sodium carbonate before addition of cobalt nitrate.

For granular catalysts (broken filter cake), the external volume of the particles as measured by displacement of mercury was approximately equal to the bulk volume of kieselguhr in the sample. Most of the cobalt basic carbonate-promoter complex was precipitated in the larger pores or void space of the kieselguhr, as indicated by Figure 15, where the volume of mercury (at 1140 mm) displaced per gram of catalyst is a linear function of the volume of mercury displaced by the kieselguhr in a gram of catalyst. The two points on the vertical axis are the volumes of mercury displaced by preparations without kieselguhr, corrected to the proper weight basis. The volume of the kieselguhr to a large extent determines the volume of the resulting granular catalyst. The kieselguhr acts as a "brush heap," with

TABLE 21. SURFACE AREAS AND PORE VOLUMES OF RAW COBALT CATALYSTS^a

No.	Form ^b	Composition			Per Cent Co	Kieselguhr		Surface Areas (m ² /g)		Densities (g/cc)		Pore Volume ^e (cc/g)	Average Pore Diameter ^f
		Co	ThO ₂	MgO	Kg	Type ^c	Area (m ² /g)	Catalyst	Complex ^d	Mercury	Helium		
	G	100	—	—	—	None	—	126.2	126.2	0.925	3.81	0.82	293
	G	100	—	—	200	F.C.	22.2	75.6	124.7	.457	2.71	1.75	926
	G	100	—	12	—	None	—	142.6	142.6				
	G	100	6	—	—	None	—	171.0	171.0				
	G	100	6	12	—	None	—	154.8	154.8	.781	3.62	1.00	259
	G	100	6	12	—	None	—	149.0	149.0	.676	3.80	1.22	327
89I	G	100	6	12	200	H.S.C.	1.9	83.6	165.2	.511		1.60	766
89H	P	100	6	12	200	H.S.C.	1.9	67.2	132.5	1.20	2.74	.47	280
89J	G	100	6	12	200	F.C.	22.2	104.1	186.0	.428	2.87	1.98	760
	P	100	6	12	200	F.C.	22.2	88.7	155.2	.974	2.76	.66	297
89K	G	100	6	12	200	Port.	17.5	101.1	185.0	.611	2.77	1.28	506
	P	100	6	12	200	Port.	17.5	88.8	160.1	1.20	2.77	.47	212
89U	G	100	6	12	200	Germ.	14.9	109.3	203.9	.445		1.89	692
	P	100	6	12	200	Germ.	14.9	86.2	157.5	1.10	2.80	.55	255
108B	G	100	18	—	100	F.C.	22.2	84.1	115.4	.48		1.56	742
	P	100	18	—	100	F.C.	22.2	71.6	96.6	1.13	3.08	.56	313
108H	P	100	18	—	100	F.C.	22.2	125.0	170.0				

^a From Ref. 7.^b G = broken filter cake; P = pellets.^c H.S.C. = Johns Manville "Hyflo-Super-Cel"; F.C. = Johns Manville "Filter-Cel"; Port. = Portuguese kieselguhr; Germ. = German kieselguhr.^d Area of cobalt basic carbonate-promoter complex computed on an additive basis per gram of complex.^e The reciprocal of mercury density minus the reciprocal of the helium density.^f Average pore diameter = $4 \times$ pore volume/surface area.

the cobalt basic carbonate-promoter complex being deposited in the void space and larger pores. In pelleted catalysts, the mercury volume of the catalyst is much less than the bulk volume of the kieselguhr and the brush-pile structure of the kieselguhr is compressed.

The surface areas of the cobalt-promoter complex of the raw catalysts in Table 21 are of the same order of magnitude; however, after reduction in hydrogen, the effectiveness of promoters and kieselguhr in retarding sinter-

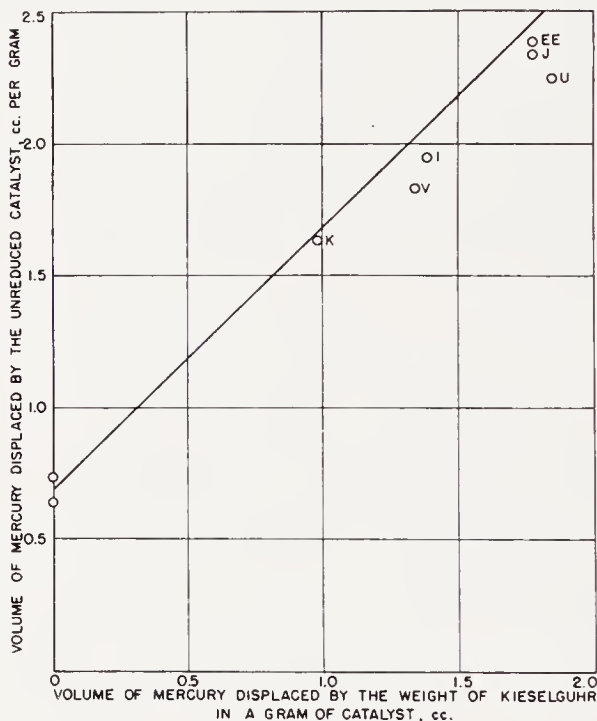


Figure 15. The volumes of mercury displaced per gram of unreduced cobalt Fischer-Tropsch catalysts of the 89-type in granular form plotted against the volume of mercury displaced by the weight of kieselgur per gram of catalyst. The mercury displacement experiments were made at an absolute pressure of 1,140 mm Hg. (Reproduced with permission from Ref. 7)

ing is clearly evident, as indicated by Table 22. In reduction, the area of cobalt-promoter complex of Co-ThO₂-MgO-kieselguhr catalysts decreased to about 60 per cent of its area in the raw state, while for Co-ThO₂-kieselguhr catalyst the area decreased to 40 per cent of its original value. Of the promoters, magnesia was more effective in retarding sintering than thoria. Kieselguhr was about as effective in retarding sintering as the thoria. The natural kieselguhr (F.C.) was more effective than the flux-calcined support (H.S.C.). Data in Table 23 indicate that the surface area changes are the result of two processes: (a) the thermal decomposition of the cobalt basic

TABLE 22. SURFACE AREAS OF UNREDUCED AND REDUCED COBALT FISCHER-TROPSCH CATALYSTS^a

Catalyst	Form ^b	Kieselguhr ^c	Method of reduction ^d			Surface Areas of Catalysts (m ²)				Ratio of Areas of Complex After to Before Reduction
			Temp. (°C)	Hours	Per cent Weight Loss	Unreduced		Reduced		
						Total per gram	Complex per gram of complex	Total ^e per Gram	Complex ^f per Gram of Complex	
Co:ThO ₂ :MgO: kieselguhr = 100:6:12:200										
89H	P	H.S.C.	400	2	19.8	67.2	127.2	41.9	83.8	0.620
89J	P	F.C.	400	2	17.4	85.5	155.4	62.0	99.6	.640
89K	P	Port.	400	2	19.7	88.8	160.3	62.7	105.5	.651
89K	G	Port.	400	2	17.7	101.1	185.0	62.2	104.5	.580
89U	P	Germ.	400	2	19.3	86.2	157.5	37.8	59.6	.374
89BB	P	JM-II	400	2	18.9	66.2	121.5	46.2	84.6	.690
89FF	P	FCX	400	2	16.7	102.9	177.5	80.2	133.2	.751
Co:ThO ₂ :kieselguhr = 100:18:100										
108B	P	F.C.	360	2	24.4	71.6	96.2	32.4	50.0	.390
Co:ThO ₂ :MgO = 100:6:12	G	None	400	2	37.7	154.8	154.8	52.8	52.8	.341
Co:ThO ₂ = 100:6	G	None	400	2	38.7	171.0	171.0	14.6	14.6	.085
Co:MgO = 100:12	G	None	400	2	41.6	142.6	142.6	35.2	35.2	.247
Co:kieselguhr = 100:200	G	F.C.	400	2	21.1	75.6	124.7	18.3	14.2	.109
Co:kieselguhr = 100:200	G	H.S.C.	400	2	21.2	77.2	152.4	6.9	12.0	.078
Cobalt basic carbonate	G	None	400	2	44.2	126.2	126.2	2.5	2.5	.020

^a From Ref. 8.^b G = granules, broken filter cake; P = pellets (1.6 mm. long by 3.2 mm. diameter).^c H.S.C. = Johns Manville "Hyflo-Super-Cel"; F. C. = Johns Manville "Filter-Cel"; Port. = Portuguese kieselguhr; JM-II = Johns Manville II, FCX = acid extracted Filter-Cel.^d All reductions were made with hydrogen at space velocities per hour of 6,000.^e Per gram of unreduced catalyst.^f Per gram of complex in unreduced catalyst.

carbonate while the catalyst was heated to reduction temperature in nitrogen, and (b) during reduction of the cobalt oxide or basic carbonate to metal. For the Co-ThO₂-MgO preparation, both with and without kieselguhr, the largest surface area diminution occurred in step (a). For preparations without promoters, a large degree of sintering occurred in both steps, the preparation supported on kieselguhr being more resistant to sintering.

Although kieselguhr is somewhat effective in preventing excessive diminution of surface area during reduction, its principal function is to prevent

TABLE 23. CHANGES IN SURFACE AREA DURING HEATING AND REDUCTION^a
(All data per gram of original unreduced catalyst or complex)

Catalyst	Catalyst							
	Original		Heated ^b		Evacuated ^b		Reduced ^b	
	Area (m ² /g)	Area of Complex per Gram Complex	Area (m ² /g)	Area of Complex per Gram Complex	Area (m ² /g)	Area of Complex per Gram Complex	Area (m ² /g)	Area of Complex per Gram Complex
Co:ThO ₂ :MgO:kieselguhr = 100:6:12:20, 89J	85.5	155.4	65.5	108.9	67.0	109.8	62.0	99.6
Co:ThO ₂ :MgO = 100:6:12	154.8	154.8	68.3	68.3	61.1	61.1	52.8	52.8
Co:kieselguhr ^c = 100:200	75.6	124.7	37.1	52.4	35.5	49.2	18.3	14.2
Cobalt basic carbonate	126.2	126.2	24.2	24.2	21.6	2.5	2.5	2.5

^a From Ref. 8.

^b Area of catalyst and complex per gram of catalyst and per gram of complex in the original unreduced catalyst, respectively.

^c Contains "Filter-Cel."

excessive shrinkage of the particle, as shown by mercury density data in Table 24. Although mercury wetted and penetrated the particles of reduced cobalt basic carbonate, mercury did not wet or penetrate the particles of the samples containing either promoters or kieselguhr. On reduction, the volume of mercury displaced per gram of catalyst (in the unreduced state) decreased by less than 5 per cent for samples containing kieselguhr, whether or not the catalyst contained promoters and whether the samples were in the form of granules or pellets. The volume of mercury displaced by the unsupported catalyst decreased on reduction to less than half of the initial volume. The pore volumes (Table 24) of all preparations containing kieselguhr increased on reduction; however, those of unsupported samples decreased. Average pore diameters computed from the equation of Emmett

TABLE 24. MERCURY AND HELIUM DENSITIES OF UNREDUCED AND REDUCED COBALT CATALYSTS^a

Catalyst	Form ^b	Unreduced Catalysts					Reduced catalysts					Mercury Volumes per Gram of Unreduced Catalyst (cc)	
		Densities		Pore Volume (cc/g)	Area (m ² /g)	\bar{d}_v (Å) ^c	Densities		Pore Volume (cc/g) ^e	Area (m ² /g) ^e	\bar{d}_v (Å) ^c	Before	After
		Hg	He				Hg	He ^d					
Co:ThO ₂ :MgO: kieselguhr = 100:6:12: 200													
89H	P	1.20	2.74	0.47	67.2	280	0.993	3.10	0.68	51.8	527	0.833	0.816
89J	P	0.974	2.76	.66	88.7	297	.780	3.07	.95	76.6	500	1.026	1.037
89K	P	1.20	2.77	.47	88.8	212	1.045	3.08	.63	77.4	327	.833	.768
89K	G	.611	2.77	1.28	101.1	506	.537	3.13	1.54	76.8	804	1.635	1.530
89U	P	1.10	2.80	.55	86.2	255	.901	3.08	.79	46.7	672	.909	.896
89FF	P	1.295	<i>f</i>	.41	102.9	160	1.138	3.03	.55	99.0	222	.772	.712
Co:ThO ₂ :kie- selguhr = 100:18:100													
108B	P	1.13	3.08	.56	71.6	313	.905	3.69	.73	42.3	693	.885	.836
Co:ThO ₂ :MgO = 100:6:12	G	.781	3.62	1.00	154.8	259	1.057	6.72	.80	84.1	379	1.280	.593
Co:kieselguhr = 100:200	G	.457	2.71	1.75	75.6	926	.378	3.00	2.31	22.8	4060	2.189	2.082
Cobalt basic carbonate	G	.925	3.81	.82	126.1	293	4.476 ^g	9.00	.112	4.2	1070	1.081	.125

^a From Ref. 8.^b P = pellets (1.6 mm long by 3.2-mm diameter); G = granules, broken filter cake.^c Average pore diameters computed from $\bar{d} = 4V/A$, where V is the pore volume and A the surface area per gram.^d Helium densities calculated from compositions of reduced catalysts: 89-type, 3.12; 108B, 3.69; Co:ThO₂:MgO = 100:6:12, 7.79; Co:kieselguhr = 100:200, 3.06; and cobalt basic carbonate, 8.9.^e Pore volumes and surface areas per gram of reduced catalyst.^f Not determined, assumed to be 2.77.^g This sample wet by mercury.

and DeWitt⁴⁴ ($d = 4 \times$ pore volume/surface area) increased on reduction, because the decrease in surface area was always of a greater magnitude than the changes in pore volume.

At -195°C , carbon monoxide seems to be chemisorbed only on the metallic cobalt in the catalyst surface. Actually, the isotherm at this temperature is a composite of chemical and physical adsorption; and the volume of chemisorbed carbon monoxide is obtained by subtracting the adsorption

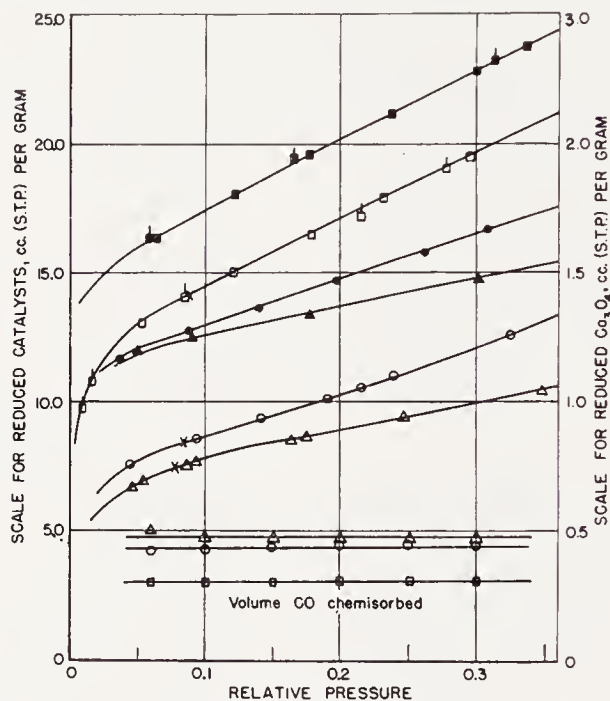


Figure 16. Sorption of nitrogen and carbon monoxide at -195°C on reduced pelleted catalysts 89H and 89J and reduced cobalt oxide powder where open points represent nitrogen and solid points represent carbon monoxide isotherms. Points of reduced 89 H are given by \circ , two samples of reduced 89 J by \square and \square , and the reduced cobalt oxide by \triangle . The volumes of chemisorbed carbon monoxide are given in lower part of the graph. (Reproduced with permission from Ref. 9)

isotherm of nitrogen from the total carbon monoxide isotherm, with both isotherms being plotted on a relative pressure basis as shown in Figure 16. This approximation is permissible, since the physical properties of the two molecules, including molecular size, are nearly identical. For the samples without kieselguhr or promoters, which in the reduced state were essentially pure cobalt, the ratio of chemisorbed carbon monoxide (V_{Co}) to the nitrogen monolayer (V_{m}) was about 0.65 (Table 25). Possibly this ratio arises from the steric factors involved in chemisorption on fixed sites. For all promoted and/or supported catalysts, the ratio of V_{Co} to V_{m} for the complex was lower than 0.65. The lowest values of this ratio were obtained

for promoted and supported catalysts, and for these samples it may be inferred that more than 30 per cent of the surface of the complex contained material other than metallic cobalt.

The changes in surface area and carbon monoxide chemisorption on Co-ThO₂-kieselguhr catalyst 108B and Co-ThO₂-MgO-kieselguhr catalyst

TABLE 25. CHEMISORPTION OF CARBON MONOXIDE ON REDUCED COBALT FISCHER-TROPSCH CATALYSTS^a

(All data per gram of unreduced catalyst)

Catalyst	Form ^b	V _m , (cc)	V _{CO} , (cc) ^c	Complex per Gram of Complex (cc)		$\frac{V_{CO}}{V_m}$ (complex)	Co Atoms in Surface (%)
				V _m	V _{CO}		
Co:ThO ₂ :MgO:kieselguhr = 100:6:12:200							
89H	P	9.58	4.40	18.72	8.80	0.470	72.3
89J	P	14.15	3.10	23.92	6.20	.259	39.9
89K	P	14.31	3.80	24.80	7.60	.306	47.1
89K	G	14.19	4.00	24.40	8.00	.328	50.4
89U	P	8.64	2.17	13.98	4.34	.311	47.9
Co:ThO ₂ :kieselguhr = 100:18:100							
108B	P	7.40	2.56	11.42	2.84	.448	69.0
Co:ThO ₂ :MgO = 100:6:12	G	12.06	6.90	12.06	6.90	.572	88.0
Co:ThO ₂ = 100:6	G	3.33	1.95	3.33	1.95	.586	90.2
Co:MgO = 100:12	G	8.03	3.70	8.03	3.70	.461	71.0
Co:kieselguhr ^e = 100:200	G	4.18	.85	3.28	1.70	.518	79.7
Cobalt basic carbonate	G	.58	.36	.58	.36	.632	97.2
Cobalt oxide powder		.73	.73	.48	.48	.648	99.7

^a From Ref. 8.

^b G = granules, broken filter cake; P = pellets.

^c V_{CO} computed from the difference the total carbon monoxide isotherms and the physical nitrogen at equal relative pressures.

^d V_{CO}/V_m-complex divided by 0.65, the value of V_{CO}/V_m-complex for cobalt metal.

^e "Filter-cel."

89K during carburization in carbon monoxide were studied⁹. In carburizations with carbon monoxide at 208°C, chiefly cobalt carbide, Co₂C, was produced, and at 275°C, chiefly elemental carbon was deposited. The surface areas of the catalyst remained essentially constant in carburizations at 208°C, but the volume of carbon monoxide chemisorbed at -195°C decreased to less than half of its original value. Most of the carbon was removed by hydrogen treatment at 208°C, and although the surface area remained constant, the volume of chemisorbed carbon monoxide increased, but not quite to the value for the original reduced catalyst.

In carburizations of catalyst 108B at 275°C, at least four times the amount of carbon corresponding to Co_2C was deposited, and only a small portion of this carbon could be removed by hydrogenation at 208°C. These facts suggest that the carbon deposited was chiefly in the elemental form⁸⁵, and this was confirmed by a 60 per cent increase in surface area. On this sample, the volume of chemisorbed carbon monoxide was greater than those observed on the catalyst in the carburized or reduced state earlier in this series. Similarly, after deposition of 16-times the carbon equivalent to Co_2C on catalyst 89K, the volume of chemisorbed carbon monoxide was 3.6 cc/g compared with 3.1 cc/g for the catalyst after the initial reduction. These data indicate that the area of the cobalt portion of the surface, as well as the total area, had increased by the deposition of elemental carbon. Presumably, a portion of the carbon is formed by the growth of nuclei of elemental carbon within the crystal lattice of the cobalt, resulting in partial disintegration of the cobalt structure and a corresponding increase in number of accessible cobalt atoms. The presence of sizable amounts of elemental carbon prevented subsequent carburization at 208°C. The elemental carbon hydrogenated very slowly, and for catalyst 108B, the carbon was not completely removed in 530 hours at 360 to 450°C. In this hydrogenation, the surface area decreased from 52.2 to 35.2 m²/g compared with 32.6 m²/g for the original reduced catalyst. Later in this chapter (p. 94), surface area and pore volume studies on a used cobalt catalyst, as well as changes in these quantities during regeneration in hydrogen, will be presented.

In the preparation of cobalt catalysts at the Bureau of Mines, the time of contact of reacting solutions and kieselguhr was as short as possible, and there was little evidence for interaction between cobalt oxide or basic carbonate and kieselguhr. However, many nickel catalysts supported on kieselguhr appear to contain sizable amounts of nickel hydrosilicate. DeLange and Visser³⁸ observed that nickel-kieselguhr catalysts were active in hydrogenation reactions when reduced at 500°C, whereas nickel hydroxide reduced at this temperature was inactive. Further, after heating in nitrogen at 500°C, the surface area of the nickel-kieselguhr catalyst greatly exceeded the areas of the heated nickel hydroxide and kieselguhr, as shown by the following data: kieselguhr 10 m²/g, NiO 30 m²/g, NiO-kieselguhr (20 per cent Ni by weight) 270 m²/g. X-ray data confirmed the presence of nickel hydrosilicate. Hydrothermal treatment increased the formation of nickel hydrosilicate to such an extent that the structure of the kieselguhr was destroyed. Co-ThO₂-MgO-kieselguhr catalysts prepared by Craxford³⁴ had larger surface areas after reduction than corresponding Bureau of Mines preparations, and Craxford suggested that interaction of cobalt oxide with the kieselguhr was responsible for the high areas.

Workers in M. Prettre's laboratory have presented numerous papers^{121, 122, 182, 183, 186, 187, 188, 189} on Ni-Al₂O₃-MnO-kieselguhr and nickel aluminate catalysts for which there is substantial evidence for the formation of nickel hydrosilicate and hydroaluminate bonds. Trambouze^{188, 189} developed a method based on selective solubility for estimating the fraction of nickel present as hydroaluminate and hydrosilicate. Nickel as oxide, hydroxide, or basic carbonate was dissolved by a concentrated aqueous ammonia solution. Nickel as hydroaluminate, as well as the phases listed in the previous sentence, was removed by concentrated nitric acid solution. Nickel as hydrosilicate was insoluble in the above reagents, but could be dissolved by alkali fusion methods. Table 26 presents the fractions of nickel in

TABLE 26. FRACTION OF NICKEL PRESENT AS HYDROALUMINATE OR HYDROSILICATE IN Ni-Al₂O₃-MnO-KIESELGUHR CATALYSTS^a

Treatment	Nickel Present as		
	Hydroxide, Oxide, or Basic Carbonate (%)	Hydroaluminate (%)	Hydrosilicate (%)
Cold precipitation	100	0	0
Precipitate boiled	63	37	0
Dried in air	63	37	0
Evacuated at 150°C ^b	63	37	0
N ₂ at 220°C for 2 hours	59	13	28
N ₂ at 320°C ^b	18	46	36
N ₂ at 450°C ^b	16	40	44

^a From Refs. 186 and 188.

^b To constant weight.

Ni-Al₂O₃-MnO-kieselguhr catalysts present as hydroaluminate or hydrosilicate after various treatments, as estimated by this method. The nickel hydroaluminate was formed in sizable amounts at 100°C, while the hydrosilicate was formed only at temperatures of 220°C and above.

Teichner¹⁸² studied the changes in surface areas of Ni-Al₂O₃-MnO-kieselguhr catalysts on evacuation at various temperatures and on reduction in hydrogen at 450°C. The surface areas of preparations that were not boiled after precipitation usually decreased during heat treatment or reduction in somewhat the same manner as the areas of cobalt catalysts studied at the U. S. Bureau of Mines. However, the behavior of preparations that were boiled after precipitation was very different and apparently characteristic of nickel hydroaluminate. For example, the surface area of a catalyst of this type increased on evacuation at 180°C and further on reduction in hydrogen at 450°C. The areas per gram (based on weight after

evacuation at 180°C) were 30, 39, and 75 m² after evacuation at 20 and 180°C and reduction at 450°C, respectively. Surface areas of similar preparations which had been boiled after precipitation are given in Table 27. The first preparation, Ni-MnO, indicates that oxides of manganese are not effective structural promoters. The area of sample with Al₂O₃ and MnO increased upon reduction in the same manner as Ni-Al₂O₃-MnO-kieselguhr catalyst described previously. The catalyst that was precipitated by a special method in which the pH was maintained constant had a larger surface area than the similar catalyst precipitated as variable pH.

Teichner also studied surface area changes in nickel hydroaluminate during various thermal treatments and reduction, as shown in Table 28. The

TABLE 27. SURFACE AREAS OF Ni-MnO-Al₂O₃-KIESELGUHR CATALYSTS^a

Components	Evacuated at				Reduction at 450°C	
	20°C		150°C			
	Weight Loss (%) ^b	Surface Area (m ² /g) ^c	Weight Loss (%) ^b	Surface Area (m ² /g)	Weight Loss (%) ^b	Surface Area (m ² /g) ^c
Ni-MnO ^d			2.2	125	47.0	1.6
Ni-MnO-Al ₂ O ₃ ^d			12.7	35	32.9	63
Ni-MnO-Al ₂ O ₃ -kieselguhr ^e	2.1	130	11.0	118	27.6	114

^a From Ref. 182.

^b Loss in weight based on initial dried sample.

^c Areas corrected to correspond to 1 gram of catalyst after evacuation at 150°C.

^d "Solution" heated to boiling after precipitation.

^e Precipitated from boiling solution with pH maintained constant at 9.

surface area changes of this material parallel those of catalysts containing sizable quantities of the hydroaluminate.

The chemisorption of carbon monoxide at -195°C was determined on some of the samples described in Tables 27 and 28 by the method used at the Bureau of Mines (p. 76). The results for samples that did not contain appreciable amounts of nickel hydroaluminate were essentially the same as those of the Bureau of Mines. Carbon monoxide was apparently chemisorbed only upon reduced nickel and gave an indication of the extent of metal in the surface. However, samples containing sizable quantities of nickel hydroaluminate (Table 29) chemisorbed appreciable quantities of carbon monoxide in the unreduced state, apparently on the nickel hydroaluminate. In the last sample in this table, the chemisorption was zero, although 79 per cent of the nickel was present as metal. It was postulated that this was due to the migration of nickel atoms into the interior of the

TABLE 28. CHANGES OF SURFACE AREA DURING TREATMENT OF NICKEL HYDROALUMINATE^a(Approximate composition $2\text{NiO} \cdot \text{Al}_2\text{O}_3 \cdot 6\text{H}_2\text{O}$)

Treatment	Temp. (°C)	Weight Loss (%) ^b	Surface Area (m ² /g) ^c
Evacuation	100	11.9	88
Evacuation	170	11.9	48
Evacuation	220	21.5	160
Reduction	450	39.2	206
Air	450	38.2	230
Air	450}	43.7	131
Reduction	450}		

^a From Ref. 182.^b Loss in weight based on initial dried sample.^c Areas corrected to correspond to 1 gram sample after evacuation at 170°C.TABLE 29. CHEMISORPTION OF CARBON MONOXIDE ON NICKEL CATALYSTS AND NICKEL HYDROALUMINATE^a

Components	Treatment	Temp. (°C)	V _m (cc/g) ^b	V _{CO} (cc/g) ^b	V _{CO} /V _m	Nickel as Metal (%)
Ni-MnO-Al ₂ O ₃ ^c	Reduction	450}	18.9	10.1	0.53	^d
	Evacuation	150}				
Ni-MnO-Al ₂ O ₃ -kieselguhr ^c	Evacuation	150	36.3	6.2	.17	0
	Reduction	450}	32.1	3.5	.11	^d
	Evacuation	150}				
Nickel hydroaluminate ^e	Evacuation	100	20.2	4.2	.21	0
	Evacuation	220	41.5	7.8	.19	0
	Reduction	450}	69.2	16.3	.24	14
	Evacuation	150}				
	Air	450}	76.0	12.5	.16	0
	Evacuation	150}				
	Air	450}	47.3	0	0	79
	Reduction	450}				
	Evacuation	150}				

^a From Ref. 182.^b Per gram sample after pretreatment.^c The same samples as in Table 27.^d Values not given, but the nickel as metal probably approached 100 per cent.^e The same samples as in Table 28.

alumina phase. The unreduced samples were inactive in the synthesis even though many of them chemisorbed carbon monoxide, and hence there appears to be considerable uncertainty as to the significance of studies of the chemisorption of carbon monoxide at -195°C on this type of nickel catalysts.

Reduction and Pretreatment of Cobalt and Nickel Catalysts

Reduction. Precipitated oxides or basic carbonates of cobalt or nickel are readily reduced in hydrogen at relatively low temperatures, such as 200 or 250°C . Structural promoters,* such as magnesia, thoria, and alumina, usually make the reduction of the active metal in the catalyst more difficult. This may be entirely a kinetic effect, but in some instances, such as when compound or mixed crystal formation between promoter and active metal oxide is possible, for example, the formation of nickel hydroaluminate or hydrosilicate, the free energy of the transformation from oxide to metal, becomes more positive. Carriers may make reduction more difficult due to kinetic effects or, in some cases, to compound formation between the carrier and active metal oxide. The presence of easily reducible oxides, such as those of copper or silver, usually increases the rate of reduction. This phenomenon has been attributed to the rapid formation of copper or silver atoms that act as nuclei for reduction of the cobalt or nickel oxides.

Usually the rate of reduction increases with temperature. For example, under the same conditions and time with $3\text{H}_2 + 1\text{N}_2$ gas, a $100\text{Co}:5\text{ThO}_2:10\text{MgO}:200$ kieselguhr catalyst was 15 per cent reduced at 300°C , 45 per cent at 325°C , and 75 per cent at 350°C ⁷¹. In general, the catalysts that are difficult to reduce have the higher surface areas after reduction and the greater activity in the Fischer-Tropsch synthesis. For cobalt catalysts, the difficulty of reduction and surface area increase in the following order of promoters; ThO_2 , MgO-ThO_2 , MgO . Data from Ruhrchemie (Table 30) illustrate the effect of promoter as well as the amount of kieselguhr. For preparations with ThO_2 or $\text{ThO}_2\text{-MgO}$ as promoters, the extent of reduction decreased sizably with increasing kieselguhr content. However, for catalysts promoted with MgO , the reduction did not decrease appreciably as the content of kieselguhr increased. Possibly the behavior of catalysts promoted with only magnesia can be related to solid solution or formation between cobaltous and magnesium oxides, as postulated by Roelen. Both oxides have a wustite structure.

The presence of copper increases the rate of reduction of standard cobalt and nickel catalysts containing promoters such as thoria and the usual

* Additives that facilitate the formation of a structure of high surface area during preparation or pretreatment and stabilize this structure during the use of the catalyst.

amounts of kieselguhr, so that reduction in hydrogen can be accomplished at 200°C rather than temperatures above 350°C for copper-free preparation. Further, some copper-promoted catalysts can be reduced directly in synthesis gas at about 200°C. In the synthesis, the copper-promoted catalysts lost activity rapidly, and the German workers had abandoned copper as a promoter for cobalt and nickel catalysts as early as 1934. The rapid loss of activity is believed to be due to a rapid rate of sintering, involving a decrease in surface area. Unfortunately, surface areas have not been deter-

TABLE 30. REDUCIBILITY OF PRECIPITATED COBALT CATALYSTS^a
(Space velocity of 30,000 hr⁻¹ of 3H₂ + 1N₂ gas at 400°C)

Catalyst Composition				Reduction Time (min.)	Cobalt Reduced to Metal (%)
Co	ThO ₂	MgO	Kieselguhr		
100	15	—	100	5	79
			200		73
			600		47
			1000		28
			2000		36
100	5	10	200	15	78
			600		70
			1000		25
			2000		33
100	—	15	100	15	64
			200		64
			600		63
			1000		62
			2000		53

^a From Ref. 71.

mined on preparations of this type. Copper appears to render the structural promoter ineffective with respect to both ease of reduction and stability in the synthesis.

Since in many catalysts, cobalt and nickel are present initially as basic carbonates, the reduction process is complicated by the decomposition of the basic carbonate to water and carbon dioxide. The carbon dioxide liberated is partly hydrogenated to methane, as shown by Ruhrchemie experiments¹⁴⁴ in Table 31. These data also demonstrate inhibition of reduction by water and carbon dioxide.

German workers believed that the presence of compounds containing oxygen had undesirable effects other than decreasing the rate of reduction. The postulate was made that an alternate oxidation-reduction process oc-

curs on active points of the catalyst, resulting in their deactivation. However, activity tests to demonstrate this effect are apparently not available. In any case, if only on the basis of reduction rate, it was desirable to use hydrogen with a very low concentration of oxygen-containing gases at a sufficiently high space velocity to keep the percentage of these components

TABLE 31. REDUCTION OF COBALT CATALYST WITH $3\text{H}_2 + 1\text{N}_2$ IN PRESENCE OF H_2O VAPOR AND CO_2^a

(2-3 mm granules, catalyst layer 20 cm long and 2.1 cm deep, 150 liters of $3\text{H}_2 + 1\text{N}_2$ gas per hour at 350°C)

Reduction		Off-gas Analyses				
Time (min.)	% Co as Metal	CO_2	CO	H_2	CH_4	N_2
(a) $3\text{H}_2 + 1\text{N}_2 + 1$ per cent H_2O^b						
25	33	1.6	0	72.4	2.1	24.9
50	50	—	—	—	—	—
100	61.5	2.0	0	71.3	1.1	25.4
180	66	—	—	—	—	—
(b) $3\text{H}_2 + 1\text{N}_2 + 3$ per cent CO_2						
0	0	2.9	0.2	72.2	0.7	24.0
50	8	1.0	0	67.2	3.6	29.2
100	11.5	.4	0	68.1	4.6	26.8
180	11.5	0	0.2	69.5	2.8	27.7
(c) $3\text{H}_2 + 1\text{N}_2$						
35	62	—	—	—	—	—
50	81	—	—	—	—	—
65	85	—	—	—	—	—

^a From Ref. 144.

^b Gas saturated with water vapor at 3°C (8 g H_2O per m^3).

formed in the reduction process at a low value. Japanese studies¹¹⁸ of the productivity of Co- ThO_2 -MgO-kieselguhr catalysts, as a function of duration of reduction and flow of hydrogen, are given in Table 32. These data indicate that optimum yields result from a reduction time of 1.5 to 2 hours and that yields increased with increasing space velocity of hydrogen. In many cases, the actual reduction conditions may not be too important, provided that a moderate extent of reduction is attained. Ruhrchemie¹⁵⁶ reported tests of a 100Co:18 ThO_2 :200 kieselguhr catalysts reduced under the following conditions:

(a) 350°C, 300 liters $3\text{H}_2 + 1\text{N}_2$ gas per hour for 45 minutes.

(b) 400°C, 300 liters $3\text{H}_2 + 1\text{N}_2$ gas per hour for 2 hours.

(c) 350°C, 8 liters $3\text{H}_2 + 1\text{N}_2$ gas per hour for 15 hours.

In atmospheric tests of 3,800 hours, no significant differences were observed in synthesis activity or selectivity. Similarly, Bureau of Mines tests¹⁸¹ of Co-ThO₂-kieselguhr and Co-ThO₂-MgO-kieselguhr catalysts, after a variety of reduction and induction procedures, showed virtually no differences in synthesis behavior at 1 and 7.8 atmospheres (absolute). These results indicate that for standard catalysts, reduction conditions within

TABLE 32. EFFECT OF REDUCTION CONDITIONS OF 100Co:3ThO₂:8MgO:200 KIESELGUHR ON PRODUCTIVITY^a

Synthesis conditions: $2\text{H}_2 + 1\text{CO}$ gas, space velocity = 100 at atmospheric pressure and 190°C.

Reduction conditions: Hydrogen at 380 to 385°C.

A. Duration of reduction (space velocity of hydrogen = 3750)

Hours	1	1.5	2	3
Contraction, (%)	84	87	87	75
C ₅ ⁺ , cc/m ³	152	160	158	121

B. Space velocity (time of reduction = 1.5 hours)

Space velocity, hr ⁻¹	25	1250	2500	3750
Contraction, (%)	82	85	86	87
C ₅ ⁺ , cc/m ³	101	121	149	149

^a From Ref. 118.

rather broad ranges are not too critical. Possibly this results from the use of catalysts containing adequate structural promoters to prevent major variations of catalyst geometry and chemical properties in the range of conditions normally employed. Unpromoted cobalt-kieselguhr catalysts must be carefully reduced at low temperatures to attain high activity.

Roelen⁷² believed that complete reduction of cobalt catalysts was neither necessary nor desirable. Although high activity was observed in catalysts in which 40 to 90 per cent of the cobalt was reduced to metal, the maximum activity was observed between 65 and 70 per cent reduction. It was suggested that portions of unreduced cobalt oxide act as a structural promoter to prevent excessive sintering. Catalysts for the industrial synthesis were reduced 55 to 65 per cent. Apparently, the somewhat lower initial activity of these samples was advantageous for industrial scale reactors,

since the possibility of overheating (bolting) in the induction period was minimized.

In Germany, catalysts for industrial synthesis were reduced in a separate reduction unit and stored under carbon dioxide in a special vessel for shipment to the synthesis plant. The catalyst was cooled to about room temperature before admitting the carbon dioxide. If carbon dioxide was introduced at temperatures above 100°C , the catalytic activity was impaired, and sometimes even at lower temperatures heat was generated in the catalyst. The exact nature of this deactivation process is not known, but it is possible that both oxidation and carbide formation may occur. When the catalyst was cooled to a sufficiently low temperature before admission of carbon dioxide, the method was entirely successful. The reduced catalyst after saturation with carbon dioxide could tolerate moderate exposure to air without adverse effect. The carbon dioxide stabilization has been used extensively in the Bureau of Mines catalyst testing program; however, here it was used only as a precautionary measure, since procedures for the transfer of catalysts were designed to preclude exposure of the reduced catalyst to air. German laboratory tests showed that reduced catalysts were adequately protected by immersion in synthesis oil or impregnation with wax; however, this method was not used in handling reduced catalysts in the commercial plants.

Carburization of Cobalt and Nickel Catalysts. Carbides* of cobalt (Co_2C) and nickel (Ni_3C) can be easily prepared by treating the reduced catalyst with carbon monoxide at about 200°C . However, since these carbides are relatively inactive compared with corresponding reduced catalyst, this pretreatment has no practical value. Nitrides and carbonitrides of cobalt and nickel are difficult to prepare, and numerous attempts at the Bureau of Mines to find methods of preparing these interstitial compounds in conventional cobalt and nickel catalysts have been unsuccessful.

Weller, Hofer, and Anderson²⁰¹ observed that cobalt catalysts converted to Co_2C by carburizing the reduced catalyst with carbon monoxide at about 200°C had a low activity in the synthesis. The effect was reversible in that after removal of the carbidic carbon by hydrogenation at about 200°C , the activity was substantially restored to the value obtained for a reduced catalyst. The carbide was apparently stable in the synthesis for at least moderately long periods of synthesis; however, x-ray diffraction patterns of Co_2C were only found in used cobalt catalysts that had been carbided before synthesis. Furthermore, in catalysts reduced at 400°C , the

* The stoichiometry of interstitial compounds of iron group metals is difficult to determine and the formulas are often not simple. For example, the more recent work on cobalt carbide indicates that the formula is Co_{20}C_9 rather than Co_2C . However, for simplicity the approximate formula Co_2C is used.

cobalt had a disordered crystal structure with a characteristic diffraction pattern. After carburization and subsequent hydrogenation, both at about 200°C, the cobalt had been transformed into a hexagonal, close-packed structure, the thermodynamically stable phase at temperatures below 400°C. However, all of the reduced catalyst examined after synthesis gave an identical x-ray diffraction pattern, that of disordered cobalt. Since the transformation from disordered to hexagonal cobalt accompanies the for-

TABLE 33. EFFECT OF CARBURIZATION AND HYDROGENATION ON ACTIVITY AND PRODUCT DISTRIBUTION OF COBALT CATALYST 108B^a

(Space velocity of 2H₂ + 1CO gas, 100 hr⁻¹ at atmospheric pressure)

Part a					Part b						
Period	Catalyst Pretreatment				Hours	Average Temp. (°C)	Synthesis Gas Reacted (%)	Products, g/m ³ of Synthesis Gas Reacted			
	Gas	SVH	Temp. (°C)	Hours				CH ₄	C ₃ + C ₄	C ₁ - C ₄	Liquids + Solids
a	H ₂	3000	360	2	73	173	67	22	27	56	106
b	CO	100	208	16	126	195	47	42	38	90	64
c	H ₂	100	208	16	149	190	64	28	39	73	107
d	CO	100	208	16	149	191	33	42	33	82	—
e	H ₂	100	208	16	127	190	52	35	—	—	82
f	CO	100	208	16	176	193	23	84	—	—	—
g	H ₂	100	208	16	126	190	42	—	—	—	—
h	CO	100	208	16	125	191	17	123	54	189	47
i	CO	100	274	15	149	191	19	106	18	132	11
j	H ₂	100	208	16	119	191	56	73	34	108	16
k	H ₂	100	200	2	165	189	49	83	47	137	18
l	H ₂	3000	360	2	166	190	64	37	46	99	76

^a From Ref. 9.

mation and hydrogenation of cobalt carbide, it must be concluded that appreciable concentrations of Co₂C were never present in the catalyst.

Anderson, Hall, Krieg, and Seligman⁹ extended this series of experiments with synthesis tests after carburization of a cobalt-thoria-kieselguhr catalyst at 208 and 274°C. Carburization at 274°C produced chiefly elemental carbon and only small amounts of cobalt carbide. After the initial reduction and a synthesis period of 73 hours (Table 33, part a), the catalyst was converted to cobalt carbide. The carbided sample (a) had a lower activity and produced more gaseous hydrocarbons. After hydrogenation c, the activity and selectivity were partially restored. In subsequent carburization and hydrogenation cycles d to h, the activity and selectivity of the hydrogenated catalyst were always better than those of the previous car-

bided sample. However, if only the reduced or the carbided catalysts are compared, there was a gradual decrease in activity and greater production of gaseous hydrocarbons as the number of carbiding-hydrogenation cycles increased. After carburization at 274°C, i, the activity was low and the percentage of gaseous hydrocarbons was high. Subsequently, hydrogenation at 208°C, j, which should remove the carbidic carbon but not elemental carbon, resulted in greatly increased activity as well as a moderate improvement of selectivity. Further hydrogenation, l, at 360°C, which

TABLE 34. CARBURIZATION CONDITIONS FOR Ni-Mn-Al₂O₃-KIESELGUHR CATALYSTS^a

Test	Catalyst	Carburization Conditions				Comments
		Gas	Flow (cc/hr) ^b	Temp. (°C)	Time (hr)	
G	C.I. 10	Used directly in synthesis				Catalyst completely carbided
J	C.I. 12	Used directly in synthesis				
L	C.I. 10	CO	350	175	36	
M	C.I. 12	CO	300	175	18	Catalyst about 75 per cent carbided. After 25 hours of synthesis, catalyst was hydrogenated at 175°C for 17 hours, and then after 3½ hours of synthesis hydrogenated at 185°C for 40 hours
N	C.I. 12	1CO + 3N ₂	1100	180	4	
						Catalyst only slightly carbided.

^a From Ref. 122.

^b Presumably per 40 cc of catalyst.

should remove all carbidic carbon and most of the elemental carbon, restored the activity to that observed in period c; however, the fraction of gaseous hydrocarbons was greater than in week c. These results indicate that carbidic carbon decreased activity and increased the formation of gaseous hydrocarbons, whereas elemental carbon also increased the gaseous hydrocarbons, but did not influence activity greatly.

Perrin¹²² studied the effect of precarbiding Ni-Mn-Al₂O₃-kieselguhr catalysts in the synthesis with 2H₂ + 1CO gas at atmospheric pressure in a glass reaction tube. The heat transfer properties of this reactor appear to have been rather poor, since temperatures, in the catalyst bed at times exceeded those of the reactor by more than 40°C; this factor, however, does not invalidate the conclusions drawn from this work. After an initial

reduction at 450°C, the catalyst was either used directly in the synthesis or carburized, as shown in Table 34. The activities of these samples in the synthesis, as indicated by apparent contractions, are plotted as a function of time in Figure 17. The catalysts in tests L and M, which were carbided to sizable extents, were relatively inactive in the synthesis compared with corresponding reduced catalysts and produced no oil. After hydrogenation in test M, the activity was increased sizably. The slightly carbided sample in test N was as active as the corresponding reduced catalyst in the first hour, but the activity decreased rapidly to a value lower than that of the reduced preparation.

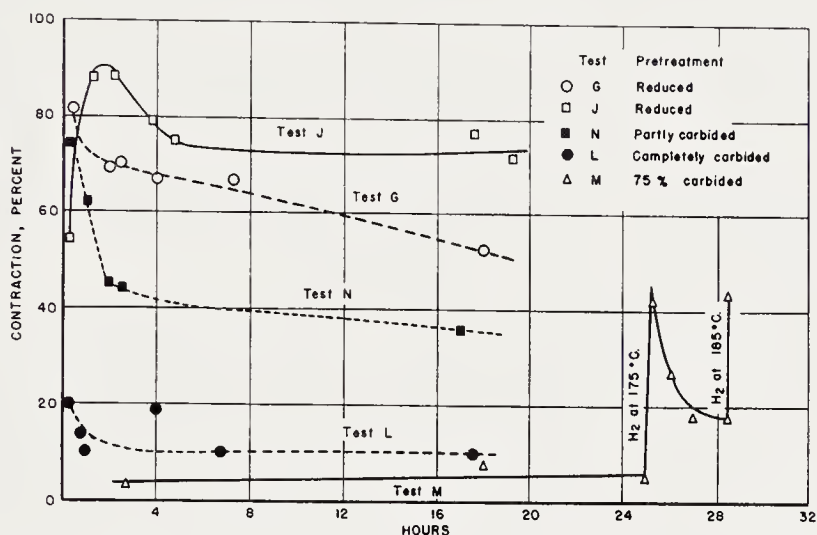


Figure 17. The effect of carbiding on activity of Ni-Mn-Al₂O₃-kieselguhr catalysts. (From data of Ref. 122)

The Course of the Synthesis on Precipitated Cobalt Catalysts and Methods of Reactivation

The behavior of standard precipitated cobalt catalysts in the synthesis at atmospheric pressure (normal pressure synthesis) and at 5 to 20 atmospheres (medium-pressure synthesis) is sufficiently distinctive to merit individual consideration. In the next few pages, several pertinent experiments illustrating the characteristics of the normal and medium-pressure syntheses will be described.

Atmospheric-pressure Synthesis. Roelen^{71, 157} at Ruhrchemie reported a comparison of two reduced Co:ThO₂:kieselguhr (100:18:200) catalysts in the atmospheric-pressure synthesis. Although the experiments were made to test two kieselguhrs as carriers (S. 11, a natural kieselguhr, and S. 120, a calcined variety), the data also illustrate some of the essential features of the normal-pressure synthesis. The flow of 2H₂ + 1CO gas was

maintained at 1 liter per gram of cobalt per hour and the temperature was varied as required between 185 and 195°C. Periodically, probably when the conversion fell below a desired value, the catalyst was activated by hydrogenation with $3\text{H}_2 + 1\text{N}_2$ gas at 5 to 7°C above the previous operating temperature. In the course of 160 days of synthesis, the catalysts were activated 8 times, the periods of synthesis between activations becoming shorter as the tests progressed, as shown by temporal plots of contraction

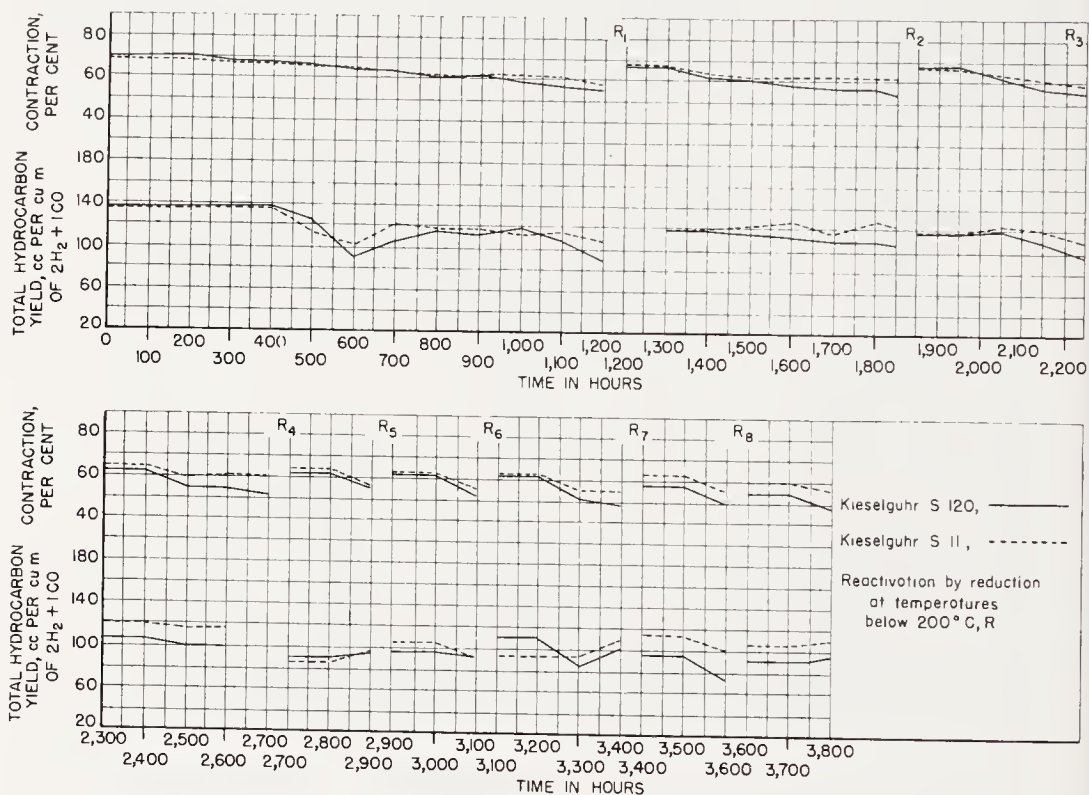


Figure 18. Effect of type of kieselguhr upon life and yields of cobalt catalysts, Ruhrchemie, 1938. (100 Co-18ThO₂-200 kieselguhr catalyst operated at atmospheric pressure of $2\text{H}_2 + 1\text{CO}$ and 185–195°C). (From Ref. 157)

and condensed hydrocarbon yields in Figure 18. In the first period (50 days), the two catalysts had essentially the same activity and selectivity, but thereafter the preparation with natural S. 11 was better than that with calcined S. 120.

The hydrogenation removed a sizable amount of wax from the catalyst, partly as such and partly as lower hydrocarbons, including large yields of methane, by hydrocracking of the adsorbed wax. This hydrogen treatment, however, removed only part of the organic material on the catalyst. Following the hydrogenation, extraction of the catalyst in benzene yielded a dark brown wax called "Restbeladung." This material melted at about

90°C and had the odor of oxygenated organic molecules. Data are not given to indicate if an appreciable amount of carbonaceous material remained after this extraction.

A study of the deposition of wax on these two catalysts was made. The catalysts were removed after the periods shown in Table 35. One portion was hydrogen-treated and then extracted in benzene to give, respectively, the weight of wax removable in hydrogen and the Restbeladung. The other portion was given only the hydrogen treatment and then returned to the synthesis. Thus, Restbeladung was an accumulation from the beginning of the experiment, while the wax removable in hydrogen was deposited in the last period of operation. The Restbeladung (Table 35) increased to about

TABLE 35. DEPOSITION OF WAX ON A $\text{Co}:\text{ThO}_2$:KIESELGUHR CATALYST DURING ATMOSPHERIC PRESSURE SYNTHESIS^a

Synthesis Period	Reactivation Temp. (°C)	Cumulative Time (days)	Catalyst Wax, g per 4 g Co					
			Kieselguhr S. 120			Kieselguhr S. 11		
			Remov-able in H_2	Rest-beladung	Total	Remov-able in H_2	Rest-beladung	Total
1	188	50	10.1	12.0	22.1	13.7	7.8	21.5
2	190	78	6.5	15.0	21.5	8.6	10.0	18.6
3	190	96	3.6	16.8	20.4	5.7	10.8	16.5
4	192	112	4.5	17.0	21.5	4.5	10.2	15.7
5	193	121	2.8	15.6	18.4	2.9	9.6	12.5
6	194	131	2.9	15.8	18.7	2.4	11.0	13.4
7	194	144	2.2	15.4	17.6	1.8	12.0	13.8
8	200	155	2.0	17.0	19.0	2.5	13.5	16.0

^a From Ref. 157.

constant values in the first 78 days of synthesis. The weights of wax removable in hydrogen, as well as the total wax, fluctuated rather widely. However, the weights of wax removable in hydrogen were approximately proportional to the length of the previous operating period. The rate of deposition of this type of wax varied from 0.2 to 0.3 gram of wax per day per 4 grams of cobalt. The higher Restbeladung values for preparations with calcined kieselguhr S. 120, compared with those with natural S. 11, were believed to be related to the greater activity of the catalyst with S. 11 in the last 100 days of synthesis.

Other Rurhchemie data⁷¹ describe the influence of promoters— ThO_2 , $\text{ThO}_2\text{-MgO}$, and MgO —on deposition of wax on precipitated cobalt catalysts, as shown in Table 36. Thoria favors deposition as well as production of heavy wax, whereas magnesia-promoted catalysts are virtually free of heavy wax (Restbeladung) in the synthesis.

In the synthesis, the catalyst can contain a remarkably great amount of wax without any great decrease in catalytic activity. According to Ruhr-chemie data an amount of catalyst corresponding at 4 gram of cobalt had a bulk volume of 44 cc. After 50 to 65 days of synthesis, thoria-promoted catalysts contained from 22 to 25 grams of wax, corresponding to a volume at room temperature of 24 to 28 cc. For a similar Bureau of Mines preparation (89 K-granules of Table 24), reduced catalyst containing 4 grams of cobalt had a bulk volume of 50 cc and a volume of pores with openings smaller than 5 microns of 30 cc. Although an accurate comparison between volume of wax and pore volume cannot be made, these data indicate that the catalyst pores must be nearly filled with wax after an extended period of operation.

TABLE 36. EFFECT OF PROMOTER ON WAX DEPOSITION^a
(100Co:200 kieselguhr at atmospheric pressure)

Synthesis Period	Cumulative Time (hr)	Catalyst Wax, g per 4 g Co								
		15ThO ₂			5ThO ₂ -10MgO			15MgO		
		Remov-able in H ₂	Rest-bela-dung	Total	Remov-able in H ₂	Restbela-dung	Total	Remov-able in H ₂	Restbela-dung	Total
1	1550	4.0	22.0	26.0	11.4	8.4	19.8	8.6	0.4	9.0
2	1850	6.0	20.6	26.6	7.0	5.6	12.6	2.0	.4	2.4
3	2250	3.6	21.6	25.2	5.6	6.0	11.6	1.8	.8	2.6

^a From Ref. 71.

Hall and Smith⁷⁶ made a detailed life test of a Co-ThO₂-MgO-kieselguhr (100:6:12:200) catalyst at atmospheric pressure. Granules (broken filter cake) of 7- to 14-mesh size were used at a space velocity 67 hr⁻¹ of 2H₂ + 1CO gas, corresponding to 1 liter per gram of Co per hour. 100 cc of catalyst weighed 26.6 grams and contained 6.7 grams of cobalt. The catalyst was reduced for 2 hours at 200°C in dry hydrogen at a space velocity of about 900 hr⁻¹. By suitable activations, the yields of condensed hydrocarbons were maintained above 100 g/m³ for about 400 days of synthesis. Figure 19 summarizes operating data for the entire test. The gaps in the curves denoted by "RR₁, RR₂, etc." represent re-reduction of the catalyst in hydrogen at 400°C under essentially the same conditions as the initial reductions. Gaps in only the temperature curves indicate an activation by hydrogen treatment at 195°C. After the initial reduction, the catalyst was operated briefly at 175 and 180°C, as shown in Figure 20, an expanded section of the previous graph, and then the temperature was maintained at 185°C. After about 19 days of synthesis, the contraction

and yields decreased sharply and the catalyst was reactivated by treatment with hydrogen for 6 hours at 195°C. This regeneration was followed by a period of about 18 days of high activity and productivity at 185°C, after which the conversion fell sharply, necessitating another hydrogenation at 195°C. Following this, high conversions were attainable at 185°C for 11 days, but after subsequent activations high conversions at 185°C were not

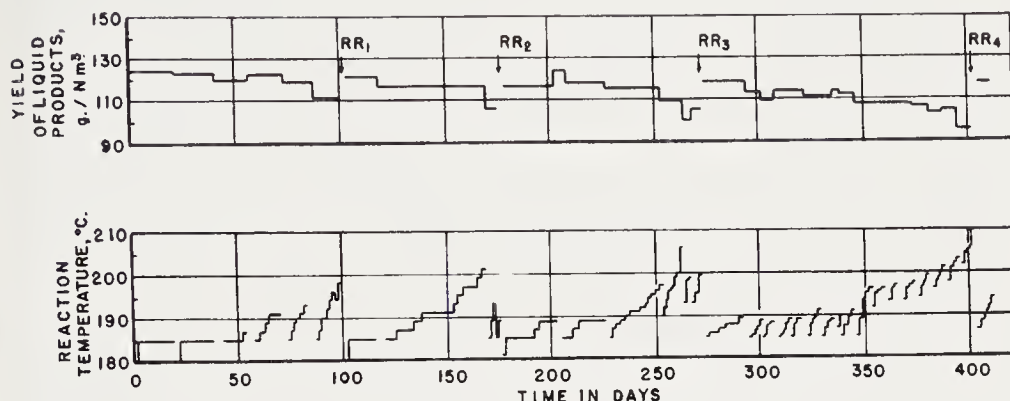


Figure 19. Durability test of 100Co-6ThO₂-3MgO-200 kieselguhr catalyst at atmospheric pressure of 2H₂ + 1CO gas (British Fuel Research Station). (Reproduced with permission from Ref. 76)

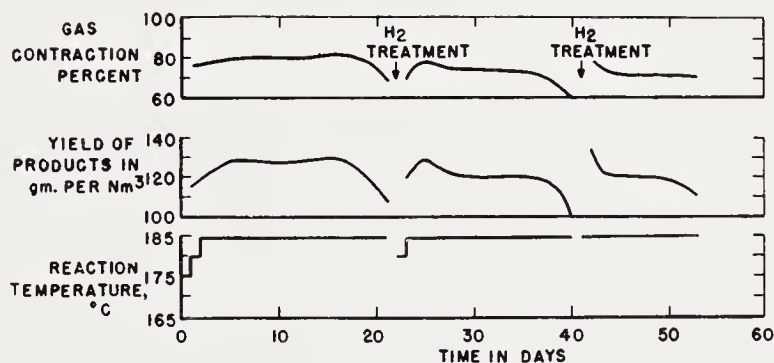


Figure 20. Synthesis data for first 50 days of test of Co-ThO₂-MgO-kieselguhr catalyst at atmospheric pressure. (Reproduced with permission from Ref. 76)

obtained for appreciable periods and the temperature had to be increased. Thus, as the experiment progressed, the effectiveness of the reactivation at 195°C decreased, and finally at 100 days, catalyst temperatures of 200°C were required to maintain the desired conversion.

At this time the catalyst was rereduced at 400°C in hydrogen at a space velocity of 6000 hr⁻¹ for 2 hours. The catalyst was restored to its initial activity and at 185°C yields of condensed hydrocarbons exceeding 120 g/m³ were obtained for 16 days. Following a low-temperature hydrogenation, a continuous period of operation of 50 days at high productivity was

obtained by increasing the temperature. After a second 195°C activation, the yields were low, and the second rereduction was made at a slightly higher temperature, 430°C. Again a substantial restoration of activity was observed and several 20-day periods of operation followed by hydrogen activations at 195°C were possible.

After a third rereduction at 425°C, the activity was lower and the decrease in activity with time was more rapid than after previous rereductions. At this point a series of 7-day operating periods followed by low-temperature activations were tried. Although the temperature had to be increased rapidly within each operating period, productivity was maintained high for about 100 days. Finally, when high yields were no longer attainable, a fourth rereduction, this time at 450°C, was made. This treatment was less effective than previous rereductions. Although the activity was still high enough for continued operation, the catalyst was extracted with a hydrocarbon fraction in the presence of carbon dioxide at 100 to 150°C. This treatment decreased the activity to a very low value, and attempts to reactivate the catalyst were unsuccessful. Upon removal from the reactor, the catalyst was still in a granular form and was mechanically robust. Chemical analysis indicated 0.2 per cent sulfur, 2.2 per cent carbon, and 28.9 per cent cobalt. The sulfur and carbon contents were probably too low to account for the low final activity.

Anderson, Hall, Krieg, and Seligman⁹ determined surface areas and helium and mercury densities of a pelleted Co:ThO₂:MgO:kieselguhr (100:6:12:200) catalyst after use in the synthesis at atmospheric pressure and after hydrogen treatments at 200 and 400°C. The catalyst was initially reduced in hydrogen at 400°C for 2 hours. In the synthesis, the catalyst was operated with 2H₂ + 1CO gas at an average temperature of 183°C for 11 periods of 5 days each, followed by a 2-hour treatment in hydrogen at 195°C and a 44-hour period in a slow flow of hydrogen at 150°C. Although the activity decreased somewhat during each period, the average activity of the periods was the same for all 11 weeks. The catalyst was removed in an inert atmosphere after 4 days of synthesis in the 12th week. Since, as shown in Table 37, about 90 per cent of the wax on the catalyst was removed by hydrogenation at 200°C, most of the wax on the catalyst was deposited during the last 4 days of synthesis. Data of adsorption and helium and mercury densities are given in Tables 37 and 38.

After use in the synthesis, the area of the catalyst was 4.4 m²/g compared with 80.0 m²/g, after the initial reduction. The hydrogen reactivation at 200°C for 2 hours decreased the weight by 23.5 per cent and increased the surface area to 70.5 m²/g. Further reduction at 200°C for 20 hours produced only a slight additional weight loss and a small increase in area. Rereduction at 400°C caused only a slight loss in weight, but the area in-

creased to nearly that of the original reduced catalyst. The ratio of the volume of chemisorbed carbon monoxide, V_{CO} , to the volume of physically adsorbed nitrogen corresponding to a monolayer, V_m , was increased from 0.13 to 0.21 by the hydrogen treatment. Since the catalyst as removed from the reactor chemisorbed carbon monoxide, it must be inferred that some cobalt atoms were accessible in spite of the large amount of wax on the catalyst.

The helium density of the used catalyst was 1.891 g/cc and after hydrogenation at 400°C, 3.007 g/cc, which is nearly equal to that of the original reduced catalyst. The mercury density decreased from 1.471 to 1.112 in the

TABLE 37. ADSORPTION DATA FOR REDUCED AND USED COBALT CATALYST 89FF^{a, b}
(All adsorption data per gram of unreduced catalyst)

Treatment	Cumulative Weight Loss (%) ^c	Surface Area (m ² /g)	V_m^d (cc/g)	V_{CO}^e (cc/g)	V_{CO}/V_m
a. Reduced 2 hr of H ₂ at 400°C, SVH = 6000 ^f	—	80.8	18.45	3.2	0.173
b. Used (a) plus 12 wks of synthesis	0.0	4.36	1.00	0.13	.130
c. (b) plus 2 hr of H ₂ at 200°C, SVH = 200	23.5	70.5	16.1	2.7	.168
d. (c) plus 20 hr of H ₂ at 200°C, SVH = 200	23.7	74.2	16.9	3.2	.189
e. (d) plus 2 hr of H ₂ at 400°C, SVH = 6000	25.3	79.1	18.1	3.8	.210

^a From Ref. 9.

^b Cobalt:thoria:magnesia:kieselguhr = 100:6:12:200.

^c Weight based on weight of used catalyst as removed from converter.

^d Volume of nitrogen corresponding to a physically adsorbed monolayer.

^e Volume of carbon monoxide chemisorbed at -195°C.

^f Space velocity per hour, volumes of gas (S.T.P.) per volume of catalyst per hour.

hydrogenation at 400°C, while the pore volume (volume of pores not penetrated by mercury, i.e., pores of smaller diameter than about 5 microns) increased from 0.201 to 0.566 g/cc of unreduced catalyst. After the hydrogenation at 400°C, the surface area, densities, and pore volumes of the used catalysts were nearly the same as those of the original reduced catalyst. Hence, there was no change in the pore geometry of the catalyst in 12 weeks of synthesis.

The volumes of mercury displaced by the used catalyst per unit weight of cobalt before and after hydrogenation at 400°C were identical, indicating that the adsorbed hydrocarbons were located in the pores not penetrated by mercury and not on the external surface of the pellet. At 30°C, 65 per cent of the pore volume of the used catalyst was filled with hydrocarbons. The density of the hydrocarbons removed from the pores, as calculated

from the changes in weight and in the volume of helium displaced, was 0.90, which compared favorably with the densities of soft and hard wax of 0.90 and 0.93, respectively, reported by Pichler for waxes from normal-pressure synthesis¹²⁴. The weight ratio of wax removed by hydrogenation at 200°C to cobalt was 1.01 and the ratio of total wax removed on hydrogenation to cobalt was 1.08. These ratios are considerably lower than those observed in Ruhrchemie experiments (ratios as high as 5), and the difference probably results from the smaller pore volume of the pelleted catalyst compared with the granular Ruhrchemie preparation. The pore volume of

TABLE 38. DENSITY AND PORE VOLUME DATA ON REDUCED AND USED COBALT CATALYST 89FF^{a, b}

Treatment	Cumulative Weight Loss ^c (%)	dHe (g/cc)	dHg (g/cc)	Pore Volume (cc/g)
a. Reduced 2 hr at H ₂ at 400°C, SVH ^d = 6000	—	3.031	1.138	0.549 ^e
b. Used (a) plus 12 weeks of synthesis	0.0	1.891	1.471	.151 ^f (0.201) ^e
c. (b) plus 2 hr at H ₂ at 200°C, SVH = 200	23.8	2.881	—	—
d. (c) plus 2 hr of H ₂ at 400°C, SVH = 6000	25.5	3.007	1.112	.566 ^e

^a From Ref. 9.

^b Cobalt:thoria:magnesia:kieselguhr = 100:6:12:200.

^c Weight based on weight of used catalyst as removed from converter.

^d Space velocity per hour, volumes of gas (S.T.P.) per volume of catalyst per hour.

^e Pore volume in cc per gram of reduced catalyst.

^f Pore volume in cc per gram of catalyst as removed from converter.

a typical reduced granular catalyst was about three times as great as that of a corresponding pelleted sample (Table 24).

Sastri and Srinivasan¹⁶³ observed that a large fraction of hydrocarbons adsorbed on a used cobalt catalyst could be removed by evacuation at 200°C, and this method was employed to dewax a used catalyst for adsorption studies at -187°C. The used and evacuated catalyst chemisorbed carbon monoxide in a manner similar to reduced cobalt surfaces, and it may be inferred that the active surface is in a reduced state and not present as carbide. These data are considered in detail in Chapter 3, p. 326.

In Ruhrchemie catalyst assaying⁷¹ the reduced samples were started in the synthesis at 185°C, presumably with the normal flow of synthesis gas. In the first 4 hours, all catalysts produced chiefly methane, but the methane production had usually diminished to the normal value in the next 32

hours. Catalysts that produced methane for longer periods were considered undesirable. Herington and Woodward⁸² also observed that initially most reduced catalysts produced chiefly methane when started directly at the desired synthesis temperature, but found that the methane production could be avoided by starting the catalyst at a low temperature, such as 150°C, and gradually raising the temperature to the desired value over a period of several days.

Similarly, in Bureau of Mines experiments in which the catalyst temperature was gradually increased to the desired operating value over a 1- or 2-day period, the initial formation of light hydrocarbons was not observed. Herington and Woodward⁸² postulated two types of active centers; the first, presumed to be cobalt carbide, was postulated to be responsible for production of higher hydrocarbons, while the second, assumed to be cobalt metal, produced gaseous hydrocarbons. The induction procedures involving gradual temperature increase apparently favored the formation of carbide sites. This explanation is probably incorrect, especially in view of the wealth of evidence that has accumulated to demonstrate that the carbide phase is neither an active catalyst nor an intermediate. Probably the best explanation is the following: The reduced catalyst is highly active and at synthesis temperatures hydrogenates most of the carbon monoxide all the way to methane and catalyzes the water-gas shift reaction. However, some wax is produced and sorbed on the catalyst and eventually decreases the accessibility of the catalyst sufficiently to diminish the activity to a moderate value. Induction at low temperature should favor wax production. The accumulation of wax on the catalyst as well as selective poisoning by carbon monoxide eventually changes the selectivity to favor the production of higher hydrocarbons.

In addition, the high initial activity may cause hot spots in the catalyst bed and very high conversions of synthesis gas, and the high initial yield of gaseous hydrocarbons may result from these factors. Thus, Craxford³⁵ observed that the production of condensed hydrocarbons (in g/m³) by a Co-ThO₂-MgO-kieselguhr catalyst at 185°C increased to a maximum and then decreased as the flow of synthesis gas was decreased, that is, as the conversion was increased. This observation was attributed to hydrocracking of higher hydrocarbons under conditions where most of the carbon monoxide was consumed.

The atmospheric-pressure synthesis with typical precipitated cobalt catalysts is characterized by a brief period of high activity, sometimes accompanied by formation of principally gaseous hydrocarbons, then a period of essentially constant activity, often extending for periods longer than 20 days, and finally a relatively rapid decline in activity. In the intermediate portion of constant activity and high productivity the catalyst contains

large quantities of wax. Although the wax content apparently increases with the time of synthesis, the activity in the intermediate interval is essentially constant. Hydrogenation of the used catalyst at 190 to 200°C removes only a portion of this wax, but in the early part of the synthesis the activity is restored to essentially its original value by this treatment. The effectiveness of the low-temperature hydrogenation decreases with time of testing. The residual organic material, Restbeladung, on the catalyst can be removed by solvent extraction or by hydrogenation at about 400°C. The latter method was not employed in the German industrial synthesis, since the reactors could not attain this temperature. Both treatments result in a sizable increase in activity, the rereduction procedure in the first 200 days of synthesis restoring the activity to its initial value.

Hence, the organic material on the catalyst may be divided into two groups based upon its ease of hydrogenation. Possibly the decrease in effectiveness of the low-temperature hydrogenation with time of synthesis is related to the accumulation of wax not removable under these conditions. Hall and Smith⁷⁶ have suggested that the accumulation of both types of wax is minimized by low-temperature hydrogenation at short, regular intervals, such as every 7 days, and they believed that optimum life and productivity may be attained in this way. Bureau of Mines tests⁹, in which the catalyst was treated with hydrogen at 195°C on every sixth day of synthesis, showed only very small quantities of wax that was not removable by the low-temperature hydrogenation. Craxford³⁵ suggested that the final rapid decrease in activity occurred when the pores of the catalyst were completely filled with wax. This may offer an explanation of why Co-ThO₂-MgO-kieselguhr catalysts are superior to the Co-ThO₂-kieselguhr catalyst, since the thorium-promoted catalyst deposited wax at a more rapid rate than ThO₂-MgO-promoted catalysts. Magnesia-promoted preparations deposit only small quantities of wax, and possibly the undesirable sensitivity of this preparation to temperature changes may be related to the absence of appreciable amounts of wax on the catalyst. It should be emphasized that other than this temperature sensitivity of the magnesia catalyst, there are no major differences in the activity of ThO₂, ThO₂-MgO, or MgO-promoted preparations in the first few weeks of synthesis; however, catalysts that produce smaller amounts of Restbeladung may have longer lives if the deleterious effects of overheating can be avoided.

As the final topic of this discussion, the synthesis schedule of the two-stage, normal-pressure commercial plant of Ruhrchemie at Sterkrade-Holten⁷¹ will be described. This operational procedure is typical of the atmospheric synthesis in Germany up to 1944. The fresh reduced catalyst was introduced into Stage II, where it was flushed with Stage II gas and then heated to 100 to 125°C without gas flow. After 5 hours at this tem-

perature, the gas flow was started at a rate of 250 m³ per hour. The temperature was increased 5°C per hour to 160°C and thereafter at 1°C per hour until a contraction of 60 per cent was attained. The gas rate was then increased to 500 m³/hr, causing the contraction to decrease to 40 per cent, the the temperature was increased 1°C per hour to increase the contraction to 45 per cent. Then the gas rate was further increased to 1,000 m³/hr and the temperature was increased 1°C per hour to restore the contraction to 45 per cent. At this point, the gas flow was increased to its final value, 1,400 m³ per hour, and the temperature increased 1°C per hour until the contraction attained 55 to 60 per cent. Thereafter, the contraction was maintained within this range by increasing the temperature. The gradual increase of both gas flow and temperature, as well as initial operation in Stage II, was designed to prevent overheating of the fresh catalyst.

TABLE 39. GAS COMPOSITION TWO-STAGE ATMOSPHERIC OPERATION, RUHRCHEMIE 1943-44^a

	Fresh Gas	Stage II Gas	Residual Gas
CO ₂	14.4	29.6	44.2
Gaseous hydrocarbons above CH ₄	0.0	1.5	2.0
CO	26.7	17.8	9.7
H ₂	53.2	33.7	16.0
CH ₄	0.4	7.0	13.2
N ₂	5.3	10.4	14.9

^a From Ref. 71.

When the reactor temperature had reached 190 to 191°C (after about 30 days), the catalyst was regenerated by solvent extraction of catalyst wax, which may be followed by hydrogenation. After 2 days in Stage II at 175°C, this reactor was transferred to Stage I with a flow of 1,000 to 1,200 m³/hr of fresh gas. The first regeneration in Stage I occurred when the temperature had increased to 192°C, and the synthesis was resumed on the activated catalyst at 180°C. Subsequent reactivations were made when the catalyst temperature reached 193, 195, 198, 200, and 203°C for the second to sixth regenerations, respectively. The period between activations was about 20 days. In the course of the synthesis in Stage I, the gas flow was decreased about 100 m³/hr per month to a final value of 800 m³/hr. Typical analytical data for the composition of fresh gas, Stage II gas, and the residual gas are given in Table 39.

In most German plants, solvent extraction was considered adequate for the first few reactivations, but later in the catalyst life extraction followed by hydrogenation at about 200°C was considered desirable. The useful life of catalysts in industrial plants was about 4 months; however, the life

could be extended to 6 or 8 months by more frequent activations. Although Ruhrchemie had investigated a procedure which was essentially the same as the rereduction studied by Hall and Smith⁷⁶ (p. 92), and which extended catalyst life to 12 to 14 months, this method was not used due to the shortage of hydrogen at Ruhrchemie and to the inability of the commercial synthesis reactors to be heated to 400 or 450°C. When the catalyst was removed from the reactor, it was considered desirable to return the spent catalyst to the catalyst preparation factory and start with a fresh preparation.

Medium-pressure Synthesis. In 1939 Fischer and Pichler⁵⁶ reported the discovery that the optimum-pressure range for normal Fischer-Tropsch

TABLE 40. PRODUCTS FROM SYNTHESIS AT DIFFERENT PRESSURES^a
(Average of 4-week tests with standard Co-ThO₂-kieselguhr catalysts)

Pressure (atm. gage)	Hydrocarbon Products (g/m ³)					
	Total Hydrocarbons	C ₁ -C ₄	Liquid plus Solids			
			Total	Gasoline <200°	Diesel Oil >200°	Wax
0	155	38	117	69	38	10
1.5	181	50	131	73	43	15
5	183	33	150	39	51	60
15	178	33	145	39	36	70
50	159	21	138	47	37	54
150	144	31	104	43	34	27

^a From Ref. 56.

catalysts was 5 to 20 atmospheres rather than atmospheric pressure. Since these pressures are intermediate between those of the usual atmospheric Fischer-Tropsch process (normal pressure synthesis) and the high-pressure syntheses of alcohols and synthol, the process at 5 to 20 atmospheres was termed the "medium-pressure synthesis." Previous studies^{50, 55} in this range of operating pressure, due to either the type of catalyst or mode of operation, had indicated that both the catalytic activity and life were inferior to the normal-pressure synthesis.

Fischer and Pichler determined the highest yields obtainable* from a standard precipitated cobalt-thoria kieselguhr catalyst at 0, 1.5, 5, 15, 50, and 150 atm. gage and a flow of 1 liter (S.T.P.) of 2H₂ + 1CO gas per gram of Co. The catalyst was operated for a brief period at atmospheric pressure and 185 to 190°C; then the temperature was decreased below the synthesis range, the pressure increased to the desired value, and the temperature increased to give the maximum yields of liquid and solid hydrocar-

bons. The products from 4-week tests are given in Table 40. The selectivity of the catalyst for production of total condensed hydrocarbons as well as wax increased to a maximum at 5 to 15 atmospheres and then decreased. In extended tests, the life of the catalyst was at a maximum in the same range of pressure, as shown in Figure 21. In the life tests, the temperature was varied to give the maximum yields of condensed hydrocarbons. At all pressures these maximum yields of total condensed hydrocarbons as well as wax decreased with time; however, at 5 and 15 atmospheres the initial

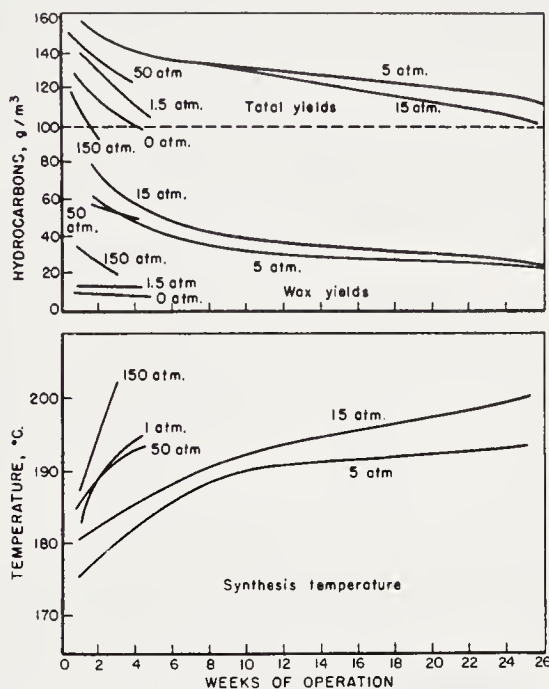


Figure 21. Effect of operating pressure on temperature and productivity of a Co-ThO₂-Kieselguhr catalyst. Temperature varied to maintain maximum yields of condensed hydrocarbons. (Reproduced from Ref. 56)

values were higher and their decrement with time was smaller. Similarly, in all experiments the temperature of operation had to be increased with time from initial values of 175 to 185°C; however, less rapid increases were required at 5 and 15 atmospheres. In this pressure range, yields of liquid plus solid hydrocarbons exceeding 100 g/m³ were possible for 26 weeks, whereas at atmospheric pressure and 150 atmospheres yields of 100 g/m³ were possible for only 4 and 2 weeks, respectively. The rapid decline in activity at pressures of 50 to 150 atmospheres was attributed to the removal of catalyst metal by carbonyl formation, and appreciable amounts of cobalt carbonyl were found in the reaction products. It was also suggested that the rapid diminution in activity may be related to the increased yields of oxygenated organic molecules at pressures from 50 to

150 atmospheres. In regard to carbonyl corrosion, the authors stated that synthesis in the medium-pressure range was not possible with precipitated nickel catalysts due to removal of nickel as carbonyl.

Medium-pressure tests of a variety of catalysts other than the standard cobalt-thoria-kieselguhr catalysts were described. As in the atmospheric synthesis, catalysts containing copper did not require the usual high temperature reduction; however, their activity decreased very rapidly with time compared with copper-free catalysts. Somewhat lower yields were obtained with preparation containing uranium oxide rather than thoria. Although thoria and alkali (e.g., K_2CO_3) were effective promoters for in-

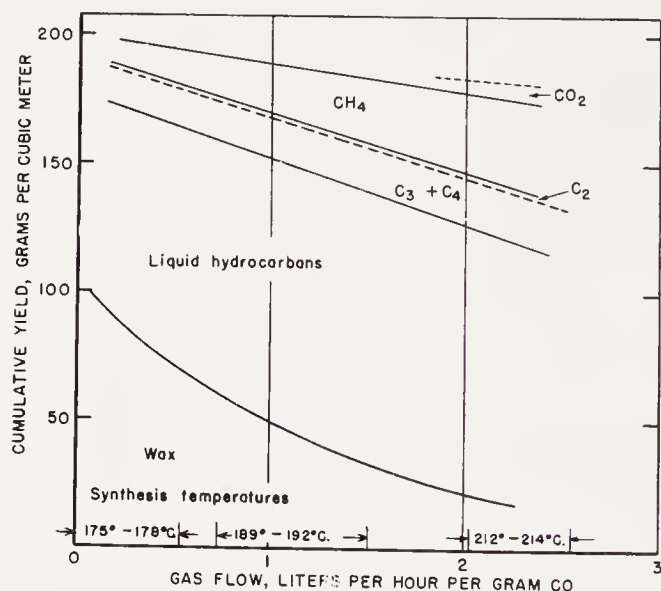


Figure 22. Selectivity of Co-ThO₂-kieselguhr catalyst as a function of flow. $2H_2 + 1 CO$ gas, 10 atm. in two-stage reactor. (From Ref. 57)

creasing the yield of wax in the atmospheric-pressure synthesis, the wax production was high with all cobalt catalysts in medium-pressure synthesis and the presence or amount of these promoters was not very important for wax production. A cobalt-kieselguhr catalyst gave high wax yields in the middle-pressure synthesis; however, its life was short. The presence of small amounts of thoria (2 to 6 per cent Th) prevented the rapid catalyst deterioration without any major effect on wax production.

In a later paper in 1939, Fischer and Pichler⁵⁷ attempted to approach the theoretical yield of hydrocarbons at 10 atmospheres of $2H_2 + 1CO$ gas on a standard Co-ThO₂-kieselguhr catalyst in a two-stage water cooled reactor (Figure 2). At low gas flows (0.25 l/g Co/hr) and low temperatures (177°C), 98 per cent of the carbon monoxide was consumed and the yield of C₃₊ was 185 g/m³, corresponding to an 89 per cent conversion of $H_2 +$

CO to usable hydrocarbons. These and additional data at higher flows and temperatures in Figure 22 illustrate that formation of higher hydrocarbons is favored by lower operating temperatures, although the production of total condensed hydrocarbons per unit time (space-time-yield) is increased by increasing the temperature and flow.

Although selectivity and life of cobalt Fischer-Tropsch catalysts were greatly improved by operation in the medium-pressure range, the conversion of $H_2 + CO$ was essentially independent of pressure. Data of Roelen¹⁴⁵ on a Co:ThO₂:MgO:kieselguhr catalyst at pressures from 0.2 to 7.0 atmospheres (gauge) in Table 41 illustrated the constancy of conversion as

TABLE 41. EFFECT OF OPERATING PRESSURE ON SYNTHESIS
WITH Co:ThO₂:MgO:KIESELGUHR CATALYST^a

Synthesis gas composition, per cent = 54 H₂, 28 CO, 14 CO₂

Pressure, absolute atm.	0.2	1.0	2.0	3.0	4.0	5.0	6.0	7.0
Duration, hr	6	3	11	11	11	18	7	8
Space velocity, hr ⁻¹	100	103	105	103	101	102	99	103
Temperature, °C	191	191	192	187	188	188	192	196
Contraction, (%)	60	56	59	58	60	59	59	59
Per cent of CO entering								
Total converted	77	70	74	73	76	74	73	74
To oil	60	51	56	59	61	62	59	57
To CH ₄ + gasol	17	19	18	12	13	12	13	14
To CO ₂	0	0	0	1.8	2.0	0.9	0.9	1.8
Condensed hydrocarbons, g/m ³ of 2H ₂ + CO	—	107	119	125	128	128	125	120
Usage ratio, H ₂ :CO	2.5	2.12	2.12	2.13	2.08	2.09	2.14	2.11

^a From Ref. 145.

the pressure was varied. Bureau of Mines data⁹ similarly demonstrate that the synthesis rate was independent of pressure. Pelleted catalysts produced more methane and gaseous hydrocarbons at 7.8 atmospheres than at 1 atmosphere.

Hall and Smith⁷⁵ made life tests of Co:ThO₂:MgO:kieselguhr (100:6:3:200) catalysts at 10 atmospheres and studied methods of regeneration. In most experiments, after the initial reduction, the catalyst was operated at atmospheric pressure for about 2 days. This procedure was desirable, since it decreased the risk of overheating and premature deterioration of the catalyst. In one test (8/3) after the initial period at atmospheric pressure, yields of condensed hydrocarbons of 130 g/m³ were obtained for 64 days. In the first 20 days, decreasing activity necessitated increasing the temperature from 182 to 189°C, while from 20 to 64 days an increase from 189 to 194°C was required, as shown in Figure 23. At 64 days the pro-

ductivity declined and the catalyst was hydrogenated at synthesis pressures and 200°C for 17 hours (treatment A). The catalyst activity was partially restored and for 24 days yields of condensed hydrocarbons from 125 to 130 g/m³ were attained. Reactivation B (also at 10 atmospheres) with high hydrogen flow for 2 hours at 194°C increased the activity somewhat, but high productivity was possible for only 6 days. The next activation, C, the same as A, did not increase the activity. The temperature was raised to increase the conversion, but this had an adverse effect on selectivity, with the yield of condensed products decreasing to 120 g/m³. In ensuing periods, the catalyst was treated with nitrogen at 220°C and 10

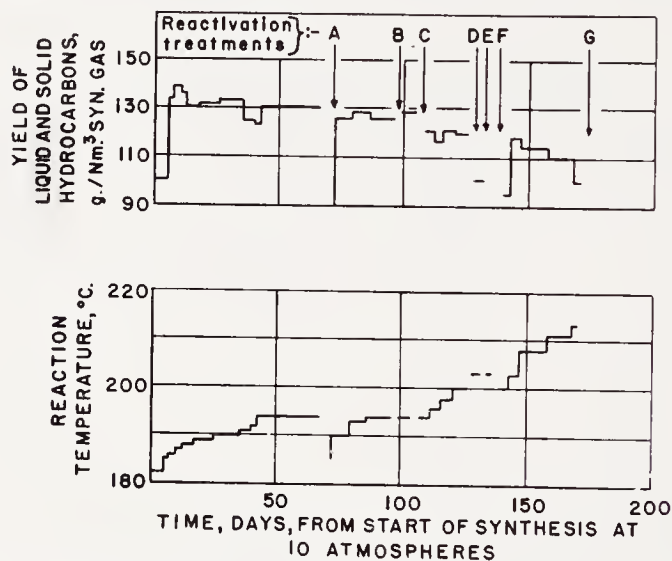


Figure 23. Durability test of 100Co-6ThO₂-3MgO-200 kieselguhr catalyst at 10 atmospheres pressure of 2H₂ + 1CO gas. (Reproduced with permission from Ref. 75)

atmospheres (treatment D) and then with hydrogen at 220°C and 10 atmospheres (treatment D). The activity after D and E was low and yields of 100 to 110 g/m³ were obtained at 203°C. Following this, the catalyst was hydrogenated at 10 atmospheres and 220°C followed by a rereduction in hydrogen at 400°C and atmospheric pressure for 2 hours (treatment F). After a brief synthesis period at atmospheric pressure in which the activity was quite low, the medium-pressure synthesis was resumed. The activity and yield were only slightly improved. In this synthesis period the activity decreased rapidly, necessitating increasing the temperature to 213°C in a period of 27 days of synthesis. Solvent treatment G removed a sizable amount of hard wax, but also caused a marked decrease in catalytic activity. An attempt to reactivate the catalyst by hydrogenation at 230 and 400°C was unsuccessful.

Further studies of reactivation by hydrogen were made in experiment

10 A/4 employing a similar but not identical catalyst to that used in test 8/3. The first 35 days of synthesis in test 10 A/4 were essentially the same as in 8/3. At this time, the flow of synthesis gas was reduced to half the normal rate (1 liter/g Co/hr). Although the yield per cubic meter of synthesis gas was equally high at this lower flow, the subsequent activity at the normal flow rate was sizably decreased. After two periods at low gas flow, the catalyst was considered to be sufficiently deactivated to be a useful subject for activation studies. The various activation procedures summarized in Table 42 had virtually no effect. The high-pressure hydro-

TABLE 42. HYDROGEN REACTIVATION OF Co-ThO₂-MgO-KIESELGUHR CATALYST IN SYNTHESIS AT 10 ATMOSPHERES^a

	Days of Synthesis before Treatment	Hydrogen treatment				Activity in synthesis ^b			
		Duration (hr)	Temp. (°C)	Flow (l/hr)	Pressure (atm. absolute)	Before treatment		After treatment	
						Temp (°C)	Contraction (%)	Temp. (°C)	Contraction (%)
J	74	8	205	14	31	195	57	195	63
K	78	16	205	14	1	195	63	195	57
L-M	85	16	205	14	1	195	57	197	60
		16	205	14	0.1				
N-O	90	16	207	14	1	197	60	201	64
		^c	150	^c	1				

^a From Ref. 75.

^b Flow of 2H₂ + 1CO gas of 1 liter per gram Co per hour.

^c Extraction with 500 cc of 150 to 200°C fraction.

genation J removed only 2 grams of hydrocarbon material from the catalyst, whereas atmospheric hydrogenation K removed more than 20 grams. Treatment L-M removed a total of 21 grams and the solvent treatment removed 5 grams of wax that remained after the hydrogenation at 1 atmosphere.

In other tests, it was shown that hydrogen treatment early in the life of a catalyst at 10 atmospheres was more effective than after a prolonged period of synthesis without activation. Although atmospheric hydrogenation removed more wax from the catalyst than in a similar treatment at 10 atmospheres, the pressure activation produced the greatest increase in activity. However, in all cases the effect of hydrogenation in the medium-pressure synthesis was less than in the atmospheric synthesis. Hall and Smith concluded that the maximum useful life of catalysts in the medium-

pressure synthesis was about 6 months compared with 18 months for the same catalysts in the atmospheric synthesis, due to the inability to reactivate catalysts used in the medium-pressure synthesis.

Hall and Smith⁷⁵ analyzed the waxes extracted from used cobalt catalysts after synthesis at atmospheric pressure and 10 atmospheres. These data demonstrate the unexpected fact that the average molecular weight of the catalyst wax in the atmospheric-pressure synthesis was greater than that of the wax of the medium-pressure synthesis. This situation apparently

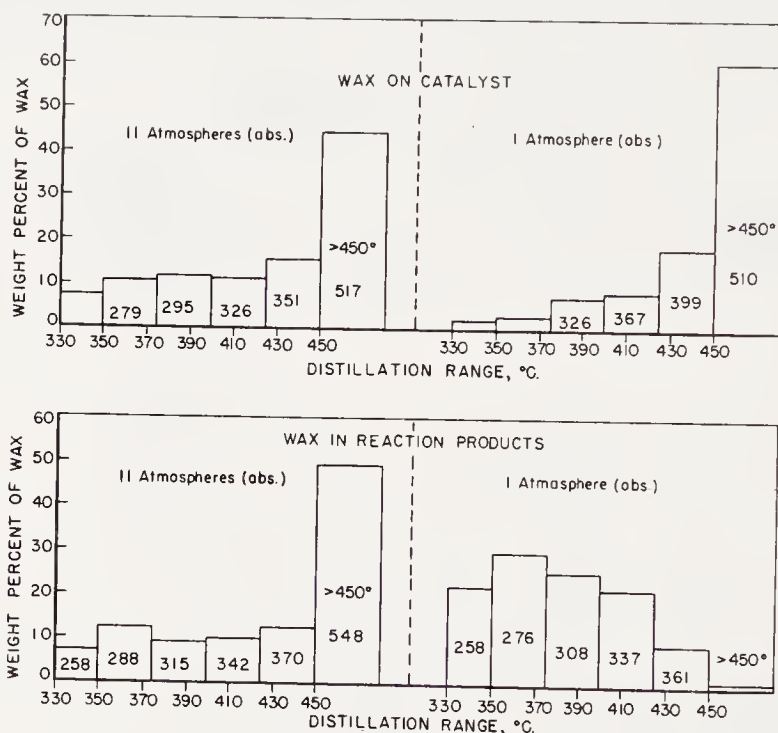


Figure 24. Comparison of catalyst wax with wax in synthesis products. Numbers in blocks are the average molecular weights. (From data of Ref. 75)

results from the fact that in the pressure synthesis a sizable fraction of the hydrocarbons are present as liquids which continually flow over the catalyst. On this basis the composition of the catalyst wax should be approximately the same as that of the wax in the reaction products, as is shown in Figure 24. In the atmospheric-pressure synthesis, however, due to the low operating pressure as well as to the lower average molecular weight of the products, most of the hydrocarbons pass over the catalyst as vapor and only the very high molecular weight waxes are adsorbed in sizable amounts.

Hall and Smith⁷⁵ stated that although the initial deterioration of cobalt catalysts at atmospheric pressure may not be due to the presence of wax, the rate of decline of catalytic activity can be closely correlated to the rate

of deposition of wax. Whatever the cause may be, the activity can be essentially restored by treatments (hydrogenation or solvent extraction) that remove wax. In the medium-pressure synthesis the catalyst is always saturated with wax, as shown by data of Roelen¹⁴⁸ in Table 43, and the

TABLE 43.—WAX CONTENT OF CATALYST IN THE MEDIUM-PRESSURE SYNTHESIS^a
(2H₂ + 1CO gas at 10 atmospheres)

Catalyst Composition	Hours of Synthesis	Temp. (°C)	Wax on Catalyst ^b (g/g Co + Ni)
100Co:13.5ThO ₂ :225 kieselguhr	353	175-185	6.4
90Co:10Ni:15ThO ₂ :200 kieselguhr	543	170-190	6.1

^a From Ref. 148.

^b Grams of wax per gram of Co + Ni. Wax extracted from catalyst with benzene.

TABLE 44. ALTERNATE OPERATION AT 1 AND 7.8 ATMOSPHERES OF PELLETED
Co-ThO₂-KIESELGUHR CATALYST 108B^a
(Operating periods 5-6 days, space velocity = 100/hr)

Operating Periods ^b	Pressure (atm.)	Average Temp. (°C)	Apparent Contraction (%)	Products (%)			
				CH ₄	C ₃ + C ₄	C ₁ - C ₄	Liquids and Solids
e	1	187	72	15	11	32	68
f	1	186	70	15	16	34	66
g	7.8	186	67	21	13	35	65
h	1	191	70	19	10	36	64
i	7.8	188	70	25	13	42	57
j	1	198	69	—	—	—	—
k	7.8	198	71	41	10	54	46
l	1	207	69	25 ^c	—	—	—

^a From Ref. 9.

^b A 2-hour hydrogen activation at 10° higher than the previous operating temperature preceded operating periods.

^c Approximate.

presence of wax can hardly be blamed for the eventual decline in activity. Similarly, removal of wax by solvent extraction or hydrogenation is in the medium synthesis largely ineffective in reactivating the catalyst. Hall and Smith suggest that unknown "complex bodies" are produced in the medium-pressure synthesis that cause a permanent poisoning of the active portions of the catalyst. Evidence for a permanent loss in catalytic activity is given by experiments in which the activity in the synthesis at atmospheric pres-

sure was found to be very low after the catalyst had been used in the synthesis at 10 atmospheres, even when the catalyst had been reduced in hydrogen at 400°C to remove catalyst wax after the 10 atmospheres synthesis. This effect is also shown by Bureau of Mines data⁹ (Table 44) from experiments in which the catalyst was activated with hydrogen at atmospheric pressure and about 200°C at the time the operating pressure was changed. In each case, the activity of the catalyst in atmospheric synthesis was considerably less than in the previous operation at 7.8 atmospheres.

In the medium-pressure commercial synthesis of Ruhrchemie⁷¹ three stages were employed. The reactor charged with fresh reduced catalyst was started in Stage III. The pressure was increased to desired pressure, 5 to 10 atmospheres, and the reactor heated to 125°C with no gas flow.

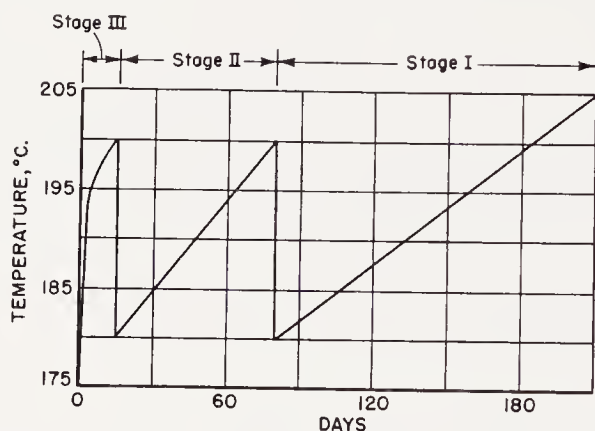


Figure 25. Method of conducting medium-pressure synthesis. (From Ref. 71)

Then at a flow of $500 \text{ m}^3/\text{hr}$ the temperature was increased 5°C per hour to 160°C , and above this at 1°C per hour until the contraction reached 45 per cent. The gas rate was then doubled and the temperature was increased 1°C per hour to restore the contraction to 45 per cent. Finally, the flow was increased to its normal value, $1,500 \text{ m}^3/\text{hr}$, and the temperature increased to give a contraction of 40 per cent. Figure 25 shows the course of a typical middle-pressure operation. The catalyst remained in Stage III for about 15 days and in Stage II for 70 days before being changed to Stage I. In the stage operation, the conditions were varied to maintain the same daily productivity per each reactor. The conversion of $\text{H}_2 + \text{CO}$ in stages I, II, and III was 63, 69, and 54 per cent, respectively. Since the usage ratio H_2/CO remained about 2 for all synthesis gas compositions normally employed, it was desirable to add hydrogen between stages when $1.5\text{H}_2 + 1\text{CO}$ gas was employed to increase the H_2/CO ratio of II and III stage gas to that of the fresh gas.

Products from the Synthesis on Cobalt Catalysts

The discussion of the selectivity of cobalt catalysts begins with a consideration of available detailed characterizations of synthesis products, the carbon number and isomer distributions of hydrocarbons and alcohols. Then the production of other oxygenated products, including water and carbon dioxide, is described, and finally the influence of catalyst composition and mode of operation.

Detailed Characterization of Hydrocarbons and Alcohols. The carbon number distribution curves of Martin^{111, 194} for hydrocarbons from the normal- and medium-pressure syntheses (Figure 26) demonstrate the characteristics of available data of this type. The yield of methane was

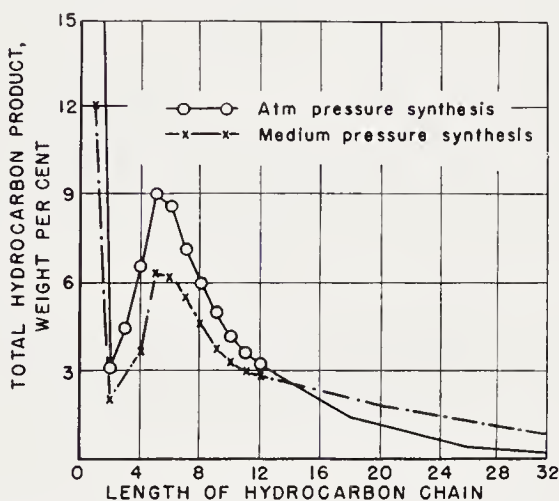


Figure 26. Distribution of hydrocarbon products from cobalt catalysts in the atmospheric and medium-pressure syntheses. (From Ref. 111)

high, followed by a low value at C_2 , then the yield increased with carbon number to a maximum in the range C_4 to C_8 , and finally decreased monotonically with increasing carbon number. The distribution curves for both the normal- and medium-pressure syntheses have the same characteristics; however, their relative positions reflect the higher average molecular weight of the medium-pressure products. Although these curves indicate the general trend in carbon number distribution, the accuracy of the experimental points cannot be judged, since no details are given regarding the method of separation (also there is no point for C_3 on the medium-pressure curve). The maximum at C_5 is sharper than observed by other workers.

Usually over a considerable range of carbon number, above C_2 or C_3 , $\Phi_{n+1}/\Phi_n = \alpha$ where Φ_n and Φ_{n+1} are, respectively, the number of moles in carbon numbers n and $n + 1$, and α is a constant less than unity⁶⁴. Thus,

the moles of carbon number n may be expressed in general terms as $\Phi_n = \Phi_1 \alpha^{n-1}$, and a plot of $\log \Phi_n$ against n should be linear. Available data plotted in Figure 27 approximate straight lines for normal- and medium-pressure data with standard granular catalysts at usual operating temperatures^{152, 197} as well as medium-pressure data for both alcohols and hydrocarbons obtained with standard granular catalysts under low temperature-low conversion operating conditions⁶⁶; the values of α were about 0.75. The only

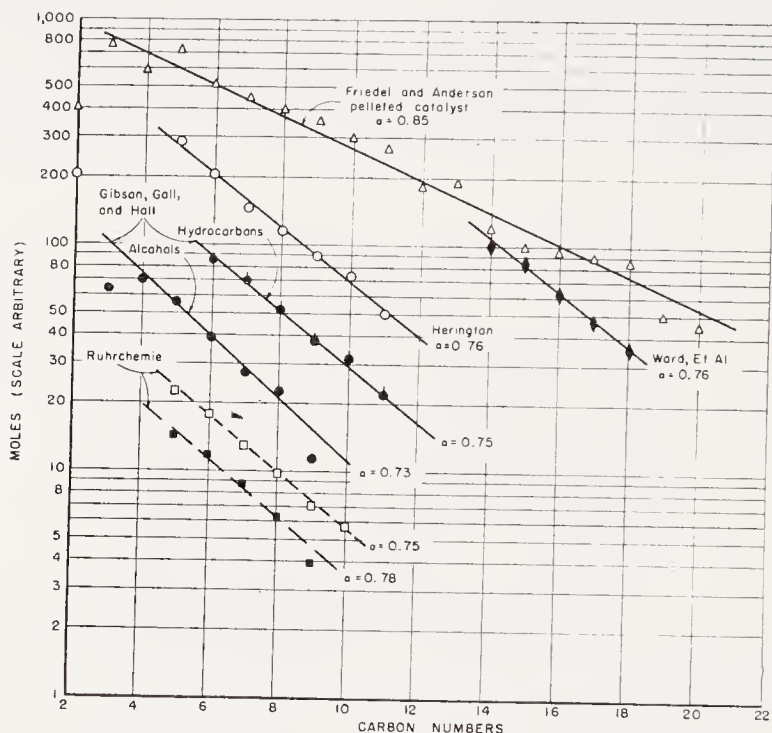


Figure 27. Semi-logarithmic carbon number distribution curves for hydrocarbons and alcohols from the normal (open symbols) and medium (solid symbols) pressure syntheses with cobalt catalysts. Data for hydrocarbons unless otherwise indicated.

exception was the plot for products from an atmospheric test of a pelleted catalyst with frequent hydrogen treatments⁶⁴ for which a value of α of 0.85 was found. The constant α should increase with the average molecular weight of the product, and it is not unexpected that the dense pelleted catalyst would yield a product of higher molecular weight than granular catalysts, since dense catalysts containing only 12.5 kieselguhr to 100 Co (Table 9) produced high yields of wax. For the data available, the values of α do not properly express differences in selectivity between the atmospheric and medium-pressure syntheses.

The olefin content of hydrocarbons from cobalt catalysts is essentially zero for C_2 and increases to a maximum for C_3 or C_4 and then decreases

monotonically with increasing carbon number. In Bureau of Mines tests⁶⁴ at atmospheric pressure, the percentages of olefin in gaseous hydrocarbons were C₂ 0, C₃ 39, C₄ 47, and C₅ 43. Data from products of tests with Co-ThO₂-

TABLE 45. OLEFIN CONTENT OF LIQUID PRODUCTS
(Co-ThO₂-kieselguhr catalysts at atmospheric pressure)

Boiling Range of Fraction (°C)	Part A ^a		Part B ^b	
	Carbon Number Range	Olefin Content (%)	Carbon Number	Olefin Content (%)
35-100	5-7	24.0	5	38.5
100-125	7-8	24.3	6	30.5
125-150	8-9	22.5	7	25.6
150-175	9-10	11.8	8	18.3
175-200	11	10.2	9	14.1
200-225	12-13	7.3	10	9.1
225-250	13-14	4.6	11	6.9
250-275	14-15	3.8		
275-305	16-18	4.0		

^a From Ref. 109.

^b From Ref. 81.

TABLE 46. GENERAL OLEFIN TYPES, C₆-C₈^a
(Cobalt catalyst at 1 atmosphere)

Fraction	Volume Per cent		
	α -olefins	Internal Double Bond Olefins	
		<i>trans</i>	<i>cis</i>
C ₆ ^b	36 \pm 2	39 \pm 3	25 \pm 3
C ₇	28 \pm 2	42 \pm 5	30 \pm 5
C ₈	18 \pm 2	52 \pm 5	30 \pm 5

^a From Ref. 64.

^b The equilibrium concentration of straight chain hexenes in mole per cent at 227°C is hexene-1, 4.7; *trans* hexenes, 64; and *cis* hexenes, 31.

kieselguhr catalysts in Table 45 indicate a decrease in olefin content as the carbon number increases. Table 46 presents data⁶⁴ for the position of the double bond in the C₆-C₈ olefin fractions. Internal double-bond olefins predominate; however, it should be noted that the percentages of α -olefins exceed those corresponding to thermodynamic equilibrium between the olefin isomers.

Molecules with straight carbon chains are the principal components of

Fischer-Tropsch products, and monomethyl isomers are present in small to moderate amounts. Considerably fewer molecules with dimethyl-substituted carbon chains are found. Detailed analyses of hydrocarbons through C_8 indicate that molecules containing ethyl-substituted carbon chains or chains containing quaternary carbon atoms are not present in appreciable amounts. By distillation methods, von Weber¹⁹⁵ estimated that the fractions of branched hydrocarbons in the C_6 , C_8 , and C_{10} ranges were 0.15, 0.27, and 0.40, respectively. Koch and Hilberath⁹⁷ showed the

TABLE 47. MASS SPECTROMETRIC ANALYSES OF PARAFFINS FROM COBALT CATALYST AT ATMOSPHERIC PRESSURE^a

Component	Composition (Vol. %)	Component	Composition (Vol. %)
<i>n</i> -Pentane	94.9	<i>n</i> -Octane	84.5
Isopentane	5.1	2-Methylpentane	3.9
		3-Methylpentane	7.2
<i>n</i> -Hexane	89.6	4-Methylpentane	4.4
2-Methylpentane	5.8	3-Ethylhexane	0.1
3-Methylpentane	4.6	2,3-Dimethylhexane	^b
2,2-Dimethylbutane	^b	2,4-Dimethylhexane	^b
2,3-Dimethylbutane	0.04	2,5-Dimethylhexane	^b
<i>n</i> -Heptane	87.7		
2-Methylhexane	4.6		
3-Methylhexane	7.7		
3-Ethylpentane	^b		
2,3-Dimethylpentane	^b		
2,4-Dimethylpentane	^b		

^a From Ref. 64.

^b Values computed actually very slightly negative, and hence may be regarded as zero.

presence of various monomethyl isomers in the C_5 - C_7 paraffins. Traces of more highly-branched paraffins were reported, but none containing quaternary carbon atoms was found. Friedel and Anderson⁶⁴ determined the isomer distribution of paraffin fractions in the range of C_5 - C_8 , as shown in Table 47. Although the fraction of branched hydrocarbons was lower than estimated by the previous work, the results were qualitatively similar. The fraction of branched isomers increased with increasing carbon number and monomethyl isomers were the only ones found in appreciable amounts.

Oxygenated organic molecules are produced in only trivial amounts (about 1 per cent) in the atmospheric-pressure synthesis with cobalt catalysts and in only slightly greater amounts in the medium-pressure synthesis. These statements apply to the usual range of operating tempera-

tures, 180 to 200°C, and moderately high conversions per pass. However, on a standard Co-ThO₂-MgO-kieselguhr catalyst, at low temperatures,

TABLE 48. DISTRIBUTION OF LIQUID PRODUCTS FROM COBALT CATALYSTS^a
(2H₂ + 1CO gas at 150 psig and 160 to 175°C)

Type of Compound	Weight-Per cent of Liquid Products Exclusive of Water	Weight-Per cent of Oxygenated Molecules
Alcohols	40.0	92.4
Acids	0.5 ^b	1.2 ^b
Esters	0.8 ^c	1.8 ^c
Carbonyl compounds	2.0	4.6
Hydrocarbons	56.7	—

^a From Ref. 66.

^b Calculated as acetic acid.

^c Calculated as ethyl acetate.

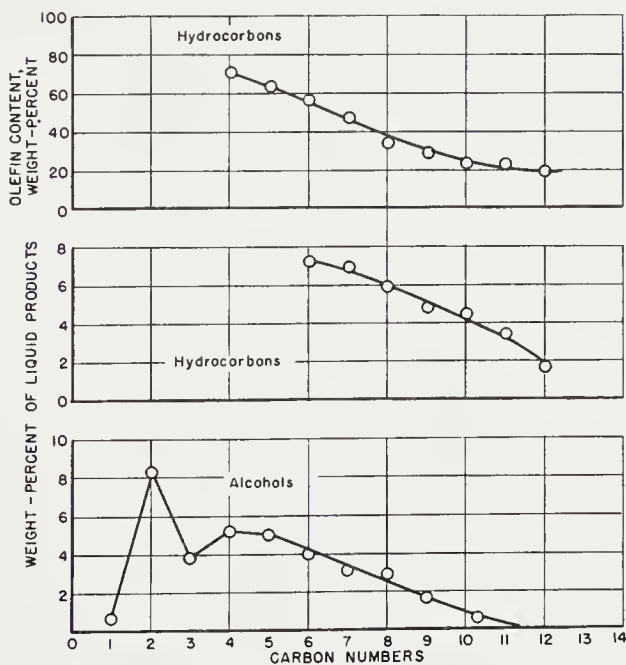


Figure 28. Distribution of product from medium pressure synthesis with Co-ThO₂-MgO-kieselguhr catalysts at low temperatures and low conversions. (From Ref. 66)

160 to 175°C, and low conversions, Gall, Gibson, and Hall⁶⁶ obtained high yields of oxygenates, as shown in Table 48. Alcohols comprised 92.4 per cent of the oxygenated organic molecules. Only primary straight-chain alcohols were identified in these products. The carbon number distributions of alcohols and liquid hydrocarbons are shown in Figure 28. The distribution of alcohols is different from that usually observed for hydrocarbons

showing a low value for C_1 , a maximum at C_2 , and a second maximum at C_4 followed by a monotonic decrease with increasing carbon number. Plots of these data in Figure 27 for both alcohols and hydrocarbons are linear except for the first and last points, and the values of the growth constant were about 0.75 for both components. The olefin content of the hydrocarbons (also shown in Figure 28) were considerably higher than those reported in Table 45, but they decreased with increasing carbon number in a similar manner.

With cobalt and nickel catalysts, water is the principal oxygenated product at usual operating temperatures, with the amount of carbon monoxide appearing as carbon dioxide being less than 1 per cent. Under conditions in which the conversion attains very high values, that is, low gas flow and/or high temperatures, sizable yields of carbon dioxide are obtained. In these experiments, most of the carbon dioxide is produced by a subsequent water-gas-shift reaction. The relative production of water and carbon dioxide will be considered in detail in Chapter 3.

Effect of Operating Pressure and Catalyst Composition on Selectivity of Cobalt Catalysts. With cobalt catalysts, more drastic changes in selectivity are usually produced by increasing the pressure from atmospheric to the medium-pressure range, 5 to 15 atmospheres, than by changing the amount or type of promoters or carriers; for this reason, it is desirable to examine the effect of operating pressure on selectivity before considering the effect of various additives. Data for the selectivity of Co-ThO₂-MgO-kieselguhr¹³¹ at 1 and 7 atmospheres in Figure 29 show that the average molecular weight of the products as well as the total yield are increased by increasing the operating pressure. The yield of wax ($>C_{18}$ fraction) was sizably increased and gasoline (C_5 - C_{11} fraction) and gaseous hydrocarbons were decreased, but the diesel oil fraction (C_{12} - C_{18}) remained virtually constant. The increased wax yield and the higher molecular weight of the wax in the medium-pressure synthesis are shown in Figures 29 and 24, respectively. The olefin content of the fractions was lower at 7 atmospheres than at 1 atmosphere. Research octane numbers for the gasoline fractions from the normal and medium-pressure syntheses were 52 and 28, respectively, the lower value for the medium-pressure gasoline apparently reflecting its lower olefin content. The diesel fuel fractions from both syntheses have cetane numbers of 100. Ward, Schwartz, and Adams¹⁹⁷ made a detailed characterization of a diesel oil fraction from the medium-pressure plant at Harnes, France. Cetane numbers increased from 60 for C_9 to values slightly in excess of 100 for C_{19} . Distillation and infrared analyses indicated that the product was predominantly paraffinic. Of the olefins present, 85 per cent was estimated to have internal double bonds.

In the atmospheric synthesis, the presence of a variety of promoters

increased average molecular weight of the products and the yield of wax. Of these, thoria and potassium carbonate were the most successful. However, the increase in average molecular weight produced by varying the amount or type of promoter was small compared with that observed by increasing the operating pressure to 5 to 15 atmospheres. The effectiveness of promoters in increasing the average molecular weight of medium-pressure-synthesis products was slight. For example, small additions of alkali had no significant effect on the selectivity of a Co-kieselguhr catalyst, as

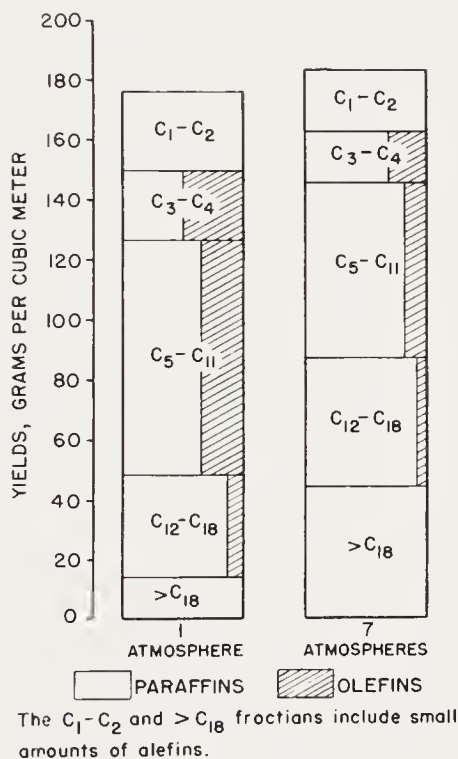


Figure 29. Typical yields with Co-ThO₂-MgO-kieselguhr catalyst at 1 atmosphere and 7 atmospheres. (Reproduced with permission from Ref. 131)

shown in Table 49. The data in this table also show that in the medium-pressure synthesis, high wax yields are obtained from essentially unpromoted catalysts.

The yield of wax in the medium-pressure synthesis under similar operating conditions varied inversely with the kieselguhr content, as shown in Table 16. In accord with these data, the "wax-producing catalysts" of Ruhrchemie contained only 12.5 parts of kieselguhr to 100Co (Table 9).

Apparently no detailed characterization data are available for products from nickel catalysts, but available information indicates the hydrocarbons from nickel catalysts have lower average molecular weights and are more saturated than those from cobalt catalysts, presumably due to the greater

hydrogenation ability of nickel. This tendency is also found in cobalt-nickel catalysts, the average molecular weight and the degree of unsaturation decreasing with increasing nickel content (Table 13).

Effect of Operational Variables on Selectivity. The influence of operating pressure on selectivity has been described previously. The average molecular weight of hydrocarbon products decreased with increasing temperature of operation, as shown in Table 50, and the fraction of gaseous

TABLE 49. EFFECT OF ALKALI CONTENT ON SELECTIVITY OF Co-KIESELGUHR CATALYSTS^a

(1 liter 2H₂ + 1CO gas per gram Co per hour at 12 atmospheres)

Parts K ₂ O per 100 Co	Temp. (°C)	CO Consumed (%)	CH ₄ in Off Gas (%)	Solid + Liquid Hydrocarbons (g/m ³)	Wax Content, % of Condensed Hydrocarbons	
					>320°C	>450°C
0.8	190	71	6.5	139	61	37
0.2	189	71	8.0	135	67	40
0.4	182	67	5.6	130	60	34
0.1	188	73	8.8	137	61	37
0.1	180	75	9.5	133	58	29

^a From Ref. 165.

TABLE 50. EFFECT OF TEMPERATURE ON SELECTIVITY OF Co-MgO-KIESELGUHR CATALYSTS^a

(2.5H₂ + 1CO gas at atmospheric pressure, space velocity = 125 hr⁻¹)

Temp. of Operation (°C)	Condensed Hydrocarbons (%)		
	35 to 200°C	200 to 320°C	>320°C
185-191	46.4	35.6	18
170	29.5	33.2	37.3

^a From Ref. 109.

hydrocarbons increased. Data for the medium-pressure synthesis with Co-kieselguhr catalysts using 2H₂ + 1CO gas (Table 51) indicates that the paraffin yield decreased when the temperature was increased from 170 to 180°C. Further, in the range 160 to 180°C the percentage of olefins in the distillation fractions either remained constant or decreased, while the percentages of alcohols decreased with temperature. When 1H₂ + 1CO gas was used, the percentage of olefins increased, whereas the percentage of alcohols decreased with increasing temperature in the range 175 to 195°C. That greater alcohol yields are obtainable at lower operating temperatures was also shown by data in Table 48.

The effect of hydrogen to carbon monoxide ratio on products from cobalt catalysts is shown in Table 51, where the yields of both olefins and alcohols were greater for $1\text{H}_2 + 1\text{CO}$ gas than for $2\text{H}_2 + 1\text{CO}$. Data in

TABLE 51. PRODUCTS FROM COBALT-KIESELGUHR CATALYSTS IN THE MEDIUM-PRESSURE SYNTHESIS^a

Temp. (°C)	Contraction (%)	CO Con- version (%)	Yields (g/m ³)	Per cent Paraffins (>320°C)	Composition of Boiling Ranges					
					195-250°C		250-320°C		320-450°C	
					Olefins	Alcohols	Olefins	Alcohols	Olefins	Alcohols
					(%)					
<i>2H₂ + 1CO gas</i>										
160	55	50	97	53	12	15	9	—	9	25
170	—	56	93	69	10	10	6	9	3	5
180	72	71	138	58	10	8	3	3	3	3
<i>1H₂ + 1CO gas</i>										
170	47	38	71	49	29	27	19	21	17	17
175	50	49	96	58	33	29	19	23	14	17
195	62	62	115	54	38	19	23	8	16	8

^a From Ref. 165.

TABLE 52. EFFECT OF H₂:CO RATIO ON PRODUCTS FROM COBALT CATALYSTS^a
(Atmospheric pressure, space velocity = 125 hr⁻¹, temperature = 190 – 192°C)

Synthesis Gas	Condensed hydrocarbons				
	35-200°C		200-320°C		>320°C Weight (%)
	Weight (%)	Bromine Number	Weight (%)	Bromine Number	
1.2H ₂ + 1CO	30.4	72	22.6	33	47
2.5H ₂ + 1CO	51.0	34	37.0	10	12

^a From Ref. 109.

Table 52 indicate that olefin content and the average molecular weight increased when $1.2\text{H}_2 + 1\text{CO}$ gas was used instead of $2.5\text{H}_2 + 1\text{CO}$. This effect is also shown for Co-Ni catalysts in Table 53.

There is evidence to indicate that the olefin content is greater when cobalt and nickel catalysts are operated at conditions of high flow and/or low conversions. For cobalt-nickel catalysts the unsaturation of liquid hy-

drocarbons increased with increasing flow or decreasing conversion¹¹⁶. The same trend was observed with cobalt catalysts at the Bureau of Mines¹¹. This effect is most significant with $2\text{H}_2 + 1\text{CO}$ gas. With other feed compositions the average ratio of $\text{H}_2:\text{CO}$ varies widely with conversion, and the selectivity is more strongly dependent upon average $\text{H}_2:\text{CO}$ ratio than on conversion or flow.

In Ruhrchemie recycle experiments on cobalt catalysts at 7.5 atmospheres of $1\text{H}_2 + 1\text{CO}$ gas, the olefin content increased with increasing recycle ratio. However, Pichler¹³¹ has demonstrated that the increase in

TABLE 53. EFFECT OF $\text{H}_2:\text{CO}$ RATIO OF SELECTIVITY OF Co-Ni CATALYSTS^a
(Co:Ni:ThO₂:Mn:kieselguhr = 50:50:15:2:200)
(Pressure = 10 atm., temperature = 193°C)

Gas composition	$2\text{H}_2 + 1\text{CO}$	$1\text{H}_2 + 1\text{CO}$
Contraction, %	49	39
Carbon monoxide consumed, (%)	64	38
Carbon monoxide to CH_4 , (%)	30	12
Usage ratio, H_2/CO	2.16	1.84
Yields, g/m ³		
Gasol	10	5
Condensed hydrocarbons	75	55
Distillation data, wt-%		
< 200°C	72	70
200°-320°C	24	24
> 320°C	4	6
Olefins, vol%		
< 200°C	22	53
200°-320°C	11	36
Octane number, < 200°C	31	56

^a From Ref. 153.

unsaturation can be entirely explained on the basis of the $\text{H}_2:\text{CO}$ ratio of the gas entering the catalyst bed (Figure 30). Due to higher over-all conversion and a slightly higher usage ratio under recycle conditions, the $\text{H}_2:\text{CO}$ ratio of the gas entering the catalyst bed was considerably lower than that of the fresh feed. When the flow of synthesis gas is decreased to very low values (or when the conversion is very nearly complete), two side reactions become important^{35, 116}. First, water produced in the synthesis reacts with carbon monoxide by the water-gas reaction, producing large amounts of carbon dioxide and hydrogen. Second, hydrocracking of higher hydrocarbons occurs, causing a decrease in the yield of oil per cubic meter and an increase in methane. Under these conditions chiefly saturated higher hydrocarbons are produced¹¹⁶.

IRON CATALYSTS

In general the synthesis on iron catalysts is more complicated than on cobalt or nickel. With cobalt and nickel catalysts, there is little tendency for oxidation or carburization of the reduced metal or deposition of elemental carbon, whereas these reactions occur to varying degrees with all iron catalysts, and result in some cases in loss of activity and/or disintegration of the catalyst. However, the availability and low cost of iron, the wide range of selectivity and operating conditions, and the general desirability of the synthesis products have provoked abundant research on iron catalysts, especially since the discovery of the medium-pressure syn-

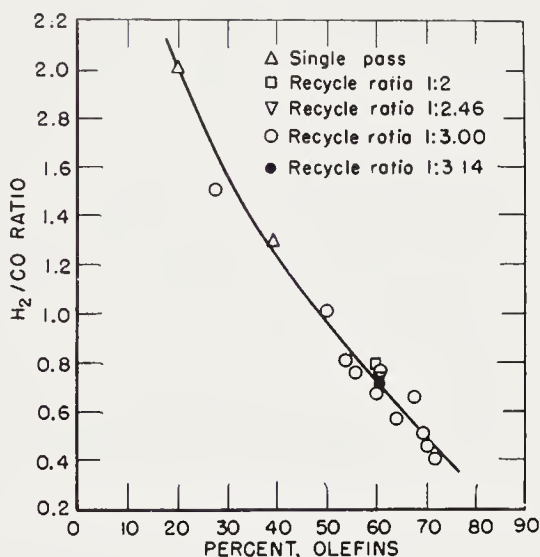


Figure 30. Influence of H_2 -CO ratio on olefin content of synthetic hydrocarbons. (Reproduced with permission from Ref. 131)

thesis on iron by Fischer and Pichler in 1937¹³¹. Before this time, iron catalysts had been tested at atmospheric pressure but the results were without exception poor. Data for the preparation and testing of various types of iron catalysts, precipitated, fused, sintered, etc., will be considered here, followed by a discussion of surface areas and pore volumes of iron catalysts. Then the methods of pretreatment, the changes in catalysts during synthesis, and finally the selectivity of iron catalysts will be considered.

Precipitated Iron Catalysts

In most precipitated iron catalysts, the iron is present initially as ferric oxide or magnetite gels. Due to the complex colloid chemistry involved, elaborate methods of preparation were developed. Although in many cases these procedures seem very complicated, they were usually the result of

laborious empirical research and represent practical ways of attaining the desired gel structure and obtaining precipitates that can be filtered and washed free of foreign ions without undue effort. However, the cost of preparing precipitated catalysts by any of the procedures is relatively high.

Solutions of ferric nitrate or mixtures of ferric and ferrous nitrate were used in the preparation of most precipitated iron catalysts. Pichler¹²⁵ used ferric nitrate prepared by dissolving iron in small portions in nitric acid of an initial density of 1.18 at temperatures below 40 to 50°C. Solutions containing ferrous nitrate were made by the action of more dilute nitric acid (maximum density = 1.05) on iron shavings. In the preparation of Pichler's standard catalysts of about 1940, an iron nitrate solution containing 1 kg of iron per 30 liters was used. The solution was preneutralized at room temperature with an amount of sodium carbonate solution just insufficient to produce a permanent precipitate. The solution was heated to 100°C in the case of ferric nitrate and 70 to 75°C for ferrous nitrate, and the precipitation was accomplished with hot sodium carbonate solution. Then the mixture was heated to boiling and maintained at this temperature for a few minutes, filtered, and washed free of alkali with hot distilled water. The moist precipitate was repulped in distilled water, and the desired amount of alkali (usually as potassium carbonate solution) was added. The mixture was evaporated on a water bath and the solid was dried overnight at 110°C. Catalysts from ferric nitrate were dense, brownish-black with a glassy fracture, whereas preparations from ferrous nitrate were voluminous and earthen-brown in color.

Early Fe-Cu-Al₂O₃-K₂CO₃ catalysts of Scheuermann¹⁶⁵ at I.G. Farbenindustrie were made by a slow precipitation extending for 48 hours. For similar catalysts containing magnesia rather than alumina, the precipitation could be accomplished rapidly. A solution of the metal nitrates and the alkali carbonate solution were introduced by a mixing nozzle with the pH maintained constant. If desired, the precipitate was mixed with an aqueous slurry of kieselguhr or silica gel and then heated for about 10 minutes. The precipitate settled rapidly and was easy to wash. Lurgi Fe-Cu-Al₂O₃-SiO₂-K₂CO₃ catalysts⁷¹ were precipitated from a hot aqueous solution of metal nitrates with sodium carbonate, and freshly prepared silica gel was stirred into the precipitate. The precipitate was filtered, washed, and impregnated with the desired amount of potassium carbonate. In the pretreatment of Rheinpreussen Fe-Cu-dolomite-K₂CO₃ catalysts⁷¹, powdered dolomite was added to boiling solution of iron and copper nitrates and the precipitation was accomplished with a boiling sodium carbonate solution. After being filtered and washed, the wet precipitate was impregnated with an aqueous potassium carbonate solution. Ruhrchemie Fe-Cu-CaO-kieselguhr-K₂O catalysts^{71, 72} were prepared from a solution of iron, calcium, and copper nitrates by precipitation with hot sodium car-

bonate solution. The amount of sodium carbonate was chosen so that after precipitation the pH was 6.8–7.0. Kieselguhr was stirred into the precipitate, which was then filtered and washed with hot water until the sodium nitrate content was reduced to 0.5–0.7 parts per 100Fe. The desired amount of alkali promoter, KOH, K_2CO_3 , or K_2SiO_3 , was impregnated into the wet filter cake by repulping in a kneading machine and then filtering. The filter cake was dried at 110°C, crushed, and screened to 2 to 3 mm particles. One of the most active KWI catalysts¹³¹, Fe-Cu- K_2CO_3 , was prepared from a mixture of ferrous and ferric chloride. A solution, in which 75 per cent of the iron was present as ferrous chloride and 25 per cent as ferric chloride together with cupric chloride, was heated to 70°C, and precipitation was accomplished by adding a boiling sodium carbonate solution as rapidly as possible. The precipitate was washed free of salts and alkalized with potassium carbonate solution. The mixture was evaporated, dried at 105°C, and granulated.

This account of methods of preparing precipitated iron catalysts is very brief, but it illustrates many factors that were considered essential. A few of the more important generalizations follow:

1. Usually dilute aqueous solutions, less than 10 per cent by weight, were used.

2. For starting materials, iron salts can be used; however, solutions containing ferrous nitrate must be obtained by careful dissolution of iron in dilute nitric acid. Sodium carbonate was usually used as a precipitating agent. Potassium carbonate would be equally effective, but was too expensive.

3. Precipitation was usually accomplished using hot or boiling solutions with rapid addition of the sodium carbonate solution to the solution of iron salts, with efficient stirring. The use of hot solutions usually resulted in dense, easily filterable precipitates.

4. Kieselguhr or other carriers, if employed, were mixed with the wet precipitate. The presence of kieselguhr usually facilitated filtration and was considered desirable by some laboratories, if for only this purpose.

5. Violent agitation of the wet precipitate, as well as extrusion through dies, was considered by some workers to be deleterious to the gel structure of the catalyst.

6. Although many precipitated catalysts are very hard in the raw state, most of their mechanical strength is usually lost during pretreatment.

7. Catalysts prepared from iron sulfates usually had poor activity, apparently due to residual sulfate ion on the resulting catalyst¹⁸⁰. Active iron catalysts can be prepared from ferrous chloride or mixtures of ferrous and ferric chlorides, but not from ferric chloride⁸³. This topic will be more fully considered later.

For catalysts from ferric nitrate, Pichler¹²³ found that a brief period of

boiling immediately after precipitation was desirable regardless of the temperature of precipitation. Possibly the nature of the iron oxide gel after boiling is such that impurities can be readily removed by washing. For supported catalysts, the order of addition of kieselguhr was critical. KWI data in Figure 31 demonstrate that the catalyst prepared by the addition of kieselguhr after precipitation and alkalization was superior to addition of kieselguhr to either of the precipitating solutions. As in the preparation of the cobalt catalysts, it appears desirable to keep the contact between kieselguhr and solutions as brief as possible.

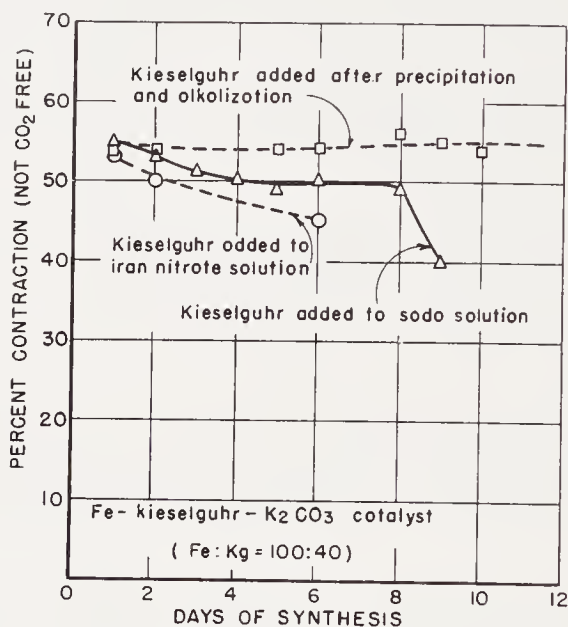


Figure 31. Effect of order addition of kieselguhr in preparation of iron catalysts. $1\text{H}_2 + 1.5\text{CO}$ gas at 15 atm. and 235°C . (From Ref. 123)

The activities of catalysts from iron chlorides and nitrates are summarized:

ACTIVITY IN MEDIUM-PRESSURE SYNTHESIS

	Nitrate	Chloride
Fe^{++}	Moderate	Moderate
$\text{Fe}^{++}, \text{Fe}^{+++}$	High	High
Fe^{+++}	High	Very low

Catalysts prepared from ferrous chloride or nitrate had moderate and approximately equal activities¹²⁵, but to maintain high conversions for long periods, the temperature had to be increased to at least 260°C . The ferri-ferrous chloride preparations of Pichler and Weinrotter¹³¹, $\text{Fe}^{+2}:\text{Fe}^{+3}:\text{Cu}:\text{K}_2\text{CO}_3 = 75:25:20:1$ or $50:50:1:0.25$, were excellent catalysts maintaining high conversion and desirable selectivity at 200°C at 10 atmospheres.

On the other hand, at the Bureau of Mines repeated attempts to prepare active catalysts from ferric chloride solutions were unsuccessful¹⁸¹, whereas similar catalysts from ferric nitrate were moderately active.

A systematic study of chloride catalysts^{83, 86} led to the data in Table 54. Here again catalysts prepared from ferric chloride were inactive, whether promoted with copper or not. For these inactive preparations, the usage ratios, H_2/CO , were high compared with those for the active catalysts. X-ray diffraction and chemical analyses of the catalysts resulted in the data in Table 55. Raw catalysts prepared from ferric chloride gave the x-ray diffraction pattern of $\beta\text{-Fe}_2\text{O}_3 \cdot 3\text{H}_2\text{O}$, whereas catalysts from ferrous chloride or ferrous-ferric chloride gave patterns of Fe_3O_4 . It is difficult to attribute the large differences in activity to the presence of different phases in the raw catalyst, since all catalysts were reduced at least to magnetite in the induction. Chemical analyses revealed that the catalysts containing $\beta\text{-Fe}_2\text{O}_3 \cdot \text{H}_2\text{O}$ in the raw state had a considerably greater amount of residual chloride ion than samples containing magnetite. This behavior is consistent with published data^{104, 199} that the $\beta\text{-Fe}_2\text{O}_3 \cdot \text{H}_2\text{O}$ phase tenaciously retains chloride ions, so that it is virtually impossible to remove them by washing. The chloride content of the catalyst was retained during the induction procedure, and the surface areas after induction were essentially the same for both the active and inactive catalysts. These data suggest that the inactivity of catalysts prepared from ferric chloride solutions results from poisoning by residual chloride ion. The high values of the usage ratio observed for the inactive catalysts must result at least in part from this poisoning effect.

Raw catalysts from ferric nitrate contain $\alpha\text{-Fe}_2\text{O}_3$ and/or $\alpha\text{-Fe}_2\text{O}_3 \cdot \text{H}_2\text{O}$, and these preparations had high activities. Catalysts precipitated at 70°C or higher usually had the following physical characteristics:

Iron Solution	Appearance	Mechanical Strength
Ferric nitrate or chloride	Black, glassy gel	Hard
Ferric-ferrous nitrates or chlorides	Dull brown	Moderate
Ferrous nitrate or chloride	Dull brown	Soft

The mechanical strength of all of these preparations decreased considerably upon induction and use in the synthesis. At the Bureau of Mines the preparations from ferrous chloride disintegrated to such an extent that operation in small vertical fixed-bed laboratory reactors was terminated after about one week due to plugging of the catalyst tube. Although long periods of synthesis were possible with the other catalysts, it is questionable whether they would have sufficient mechanical strength for use in commercial-scale, fixed-bed units unless special precautions are taken.

Promoters. *Alkali.* Pichler¹²³ observed that the activity of iron oxide catalysts precipitated from iron nitrate solutions was independent of the

TABLE 54. SYNTHESIS TESTS OF CATALYSTS PREPARED FROM IRON NITRATE AND CHLORIDE SOLUTIONS^a
(1H₂ + 1CO gas at 7.8 atm. Induction in 1H₂ + 1CO gas at atm. pressure for 24-25 hr)

Catalyst Number	2001	2002	2003	3008	3008	3006	3004	3003.24
Catalyst composition								
Fe ²⁺	100 ^b	0	0	100	100	0	75	0
Fe ³⁺	0	100	100	0	0	100	25	100
Cu	0	0	0	20	20	20	20	10
K ₂ CO ₃	0.2	0.2	0.2	0.2	0.2	0.2	0.2	0.5
Source of iron	Nitrate	Nitrate	Chloride	Chloride	Chloride	Chloride	Chloride	Nitrate
Induction temperature, °C	260	260	260	224	225	227	226	230
Synthesis temperature, °C	238	244	263	222 ^c	227 ^c	282	229	221
Contraction, % ^d	64	63	28	65	66	37	66	65
Space velocity, hr ⁻¹	91	103	97	86	74	100	100	100
Usage ratio, H ₂ /CO	0.74	0.75	1.44	0.63	0.68	1.51	0.65	0.57
Activity ^e	100	69	15	243	181	11	159	131
Products, g/m ³								
CH ₄	13	11	8	8	—	9	8	5
C ₂	11	9	3	5	—	13	7	5
C ₃ + C ₄	28	24	22	12	—	16	33	9
Liquids + solids	74	55	16	76	67	13	88	103

^a From Ref. 83.

^b Prepared by dissolving iron in dilute nitric acid at low temperatures.

^c These tests terminated after about 7 days due to catalyst disintegration resulting in plugging of the reactor.

^d CO₂-free.

^e Activity defined as cc of synthesis gas reacted per hour per gram of iron at 240°C.

alkali content, as shown in Table 56. The first catalyst of the series was precipitated with ammonia, whereas sodium carbonate was used for the remainder of the series. Alkalization was accomplished with potassium carbonate or other potassium salts after precipitation and washing. Catalysts impregnated with other potassium salts were as active as those containing potassium carbonate; however, the activity of the sample with potassium

TABLE 55. PHYSICAL PROPERTIES AND CHEMICAL ANALYSES OF PRECIPITATED IRON CATALYSTS^a

State	Catalyst			
	L-2003	L-3006	L-3004	L-3008
Raw				
Diffraction analysis	$\beta\text{-Fe}_2\text{O}_3 \cdot \text{H}_2\text{O}$	$\beta\text{-Fe}_2\text{O}_3 \cdot \text{H}_2\text{O}$	Fe_3O_4	Fe_3O_4
Chloride content, %	0.56	0.92	0.04	0.02
Potassium content, %	.12	.10 ^b	.07	.09
Used				
Diffraction analysis	Fe_3O_4	$\text{Fe}_3\text{O}_4\text{:Cu}$	$\text{Fe}_3\text{O}_4\text{:Cu}$	$\text{Fe}_3\text{O}_4\text{:Fe}_2\text{C-}$ (h.c.p.):Cu
Inducted				
Chloride content, %		1.08	0.03	
Carbon content, %		0.97	1.85	
Surface area, g/m ²		21.0	23.8	

^a From Ref. 83.

^b Sodium content was less than 0.001 per cent.

monohydrogen phosphate declined more rapidly than that of the other preparations. Potassium chloride was not included in this series.

Although the activity was unaffected by the alkali content, the selectivity was considerably altered, as indicated by the composition of the C₃+ fraction as shown in Figure 32. The average molecular weight of the product, and especially the percentage of wax, increased with alkali to approximately constant values at 1 part K₂CO₃ per 100Fe and higher. Catalysts containing potassium salts (listed in Table 56) equivalent to 1K₂CO₃ per 100Fe had approximately the same selectivity as the one impregnated with potassium carbonate.

Similar results were obtained in Bureau of Mines tests¹⁵ with precipitated Fe₂O₃-CuO-K₂CO₃ catalysts at 7.8 atmospheres with 1H₂ + 1CO gas, as

shown in Figure 33. Although these preparations, for some unknown reason, were considerably less active than average preparations of this type, the results are believed to be valid. In these tests the activity increased linearly with alkali content; however, the increase was small (about 50 per cent over the range investigated). The average molecular weight increased with alkali content to the highest value studied.

TABLE 56. EFFECT OF ALKALI CONTENT ON ACTIVITY OF PRECIPITATED IRON OXIDE CATALYST^a

($2\text{H}_2 + 3\text{CO}$ gas at 15 atm. and 235°C . Flow of feed gas not stated, but it is assumed to be 4 l/10 g Fe/hour. Catalysts precipitated with Na_2CO_3 , unless otherwise indicated)

Alkali Added ^b		Per cent Contraction ^c at the Following Days of Synthesis								
Compound	K_2CO_3 per 100Fe	1	2	5	10	20	30	40	50	100
K_2CO_3	0 ^d	50	50	50	50	50	49	51	51	53
	0	53	50	48	49					
	0.25	47	50	50	51	55	56	54	54	
	0.5	54	—	54	47	—	45			
	1.0	40	—	54	53	50				
	1.0	45	45	45	52	48	48	47		
	2.0	45	45	47	46	47	50			
	5.0	—	—	45	50	50	51	50	40	
	<10.0	—	50	47	50	45	42			
KMnO_4	1.0	40	—	50	51	55	50			
K_2F_2	1.0	—	57	53	55	48				
K_2SiO_3	1.0	—	54	53	46	50				
K_2HPO_4	1.0	55	46	—	46	40				

^a From Ref. 123.

^b When other salts than K_2CO_3 were employed, the alkali content is expressed as the equivalent content of K_2CO_3 .

^c Contractions determined without removal of CO_2 from exit gas.

^d This catalyst precipitated with ammonia.

With precipitated iron or iron-copper catalysts, the yield of wax usually approaches a high constant value when the potassium carbonate content is increased to 1 or 2 parts per 100Fe. When other promoters or carriers are used, the alkali content required for high-wax yields may be drastically altered, and in some cases the activity increases greatly with alkali. When acidic, high-area supports such as kieselguhr or silica gel are used, the alkali content must be greatly increased to achieve high-wax yields. Precipitated catalysts described by Scheuermann¹⁶⁵ having the composition 100Fe:25Cu:(36 to 95)MgO:(50 to 95)SiO₂ (as silica gel or kieselguhr):(10 to 18)K₂CO₃ produced wax yields 52 to 78 per cent (presumably of con-

densified hydrocarbons) in the temperature range 210 to 230°C at 12 atmospheres. One of the most active Ruhrchemie catalysts^{45, 71} contained 100Fe:5Cu:8CaO:30 kieselguhr:(3.0 to 3.5)KOH. The Lurgi catalyst used in the Schwarzheide tests contained 100Fe:10Cu:9Al₂O₃:30SiO₂:2.9K₂CO₃. Cor-

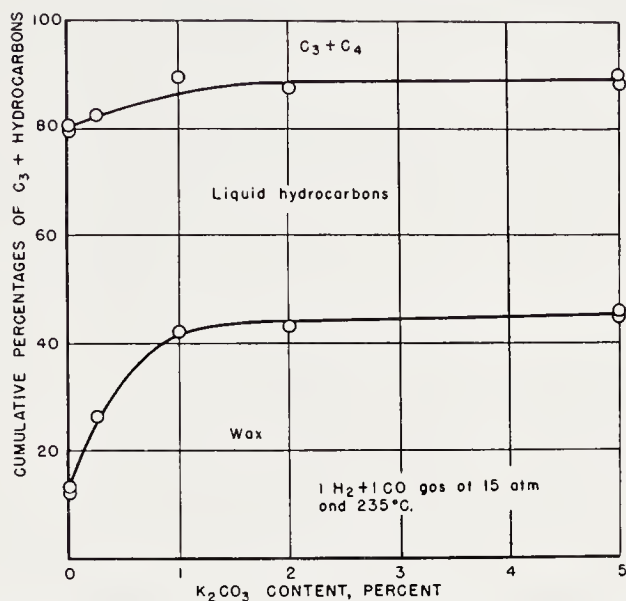


Figure 32. The distribution of C₃+ hydrocarbons as a function of K₂CO₃ content of precipitated Fe₂O₃-K₂CO₃ catalyst. (From Ref. 123)

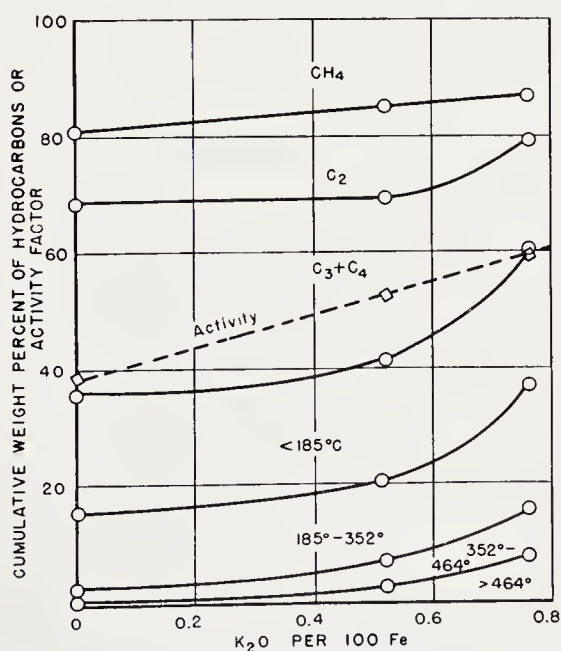


Figure 33. Selectivity and activity of a precipitated iron-copper catalyst as a function of alkali. 1H₂ + 1CO gas at 7.8 atmosphere. (Reproduced with permission from Ref. 15)

responding precipitated catalysts that did not contain silica were promoted with from 0.5 to 1.0 parts K_2CO_3 per 100Fe. The most complete account of the influence of alkali on precipitated iron catalysts containing kieselguhr are tests of 100Fe:25Cu:125 kieselguhr preparation performed at Kyoto Imperial University⁹⁸. Tests of catalysts containing from 2 to 8 K_2CO_3 per 100 Fe were made under the following conditions:

Catalyst pretreatment— $1\text{H}_2 + 1\text{CO}$ for 24 hours at 250°C and atmospheric pressure. Operating conditions—synthesis gas, $1\text{H}_2 + 1\text{CO}$; space velocity, 100 hr^{-1} ; temperature, 210°C ; and operating pressure, atm.—2.9, 5.8, 9.7, 14.5, and 19.5. As the alkali content was increased, the con-

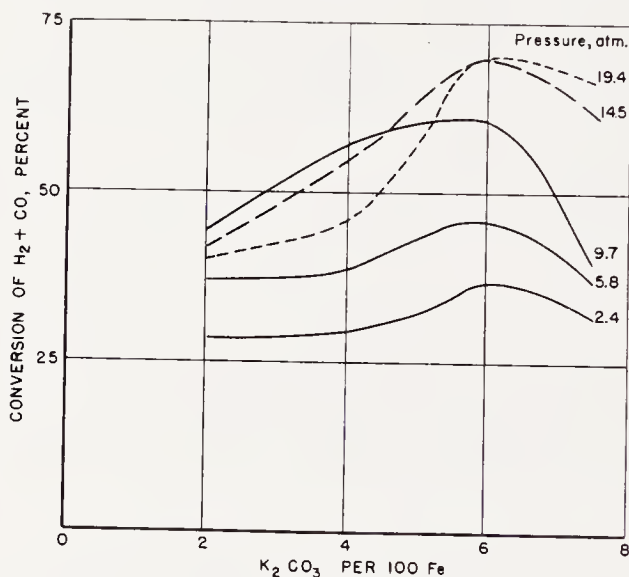


Figure 34. Conversion as a function of alkali content for Fe-Cu-kieselguhr catalysts at 210°C . (From data of Ref. 98)

version at a given pressure increased to a maximum at $6\text{K}_2\text{CO}_3/100\text{Fe}$ and then decreased (Figure 34). The fraction of wax in the C_{5+} product increased with increasing alkali content at operating pressures of 5.8 and 9.7 atmospheres, but remained essentially constant at 14.5 and 19.4 atmospheres, as shown in Figure 35.

In this discussion most of the synthesis studies at atmospheric pressure have been omitted, because both the activity and life of catalysts were poor. A detailed account of KWI research, before the discovery of the medium-pressure synthesis, is found in Reference 123. However, some data of Japanese workers on the atmospheric synthesis are described, since they demonstrate effects of promoters rather well. Murata¹¹⁷ made short tests of the effect of potassium carbonate and boric acid content of complex catalysts containing 100Fe:25Cu:2Mn:125 kieselguhr at atmospheric

pressure and 252°C with $1\text{H}_2 + 1\text{CO}$ gas. In the Japanese atmospheric-pressure tests described here the catalysts were reduced in hydrogen and tested with a flow of 1 liter $1\text{H}_2 + 1\text{CO}$ gas per 4 grams of Fe per hour.

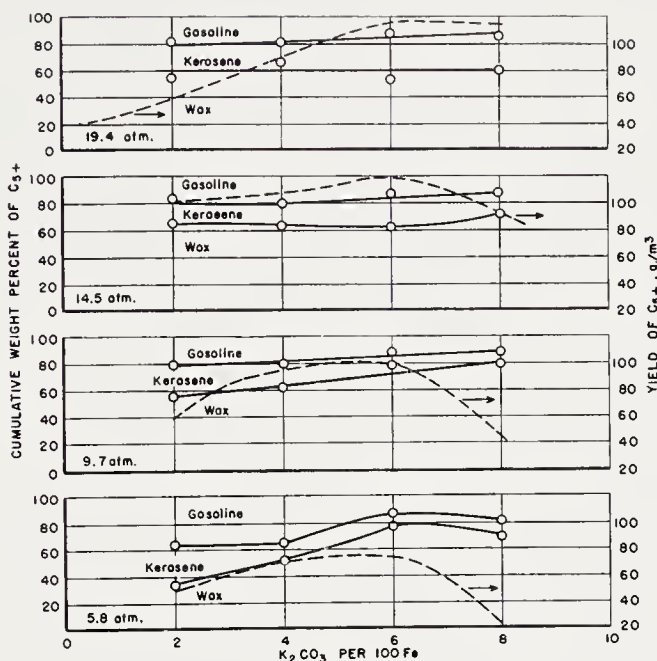


Figure 35. Influence of alkali on activity and selectivity of precipitated Fe-Cu-kieselguhr catalyst at 210°C . (From data of Ref. 98)

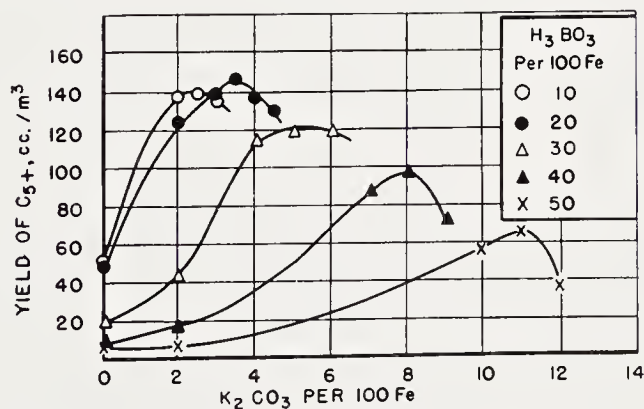


Figure 36. Influence of K_2CO_3 and H_3BO_3 on productivity of Fe-Cu-Mn-kieselguhr catalysts at atmospheric pressure and 252°C . (Reproduced from Ref. 117)

The yields of C_5+ hydrocarbons are shown as a function of these promototers in Figure 36. As the boric acid content was increased, the alkali content for maximum yields increased. The highest yield, $145 \text{ cc}/\text{m}^3$, was obtained with $20\text{H}_3\text{BO}_3$ and $3.5 \text{ K}_2\text{CO}_3$ per 100Fe. In other atmospheric-pressure tests with $100\text{Fe}:25\text{Cu}:2\text{Mn}:125$ kieselguhr, the effect of various

alkali compounds on productivity at 250°C was studied. The yields of C_5+ are plotted against the gram moles of alkali oxide as M_2O in Figure 37, where the highest yields were obtained with $KMnO_4$ and KNO_3 , intermediate yields with Na_2CO_3 and $NaOH$, and the lowest yields with Li_2CO_3 . For each alkali promoter, maximum yields were obtained with 2 to 3.3 gram moles of alkali oxide per 10,000 grams of Fe. Optimum concentrations by weight are 0.6 Li_2O , 1.5–2.0 Na_2O , and 2.1–2.4 K_2O per 100Fe.

In further atmospheric experiments⁹⁹, the effect of kieselguhr, boric acid, and potassium carbonate contents on the productivity of 100Fe:25Cu:2Mn was investigated, as shown in Table 57. As the content of the acidic components, H_3BO_3 and kieselguhr, was increased, the alkali content for op-

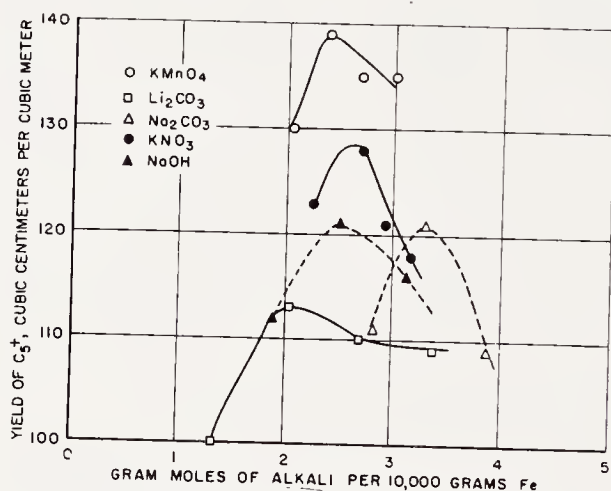


Figure 37. Influence of type and concentration of alkali on productivity of a precipitated iron catalyst. $1H_2 + 1CO$ gas at atmospheric pressure. (From data of Ref. 117)

timum yields increased. The best catalyst contained 125 kieselguhr: $20H_3BO_3:4K_2CO_3$. Kodama⁹⁹ tested this catalyst at 10 atmospheres, but found that the optimum alkali composition was 7 rather than 4 parts K_2CO_3 . In the temperature range 230 to 255°C, yields of 90 g/m³ were obtained for 180 days. Catalysts without boric acid (100Fe:25Cu:125 kieselguhr: $4K_2CO_3$) were more active, producing 116 g/m³ at 220°C and 84 g/m³ at 210°C.

Koelbel¹⁰⁰ reported that iron-dolomite catalysts without alkali operate at 250 to 260°C, whereas for similar preparations with 1 to 10 per cent alkali, the temperature could be decreased to 230 to 240°C.

The present survey indicates that the average molecular weight of synthesis products increases with alkali content; the effectiveness of alkali in changing selectivity decreases with operating pressure. For some catalysts, the activity remained essentially constant as the alkali content was varied,

TABLE 57. TESTS OF IRON CATALYSTS AT ATMOSPHERIC PRESSURE^a
 (4 l/hr per g Fe of 1H₂ + 1CO gas at 250°C)
 100Fe:25Cu:2Mn

Parts per 100 Fe			Apparent Contraction (%)	C ₆ ⁺ , cc/m ³	Light Oil, ^b % of C ₆ ⁺
Kieselguhr	H ₃ BO ₃	K ₂ CO ₃			
0	0	0	27	32	47
		1	30	52	52
		2	24	35	63
	15	3	47	101	68
75	0	1	33	61	44
		2	33	67	45
	15	3	41	119	70
	20	3	46	115	70
		4	46	122	66
125	20	4	48	130	66
200	0	3	21	38	45
	15	3	40	101	63
		4	42	101	67
	20	4	42	106	58
		5	44	117	69
		6	40	92	62
	25	5	37	98	73
	30	5	34	80	74
		6	35	81	72
300	0	3	19	24	33
		4	22	36	33
		5	20	34	33
	15	6	46	81	67
		7	41	86	67
	20	6	45	106	63
		7	46	109	65
		8	44	101	67
	25	7	49	96	64
		8	41	93	67

^a From Ref. 99.

^b Condensed hydrocarbons divided into two fractions, benzine and light oil.

while for others the activity increased to a maximum and decreased as alkali was increased. Apparently the composition and pretreatment of the catalyst determine the relationship between activity and alkali content; however, the available data are insufficient to provide a simple explanation.

The data of Pichler in Table 56 demonstrate that pure iron oxide precipitated with ammonia is active in the synthesis and produces higher hydrocarbons. The selectivity of these preparations is improved by addition of alkali. Thus, if the catalysts are properly pretreated, the only necessary components for precipitated iron catalysts are iron and alkali. Other promoters may be desirable for facilitating the induction, improving the mechanical properties, or modifying the selectivity by a small amount; however, their effects are usually small.

Copper. The action of copper in precipitated iron catalysts is similar to that described for cobalt and nickel catalysts; with iron, however, copper does not usually shorten the catalyst life*. Specifically, copper increased the rate of induction of precipitated catalysts—reduction or carburization—so that lower temperature or shorter time of pretreatment was possible. The activity of catalysts containing high amounts of copper (20Cu:100Fe) was reported to decrease rapidly at temperatures above 250°C. Although this effect has been attributed to formation of iron-copper solid solutions, it may equally well be due to excessive sintering of the iron in the presence of sizable amounts of metallic copper. Small amounts of copper, such as 1Cu:100Fe, have been reported to increase the reproducibility of catalyst preparations. Pichler¹²³ demonstrated that when properly inducted, in this case with pure carbon monoxide at 0.1 atmosphere and 325°C, catalysts containing no copper and those with 100Fe:20Cu had about the same activity at 235°C in the medium-pressure synthesis. According to Koelbel¹⁰⁰, an iron-dolomite-1 per cent K₂CO₃ preparation operated at 230 to 240°C, whereas when 10 per cent copper was added the temperature could be decreased to 210 to 230°C. Data of Murata¹¹⁷ for the synthesis at atmospheric pressure on a variety of iron catalysts (Figure 38) indicated that the yield of liquid hydrocarbons increased with addition of copper to about 10Cu:100Fe and then remained approximately constant.

Difficulty Reducible Oxides. Scheuermann¹⁶⁵ reported tests of catalysts promoted with alumina and magnesia, as shown in Table 58. Although the alumina catalyst had the highest activity, the slow precipitation procedure used in its preparation prevented its consideration for large-scale use. Conditions of the preparation of the magnesia catalyst were less critical and the precipitation could be accomplished rapidly. Koelbel¹⁰⁰ stated the

* This observations may be related to the fact that the solubility of copper in iron is very much lower than in cobalt or nickel.

function of magnesia was not to increase the activity, but to increase the strength of the particles. Similarly, for a 100Fe:20Al:1K₂CO₃ catalyst, the activity was not exceptionally high (operating temperature 225 to 260°C); however, the alumina apparently contributed to the mechanical stability of the catalyst so that its particles were intact after 1,500 hours of synthesis. Although dolomite, added in sizable amounts to precipitated catalysts at Rheinpreussen, was called a support, Koelbel¹⁰⁰ states that the calcium oxide in the dolomite increased the activity and possibly increased the molecular weight of the product. Calcium oxide was a standard promoter in Ruhrchemie catalysts. Other Ruhrchemie preparations containing cerium

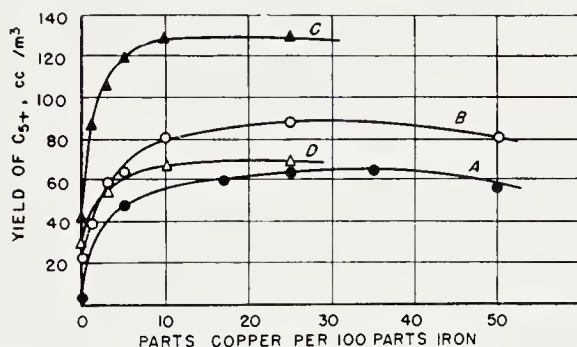


Figure 38. Influence of copper on productivity of precipitated iron catalysts at atmospheric pressure. (Reproduced from Ref. 117)

A Fe-kieselguhr-K₂CO₃, 2H₂ + 1CO

B Fe-kieselguhr-Mn-K₂CO₃, 1H₂ + 1CO

C Fe-kieselguhr-Mn-H₃BO₃-K₂CO₃, 1H₂ + 1CO

D Fe-kieselguhr-H₃BO₃-K₂CO₃, 2H₂ + 1CO

or vanadium oxides in addition to copper and kieselguhr were reported to favor alcohol and ester formation in synthesis at 100 atmospheres⁴⁵.

Carriers. *Kieselguhr.* For precipitated iron catalysts, the beneficial effects of kieselguhr observed for cobalt and nickel were not found. Experiments indicated that not only was the activity inferior for catalysts containing kieselguhr but the product distribution was shifted to a lower average molecular weight with high yields of gaseous hydrocarbons. As described in the previous discussion of alkali promoters, kieselguhr appears to adsorb or react with alkali and thus prevents the usual desirable promoter effects.

After the discovery of the medium-pressure synthesis with iron catalysts and the development of improved methods of pretreatment, Pichler¹²³ investigated the preparative procedure for catalysts supported on kieselguhr. As described on p. 121, the best catalysts resulted from mixing kieselguhr with the moist precipitate after washing and alkalization. This

preparation after induction with carbon monoxide at 0.1 atmosphere and 325°C was very active at 235°C in the medium-pressure synthesis; however, the selectivity was inferior to that for similar preparations without kieselguhr. Figure 39 compares the supported catalyst with a similar unsupported preparation and with an alkali-free catalyst precipitated with aqueous ammonia. The products from the supported preparation had a lower average molecular weight than even the alkali-free catalyst. The supported catalyst, however, had considerably improved mechanical properties compared with Pichler's standard iron catalyst, and could be operated fairly satisfactorily in vertical tube reactors. Similarly, Koelbel¹⁰⁰ found that granules of a 100Fe:0.5Cu:2Mn:1K₂CO₃:100 kieselguhr preparation

TABLE 58. COMPARISON OF TESTS WITH Fe-Cu-Al₂O₃-K₂CO₃ AND Fe-Cu-MgO-K₂CO₃ CATALYSTS^a

(1H₂ + 1CO gas at space velocity of 240 hr⁻¹ and 12 atm.)

	Promoter	
	Alumina	Magnesia
Temperature, °C	210	235
CO conversion, %	80	70
Yields, g/m ^{3b}	82	90
Boiling fractions, °C		
<195	23	40
195-320	18	15
320-450	24	20
>450	35	25

^a From Ref. 165.

^b Presumably liquid + solid hydrocarbons.

were intact after 1,100 hours of medium-pressure synthesis with 1.2H₂ + 1CO gas at 220 to 250°C. This catalyst produced no wax. The Ruhrchemie catalyst employed in the Reichsamtversuch (p. 160) contained 50 kieselguhr per 100Fe.

A series of supported iron-copper catalysts containing natural "Filter-Cel" and flux-calcined "Hyflo-Super Cel" (see p. 60) were tested at the Bureau of Mines¹⁷⁶. Although the two kieselguhrs had approximately the same bulk density, the surface area of the flux-calcined sample was only 10 per cent of that of the natural sample, and the available area of the flux-calcined material presumably was less reactive to alkali due to the high-temperature alkali treatment. The tests (Table 59) were made at essentially constant space velocities, and activities at 240°C¹⁵ per gram of iron and per cc of catalyst were computed. For granular catalysts with "Filter-

Cel" (X122) and "Hyflo-Super-Cel" (X106), the weight of iron per 50 cc of catalyst space was 7.8 grams compared with 45.4 grams for the carrier-free preparation (X101). Although the activity per cc was lower for the supported preparations, the activity per gram Fe was greater. However, the products of supported catalysts had a considerably lower molecular weight than the carrier-free preparation and were characteristic of alkali-deficient catalysts. The products from the sample containing the flux-calcined carrier had a higher average molecular weight than those from the preparation with the natural kieselguhr, indicating that although both catalysts were

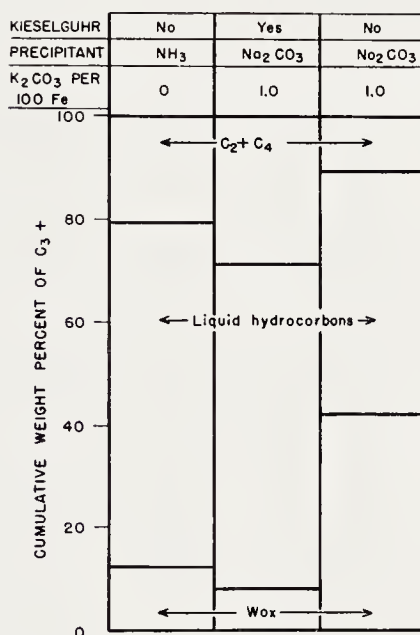


Figure 39. Comparison of products from carrier-free and kieselguhr containing precipitated iron catalysts. Medium-pressure synthesis at 235°C. (From data of Ref. 123)

deficient in alkali, the preparation with natural kieselguhr appeared to be more deficient. On the basis of these tests, the preparation with the flux-calcined carrier appeared more amenable to improvement of selectivity by further alkali addition. In test X239 the alkali content was increased to 1.91K₂O per 100Fe. This resulted in an increase of activity per gram of Fe to 516, one of the highest activities observed in the Bureau of Mines testing program; however, the activity per cc was 92 compared with 135 for the unsupported preparation (X101). The product in X239 nevertheless had a lower molecular weight than that from X101. Attempts were made to increase the activity per cc of high-alkali-content catalysts supported on "Hyflo-Super-Cel" by increasing the bulk density by pelleting (test X254, X272, X284). This procedure, however, resulted in lower

TABLE 59. BUREAU OF MINES' TESTS OF PRECIPITATED CATALYSTS (100Fe:10Cu) SUPPORTED ON KIESELGUHR
(1H₂ + 1CO gas at 7.8 atm.)

Test	X101	X122	X106	X239	X254	X272	X284	X245
K ₂ O/100Fe	0.44	0.87	0.79	1.91	1.48	2.36	3.13	0.44
Kieselguhr/100Fe	None	100 F.C. ^a			100 H.S.C. ^b			None
Grams Fe per 50 cc catalyst	45.4 ^c	7.8 ^c	7.8 ^c	9.0 ^c	19.7 ^d	17.6 ^d	16.6 ^d	44.7 ^c
Induction ^e								
Gas			1H ₂ + 1CO				H ₂	H ₂
Temperature, °C							200-300	313
Time, hours							25	17
Space velocity, hr ⁻¹							100	135
Temperature, °C							238	229
Contraction, %							63	65
Average activity ^f								
Per gram Fe								
Per cc								
Products, wt-%								
CH ₄								
C ₂								
C ₃ + C ₄								
Liquids + solids								
Distillation data, wt%								
<185°C								
185°-352°C								
352°-464°C								
>464°C								

Infrared analysis of fractions ^a									
<185°C									
CO + COOH	1.6	0.01	0.4	0.8	0.6	1.9	3.5		
COO	0.5	.02	.01	.2	.2	0.87	0.83		
OH	3.1	.16	.16	2.9	1.1	12.2	10.5		
C=C	3.8	6.3	6.8	7.6	7.8	5.1	4.3		
185-352°C									
CO + COOH	1.0	0.08	0.10	0.3	0.2	1.0	1.4		
COO	0	.03	.05	.2	.1	1.4	1.9		
OH	0.69	0	0	.5	.1	6.4	2.2		
C=C	3.2	2.4	2.3	3.9	2.7	2.3	4.1		

^a F.C. = "Filter Cel," natural kieselguhr.

^b H.S.C. = "Hyflo Super Cel," flux-calcined kieselguhr.

^c Broken filter cake.

^d Pelleted catalyst.

^e Induction at atmospheric pressure.

^f Activity expressed as cc of gas converted at 240°C.

^g Expressed as weight-per cent of functional group.

activities per cc than observed in X239. The best results of this series were obtained in test X284, in which the catalyst was reduced in hydrogen rather than inducted in synthesis gas. However, the activity per cc and the selectivity of this catalyst were inferior to those of a corresponding reduced, unsupported catalyst in test X245.

These experiments demonstrate that catalysts containing kieselguhr require greater quantities of alkali to produce the desired promoter effect. With the relatively inert flux-calcined kieselguhr, good yields were obtained in the range 1.9 to 3.1K₂O per 100Fe, although the average molecular weight may not have reached its maximum in this range. Presumably greater amounts of alkali would be required for natural "Filter-Cel." For granular catalysts (broken filter-cake), the activity per gram of iron for the supported catalysts was greater than for corresponding preparations without kieselguhr; therefore, the pore structure produced by the presence of the support may have a desirable effect on synthesis rate. The presence of kieselguhr in an amount equal to the iron content, however, decreases the amount of iron per unit volume by a factor of 6, so that the activity of supported catalysts per cc was lower than that of unsupported catalysts. Increasing the bulk density by pelleting supported catalysts did not improve the activity per unit volume. Possible improvements might result from reducing the kieselguhr content to 20 to 30 parts per 100Fe. In contrast to the results with cobalt and nickel catalysts, (p. 55) the best iron catalysts were obtained with flux-calcined rather than with natural kieselguhr.

Ruhrchemie experiments in 1944¹⁵¹ were apparently directed in the same general direction. Kieselguhr was boiled for a short time in aqueous solutions of various alkalis before incorporation into catalysts containing 100Fe:5Cu:10CaO:5 to 50 kieselguhr. The catalysts were impregnated with KOH or potassium water glass. However, these preparations with few exceptions were less active than samples containing raw kieselguhr, and usually the samples supported on treated kieselguhr produced larger yields of methane.

Silica Gel and Water Glass. Herbert^{31, 87} of Lurgi described catalysts supported on freshly precipitated silica gel, the best composition being 100Fe:25Cu:9Al₂O₃:2K₂O:30SiO₂. A metal oxide precipitate was prepared by the rapid addition of a dilute solution of nitrates of iron, copper, and aluminum at 70°C. Freshly precipitated silica gel from water glass plus a mineral acid was added to the metal oxide precipitate and stirred for one minute. The mixture was filtered, washed until the pH of the wash water was 8, and then impregnated to the proper alkali content with potassium carbonate. The material was extruded, cut into pieces of the desired length, and dried at 100°C. The resulting catalyst was hard and had a long life; the good mechanical properties were attributed to the formation of potas-

sium silicate. These catalysts were reduced with hydrogen at a space velocity of $1,000 \text{ hr}^{-1}$ for 1 to 3 hours at 250 to 300°C in the synthesis reactors. In a conventional, externally-cooled, double-tube pilot plant⁶⁸ with $1\text{H}_2 + 1\text{CO}$ at a space velocity of 100 hr^{-1} , 20 atmospheres, and a 2.5:1 recycle ratio, yields of C_3+ of 136 g/m^3 were obtained in tests of 3 months' duration. However, the catalyst was still active at the termination of the experiment and a life of one year was predicted. In the 3 months of synthesis, the catalyst temperature had to be increased from 220 to 230°C . For a two-stage operation, the following data were estimated:

Over-all Distribution	g/m ³	Distribution of C_6+		
		Fraction	Weight %	Olefin Content (%)
$\text{C}_1 + \text{C}_2$	18	$< 200^{\circ}\text{C}$	20	60
$\text{C}_3 + \text{C}_4$	15	$300^{\circ}\text{--}320^{\circ}\text{C}$	20	45
C_4+	146	$320^{\circ}\text{--}460^{\circ}\text{C}$	15	
Alcohols	9	$> 460^{\circ}\text{C}$	45	

The high yields of wax ($> 320^{\circ}\text{C}$) seem to indicate that the catalyst was not deficient in alkali.

Ruhrchemie¹⁵¹ described catalysts of the composition $100\text{Fe}:5\text{Cu}:10\text{CaO}:6.5\text{SiO}_2$, which were prepared by a method similar to that of the Lurgi catalysts, except that the precipitated oxides of iron and promoters were filtered, washed, and then suspended in a potassium water-glass solution. After filtering, the catalyst was dried at 100°C .

Dolomite. Koelbel^{73, 100} of Rheinpreussen developed catalysts containing dolomite as a support to improve the mechanical strength and stability. The dolomite was selected to be free of sulfur and phosphates. It was further desirable that ratio, CaO/MgO , lie between 1.45 and 1.70 and that the content of silica be low. The dolomite was roasted at 700°C and crushed to particles about 0.1 mm in diameter. Apparently this treatment removed most of the carbon dioxide. In the catalyst preparation, iron was dissolved in a quantity of nitric acid somewhat in excess of that required, and copper nitrate was added to the solution. The solution was heated to boiling with the powdered dolomite added either before or after the solution was heated, and the precipitation was accomplished with sodium carbonate solution. Apparently a large fraction of the dolomite dissolved before the precipitation. The sodium carbonate was added to only a slight excess of that required by the iron so that dissolved magnesia would be incompletely precipitated. After precipitation, the catalyst was washed with hot water, filtered, and the moist cake impregnated with potassium carbonate.

A catalyst of this type, $100\text{Fe}:0.1\text{Cu}:80 \text{ dolomite}:3\text{K}_2\text{CO}_3$, was used in a fixed-bed pilot plant (8.2 kg of catalyst) with $1\text{H}_2 + 1.6\text{CO}$ at 12 atmos-

pheres, space velocity of 109, and 245°C. The catalyst was pretreated with CO₂-free synthesis gas at 245°C and atmospheric pressure for 47 hours, and then the pressure was gradually increased to 12 atmospheres. After 600 hours, the catalyst was easily removed from the reactor and found to be intact. It was then extracted with a gasoline fraction and put into the synthesis for another 600 hours. The catalyst was readily removed at the termination of the experiment. The products from similar pilot-plant tests are given in Table 60.

There is considerable uncertainty as to whether or not dolomite in these catalysts should be classed as a support or as a promoter. According to Koebel¹⁰⁰, the fact that these catalysts operate without plugging or extensive mechanical disintegration must be attributed to the magnesia content while the calcium oxide increased the activity. Possibly the reason for re,

TABLE 60. PRODUCTS FROM PILOT-PLANT EXPERIMENTS WITH
Fe-Cu-DOLOMITE-K₂CO₃ CATALYSTS^a
(1H₂ + 1.6CO gas at 240°C and 12 atm.)

Fraction	Weight (%)	Olefin Content (vol. %)	Octane Number
C ₃ + C ₄	10-20	50-70	74
40°-150°C	34	55-65	
150°-360°C	27-30	30-50	
360°-450°C	21-22		
>450°C	14-16		

^a From Ref. 100.

garding dolomite as a support is that it is present in greater amounts than components normally classed as promoters. In contrast to these reports, a Rheinpreussen catalyst of similar composition encountered considerable "coking" troubles in the Schwarzheide comparative tests (p. 160).

Fused Iron Catalysts

This type of catalyst is used in the ammonia synthesis, and its preparation and properties have been described in the literature of this process. For recent reviews, see Nielsen¹¹⁹ and Zwietering²⁰⁷. Successful iron ammonia catalysts usually contain small amounts, about 3 per cent, of a structural promoter, such as alumina or magnesia, and potassium oxide as a chemical promoter. These catalysts are prepared by fusing a mixture of magnetite and promoters in an electric resistance furnace by passing the current between water-cooled iron electrodes directly through the catalyst mixture^{23, 106}. The fusion is accomplished in a container lined with magnetite so that there is no problem of contamination. In Germany, fused catalysts were frequently prepared by oxidizing metallic iron in a stream of

oxygen^{88, 136}. To start the oxidation, a portion of the iron must be heated to a high temperature. Promoter oxides were added to the molten magnetite. Many fused preparations have a spinel-structure composed of a solid solution of magnetite and structural-promoter oxide. In the raw state, these catalysts have virtually no internal surface area or pore volume, the pore structure being developed during reduction. The reduction and pore structure of these catalysts will be discussed later in this chapter.

As a starting material, any oxide of iron may be used since all of them will revert to magnetite in the presence of oxygen at fusion temperatures. Small amounts of impurities, such as most metal and nonmetal oxides (up to 3 per cent), usually produce no serious diminution of catalyst activity since they are either volatilized in the fusion or serve as structural promoters. A purified, commercially available ore, Alan Wood magnetite, has been used extensively for the preparation of fused catalysts at the Bruceton laboratory of the Bureau of Mines, and these catalysts are usually more active in the Fischer-Tropsch synthesis than commercial synthetic ammonia catalysts. Mill scale was used at the Bureau of Mines demonstration plant at Louisiana, Missouri, with good results. It has been reported that active catalysts may be prepared from oxides produced by roasting and oxidizing iron sulfide ores¹⁶⁸. Oxides with lower contents of impurities, or at least different impurities than encountered in natural ores, may be obtained by burning relatively pure iron such as Armco, commercially available refined iron, or iron scrap in oxygen. At the Tennessee Valley Authority, Wilson Dam,²³ a low-silica content magnetite for catalyst manufacture was prepared in the following way: A finely crushed magnetite ore was concentrated by removing the high silica-content particles by a tabling procedure. To this concentrate was added sufficient synthetic magnetite made by burning "Armco" iron rods in oxygen to decrease the silica content below the desired limit. It should be noted, however, that small amounts of silica in fused Fischer-Tropsch catalysts are not undesirable, and many workers believe that silica causes no bad effects in catalysts for the ammonia synthesis. Typical analyses of roasted pyrites, mill scale, and Alan Wood magnetite are given in Table 61.

Alkali as potassium hydroxide, carbonate, or nitrate may be incorporated into the fusion mixture, or it may be added subsequently by immersing the catalyst in a solution of the potassium compound, as described by Brunauer and Love¹¹⁰. In the latter method, the amount of alkali retained by the catalyst depends upon the concentration of the solution in which it is immersed. In the ammonia synthesis, the method of alkali addition produces no differences in the resulting activity of the catalysts. This appears to be the case in the Fischer-Tropsch synthesis; however, the effect has not been thoroughly investigated.

Details of the preparation of the Leuna fused catalyst WK17^{108, 138, 202}, by

oxidation of the metallic iron follow: 19 kg of iron were placed in a shallow water-cooled pan (50 x 15 cm). Presumably a portion of the iron was preheated to initiate the reaction with oxygen. Pure oxygen from two nozzles was directed at the iron and sufficient heat was evolved to melt the mass in about 10 minutes. The promoters as nitrates were added and the oxidation continued. After a total of 30 minutes, the oxidation was completed and the molten catalyst was poured into an iron pan and cooled slowly. The Leuna fused catalyst prepared by this method was said to be somewhat inhomogeneous. Remelting the finely-crushed catalyst in an electric resistance furnace, as described previously, made the material more homo-

TABLE 61. COMPOSITION OF VARIOUS INEXPENSIVE FORMS OF IRON

	Weight Per cent			
	Mill Scale ^a	Roasted Pyrites ^a	Alan Wood Magnetite ^b	
Fe	74.5	68.0	71.4	69.0
Mn	0.4	0.09	0.4	
Cu	Trace	.12	—	
Ni	.09	—	—	
Si	.1	—	.20	0.35
Zn	—	.24	—	
MgO	—	.65	—	.15
CaO	—	.6	—	
Al ₂ O ₃	—	.5	.04	
S	—	.06	—	
P	—	.006	—	

^a Analytical data from Ref. 168.

^b Analytical data of the Bureau of Mines.

geneous. This procedure improved the catalyst for use in the ammonia synthesis; however, there are contradictory statements as to whether or not remelting was desirable for the Fischer-Tropsch catalysts. For the Fischer-Tropsch synthesis, the best results were obtained by melting a mixture of crushed catalyst and carbonyl iron in an atmosphere of oxygen.

For many years, alkali oxides have been known to be promoters for fused iron catalysts in the ammonia synthesis^{41, 114}. In the Fischer-Tropsch synthesis, with catalysts of this type, both the activity and selectivity are drastically changed by the alkali content. Scheuermann¹⁶⁵ described a detailed study of catalysts containing varying amounts of magnesia, silica, and potassium oxide. The goal of these experiments was the production of high-molecular weight olefins, and unfortunately, for most experiments data on lower-molecular weight products are not available. Four series of catalysts were studied: (a) 100Fe:4.8MgO with variable amounts of K₂O,

(b) 100Fe:4.8MgO with variable SiO_2 , (c) 100Fe:4.6MgO:0.4K with variable SiO_2 , and (d) 100Fe:4.5MgO:2.7 SiO_2 with variable K_2O . All tests were made at 12 atmospheres, series a, b, and c with $2\text{H}_2 + 1\text{CO}$ gas at a space velocity of 480 hr^{-1} and series d with $1\text{H}_2 + 1\text{CO}$ at a space velocity of 240 hr^{-1} . All catalysts were reduced in a high flow of hydrogen at 500°C for 48 hours. Since the tests were not made at constant temperature, the activity per unit volume of catalyst at 240°C was estimated using the empirical equation developed by Bureau of Mines workers¹⁵. Data for series a and d (Figure 40) indicate that for both the Fe-MgO and Fe-MgO- SiO_2 the activity increased to a maximum corresponding to 0.7K/100Fe. For series b and c (Figure 41) the activity decreased with increasing silica

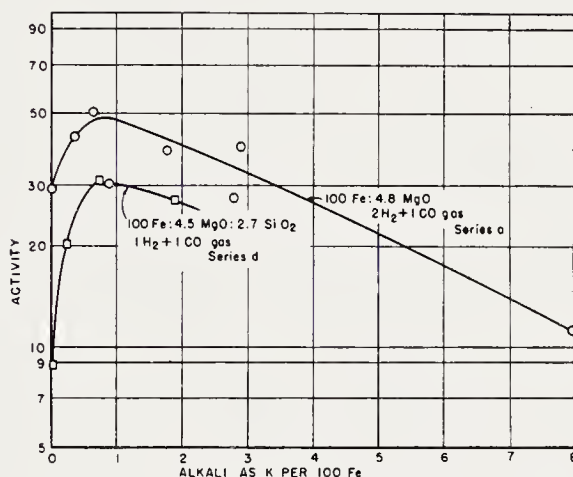


Figure 40. Activity of fused iron catalysts as function of alkali at 12 atm. (From data of Ref. 165)

content, and in the case of series b passed through a minimum and increased. Catalysts containing K_2O (series c) were more active at a given silica content than alkali-free preparations (series b). Data for the per cent of wax (b.p. $>320^\circ\text{C}$) in the C_5+ fraction as a function of K and SiO_2 content in Figure 42 are difficult to interpret, because the wax formation is a function of synthesis temperature (which was not held constant except in series d) as well as catalyst composition. As alkali was increased in series a, the per cent wax increased to a maximum at about 1K/100Fe and then decreased to a relatively constant value. For series d (at constant temperature) the wax increased with alkali content, but did not reach a maximum in the range studied. With silica, the wax yield decreased with increasing promoter concentration and then increased. Series d affords unambiguous data for the effect of K_2O and SiO_2 on selectivity, and more detailed data are available, as shown in Figure 43. The olefin content of distillation fractions decreased with addition of silica and increased with alkali content to a

relatively constant value at about 0.7K/100Fe. The alcohol content of the fractions, excluding the 320 to 450°C data, decreased with silica content and increased with alkali to the highest value studied.

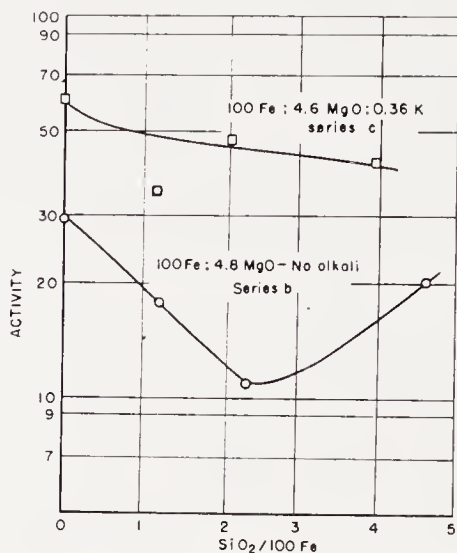


Figure 41. Variation of activity of fused iron catalysts with silica content. (From data of Ref. 165)

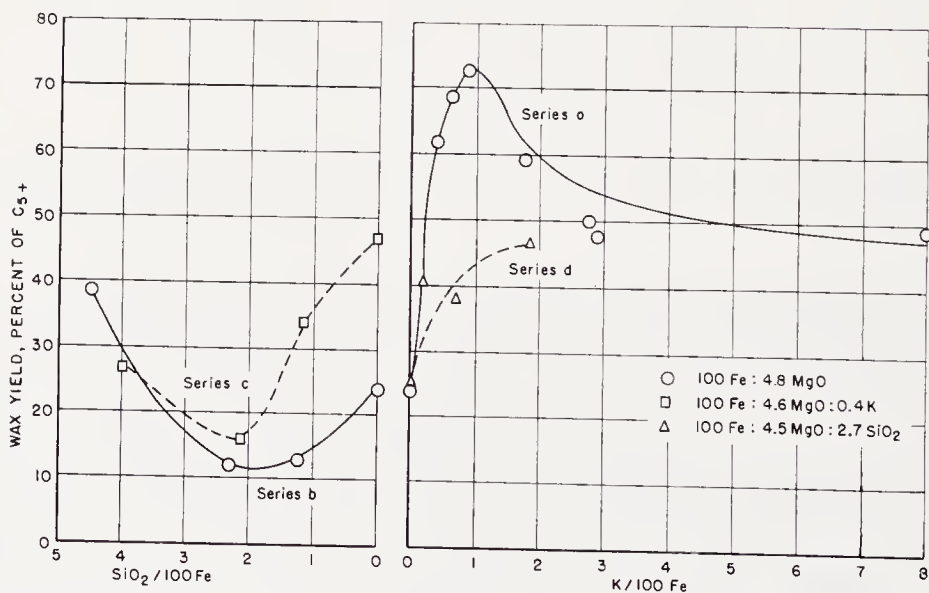


Figure 42. Wax yields from fused catalysts as functions of alkali and silica content. (From data of Ref. 165)

Bureau of Mines studies¹⁷² of a fused iron catalyst (100Fe:4.5Al₂O₃) with 1H₂ + 1CO gas at 7.8 and 21.4 atmospheres demonstrate a similar activating effect for the addition of K₂O (as K₂CO₃), as shown in Figure 44. One group of catalysts was reduced in hydrogen and a second reduced in

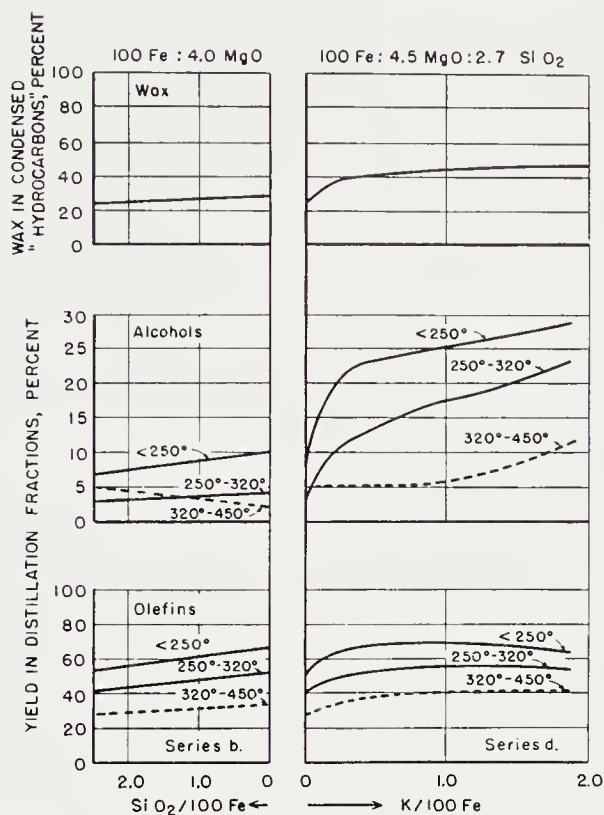


Figure 43. Selectivity of fused iron catalysts as function of silica and potassium oxide. $1\text{H}_2 + 1\text{CO}$ gas at 12 atm. and 230°C . (From data of Ref. 165)

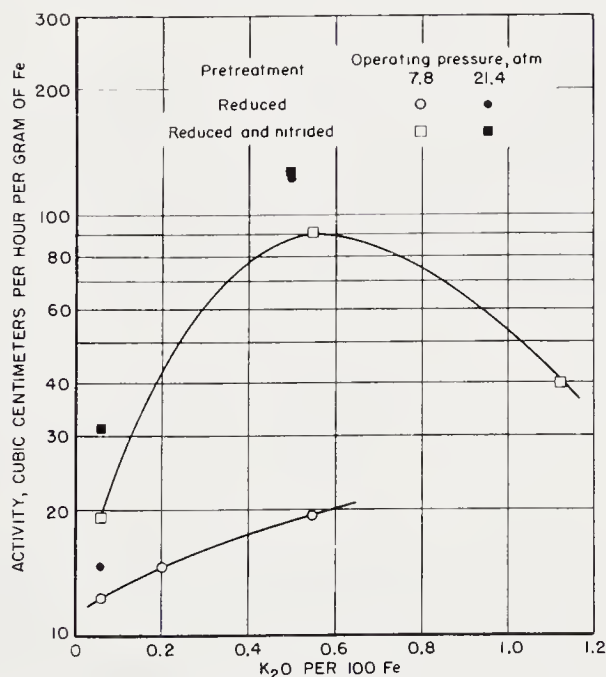


Figure 44. Activity of reduced and nitrided fused iron catalyst as a function of potassium carbonate content with $1\text{H}_2 + 1\text{CO}$ gas.

hydrogen and nitrated in ammonia pp. 188 and 192). Essentially the same effect of promoter on activity was observed for both reduced and reduced-and-nitrated preparations. For nitrated catalysts at 21.4 atmospheres, a maximum activity was observed at about $0.6\text{K}_2\text{O}$ per 100Fe . In other series, the highest alkali content was only $0.55\text{K}_2\text{O}$ per 100Fe , and a maximum in the activity-alkali curve was not observed. Since these experiments were made at different temperatures, the selectivity data do not clearly demonstrate the effect of alkali. Further unpublished work indicates that lithium and sodium oxides have only a slight activating effect on reduced fused catalysts; potassium oxide is a good promoter, and rubidium oxide is still more effective. Thus, the effectiveness of alkali oxides increases with the atomic weight of the alkali metal.

On the basis of numerous tests of fused catalysts of different compositions (Figures 40 to 43), Scheuermann¹⁶⁵ concluded that the ratio of K_2O to structural promoter, as well as the ratio of K_2O to Fe , was critical in determining the catalytic behavior. This conclusion was based on the olefin content of the wax fraction obtained in experiments performed at widely different temperatures. Possibly the observed variation of the olefin content resulted from a fortuitous combination of the effects of alkali content and temperature. The activity- and wax production-alkali content plots in Figures 40 and 42 indicate that the activity and selectivity were primarily related to the K_2O to Fe ratio.

The data presented in this section demonstrate that the K_2O content has a larger effect on activity of fused catalysts than observed for some precipitated iron catalysts (p. 126).

A report from Oppau¹²⁰ describes a detailed study of fused iron oxide catalysts for hydrogenation of carbon monoxide. Unfortunately the conditions of catalyst testing were not those normally employed for the Fischer-Tropsch synthesis, and the results were poor. After reduction in hydrogen at 550 or 650°C , the catalysts were tested with 3 or $4\text{H}_2 + 1\text{CO}$ gas at 100 atmospheres and the temperatures and flow were varied according to the following schedule:

Days	Temp. ($^\circ\text{C}$)	Space Velocity, hr^{-1} (exit gas)
0-2	280	100-250
2-4	290	500
4-6	300	750
6-8	310	1000
etc.		

Promoters in varying combinations were SiO_2 , TiO_2 , ZrO_2 , MnO , CuO , CaO , and K_2O . The authors divided the promoters into two classes, alkaline and acidic, and summarized their results as follows:

1. Alkaline or basic promoters (K_2O , CuO , CaO), especially K_2O , dispose the catalyst to form hydrocarbons. Copper oxide was said to suppress carbon formation.

2. Acidic components (SiO_2 , TiO_2 , ZrO_2) promoted the formation of alcohols and other oxygenated molecules. The effectiveness of the acidic component increased with increasing molecular weight; thus ZrO_2 was more effective than TiO_2 .

Samples of these catalysts, in the raw state, were polished and subjected to petrographic analysis. The best catalysts had the most simple microscopic structure and were characterized by large, well developed crystals. Apparently in good catalysts the promoters are homogeneously dispersed in the magnetite phase. The authors concluded that the petrographic studies of raw catalysts were a better criterion for predicting the activity of the reduced catalyst than x-ray analysis (of raw catalysts), which usually gave only diffraction patterns of magnetite.

These studies were extended by Linckh and Klemm²⁰⁶ to experiments in a hot-gas-recycle pilot plant. Gas containing 20 per cent carbon monoxide and 60 to 80 per cent hydrogen, with sufficient recycle gas to decrease the carbon monoxide in the entering gas to 10 per cent, was used at 100 to 180 atmospheres and 290 to 320°C. The catalyst based on the studies described above was prepared by fusing in oxygen a mixture of 89.5 per cent iron powder, 2.24 per cent TiO_2 , 2.24 per cent silicon powder, 2.24 per cent MnO , 2.03 per cent copper powder, and 1.8 per cent KOH . Metallic copper was said to enter the melt homogeneously, whereas copper oxide decomposed to form globules of metallic copper. The catalyst was reduced in hydrogen (space velocity = 500–700 hr^{-1}) at 650°C for 3 days. Carbon deposition, which usually occurred at the gas inlet portion of the catalyst bed, was suppressed by copper-plating the inlet portion of the catalyst with a dilute copper-nitrate solution. It was not stated whether this treatment was made on the raw or reduced catalyst; however, the copper-plating did not impair the activity of the catalyst. Yields of 58 g/m^3 were obtained, the product containing in per cent: 23 heavy oil, 5.6 light oil, 12.6 gasoline, 8.5 $C_3 + C_4$, and 49.5 alcohols. The yield of alcohol increased with pressure, for example, in comparable experiments the condensable products (exclusive of water) in g/m^3 and the per cent of alcohol in this material, respectively, were 42 and 31 at 100 atmospheres and 44 and 84.5 at 180 atmospheres.

A similar catalyst²⁰⁶, prepared by fusing a mixture of 100Fe:2.5Si:2.5 TiO_2 :5 $KMnO_4$ in oxygen, was employed in the Duftschmid oil-circulation process. Oxides of manganese plus potassium hydroxide could be used in place of potassium permanganate. After reduction in hydrogen at 450 to 500°C for 5 to 6 days, this catalyst was operated at temperatures from 240 to 290°C with 0.9 $H_2 + 1CO$ gas at 20 atmospheres. The C_3+ products

from this catalyst were:

Fraction	Weight-Per cent	Olefins (Vol.-per cent)
$C_3 + C_4$	14	80
$<100^\circ\text{C}$	19	50-65
$100^\circ\text{--}150^\circ\text{C}$	11	40-55
$150^\circ\text{--}175^\circ\text{C}$	4	35-45
$175^\circ\text{--}325^\circ\text{C}$	19	20-35
$325^\circ\text{--}400^\circ\text{C}$	11	20
$>400^\circ\text{C}$	17	—
Alcohol in aqueous phase	5	—

A catalyst of this composition was prepared and tested at the Bureau of Mines. Although this preparation was satisfactory, it was not exceptional with respect to either activity or selectivity.

Scheuermann¹⁶⁵ stated that a variety of structural promoters other than magnesia and silica were tried; however, no details are available. With respect to catalytic activity, alumina was a somewhat better promoter than magnesia, but the magnesia-promoted catalyst was considered more desirable on the basis of the amount and quality of high-molecular-weight olefins. The olefins from magnesia-promoted catalysts, were more suitable for manufacture of synthetic soap. Certain fluorides, CaF_2 , AlF_3 , and FeF_3 , were said to lower the molecular weight of the products so that low-boiling products were obtained at low temperatures (170 to 200°C). The conversion at these temperatures were low. Arsenic oxide was reported to promote the formation of esters²⁰²; however, in later work at the same laboratory¹³⁷ high ester yields were not obtained with catalysts containing either arsenic or antimony oxides.

In unpublished research at the Bureau of Mines about twenty fused catalysts containing a number of oxides in varying amounts were tested in the Fischer-Tropsch synthesis at 300 psig after reduction or reduction plus nitriding. Alan Wood magnetite was used as a starting material in these preparations, and in all cases the catalysts contained about $0.5\text{K}_2\text{O}$ per 100Fe . The results of these experiments may be tentatively summarized as follows:

(a) Most of the catalysts that contained less than 3 or 4 per cent structural promoters, as well as fused Alan Wood magnetite (about 0.7 per cent structural promoter as impurities, see Table 61), had high activities of at least the same magnitude.

(b) Above 3 to 4 per cent structural promoter, the activity usually decreased with increasing content of structural promoter.

(c) Usually the oxide used as a structural promoter does not produce major changes in selectivity.

(d) With few exceptions, catalysts containing 3 to 4 per cent of struc-

tural promoters, as well as fused Alan Wood magnetite, were more active than commercial synthetic ammonia catalysts.

In earlier studies at the Bureau of Mines¹⁸¹, six commercial ammonia synthesis catalysts were tested with $1\text{H}_2 + 1\text{CO}$ gas at 7.8 atmospheres. Two samples contained $\text{MgO} + \text{K}_2\text{O}$ as the principal promoters and the others $\text{Al}_2\text{O}_3 + \text{K}_2\text{O}$. Appreciable amounts of other oxides were present in some preparations; these oxides were probably impurities in the raw materials used for the catalysts. In this series, the catalysts promoted with magnesia were more active than those with alumina; however, alumina-promoted

TABLE 62. SYNOL OPERATION OF CATALYST WK17^a

$\text{Fe}_3\text{O}_4\text{-Al}_2\text{O}_3\text{-K}_2\text{O}$ catalyst reduced in hydrogen for 60 hr at 500°C . Synthesis with 20 atm. of water gas at space velocity of 350.

Conversion maintained at 50 per cent, yield C_3+ = 45 g/m³, and temperature $191^\circ\text{-}193^\circ\text{C}$.

Distillation of C_3+

	Days					
	7-17			20-30		
	Weight (%)	Per cent in fraction		Weight Per cent	Per cent in Fraction	
		Alcohols	Olefins		Alcohols	Olefins
$\text{C}_3 + \text{C}_4$	13.1			15.3		
$<200^\circ\text{C}$	50.0	29.5	45	43.6	34.6	42
$200\text{-}230^\circ$	2.2	34.5	35	3.8	35.7	34
$230\text{-}350^\circ$	16.5	53.5	28	11.5	59.8	25
$350\text{-}400^\circ$	4.3	37.5	24	8.1	56.5	28
$>400^\circ$	13.9			17.8		

^a From Ref. 107.

fused catalysts of activity equal to or greater than that of the magnesia-promoted catalysts have been prepared at the Bureau. The Leuna synol catalyst with Al_2O_3 , CuO , and K_2O as promoters was found to be very active. This sample which had probably been remelted with iron (the iron content was very high) was obtained as a fine powder. The high activity probably resulted largely from the small particle size, since the standard Bureau of Mines catalyst D3001 as 40- to 60-mesh particles had nearly the same activity.

Nevertheless, the synol-type preparations of Leuna must be regarded as very good fused catalysts, which were as active as precipitated catalysts. Under normal synthesis conditions, that is 210 to 230°C , low flows and relatively high conversion (70 per cent), these catalysts produce a moder-

ately high-molecular-weight product, with only a small fraction of oxygenated organic molecules; for example, in the Bureau of Mines test, the C_5+ fraction from the synol catalyst contained 8 weight per cent in the $<185^\circ\text{C}$ fraction, 24 per cent from 185 to 352°C , 16 per cent from 352 to 464°C , and 52 per cent from $>464^\circ\text{C}$. (See also this catalyst in Schwarzheide tests, p. 162). In the typical synol operation at 190 to 200°C with high flows and 50 per cent conversion, these catalysts yielded a lower-molecular-weight product containing a large fraction of oxygenated molecules. Data for the synol operation are given in Table 62.

Sintered, Cemented, Impregnated, and Miscellaneous Types of Iron Catalysts

This section describes the preparation and synthesis tests of all types of iron catalysts other than fused or precipitated. Since some of the catalyst types overlap, the following definitions as used here may be helpful: "Sintered" refers to materials heated to a high temperature to form coherent granules without the addition of substances known to be bonding agents, and "cemented" to preparations to which bonding agents were added, either with or without high-temperature treatment. "Impregnated" refers to materials impregnated with promoters but usually not heat-treated. Ordinary impregnated catalysts, in which the active component is impregnated on a porous, relatively inert material, have not been thoroughly studied. Studies of catalysts prepared from various inexpensive forms of iron oxide, such as ores and industrial residues, will be described first followed by the preparations made from metallic iron.

Sintered magnetite catalysts were studied at the Bureau of Mines¹⁵. Spheres of magnetite particles were prepared by compacting a wet paste of powdered Alan Wood magnetite in a high-frequency vibrator and extruding it through a perforated plate. The extruded material was rolled into rough spheres, sintered in air at 1200°C , crushed and impregnated with potassium carbonate. A series of catalysts with varying alkali content were tested after reduction in hydrogen (space velocity = $1,500\text{ hr}^{-1}$) at 400°C for 20 hours. The most active sample containing 0.45 K_2O per 100 Fe gave high conversions (70 per cent) of $1\text{H}_2 + 1\text{CO}$ at a space velocity of 352 hr^{-1} and 226°C . The variation of activity with alkali content (Figure 45) shows a ten-fold increase in activity as the alkali content was increased from 0.06 to 0.45 K_2O per 100Fe, followed by decreasing activity with higher alkali content. Since this series was performed at nearly constant temperatures (226 to 229°C) and conversions, these data demonstrate the influence that alkali has on selectivity. As shown in Figure 46, the average molecular weight increased with increasing alkali content up to 0.5 K_2O per 100Fe and remained essentially constant for greater amounts of alkali.

The maximum alcohol content of the distillation fractions was observed for 0.45K₂O per 100Fe, whereas the olefin content was essentially constant. Although these catalysts were robust in the raw state, their mechanical strength after reduction and after synthesis was too low for use in most

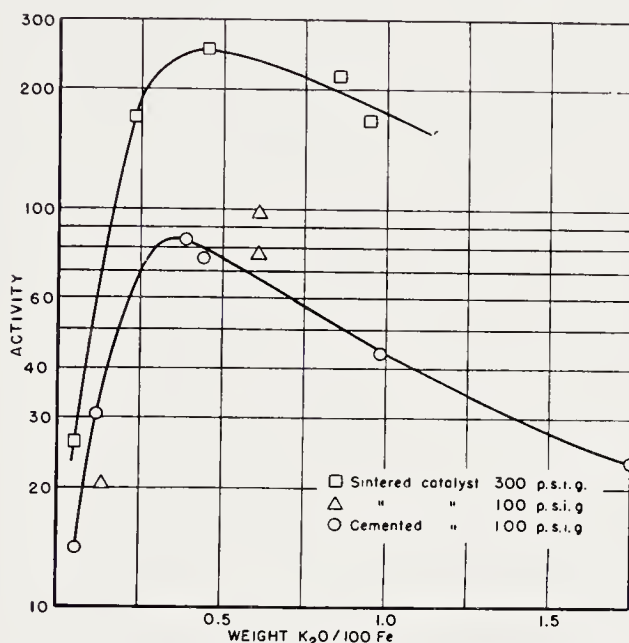


Figure 45. Variation of activity of iron catalysts with alkali content with 1H₂ + 1CO gas. (Reproduced with permission from Ref. 15)

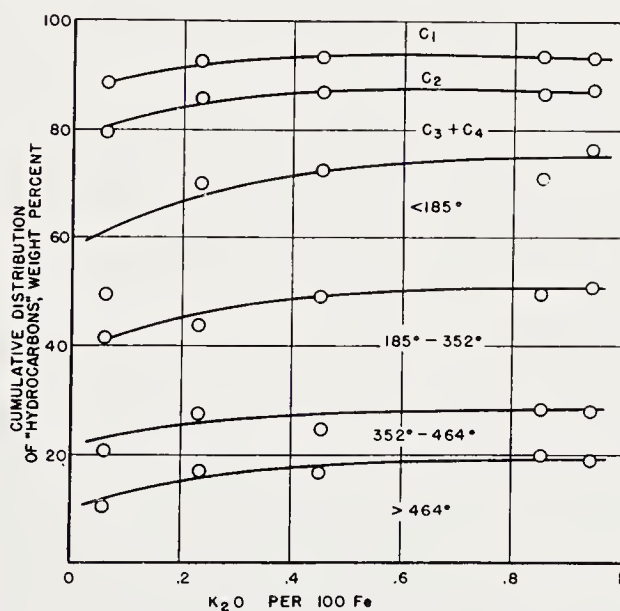


Figure 46. Variation of selectivity with alkali content for a sintered magnetite catalyst, 1H₂ + 1CO gas at 300 psig and 226-229°C. (From data of Ref. 15)

TABLE 63. SYNTHESIS BEHAVIOR OF CEMENTED IRON CATALYSTS

(1H₂ + 1CO gas at 7.8 atm. All catalysts contain about 0.5K₂CO₃ per 100Fe, except preparation with borates and silicates)

Test	166	153	134	165	175	156	187
Iron oxide	A.W. ^a	A.W. ^a	Pigment ^b	A.W. ^a	A.W. ^a	M.S. ^c	A.W. ^a
Bonding agent per 100 Fe	None	3.0Al ₂ O ₃	4.5Al ₂ O ₃	7.5Na ₂ B ₂ O ₇	6.0K ₂ B ₂ O ₇	3.5Al ₂ O ₃	15.9 water glass
Reduction in H ₂ :							
Temperature, °C	394	450	450	450	450	450	450
Hours	41	20	38	20	20	39	40
Synthesis data:							
Space velocity, hr ⁻¹	97	98	100	97	106	100	78
Temperature, °C	234	232	236	248	296	237	300
Contraction, per cent	65	65	65	66	59	65	56
Yield, g/m ³ :							
CH ₄	8.5	6.6	15.3	14.9	21.5	13.5	31.4
C ₂	8.0	6.0	13.5	8.5	—	6.9	9.4
C ₃ + C ₄	13.8	13.6	29.0	20.5	—	16.7	17.7
Liquids + solids	103	82.9	64.8	62.5	51.5	65.4	34.2

^a A.W. = Alan Wood magnetite.^b Pigment grade iron oxide, Fe₂O₃.^c M.S. = mill scale.

fixed- or fluid-bed reactors; however, this material should be suitable for the slurry process.

In further work at the Bureau of Mines¹⁸¹, powdered iron oxide was mixed with a cementing agent and heated at temperatures from 500 to 1,100°C to convert the material to a hard cake that was crushed to the desired mesh size. Moderately satisfactory catalysts were made with alumina (from aluminum nitrate solution), borax, and ball clay. Preparations with sodium water glass had poor selectivity, while samples cemented with potassium water glass or potassium borate had a very low activity. In all of these catalysts, an attempt was made to select the content of cementing agent to give adequate mechanical strength without impairing the activity and selectivity of the catalyst. With increasing concentration of bonding agent, the mechanical strength increased, but the activity and selectivity became less desirable. The attempts to balance the two effects was only moderately successful, as shown by tests of a number of representative catalysts in Table 63.

German workers tested catalysts prepared from Lautamasse and Luxmasse, residues from aluminum refining. These materials, which are usually obtained as a moist paste, contain 50 to 56 per cent iron oxide on a dry basis. A Lurgi catalyst^{31, 87} was prepared by impregnating Lautamasse with a copper-ammonium nitrate solution. The copper was precipitated with K_2CO_3 solution, dried, and reduced in hydrogen. Although this material had low activity, the rates of carbon deposition and other processes leading to catalyst disintegration were correspondingly low, so that the catalyst operated satisfactorily at 275°C. A catalyst of Brabag, prepared by impregnating Lautamasse with alkali carbonates, also had a relatively low activity and required operating temperatures of 250 to 270°C. Ruhrchemie⁷¹ used Luxmasse in a catalyst containing 100Fe:3.5Cu:100 granosil (bleaching earth):10 kieselguhr. This preparation was induced in water-gas at atmospheric pressure. As observed for catalysts containing Lautamasse, this preparation required a relatively high temperature, 255°C, for 60 per cent conversion of water-gas at a space velocity of 100 hr⁻¹ at 15 atmospheres. At Rheinpreussen¹⁴², alkalized Lautamasse and Luxmasse catalysts were also found to require high-operating temperatures. In general, due to the high-operating temperatures as well as specific catalytic effects, these preparations gave a low-molecular-weight product with a high-olefin content. Data for tests of two German catalysts of this type and a similar preparation of the Bureau of Mines are given in Table 64.

At the Bureau of Mines, a number of iron ores have been tested in the synthesis after impregnation with alkali (K_2CO_3 or KNO_3) and reduction in hydrogen. Many of these samples were moderately active and have desirable selectivity in the synthesis, as shown by data in Table 65. Appar-

ently the requirement for active catalysts from iron oxide are the following:

- (a) The raw material should contain a high concentration of iron oxide.
- (b) The raw material should not contain high concentrations (above 15 per cent) of certain oxides, such as silica, in combination with iron oxide in

TABLE 64. TESTS OF CATALYSTS PREPARED FROM LAUTAMASSE AND LUXMASSE

	Lurgi	Ruhrchemie	Bureau of Mines
Source of iron	Lautamasse	Luxmasse	Luxmasse
Composition, %			
Cu	3 ^a	3.5 ^b	—
Granosil	—	100	(K ₂ O = 0.5)
Kieselguhr	—	10	—
Alumina	—	—	3.5 ^a
Pretreatment			
Gas	H ₂	Water gas	H ₂
Temperature, °C	^c	^c	450
Synthesis			
Gas	1H ₂ + 1.6CO	1.2H ₂ + 1CO	1H ₂ + 1CO
Space velocity, hr ⁻¹	100	100	—
Recycle ratio	3	1.5-2.5	0
Pressure, atm.	20	15	7.8
Temperature, °C	275	255	245
Conversion, %	85	60	65
Total "hydrocarbons," g/m ³	170	—	113
C ₁ + C ₂	35	(C ₂ -C ₄ 14)	33
C ₃ + C ₄	32	—	33
Alcohols	5	—	—
C ₅ +	98	63	36
Distillation of C ₅ +, wt-%; olefins, vol.-% in parenthesis			
<200°C	71 (75)	39 ^d	<185° 61
200-320°C	21 (60)	31	185-352° 35
320-350°C	8}	30	—
>350°C	0}		4

^a Based on weight of resulting catalyst.

^b Based on 100Fe.

^c Not specified.

^d Octane number = 72.

the form of compounds that are difficult or impossible to reduce at usual reduction temperatures (<600°C).

(c) The raw material should not contain high concentrations of specific poisons such as sulfates or chlorides.

For the fluidized process, a variety of catalysts prepared by impregnating inexpensive ores or mill scale with about 0.5 per cent K₂O have been de-

scribed. Roberts¹⁴³ sintered a mixture of hematite plus 2 per cent potassium carbonate at 1,000°C and then extracted the alkali until only 0.5 per cent remained. Walker¹⁹⁶ employed mill scale impregnated with aqueous potassium carbonate or nitrate solution to give 0.5 to 2.0 per cent K₂O. Iron pyrites roasted in air at high temperatures and impregnated with alkali have been described as satisfactory, inexpensive catalysts for the fluidized synthesis. The oxidation removes the sulfur rather completely, as shown by data in Table 61. Seelig, Weck, Voss, and Zisson¹⁶⁸ studied a sample of roasted pyrites in the synthesis in a fluidized reactor. One portion was used without further treatment, a second was impregnated with aqueous potassium carbonate solution (0.52 per cent K₂CO₃ corresponding to 0.53

TABLE 65. SYNTHESIS TESTS OF IRON ORES AT BUREAU OF MINES
(1H₂ + 1CO gas at 7.8 atm. All preparations contained about 0.5 K₂CO₃ per 100Fe)

Test Ore	181 Goethite	233 Siderite	202 Limonite	232 Alabama Ore
Reduction in H ₂				
Temperature, °C	450	400	450	400
Hours	24	40	24	40
Synthesis data:				
Space velocity, hr ⁻¹	100	98	93	99
Temperature, °C	230	232	294	256
Contraction, %	65	66	9	66
Yield, g/m ³ :				
CH ₄	7.9	4.6	—	12.0
C ₂	7.9	4.8	—	7.9
C ₃ + C ₄	17.5	11.4	—	22.2
Liquids + solids	68.3	72.2	—	83.7

K₂O per 100Fe), and a third was mixed with 0.1 per cent powdered potassium carbonate, and at 72-hour intervals further additions of this amount of powdered potash (each corresponding to 0.1 per cent K₂CO₃ based on catalyst weight) were made to the reactor, so that the final alkali in the system was 0.47 per cent K₂CO₃. The catalysts were reduced in hydrogen (space velocity = 1,000–1,500 hr⁻¹) at 17 atmospheres and 371°C until the formation of water ceased. Testing conditions were 315°C and 18 atmospheres of 2H₂ + 1CO gas at fresh feed space velocities of 1,000–1,500 hr⁻¹ and a recycle ratio of 2. The activity represented by carbon monoxide-conversion and the alkali content as a function of time are given in Figure 47. The conversion for the alkali-impregnated preparation (solution-promoted) was about 99 per cent. For the sample promoted by addition of solid potassium carbonate, the conversion increased with alkali addition, approaching the activity of the solution-promoted sample. Selectivity data

in terms of carbon balances are shown in Figure 48. Here the yield of liquid hydrocarbons and oxygenated organic molecules increased with increasing alkali content. It appears from Figures 47 and 48 that the mode of alkali-

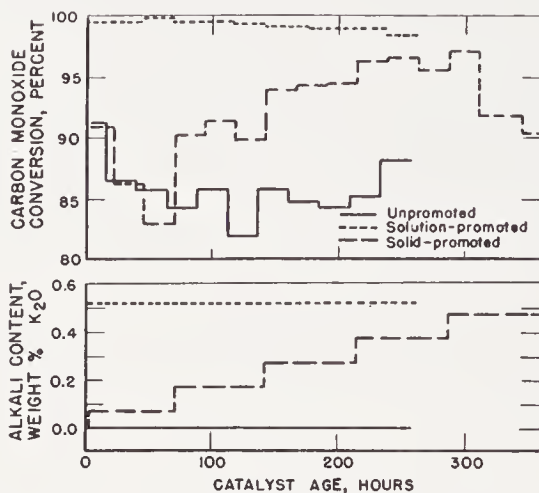


Figure 47. Variation of activity and alkali content in fluidized tests of roasted pyrites catalysts. (Reproduced with permission from Ref. 168)

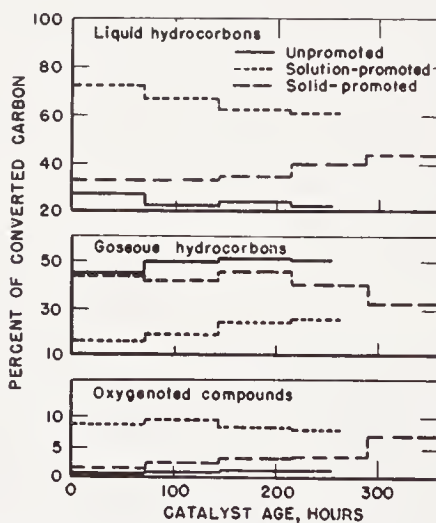


Figure 48. Selectivity as a function of amount and mode of addition of alkali. Roasted pyrites catalyst in fluidized reactor. (Reproduced with permission from Ref. 168)

addition, impregnation from solution or addition of powdered alkali to the reactor, does not give greatly differing results.

The impregnated catalysts described in this section have been prepared by adding a solution of promoters to various forms of iron or iron oxide, and are not the usual type in which porous material is treated with solutions of iron salts. Little attention has been given to the latter type of impreg-

nated catalyst, apparently for the following reasons: (a) These catalysts are not very active, and (b) the active metal, iron, is the least expensive of the catalyst materials, and hence there is no advantage to be gained by minimizing the amount of iron used.

Decomposition catalysts were used in early experiments of Fischer and Tropsch, but have not been given much consideration by later workers. These materials have relatively low activity and are usually obtained as fine powders that require shaping into granules for use in fixed-bed reactors. Fischer and Tropsch⁶² in 1926 studied the effect of alkali on iron decomposition catalysts in the synthesis at atmospheric pressure. Although only low conversions and short lives were obtained, the influence of alkali was

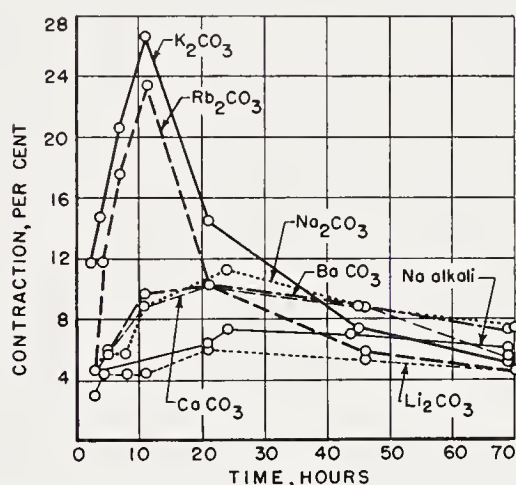


Figure 49. Effect of adding 0.5 per cent alkali on activity of 4 grams of Fe-Cu (4:1) catalyst. (From Ref. 62)

clearly and accurately defined. For potassium carbonate, maximum activity and useful life were obtained at concentrations of 0.32 per cent. The effectiveness of the addition of 0.5 per cent various alkali and alkaline-earth carbonates is shown in Figure 49. For the series of alkali carbonates, the activity increased in the order lithium, sodium, potassium, and rubidium; the yields of wax increased in the same order. Lithium and sodium carbonates, as well as alkaline-earth carbonates, gave equal or poorer results than the preparation containing no alkaline promoter.

The catalysts described thus far have been prepared by sintering, cementing, or impregnating various forms of iron oxide. Another type of catalyst employs metallic iron as a starting material. Michael^{71, 89, 206} prepared a catalyst by sintering carbonyl iron (2–5 micron particles) impregnated with a concentrated solution of borax (1 per cent Na₂B₄O₇ based on iron) for use in the hot-gas-recycle process. The impregnated iron was formed into 1 cm cubes and sintered in hydrogen at 850°C for 4 hours. The sintered cubes

were cooled in hydrogen and transferred in carbon dioxide to the reactor. This material had a relatively low activity, giving conversions of 78 to 82 per cent of $0.9\text{H}_2 + 1\text{CO}$ gas at 20 atmospheres and $320\text{--}330^\circ\text{C}$ with a recycle ratio of 100. The products from this process in grams per cubic meter were: Methane plus ethane, 35; ethylene, 10; C_3 , 17 (70–80 per cent olefin); C_4 , 14 (70–80 per cent olefin); gasoline (to 200°C), 83; diesel oil ($200\text{--}320^\circ\text{C}$), 21; wax, 1.5; oxygenated molecules (largely ethanol plus propanol), 14. The life of these catalysts at best was only slightly in excess of 2 months. It should be noted that hard, porous granules can be prepared from powdered iron by the sintering treatment employed by Michael without the presence of sodium borate. These sintering techniques are well known in powder metallurgy for the production of porous iron for bearings, etc. The possibility of sintering powdered iron into robust, porous granules of desired shapes by these techniques, together with suitable activation procedures involving oxidation, reduction, and carburization, has not been investigated.

Recently at the Bureau of Mines, very promising massive iron catalysts^{19, 172} from steel shot or turnings have been developed for the oil-circulation process. The steel was oxidized with steam at $550\text{--}600^\circ\text{C}$, the temperature being the highest that can be employed without causing the oxide film to cement the particles together. For steel spheres, only 1–3 per cent of the iron was oxidized, while for the steel turnings 10–20 per cent. The oxidized material was alkalinized by immersion in an aqueous potassium carbonate solution, dried, and reduced in hydrogen at 400 to 450°C . The concentration of alkali for maximum activity was only about one-tenth of that required for fused catalysts.

In small, fixed-bed units as well as in an oil-circulation pilot plant, these materials operated at temperatures from 250° to 270°C for a conversion of 65 to 70 per cent with a space velocity of 300 of $1\text{H}_2 + 1\text{CO}$ gas at 20 atmospheres. Usually the temperature can be decreased as the synthesis proceeds. The life of these catalysts appears to be very long, and the mechanical properties of the catalysts are relatively unchanged, since the core of the particles is inert massive iron that is not carburized or oxidized under synthesis conditions. The massive iron preparations are similar to the early Synthol catalysts of Fischer and Tropsch⁶¹, alkalized iron filings; however, these early preparations had not been activated by steam.

Data typical of synthesis in the oil-circulation pilot plant with oxidized steel (SAE 1018) turnings are shown in Table 66. In the second and third operating periods the yields of $\text{C}_1 + \text{C}_2$ hydrocarbons were higher than desired. Analyses of catalyst samples removed from the reactor after 855 hours indicated that the potassium oxide content had decreased from its initial value of 0.02 to 0.01 per cent. At this time an alcoholic solution of

potassium hydroxide was added to the bottom of the reactor to increase the alkali content to 0.04 per cent. The added alkali produced a permanent effect on selectivity and decreased the activity slightly. Catalyst samples were removed from the top of the reactor during the experiment. After extraction with toluene, the turnings were agitated in a mechanical shaker to dislodge the active layer. In Figure 50 analyses of this material by magnetic and x-ray methods are compared with analyses of a fused catalyst

TABLE 66. SYNTHESIS WITH OXIDIZED STEEL TURNINGS IN OIL-CIRCULATION PILOT PLANT^a

(Experiment 37: 1H₂ + 1CO feed at 21.4 atm.)

	Catalyst Age (hr)						
	231- 327	423- 716	855- 879	903- 927 ^b	1239- 1287	1503- 1527	2174- 2390
Fresh feed space velocity, hr ⁻¹	401	601	600	599	674	700	401
Max. converter temp., °C	270	283	270	270	280	290	290
Temperature differential, °C	3	6	6	6	5	7	6
Gas recycle ratio	1:1	1:1	1:1	1:1	2:1	2:1	1.5:1
Usage ratio, H ₂ /CO	0.89	0.90	0.95	0.88	0.82	0.85	0.82
H ₂ + CO conversion, %	70.5	77.6	72.9	68.5	70.8	70.0	79.4
C ₁ + C ₂ yield, g/cm H ₂ + CO converted	39.7	58.3	44.2	39.0	33.6	37.5	36.9
Product distribution, wt.-% C ₃ +, as:							
Gasoline (C ₃ + to 204°C)	67.1	85.3	74.0	55.0	57.5	72.3	70.2
Diesel (204-316°C)	15.5	8.2	14.5	17.4	14.6	16.3	13.3
Heavy distillate (316-340°C)	9.5	4.5	8.5	13.6	13.3	7.6	10.4
Wax (>450°C)	7.9	2.0	3.0	14.0	14.6	3.8	6.1

^a From Ref. 19.

^b Alkali added prior to this period.

during synthesis in the same reactor. The active layer of the turnings oxidized during synthesis at a considerably lower rate.

Skeletal iron catalysts have not been investigated thoroughly. Fischer and Meyer⁵³ found that skeletal iron-silicon or iron-aluminum catalysts were inactive at temperatures up to 260°C. However, in a patent, Black and Kearby²¹ claim satisfactory activity and selectivity and low-carbon deposition for iron-silicon and iron-aluminum preparations. In tests of Fe-Si catalysts the activity was essentially independent of extent of leaching, whereas the optimum selectivity was attained at a low value of silica removal. A similar optimum in selectivity was claimed for small extents of extraction of iron-aluminum preparations. The selectivity of these catalysts was good for the high-synthesis temperatures employed, 316 to 343°C;

however, the activity was relatively low compared with precipitated or fused-iron catalysts.

Schwarzheide Tests

With the advent of World War II, the German supply of cobalt from the Belgium Congo was drastically curtailed, and in 1943 plans were made for employing iron catalysts in the existing synthesis plants designed for cobalt catalysts. The companies actively engaged in Fischer-Tropsch research were requested to develop catalysts for use under the rather restricted reaction conditions imposed by the existing plants. The task of choosing the best catalyst was difficult, and the Reichsamt für Wirtschaftsaufbau arranged a

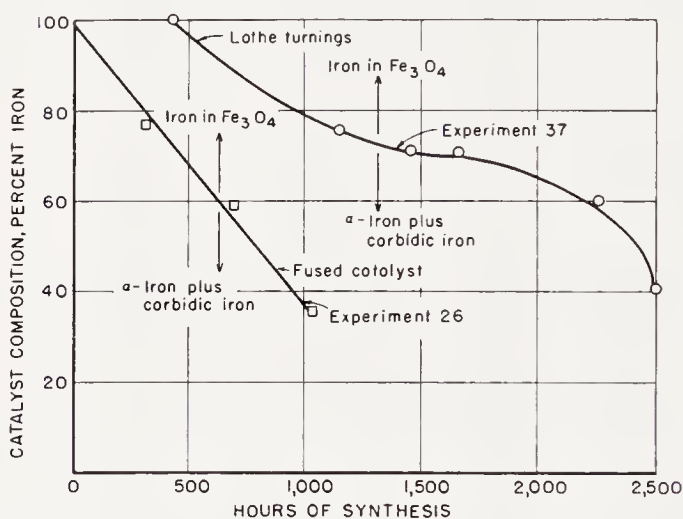


Figure 50. Change in catalyst composition during synthesis in the pilot plant. (Reproduced with permission from Ref. 19)

comparative experiment, the "Reichsamtversuch," at the Braunkohle-Benzol A. C. plant in Schwarzheide-Ruhland in September 1943.

The tests were performed in a reactor of 5-liter capacity of the same dimensions as the water-cooled, double-tube, standard medium-pressure reactors (identical to a single-tube of a medium-pressure reactor). The catalyst was placed in the annular space between 24-mm O.D. and 44-mm I.D. tubes; the depth of the catalyst charge was 5 m. The conditions for the comparative tests were:

1. Standard water-gas ($1.25H_2 + 1CO$ with 12 per cent inerts) in one stage without recycle.
2. Synthesis pressure = 10 atm.
3. Maximum temperature = $225^\circ C$.
4. The desired duration of the test without reactivation of the catalyst was 3 months.

5. The products should be as similar as possible to those from the medium-pressure synthesis with cobalt catalysts.

TABLE 67. COMPOSITION AND PRETREATMENT OF CATALYSTS USED IN SCHWARZHEIDE TESTS

Company	Promoters per 100Fe			Carrier per 100Fe	Apparent Density (g/cc)	Pretreatment (at Atmospheric Pressure Unless Specified)
	Alkali	Copper	Other			
Kaiser-Wilhelm Institut	$K_2CO_3^a$ 1.0	1	—	None	1.02	Water gas, 325°C, 0.1 atm. 24 hours
	$K_2CO_3^b$ 0.75	1	—	None		
Lurgi	$K_2SiO_3^a$ 30 K_2O 9	10	—	—	0.79	H_2 , 250–300°C to 30 per cent reduction
Brabag	$K_2CO_3^a$ 0.5	10	—	None	1.37	Water gas, 230–240°C, 48 hours
	$K_2CO_3^b$ 0.5	10	Zn 10	None		
I.G. Farben	$K_2CO_3^{a, b}$ 1.0	None	Al_2O_3 - CaO 2.0	None	2.27	H_2 , 450–500°C
Ruhr-chemie	$K_2CO_3^{a, b}$ 0.5–2.0	5	—	Kieselguhr	0.44	H_2 , 300°C
	$K_2CO_3^c$ 0.5–2.0	5	CeO_2 10	Kieselguhr 50		
Rhein-preussen	$K_2CO_3^{a, b}$ 0.5–1.0	5	—	Dolomite	0.68	H_2 , 300–400°C plus water gas, 245°C

^a From Ref. 68.

^b From Ref. 131.

^c From Ref. 72.

6. Within the limits of items 1 to 3, the operator was permitted to vary conditions as desired.

The compositions of the catalyst were not divulged at the time of the tests, and some of the subsequent reports presenting information on components are contradictory. The six companies participating in the comparison and their catalysts and condition of pretreatment are given in Table 67. All of the catalysts were of the precipitated type, except for the fused material used by I. G. Farben. Preparative methods for many of these

catalysts have already been described. The KWI catalysts were prepared from iron-nitrate solutions containing equal amounts of ferrous and ferric ion. The first charge, which contained $0.25\text{K}_2\text{CO}_3$ per 100Fe , produced yields of gaseous and liquid hydrocarbons that were too high for the purposes of the tests. Therefore, the catalyst was replaced by one containing

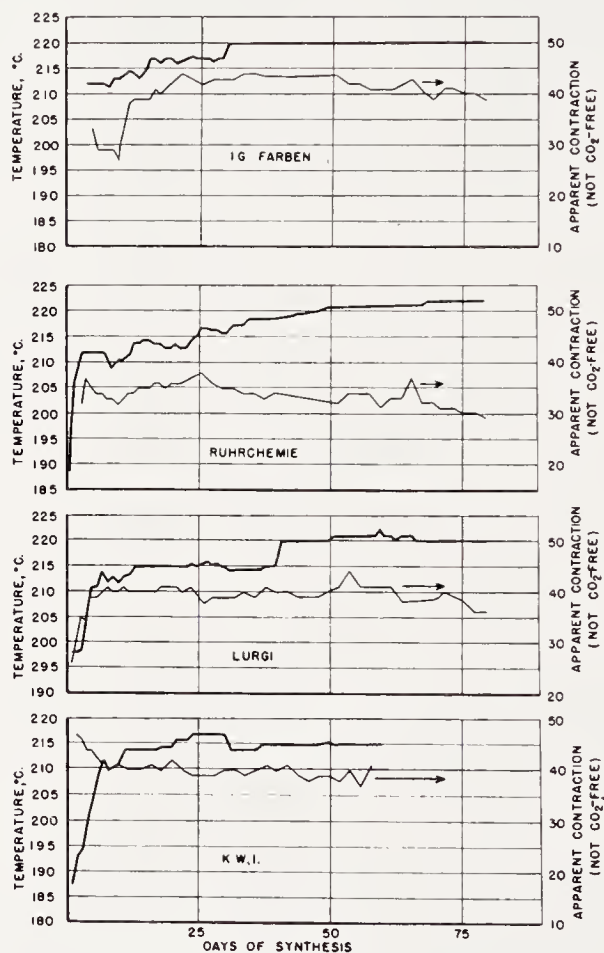


Figure 51. Temperatures (heavy curves) and conversions in Schwarzheide tests.

$0.75\text{K}_2\text{CO}_3$ per 100Fe , which had better selectivity. Initially, this catalyst operated at $180\text{--}190^\circ\text{C}$, and in the course of the 3-month test the temperature had to be increased to 224° . The Lurgi catalyst temperature had to be increased only 6°C , from 215 to 221°C , in the period of testing. The first two charges of Brabag catalyst were unsuccessful, due to catalyst disintegration, possibly due to improper pretreatment. The third charge was performed satisfactorily. The I. G. Farben. and Ruhrchemie catalysts encountered no difficulty, and the first charges operated throughout the entire testing period. The Rheinpreussen catalyst had "coking" difficulties and

had to be replaced four times. I. G. Farben. used a fused preparation at least similar to their WK17 catalyst.

Operating data for the four reactors that did not require frequent re-charging are given in Figure 51. After somewhat erratic behavior in the first few days, the conversions were maintained at moderately high values at either constant temperature or with small periodic increases in temperature. The KWI, Lurgi, and I. G. Farben. catalysts were maintained at

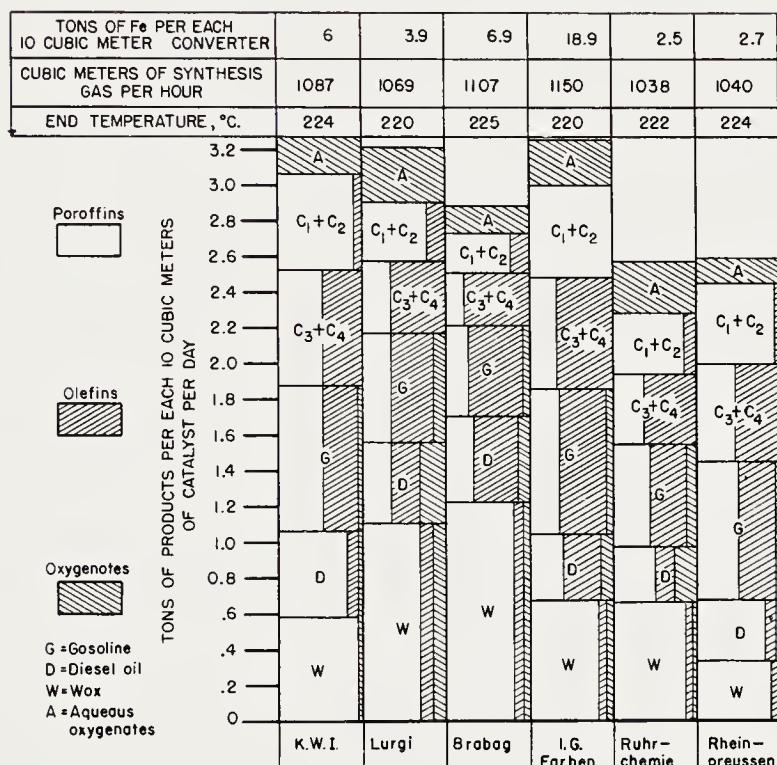


Figure 52. Productivity of catalysts in the Schwarzheide tests. (Reproduced with permission from Ref. 131)

about 40 per cent apparent contraction (not CO₂-free), while the contraction of the Ruhrchemie catalyst was held at about 35 per cent.

The synthesis products were given a detailed analysis consisting of a standard gas analysis of exit gas, low-temperature precision distillation of gasol fraction, precision distillation of condensed hydrocarbons, and chemical determinations of unsaturation, hydroxyl and ester numbers. Since the latter determinations were made on narrow-distillation fractions, it was possible to estimate the molecular weight of these components and compute the weight per cent of olefins, alcohols, and esters. Detailed carbon number distributions, as well as fragmentary information about the extent of chain branching, are presented later (p. 207). A graphical comparison of products from these tests in terms of space-time yields is given in Figure 52.

The highest space-time yields were obtained from the KWI and I. G. Farben. catalysts, with the Lurgi catalyst a close third. The lowest yields were obtained from the Ruhrchemie catalyst. The catalysts of Lurgi and Brabag produced the lowest percentage of methane and the highest percentage of wax. In general, the selectivity of all preparations was quite good and possibly small adjustment of the alkali content would have improved the selectivity of the catalysts producing the highest yields of methane.

The results of the tests have been summarized by Pichler¹³¹ as follows:

"1. The total yields per volume of catalyst (not per unit weight, however) were of the same magnitude in spite of the use of very different types of iron catalysts.

2. The synthetic products were composed of paraffins, olefins, and oxygenated products. The amount of these components varied over wide limits. In all cases the olefin content of the product decreased with increasing molecular weight of the hydrocarbon, while the oxygenates seemed to have a maximum in the low range (C_2) and a second maximum in the diesel-oil fraction.

3. No promoters are known (except alkali) which are indispensable for the activities of iron catalysts. In contrast to cobalt catalysts, supports are not decisive for the results obtained.

4. Iron catalysts for medium pressure require pretreatment with reducing gases. A very cautious reduction of fused-iron catalysts with very pure hydrogen was necessary, while active (precipitated) catalysts could be pretreated with synthesis gas only."

In addition the tests demonstrated that the activity of a fused catalyst per unit volume was as high as those of precipitated preparations. The space-time-yield from iron catalysts under the conditions of the comparative test were equal to those of the medium-pressure synthesis with cobalt catalysts. A second Reichsamtversuch, in which only Ruhrchemie and I. G. Farben. participated, was held, but these tests were terminated after 170 hours due to circumstances related to the war⁷². Ruhrchemie employed a 100Fe:5Cu:10CaO:50 kieselguhr at 10 atmospheres and 220°C with a recycle ratio of 0.62 to 1. Apparently no other information about these tests is available.

The Reichsamtversuch was indecisive in that no iron catalyst was chosen as a successor to the cobalt catalysts. The results, however, demonstrated that major improvements had been made in iron catalysts in the period 1938 to 1943. Most of the iron catalysts employed in the tests had a more desirable selectivity than cobalt catalysts for the production of gasoline, although the products of iron catalysts were considered inferior to cobalt for the production of synthetic soap required by the German war economy.

Surface Areas and Pore Volumes of Iron Catalysts

Surface areas of fused-magnetite (ammonia synthesis) catalysts have been studied in several laboratories, and it was the investigations of the adsorption of various gases on catalysts of this type that led to the develop-

TABLE 68. SURFACE AREAS AND ACTIVITIES OF IRON SYNTHETIC AMMONIA CATALYSTS^a

Catalyst			Reduction Conditions		Surface Area (m ² /g) ^b	Activity, (%) NH ₃ ^c
Number	Composition (weight-per cent)					
	Al ₂ O ₃	K ₂ O	Hours	Temp. (°C)		
973	0.15	None	124	300-350	0.38	3.3
			54	375-500		
973	0.15	None	96	300-400	0.94	—
954	10.2	None	48	350-450	8.4	8.2
			48	450-500		
930	None	1.07	48	350-450	0.43	5.3
958	0.35	0.08	36	350-450	1.9	10.4
			36	450-500		
931	1.30	1.59	18	300-350	3.3	12.3
			65	350-450		
			18	450-530		
931	1.30	1.59	Same as above plus several partial oxi- dations and reduc- tions at 450°C.		2.5	—

^a Data from Ref. 43.

^b Estimated by "point B" method.

^c Per cent ammonia produced in exit gas at 450°C, 100 atm., and a space velocity of 3H₂ + 1N₂ gas of 5,000. Equilibrium percentage of NH₃ = 16.4.

ment of BET method²⁷ of estimating surface area from physical adsorption isotherms. Studies of precipitated and other types of iron catalysts are less numerous.

Raw, fused-magnetite catalysts have virtually no internal surface, and the porosity and surface area are developed in the reduction. The surface area of fused catalysts depends upon the type and amount of the structural promoters as well as the reduction conditions. Data of Emmett and Brunauer⁴³ (Table 68) demonstrate the effect of alumina and potassium oxide

content and of reduction conditions on surface area and productivity of catalysts in the ammonia synthesis. The surface area increased with the alumina content, but not with the alkali content. For a given catalyst lower

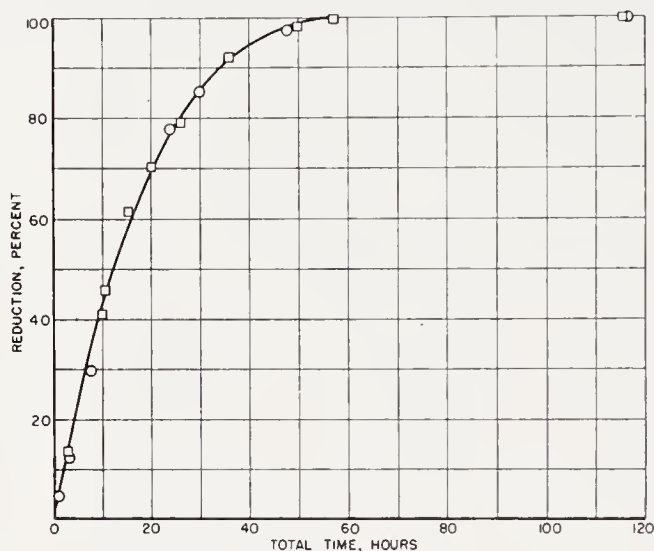


Figure 53. Extent of reduction of catalyst D-3001 at 450° and 1000 space velocity as a function of time. Circles represent data taken progressively on a single sample for surface area measurements and squares represent independent determinations on separate samples for pore volume measurements. (Reproduced with permission from Ref. 78)

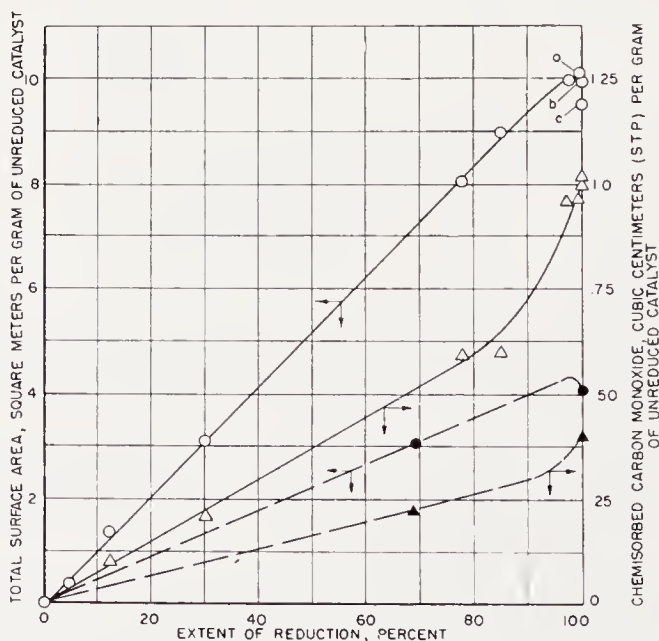


Figure 54. Variation of surface area and of carbon monoxide chemisorption with extent of reduction. The surface areas of samples reduced at 450°C are represented by \circ and their carbon monoxide chemisorptions by Δ . The solid points represent samples reduced at 550°C. (Reproduced with permission from Ref. 78)

surface areas were observed as the temperature of reduction was increased, and the area was also decreased by sintering at high temperatures and by partial oxidation and reduction. The yields of ammonia did not parallel the surface areas, but were considerably greater per unit surface area for catalysts containing alkali. These and other data demonstrate that alumina and other similar oxides are structural promoters responsible for production of high-area structures upon reduction. Alkali does not increase the surface

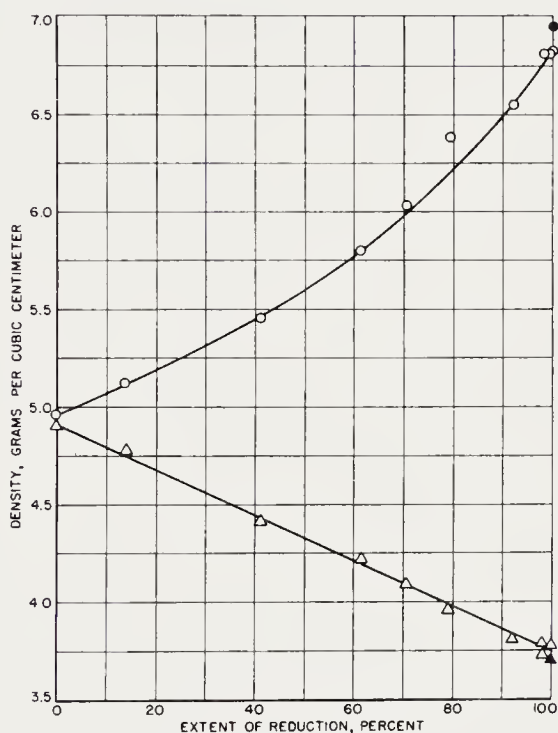


Figure 55. Variation of mercury and helium densities with extent of reduction. Absolute densities of catalysts reduced at 450°C measured by displacement of He, are represented by O; their densities measured by displacement of Hg are represented by Δ. Solid points represent a 550°C reduction. (Reproduced with permission from Ref. 78)

area, but does advantageously modify the chemical nature of the catalyst both for the ammonia and hydrocarbon syntheses.

Hall, Tarn, and Anderson⁷⁸ determined surface areas and pore volumes of fused 100Fe:6.9MgO:0.9K₂O catalyst (D3001) that has been used as a standard in many of the synthesis tests at the Bureau of Mines. First, the change in pore geometry as a function of extent of reduction was investigated. The course of the reduction, shown in Figure 53, indicates that the rate of oxygen removal decreases with extent of reduction, the process being essentially complete in 60 hours. Figure 54 shows the variation of surface area and carbon monoxide chemisorption at -195°C. For reduction at 450°C (open circles), the surface area increased linearly with extent of

reduction to about 90 per cent. Above this value, the slope of the curve decreases and becomes negative near 100 per cent. Point *a* corresponds to 99.4 per cent reduction at 63 hours, and points *b* and *c* to complete reduction at 85 and 116 hours, respectively. The chemisorbed carbon monoxide increased linearly with reduction up to about 85 per cent, and for greater reduction the curve bends sharply upward. Fragmentary data for reduction at 550°C (solid circles and triangles) suggests that the process follows the same pattern as 450°C, but the surface areas are only 40 per cent of those obtained at 450°C. Experimental values for mercury (determined at an

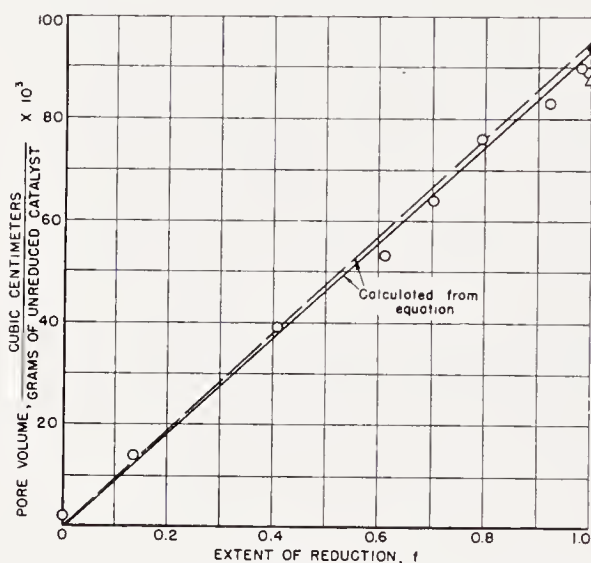


Figure 56. Variation of pore volume per gram of unreduced catalyst with extent of reduction of catalyst D-3001, where \circ represents reduction at 450°C, \bullet represents reduction at 550°C and \triangle represents a 115 hour reduction and sintering at 450°C. (Reproduced with permission from Ref. 78)

absolute pressure of 1,150 mm Hg) and helium densities are given in Figure 55, where the helium densities increased with extent of reduction and the mercury densities decreased. The pore volumes, the differences of the reciprocals of the mercury and helium densities, were directly proportional to the extent of reduction, as shown by the experimental points in Figure 56. Data from the smoothed curves of Figures 54 and 55 have been used for computing average pore diameters by the equation of Emmett and DeWitt for even decades of reduction in Table 69. The average pore diameter for reduction at 450°C varied from 330–350 Å and increased slightly near 100 per cent reduction due to deviation of the area-reduction curve from a straight line. The values for the volume of mercury displaced per gram of unreduced catalyst remain essentially constant as the reduction proceeds. Apparently the mercury does not penetrate or wet the catalyst,

and the constancy of the values indicates that the external volume of the catalyst particles remains unchanged in the reduction. If this is the case, the

TABLE 69. DENSITY AND ADSORPTION DATA OF CATALYST D-3001 AS A FUNCTION OF THE EXTENT OF REDUCTION^a

Per cent Reduction	d_{He} (cc/g)	d_{Hg}^b (cc/g)	Volume ^c of Hg Displaced (cc/g Unreduced Catalyst)	Pore ^d Volume (cc/g Unreduced Catalyst)	\bar{d}^e Å	Surface Area (m ² /g Unreduced Catalyst)	V_m^f (cc/g) (STP)	V_{CO}^g (cc/g) (STP)	V_{CO} V_m
0.0	4.96	4.91	0.203	0.002	—	0.0	0.0	0.0	—
10.0	5.07	4.80	.203	.010	400	1.0	.23	.09	0.39
20.0	5.18	4.68	.203	.018	343	2.1	.48	.16	.33
30.0	5.32	4.56	.203	.027	348	3.1	.71	.22	.31
40.0	5.45	4.45	.202	.035	333	4.2	.96	.29	.30
50.0	5.60	4.33	.204	.043	331	5.2	1.29	.36	.28
60.0	5.77	4.22	.201	.052	330	6.3	1.44	.43	.30
70.0	5.98	4.10	.200	.061	334	7.3	1.67	.50	.30
80.0	6.22	3.98	.200	.071	338	8.4	1.92	.57	.30
90.0	6.50	3.87	.199	.082	349	9.4	2.15	.67	.31
95.0	6.65	3.81	.199	.086	348	9.9	2.26	.83	.37
100.0	6.82	3.75	.198	.089	352	10.1	2.31	1.00	.43
100.0 ^h	6.82	3.78	.197	.088	371	9.5	2.20	1.00	.45
100.0 ⁱ	6.95	3.71	.201	.094	917	4.1	.94	.38	.40
68.9 ⁱ	—	—	—	—	832	3.1	.71	.22	.31
KCl ^j	1.983	1.978		.000					
	1.984	—							

^a All reductions were made with a flow of 1,000 volumes of pure H₂ gas per volume of catalyst space per hour and at 450°C except where otherwise noted. The catalyst was in all cases 6 to 8 mesh. From Ref. 78.

^b Determined at an absolute pressure of 1,100 mm of Hg.

^c $V_x = (1 - f)d_x$, where d_x is the helium or mercury density, and f is the fractional weight loss on treatment.

^d Difference between the volume of Hg and He displaced.

^e $\bar{d} = 4(\text{pore volume})/\text{surface area}$, (c.f. Ref. 44).

^f Volume of nitrogen corresponding to a monolayer, per gram of unreduced catalyst.

^g Volume of carbon monoxide chemisorbed at -195°C per gram of unreduced catalyst.

^h This row of data was obtained on a sample reduced for 116 hours at 450°C.

ⁱ These data were obtained on samples reduced at 550°C.

^j KCl was used to check our calibrations; the observed values are shown in the upper row and the literature value is below.

pore volume can be computed directly from the equation

$$\text{Pore volume} = (V_0 - V_F) f$$

where V_0 and V_F are the volumes of helium displaced by the raw catalyst

and the completely reduced catalyst per gram of raw catalyst, respectively, and f the extent of reduction. V_0 and V_F may be determined experimentally or computed from the density of components. The equation fits the experimental data very well as shown by the solid and broken lines in Figure 56.

A simple explanation of the above results involves the following premises: (a) The external volume of the catalyst does not change during reduction, the pore structure results from the removal of oxygen. (b) Once initiated the reduction proceeds very rapidly in that portion, nearly but not quite, to

TABLE 70. DENSITY AND ADSORPTION DATA OF SYNTHETIC-AMMONIA-TYPE CATALYSTS AS A FUNCTION OF REDUCTION TEMPERATURE^a

Catalyst	Reduction Temp. ^b	V_m cc/g (STP)	V_{CO} cc/g (STP)	$\frac{V_{CO}}{V_m}$	Surface Area (m ² /g)	Volume of Hg Displaced (cc/g)	Pore ^c Volume, (cc/g)	\bar{d} ^d Å
D-3001	450	2.31	1.00	0.43	10.1	0.198	0.089	371
D-3001	550	0.94	0.38	.40	4.1	.201	.094	917
D-3006	450	2.15	.72	.34	9.4	.194	.086	366
D-3006	500	1.21	.42	.35	5.3	.198	.091	687
D-3006	550	1.02	.32	.31	4.5	.195	.090	800
D-3006	600	0.46	.10	.22	2.0	.193	.092	1840
D-3006	650	.38	.12	.32	1.6	.199	.097	2420
D-3006 ^e	—	—	—	—	—	.201	—	—

^a All data given in terms of grams of unreduced catalyst. From Ref. 78.

^b The D-3006 samples were 4- to 6-mesh U. S. Standard screen fractions reduced in pure dry H₂ flowing at a rate of 2,000 volumes of gas per volume of catalyst space per hour.

^c Difference between the volumes of Hg and He displaced.

^d $\bar{d} = 4(\text{pore volume})/(\text{surface area})$, (c.f. Ref. 44).

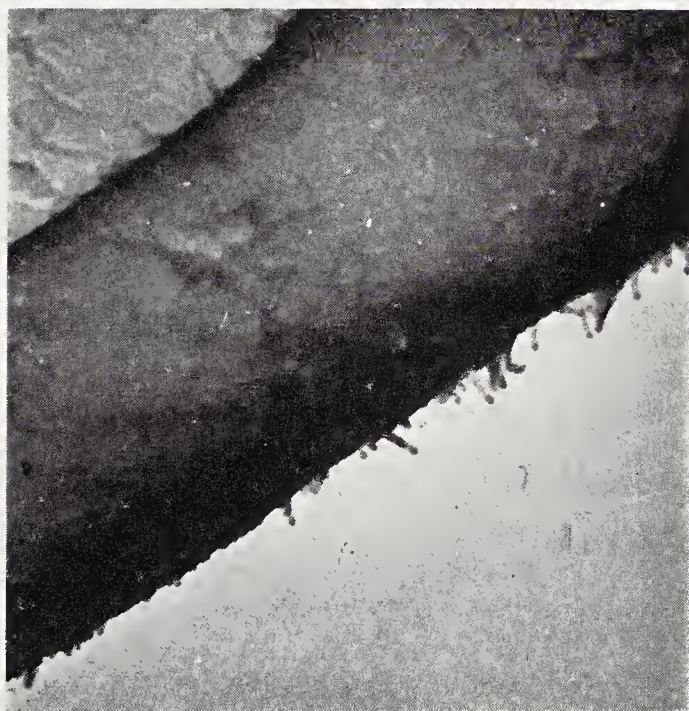
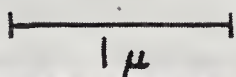
^e This was an unreduced sample.

completion. The reduction proceeds directly from Fe₃O₄ to Fe. (c) The reduced portion is quickly transformed to a relatively stable structure with a constant pore diameter. (d) On a macroscopic scale the reduction begins at the external surface and moves uniformly inward. (e) Residual iron oxide not reduced initially may act as a structural promoter, and on its removal the surface area decreases slightly.

As the temperature of reduction was increased, the surface area decreased, but the external volume of the catalyst particles still remained unchanged as shown for data in Table 70 for catalyst D-3001 and a preparation of similar composition, D-3006. Variation of the reduction temperatures of fused catalysts provides a method for "tailor-making" catalysts of desired average pore diameters.



a



b

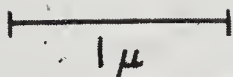


Figure 57. Electron micrographs of silica replicas of reduced fused iron catalysts. Folded specimen in b shows the profile of replica surface. (Reproduced with permission from Ref. 113)

McCartney and Anderson¹¹³ prepared electron micrographs of replicas stripped from polished surfaces of particles of catalyst D-3001. The replicas from raw catalysts showed no structure whereas the replicas from particles reduced at 450 or 550°C showed a variety of peaks and ridges whose shortest dimension varied between 500 and 800Å as shown in Figure 57. No particular differences were observed for samples reduced at 450 or 550°C.

Hall, Tarn, and Anderson⁷⁹ investigated the changes of surface area and pore volume of a reduced catalyst during oxidation with water vapor in nitrogen, carbiding in carbon monoxide, and nitriding in ammonia. The course of the initial reduction in hydrogen, oxidation by saturated water

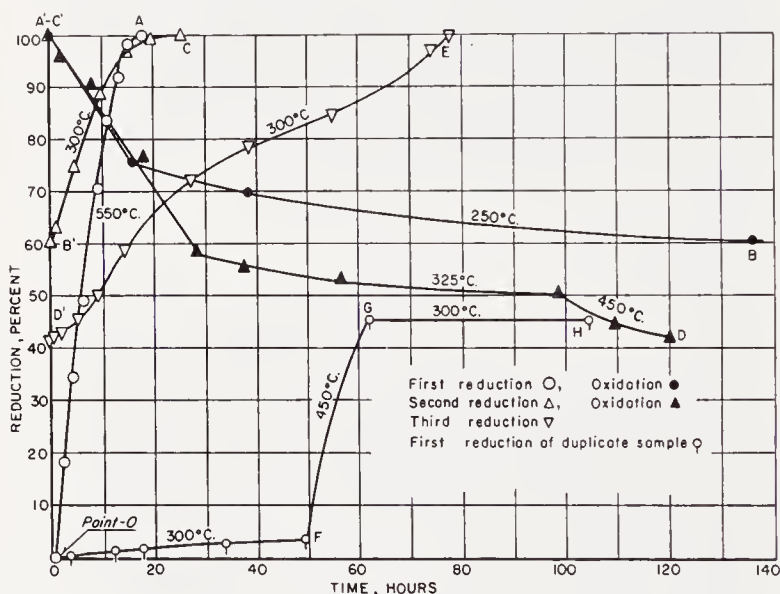


Figure 58. Oxidation and reduction of fused iron catalyst D-3001. (Reproduced with permission from Ref. 79)

vapor in a stream of nitrogen, and subsequent rereduction in hydrogen is shown in Figure 58. The initial oxidation at 250°C proceeded rapidly to about 25 per cent and thereafter was relatively slow. Subsequent reduction at 300°C had about the same initial rate as at 250°C, but the initial rapid portion extended to 40 per cent followed by a slow period. Further oxidation at 450°C was more rapid than the previous oxidation at 325°C, but considerably less than the initial rate at 325°C. The reoxidized catalysts reduced more rapidly than raw catalysts as shown by reduction data at 300°C. Surface areas and carbon monoxide chemisorption data for the preparations in Figure 58 are given in Table 71. The surface areas decreased more rapidly than the extent of reduction. Two simplified hypotheses involving long open-end cylindrical pores were considered, but neither of them explains the fact that the surface area decreased more rapidly than the

extent of reduction. In the first, the oxidation was assumed to decrease the length of the pores, and surface area (A) is proportional to extent of reduction (f) or $A/f = \text{constant}$. In the second, the diameter of the pores decreases uniformly, and $A/f^{1/2} = \text{constant}$. The most simple explanation is that the pore diameter is larger than the value calculated from equations for smooth cylindrical pores and that the pore walls are rough. In the initial

TABLE 71. ADSORPTION MEASUREMENTS ON REDUCED AND REOXIDIZED CATALYST D-3001^a

Treatment				Extent of Reduction (%)	Surface Area (m ² /g of Un-reduced Catalyst)	V_m^b cc/g (STP)	V_{CO}^c cc/g (STP)	V_{CO}/V_m	Area ^d f	Area ^d $f^{1/2}$
Gas	Temp. (°C)	Time (hr)	Point on Figure 58							
—	—	—	O	0.0	0.0	0.0	0.0	—	—	—
H ₂ ^e	550	18	A	99.7	4.7	1.07	.4	0.4	4.7	4.7
N ₂ + H ₂ O	250	136	B	60.4	2.6	.59	.1	.2	4.3	3.3
H ₂	300	27	C	100.0	4.5	1.04	.5	.5	4.5	4.5
N ₂ + H ₂ O	325	98	D	42.1	1.7	.39	.04	.1	4.1	2.6
	450	21.5								
H ₂ ^e	550	19	—	99.9	—	—	—	—	—	—
N ₂ + H ₂ O	250	70	— ^f	68.4	2.9	.66	—	—	4.2	3.5
H ₂ ^e	550	18.5	— ^f	99.8	—	—	—	—	—	—
N ₂ + H ₂ O	250	66	— ^f	68.2	2.8	.64	—	—	4.1	3.4
H ₂ ^e	450	56	—	98.0	8.2	1.88	—	—	8.4	8.3
	500	5								
N ₂ + H ₂ O	250	65	—	49.8	3.9	.89	—	—	7.8	5.5

^a From Ref. 79.

^b Calculated by use of the simple BET equation (per gram of raw catalyst).

^c Difference between the N₂ and CO isotherms at -195°C per gram of raw catalyst.

^d f = extent of reduction.

^e Original reduction of raw catalyst.

^f Density measurements were made on this sample.

part of oxidation, the entire surface is oxidized but probably to a greater extent at the pore openings. This process decreases the surface roughness with the result that the surface area decreases more rapidly than the extent of reduction. This concept of larger pores with considerable surface roughness is consistent with the observation that the same surface area and average pore diameter are attained if (a) a catalyst sample is reduced at 550°C, or (b) reduced at 450°C and then sintered in helium at 550°C. It is difficult to explain the transition of a system of cylindrical pores of 330 to 830Å during sintering in helium.

Density and pore volume data (Table 72) indicate that equal densities

were obtained for the same extent of reduction for both the initial reduction of a raw catalyst or partial oxidation of a completely reduced catalyst. The external volume of the catalyst per unit weight in raw state as indicated by displacement of mercury remained constant in reduction and oxidation; hence in oxidation the pores created in the reduction are filled. On the other

TABLE 72. STRUCTURAL DATA AS A FUNCTION OF SOLID PHASE IN CATALYST D-3001^{a, b}

Treatment of Catalyst	Phases Present (X-ray Analysis)	d_{He} (g/cc)	d_{Hg} (g/cc)	V_{Hg} (cc/g Unreduced Catalyst)	Pore Volume ^c (cc/g Unreduced Catalyst)	Pore Volume Calcd. from Eq. on p. 169, (cc/g Unreduced Catalyst)	Porosity ^b (%)	Surface Area (m ² /g Unreduced Catalyst)	Average Pore Diameter (Å)
None (raw)	Fe ₃ O ₄	4.96	4.91	0.203	0.002	0.00	1	0.0	—
Reduced at 550°C	α-Fe	6.95	3.71	.201	.093	.093	46	4.7	785
Reoxidized ^e ($f = .684$)	α-Fe, Fe ₃ O ₄	5.94	4.13	.200	.061	.064	30	2.9	820
Reoxidized ^e ($f = .682$)	—	5.93	4.13	.200	.061	.063	30	2.8	860
Carbided ^f	Hägg-Fe ₂ C, α-Fe(?)	6.28	3.63	.225	.096	—	43	^g	(820) ^g
Nitrided ^h	ε-Fe ₂ N	6.37	3.48	.237	.107	—	45	4.8	898

^a From Ref. 79.

^b Except for the raw catalyst, all samples were reduced for 19 hours at 550°C and at a space velocity of 1,000 volumes H₂/volume catalyst/hour.

^c Pore volume is the differences of the reciprocals of the helium and mercury densities per gram of unreduced catalyst.

^d Porosity = 100 × pore volume/mercury volume.

^e See footnote *f*, table 71.

^f Atom ratio, C/Fe = 0.494.

^g Surface area not determined; several other samples showed no change in surface area with carbiding for this catalyst. The surface area was assumed unchanged, and the pore diameter was calculated on this basis.

^h Atom ratio, N/Fe = 0.482.

hand, in nitriding and carbiding the external volume of the catalyst as well as the pore volume increased, but the porosity (100 times volume of pores divided by external volume of catalyst) remained constant. This behavior would be expected in carbiding or nitriding a block of massive iron containing a hole.

Surface area studies of precipitated iron catalysts have been made only on preparations without structural promoters and carriers. These preparations are usually high area-small pore gels⁶ of ferric oxide or magnetite;

however, in treatment with hydrogen, synthesis gas, or carbon monoxide prior to or during synthesis, the pore geometry is drastically altered. For example, in reduction with hydrogen the surface area of a $\text{Fe}_2\text{O}_3\text{-K}_2\text{CO}_3$

TABLE 73. ISOTHERM DATA OF HEAT-TREATED AND REDUCED PRECIPITATED CATALYST P-3003.24^a

Sample	Treatment				Type of Isotherm ^b	Area (m ² /g of Unreduced Catalyst)	V _s ^c (cc of liquid N ₂ /g Unreduced Catalyst)
	Gas	Temp. (°C)	Time (hr)	Weight Loss (%)			
1	Evac.	100	1	1.7	IV	184.0	0.140
2	N ₂	300	16	5.0	IV	97.4	.150
3	N ₂	450	16	5.9	IV	23.4	.110
4	N ₂	550	16	6.4	II	8.4	—
5 ^d	H ₂	300	17	33.0 ^e	II	6.3	—
6	H ₂ -H ₂ O ^f	250	19	9.2	II	11.3	—

^a From Ref. 78.

^b Classification of Brunauer, Ref. 25.

^c Nitrogen adsorbed at p_0 .

^d Sample after treatment 2.

^e Sum of 2 + 5.

^f H₂ gas was saturated with H₂O at 26°. Under these conditions it is not possible thermodynamically to reduce the oxide beyond magnetite.

TABLE 74. MERCURY AND HELIUM DENSITIES, PORE VOLUMES AND PORE DIAMETERS OF CATALYST P-3003.24^a

Sample	Gas	Temp. (°C)	Time (hr)	Weight Loss (%)	d_{Hg} ^b (cc/g)	d_{He} (cc/g)	Volume ^c Displaced (cc/g of Unreduced Catalyst)		Pore ^d Volume (cc/g of Unreduced Catalyst)	Pore Diameter, ^e \bar{d} (Å)	Porosity ^f (%)
							V_{Hg}	V_{He}			
7	Evac.	100	1	1.6	2.83	4.43	0.347	0.222	0.125	27	36
8	N ₂	300	16	5.5	2.79	4.84	.338	.196	.151	59	45
9	N ₂	450	16	6.1	3.14	5.04	.299	.186	.113	193	38
10	N ₂	550	16	6.5	3.20	5.11	.293	.183	.109	519	37
11	H ₂	300	17	32.6	2.73	7.60	.247	.089	.155	968	63
12	H ₂ -H ₂ O	250	18	12.7	2.75	5.25	.317	.166	.151	536	48

^a From Ref. 78.

^b Determined at an absolute pressure of 1,100 atm.

^c $V_x = (1 - f)d_x$, where d_x is the helium or mercury density, and f is the fractional weight loss on treatment.

^d Difference between the volume of Hg and He displaced.

^e $\bar{d} = 4(\text{pore volume})/\text{surface area}$, surface areas obtained from Table 73.

^f Pore volume divided by the mercury volume, V_{Hg} .

catalyst decreased from 169 to 9 m²/g¹⁸⁰. In further Bureau of Mines studies⁷⁸ with Fe₂O₃-CuO-K₂CO₃ catalyst P-3003.24 (Tables 73 and 74) it was demonstrated that serious thermal sintering does not occur at 300°C in nitrogen, whereas in the presence of hydrogen even when the sample was reduced only to magnetite, extensive sintering occurred at 250°C. Unlike the fused catalyst the external volume of the precipitated catalyst decreased with sintering and reduction. In Table 74 the porosity of all sintered and reduced samples was larger than that of the raw catalyst, the porosity increasing to 63 per cent for the completely reduced sample. Although the raw catalyst was hard, the mechanical strength of reduced or carburized samples was low. The surface areas of 100Fe₂O₃:20Cu:0.2K₂CO₃ catalysts after induction in 1H₂ + 1CO gas at 225°C were 21.0 and 23.8 m²/g (Table 55, p. 125).

Pretreatment of Iron Catalysts

Usually the methods of pretreating precipitated and fused catalysts are very different. Precipitated catalysts can be pretreated with hydrogen, synthesis gas, or pure carbon monoxide at temperatures in the range of those employed in the synthesis, 220–325°C, whereas fused catalysts require reduction in hydrogen at high temperatures, 400–600°C, before synthesis or further pretreatment.

Precipitated Catalysts. Before the discovery of the medium pressure synthesis with iron catalysts, a variety of pretreatments were tried at K.W.I.¹²³. Although these procedures did not lead to satisfactory atmospheric pressure operation, some of these methods were successful in the medium pressure range. In Pichler's studies¹²³ of alkalinized precipitated iron catalysts it was observed that the raw catalyst was inactive, at least initially, in the synthesis, and the activity was not improved by reduction in hydrogen at about 360°C, the temperature normally employed for standard Co-ThO₂-kieselguhr catalysts. This observation apparently led to the conclusion that reduction was undesirable for precipitated iron preparations; however, the work of numerous other laboratories has demonstrated that active catalysts result from reduction in hydrogen at lower temperatures, 200–300°C. At K.W.I. methods were developed for activating catalysts with carbon monoxide or synthesis gas. A lengthy series of tests was made in which the temperature and pressure of induction in carbon monoxide or 1H₂ + 1.5CO gas were varied. The length of induction was usually 25 hours with a gas flow of 0.4 liters per gram of iron, and subsequent synthesis was conducted with 1H₂ + 1.5CO gas at 15 atmospheres and 235°C. The optimum pretreatment conditions were 325°C and 0.1 atmosphere with carbon monoxide being somewhat better than synthesis gas as a pretreating agent. Synthesis data showing the effect of varying conditions

from the optimum ones are given in Figures 59, 60, and 61. Figure 59 shows that the optimum pretreatment pressure was 0.1 atmosphere (absolute) with both CO and $1\text{H}_2 + 1.5\text{CO}$ gas; however, induction at 1 atmosphere

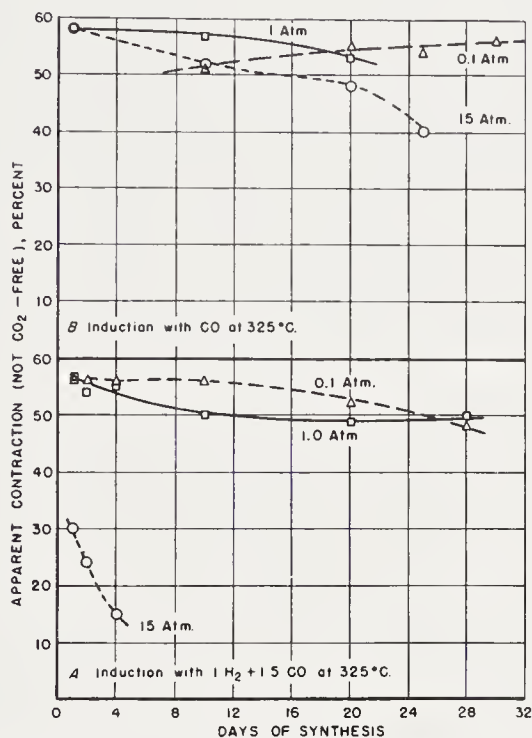


Figure 59. Activity of precipitated iron oxide- K_2CO_3 catalysts as a function of induction pressure. Length of induction 25 hours. (From Ref. 123)

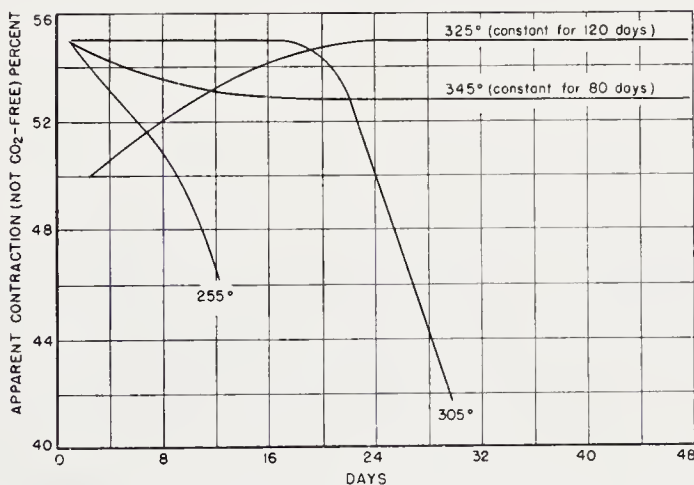


Figure 60. Influence of induction temperature upon the activity of the catalyst during medium-pressure synthesis after induction with CO at 0.1 atm. pressure. (From Ref. 123)

was not greatly inferior. Figure 60 demonstrates that 325°C was the optimum pretreatment temperature. Life tests in Figure 61 show the temperatures required to maintain an apparent contraction of 50 per cent (not CO₂-free) for catalysts induced in CO at 0.1 atmosphere and 255 and 325°C. The sample induced at 255°C required progressive increases in temperature to 273°C at the end of 300 days; however, at this time the activity had increased sufficiently so that the temperature could be lowered to 254°C. For the catalyst pretreated at 325°C, contractions of about 50 per cent were possible for 350 days. The synthesis temperature was 235°C for the first 135 days, after which progressive increases in temperature to 270°C at 350 days were required to maintain the desired conversion. Prod-

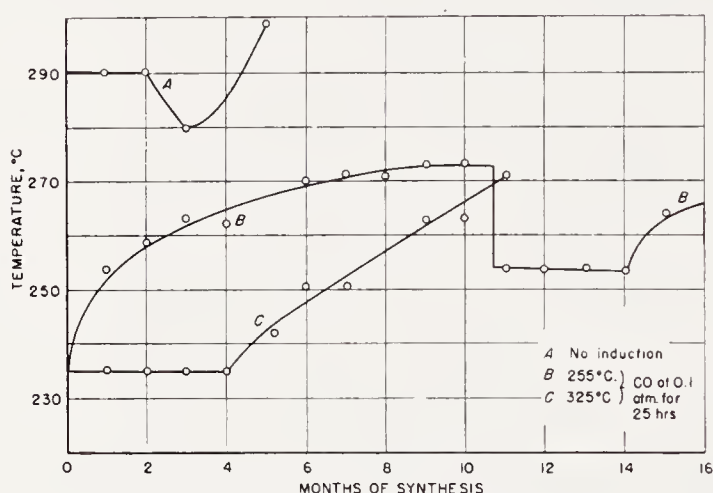


Figure 61. Influence of induction procedure on activity (expressed as temperature required to maintain a constant conversion). (From Ref. 123)

ucts in this life test were

	Days	40	70	100	300
$\text{g/m}^3 \left\{ \begin{array}{l} \text{C}_5+ \\ \text{C}_3 + \text{C}_4 \end{array} \right.$		108	105	110	110
		44	45	47	

A catalyst sample that was started directly in the synthesis operated for almost 5 months; however, temperatures of 280–300°C were required. A similar catalyst pretreated with 1H₂ + 1.5CO gas at 325°C and 0.1 atmosphere operated for 200 days with the contraction (not CO₂-free) averaging 50 per cent. After 30 days at 235°C, the temperature had to be progressively increased to 278°C at 180 days.

In the pretreatment, the gel was first reduced to magnetite and part of the magnetite was then converted to Hägg carbide. In most instances, free carbon was also deposited in the catalysts. In these steps, drastic changes in surface area, pore volume, and mechanical strength occurred, and most

of Pichler's catalysts lacked sufficient mechanical strength for use in vertical catalyst tubes. Large yields of CO_2 were produced in the initial portion of the induction, and then the CO_2 decreased gradually to a low value. In two pretreatments, a total of 11 and 16 liters of CO_2 per catalyst containing 10 grams Fe were produced. The reaction $\text{Fe}_2\text{O}_3 + 5\text{CO} = \text{Fe}_2\text{C} + 4\text{CO}_2$ requires the formation of 16 liters of CO_2 per 10 grams of Fe. However, other experiments, described below, indicate that the reaction may not follow this path. Sizable amounts of free carbon were produced and the catalyst was converted to a mixture of Hägg carbide and magnetite.

TABLE 75. THE INFLUENCE OF PRESSURE AND TEMPERATURE OF CARBURIZATION OF ALKALIZED IRON OXIDE CATALYSTS^a

(25 hr of treatment with carbon monoxide at 4 liters per 10 gram Fe per hr)

A. Temperature = 325°C

Pressure (atm.)	Atom Ratio, C/Fe	
	Free Carbon	Carbide ^b
0.1	1.03	0.21
1.0	1.97	.16
15	—	.05

B. Pressure = 0.1 atm.

Temp. (°C)		
175	0.00	0.001
225	.03	.002
275	.41	.166
325	1.03	.211
425	4.67	.008

^a From Ref. 129.

^b Carbide carbon determined by the acid decomposition method.

Pichler and Merkel^{129, 130} made a detailed study of the carburization of precipitated iron catalysts in which carbides were determined by acid decomposition and thermomagnetic methods. An objective of this research was to determine why 325°C and 0.1 atmosphere were the optimum conditions for catalyst pretreatment. It appears that under these conditions the greatest amount of carbide (Hägg) is produced. Table 75 illustrates the effect of pressure and temperature of carburization. These data indicate that even under the optimum conditions less than one fourth of the carbon deposited was present as carbide; however, the values for carbide carbon determined by acid decomposition *may be low*. Table 76 relates the tem-

perature of carburization with carbon monoxide at 0.1 atmosphere to the activity and life of precipitated iron catalysts in synthesis at 235°C and 15 atmospheres. With induction at 325°C contractions (not CO₂-free) exceeded 50 per cent for 365 days.

The highly active catalysts of Pichler and Weinrotter¹³¹ prepared from mixtures of ferrous and ferric chlorides, for example 75Fe⁺⁺:25Fe⁺⁺⁺:20Cu:1K₂CO₃, were pretreated with 2H₂ + 1CO gas at a space velocity of 500 hr⁻¹, atmospheric pressure, and 225°C. After 48 hours the catalyst was extracted with a 230–280°C fraction of synthesis oil to remove wax. The induction was terminated by a second extraction after an additional 24-hour

TABLE 76. EFFECT OF INDUCTION TEMPERATURE ON CATALYST LIFE
WITH A PRECIPITATED IRON CATALYST^a

Induction conditions: 4 liters of carbon monoxide per 10 gram Fe per hour at 0.1 atm. for 24 hr.

Synthesis conditions: 235°C, 15 atm. of 1H₂ + 1.5CO gas at a flow of 4 liters per 10 grams Fe per hour.

Induction Temp. (°C)	Carbide Carbon Atom Ratio C/Fe	Days During Which Contraction Exceeded ^b 50 Per cent
255	0.03	2
285	.18	10
305	.20	24
315	.20	50
325	.21	365
355	.20	20
450	.005	^c

^a From Ref. 129.

^b Not CO₂-free contraction.

^c Contraction never exceeded 10 per cent.

period, and the catalyst was ready for use in either atmospheric or medium-pressure syntheses. In the atmospheric synthesis extractions at 2–3 day intervals were required for the catalyst containing 1K₂CO₃:100Fe and less frequently for preparations containing lower alkali contents. In the medium pressure synthesis extraction was not required during the synthesis. The activity, selectivity, and life of these catalysts were very good. Typical data for synthesis with water gas are presented in Table 77.

Scheuermann¹⁶⁵ reported pretreatment studies of a precipitated Fe-Cu-MgO-K₂CO₃ catalyst (Table 78). This preparation was moderately active when used directly in the synthesis, and the activity was not improved by reduction in hydrogen at 300°C. Reduction in hydrogen at lower temperatures, 180–220°C resulted in improved activity. The most active sample in this series was obtained by treatment with 2H₂ + 1CO gas at 200–250°C.

Reduction in $3\text{H}_2 + 1\text{N}_2$ for about 1 hour at 300°C was the standard method of pretreatment at Ruhrchemie. It was desirable not to reduce the catalyst completely, 65–75 per cent being the reduction value for optimum catalytic activity⁶⁸. Later work showed advantages for pretreatment with water gas at atmospheric pressure. Data for synthesis tests in 5 liter-double tube reactors after induction in hydrogen-nitrogen mixture (pretreatment

TABLE 77. SYNTHESIS DATA FOR $75\text{Fe}^{++}:25\text{Fe}^{+++}:20\text{Cu}:1\text{K}_2\text{CO}_3$ CATALYST^a

Synthesis pressure, atm. absolute	1	10
Temperature, $^\circ\text{C}$	211	200
Space velocity, hr^{-1}	50	100
Yield, g/m^3	135	137
Product distribution, wt.-%		
CH_4	2.4	3.2
$\text{C}_2\text{—C}_4$	10.1	9.0
Liquid hydrocarbons $<180^\circ\text{C}$	13.5	10.0
Liquid + solid hydrocarbons $>180^\circ\text{C}$	74.0	77.8
Interval of extraction, days	2–3	Not required

^a From Ref. 131.

TABLE 78. EFFECT OF INDUCTION ON $\text{Fe-Cu-MgO-K}_2\text{CO}_3$ CATALYSTS^a,
($1\text{H}_2 + 1\text{CO}$ gas at 12 atm. Presumably space velocity = 240 hr^{-1})

Pretreatment				Synthesis				
Gas	Temp. ($^\circ\text{C}$)	Space Velocity	Duration (hr)	Temp. ($^\circ\text{C}$)	CO-Converted (%)	Liquid + Solids, (g/m^3)	Per cent Wax (320°C)	CH_4 , (g/m^3)
—	None	—	—	240	77	97	53	14
H_2	300	400	15	238	75	73	39	24
H_2	180–220	5000	15–20	222	64	88	60	14
$2\text{H}_2 + 1\text{CO}$	200–250	5000	15–20	214	62	82	60	16

^a From Ref. 165.

A) and water gas (B) are compared in Table 79. Although the activities were about the same, the catalysts inducted in water gas produced less methane and had a higher usage ratio than samples reduced in hydrogen. Roelen⁷² stated that the advantageous effects of pretreatment of catalysts with water gas at 0.1 atmosphere as done at K.W.I. could be reproduced by using a 10 per cent water gas plus 90 per cent nitrogen mixture at atmospheric pressure.

The Rheinpreussen catalyst in the Schwarzheide tests was reduced in hydrogen at $300\text{--}400^\circ\text{C}$ and then treated with water gas at 245°C , both steps at atmospheric pressure. In the comparative tests these catalysts

encountered severe coking troubles. The most successful pretreatment of Rheinpreussen was the "typhoon" induction¹⁴². The catalyst was treated with dry, CO₂-free 2H₂ + 1CO gas at 280–320°C and atmospheric pressure for 6 hours. The gas velocity was 20 times the usual synthesis rate, and if desired the gas could be recycled provided carbon dioxide and water were removed.

TABLE 79. EFFECT OF PRETREATMENT ON SYNTHESIS WITH 100Fe:5Cu:8Ca:30 KIESELGUHR: x K₂O CATALYSTS^a

(Fresh feed space velocity of water gas 100 hr⁻¹ at 10 atm.)

Catalyst Potassium compound K per 100 Fe	PN43 K ₂ SiO ₃ 1.2			PN47 KOH 1.8		
	A ^b 0	B ^b 0		A ^b 3.0	B ^b 3.0	
	Recycle ratio			Recycle ratio		
Time, hours	251	36	717	310	120	743
Temperature, °C	214	201	220	213.5	214	221.5
Usage ratio, H ₂ /CO	0.90	1.21	1.11	0.98	1.35	1.15
CH ₄ , per cent of CO reacted	22.2	4.1	15.0	17.1	75	14.6
Contraction, %	56	45	55	69	62	70
C ₅ ⁺ , g/m ³	79	77	85	105	103	107
Distillation of C ₅ ⁺ , wt-%						
<200°C	67.8	63.0 ^c	58.4	57.0		44.7
200°-290°C	18.2	19.2	9.2	18.4		13.9
290°-320°C	5.8	9.6	7.3	5.0		4.5
320°-460°C	7.6	6.9	22.7	13.4		18.4
>460°C	0.6	1.3	1.5	5.3		17.7

^a From Refs. 147, 151.

^b Induction procedure A: 3H₂ + 1N₂ gas at space velocity of 60 hr⁻¹, atmospheric pressure, and 300°C for 1 hour. Induction procedure B: 1.3H₂ + 1CO gas at space velocity of 100 hr⁻¹, atmospheric pressure, and 250°C for 24 hours.

^c Analyses after 180 hours.

Based on the German experience the following conditions were chosen for routine testing of precipitated catalysts at the Bureau of Mines laboratory:

(a) For preparations containing no copper or only small amounts such as 1 per cent, the catalyst was treated with 1H₂ + 1CO gas at atmospheric pressure, a space velocity of 100 hr⁻¹, and 260°C for 24 hours.

(b) For preparations containing larger amounts of copper a temperature of 230°C was used with the other conditions the same as in (a).

Typical testing data in Table 54 indicate that these induction procedures produced catalysts of comparable activity and selectivity to many of the German preparations.

Samples of catalyst P3003.24 ($100\text{Fe}:10\text{Cu}:0.5\text{K}_2\text{CO}_3$) were tested in the synthesis with $1\text{H}_2 + 1\text{CO}$ gas at 7.8 atmospheres and space velocities of 100 hr^{-1} after the following pretreatments¹⁷¹:

Test, X	Gas	Space Velocity, (hr^{-1})	Temp. ($^{\circ}\text{C}$)	Hours	Atom Ratio N/Fe
149	$1\text{H}_2 + 1\text{CO}$	100	230	23	0.0
245	H_2	1480	300	18	.0
220	H_2	1420	300	16	.25
	NH_3	1000	300	8	
273A	H_2	1350	300	25	.48
	NH_3	900	300	15	
273B	H_2	1000	300	9	0

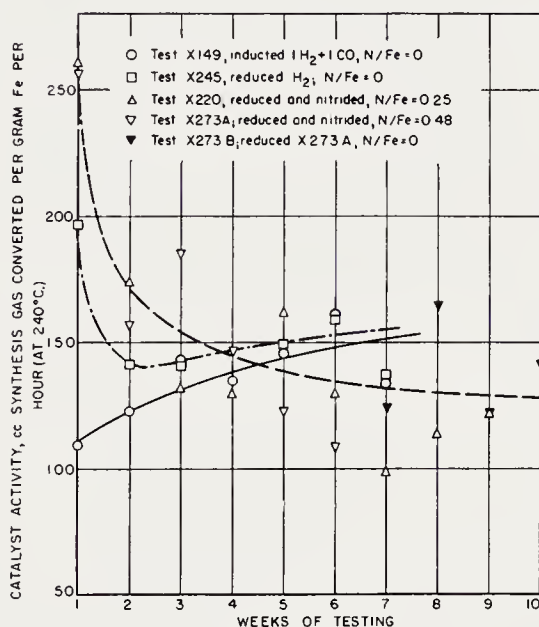


Figure 62. Variation of activity of precipitated catalyst P3003.24 with method of pretreatment. (Reproduced with permission from Ref. 171)

In the pretreatment with synthesis gas (X149) the ferric oxide was converted to magnetite and part of this to Hägg carbide. In X245, X220, and X273A the catalyst was fairly completely reduced in the hydrogen treatment (c.f. Table 73, p. 175). After 6 weeks of testing in X273A the catalyst was hydrogenated at 300°C to remove nitrogen, and the subsequent portion of the test was designated as X273B.

The average activities in these experiments were about equal as shown in Figure 62; however, the activity of the nitrided catalysts decreased with time while the activity of the sample pretreated with synthesis gas increased. Although the average activity was about the same, the selectivity

changed remarkably as shown in Figure 63. The sample inducted in synthesis gas (X149) yielded a high molecular weight product of which 92 per cent was C_3+ and 51 per cent boiled above 464°C . In the products from the reduced catalyst 84 per cent was C_3+ and 18 per cent boiled above 464°C . The reduced and nitrided catalysts (X220 and X273A) produced a still lower molecular weight product with practically no wax boiling above 464°C . Hydrogenation of the catalyst in X273A after 6 weeks produced no

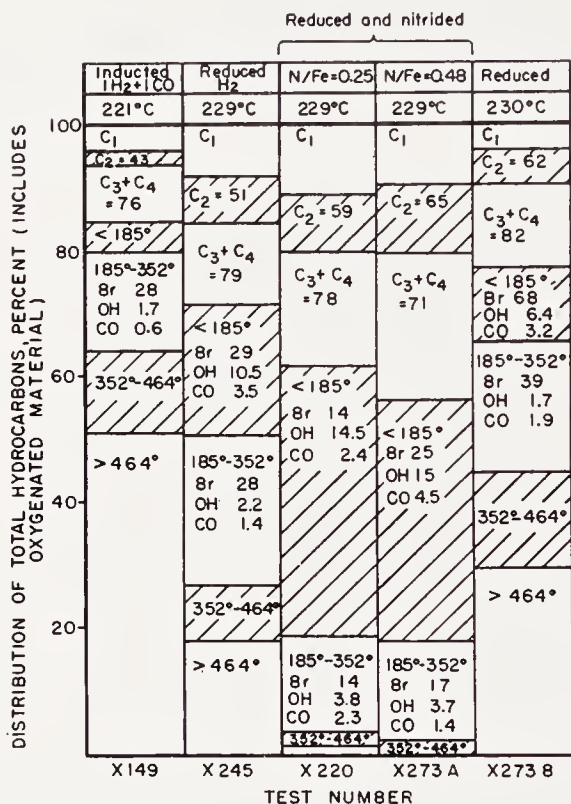


Figure 63. Effect of pretreatments of precipitated catalyst P 3003.24 on the composition of products obtained from it. (Reproduced with permission from Ref. 171)

significant change in activity, but increased the average molecular weight of the products so that these products appear intermediate between those from the inducted (X149) and reduced (X245) samples. The liquid products from nitrided catalysts contained larger quantities of alcohols and correspondingly smaller amounts of olefins than non-nitrided samples.

Attempts were made to nitride the raw $\text{Fe}_2\text{O}_3\text{-CuO-K}_2\text{CO}_3$ catalyst directly with ammonia, a process analogous to the preparation of carbides by treating iron oxide with carbon monoxide. However, at $300\text{--}400^\circ\text{C}$, ammonia only reduced the precipitated catalysts from Fe_2O_3 to Fe_3O_4 .

Pretreatment of Fused, Sintered, and Cemented Iron Catalysts. In general catalysts composed of iron oxides other than the high-surface

area forms, such as iron oxide gels prepared by precipitation, require reduction in hydrogen before either use in the synthesis or other pretreatment steps. These oxides are usually sufficiently inert to require temperatures of at least 400°C for reduction to proceed at a reasonable rate. At these high temperatures synthesis gas or carbon monoxide would deposit excessive amounts of free carbon. The methods of reduction employed in the ammonia synthesis have served as a starting point for reduction studies of fused catalysts. In the ammonia synthesis very complete reduction of iron catalysts is required for high activity, because traces of residual oxygen adversely affect the rate of synthesis. Hydrogen or ammonia synthesis gas ($3\text{H}_2 + 1\text{N}_2$), carefully freed of H_2O , CO , CO_2 and other compounds containing oxygen, is used for the following reasons:

(a) The last traces in iron oxide cannot be removed in the presence of small amounts of compounds containing oxygen^{2, 26}.

(b) The catalyst is believed to sinter more rapidly in the presence of compounds containing oxygen.

(c) Compounds containing oxygen decrease the rate of reduction. Hence, conditions are chosen to keep the water produced in the reduction at a minimum. High space velocities of hydrogen or $3\text{H}_2 + 1\text{N}_2$ are used, and frequently the temperature of reduction is increased during the process; for example, catalyst 931 of Table 68 (p. 165), was reduced 18 hours at 300–350°C, 65 hours at 350–450°C and 18 hours at 450–530°C. Usually temperatures of 450°C or higher are required for the last stage of the reduction. In the Fischer-Tropsch synthesis there is no necessity to remove the last traces of oxygen from the catalyst since sufficient water vapor and carbon dioxide are produced in the synthesis to oxidize the catalyst to an appreciable extent.

In Germany fused catalysts were investigated seriously only at the I.G. Farbenindustrie laboratories at Oppau and Leuna. With a $100\text{Fe}:2.5\text{Si}:2.5\text{TiO}_2:5.0\text{KMnO}_4$ catalyst, Linckh and Klemm²⁰⁶ found that the reduction was rapid at 650°C, and the reduced catalyst was rather insensitive to exposure to air. However, the activity was low so that reasonable conversions were attained only at operating pressures of 100 atmospheres. At temperatures of 450–500°C, the reduction required 5 to 6 days; however, this catalyst was pyrophoric and had satisfactory activity at synthesis pressures of 15 to 25 atmospheres. Duftschnid²⁰⁶ recommended the following conditions for reduction of the catalyst above for use in medium pressure synthesis:

Temperature, °C	470–500
Space velocity, hr. ⁻¹	750
Duration, days	6–8

Complete reduction was considered desirable, since carbon deposition was said to proceed more rapidly in partly reduced catalysts.

At Leuna⁶⁸, $\text{Fe}_3\text{O}_4\text{-Al}_2\text{O}_3\text{-K}_2\text{O}$ catalysts were used. The activity of the catalysts increased as the temperature of reduction was decreased, the most active preparations resulting from reduction at temperatures of 500°C or less. On the other hand the average molecular weight of the synthesis products decreased as the temperature of reduction was decreased. It was suggested that this behavior resulted from the greater hydrogenation activity of the catalyst reduced at low temperatures. Catalysts for the synol process were reduced with hydrogen at a space velocity of $2,000\text{ hr}^{-1}$ for 50 hours at 450°C . For $\text{Fe}_3\text{O}_4\text{-MgO-K}_2\text{O}$ catalysts, Scheuermann¹⁶⁵ employed similar conditions, except that the temperature was 500°C . The extent of reduction was believed to be of secondary importance, since equal

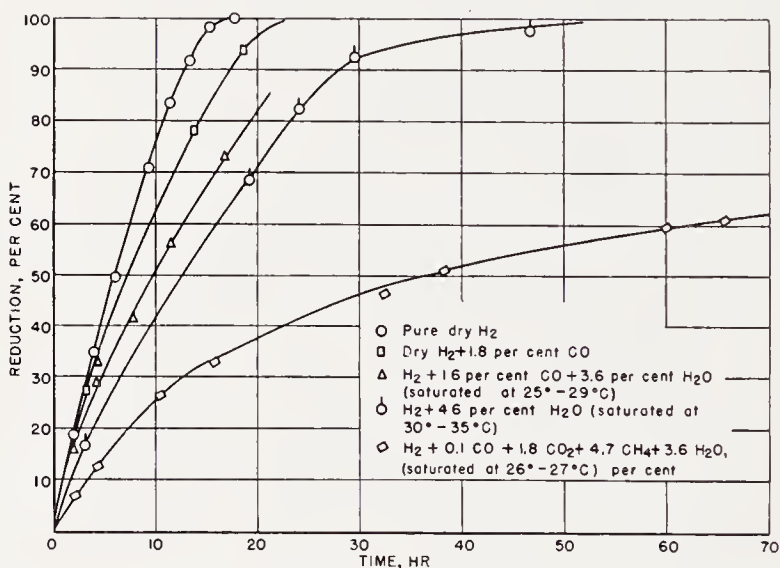


Figure 64. Rate of reduction of fused synthetic ammonia-type catalyst D-3001 at 550°C in pure dry H_2 and in H_2 containing various amounts of CO , CO_2 , CH_4 , and H_2O . (Reproduced with permission from Ref. 181)

activity and selectivity were obtained for samples reduced from 30 to 100 per cent.

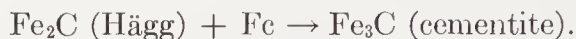
At the Bureau of Mines several aspects of the reduction of fused iron catalysts have been studied. Data on the rate of reduction and the development of pore structure during reduction were described previously (pp. 165 to 174). The effect of compounds containing oxygen in hydrogen on the rate of reduction is shown in Figure 64. Water vapor and carbon dioxide appear to inhibit the reduction more than carbon monoxide. In general the ease of reduction of fused catalysts decreased with increasing concentration of structural promoters, and preparations containing alumina were usually more difficult to reduce than those promoted with magnesia. Sintered and cemented preparations as well as many ores can be reduced at lower temperatures than fused catalysts.

Bureau of Mines studies^{78, 79} of the rate of reduction and pore geometry of fused catalyst D3001 ($\text{Fe}_3\text{O}_4\text{-MgO-K}_2\text{O}$) indicate that reduction proceeds uniformly inward from the external surface. To study the effect of extent of reduction on the synthesis, 6- to 8-mesh catalyst was reduced at 400°C to insure that the entire bed was approximately equally reduced. Although the selectivity was essentially constant, the activity increased with extent of reduction to a constant value at about 25 per cent. For this extent of reduction the average depth of the zone of reduced iron was about 0.13 mm. This result suggests that only the external surface of the particles is effective in the synthesis, and agrees with tests of catalysts of different particle size. Further, a catalyst prepared by oxidizing a completely reduced sample with steam until the extent of reduction decreased to 45 per cent had a considerably lower activity than a catalyst directly reduced to this extent. Reduction of catalyst D3001 in hydrogen at a space velocity of 2,500 hr^{-1} according to the schedule used in the ammonia synthesis (24 hours at 400°C, 24 hours at 450°C, 12 hours at 500°C, and 12 hours at 525°C) resulted in only a slight improvement in activity over catalysts reduced at 450°C for 40 hours.

Synthesis tests at 7.8 atmospheres on a 6- to 8-mesh sample of goethite ore impregnated with K_2O , showed that pretreatment in $1\text{H}_2 + 1\text{CO}$ gas at 325°C resulted in activity nearly as great as reduction in hydrogen at 450°C. Samples treated with synthesis gas at lower temperatures than 325°C were less active.

Usually the activity of reduced fused iron catalysts is increased by conversion of the iron to interstitial compounds. Catalysts ($\text{Fe}_3\text{O}_4\text{-MgO-K}_2\text{O}$) converted to Hägg carbide (approximate composition Fe_2C) and cementite (Fe_3C) were more active than reduced catalysts, but their selectivity was about the same. At 7.8 atmospheres with $1\text{H}_2 + 1\text{CO}$ gas these carbides have high constant activity whereas at 21.4 atmospheres the high initial activity decreased with time so that after 5 weeks of synthesis the carbides had an activity equal to or lower than the reduced samples. Reduced fused catalysts may be converted to Hägg carbide with carbon monoxide or synthesis gas at atmospheric pressure and a constant temperature in the range 225 to 275°C; however, carburization at a fixed temperature is usually a slow process since the rate declines rapidly with extent of carbiding. In addition, in the initial rapid period, free carbon deposition and magnetite formation may occur due to the high concentration of carbon dioxide and possible overheating due to the exothermic reactions. Thus, Podgurski, Kummer, DeWitt and Emmett¹³² prepared Hägg carbide by treating a reduced fused catalyst with carbon monoxide at 225°C for 22 hours followed by 35 hours at 275°C. Hall, Tarn, and Anderson⁷⁹ used a procedure in which the catalyst temperature was increased as required, to maintain the concentration of carbon dioxide in the exit gas at about 20 per cent. The

higher temperatures are reached at a time when the catalyst has been largely converted to Hägg carbide, and this phase is stable at 325°C if only small amounts of metallic iron are present. Cementite may be prepared by the thermal reaction of Hägg carbide and metallic iron in a partly carburized sample according to the equation*



This reaction, which usually goes to completion in about 2.5 hours at 450°C^{84, 132}, is more rapid than the thermal decomposition of relatively pure Hägg carbide.

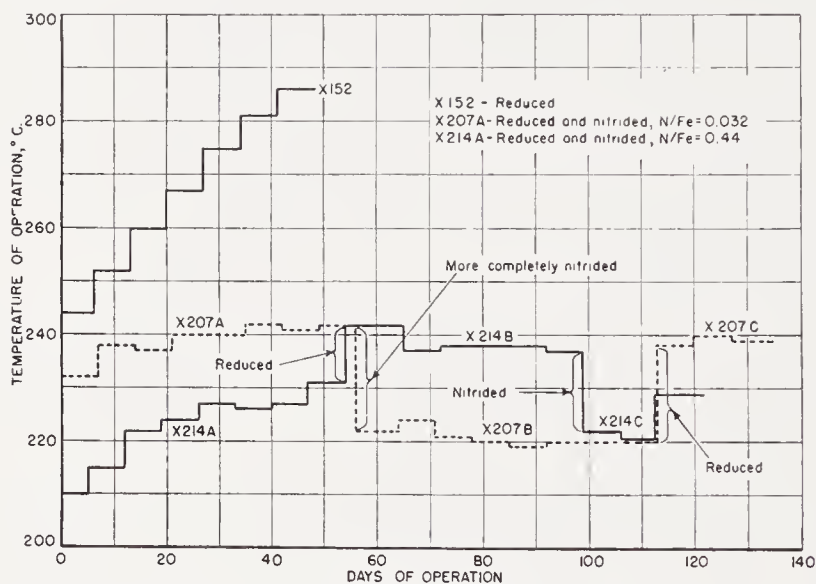


Figure 65. Temperatures of operation required to maintain constant conversions on reduced and nitrided samples of catalyst D3001 at 7.8 atm. (Reproduced with permission from Ref. 17)

Iron nitrides have unusual properties in the Fischer-Tropsch synthesis^{4, 16, 17, 171}. The selectivity of nitrided fused catalysts is always greatly different from reduced or carburized samples, and nitrides often have greater activity. Figures 65 and 66 compare activities of reduced and nitrided catalyst D3001 in the synthesis with $1\text{H}_2 + 1\text{CO}$ gas at 7.8 and 21.4 atmospheres, respectively. Here the activities are expressed as temperatures required to maintain a constant conversion, the higher temperatures corresponding to the lower activities. At 7.8 atmospheres (Figure 65) nitriding to a nitrogen-to-iron atom ratio of only 0.032 increased the activity, but a greater increase was caused by nitriding to a N/Fe ratio of 0.44. In these tests and those of Figure 66 the activity increased after nitriding and de-

* See footnote on p. 86.

creased after reduction in hydrogen at 350°C; these changes apparently occur at any stage of the synthesis. In many cases the activity of a nitrified catalyst after reduction in hydrogen was greater than that of reduced catalysts. This enhanced activity apparently results from cementite produced in the hydrogenation of ϵ -carbonitriles formed in the synthesis. Figure 67 shows the variation of operating temperature in a life test at 7.8

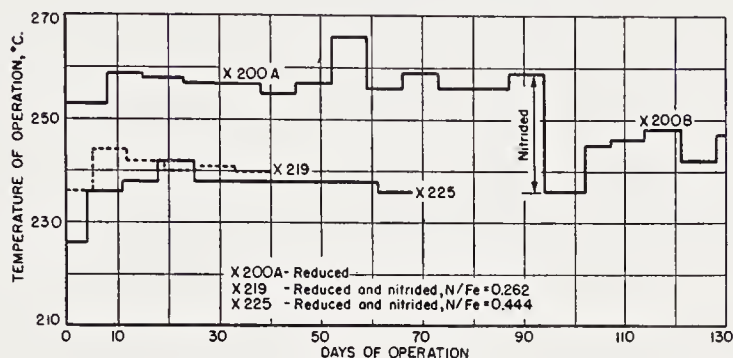


Figure 66. Temperatures of operation required to maintain constant conversions on samples of reduced and nitrified catalyst D3001 at 21.4 atm. (Reproduced with permission from Ref. 17)

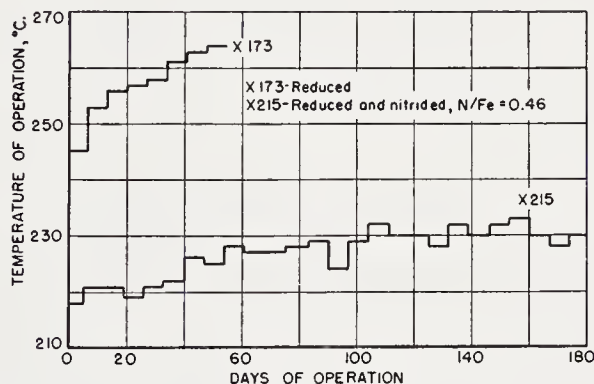


Figure 67. Temperatures of operation required to maintain constant conversions on samples of reduced and nitrified catalyst D3001 at 7.8 atm. (Reproduced with permission from Ref. 17)

atmospheres. Figure 68 compares the activities at 7.8 and 21.4 atmospheres of $1\text{H}_2 + 1\text{CO}$ gas (expressed as volumes of synthesis gas converted at 240°C) of two nitrified fused catalysts, D3001, $\text{Fe}_3\text{O}_4\text{-MgO-K}_2\text{O}$, and D3008, $\text{Fe}_3\text{O}_4\text{-Al}_2\text{O}_3\text{-K}_2\text{O}$. The magnesia-promoted catalyst was more active than the alumina-promoted preparation both reduced and nitrified. The activity of the nitrides at 21.4 atmospheres was about twice as large as at 7.8 atmospheres. The selectivity data for these tests (Figure 69) show that although the fraction of liquid products in the total hydrocarbons plus oxygenates

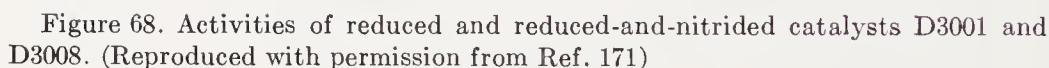


Figure 69. Average product compositions obtained from reduced and reduced-and-nitrided catalysts D3001 and D3008. (Reproduced with permission from Ref. 171)

was about the same, the composition of the liquids was very different. The condensed fractions from nitrated catalysts contained large concentrations of alcohols (expressed as weight per cent OH-group in fraction), aldehydes and ketones (weight per cent of CO-group), and esters (not indicated in block diagram) compared with reduced catalysts; however the concentration of olefins (indicated by bromine numbers, Br) in these fractions from nitrated catalysts were lower than from reduced catalysts. Hydrogenation of nitrated catalyst D3008 at 385°C after 7 weeks of testing converted the catalyst to a mixture of α -iron, cementite, and magnetite. Although the removal of nitrogen caused essentially no change in activity, the average molecular weight and olefin content of the product was greatly increased, and the fraction of oxygenated molecules was decreased.

Despite the large differences in selectivity of nitrated and reduced catalysts, the relative usage of hydrogen and carbon monoxide was virtually the same, as shown in Table 80.

The results of Bureau of Mines' tests of fused catalysts nitrated to varying extents, now in progress, may be tentatively summarized as follows:

Atom Ratio N/Fe	Activity	Selectivity
0.03-0.09	Equal and in some cases greater than reduced catalysts	Same as reduced catalysts
0.10-0.17	Greater activity than reduced catalysts	Same as reduced catalysts
0.18-0.51	Greater activity than reduced catalysts	Typical of nitrated catalysts described on previous pages

These data suggest that catalysts nitrated to N/Fe atom ratios of 0.10-0.18 have enhanced activity and greater stability and life than reduced catalysts, and yet have a selectivity similar to reduced catalysts. Apparently the selectivity of nitrated catalysts, relatively low average molecular weight products with a high concentration oxygenated molecules, results from catalysts containing ϵ -iron nitride or ϵ -carbonitride as the principal phase. The use of various types and amounts of structural promoters in fused catalysts produced only small changes in activity and selectivity of nitrated as well as reduced catalysts. Apparently changes in catalytic behavior with the amount of potassium oxide are similar for both reduced and nitrated catalysts. The selectivity of nitrated catalysts as shown in Figure 69 represents about the optimum (highest average molecular weight product) that can be achieved by changing the alkali content.

Jack⁹¹ and Hall, Dieter, Hofer, and Anderson⁷⁷ have described the preparation and reactions of iron carbonitrides. The carbonitrides have the same arrangement of iron atoms with some nitrogen atoms replaced by carbon. ϵ -carbonitrides may be prepared by treating ϵ - or γ' -nitrides with carbon monoxide or hydrogen-carbon monoxide mixtures at atmospheric pressure

and 350 to 400°C. The ϵ -carbonitride phase persists until about 75 per cent of the nitrogen in Fe_2N is replaced by carbon. With further replacement of nitrogen atoms by carbon, carbide phases (Hägg or cementite) appear. Carbonitrides may also be prepared in the reverse order by nitriding Hägg carbide or cementite (either completely or partly carbided) with ammonia at 350–400°C. Nitrides are converted to carbonitrides in the synthesis at a slow rate. In the synthesis ϵ -carbonitrides prepared either by carburizing nitrides or nitriding carbides gave essentially the same results as ϵ -nitrides.

TABLE 80. RELATIVE USAGE OF HYDROGEN AND CARBON MONOXIDE ON
NITRIDED AND REDUCED FUSED CATALYSTS
($1\text{H}_2 + 1\text{CO}$ gas; conversion about 65 per cent)

Test	Pressure (atm)	Average Temp. (°C)	Initial Atom Ratio, N/Fe	Usage Ratio $\text{H}_2:\text{CO}$
D3001 ($\text{Fe}_3\text{O}_4\text{-MgO-K}_2\text{O}$)				
X173	7.8	258	0	0.72
X200	21.4	257	0	.72
X214A	7.8	225	0.44	.75
X214B	7.8	238	0	.75
X215	7.8	222	0.46	.74
X218	7.8	218	.43	.71
X219	21.4	242	.26	.77
X225	21.4	238	.44	.79
D3008 ($\text{Fe}_3\text{O}_4\text{-Al}_2\text{O}_3\text{-K}_2\text{O}$)				
X127	7.8	271	0	.69
X253	7.8	230	0.47	.69
X337A	21.4	243	.46	.73
X337B	21.4	240	~0	.72

The pertinent facts regarding the pretreatment of fused and sintered catalysts may be summarized as follows: Most catalysts of this type require reduction in hydrogen, although some catalysts such as ores may be activated with synthesis gas at high temperatures. Conditions of reduction are not as critical as those for ammonia synthesis with respect to either extent of reduction or purity of hydrogen; however, the reduction can be accomplished more rapidly with pure dry hydrogen. Conversion of reduced catalysts to carbides or nitrides increases their activity in the synthesis. Carbides have essentially the same selectivity as reduced catalysts; however, nitrides yield products that differ greatly.

The Course of Synthesis on Iron Catalysts

In the synthesis iron catalysts differ in many ways from cobalt catalysts, particularly with respect to changes in the catalyst phases. Furthermore, it is advantageous to convert the iron to carbides or nitrides. Although most iron catalysts have low activity and short lives in the atmospheric pressure synthesis, a few are somewhat effective if carefully pretreated and frequently extracted. In the medium-pressure synthesis iron catalysts are similar to cobalt catalysts to the extent that the nature and amount of wax on the catalyst apparently have little effect on activity, and reactivation procedures such as hydrogenation or extraction are relatively ineffective. With iron catalysts operation at moderate pressures is advantageous since the activity increases approximately linearly with pressure at least to 30 atmospheres, and optimum catalyst life in terms of catalyst productivity is usually found in the pressure range 15–30 atmospheres.

TABLE 81. ATMOSPHERIC SYNTHESIS WITH PRECIPITATED IRON CATALYSTS^a
(Space velocity of water gas of 80 hr.⁻¹)

Total Time (hr)	Temp. (°C)	Contraction (not CO ₂ -free) (%)	Carbon Monoxide Conversion (%)	Total Hydrocarbons (g/m ³)	C ₁ + C ₂ Hydrocarbons (g/m ³)
102	228	44	96	145	7
608	229	44	95	142	6
1105	230	44	95	143	6
1604	231	42	93	140	5
2104	231	43	93	141	5

^a From Ref. 101.

The Atmospheric-pressure Synthesis. The results of early tests of iron catalysts were uniformly poor with respect to both activity and life¹²³. Some improvements have been made since the discovery of the medium pressure synthesis, especially for the purpose of substituting iron for cobalt catalysts in the German atmospheric plants. The catalysts of Pichler and Weinrotter¹³¹ (Fe-Cu-K₂CO₃) described on p. 181 (Table 77) had satisfactory activity and life in atmospheric synthesis with 1.2H₂ + 1CO gas, provided the catalyst was extracted with a 230–280°C synthesis fraction at 2 or 3 day intervals. Koelbel¹⁰¹ was able to obtain long lives and desirable selectivity from precipitated Fe₂O₃-MgO-CuO-K₂CO₃-kieselguhr catalysts in the atmospheric synthesis. Data for an experiment with water gas in a conventional reactor without recycle are given in Table 81. Here the catalyst was given no special pretreatment and apparently was not extracted. By using 2H₂ + 1CO gas with recycle at 200–220°C lives of more than 4 months were obtained.

Koelbel and Engelhardt¹⁰³ concluded that in the synthesis iron catalysts are chiefly oxidized by water vapor and reduced by carbon monoxide. At synthesis temperatures a reduced precipitated iron-copper catalyst was not oxidized by a carbon monoxide-steam mixture until the ratio $p_{\text{CO}}/p_{\text{H}_2\text{O}}$ became less than 2. The oxidation of precipitated iron-copper catalysts in the atmospheric pressure synthesis with $2\text{H}_2 + 1\text{CO}$ gas was studied as a function of position of catalyst in the bed and duration of the synthesis. The reactor was arranged so that the 30-cm bed of catalyst could be removed in 6 or 8 sections of equal length. These sections were analyzed for "reduced iron" which included metallic iron and carbides. Figure 70 shows the fraction of iron in the reduced state as a function of bed length for a

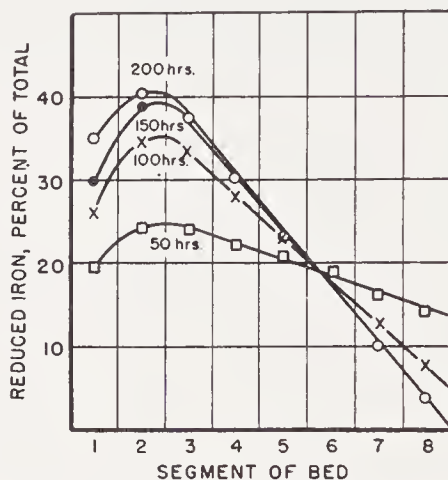


Figure 70. Reduced iron in supported iron-copper-kieselguhr catalysts as a function of bed length and time. $2\text{H}_2 + 1\text{CO}$ gas at 230°C and atmospheric pressure. (Reproduced with permission from Ref. 103)

precipitated iron-copper-kieselguhr catalyst used in the atmospheric synthesis without pretreatment. At 50 hours the analyses showed a maximum amount of "reduced iron" in the inlet portion of the catalyst bed. As the synthesis continued, the maximum remained in the same place; however, the content of "reduced iron" at the maximum increased while the extent of reduction at the outlet end of the bed decreased. The reduction reached a maximum at 200 hours. In another test a supported iron-copper catalyst was pretreated by an unspecified method to produce "reduced iron" to the extent of 50 to 60 per cent throughout the catalyst bed. Analysis of this catalyst after 1,000 hours of atmospheric synthesis at 230°C showed that the extent of reduction had increased slightly in the inlet portions of the catalyst bed but had decreased with bed length to a very low value at the outlet of the bed. These observations suggest that the ratio of partial pressures of carbon monoxide to water vapor were sufficiently high in the

inlet portion to reduce and/or carbide the catalyst, but due to the consumption of carbon monoxide and the production of water this ratio decreased so that the catalyst was oxidized in the remainder of the bed. The authors noted that the maximum amount of "reduced iron" always occurred at the same position in the bed, and believed that processes of inactivation of the catalyst such as sintering were not involved in producing the reduction-bed length pattern. If such an inactivation determined the reduction pattern, the position of the maximum should progress from the inlet to outlet ends of the bed with time of synthesis. These facts suggest that the eventual decrease in catalyst activity may be related to the oxidation of the outlet end of the catalyst bed; however, other factors such as accumulation of wax may decrease the activity in the atmospheric synthesis.

Pichler and Merkel¹²⁹ followed the composition changes of precipitated iron catalysts in atmospheric synthesis with $2\text{H}_2 + 1\text{CO}$ gas by thermomagnetic analysis. The composition of the catalysts follow:

A. $100\text{Fe}:0.25\text{Cu}:0.25\text{K}_2\text{CO}_3$ (alkali content not stated, but it may be inferred that this was their so-called standard preparation)

B. $100\text{Fe}:20\text{Cu}:0.25\text{K}_2\text{CO}_3$

C. $100\text{Fe}:20\text{Cu}:1.5\text{K}_2\text{CO}_3$

The samples were started directly in the synthesis at 235°C for catalysts A and B and 225°C for catalyst C without any pretreatment, and in the first hour or two the catalysts were reduced to magnetite. Following this reaction the contraction fell to a low value and then increased slowly. With catalyst A the contraction increased gradually for the first 49 hours, and this change was paralleled by a corresponding increase in the content of Hägg carbide (Curie point 265°C). However, the Hägg carbide content increased after the maximum contraction was attained, the iron as carbide being about 40 per cent after 120 hours of synthesis. The activity and composition data for catalyst B were similar except that a small amount of hexagonal carbide (Curie point 380°C), in addition to Hägg carbide and magnetite, was detected. Catalyst C was the most active of the group; however, due to the production of a high molecular weight product caused by the higher alkali content, frequent solvent extractions were necessary. Catalyst C carburized more rapidly and completely than the other samples, and sizable amounts of both Hägg and hexagonal carbides were present after 3 days. The magnetic curves for catalysts A, B, and C contained, in addition to Curie points for the phases described, plateaus and points of inflection that could not be explained. The authors concluded that the activity was proportional to the amount of carbide present in the catalysts with hexagonal carbide being more effective in increasing the activity than Hägg carbide.

The Medium-pressure Synthesis. The medium-pressure-synthesis

data announced by Fischer and Pichler in 1937^{123, 131} demonstrated that the synthesis with iron catalysts was more attractive in many respects than with cobalt catalysts. At the Kaiser Wilhelm Institut studies were made to establish the optimum pressure for the precipitated alkalized iron oxide gel catalysts. As shown in Figure 71, the optimum pressure for synthesis with $1\text{H}_2 + 1.5\text{CO}$ gas was between 10 and 20 atmospheres, and usually 15 atmospheres was chosen for subsequent synthesis tests¹²³. Although most iron catalysts operate satisfactorily at 15 atmospheres, the productivity, space-time-yield, of some other types of catalysts can without impairing

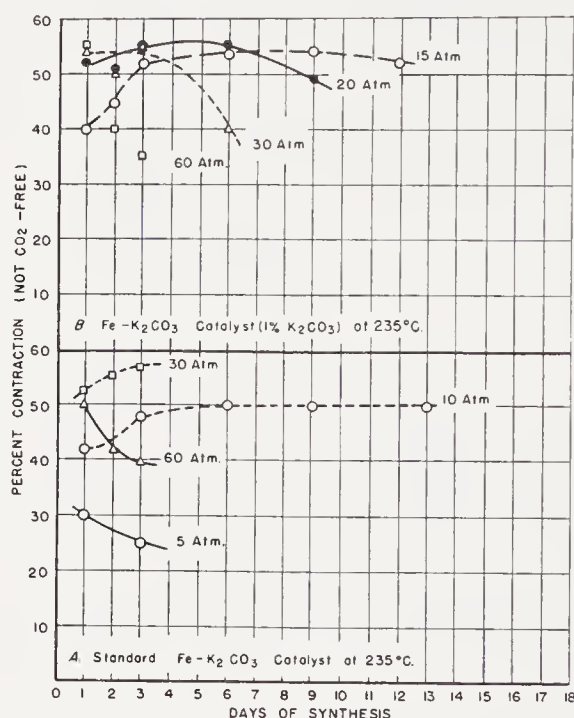


Figure 71. Variation of activity of precipitated iron catalysts with synthesis pressure. Constant flow of $1\text{H}_2 + 1.5\text{CO}$ gas. (From Ref. 123)

catalyst life be increased by employing higher pressures. Bureau of Mines tests¹⁵ compare the activity of several types of catalysts at 7.8 and 21.4 atmospheres as shown in Figure 72. In all cases the average activity was increased more than two-fold by increasing the synthesis pressure from 7.8 to 21.4 atmospheres. The activity of the precipitated catalyst declined more rapidly with time at the higher operating pressure, while the activity of the fused catalysts declined rapidly at 7.8 atmospheres, but was constant at 21.4 atmospheres. Sintered catalysts as well as nitrided fused catalysts had relatively constant activities at both pressures. The optimum pressure for reduced fused and sintered catalysts probably lies between 30 and 40 atmospheres, but this upper limit has not been carefully investigated.

The ultimate lives of many of the better iron catalysts are considerably longer than six months, and in most cases the tests have not been continued until the catalyst failed due to loss of activity, or factors related to loss of mechanical stability such as excessive spalling or plugging of the catalyst tubes. Most of the catalysts of the Schwarzheide tests (pp. 160 to 164) operated for 3 months with maximum temperatures of about 220°C, and if higher operating temperatures had been permitted, lives of at least 6 or 9 months might have been expected. The activity and mechanical proper-

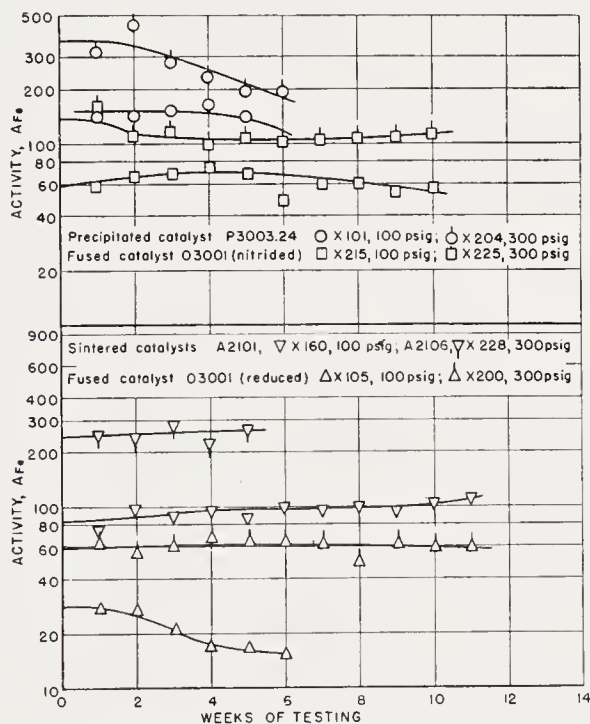


Figure 72. Activity of iron catalyst with 1H₂ to 1CO gas at 100 and 300 psig, (Reproduced with permission from Ref. 15)

ties of a nitrided fused catalyst (Figure 67) were unchanged after 6 months of operation. In the fluidized synthesis at high temperatures the catalyst life is relatively short, 2 to 3 weeks; however, the total productivity per unit weight of catalyst is relatively high, since the space velocity is 10 to 20 times higher than in the conventional fixed-bed synthesis. In the Bureau of Mines oil-circulation reactor³⁶ lives of reduced fused iron catalysts of 4 months have been attained. In these experiments the catalyst was given occasional reactivations with hydrogen under pressure. In this reactor massive iron catalysts activated by oxidation with steam and reduction with hydrogen both before and during the synthesis had a life of more than 6 months.

With Pichler's standard precipitated iron catalysts¹²³ lives as long as 15 months were obtained in tests with $1\text{H}_2 + 1.5\text{CO}$ gas at 15 atmospheres. These experiments, which are described on p. 178, demonstrate that catalysts that were not pretreated with carbon monoxide or synthesis gas at atmospheric or subatmospheric pressure had low activity and relatively short life. Presumably nearly horizontal tubes that were only partly filled with catalysts were used, and probably these long lives could not be achieved in vertical tubes. Koelbel¹⁰¹ described a three year test of a carrier-free precipitated iron catalyst in the medium pressure range with $1\text{H}_2 + 1.6\text{CO}$ gas. The catalyst was occasionally extracted with a hydrocarbon fraction.

For iron catalysts in the medium-pressure synthesis, reactivation procedures are usually ineffective and in most cases unnecessary; similar results were observed for cobalt catalysts in the medium pressure synthesis. Pichler¹²³ found that, after long periods of synthesis especially after the catalytic activity had declined, the catalyst could not be reactivated by treatment with hydrogen at 325°C or by repeating the induction procedure (carbon monoxide at 325°C and 0.1 atm.). If, however, the catalyst was reactivated with hydrogen frequently (at intervals of 5 to 10 days) some improvement in activity resulted. Pichler concluded that if activation of precipitated catalysts with hydrogen is desired, the reduction must be done as soon as the catalytic activity begins to decrease. For fused catalysts in the oil circulation reactor (granular catalyst submerged in oil) of the Bureau of Mines³⁶, reactivation with hydrogen at synthesis pressure and 250 to 300°C either with the catalyst submerged in cooling oil or with the oil removed was very effective in activating the catalyst, whereas similar treatment at atmospheric pressure did not improve the catalytic activity. The catalyst, after about a month of synthesis, contained large amounts of magnetite as well as small quantities of Hägg carbide. Both oxygen and carbidic carbon were quite completely removed in the pressure reactivation, although the temperature was at least 150°C lower than that required for the initial reduction. These results are in agreement with the experiments described on p. 172, in which reoxidized, fused catalysts were shown to reduce more readily than raw catalysts. In fixed-bed tests of reduced fused catalysts, hydrogen treatment at atmospheric pressure and 250 to 300°C apparently does not reduce either magnetite or carbides, nor does it remove the wax from the catalyst. Apparently hydrogen under moderate pressure is necessary for reduction to proceed to a significant extent; possibly pressure is required for hydrogen to penetrate wax-filled pores of the catalyst. This explanation may be a valid explanation for the observations of Pichler.

At Leuna²⁰² used ammonia-type catalysts were refused by the following

procedure: Before removal of catalyst from the reactor, wax was extracted and the catalyst was reduced in hydrogen. The catalyst was then stabilized by a slight oxidation with inert gas containing only small concentrations of oxygen to destroy the pyrophoric tendencies so that the material could be handled in air. Subsequently, the catalyst was remelted in oxygen in the manner employed in the initial preparation.

Ruhrchemie documents¹⁵⁰ describe the extraction of precipitated iron catalysts after use in the synthesis. Apparently these studies were made to establish a method for recovering the adsorbed wax and facilitating the removal of the catalyst from the reactor. After 45 days of synthesis with a wax-producing catalyst in a reactor having a volume of 127 liters, the catalyst was extracted at 140°C with a 150–210°C fraction of synthesis oil. Apparently, the reactor was merely filled with oil, and after an unspecified time the oil was drained from the unit. A sizable fraction of hydrocarbon boiling above 220°C was found in solvent after the first and second extractions, 29 and 18 per cent, respectively, but in subsequent extractions the distillation range was about the same as the original solvent. Hence only the first two extractions of this type were effective in removing absorbed wax. After the solvent from the last filling was drained from the reactor, the temperature was increased to 200°C with the result that 46.7 kg of solvent was displaced from the catalyst. Steam distillation at 200°C and 0.33 atmospheres (absolute) removed another 6 kg of solvent. Thus, the catalyst after the final extraction retained 52.7 kg of solvent corresponding to 71 liters per 127 liters of catalyst. Nitrogen was passed over the catalyst and the temperature was lowered to 120°C. Then the catalyst was treated with carbon dioxide and removed from the reactor with only light hammering. The catalyst was in good mechanical shape and was not pyrophoric. Extraction of a sample of this material with benzene in laboratory apparatus showed that the catalyst still contained 3.8 weight per cent of heavy wax.

Phase changes of iron catalysts in the medium-pressure synthesis are similar to those described for the atmospheric synthesis (pp. 193–195). Reduced catalysts are carburized and oxidized. Catalysts converted to carbide phases are also oxidized; however, at lower synthesis pressures carbides oxidize more slowly than reduced catalysts. Nitrided catalysts oxidize at a slow rate at all pressures investigated, and during the synthesis nitrides are converted to carbonitrides by carbon atoms replacing nitrogen. At higher synthesis temperatures such as those employed in fluidized reactors deposition of elemental carbon is the principal cause of catalyst disintegration, but at lower synthesis temperatures (less than 270°C) carbon deposition is usually not excessive.

Pichler and Merkel¹²⁹ studied the changes in composition of precipitated

iron catalysts by thermomagnetic and acid decomposition methods. An alkalized catalyst containing only a small amount of copper was pretreated with carbon monoxide (8 liters per 20 grams of iron per hour) at 325°C and 0.1 atmosphere for 24 hours (Pichler's standard induction procedure). Samples were taken from the inlet portion of the catalyst bed before and during synthesis at 235°C and 11 atmospheres (gas composition was presumably $1\text{H}_2 + 1.5\text{CO}$), and subjected to thermomagnetic analysis. The thermomagnetic curves indicated only the presence of Hägg carbide (Curie point = 265°C) in the samples taken after induction, and during the first 18 hours of synthesis. Samples at 40 and 62 hours showed the presence of magnetite in addition to Hägg carbide. After 109 hours of synthesis the catalyst contained sizable amounts of magnetite, roughly half Hägg carbide and half magnetite. The catalytic activity began to decrease after 62 hours, and this decrease was believed to be related to the progressive conversion of Hägg carbide to magnetite. The analyses indicated that α -iron, hexagonal carbide and cementite were not present. A similar catalyst was inducted with $1\text{H}_2 + 1\text{CO}$ gas at 325°C and 0.1 atmosphere, and operated in the synthesis at 215°C and 12 atmospheres for 400 hours. Samples taken before and after this period of synthesis contained chiefly Hägg carbide.

Acid decomposition studies of a series of active precipitated catalysts inducted in carbon monoxide at 325°C and 0.1 atmosphere indicated that the amount of carbidic carbon decreased 10 to 30 per cent in the first 7 days of synthesis (235°C and 15 atm.), and then remained essentially constant for periods as long as 112 days. In this period the oxygen content increased only slightly. The authors believed that catalysts pretreated to contain sizable amounts of Hägg carbide resisted chemical change, whereas if the pretreatment was not adequate or if the synthesis temperatures were too high, the content of carbidic carbon decreased rapidly and the amount of magnetite increased.

Herbst, Halle, and Brill^{80, 129} of I.G. Farbenindustrie found hexagonal and Hägg carbide in fused and precipitated iron catalysts after use in the synthesis. Precipitated catalysts, especially those containing copper, gave x-ray diffraction lines for hexagonal carbide. Hägg carbide was usually the only interstitial phase found in used fused catalysts; however, a fused catalyst (containing 87.6 per cent Fe, 3.42 Al_2O_3 , 3.6 CaO, and 0.52 K_2O in the raw state) used in the synol process at low temperatures ($\sim 200^\circ\text{C}$) contained large quantities of hexagonal carbide and a small amount of Hägg carbide. Apparently the presence of copper favors the formation of hexagonal carbide and stabilizes this phase. In copper-free catalysts, hexagonal carbide is found only in samples operated at low temperatures. The authors of these documents believed that the presence of hexagonal carbide was a necessary but not a sufficient condition for catalysts of high activity.

Jellinek and Fankuchen⁹² reported x-ray analyses of two reduced iron catalysts, presumably used in a fluidized reactor. After synthesis one active catalyst showed only the diffraction pattern of magnetite, while another catalyst which was somewhat more active and had been used for a longer period gave only the diffraction pattern of a carbide, presumed to be Hägg carbide. The authors were puzzled to find such dissimilar phases in two active catalysts. Eckstrom and Adcock³⁹ found a new iron phase, presumably a carbide of higher carbon content than Fe_2C , in catalysts used in the fluidized synthesis. Phase changes occurred in the following order: The reduced catalyst was rapidly and completely converted to Hägg carbide the first few days of synthesis. Then at a somewhat slower rate the Hägg carbide was converted to magnetite. When the Hägg carbide content had decreased to a low value, the magnetite was converted to this new phase. Despite these major changes in catalyst phases, the activity remained about the same. Seelig¹⁶³ and coworkers found that reduced catalysts in the fluidized synthesis were carburized and oxidized, and it was suggested that for most of the synthesis the iron of the catalyst could be assumed to be present as either Hägg carbide or magnetite.

At the Bureau of Mines composition and phase changes of catalyst D3001 ($\text{Fe}_3\text{O}_4\text{-MgO-K}_2\text{O}$) in the synthesis with $1\text{H}_2 + 1\text{CO}$ gas after reduction and after conversion to Hägg carbide, cementite, and ϵ -nitride were determined as a function of duration of synthesis. The entire catalyst charge was dropped into heptane, stirred, sampled, and replaced in the reactor. The samples were subjected to chemical, x-ray diffraction, and thermomagnetic analysis. Figure 73 shows the composition changes of a reduced catalyst during synthesis at 7.8 atmospheres¹⁰, obtained by a combination of analytical methods. After 46 hours at 235°C , the catalyst temperature was held at $257 \pm 2^\circ\text{C}$ with the flow of gas varied to maintain conversions of about 62 per cent. After about 1,900 hours the temperature was increased in several steps to 300°C . Catalyst activities corrected to 240°C were essentially constant during most of the test. In the first 46 hours of synthesis the total carbon to iron atom ratio (by chemical analysis) increased to about 0.2 and remained essentially constant until the synthesis temperature was increased near the end of the experiment. The x-ray and magnetic analyses, upper portion of Figure 73, indicated that the iron as Hägg carbide increased to 29 per cent early in the synthesis and then decreased at a slow rate. The iron as magnetite increased rapidly in the initial portion of the synthesis and then at a slower rate. Magnetite was produced chiefly at the expense of α -iron. Since the magnetic analysis was performed at a relatively low field strength, some of the magnetic phases were probably not saturated. This results in an incomplete accounting for iron phases, represented by the non-magnetic iron field of the composition diagram.

Operation at higher temperatures increased total carbon and magnetite, and decreased Hägg carbide. The amount of free carbon was not large at any time, and most of this carbon was apparently produced by the oxidation of Hägg carbide. Reduced catalysts oxidized more rapidly at 21.4 than at 7.8 atmospheres; however, at 21.4 atmospheres the activity remained essentially constant for long periods (see test X200 of Figure 72).

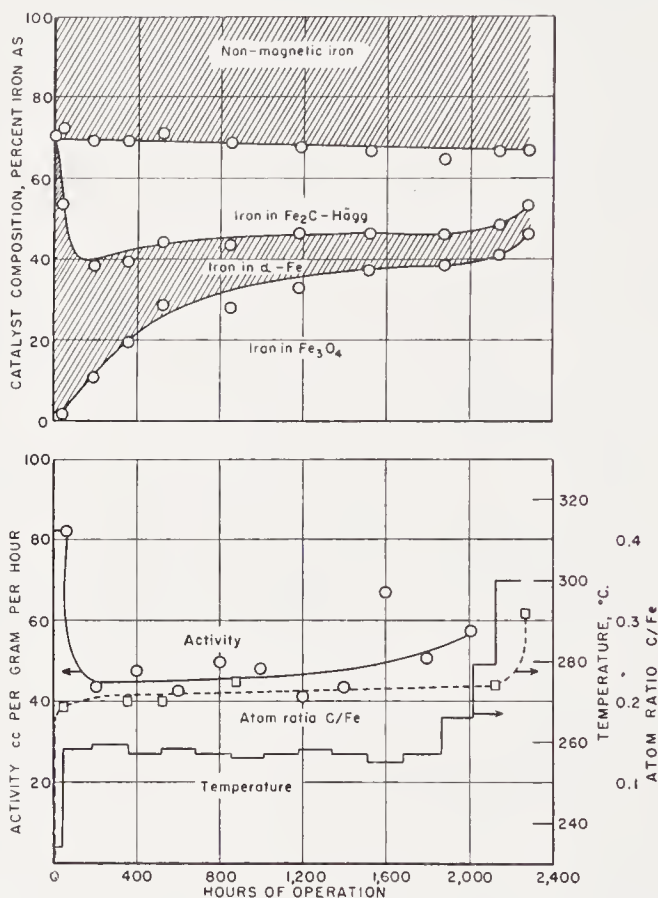


Figure 73. The variation of catalyst composition, activity and temperature with time: Fe_3O_4 -MgO- K_2O catalyst at 7.8 atmospheres at $1\text{H}_2: 1\text{CO}$ gas. (Reproduced with permission from Ref. 10)

Fused catalysts converted to Hägg carbide or cementite oxidize more slowly than reduced catalysts in the synthesis at 7.8 atmospheres, the carbides being oxidized to magnetite and free carbon. However, at 21.4 atmospheres the carbides oxidize at about the same rate as reduced catalyst. In the synthesis at 7.8 atmospheres the ratio of total carbon to iron increased during the tests; however, at higher pressures this ratio decreased. Table 82 illustrates the magnitude of the oxidation of reduced and carbided catalysts.

Nitrided iron catalysts have remarkable stability toward both oxidation and deposition of elemental carbon in the synthesis at both 7.8 and 21.4 atmospheres. Shultz, Seligman, Lecky, and Anderson¹⁷⁰ described composition changes of several types of nitrided iron catalysts in the synthesis. In test X218 with fused catalyst D3001 ($\text{Fe}_3\text{O}_4\text{-MgO-K}_2\text{O}$) using $1\text{H}_2 + 1\text{CO}$ gas at 7.8 atmospheres, the catalyst was sampled by the method described above. Only x-ray diffraction patterns of ϵ -iron nitride or carbonitride were observed, except for weak patterns of magnetite in a few samples. The changes in atom ratios of nitrogen, total carbon, elemental carbon, and oxygen to iron as well as the fraction of iron as ϵ -carbonitride and magnetite are given in Figure 74. In this figure the carbonitride phase was arbitrarily assumed to be composed of Fe_2C and Fe_2N to show the relative quantities of carbon and nitrogen in the ϵ -phase. During the first 98

TABLE 82. RATE OF OXIDATION OF REDUCED AND CARBIDED IRON CATALYSTS^a
($\text{Fe}_3\text{O}_4\text{-MgO-K}_2\text{O}$ with $1\text{H}_2 + 1\text{CO}$, conversion about 68 per cent)

Initial Phase	Increase in Iron as Magnetite in 35 to 40 Days of Synthesis, per cent of total Fe	
	7.8 atm.	21.4 atm.
α -iron (reduced)	40-70	78
Hägg carbide (>90%)	12	89-100
Cementite (>90%)	8	93

^a From Ref. 169.

days of synthesis, the temperature was maintained at 217°C, and the activity was essentially constant. The nitrogen content decreased while the carbon content increased, at rapid rates in the beginning of the synthesis and thereafter at lower rates. In this period the atom ratio of elemental carbon to iron increased from 0 to 0.10. The amount of iron present as magnetite was only about one fourth as great as in the test of the reduced catalyst in Figure 73. From 99 to 139 days the temperature was increased to 240° and finally to 258°C. The elimination of nitrogen and the deposition of both interstitial and elemental carbon were accelerated, but the rate of oxidation remained about constant.

Analytical data for other tests with nitrided catalyst D3001 at 7.8 and 21.4 atmospheres are given in Table 83. After 203 days of synthesis at 7.8 atmospheres in test X215, the catalyst contained only small amounts of magnetite and elemental carbon, and gave only the x-ray diffraction pattern of the ϵ -phase. Although the activity was still high, the catalyst was re-nitrided with ammonia at 350°C after 203 and 238 days of synthesis. After these ammonia treatments and subsequent synthesis, the catalyst still

produced only the x-ray diffraction pattern of ϵ -carbonitride. In test X349 at 21.4 atmospheres with $1\text{H}_2 + 1\text{CO}$ gas the catalyst composition changed more rapidly than at 7.8 atmospheres, especially the elimination of nitrogen and oxidation of the catalyst. After 37 days of synthesis 36 per cent of the iron was present as magnetite. In tests with $1\text{H}_2 + 1.5\text{CO}$ gas at 7.8 atmospheres (X236) and $2\text{H}_2 + 1\text{CO}$ gas at 21.4 atmospheres (X226)

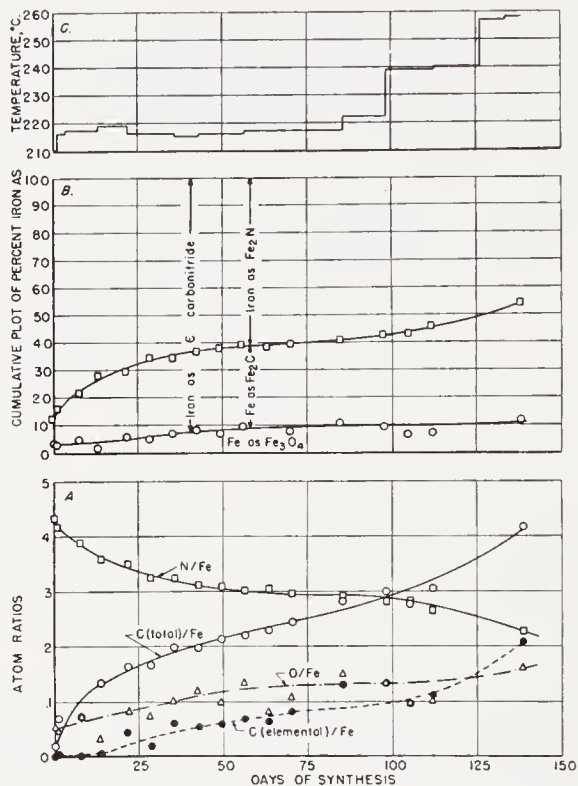


Figure 74. Composition changes of catalyst D3001 with days of synthesis with $1\text{H}_2 + 1\text{CO}$ gas at 100 psig in test X 218. Part A. presents atom ratios of nitrogen, total carbon, elemental carbon, and oxygen to iron. Part B. shows the distribution of iron as carbonitride and magnetite. Part C. presents the temperatures of synthesis. (Reproduced with permission from Ref. 170)

the changes in composition during synthesis appear to be about the same as in corresponding tests with $1\text{H}_2 + 1\text{CO}$ gas, although there is some uncertainty in comparing the catalyst composition of tests of different duration.

Nitrided catalysts of the fused type with alumina or zirconia as structural promoters oxidized less rapidly than magnesia-promoted catalyst D3001. In the synthesis at 7.8 atmospheres a nitrided sintered catalyst ($\text{Fe}_3\text{O}_4\text{-K}_2\text{O}$) and a nitrided precipitated catalyst ($\text{Fe}_2\text{O}_3\text{-CuO-K}_2\text{CO}_3$) oxidized at a very slow rate.

TABLE 83. COMPOSITION CHANGES IN NITRIDED CATALYST D3001 DURING SYNTHESIS^a

Test	Previous Treatment ^b	Total Days of Synthesis	Conditions of Previous Period of Testing		Phases from X-ray Diffraction ^e	Atom Ratios to Iron			Per cent Iron as		
			Temp. (°C)	Space Velocity, ^c		Carbon	Nitrogen	Oxygen	Fe ₂ C	Fe ₂ N	Fe ₃ O ₄
Operating pressure = 7.8 atmospheres (absolute)											
X215	RN	0	—	—	ε	0	0.46	0	0	92.0	—
	RNU	203	227	65	ε	.324	.194	.192	46.8	38.8	14.4
	RNUN ^f U	238	217	64	ε	.355	.266	.146	35.9	53.2	10.9
	RNUN ^f UN ^f U	252	223	63	ε	.358	.276	.140	34.3	55.2	10.5
	RN	0	—	—	ε	0	.46	0	0	92.0	—
X236 ^g	RNU	50	230	64	ε	.257	.302	.117	30.2	60.4	8.8
Operating pressure = 21.4 atmospheres (absolute)											
X349	RN	0	—	—	ε	0	.432	.082	0	86.4	6.2
	RNU	37	241	64	ε, M, α	.239	.138	.487	36.0	27.6	36.4
X226 ^h	RN	0	—	—	ε	0	.452	.068	0	90.4	5.1
	RNU	64	241	54	ε, M, α	.224	.140	.329	44.8	28.0	27.2

^a From Ref. 170.^b R = reduced in hydrogen, N = nitrided with ammonia, U = used in synthesis.^c Space velocity defined as volumes of synthesis gas (S.T.P.) per volume of catalyst space per hour.^d Apparent carbon dioxide free gas contraction.^e α = α-iron, ε = ε-nitride or carbonitride, M = magnetite. Phases are listed in order of decreasing amounts.^f Renitrided at 350° and a space velocity of ammonia of 1,000 for 6 hours.^g Synthesis with 1H₂ to 1.5CO gas.^h Synthesis with 2H₂ to 1CO gas.

Hydrogenation of nitrided catalysts after use in the synthesis removed virtually all of the nitrogen, but the carbon content was essentially unchanged and the oxygen decreased only slightly. In some cases the used-and-reduced catalysts contained cementite or Hägg carbide in addition to α -iron and magnetite; the carbide phase produced apparently depends upon the temperature of the reduction. After hydrogenation of the catalyst the synthesis products were characteristic of reduced catalysts, and the catalysts oxidized rapidly.

In this study of composition changes of nitrided catalysts¹⁷⁰, it was recognized that the presence of siderite (FeCO_3) or promoter carbonates would greatly complicate the interpretation of data from chemical analysis. On this basis the carbon dioxide content of the samples described in Table 83 were determined by digesting the used catalyst in hydrochloric acid. The carbon dioxide liberated was less than one per cent by weight for all catalysts except D3001 which contained magnesia, and for this catalyst the percentage of carbon dioxide exceeded four per cent in tests at 21.4 atmospheres. In this case it appears probable that most of the carbon dioxide was associated with the magnesia. In x-ray analysis of reduced catalysts after use in the synthesis, occasional samples, especially those from tests at pressures higher than those normally used in the medium pressure synthesis, gave diffraction lines corresponding to siderite. In any case the amount of siderite in used catalysts is usually small. Michael¹¹², however, reported that in the slurry process a scale of siderite deposited on the walls of reactors.

The Selectivity of Iron Catalysts

The products from iron catalysts are qualitatively similar to those from cobalt with only a few exceptions; the most important quantitative differences are the greater degree of branching of the carbon chain and the larger fractions of olefins and oxygenated molecules in products from iron catalysts.

Detailed Characterization of Hydrocarbons and Oxygenated Molecules. The products from the Schwarzheide tests (pp. 160 to 164) were characterized by a combination of precision distillation and chemical methods¹⁶⁶; however, an uncertain feature of these separations was that the oxygenated molecules dissolved in the hydrocarbon phases were not removed before the distillation, but were determined by chemical methods on the fractions. In the presence of oxygenated molecules, distillation data for hydrocarbons may be difficult to interpret. Apparently there was no analysis for aromatic hydrocarbons and no detailed determination of oxygenated molecules. Table 84 presents the carbon number distributions for hydrocarbons, the data being averages of the analyses of 3 or 4 samples

taken during the course of the tests. Included for comparison is the distribution of hydrocarbons from the fluidized-iron synthesis²⁰⁰. Products from the Lurgi and Brabag catalysts had the highest average molecular

TABLE 84. CARBON NUMBER DISTRIBUTIONS FOR HYDROCARBONS FROM SYNTHESIS WITH IRON CATALYSTS

Carbon Number	Weight Per cent of Total Hydrocarbons						
	K.W.I.	Lurgi	Brabag	I.G. Farben.	Ruhr-chemie	Rhein-preussen	Fluid Reactor ^a
1	8.5	7.1	6.6	10.4	9.4	9.6	8.9
2	9.0	7.0	6.9	9.3	8.3	9.5	7.8
3	11.7	8.5	8.7	12.7	10.8	12.9	15.9
4	9.2	6.8	7.0	9.1	8.2	10.2	13.9
5	6.2	6.0	5.8	7.4	5.4	7.8	11.5
6	5.7	4.4	5.5	5.3	5.2	6.0	8.6
7	4.3	3.6	4.1	3.6	4.0	5.1	6.6
8	4.0	3.2	3.1	3.7	3.7	4.4	5.0
9	3.1	2.4	3.3	2.8	3.0	3.6	3.9
10	3.2	2.7	3.6	2.8	2.9	3.3	3.0
11	4.5	3.4	4.8	3.3	4.1	4.1	2.4
12							1.8
13	4.1	3.8	5.0	2.8	3.0	4.0	1.4
14							1.1
15	3.0	3.3	4.7	2.7	3.0	4.4	1.0
16							0.9
17	3.2	3.0	4.4	2.4	2.9	2.5	6.3 ^b
18							
19-27	7.7	8.3	10.0	5.9	8.3	6.6	
>27	12.6	26.5	16.5	15.8	17.8	6.0	
C ₁ -C ₄	38.4	29.4	29.2	41.5	36.7	42.2	46.5
C ₂ -C ₄	30.1	22.3	22.5	30.9	27.3	32.6	37.6
C ₅ ⁺	61.6	70.6	70.8	58.6	63.4	57.8	53.5
C ₅ -C ₁₂	31.0	25.7	30.2	28.9	28.3	34.3	42.8
C ₁₃ -C ₁₈	10.3	10.1	14.1	7.9	8.9	10.9	
C ₁₉ ⁺	20.3	34.8	26.5	21.7	26.1	12.6	
C ₁₃ ⁺	30.6	44.9	40.6	29.6	35.0	23.5	10.7

^a From Ref. 200.

^b Average carbon number of 30.

weight and those from the I.G. Farben. and Rheinpreussen catalysts the lowest. Table 85 also compares the hydrocarbon distribution for the Schwarzheide tests and the fluidized synthesis. The fluidized synthesis produced larger yields of C₂-C₄ hydrocarbons and gasoline but smaller yields of diesel oil and wax. All of the distributions in Table 84 have maxima

at C_3 . The yield of C_2 is usually equal or less than C_1 or C_3 , whereas above C_3 the yields decrease monotonically with increasing carbon number.

The carbon number distributions of Table 84 are plotted as the logarithm

TABLE 85. COMPARISON OF SCHWARZHEIDE AND FLUIDIZED SYNTHESIS PRODUCTS

	Per cent of total Hydrocarbons	
	Range for Products from Schwarzheide Tests	Fluidized Synthesis (Weitkamp)
C_1	8.5-10.4	8.9
C_2 - C_4	22.3-32.6	37.6
Gasoline	25.7-34.3	42
Diesel oil	7.9-14.1	10.7
Wax	12.6-34.8	
	20.5-48.9	

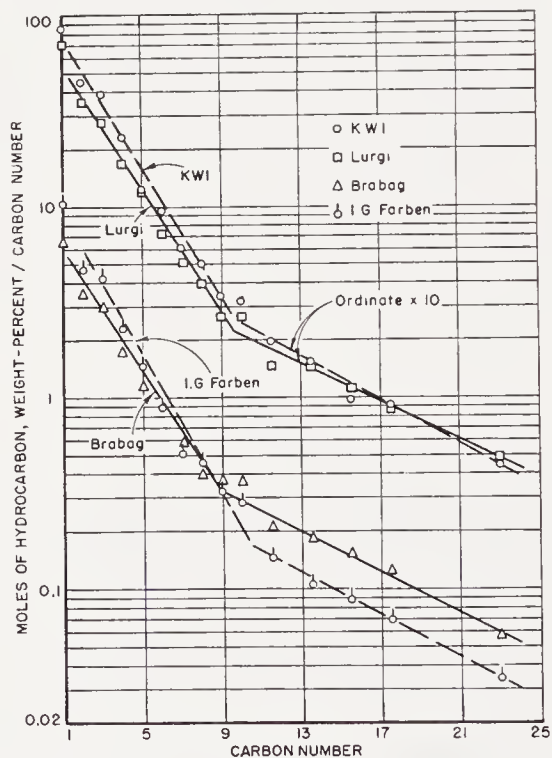


Figure 75. Logarithmic plots of moles against carbon number for hydrocarbons from Schwarzheide tests.

of moles in carbon number fractions against carbon number in Figures 75 and 76. The data can be approximated by two straight lines, one portion extending from carbon numbers 3 to 9 and the other from 10 to 21.

In the Schwarzheide products, the olefin content of the fractions was low at C_2 and then increased to a maximum at C_3 to C_6 , as shown in Figure 77.

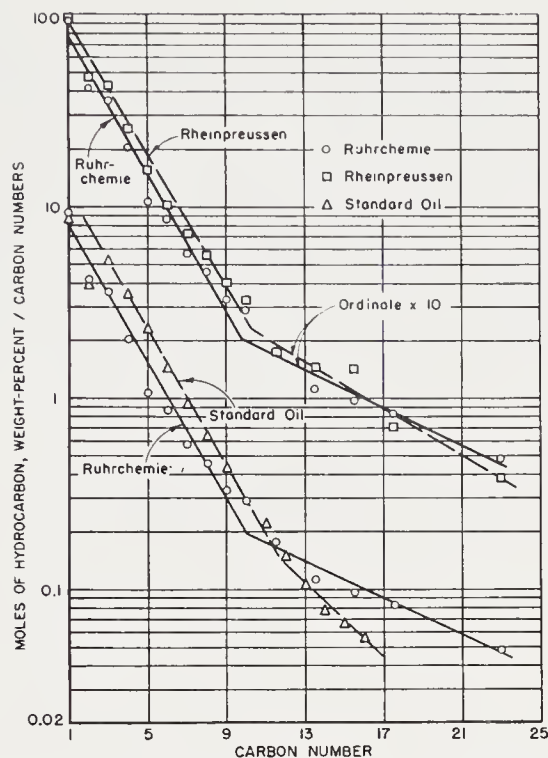


Figure 76. Logarithmic plots of moles against carbon number. Hydrocarbons from Schwarzheide tests compared with those from fluidized synthesis.

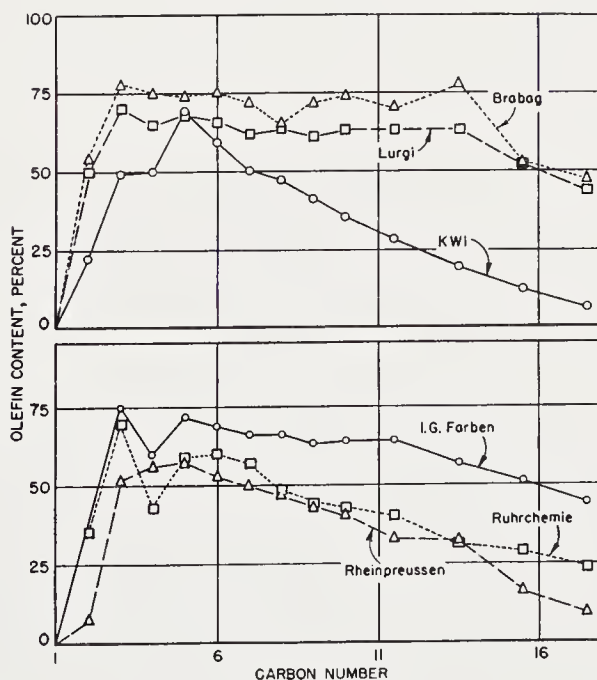


Figure 77. Olefin content as a function of carbon number for products from the Schwarzheide experiments.

Above C_5 or C_6 the olefin content decreased with increasing carbon number except for Lurgi and Brabag products, for which the unsaturation remained essentially constant from C_3 to C_{12} .

The extent of branching of C_4 , C_6 , and C_7 hydrocarbons from the Schwarzheide tests (Table 86) was determined by precision distillation. These characterizations are not as accurate or detailed as those determined by a mass spectrometer. For example, the increase in branching from C_6 to C_7 fractions appears to be smaller than would be expected on the basis of other available data, and the branching of the C_6 and C_7 fractions from cobalt catalysts, 10.4 and 12.3, respectively, agrees only approximately with the values of Friedel and Anderson⁶⁴ (p. 112).

TABLE 86. THE EXTENT OF BRANCHING OF HYDROCARBONS FROM THE SCHWARZHEIDE TESTS^a

	Per cent Branched Hydrocarbons in Following Fractions		
	C_4	C_6	C_7
Brabag	—	13	13
Ruhrchemie	9.6	11	11
Lurgi	—	13	13
Kaiser Wilhelm Institut	6.7	14.5	17
	7.9		
I. G. Farben.	—	16	18
Rheinpreussen	—	11	12
Normal cobalt catalyst	—	12.5	16.5

^a From Ref. 166.

In the last few years, American petroleum companies have published excellent detailed analyses of products from the fluidized synthesis. These studies have employed modern techniques of fractionation and separation, together with spectroscopic analyses. The carbon number distribution of products from this process at 315°C and 18 atmospheres of $2H_2 + 1CO$ gas determined by Weitkamp and co-workers²⁰⁰ was shown in Table 84 and Figure 76. Although the products were qualitatively similar to those of the Schwarzheide tests, the average molecular weight of hydrocarbons from the fluidized synthesis was lower. The distribution of hydrocarbons into paraffins, olefins, and aromatics is given in Figure 78. Although the aromatics in the fractions of higher carbon number were as high as 20 per cent, the aromatics based on total hydrocarbons was only 2.3 per cent by weight. As in the German data, the olefin content of fractions above C_5 decreased with increasing molecular weight.

Mass spectrometric methods permit detailed analysis of lower hydro-

carbons. First to be considered is the chain branching of C_4 to C_8 aliphatic hydrocarbons. Data of Bruner²⁸, Weitkamp²⁰⁰, and Clark³² in Table 87 are remarkably consistent. The extent of branching increased with carbon number in a manner similar to that observed for products from cobalt catalysts; the extent of branching, however, was greater for hydrocarbons from iron catalysts. Dimethyl-substituted carbon chains were found, but none containing quaternary carbon atoms. The ethyl-substituted isomer, 3-ethylpentane was not found in the C_7 hydrocarbons. More detailed data for chain structure and double-bond position of C_2 to C_6 aliphatic hydro-

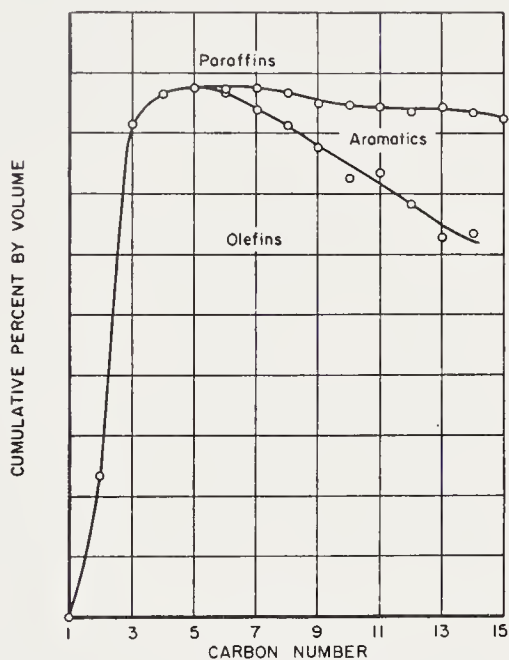


Figure 78. Composition of hydrocarbons from fluidized synthesis as a function of carbon number. (From data of Ref. 200)

carbons are presented in Table 88. In both the straight- and branched-chain olefins, the isomers with double bond in the alpha position were present in greater amounts.

Small amounts of cyclo-pentane, -pentene, -hexane and -hexene and their derivatives were found in the following percentages in the C_5 , C_6 , and C_7 fractions, respectively, 0.5, 1.8, 4.2²⁰⁰. Cady, Launer, and Weitkamp²⁹ made a detailed study of the aromatic hydrocarbons present in oils from fluid reactors. Table 89 indicates that the isomers with the longest side chains are present in the larger amounts.

Iron catalysts usually produce greater yields of oxygenated organic molecules than cobalt catalysts. High yields of these products in the fixed-bed synthesis were obtained in the synol process^{5, 139} with an alkalized, fused-

TABLE 87. CHAIN BRANCHING IN PARAFFINS PLUS OLEFINS
FLUIDIZED-IRON SYNTHESIS

	Bruner ^a	Clark ^b	Weitkamp ^c
C C C C	89.4		89.6
C C C C	10.6		10.4
C C C C C	81.2	80.4	80.3
C C C C C	18.8	19.6	19.7
C C C C C C	78.8		73.7
C C C C C C	11.2		14.1
C C C C C C	9.5		8.9
C C C C C C	0.4		3.3
C C C C C C C	66.0		70.0
C C C C C C C	13.1		10.4
C C C C C C C	19.1		17.6
C C C C C C C	1.6		1.0
C C C C C C C	0.3		1.0
C C C C C C C C	61.0		
Mono methyl	36.4		
Dimethyl	2.6		

^a From Ref. 28.^b From Ref. 32.^c From Ref. 200.

iron catalyst with a recycle ratio of 10 to 1 and $1.3\text{H}_2 + 1\text{CO}$ fresh feed at 20 atmospheres and temperatures from 190 to 210°C. Here the principal products were alcohols and olefins with moderate amounts of paraffins,

TABLE 88. CHAIN STRUCTURE AND DOUBLE-BOND POSITION OF $\text{C}_2\text{-C}_6$ ALIPHATIC HYDROCARBONS FROM THE FLUIDIZED-IRON SYNTHESIS^a

C C 72	C=C 28			
C C C 28	C C=C 72			
C C C C 12.2	C C C=C 69.8	C C=C C <i>trans</i> 4.1 <i>cis</i> 3.5		
C C C C 2.0	C C=C C 8.4			
C C C C C 8.3	C C C C=C 68.6	C C C=C C <i>trans</i> 1.5 <i>cis</i> 1.5		
C C C C C 4.3	C C C=C C 4.9	C C=C C C 0.6	C=C C C C 9.8	
C C C C C C 8.1	C C C C C=C 62.2	<u>C C C C=C C</u> <u>C C C=C C C</u> 1.3		
C C C C C C 1.4	C C C C=C C 2.8	C C C=C C C 1.5	C C=C C C C <i>trans</i> 0 <i>cis</i> —	C=C C C C C 8.0
C C C C C C 4.5	C C C C=C C 2.6	C C C=C C C <i>trans</i> trace <i>cis</i> 1.0	C C C C C C 0.5	
C C C C C C 0.9	C C C=C C C 0.9	C C=C C C C 1.4		
C C C C C C Not present	C C=C C C C Not present			

^a From Ref. 200.

aldehydes, and ketones, and minor quantities of acids and esters. Evidence was obtained for the presence of unsaturated alcohols. The carbon number distribution of alcohols, olefins, and paraffins in synol products, as computed by Storch¹⁸¹ from the data of Reisinger¹³⁹ (Table 90), shows that the yield of alcohols remained large up to rather high carbon numbers. This

fact is presented more clearly in Figure 79, where the weight per cent of alcohols is plotted.

The characterization of oxygenated products from the fluidized synthesis by American petroleum companies is the most detailed and precise of available data on Fischer-Tropsch oxygenates. Despite the high synthesis temperature, the fluidized synthesis produces high yields of oxygenated molecules. Unfortunately, in the papers on this subject, the data are not

TABLE 89. DISTRIBUTION OF AROMATIC HYDROCARBONS PRODUCED BY THE FLUIDIZED SYNTHESIS^a

Carbon Number	Weight Per cent of Total Hydrocarbons	Analysis of Fraction	
		Compound	Volume Per cent
6	0.024	Benzene	100
7	.18	Toluene	100
8	.27	{ Ethylbenzene	46
		{ <i>o</i> -Xylene	29
		{ <i>m</i> -Xylene	18
		{ <i>p</i> -Xylene	7
		{ <i>n</i> -Propylbenzene	39
9	.29	Isopropylbenzene	2
		1-Methyl-2-ethylbenzene	19
		1-Methyl-3-ethylbenzene	23
		1-Methyl-4-ethylbenzene	9
		1,2,3-Trimethylbenzene	1 (?)
		1,2,4-Trimethylbenzene	6
10	.21	1,3,5-Trimethylbenzene	1
11	.26		
12	.28		
13	.30		
14	.22		

^a From Ref. 29.

presented in a manner that permits a simple comparison of the yields of oxygenates and hydrocarbons. According to Weitkamp²⁰⁰, 66 per cent of the carbon monoxide consumed appeared as hydrocarbons and 18 per cent as oxygenated molecules, 10 per cent in the aqueous layer and 8 per cent in the oil phase. On this basis, hydrocarbons comprise approximately 72 per cent by weight of the total product, exclusive of water and carbon dioxide; oxygenated organic molecules, 17 and 11 per cent in aqueous and oil layers, respectively. The total yield of oxygenated molecules was 39 per cent of the total hydrocarbons and 73 per cent of the liquid (C₅+) hydrocarbons. The yields, of course, can be varied somewhat by changing

operating conditions and catalyst composition. The data of Morrell¹¹⁵ in Figure 80 show that the distribution of oxygenated molecules varies in a manner similar to hydrocarbons, and these workers suggested that a relationship may exist between C_n hydrocarbons and C_{n+1} oxygenates.

TABLE 90. DISTRIBUTION OF SYNOL PRODUCTS^a

Carbon Number	Mole Per cent ^b			
	Alcohols	Olefins	Paraffins	Total
1	2.35	—	37.3	39.65
2	4.36	5.98	1.37	11.71
3	4.55	9.68	2.33	16.56
4	1.47	7.41	1.79	10.67
5	0.765	2.09	0.67	3.53
6	.681	3.17	.78	4.63
7	.783	1.075	.87	2.73
8	.645	0.938	.39	1.97
9	.627	.424	.36	1.41
10	.651	.245	.19	1.09
11	.502	.125	.13	0.757
12	.460	.203	.045	.708
13	.269	.120	.032	.421
14	.209	.131	.020	.360
15	.275	.090	.019	.384
16	.203	.108	.009	.320
17	.096	.084	.008	.188
18	.141	.078	.011	.230
19	.140	.072	.007	.219
20	.123	.078	.007	.208
21	.110	.045	.006	.161
22	.191	.030	.006	.227
>22	.848	.930	.045	1.823

^a From Ref. 181.

^b 7.2 weight per cent of esters + aldehydes + ketones + acids is not included in this distribution.

The yields of water-soluble oxygenated molecules from fluidized synthesis of three groups^{40, 115, 178} are presented in Table 91. As an average, about 50 per cent of these chemical were alcohols, 25 acids, 15 ketones, 8 aldehydes, and 2 esters. In all cases the yields of these molecules were maximum at C_2 . The yields of acids were very much larger than those obtained in the fixed-bed experiments at low temperatures. Only small yields of methanol and formaldehyde were found; however, the production of these molecules may be limited by the unfavorable thermodynamics of their synthesis. Both secondary alcohols and alcohols with branched-carbon chains were

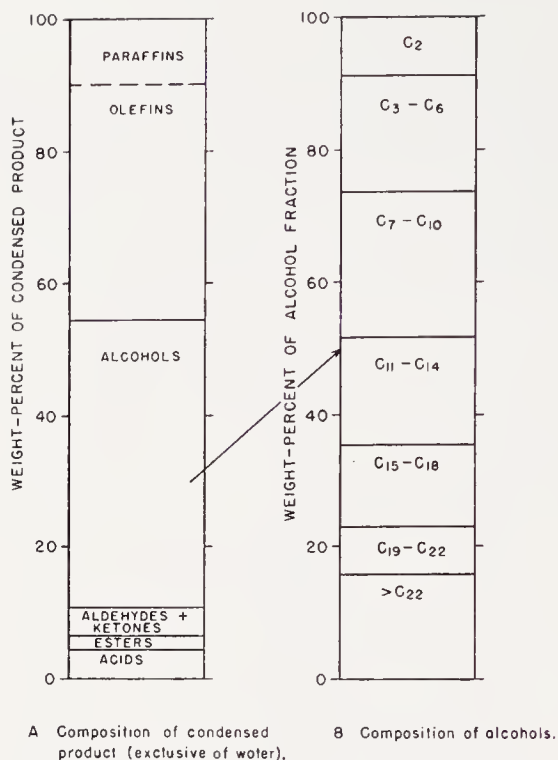


Figure 79. Products from the synol process with a fused $\text{Fe}_3\text{O}_4\text{-Al}_2\text{O}_3\text{-K}_2\text{O}$ catalyst. (From Ref. 5)

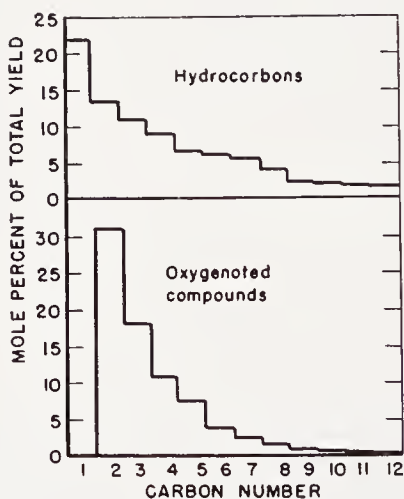


Figure 80. Comparison of the carbon number distributions of hydrocarbons and oxygenated molecules from fluid synthesis. (Reproduced with permission from Ref. 115)

found in considerably smaller amounts than the corresponding straight-chain primary alcohol. Cain³⁰ characterized many of the oxygenated compounds in the oil phase. The content of oxygenates in the oil phase was about 27 per cent, as shown in Table 92. Alcohols, acids, and carbonyl

TABLE 91. OXYGENATED COMPOUNDS IN WATER PHASE FROM FLUIDIZED SYNTHESIS

	Weight Per cent of Type Compound			Weight Per cent of Total Oxygenated Compounds			Weight per cent in Aqueous Phase		
	A ^a	B ^b	C ^c	A	B	C	A	B	C
Alcohols:				42.2	51.9	58.7	4.3	—	5.1
Methanol	0.5	0.5	0.6						
Ethanol	58.2	71.0	78.6						
1-Propanol	25.3	16.7	16.1						
2-Propanol	6.0	1.5							
1-Butanol	6.8								
2-Methyl-1-propanol	0.7	7.7	(>C ₃ 4.6)						
1-Pentanol	1.7	(>C ₄ 2.3)							
3-Methyl-1-butanol	0.8								
Acids:				30.4	27.0	20.7	3.1	—	1.8
Acetic	72	67.0	48						
Propionic	18	17.4	18						
Butyric	2	12.6	14						
C ₆ acids	2	(>C ₄ 3.0)	(>C ₄ 20)						
Ketones:				21.6	10.8	10.3	2.2	—	0.9
Acetone	75.6	69.4	73						
Butanone	18.1	20.4	25						
2-Pentanone	4.9	(>C ₄ 10.2)							
2-Hexanone	1.3								
Aldehydes:				5.8	10.3	6.9	0.6	—	0.6
Formaldehyde	trace								
Acetaldehyde	69.5	58.3	48.7						
Propionaldehyde	19.5	21.4	25.7						
Butyraldehyde	7.3	20.3	23.0						
<i>n</i> -Valeraldehyde	3.7		(>C ₄ 2.6)						
Esters:				0.04	—	3.4	0.004	—	0.3
Methyl acetate	20								
Ethyl acetate	80								
				100.0	100.0	100.0	10.2	10-20	8.7

^a From Ref. 178.^b From Ref. 40.^c From Ref. 115.TABLE 92. COMPOSITION OF OIL PHASE FROM FLUIDIZED SYNTHESIS^a

Type of Compounds	Estimated Weight per cent of Oil Phase
Alcohols	8.0
Acids	8.1
Aldehydes + ketones	9.4
Esters	1.5
Hydrocarbons	73.0

^a From Ref. 30.

compounds (aldehydes plus ketones) were present in about equal amounts, and the yield of esters was low. The yields of the three principal types of oxygenated molecules in the oil phase as a function of carbon number are shown in Figure 81. Above C₄, where solubility in aqueous phase becomes

relatively unimportant, the yields of all of these components decreased regularly with carbon number, and the molar quantities of acids was greater than either alcohols or carbonyls. The branching of the carbon chain of the alcohols was about the same as that of the corresponding olefin; for example, the C_4 alcohols contained 8 per cent 2-methyl-1-propanol and the C_{10} alcohols 52 per cent molecules with branched-carbon chains. Branching in the acids was somewhat greater than in the alcohols, and the branches on the carbon chain appeared to be located near the carboxyl group. A sizable concentration of unsaturated alcohols and acids was found, increasing from about 2 per cent at C_5 to 20 per cent at C_{10} . Bifunctional molecules, such as dibasic acids or acids containing hydroxyl or carbonyl groups, were not found; however, a variety of oxygenated compounds

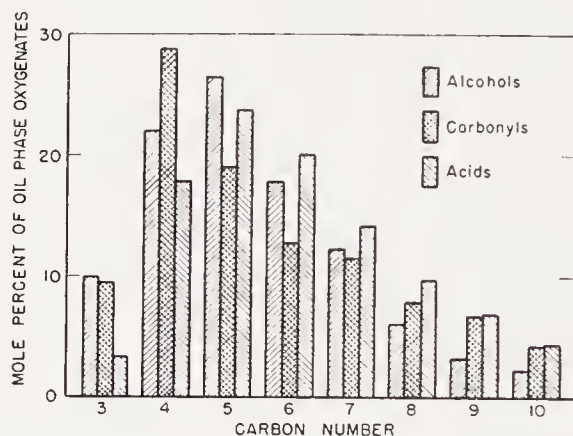


Figure 81. Distribution of types of oxygenated molecules in oil phase from fluid synthesis with iron catalysts. (Reproduced with permission from Ref. 115)

containing aromatic structures or unsaturated bonds were present in trace amounts.

Products from two nitrided iron catalysts were characterized in some detail at the Bureau of Mines⁵. Samples of the oil phases were distilled into 100°C fractions from 50 to 450°C. These fractions were separated into hydrocarbon and oxygenated portions by chromatography, and the oxygenated material was characterized for functional groups by chemical and spectrometric methods. From those data and an analysis of the aqueous phase, the product distribution diagrams in Figures 82 and 83 were constructed. For some fractions, the analyses did not account for the entire product and these differences are indicated by question marks. In addition, alcohols were separated from the oil and aqueous phases by formation of half-acid phthalates. In the separation procedure, esters in the aqueous phase were hydrolyzed and acids and ketones in the oil phase were not separated. The yields of alcohols actually separated (Table 93) were slightly

lower than those derived from functional group analysis in Figures 82 and 83. Alcohols were apparently chiefly straight-chain, primary type. Esters were present in sizable amounts in products from the fused catalyst promoted with alumina. Yields of aldehydes, ketones, and organic acids were relatively small. The main differences between the synol and nitrided products were the rather rapid decrease in alcohol yield with increasing carbon number and the higher yields of esters from the alumina-promoted nitrided catalysts.

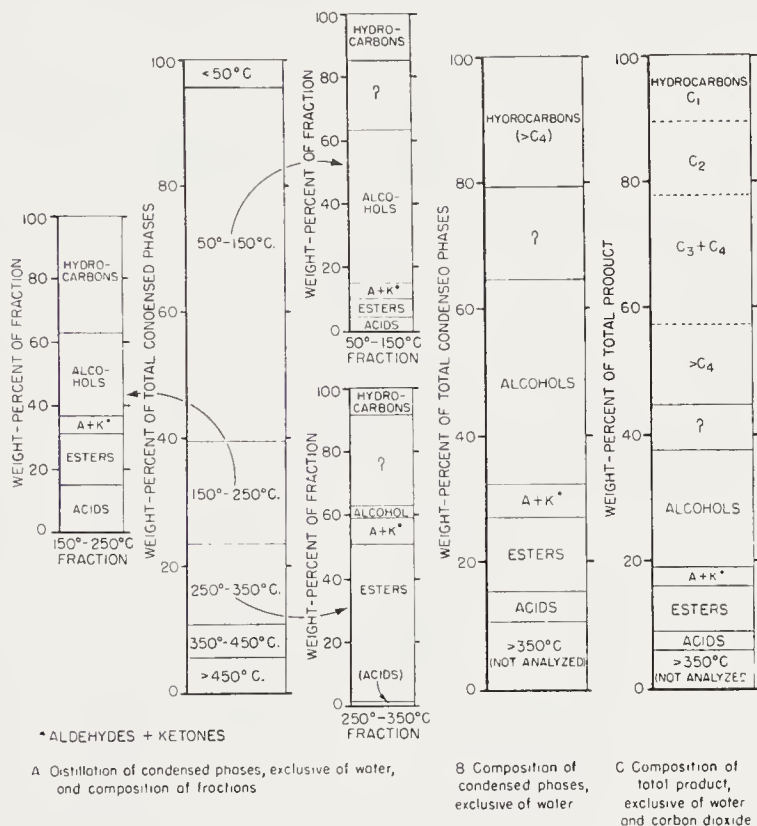


Figure 82. Product from Fischer-Tropsch synthesis with nitrided fused $\text{Fe}_3\text{O}_4\text{-Al}_2\text{O}_3\text{-K}_2\text{O}$ catalyst. $1\text{H}_2 + 1\text{CO}$ gas at 21.4 atm. (Reproduced with permission from Ref. 5)

Selectivity as a Function of Composition and Pretreatment of Iron Catalysts. In these and the subsequent pages, the factors determining selectivity—catalyst composition, pretreatment, and operating variables (temperature, pressure, flow, gas composition, etc.)—are considered. Depending upon the combination of circumstances, any of these factors may control the selectivity. On this basis, selectivity data must be carefully evaluated.

Alkali, usually potassium compounds such as KOH , K_2CO_3 , and KNO_3 ,

is the most important and probably the only necessary promoter for iron catalysts. The use of a variety of potassium salts had essentially the same effect on the selectivity of precipitated iron catalysts^{123, 131}. K.W.I.¹²³ and Bureau of Mines tests¹⁵ of precipitated iron or iron-copper catalysts (Figures 32 and 33) indicated that the average molecular weight of the product increased with increasing alkali content to 1 part K_2CO_3 per 100Fe for the experiments at 15 atmospheres and to the highest alkali content employed in tests at 7.8 atmospheres. Similarly, the average molecular weight of

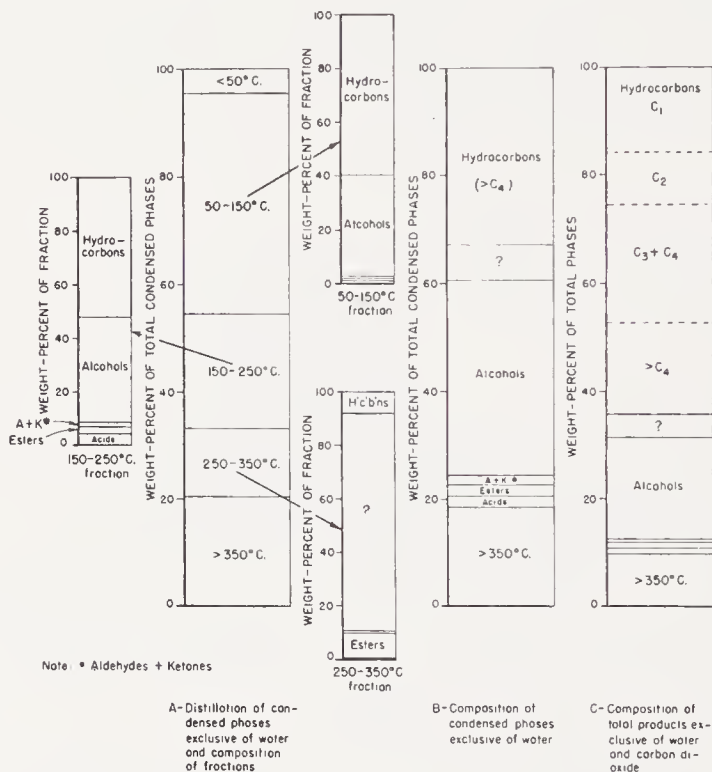


Figure 83. Product from Fischer-Tropsch synthesis with nitrated fused Fe_3O_4 - MgO - K_2O catalyst. $1H_2 + 1CO$ gas at 21.4 atm.

products from precipitated Fe-Cu-kieselguhr catalysts⁹⁸ increased with alkali content to 6 or $8K_2CO_3$ per 100Fe at 5.8 and 9.7 atmospheres, but was essentially constant at 14.5 and 19.4 atmospheres in the range 2 to $8K_2CO_3$ per 100Fe. With fused and sintered catalysts, the average molecular weight of hydrocarbons increased to a maximum at about $0.5K_2O$ per 100Fe and then remained essentially constant (Figure 44 and Figure 47). Figure 84 presents the analysis of product fractions (expressed as weight-per cent functional group in liquid fractions) from a sintered iron catalyst at 21.4 atmospheres as a function of alkali content. The overall distribution of products in this series of tests is shown in Figure 47. The alcohol content

of fractions increased with alkali concentration to about 0.5K₂O per 100Fe and then decreased. The olefin content increased to about 0.25K₂O per 100Fe and then decreased. α -Olefins predominated in all samples, and the

TABLE 93. ALCOHOLS SEPARATED FROM PRODUCTS OF NITRIDED IRON CATALYSTS

Test Number	X337A			X349		
Catalyst	Fe ₃ O ₄ -Al ₂ O ₃ -K ₂ O			Fe ₃ O ₄ -MgO-K ₂ O		
Component	Composition, Weight Per cent in					
	Oil Phase	Aqueous Phase	Total Condensed Product (exclusive of H ₂ O)	Oil Phase	Aqueous Phase	Total Condensed Product (exclusive of H ₂ O)
Acids	<i>a</i>	5.28	1.74 ^b	<i>a</i>	1.93	0.69 ^b
Acetone	<i>a</i>	0.12	0.04 ^b	<i>a</i>	0.25	.09 ^b
Methylethyl ketone	<i>a</i>	.09	.03 ^b	<i>a</i>	.11	.04 ^b
Methyl propyl ketone	<i>a</i>	.06	.02 ^b	<i>a</i>	.08	.04 ^b
Alcohols	20.46 ^c	14.32 ^d	23.80	19.49 ^c	28.72 ^d	28.52
Methanol	0.06	0.51	0.23	0.11	3.30	2.18
Ethanol	5.70	11.53	9.12	3.78	17.03	9.47
<i>n</i> -Propanol	3.28	1.51	3.54	3.64	5.01	5.03
<i>i</i> -Propanol	0.08	—	0.07	0.40	0.67	0.59
<i>n</i> -Butanol	2.85	0.48	2.82	2.56	1.65	2.87
<i>i</i> -Butanol	0.01	—	0.01	—	—	—
<i>n</i> -Pentanol	2.29	0.23	2.22	3.08	0.76	3.01
<i>n</i> -Hexanol	1.89	.06	1.78	1.92	.30	1.82
<i>n</i> -Heptanol	1.54	—	1.44	0.14	—	0.12
<i>n</i> -Octanol	0.95	—	0.88	.03	—	.02
<i>n</i> -Nonanol	.63	—	.59	3.26 } C ₉ ⁺	—	2.90
C ₁₀ ⁺ alcohols	1.18	—	1.10			
	—	—	—	0.57 ^e	—	0.51 ^e
Total oxygenated molecules separated	20.46	19.87	25.63	19.49	31.09	29.38

^a These organic molecules were not separated from oil phase.

^b Only from aqueous phase.

^c Does not include alcohols combined in esters.

^d Includes alcohols combined in esters.

^e Secondary alcohols.

amount of internal olefins decreased with alkali content. The olefin content of the C₃ and C₄ fractions remained essentially constant. For C₂ hydrocarbons, the olefin content increased slightly up to 0.2 K₂O per 100Fe and then remained constant. In fluidized tests^{168, 200} the alkali content had

a more pronounced influence on the olefin concentration of the gaseous hydrocarbons, as shown in Table 94. Weitkamp²⁰⁰ reported similar data in which the C₂-C₄ hydrocarbons were characterized in detail, as shown in Table 95. The olefin content of the gaseous hydrocarbons from the alkalized

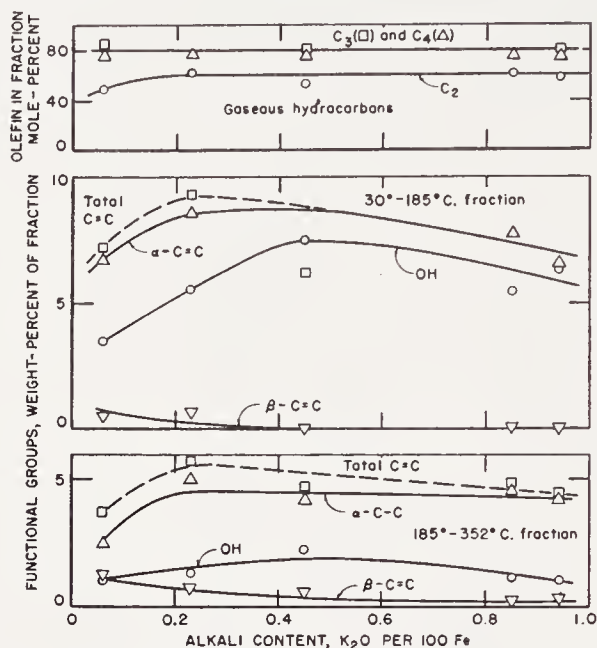


Figure 84. Analysis of distillation fractions from a sintered iron catalyst as a function of alkali content. (From Ref. 15)

TABLE 94. THE INFLUENCE OF ALKALI CONTENT ON OLEFIN CONTENT OF GASEOUS HYDROCARBONS FROM FLUIDIZED SYNTHESIS^a

K ₂ O (%)	Olefin Content of C ₃ + C ₄ Hydrocarbons (%)
0.07	14.4
.17	29.9
.27	39.5
.37	46.4
.47	54.9

^a From Ref. 168.

catalyst was much greater than from the alkali-free material. No olefins are found in the C₂ and C₃ fractions from the alkali-free catalyst. Although the olefin content of the C₄ fraction was strongly influenced by the presence or absence of alkali, the extent of branching of the carbon chain remained about the same. Further, the distribution of the double-bond position isomers of the *n*-C₄ olefins from the alkali-free catalyst more nearly approached the equilibrium concentrations than the corresponding olefins from the

alkalized sample. The fraction of branched hydrocarbons in the C₄ fraction was the same for catalysts with and without alkali, showing that chain branching probably results from some fundamental step in the reaction mechanism that is relatively unaffected by subsequent reactions. The usage ratio, H₂/CO, for alkali-free catalysts was usually higher than for alkalinized preparation; however, the usage ratio was constant for catalysts containing alkali in excess of 0.1–0.2K₂O/100Fe.

The effects of promoters other than alkali are more difficult to define. For a given alkali content, the average molecular weight of the product from precipitated catalysts decreased with increasing content of active

TABLE 95. EFFECT OF ALKALI ON COMPOSITION OF C₂–C₄ HYDROCARBONS^a

Percentage in carbon number fractions. Numbers in brackets [] refer to alkalinized catalysts; numbers in parentheses () refer to alkali-free catalysts.

C C	C=C			
[72]	[28]			
(100)	(0)			
C C C	C C=C			
[28]	[72]			
(100)	(0)			
C C C C	C C C=C	<i>cis</i> C C=C C	<i>trans</i> C C=C C	total <i>n</i> -C ₄
[12.2]	[69.8]	[3.5]	[4.1]	[89.6]
(74.5)	(4.4)	(3.8)	(5.8)	(88.5)
C C C	C C=C			total <i>i</i> -C ₄
C	C			
[2.0]	[8.4]			[10.4]
(8.5)	(3.0)			(11.5)

^a From Ref. 200.

forms of silica such as silica gel, kieselguhr, or clay. In most cases, however, these results may be explained by a decrease in the effective alkali content caused by the alkali reacting with the silica. In fused catalysts, small amounts of silica do not appear to produce this effect, since the alkali content required for maximum activity and for the formation of a high-molecular-weight product was about the same in the presence or absence of silica (Figures 41 and 44). Calcium oxide as an additive to precipitated catalysts of Ruhrchemie and Rheinpreussen (CaO from dolomite) was said to increase the average molecular weight of the hydrocarbon; however, testing data are not available to substantiate this statement. Furthermore, in the Schwarzheide comparative tests (Figure 52), the products from the Rheinpreussen catalyst had the lowest average molecular weight. Scheuer-

mamm¹⁶⁵ stated that fused alkalized iron catalysts promoted with alumina gave products containing a greater fraction of branched hydrocarbons and less olefins than similar catalysts promoted with magnesia. The chemical method employed to estimate the extent of branching is not very reliable, and the validity of the results on which this conclusion was made may be questioned. No other data relating chain branching to promoters other than alkali are available. The addition of fluorides, such as CaF_2 , AlF_3 , and FeF_3 was said to lower the average molecular weight of the hydrocarbons¹⁶⁵. Davis and Wilson³⁷ claimed that small amounts of organic halogen compounds, such as ethylene dichloride, added to the synthesis gas, continuously or intermittently, sizably increased the yield of $\text{C}_2\text{--C}_4$ olefins.

The method of pretreatment of iron catalysts can frequently produce more drastic changes in selectivity than variation of the catalyst composition. Since these data have been presented in the previous discussion on catalyst pretreatment, pp. 176 to 192, only a summary is given here. Precipitated iron catalysts of at least moderate activity can be obtained by treatment with carbon monoxide, synthesis gas, or hydrogen, and in some cases without any pretreatment. Catalysts treated with hydrogen at temperatures high enough to permit the reduction of an appreciable amount of the oxide to metallic iron usually yield a lower average molecular weight product than catalysts used directly in the synthesis or those pretreated with carbon monoxide or $\text{H}_2 + \text{CO}$ mixtures, as shown in Table 77 and in Figure 63. The relative amounts of carbide and magnetite in the pretreated precipitated catalysts apparently is of minor importance in determining the selectivity.

Nearly all fused and sintered iron catalysts require a pretreatment in hydrogen at temperatures greater than 400°C . Workers at I.G. Farben. believed that fused catalysts reduced at high temperatures yielded a higher average-molecular-weight product than those reduced at lower temperatures. Since fused catalysts sinter significantly at temperatures above 500°C , it was suggested that the higher-molecular-weight product of catalysts reduced at high temperatures was related to a decrease in hydrogenating ability caused by sintering. However, Bureau of Mines studies indicated little change in selectivity of catalysts reduced at 450, 500, or 550°C . The extent of reduction in the range 30–100 per cent has little effect on selectivity. Conversion of reduced fused catalysts to Hägg carbide or cementite usually increased the average molecular weight of the product; however, since the carbided catalysts were often more active and were operated at lower temperatures, it is difficult to state whether the change in selectivity resulted from the pretreatment or the lower operating temperature. Although partial reoxidation of a reduced catalyst decreased its activity, the average molecular weight of the products was presumably increased, since

the selectivity was about the same for reoxidized sample at 280°C and a reduced catalyst at 260°C.

Conversion of all types of iron catalyst to ϵ -nitride or carbonitride produced the greatest changes in selectivity, as shown by the numerous examples presented in the text.

The effect of catalyst pretreatment on the relative usage of hydrogen and carbon monoxide is usually slight. Only in the Ruhrchemie tests (Table 78) was a major change in usage ratio observed as a result of pretreatment. In this case the ratio H_2/CO was higher after pretreatment with water gas than with hydrogen.

Selectivity as a Function of Operating Variables. Satisfactory experimental data on the influence of operating variables on selectivity are not numerous, and an effort has been made to select sound and consistent results. Usually no attempt will be made to interpret the data, for this subject will be considered in Chapter 3.

Temperature. For a given iron catalyst, the selectivity usually varies with increasing temperature in the following manner: (a) the average molecular weight of the hydrocarbons decreases, (b) the olefin content of the hydrocarbons either remains about the same or increases, and (c) the production of oxygenated organic molecules decreases. The effect of increasing the synthesis temperature on average molecular weight is shown by medium-pressure data for precipitated catalysts of Pichler¹²³.

Temp. (°C)	Wax	Per cent of C_3+ as	
		Liquids	$C_3 + C_4$
235	26	56	18
270	3	65	32

Scheuermann¹⁶⁵ reported more detailed studies of precipitated Fe-Cu-MgO-SiO₂-K₂O catalysts. In the first series, the space velocity was held at 720 hr⁻¹ and the temperature varied from 215 to 275°C, as shown in Figure 85. The over-all product distribution shows that the largest changes were obtained in the C₁-C₅ and the >350°C fractions as the temperature was varied. Analyses for the olefin and alcohol contents of distillation fractions (Figure 86) indicates that the average olefin content remained about constant, but the concentration of alcohols decreased with increasing temperature. In these tests, the conversion of carbon monoxide increased from 18 to 72 per cent as the temperature was raised. Similar results were obtained in tests in which the temperature and space velocity were varied simultaneous to maintain about constant conversion, except that the olefin content increased with temperature.

Bureau of Mines tests of fused catalyst D3001 (Fe₃O₄-MgO-K₂O) crushed to various particle sizes provide data for comparing the influence of temperature on selectivity when the conversion was held constant, as shown in

Figure 87. The gaseous hydrocarbons and the gasoline fraction ($<195^{\circ}\text{C}$) doubled as the temperature was increased from 225 to 260°C , while the amount of heavy wax ($>464^{\circ}\text{C}$) decreased sharply. The olefin content of

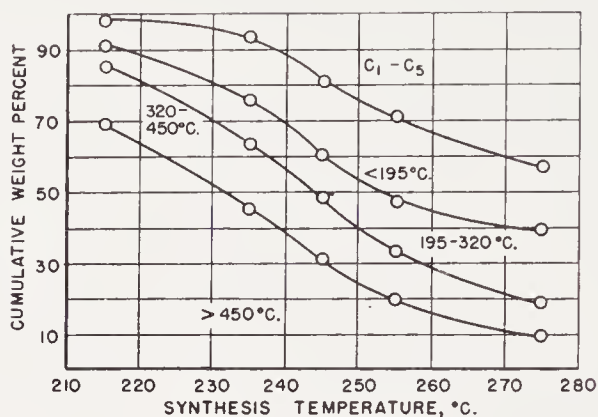


Figure 85. Selectivity as a function of temperature with precipitated iron catalyst, $1\text{H}_2 + 1\text{CO}$ gas, space velocity 720 hr^{-1} , and 12 atm. (From Ref. 165)

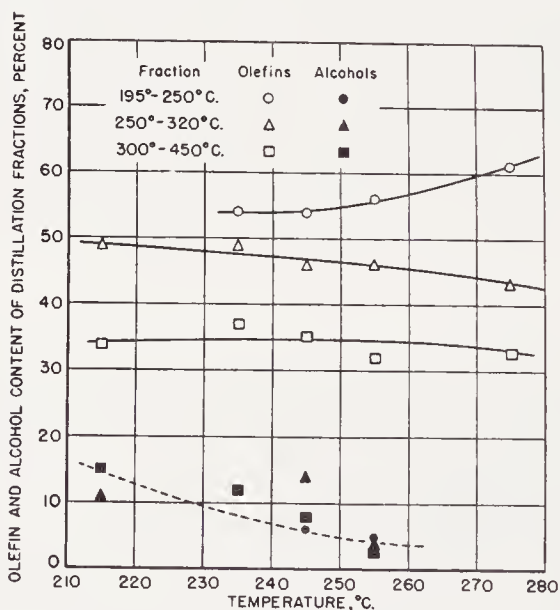


Figure 86. Alcohol and olefin content of distillation fractions in Figure 85. (From Ref. 165)

the C_2 - C_4 hydrocarbons and infrared analyses of the two lower-distillation fractions (expressed as weight per cent of functional group, OH groups in alcohols and $\text{C}=\text{C}$ in α - and internal double bond olefins) are plotted as a function of temperature in Figure 88. The olefin content of C_2 hydrocarbons decreased with temperature, but the unsaturation in the C_3 and C_4 fractions was constant. The olefin content of the distillation fractions remained essentially constant as the temperature was increased; however there was

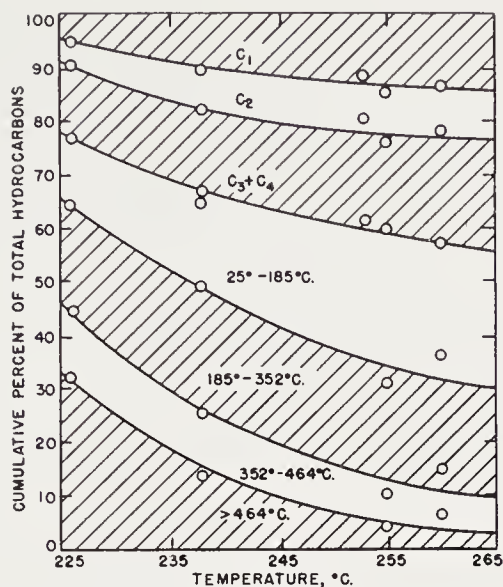


Figure 87. Variation of product distribution with temperature. Fused catalyst, $1\text{H}_2 + 1\text{CO}$ gas at 7.8 atm. (Reproduced with permission from Ref. 15)

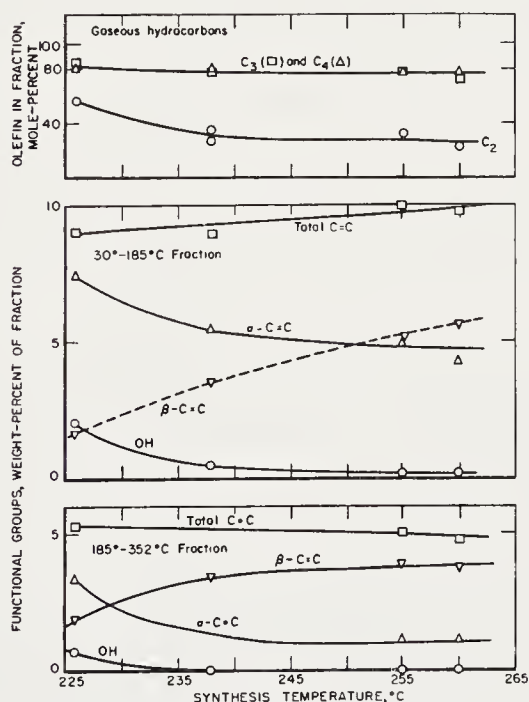


Figure 88. Temperature variation of olefin and alcohol content of fractions shown in previous figure. (From data of Ref. 15)

a gradual change from chiefly 1-olefins at 226°C to predominantly internal-double-bond olefins at 255 and 260°C . The yield of alcohol as indicated by OH group decreased sharply with increasing temperature. The yields of other oxygenated material, which were smaller than alcohols, decreased in

about the same manner as alcohols. The usage ratios, H_2/CO , were constant, with average values for 5 weeks of testing being 0.78, 0.79, 0.71, 0.79, 0.76, and 0.72 at 226, 238, 238, 253 and 260°C, respectively. The usage ratios in a large number of Bureau of Mines tests at 7.8 and 21.4 atmospheres of $1H_2 + 1CO$ gas, in which the conversion was maintained about 65 per cent, were from 0.70 to 0.80 for temperatures varying from

TABLE 96. INFLUENCE OF OPERATING TEMPERATURE ON SYNTHESIS IN
FIXED-BED AND SLURRY REACTORS^a

(Operating pressure 300 psig, $2H_2 + 1CO$ gas)

Reduced, fused Fe_3O_4 - MgO - K_2O catalyst. Recycle ratio 2.0-2.5.

Reactor Catalyst mesh size	Fixed bed 7-14		Slurry <200	
Temperature, °C	265	300	265	300
Space velocity, hr^{-1}	427	1087	—	—
Liter per gram per hr	0.21	0.53	0.64	0.89
Synthesis gas consumed per cent	89.2	89.2	66.6	84.2
Usage ratio, H_2/CO	1.86	1.81	1.40	1.72
Yield, g/m^3 (weight % of total)				
CH_4	33.0	37.5	11.5	22.6
C_2-C_4	48.1	56.9	48.6	63.3
C_5^+	80.3	75.0	71.0	78.8
Aqueous alcohol	3.2	2.1	8.0	9.5
Aqueous acids	1.3	1.9	1.6	1.6
Distillation of C_5^+ , wt-%				
<200°C	65.8	73.2	44.6	73.7
200°-300°C	20.4	14.0	21.1	16.8
>300°C	13.8	12.8	34.3	9.5
Analysis of 80-150°C fraction				
Olefins, weight per cent	51.2	68.4	59.0	64.5
OH number, mg KOH/g	42.6	52.8	122.5	52.2
Acid number, mg KOH/g	4.1	7.6	8.4	5.3
Ester number, mg KOH/g	4.3	11.5	1.8	3.8

^a From Ref. 74.

215 to 280°C. Koelbel and Engelhardt¹⁰² suggested that the usage ratio increased with decreasing temperature; however, this occurs only when the conversion decreases with decreasing temperature; for example, in tests at constant space velocity in which the temperature is varied. Since the same results are obtained when conversion is varied at constant temperature, the usage ratio is considered to be primarily a function of conversion.

Hall, Gall, and Smith⁷⁴ studied the influence of temperature on synthesis in fixed-bed and slurry reactors, as shown in Table 96. In the slurry reactor the amount of products, especially the >300°C fraction, must be inter-

preted with caution, since this material is a mixture of fresh product and suspension oil. In these experiments, the average molecular weight decreased with increasing temperature and the olefin content of the 80–150°C cut increased.

The products from the fluidized synthesis are (pp. 210 to 218) exceptional in that high yields of 1-olefins and oxygenated molecules are produced at high temperatures, 315–340°C. In addition, the usage ratio, H_2/CO , is high, often exceeding 2⁷⁴. Apparently the high space velocity together with recycle remove the products from the reaction zone before subsequent reactions occur.

Synthesis Pressure. Usually the average molecular weight of hydrocarbons increases with pressure to a maximum in the range of 10 to 30 atmospheres;

TABLE 97. SELECTIVITY AS A FUNCTION OF PRESSURE^a

(Precipitated iron catalyst with $1H_2 + 1CO$ gas, temperatures not specified)

Pressure, atm., absolute	1	3	5	10	20
Conversion of CO, %	95	75	70	75	75
Yield of C_3^+ , g/m ³	90	98	86	118	120
Liquid plus solids, wt-%					
Gasoline	57	32	30	25	22
Diesel oil	24	30	25	20	22
Wax	19	38	45	55	56
Olefin content, vol %					
Gasoline	68	64	63	62	63
Diesel oil	41	48	49	47	46

^a From Ref. 145.

however, there are some exceptions; for example, the data of Pichler¹³¹ (Table 76) indicate that the selectivity at 1 and 10 atmospheres was about the same. In the atmospheric-pressure test, however, the catalyst was solvent extracted at frequent intervals. Roelen¹⁴⁵, on the other hand, found an increase of average molecular weight with synthesis pressure up to 10 atmospheres, as shown in Table 97. (In these and tests described subsequently, the catalysts were not extracted.) Although the product distribution changed considerably, the olefin content of the gasoline and diesel oil fractions was about constant. In Bureau of Mines tests¹⁵ shown in Table 98 (activity data for these experiments are given in Figure 72), the average molecular weight of hydrocarbons from precipitated and sintered catalysts decreased slightly when the pressure was increased from 7.8 to 21.4 atmospheres, whereas for the reduced and nitrided fused catalysts, the molecular weight increased. The olefin content of the distillation fractions was approximately the same at both pressures; however, the fraction of unsatu-

TABLE 98. EFFECT OF OPERATING PRESSURE ON ACTIVITY AND SELECTIVITY^a

Catalyst: Composition Type Number	Fe ₃ O ₄ -CuO-K ₂ CO ₃ Precipitated ^b P-3003.24		Fe ₃ O ₄ -K ₂ CO ₃ Sintered ^c A-2101 A-2106.05		Fe ₃ O ₄ -MgO-K ₂ O Fused ^c D-3001			
	X101	X204	X160	X228	X152	X200	X215	X225
Pretreatment:								
Gas	1H ₂ + 1CO	1H ₂ + 1CO	H ₂	H ₂	H ₂	H ₂	NH ₃ ^d	NH ₃ ^d
Space velocity ^e	135	135	1000	1000	600	2700	5000	1000
Hours	24	24	43	24	43	40	4	6
Temperature, °C	230	230	400	400	450	450	385	350
Testing data:								
Pressure, psig	100	300	100	300	100	300	100	300
Temperature, °C	232	241	221	226	263	257	226	238
Average activity, A _{Fe} ^f	148	337	89.7	254	18.4	62.1	67.8	120.4
Usage ratio, H ₂ /CO	0.59	0.68	0.61	0.74	0.73	0.72	0.74	0.79
Product composition: hydrocarbons ^g , wt-% as:								
C ₁	4.7	5.0	4.8	6.7	13.2	11.3	16.0	16.4
C ₂	5.3	4.4	4.7	6.2	8.8	8.3	10.6	8.3
C ₃ + C ₄	8.5	9.1	11.6	13.9	20.6	12.2	22.5	17.9
C ₁ -C ₄	18.5	18.5	21.1	26.8	42.6	31.8	49.1	42.6
Liquids + solids	81.5	81.5	78.9	73.1	57.4	68.1	50.9	57.4
Acid number ^h	—	2.1	6.2	10.4	0.8	7.7	0.3	3.0
Distillation of liquids + solids wt-%								
<185°C	2.6	14.0	11.8	32.1	36.5	36.8	61.9	67.3
185-352°C	19.6	27.0	25.9	33.8	36.5	29.8	34.5	25.0
352-464°C	17.5	14.0	10.5	11.1	15.3	13.2	2.9	5.2
>464°C	60.3	45.0	49.5	23.0	11.7	20.2	0.7	2.5

Infrared analysis, weight per cent of functional group									
<185°C									
CO + COOH	1.6	2.8	3.7	4.0	0.6	1.7	1.5	1.4	
COO	0.5	0.5	1.3	1.3	.1	0.5	0.2	0.3	
OH	3.1	7.9	4.5	7.5	.2	3.4	13.5	11.7	
α -olefins (C=C)	2.8	4.1	5.7	6.2	4.9	7.0	1.5	1.7	
Other olefins (C=C)	1.0	0.3	0	0	5.1	0.9	0	0	
Bromine number	25	29	38	41	66	53	10	12	
185-352°C									
CO + COOH	1.0	1.0	1.5	1.7	0.3	0.8	0.8	1.3	
COO	0.0	1.2	2.0	2.8	.1	.9	.6	1.0	
OH	.7	1.9	0.9	2.2	0	.7	2.0	2.7	
α -olefins (C=C)	1.9	1.8	3.8	4.2	1.1	4.0	0.4	0.6	
Other olefins (C=C)	1.4	0.6	0.4	0.5	3.9	1.3	.9	.5	
Bromine number	22	16	28	28	33	35	9	8	

^a From Ref. 15.

^b 6- to 14-mesh granules.

^c 6- to 8-mesh granules.

^d Reduced in hydrogen at space velocity of 2,500 at 550°C for 20 hours, and converted to ϵ -phase nitride by the ammonia treatment.

^e Volumes of gas at standard temperature and pressure per volume of catalyst space per hour.

^f Average activity of weeks 1 to 5.

^g Total hydrocarbons and liquids + solids include oxygenated compounds dissolved in hydrocarbon phases.

^h Acid number of liquids + solids.

rates as 1-olefins increased with pressure. The yield of oxygenated molecules, especially alcohols, increased with pressure except for the nitrated catalyst, where the yield of oxygenates was high at both pressures. The usage ratio, H_2/CO , usually increased slightly with pressure (Table 75). Under comparable conditions using precipitated catalysts with $0.64-0.71 H_2 + 1CO$

TABLE 99. INFLUENCE OF OPERATING PRESSURE ON SYNTHESIS IN
FIXED-BED AND SLURRY REACTORS^a
($2H_2 + 1CO$ gas on reduced fused $Fe_3O_4-MgO-K_2O$ catalysts)

Reactor	Fixed Bed		Slurry		
Pressure, atm.	21.4	41.8	21.4 ^b	31.6	41.8
Temperature, °C	250	250	265	265	265
Space velocity, hr ⁻¹	427	821	—	—	—
Liter/g/hr	0.20	0.39	0.78	1.15	1.59
Recycle ratio	2.3	2.3	6.0	5.2	5.5
Synthesis gas consumed, %	82.1	84.8	75.9	74.7	69.6
Usage ratio, H_2/CO	1.79	1.88	1.43 ^b	1.57	1.48
Yield, g/m ³					
C ₁	29.0	24.5	18.2	14.9	12.7
C ₂ -C ₄	46.0	52.0	38.5	36.9	37.0
C ₅ +	90.5	93.6	96.0	91.0	86.0
Aqueous alcohol	—	—	10.5	9.7	7.3
Aqueous acids	—	—	2.1	2.8	4.3
Distillation of C ₅ +, wt-%					
<200°C	61.5	52.7	51.2	49.6	46.9
200-300°C	19.7	25.1	15.0	15.5	15.6
>300°C	18.8	22.2	33.8	34.9	37.5
Analysis of 80-150°C fraction					
Olefin content	43.7	42.1	72.0	62.8	50.6
Hydroxyl number, mg KOH/g	41.0	48.0	70.0	95.9	143.0
Acid number, mg KOH/g	3.9	3.9	7.7	14.1	23.0
Ester number, mg KOH/g	6.5	1.1	16.8	20.9	37.3

^a From Ref. 74.

^b In this experiment, H_2/CO of feed gas was 1.85.

gas, Pichler¹²³ observed the following usage ratios, 0.59, 0.60, 0.62, and 0.69 at 5, 15, 30, and 80 atmospheres, respectively.

Hall, Gall, and Smith⁷⁴ investigated the influence of operating pressure from 21.4 and 41.8 atmospheres on selectivity in fixed-bed and slurry reactors, as shown in Table 99. The average molecular weight increased with pressure. For slurry tests, the fraction of olefins in the 80-150°C fraction decreased and the alcohol content increased with increasing pressure. Similar trends were observed for fixed-bed products, but the magnitude of the changes was very much smaller.

Synthesis tests at 50 atmospheres and higher pressures in Table 100 indicate that both selectivity and activity are inferior with respect to synthesis at 12 atmospheres. At 50 and 200 atmospheres, the catalyst yielded a lower average molecular-weight product containing a large fraction of oxygenated material. The effect of pressure on selectivity may be tentatively summarized as follows: with increasing pressure

(a) The average molecular weight of the hydrocarbons increases to a

TABLE 100. COMPARISON OF SYNTHESIS AT 12, 50, AND 200 ATMOSPHERES ON PRECIPITATED Fe-Cu-MgO-K₂CO₃ CATALYSTS^a
(1H₂ + 1CO at space velocity of 240 hr⁻¹)

Catalyst	A	A	B	B
Pressure, atmospheres	12	50	12	200
Temperature, °C	215	225	215	265
CO conversion, %	29	30	32	31
Liquid + solid hydrocarbons ^b g/m ³	56	48	61	52
C ₁ -C ₅ , g/m ³	3	12	4	11
Distillation data, %				
<195°C	17	41	7	34
195-320°C	12	28	7	17
320-450°C	21	17	14	19
>450°C	50	12	72	30
Olefins in fractions, %				
195-250°C	48	23	—	44
250-320°C	48	20	—	39
320-450°C	36	18	41	44
Alcohols in fractions, %				
195-250°C	16	57	—	23
250-320°C	18	57	—	32
320-450°C	27	43	13	42

^a From Ref. 165.

^b Include oxygenated organic molecules.

maximum value in the range 10-40 atmospheres, the maximum probably varying with both the catalyst type and operating conditions.

(b) The olefin content of various fractions remains essentially constant at least up to the pressure corresponding to the maximum in molecular weight of hydrocarbons described in (a).

(c) The concentrations of alcohols and other oxygenated molecules in the hydrocarbon and water phases increase at least to 50 atmospheres and probably to even higher pressures.

(d) The usage ratio (H₂/CO) remains constant or increases slightly.

Gas Composition. Usually the usage ratio, H₂/CO increases, and the

average molecular weight and the olefin content of the product decrease as the H_2/CO ratio of the synthesis gas is increased. Data of Scheuermann (Figure 89) on a magnesia-promoted precipitated catalyst indicate that although the total yield of hydrocarbons was greater with $2H_2 + 1CO$ gas than with $1H_2 + 1CO$, the yield of product boiling above $320^\circ C$ was sizably diminished and the yields of C_1-C_5 hydrocarbons and gasoline were correspondingly increased. Less olefins and alcohols were found in the intermediate distillation fractions from $2H_2 + 1CO$ gas.

At the Bureau of Mines, reduced and reduced-and-nitrided fused catalysts (D3001) were tested at 21.4 atmospheres with synthesis gas having different ratios of hydrogen to carbon monoxide, as shown in Figure 90.

H_2/CO INLET GAS	1 / 1	2 / 1
TOTAL HYDROCARBONS gm./m. ³	67	82
	C_1-C_5	C_1-C_5
Olefins	<195° 195°-320°	<195°
Alcohols	320°-450°	<195° 195°-320° 320°-450° >450°
	>450°	

Figure 89. Selectivity as a function of gas composition. Precipitated iron catalyst, $250^\circ C$, 12 atm., and a space velocity of 720 hr^{-1} . (Data of Ref. 165)

The results of tests of reduced catalysts with gas of H_2/CO ratios of 0.7 and 1.0 were not greatly different; however, with $2H_2 + 1CO$ the average molecular weight of the product was appreciably decreased, the largest differences from the tests with $1H_2 + 1CO$ gas being observed in the gaseous hydrocarbon and the heavy-wax ($>464^\circ C$) fractions. The yields of olefins and oxygenates show no particular trend. Products from nitrided catalysts had a lower average molecular weight and lower olefin content when tested with $2H_2 + 1CO$ gas than with $1H_2 + 1CO$.

The usage ratio, H_2/CO , increases with increasing ratio of H_2/CO in the inlet gas, but for usual fixed-bed experiments (without recycle) at relatively high conversion, 65 to 75 per cent, the usage ratio is always somewhat less than the H_2/CO ratio of the inlet gas. Data in Figure 91, for tests of precipitated catalysts by Pichler¹²³ and for Bureau of Mines experiments with fused catalysts, are plotted as the ratio of moles of hydrogen consumed to

		REOUCEO			REOUCEO AND NITRIOEO	
INLET GAS H ₂ /CO		0.67	1.0	2.0	1.0	2.0
TEMPERATURE, °C.		240	252	248	238	241
USAGE RATIO, H ₂ /CO		0.64	0.79	0.98	0.79	1.03
DISTRIBUTION OF TOTAL HYDROCARBONS, PERCENT (INCLUDES OXYGENATED MATERIAL)		C ₁	C ₁	C ₁	C ₁	C ₁
		C ₂ = 49	C ₂ = 64			
	90	C ₃ + C ₄ = 81	C ₃ + C ₄ = 80	C ₂ = 46	C ₂ = 56	
		< 185° Br 67 OH 4.6 CO 4.0	< 185° Br 85 OH 3.3 CO 2.3	C ₃ + C ₄ = 77	C ₃ + C ₄ = 68	C ₂ = 13
	70					
		185°-352° Br 54 OH 1.1 CO 1.2	185°-352° Br 37 OH 0.51 CO 0.52	< 185° Br 59 OH 3.9 CO 1.9	< 185° Br 14 OH 12.4 CO 1.7	C ₃ + C ₄ = 58
	50		352°-464°			
		352°-464°	> 464°	185°-352° Br 32 OH 1.0 CO 0.8		< 185° Br 3 OH 15.8 CO 1.3
	30					
		> 464°		352°-464°	185°-352° Br 8 OH 2.5 CO 1.1	185°-352° Br 4 OH 4.0
	10			> 464°		
		x 297	x 282	x 230	x 225	x 226

Figure 90. Selectivity as a function of gas composition with fused iron catalyst (Fe_3O_4 - MgO - K_2O) at 21.4 atm.

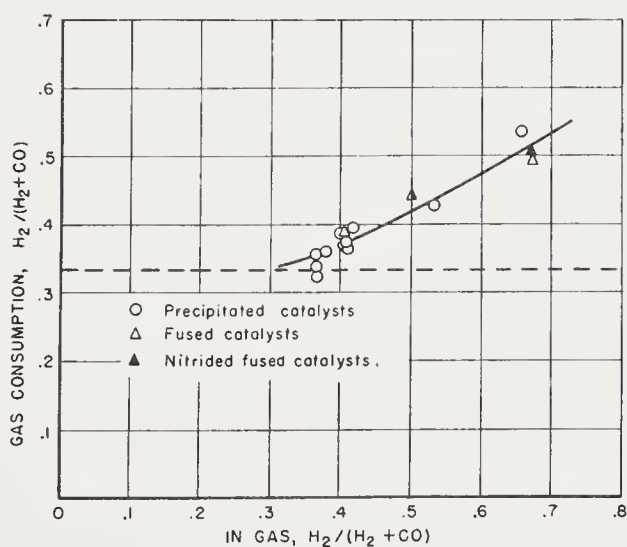


Figure 91. Relative usage of H_2 and CO as a function of gas composition with iron catalysts at 5-12 atm.

total moles of $H_2 + CO$ consumed against moles H_2 per total $H_2 + CO$ in feed gas.

*Conversion, Gas Flow and Recycle**. The effect of conversion, gas flow, and recycle on selectivity has not been completely determined. Without recycle, conversion and gas flow at a given temperature are interrelated, the fraction of the gas converted decreasing with increasing flow. Data of Scheuermann¹⁶⁵ for a precipitated iron catalyst at 240°C are erratic. The yields of gaseous hydrocarbons increased with flow over the range of space velocities studied, 240 to 2,400 hr^{-1} . The olefin and alcohol concentrations in distillation fractions varied in an irregular manner, and the only conclusion that can be drawn is that the concentration of these molecules is relatively independent of flow, possibly increasing slightly at high-space velocity. The use of moderate recycle ratios up to two volumes of recycle gas/volume of fresh feed has no effect on the olefin content of products, as shown in Figure 92. In fluidized studies²⁰⁰, a fourfold variation of recycle ratio produced no consistent variations in olefin content. However, the large alcohol yields from the synol process (Table 90) must be largely attributed to the high recycle ratio employed, since the same catalyst, operated without recycle and at somewhat higher temperature in the Schwarzheide tests (see I.G. Farben. catalyst in Figure 52), produced considerably smaller quantities of alcohols. The difference in these yields seems larger than would be expected for the same temperature increment without recycle. Less detailed synol data in Table 101 demonstrates the increase in alcohol content and the shift in production ratio, H_2O/CO_2 , with recycle. The yields of alcohols from the fluidized process are considerably greater than would be expected from an extrapolation of synthesis data at low temperatures, 200–270°C to 315–340°C, and the selectivity in the fluid synthesis probably results from the high space velocity and the moderate recycle ratio employed.

The relative usage of hydrogen and carbon monoxide is strongly influenced by the conversion. Data for tests of $1H_2 + 1CO$ on fused catalyst D3001 (Figure 93) are typical of most experiments with $1H_2 + 1CO$ gas. The usage ratio decreased with conversion from a high value, possibly approaching 2, for zero contraction and passed through a minimum at 30 to 40 per cent conversion. The usage ratio usually increases with recycle ratio, as shown by data from the Bureau of Mines oil circulation pilot plant³⁶, in Table 102. With $1.3H_2 + 1CO$ gas, the usage ratio approaches the feed ratio only at moderately high recycle. Similarly, with $1H_2 + 1CO$ gas, the usage ratio increased with recycle, but equalled or exceeded feed ratio at low-recycle ratios.

* In these experiments the recycle gas was cooled to about room temperature before reentering the reactor. In this process most of the water and liquid hydrocarbons was condensed and removed in the recycle system.

RUTHENIUM CATALYSTS

According to Pichler¹³¹, studies of the hydrogenation of carbon monoxide on ruthenium catalysts at high pressures were initiated at the Kaiser Wilhelm Institut in an attempt to produce carbohydrates. Although carbo-

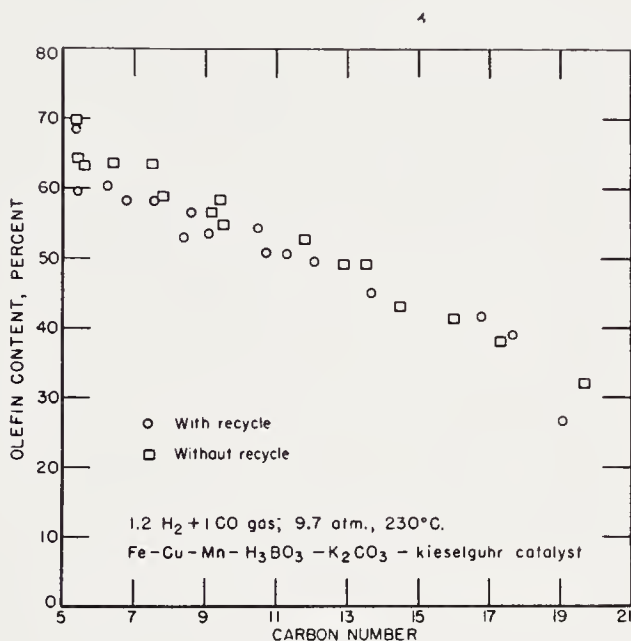


Figure 92. Variation of olefin content with carbon number for synthesis on a precipitated iron catalyst. (From data of Ref. 198)

TABLE 101. THE INFLUENCE OF RECYCLE RATIO ON SELECTIVITY^a OF FUSED-IRON CATALYST

(Space velocity (fresh feed) = 350 hr⁻¹; pressure = 25 atm.)

Recycle Ratio	Temp. (°C)	Alcohol Content in Fractions (%)		Production Ratio H ₂ O/CO ₂
		230-350°C	350-400°C	
0	189	55-60	45-55	0.7
10-15	183	70-75	70-80	9.0

^a From Ref. 137.

hydrates were not obtained, the synthesis at high pressures yielded very high-molecular-weight paraffins. Studies were also made of the high-pressure synthesis on other platinum-group metals. Rhodium and osmium were moderately active catalysts, but platinum, palladium, and iridium had low activity. Rhodium catalysts produced sizable yields of oxygenated material and less wax than ruthenium. Osmium catalysts required higher operating temperatures and produced larger yields of gaseous hydrocarbons.

Preparation and Pretreatment of Catalysts

Relatively pure ruthenium dioxide containing only traces of impurities, such as those carried over from the original ruthenium or introduced in the preparation, was one of the best catalysts. No promoters or supports were

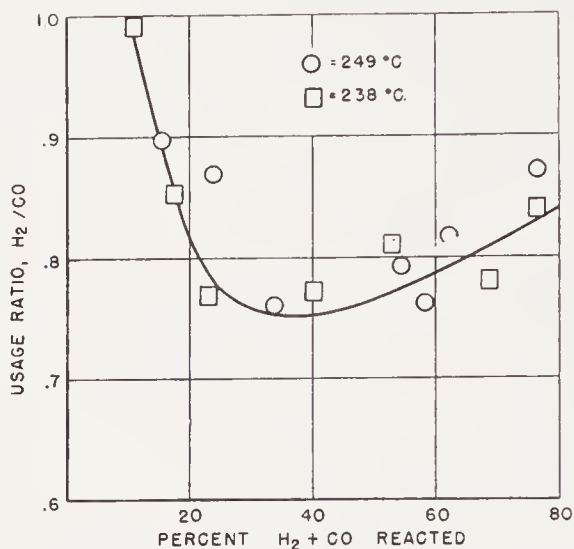


Figure 93. Variation of usage ratio with conversion on fused catalyst D3001 at 100 psig with $1H_2$ to $1CO$ gas. (Reproduced with permission from Ref. 15)

TABLE 102. VARIATION OF USAGE RATIO WITH RECYCLE RATIO^a

(Bureau of Mines oil circulation pilot plant. $1.3H_2 + 1CO$ gas at 20 atm. and 231–238°C. Space velocity of fresh feed 230 hr^{-1})

Recycle Ratio, End Gas to Fresh Gas	CO_2 in End Gas (%)	Usage Ratio, H_2/CO
1	27.4	0.99
2	25.1	1.03
3	23.4	1.15
4	22.9	1.13
5	21.5	1.15
6	20.3	1.22
7	21.5	1.21

^a From Ref. 36.

found that improved the behavior of ruthenium catalysts. Ruthenium dioxide was prepared from commercial ruthenium powder in the following way¹²⁶: A mixture of $1Ru:10KOH:1KNO_3$ was fused in a silver crucible. One to 2 hours were required to completely dissolve the ruthenium. The mass was cooled and dissolved in water to give a deep red solution of potassium ruthenate. The solution was heated to boiling and methyl alcohol

was added dropwise to reduce the potassium ruthenate to ruthenium dioxide. The finely-divided oxide settled after a few hours and was filtered on a fritted plate, washed with a nitric acid solution and finally with distilled water, and dried at 110°C. Reduction could be accomplished with either hydrogen or synthesis gas.

Operating Conditions and Selectivity

With sulfur-free $2\text{H}_2 + 1\text{CO}$ gas, long periods of operation at constant activity and selectivity were possible. In one experiment at 195°C and 100 atmospheres, the activity and selectivity were constant during a 6-month test. Although the ruthenium was not oxidized or carburized, operating conditions were favorable for the formation of the volatile carbonyl, $\text{Ru}(\text{CO})_4$; however, if carbonyl formed to any great extent, it did not

TABLE 103. SYNTHESIS WITH RUTHENIUM CATALYSTS AT VARIOUS PRESSURES^a
($2\text{H}_2 + 1\text{CO}$ gas at 180°C)

Pressure (atm)	Carbon Monoxide, Conversion (%)	Per cent of Reacted Carbon Monoxide to		
		Wax	Liquid Hydrocarbons	Gaseous Hydrocarbons
1	0	—	—	—
50	48	46	33	21
100	68	53	31	16
1000	92	59	26	15

^a From Ref. 131.

impair the activity. The selectivity of tests in which the catalyst was used in a fixed bed, or as a suspension in neutral oil, concentrated solutions of alkali, or dilute acid solutions, was about the same. In the absence of carbon monoxide, ruthenium catalysts hydrogenated carbon dioxide to methane at temperatures even below 100°C. However, appreciable hydrogenation of carbon monoxide proceeded only at temperatures above the melting point of the highest-melting waxes produced, that is, above 134°C. In the presence of carbon monoxide, carbon dioxide was not hydrogenated. The ruthenium catalysts were more susceptible to sulfur poisoning than cobalt catalysts.

Conversion increased rapidly with both synthesis temperature and pressure, as shown in Figure 94. Appreciable conversions were usually not obtained at pressures lower than 15 atmospheres. Table 103 presents typical products from the synthesis at 180°C. As the pressure was increased, the yield of wax increased at the expense of the liquid and gaseous hydrocarbons.

The usage ratio, H_2/CO , varied from 1.9 to 2.3 over a wide range of operating conditions, as shown in Table 104. In experiments at high temperatures, the greater relative usage of hydrogen to produce the large yields of methane was compensated by increased production of carbon dioxide so that the usage ratio remained about 2. In tests at 100 atmospheres and $230^\circ C$, in which the conversion was varied by changing the space velocity, the usage ratio decreased as the conversion was increased. Methane production appeared to decrease with increasing conversion. In experiments at 100 and 1,000 atmospheres, both methane and carbon dioxide production was high at temperatures of $300^\circ C$ and higher.

Waxes from ruthenium catalysts were fractionated by extraction with different solvents at various temperatures¹²⁸. Of the waxes produced at

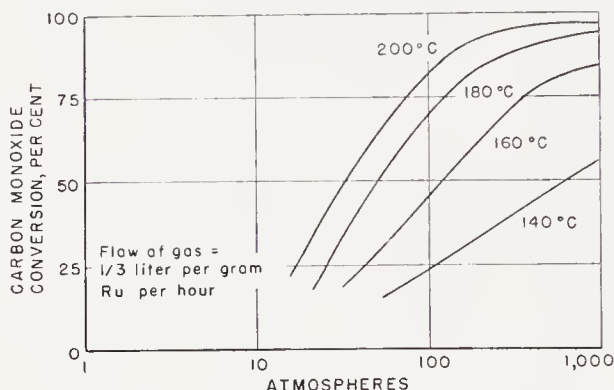


Figure 94. Variation of the extent of conversion with pressure on ruthenium catalysts. (From Ref. 126)

100 and 1,000 atmospheres, about 13 and 50 per cent, respectively, melted at temperatures above $126^\circ C$, as shown in Table 105. The physical properties of the fractions separated from the 1,000-atmosphere wax are given in Table 106. The molecular weights of these waxes, from the boiling point elevation of toluene, were remarkably high, and these are probably the highest-melting waxes ever prepared. As the molecular weight increased, the melting point increased asymptotically toward a constant value, about $134^\circ C$.

Waxes from Pichler's ruthenium catalyst were virtually oxygen-free. The elemental analyses for carbon and hydrogen, respectively, varied from 85.4–85.5 per cent and 14.2–14.5 per cent, corresponding to the empirical formula $CH_{2.00-2.04}$. Bromine and acid numbers for the waxes were zero within experimental error.

In patents, Howk and Hager⁹⁰ and Gresham⁶⁹ claimed high yields of primary straight-chain alcohols from the hydrogenation of carbon monoxide in the presence of ruthenium suspended in primary alcohols or water. A

TABLE 104. USAGE RATIO AND PRODUCTION OF CARBON DIOXIDE AND GASEOUS HYDROCARBONS ON RUTHENIUM CATALYSTS^a

Pressure (atm.)	Temp. (°C)	Usage Ratio, H ₂ /CO	Grams per m ³ In-Gas		Conversion, (%)
			CO ₂	CH ₄ ^b	
100	200	2.18	0.0	16.5	
	240	2.18	.0	22.9	
	260	2.18	11.8	35.0	
	280	2.18	25.3	55.4	
	300	2.21	35.3	71.4	
	320	2.14	88.4	127.2	
	340	1.99	123.6	133.0	
	360	1.99	123.6	134.4	
	380	2.00	131.5	145.8	
	400	2.03	143.3	144.5	
1000	300	1.92	94.2	132.0	
	400	1.96	104.0	123.0	
	500	1.97	110.0	117.1	
100	230	2.08	2.0	25.7	81
		2.12	0	32.8	79
		2.20	0	42.2	69
		2.20	0	44.3	62
		2.24	11.8	31.4	56
		2.26	0	38.6	50
		2.53	23.6	30.0	36

^a From Refs. 126 and 127.^b Gaseous hydrocarbons computed as CH₄. Carbon numbers varied from 1.0 to 1.4.TABLE 105. FRACTION OF WAX FROM RUTHENIUM SYNTHESIS^a

Pressure (atm.)	Fraction	Solvent	Extraction Temp. (°C)	Per cent Dissolved	Melting Point (°C)
100	1	Benzene	20	34	50-60
	2	Benzene	80	53	113
	3	Residue	—	13	126-128
	4	Toluene	110	^b	132
1000	1	<i>n</i> -Pentane	34	30-33	51-57
	2	<i>n</i> -Hexane	68	14-17	93-95
	3	Gasoline	90	14-16	121-123
	4	<i>n</i> -Heptane	98	20-25	130
	5	Gasoline	121	12-15	132-134

^a From Ref. 128.^b Traces of wax extracted from catalyst.

variety of active compounds of ruthenium were described including oxides, carbonyls, hydrocarbonyl, and salts of organic acids, either alone or deposited on various carriers. Ruthenium dioxide prepared by the method of Pichler was active in this synthesis. Operating conditions were essentially the same as those employed by Pichler, pressure 300–1,000 atmospheres and temperature 175–225°C. The only major difference between the wax synthesis of Pichler and this alcohol synthesis appears to be the suspension of the catalyst in a primary alcohol or water in the alcohol synthesis. Part of the alcohol suspension medium participated in the synthesis or was removed by other reactions. Gresham⁶⁹ claimed that the presence of alkaline substances, such as NaOH, KHCO₃, and NH₃, in the suspension medium to maintain the pH in the range of 7.0 to 11.5 prevented the formation of high-molecular-weight alcohols.

TABLE 106. PROPERTIES OF WAX FRACTIONS FROM THE 1000 ATMOSPHERE SYNTHESIS^a

Fraction ^b	Melting Range (°C)	Density (°C)		Average Molecular Weight	Viscosity, centistokes, (°C)	
		20	150		150	180
1	51–57	—	—	—	—	—
2	92–95	—	0.765	760	6	4
3	121–122	0.966	.778	1750	29	17
4	129–130	.978	.783	6750	870	410
5	132–134	.980	.786	23000	35600	15800

^a From Ref. 128.

^b Fractions described in Table 105.

SULFUR-POISONING OF FISCHER-TROPSCH CATALYSTS

Sulfur compounds are permanent poisons for cobalt, nickel, iron and ruthenium catalysts in the Fischer-Tropsch synthesis, as well as in other catalytic reactions such as the synthesis of methane and ammonia, the water gas shift reaction*, and the deposition of elemental carbon from carbon monoxide. Poisoning of metallic catalysts by sulfur compounds was known from earlier studies of the ammonia synthesis, and similar poisoning effects were found early in the research on Fischer-Tropsch catalysts. Actually the available literature contains few detailed studies of sulfur-poisoning of Fischer-Tropsch catalysts, and usually the workers were satisfied to establish a reasonable upper limit for sulfur concentration. Few experimental data are available that give any fundamental information regarding the mechanism of the poisoning process. Presumably sulfur com-

* Iron water-gas shift catalysts are an exception in that the tolerance to sulfur compounds is relatively high.

pounds are chemisorbed relatively permanently on the catalyst surface and migrate only slowly if at all. Thus, in a fixed-catalyst bed, the sulfur compounds may be expected to be largely removed by the inlet portion of the catalyst, and the activity will decrease only slowly until the zone of poisoning has progressed through the entire bed. Similar preferential poisoning probably occurs in the pores of catalyst particles, but its deleterious effect on activity may be more drastic²⁰⁴. Poisoning in fluid- or other moving-catalyst beds should be more serious, since all of the catalyst may be exposed to the inlet gas and usually no portion of the catalyst acts as a purifier.

Sulfur compounds are classified as hydrogen sulfide and organic sulfur, the latter including virtually all other volatile sulfur compounds; for example, carbonyl sulfide, carbon disulfide, thiophene, mercaptans, thioethers, etc. The classical purification methods, the coarse and fine purifications with iron oxide, as employed in the German Fischer-Tropsch plants, have been described by Storch¹⁸¹. Research at the Bureau of Mines laboratories^{162, 203} has shown that the removal of sulfur compounds from synthesis gas under pressure by activated charcoal is advantageous. Recently, processes for removal of sulfur compounds by low temperature (-40°C) scrubbing in liquids, such as methanol, have been described. Sulfur compounds usually arise from sulfur present in the raw material from which the synthesis gas is produced, such as coal; however, occasionally disastrous concentrations of hydrogen sulfide are produced by bacterial reduction of sulfates in gasholder water^{70, 71, 174, 175}.

For most purposes the sulfur content of synthesis gas of 0.2 gram per 100 m³ or 0.87 grains per 1,000 ft³* chosen by Fischer⁴⁸, may be regarded as a satisfactory "economic" upper limit. The amount of sulfur required to completely inactivate a catalyst is not well defined and presumably depends upon the composition and type of preparation, as well as the mode of operation. In any case, this amount of sulfur is very much less than that required to convert all of the metal to a sulfide. An experiment of Pichler and Merkel¹²⁹ demonstrates this point. An active iron catalyst, after use in the synthesis, was extracted with a diesel fuel containing sulfur compounds. This treatment rendered the catalyst completely inactive, although thermomagnetic analysis indicated that the composition of the poisoned catalyst was essentially the same as the active catalyst.

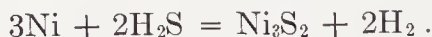
Hydrogen sulfide and organic sulfur are permanent poisons for Fischer-Tropsch catalysts; that is, after poisoning, the activity does not return to its original value when sulfur-free gas is passed over the catalyst. Relatively mild treatment of the poisoned catalyst, such as hydrogenation or oxidation with air or steam under conditions that do not drastically alter

* 1 gram/100 m³ = 4.37 grains/1000 ft³.

the properties of the catalyst, does not usually improve the activity⁶². Re-preparation of precipitated catalysts by dissolution in nitric acid and reprecipitation yields catalysts of high activity⁶² and, similarly, refusion of fused catalysts should be expected to yield materials of essentially the same activity as the original catalyst. Although the presence of sulfates in solutions used in the preparation of precipitated catalysts is usually considered undesirable, the activity is often not greatly decreased. This result is not unexpected, since efficient washing of the precipitate may remove most of the occluded sulfate ions. Roelen reported that the presence of sulfate ion in solutions at concentrations up to 8 per cent does not appreciably decrease the activity of precipitated cobalt catalysts. However, in technical preparations, the solutions usually contained calcium ions, and calcium sulfate precipitated in the catalyst had a detrimental effect on activity. Fischer and Tropsch⁶² reported that small amounts of impregnated potassium sulfate (e.g., 1 per cent) produced the same *increase* in activity of an iron catalyst as the equivalent amount of potassium carbonate, whereas potassium sulfide completely inactivated the catalyst. Experiments of Frear and Shultz⁶³ demonstrated that sulfur dioxide was only a temporary poison (similar to water and oxides of carbon) for iron catalysts in the ammonia synthesis. From these data it may be inferred that oxides of sulfur are at most mild poisons compared with hydrogen sulfide and organic sulfur.

Steinbrecher¹⁷⁷ stated that the poisoning action of organic sulfur compounds for cobalt catalysts in order of decreasing effectiveness was: Thiophene and other ring-substituted sulfur compounds, mercaptans, carbon disulfide and carbon oxysulfide. It was postulated that ring-substituted compounds are less strongly adsorbed and hence penetrate to a greater depth of the catalyst bed than molecules without the cyclic structure.

Karzhavin⁹⁴ cites Russian data on the thermodynamics of the reaction



At 180°C, under synthesis conditions, a concentration of H_2S corresponding to 0.45 g S/100 m³ is required for formation of Ni_3S_2 . Since this equilibrium concentration is more than twice the upper "economic" limit of sulfur tolerance, it was inferred that surface atoms are more reactive and adsorb sulfur compounds at considerably lower concentrations than required for producing bulk-phase sulfide. This concept is consistent with observations on the poisoning of iron catalysts in the ammonia synthesis, where the concentration of water vapor required to inactivate the catalyst was 0.1 per cent of that required to produce magnetite^{2, 26, 63}.

Cobalt and Nickel Catalysts

Herington and Woodward⁸² studied the poisoning of a pelleted Co-ThO₂-kieselguhr catalyst at atmospheric pressure. Hydrogen sulfide was added

intermittently by dropping pellets of cadmium sulfide into acid in a suitable vessel in the gas inlet system. In all cases, the hydrogen sulfide was completely adsorbed by the catalyst. The data were reported as relative yields of condensed and gaseous (average carbon number = 1.7) hydrocarbons, as shown in Table 107. Initially, as the sulfur content of the catalyst increased, the relative yields of condensed hydrocarbons increased and the formation of gaseous hydrocarbons decreased. At about 8 mg sulfur per gram of catalyst (approximately 24 mg per gram of cobalt), the catalytic activity had decreased sufficiently to require a higher reactor temperature to maintain a moderate conversion. Under these conditions, the yields of condensed hydrocarbons decreased and gaseous products increased. A similar initial increase in average molecular weight was observed in the addition of carbon disulfide. On a partly sulfur-poisoned catalyst, liquid

TABLE 107. SULFUR-POISONING OF Co-ThO₂-KIESELGUHR CATALYST^a

Sulfur Added, mg/g of Catalyst	Catalyst Temp. (°C)	Relative Yields of Hydrocarbons	
		Condensed	Gaseous
0.00	183	1.00	1.00
.67	183	2.3	1.0
3.50	183	2.1	0.8
7.94	183	—	.5
7.94	195	2.0	1.3
13.4	195	1.5	—
33.5	207	1.2	2.1

^a From Ref. 82.

hydrocarbons were produced in synthesis with $1.4\text{H}_2 + 1\text{CO}$ gas at 300°C. It must be concluded that small quantities of sulfur increased the average molecular weight of synthesis products. It has been demonstrated by Craxford³⁵ and others that hydrocracking reactions occur in the synthesis with cobalt catalysts, and with freshly reduced catalysts or at very high conversion, may decrease the average molecular weight of products appreciably. Apparently sulfur-poisoning decreases the magnitude of the hydrocracking reactions. If the conversion at the start of the experiments was very high, merely poisoning of the initial portion of the catalyst bed would be sufficient to explain the observed results; however, it is also possible that poisoning preferentially destroys the activity of portions responsible for hydrocracking. Data are not sufficient to demonstrate which mechanism is predominant; however, the following experiment seems to indicate that sulfur is strongly adsorbed at the inlet portion of the bed: A catalyst was progressively poisoned with organic sulfur in the synthesis at 200°C. By the time 19.4 mg of sulfur per gram of catalyst had been introduced, the

contraction had decreased from the initial value of 59 to 38 per cent. In an attempt to remove sulfur by hydrogenation, the sample was heated in pure hydrogen at 375°C for 14 hours. No hydrogen sulfide was evolved. After this treatment, the contraction observed in synthesis at 200°C was only 10 per cent. A similar treatment of an unpoisoned catalyst at 375°C caused no decrease in contraction. The authors postulated that a redistribution of sulfur occurred during the hydrogenation. Data of Alberts¹³¹ show the sulfur concentration of a cobalt catalyst as a function of bed length after a year of synthesis at 10 atmospheres. The inlet portion of the catalyst contained about 0.8 per cent sulfur, and the sulfur content decreased progressively to a very low value at about half of the bed length. About 40 per cent of the sulfur in the inlet portion of the bed was present as sulfate, possibly due to oxidation of sulfides by traces of oxygen in the synthesis gas.

Weingaertner¹⁷⁷ of Brabag reported analyses of a standard German cobalt catalyst after synthesis with a gas containing 0.45 g S per 100 m³. The inlet portion of the catalyst bed contained 1.62 per cent sulfur and the outlet portion 0.25 per cent. The average sulfur concentration was 0.30 per cent. The sulfur in the gas passed over the catalyst was equivalent to 0.2 per cent of the weight of the catalyst and the sulfur content of fresh catalyst was about 0.1 per cent. Thus, virtually all of the sulfur was adsorbed in the catalyst bed. On this basis, a catalyst should have a longer life in a second than in the first stage, and the author stated maximum lives of 4,000–5,000 hours in Stage II compared with 3,000 hours in Stage I. The following data for the average contraction in 2,000 hours for catalysts in the first stage as a function of sulfur content were given:

Sulfur Content, g/100 m ³	Average Contraction (%)
0.4–0.5	50
0.7–0.8	35

The poisoning of nickel catalysts by H₂S and CS₂ was studied by Fujimura, Tsuneoka, and Kawamichi⁶⁵. Data for synthesis at 200°C and atmospheric pressure (Figure 95) indicate that poisoning by H₂S and CS₂ is similar on a given catalyst; however, catalysts of different compositions do not respond in the same manner. For the Ni-Mn-ThO₂-kieselguhr preparation, the activity (expressed as apparent contraction) and the selectivity (yield of liquid hydrocarbons divided by contraction) decreased monotonically with sulfur content. The activity and selectivity of Ni-Mn-bleaching earth-kieselguhr increased to a maximum and then decreased as the sulfur content increased. The sulfur content required to decrease the contraction to half its original value was 50–100 mg S/g Ni for the Ni-Mn-ThO₂-kieselguhr catalyst and 154 for Ni-Mn-bleaching earth-kieselguhr. The increased hydrocarbon yields observed with the latter catalyst at low-

sulfur contents are similar to the results of Herington and Woodward for cobalt catalysts.

Fischer and Meyer⁵⁴ studied the poisoning of a nickel-cobalt-silicon skeletal catalyst in the synthesis with $2\text{H}_2 + 1\text{CO}$ gas containing 30 grams sulfur per 100 m^3 . The contraction decreased from 57 to 29 per cent in the first 47 hours. At this point, the catalyst was boiled in a sodium hydroxide solution for 30 minutes. The activity was partially restored, and on re-suming synthesis the contraction decreased from 53 to 27 per cent in 48 hours. After a second sodium-hydroxide treatment, the conversion dropped

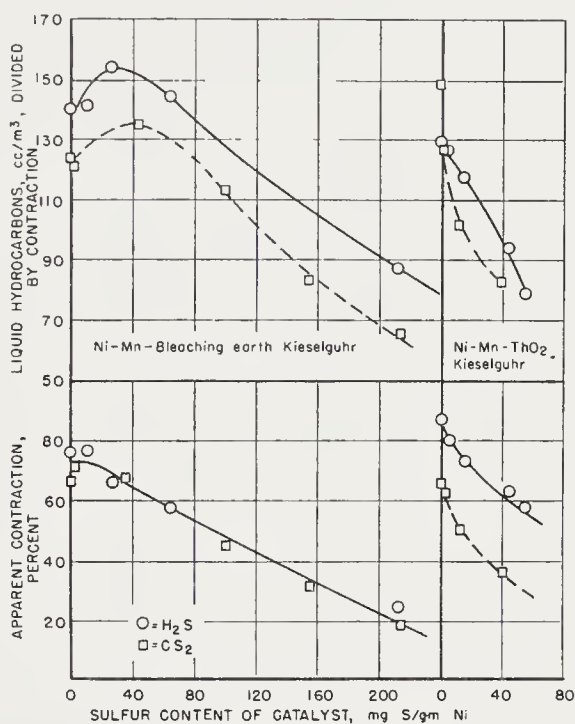


Figure 95. Sulfur poisoning of nickel catalysts. (From data of Ref. 65)

from 51 to 15 per cent in 40 hours. Further treatment with sodium hydroxide did not restore the activity. In the experiments, about 0.24 mg S was introduced per gram Co + Ni per hour, and the addition of 12 mg S per gram Co + Ni (in 48 hours) decreased the conversion to less than half. The activation by alkali-treatment may have resulted from the formation of fresh surface by further leaching of the silicon from the alloy.

Workers of the Gas Research Board^{22, 205} have studied the poisoning of nickel methanization catalysts with sulfur. Moderately long catalyst lives were obtained with synthesis gas containing no more than 0.3 grains of sulfur per 1000 ft^3 ; however, considerably better results were achieved with a gas containing 0.04 grains per 1000 ft^3 .

Iron Catalysts

Koelbel^{99a} reported a few results of sulfur poisoning of precipitated iron catalysts in the atmospheric pressure synthesis. The activity of catalysts in a typical synthesis gas containing 0.4 g sulfur per 100 m³ was, throughout the test, only about half as great as in pure gas. Systematic tests demonstrated that this type of catalyst was particularly sensitive to poisoning during the induction period. Three portions of the same catalyst were used: sample *a* was inducted with the regular synthesis gas (0.4 g S/100 m³), and samples *b* and *c* with gas scrubbed with charcoal. At 120 hours sample *c* was changed to the regular synthesis gas. Samples *b* and *c* had equal activity (contraction = 25 per cent) for the first 300 hours, but after this period the activity of sample *c* decreased at a faster rate than sample *b* so that the contractions at 1,250 hours were 19 and 14 per cent for samples *b* and *c*, respectively. Sample *a*, that was inducted with the impure gas, had low activity throughout the experiment.

Although sulfur-poisoning has not been systematically investigated at the Bruceton laboratory of the Bureau of Mines, some information was inadvertently obtained by Benson and co-workers²⁰ in pilot-plant studies of the oil-circulation process. The synthesis gas was produced by reforming natural gas. Since the natural gas contained virtually no sulfur compounds and the reformed gas consistently had a sulfur content less than 0.5 grains per 1,000 ft³, the synthesis gas was used without sulfur-purification, with analyses made at regular intervals. After three years of research on a variety of catalysts with no apparent difficulty due to sulfur-poisoning, the catalysts in the two pilot-plant units lost activity more rapidly than anticipated and did not respond to reactivation by hydrogen treatment. At the beginning of this period, the gas contained 31 grains S per 1,000 ft³ and 8 days later 120, although the natural gas was essentially sulfur-free over this period. Analyses of used catalysts from several pilot-plant experiments (Table 108) showed that catalysts with moderate to high activity contained less than 0.03 per cent sulfur. In experiment 21, in which poisoning was encountered as described above, the sulfur content was about 0.2 per cent. Apparently the sulfur compounds were produced by bacterial reduction of sulfates in the gasholder water. Following this experience, all of the synthesis gas was passed through charcoal at synthesis pressure and the sulfur content was determined continuously with a Rubicon automatic sulfur analyzer. This information appears to be about all that is available on sulfur-poisoning of iron catalysts in the Fischer-Tropsch synthesis. An upper limit of sulfur content of 0.5 grains per 1,000 cu ft seems to be adequate.

In lieu of experimental data on the Fischer-Tropsch synthesis, the studies of Frear, Shultz, and Elmore⁶³ on poisoning of iron catalysts in the am-

monia synthesis at 100 atmospheres are given. Hydrogen sulfide was a permanent poison. With a gas containing 0.1 per cent hydrogen sulfide, the conversion initially decreased only slowly as the sulfur content of the catalyst increased. At about 20 mg S per gram of catalyst, the conversion was 80 per cent of that of the fresh catalyst, but above this sulfur concentration the conversion decreased rapidly to a very low value. The sulfur content of the inlet portion of the bed was greatest, and similarly the outer layers of individual particles contained more sulfur than the interior. Water, oxygen, carbon monoxide, carbon dioxide, and sulfur dioxide were effective temporary poisons. It is remarkable that in poisoning action sulfur dioxide was similar to oxides of carbon and water rather than hydrogen sulfide. Similar results for poisoning of iron catalysts in the ammonia synthesis

TABLE 108. SULFUR CONTENT OF USED IRON CATALYSTS IN
OIL-CIRCULATION PROCESS^a
(Reduced fused Fe_3O_4 - MgO - K_2O catalysts)

Experiment	Hours of Synthesis	Sulfur (wt.-%)	Synthesis Gas	Activity
21b	750	Nil	Raw	Moderate to high
21c	800	0.2	Raw ^b	Low ^b
21c	900	0.16-0.27	Raw ^b	Low ^b
22c	2200	0.00-0.03	Charcoal scrubbed	Moderate to high
24	500	0.03	Charcoal scrubbed	Moderate to high

^a From Ref. 20.

^b High concentrations of sulfur found in synthesis gas in these periods.

were obtained by Brill²⁴. Catalysts promoted with calcium oxide, alumina, and potassium oxide were more resistant to sulfur poisoning than similar preparations without calcium oxide.

Bibliography

1. Alberts, L., private communication.
2. Almquist, J. A., and Black, C. A., *J. Am. Chem. Soc.*, **48**, 2814 (1926).
- 2a. Anderson, H. C., Wiley, J. L., and Newell, A., Vols. 1 and 2, Bureau of Mines Bulletin 544 (1954 and 1955).
3. Anderson, J. A., and Seyfried, W. C., *Anal. Chem.*, **20**, 998 (1948).
4. Anderson, R. B., "Advances in Catalysis," ed. by W. F. Frankenburg, V. I. Komarewsky, and E. K. Rideal, Vol. 5, p. 355, New York, Academic Press, Inc., 1953.
5. Anderson, R. B., Feldman, J., and Storch, H. H., *Ind. Eng. Chem.*, **44**, 2418 (1952).
6. Anderson, R. B., and Hall, W. K., *J. Am. Chem. Soc.*, **70**, 1727 (1948).
7. Anderson, R. B., Hall, W. K., Hewlett, H., and Seligman, B., *J. Am. Chem. Soc.*, **69**, 3114 (1947).

8. Anderson, R. B., Hall, W. K., and Hofer, L. J. E., *J. Am. Chem. Soc.*, **70**, 2465 (1948).
9. Anderson, R. B., Hall, W. K., Krieg, A., and Seligman, B., *J. Am. Chem. Soc.*, **71**, 183 (1949).
10. Anderson, R. B., Hofer, L. J. E., Cohn, E. M., and Seligman, B., *J. Am. Chem. Soc.*, **73**, 944 (1951).
11. Anderson, R. B., Krieg, A., Friedel, R. A., and Mason, L. S., *Ind. Eng. Chem.*, **41**, 2189 (1949).
12. Anderson, R. B., Krieg, A., Seligman, B., and O'Neill, W. E., *Ind. Eng. Chem.*, **39**, 1548 (1947).
13. Anderson, R. B., Krieg, A., Seligman, B., and Tarn, W. H., *Ind. Eng. Chem.*, **40**, 2347 (1948).
14. Anderson, R. B., McCartney, J. T., Hall, W. K., and Hofer, L. J. E., *Ind. Eng. Chem.*, **39**, 1618 (1947).
15. Anderson, R. B., Seligman, B., Shultz, J. F., Kelly, R., and Elliott, M. A., *Ind. Eng. Chem.*, **44**, 391 (1952).
16. Anderson, R. B. and Shultz, J. F., U. S. Patent 2,629,728, Feb. 24, 1953.
17. Anderson, R. B., Shultz, J. F., Seligman, B., Hall, W. K., and Storch, H. H., *J. Am. Chem. Soc.*, **72**, 3502 (1950).
18. Badische Anilin u. Soda Fabrik, German Patents 293,787 (1913); 295,202 (1914); 295,203 (1914).
19. Benson, H. E., Bienstock, D., Field, J. H., and Storch, H. H., *Ind. Eng. Chem.*, **46**, 2278 (1954).
20. Benson, H. E., Bienstock, D., Field, J. H., and Crowell, J. H., unpublished data of the Bureau of Mines.
21. Black, J. F. and Kearby, K. K., U. S. Patent 2,593,250, April 15, 1952.
22. Booth, N., Wilkins, E. T., Jolley, L. J., and Tebboth, J. A., "Catalytic Synthesis of Methane-Experimental Work of the Fuel Research Station," Gas Research Board, Copyright Pub. No. 21/11, 1948.
23. Bridges, G. L., Pole, G. R., Beinlich, A. W., Jr., and Thompson, H. L., *Chem. Eng. Progr.*, **43**, 291 (1947).
24. Brill, R., TOM Reel 300, FIAT Reel R-19, Frames 7088-7104, 1941.
25. Brunauer, S., "Physical Adsorption," Princeton University Press, 1943.
26. Brunauer, S., and Emmett, P. H., *J. Am. Chem. Soc.*, **52**, 2682 (1930).
27. Brunauer, S., Emmett, P. H., and Teller, E., *J. Am. Chem. Soc.*, **60**, 309 (1938).
28. Bruner, F. H., *Ind. Eng. Chem.*, **41**, 2511 (1949); private communication.
29. Cady, W. E., Launer, P. J., Weitkamp, A. W., *Ind. Eng. Chem.*, **45**, 350 (1953).
30. Cain, D. G., Weitkamp, A. W., and Bowman, N. J., *Ind. Eng. Chem.*, **45**, 359 (1953).
31. Chaffee, C. C., Thompson, O. F., King, J. G., Atwell, H. V., Jones, I. H., PB 12,624 (1945), 54 pp., CIOS File XXXI-23, Item 30.
32. Clark, A., Andrews, A., Fleming, H. W., *Ind. Eng. Chem.*, **41**, 1527 (1949).
33. Clark, E. L., Kallenberger, R. H., Browne, R. Y., and Phillips, J. R., *Chem. Eng. Progr.*, **45**, 651 (1949).
34. Craxford, S. R., *Fuel*, **26**, 119 (1947).
35. Craxford, S. R., *Trans. Faraday Soc.*, **42**, 576 (1946).
36. Crowell, J. H., Benson, H. E., Field, J. H., and Storch, H. H., *Ind. Eng. Chem.*, **42**, 2376 (1950).
37. Davis, H. G., and Wilson, T. P., British Patent 684,130.
38. DeLange, J. J., and Visser, G. H., *Ingenieur*, **58**, 24 (1946); private communication.

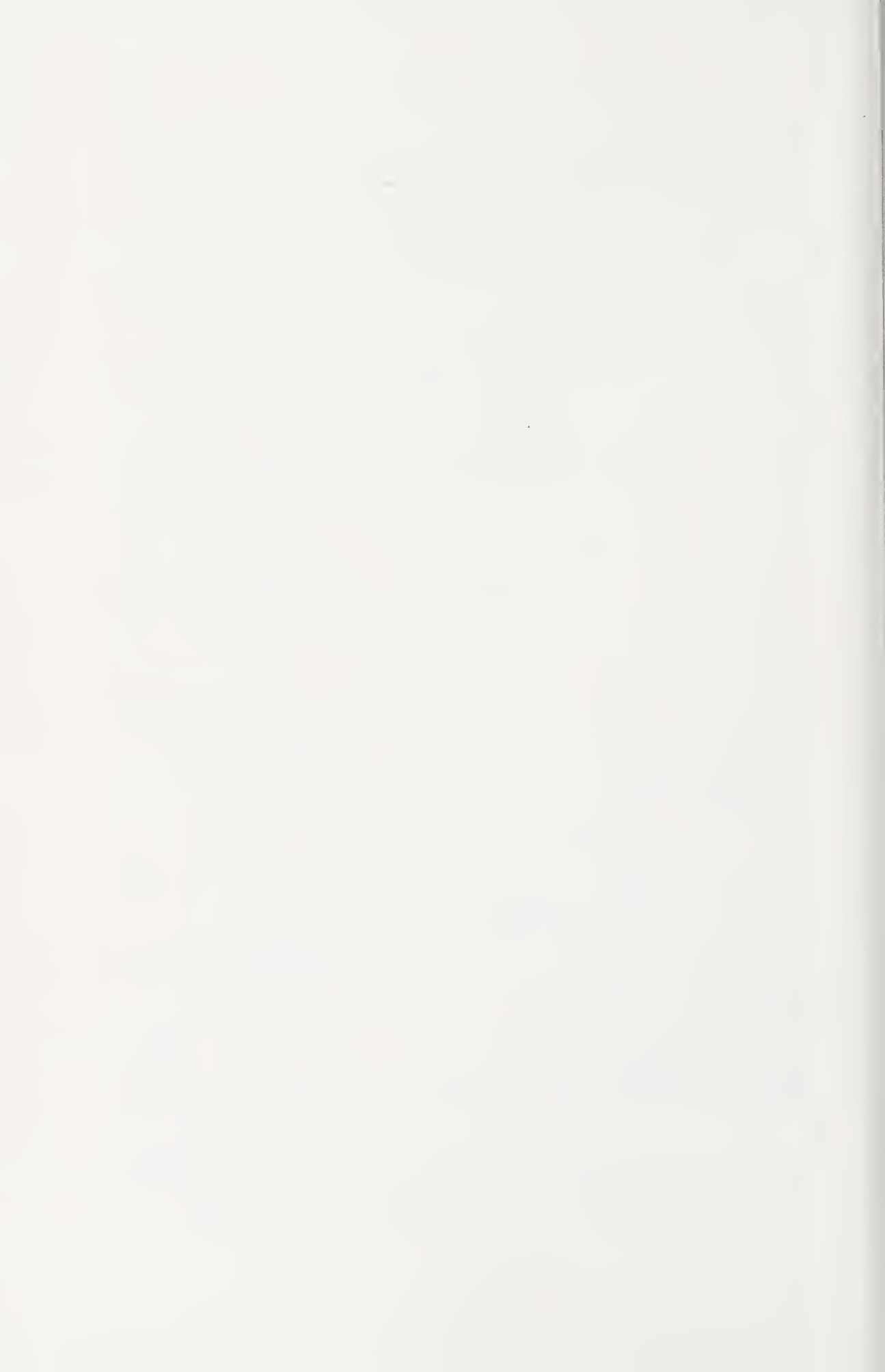
39. Eckstrom, H. C., and Adecock, W. A., *J. Am. Chem. Soc.*, **72**, 1042 (1950); paper presented at Pgh. Conference on X-ray and Electron Diffraction, 1951.
40. Eliot, T. W., Goodwin, S. C., Jr., and Pace, P. S., *Chem. Eng. Progr.*, **45**, 532 (1949).
41. Emmett, P. H., in "Fixed Nitrogen," ed. by H. A. Curtis, pp. 150-239, New York, Chemical Catalog Co. (Reinhold Publishing Corp.), 1932.
42. Emmett, P. H., "Advances in Colloid Science," Vol. I, pp. 1-36, New York, Interscience Publishers, 1942.
43. Emmett, P. H., and Brunauer, S., *J. Am. Chem. Soc.*, **59**, 310, 1553 (1937).
44. Emmett, P. H., and DeWitt, T. W., *J. Am. Chem. Soc.*, **65**, 1253 (1943).
45. Faragher, W. F., *et al.*, Supplemental Report on Ruhrchemie A.G., Sterkrade-Holten (Oberhausen-Holten) Ruhr, PB 1,366; CIOS Rept. XXXII-96, Item 30 (1946).
46. Fischer, F., *Ges. Abhandl. Kenntnis Kohle*, **10**, 501 (1930).
47. Fischer, F., *Brennstoff-Chem.*, **11**, 489 (1930).
48. Fischer, F., *ibid.*, **16**, 1 (1935).
49. Fischer, F., and Koch, H., *Brennstoff-Chem.*, **13**, 61 (1932).
50. Fischer, F., and Kuster, H., *Brennstoff-Chem.*, **14**, 3 (1933).
51. Fischer, F., and Meyer, K., *Brennstoff-Chem.*, **12**, 225 (1931).
52. Fischer, F., and Meyer, K., *ibid.*, **14**, 47 (1933).
53. Fischer, F., and Meyer, K., *ibid.*, **15**, 84 (1934).
54. Fischer, F., and Meyer, K., *ibid.*, **15**, 107 (1934).
55. Fischer, F., and Pichler, H., *Brennstoff-Chem.*, **12**, 365 (1931).
56. Fischer, F., and Pichler, H., *ibid.*, **20**, 41 (1939).
57. Fischer, F., and Pichler, H., *ibid.*, **20**, 221 (1939).
58. Fischer, F., and Pichler, H., German Patent 731,295 (1936).
59. Fischer, F., and Pichler, H., German Patent Appl. St 56,470, July 30, 1937.
60. Fischer, F., Roelen, O., and Feisst, W., *Brennstoff-Chem.*, **13**, 461 (1932).
61. Fischer, F., and Tropsch, H., *Brennstoff-Chem.*, **4**, 276 (1923); **5**, 201, 217 (1924).
62. Fischer, F., and Tropsch, H., *Ges. Abhandl. Kenntnis Kohle*, **10**, 333 (1930).
63. Frear, G. L., and Shultz, J. F., Tennessee Valley Authority Internal Report R545.
64. Friedel, R. A., and Anderson, R. B., *J. Am. Chem. Soc.*, **72**, 1212 (1950).
65. Fujimura, K., Tsuneoka, S., and Kawamichi, K., *J. Soc. Chem. Ind. Japan*, **37**, Suppl. binding 395 (1934).
66. Gall, D., Gibson, E. J., and Hall, C. C., *J. Appl. Chem.*, **2**, 371 (1952).
67. Ghosh, J. C., and Basak, N. G., *Petroleum*, **11**, 131 (1948).
68. Gordon, K., "Report on the Petroleum and Synthetic Oil Industry of Germany," BIOS Overall Rept. 1, 82 (1947).
69. Gresham, W. F., U. S. Patent 2,535,060, June 15, 1949.
70. Grossman, J. P., and Postgate, J. R., *Nature*, **171**, 600 (1953).
71. Hall, C. C., and Craxford, S. R., PB 93,498 (1946), BIOS Final Rept. 1722, Item 22, 178 pp.
72. Hall, C. C., Craxford, S. R., and Gall, D., "Interrogation of Dr. Otto Roelen of Ruhrchemie A. G." PB 77,705 (1946), 60 pp.; Final BIOS Rept. 447, Item 30.
73. Hall, C. C., Craxford, S. R., Gall, D., and Smith, S. L., "Interrogation of Dr. H. Koelbel," PB 91,925, BIOS Final Rept. 1712, Item 30.
74. Hall, C. C., Gall, D., and Smith, S. L., *J. Inst. Petroleum*, **38**, 845-876 (1952).
75. Hall, C. C., and Smith, S. L., *J. Inst. Petroleum*, **33**, 439 (1947).
76. Hall, C. C., and Smith, S. L., *J. Soc. Chem. Ind. (London)*, **65**, 128 (1946).

77. Hall, W. K., Dieter, W. E., Hofer, L. J. E., and Anderson, R. B., *J. Am. Chem. Soc.*, **75**, 1442 (1953).
78. Hall, W. K., Tarn, W. H., and Anderson, R. B., *J. Am. Chem. Soc.*, **72**, 5436 (1950).
79. Hall, W. K., Tarn, W. H., and Anderson, R. B., *J. Phys. Chem.*, **56**, 688 (1952).
80. Herbst, M., Halle, F., and Brill, R., FIAT Reel R19, Frames 7,136-47; TOM Reel 26, Bag 2,463; TOM Reel 134, Item II/10.
81. Herington, E. F. G., *Chemistry & Industry*, **1946**, 347.
82. Herington, E. F. G., and Woodward, L. A., *Trans. Faraday Soc.*, **35**, 958 (1939).
83. Hofer, L. J. E., Anderson, R. B., Peebles, W. C., and Stein, K. C., *J. Phys. Colloid Chem.*, **55**, 1201 (1951).
84. Hofer, L. J. E., and Cohn, E. M., *J. Chem. Phys.*, **18**, 766 (1950).
85. Hofer, L. J. E., and Peebles, W. C., *J. Am. Chem. Soc.*, **69**, 2497 (1947).
86. Hofer, L. J. E., Peebles, W. C., and Dieter, W. E., *J. Am. Chem. Soc.*, **68**, 1953 (1946).
87. Hollings, H., and King, J. G., PB 4,328 (1945), 13 pp.; CIOS File XXXII-91, Item 30/6.08.
88. Holroyd, R., editor, *Bureau of Mines Inform. Circ.* **7,370** (1946); PB 6,650; CIOS Rept. XXXII-107, Item 30 (1945).
89. Horne, W. A., and Faragher, W. F., *Bureau of Mines Inform. Circ.* **7,376**, 27 pp.; PB 7,745; FIAT Final Rept. 426 (1945).
90. Howk, B. W., and Hager, G. F., U. S. Patent 2,549,470, April 12, 1949.
91. Jack, K. H., *Proc. Roy. Soc. (London)*, **A195**, 41 (1948).
92. Jellinek, M. H., and Fankuchen, I., "Advances in Catalysis," ed. by W. G. Frankenburg, V. I. Komarewsky, and E. K. Rideal, Vol. I, p. 279, New York, Academic Press, Inc., 1948.
93. Johnson, M. F. L., and Ries, H. E., *J. Phys. Chem.*, **57**, 865 (1954).
- 93a. Kainer, F., "Die Kohlenwasserstoff-Synthese nach Fischer-Tropsch," Berlin, Springer-Verlag, 1950.
94. Karzhavin, V. A., *Advances in Chemistry (U.S.S.R.)*, **16**, 327 (1947).
95. Katayama, I., Murata, Y., Koide, H., and Tsuneoka, S., *Sci. Papers Inst. Phys. Chem. Research (Tokyo)*, **34**, 1, 181 (1938); *J. Soc. Chem. Ind. Japan*, **41**, Suppl. Binding 393 (1938).
96. Koch, H., and Billig, R., *Brennstoff-Chem.*, **21**, 157 (1940).
97. Koch, H., and Hilberath, F., *Brennstoff-Chem.*, **22**, 135, 145 (1941).
98. Kodama, S., in "Japanese Fuels and Lubricants, Article 7. Progress in the Synthesis of Liquid Fuels from Coal," U. S. Naval Tech. Mission to Japan; PB 53,701, p. 238.
99. Kodama, S., Tahara, H., Hukushima, I., Isoda, M., Komazawa, S., and Kimura, K., *J. Soc. Chem. Ind. Japan*, **45**, 448B, Suppl. Binding (1942).
- 99a. Koelbel, H., TOM Reel 115X, Frames 1181-1196.
100. Koelbel, H., TOM Reel 115X, Frames 1510-1592.
101. Koelbel, H., Ackermann, P., Ruschenburg, E., Langheim, R., and Engelhardt, F., *Chem.-Ing. Tech.*, **8**, 183 (1951).
102. Koelbel, H., and Engelhardt, F., *Erdol u Kohle*, **2**, 52 (1949).
103. Koelbel, H., and Engelhardt, F., *ibid.*, **3**, 529 (1950).
104. Kolthoff, I. M., and Moskowit, B., *J. Am. Chem. Soc.*, **58**, 777 (1936).
- 104a. Komarewsky, V. I., Riesz, C. H., and Estes, F. L., "The Fischer-Tropsch Process," The Institute of Gas Technology, Chicago, 1945.
105. Krieg, A., Dudash, A. P., and Anderson, R. B., *Ind. Eng. Chem.*, **41**, 1508 (1949).
106. Larson, A. T., and Richardson, C. N., *Ind. Eng. Chem.*, **17**, 971 (1925).

107. Leuna, TOM Reel 13, Bag 3043-3, 30/4.02, Frame 430.
108. Leuna, TOM Reel 86, Bag 3979, Item 78, Frames 1058-1096.
109. Leuna, TOM Reel 134, Section 1a, Item 8.
110. Love, K. S., and Brunauer, S., *J. Am. Chem. Soc.*, **64**, 745 (1942).
111. Martin, F., *Chem. Fabrik.*, **12**, 233 (1939).
112. Michael, W., in report of Zorn, H., "The CO-H₂ Synthesis at I. G. Farben.," PB 97,368 (1949); FIAT Final Rept. 1267 (1949).
113. McCartney, J. T., and Anderson, R. B., *J. Appl. Phys.*, **22**, 1441 (1951).
114. Mittasch, A., "Advances in Catalysis," ed. by W. G. Frankenburg, V. I. Komarewsky, and E. K. Rideal, Vol. 2, p. 82, New York, Academic Press, Inc., 1949.
115. Morrell, C. E., Carlson, C. S., McAteer, J. H., Robey, R. F., and Smith, P. V., *Ind. Eng. Chem.*, **44**, 2839 (1952).
116. Murata, Y., Ishikawa, S., and Tsuneoka, S., *J. Soc. Chem. Ind. Japan.*, Suppl. Binding **39**, 329 (1936).
117. Murata, Y., Sawada, Y., Takezaki, Y., and Yasuda, M., *J. Soc. Chem. Ind. Japan*, **45**, 288, 292, Suppl. Binding (1942).
118. Nakai, A., in "Japanese Fuels and Lubricants, Article 7. Progress in Liquid Fuels from Coal," U. S. Naval Tech. Mission to Japan; PB 53,701, p. 171.
119. Nielsen, A., "Advances in Catalysis," ed. by W. F. Frankenburg, V. I. Komarewsky, and E. K. Rideal, Vol. 5, p. 1, New York, Academic Press, Inc., 1953.
120. Oppau, TOM Reel 278, "Fused Iron Catalysts for the CO-H₂ Synthesis," July 1, 1944, 44 pp.
121. Perrin, M., *Compt. rend.*, **227**, 476 (1948).
122. Perrin, M., doctoral dissertation, University of Lyon, 1948.
123. Pichler, H., TOM Reel 101, PG 21,559; PG 21,574; PG 21,577; and PG 21,581, translated by M. Leva in Bur. Mines Special Rept.
124. Pichler, H., "The Synthesis of Hydrocarbons from Carbon Monoxide and Hydrogen," U. S. Bur. Mines Special Rept., 1947, translation in TOM Reel 259, Frames 467-654.
125. Pichler, H., Special Reel 427, Bur. of Mines translation by M. Leva.
126. Pichler, H., and Buffleb, H., *Brennstoff-Chem.*, **21**, 257 (1940).
127. Pichler, H., and Buffleb, H., *ibid.*, **21**, 273 (1940).
128. Pichler, H., and Buffleb, H., *ibid.*, **21**, 285 (1940).
129. Pichler, H., and Merkel, H., U. S. Bureau of Mines Tech. Paper 718 (1949).
130. Pichler, H., and Merkel, H., *Brennstoff-Chem.*, **31**, 1, 33 (1950).
131. Pichler, H., "Advances in Catalysis," ed. by W. G. Frankenburg, V. I. Komarewsky, and E. I. Rideal, Vol. 4, pp. 271-341, New York, Academic Press, Inc., 1952.
132. Podgurski, H., Kummer, J. T., DeWitt, T. W., and Emmett, P. H., *J. Am. Chem. Soc.*, **72**, 5382 (1950).
133. Powell, A. R., *Ind. Eng. Chem.*, **40**, 558 (1948).
134. Raney, M., U. S. Patents 1,563,487 (1925); 1,628,190 (1927); 1,915,473 (1933), *J. Am. Chem. Soc.*, **54**, 4116 (1932).
135. Redlich, O., Gable, C. M., Dunlop, A. K., Miller, R. W., *J. Am. Chem. Soc.*, **72**, 4153 (1950).
136. Reichl, E. H., U. S. Naval Tech. Mission in Europe Rept. 248-45 (1945); 128 pp.; PB 22,841.
137. Reisinger, Breywisch, and Geiseler, TOM Reel 55, Bag 2523, Documents 86 and 87.
138. Reisinger, TOM Reel 134, Rept. 283.
139. Reisinger, TOM Reel 13, Bag 3,043, Item 3; TOM Reel 86, Bag 3,979, Item 78.

140. Reitmeier, R. E., Atwood, K., Bennett, H. A., Jr., and Baugh, H. M., *Ind. Eng. Chem.*, **40**, 620 (1948).
141. Report of the Fuel Research Board (British), His Majesty's Stationery Office, London, reports for the years ending March 1936, p. 148; March 1937, p. 141; March 1938, p. 186; March 1939, p. 151.
142. Rheinpreussen, FIAT Reel 116-X, Frames 1717-87, 17th Communication.
143. Roberts, J. K., U. S. Patent 2,461,570, Feb. 15, 1949.
144. Roelen, O., Ruhrchemie FIAT Reel K-21, Frames 792-805, April 1937.
145. Roelen, O., TOM Reel 33, Bag 3,440, Target 30/5.01, Items 6 and 24; TOM Reel 36, Bag 3,451, Item 13.
146. Rubin, L. C., U. S. Patent 2,448,279 (1948).
147. Ruhrchemie, TOM Reel 34, Bag 3,440, Item 31.
148. Ruhrchemie, TOM Reel 37, Bag 3,451, Item 23.
149. Ruhrchemie, TOM Reel 37, Bag 3,451, Item 24.
150. Ruhrchemie, TOM Reel 39, Bag 3,450, Item 42.
151. Ruhrchemie, TOM Reel 42, Bag 3,439, Item 22.
152. Ruhrchemie, TOM Reel 45, Bag 3,441, Item 76.
153. Ruhrchemie, FIAT Reel K21, PB 70,212.
154. Ruhrchemie, FIAT Reel K21, Frame 980, March 1937.
155. Ruhrchemie, FIAT Reel K21, Frames 1010-11, 1938.
156. Ruhrchemie, FIAT Reel K21, Frames 1032-35.
157. Ruhrchemie, FIAT Reel K21, Frames 1036-39, 1938.
158. Ruhrchemie, FIAT Reel K21, Frames 1070-75.
159. Ruhrchemie, FIAT Reel K21, Frame 1104A.
160. Ruhrchemie, FIAT Reel K21, Frames 991-3, 1938; 1116-8, 1941.
161. Sabatier, P., and Senderens, J. B., *Compt. rend.*, **134**, 514 (1902); *J. Soc. Chem. Ind.*, **21**, 504 (1902).
162. Sand, A. E., Wainwright, H. W., Egleson, G. C., Bureau of Mines Rept. Investigations 4699 (1950).
163. Sastri, M. V. C., and Srinivasan, S. R., *J. Am. Chem. Soc.*, **75**, 2898 (1953).
164. Schaarschmidt, A., and Marder, H., *Brennstoff-Chem.*, **13**, 412 (1932).
165. Scheuermann, A., in report of Zorn, H., "The CO-H₂ Synthesis at I. G. Farben.," PB 97,368 (1949); FIAT Final Rept. 1267 (1949).
166. Schwarzheide tests, Reel 33, Bag 3440, Item 29.
167. Seelig, H. S., and Marschner, R. F., *Ind. Eng. Chem.*, **40**, 583 (1948).
168. Seelig, H. S., Week, H. I., Voss, D. J., and Zisson, J., Preprint of paper presented before the Division of Petroleum Chemistry of the American Chemical Society, Atlantic City, Sept. 1952.
169. Shultz, J. F., Hall, W. K., Seligman, B., and Anderson, R. B., *J. Am. Chem. Soc.*, **77**, 213 (1955).
170. Shultz, J. F., Seligman, B., Lecky, J., and Anderson, R. B., *ibid.*, **74**, 637 (1952).
171. Shultz, J. F., Seligman, B., Shaw, L., and Anderson, R. B., *Ind. Eng. Chem.*, **44**, 397 (1952).
172. Shultz, J. F., Stein, K., Abelson, M., unpublished results of the Bureau of Mines.
173. Smith, D. F., Davis, J. D., and Reynolds, D. A., *Ind. Eng. Chem.*, **20**, 462 (1928).
174. Spruit, C. J. P., and Wauklyn, J. N., *Nature*, **168**, 951 (1951).
175. Starkey, R. L., *J. Am. Water Works*, **37**, 963 (1945).
176. Stein, K., Seligman, B., and Anderson, R. B., unpublished results.
177. Steinbrecher, and Weingaertner, FIAT Reel K25, Frames 003,782-003,796, Jan. 5, 1938; PB 70,216, TOM Reel 292.

178. Steitz, A., and Barnes, D. K., *Ind. Eng. Chem.*, **45**, 353 (1953).
179. Storch, H. H., *Chem. Eng. Progr.*, **44**, 469 (1948).
180. Storch, H. H., Anderson, R. B., Hofer, L. J. E., Hawk, C. O., Anderson, H. C., and Golumbic, N., Bureau of Mines Tech. Paper 709 (1948).
181. Storch, H. H., Golumbic, N., and Anderson, R. B., "The Fischer-Tropsch and Related Syntheses," New York, John Wiley & Sons, Inc., 1951.
182. Teichner, S., Doctoral dissertation under M. Prettre at the University of Lyon, 1950.
183. Teichner, S., *Compt. rend.*, **227**, 478 (1948).
184. Teichner, S., and Pernoux, E., *Clay Minerals Bull.*, **1**, 145 (1951).
185. Thompson, J. G., *Ind. Eng. Chem.*, **21**, 389 (1929).
186. Trambouze, Y., *Compt. rend.*, **227**, 971 (1948).
187. Trambouze, Y., *ibid.*, **228**, 1432 (1949).
188. Trambouze, Y., Doctoral dissertation, University of Lyon, 1950.
189. Trambouze, Y., and Perrin, M., *Compt. rend.*, **228**, 837, 1015 (1949).
190. Tsutsumi, S., Report of the Imperial Fuel Research Institute of Japan, July 25, 1935, edited by R. C. Grass, Bureau of Mines Inform. Circ. 7594 (1951).
191. Tsutsumi, S., *Sci. Papers Inst. Phys. Chem. Research Tokyo*, **35**, 481 (1939); **36**, 47 (1939); **36**, 251 (1939).
192. Tsutsumi, S., *J. Fuel Soc. Japan*, **14**, 110 (1935); *ibid.*, **58**, 996 (1937); *Sci. Papers Inst. Phys. Chem. Research (Tokyo)*, **35**, 435 (1939); **36**, 335 (1939).
193. Tsuneoka, S., and Murata, Y., *Sci. Papers Inst. Phys. Chem. Research (Tokyo)*, **34**, 280 (1938); *J. Soc. Chem. Ind. Japan*, **41**, Suppl. Binding 52 (1938).
194. Underwood, A. J. V., *Ind. Eng. Chem.*, **32**, 449 (1940).
195. von Weber, U., *Angew. Chem.*, **52**, 607 (1939).
196. Walker, S. W., U. S. Patent 2,485,945, Oct. 25, 1949.
197. Ward, C. C., Schwartz, F. G., and Adams, N. G., *Ind. Eng. Chem.*, **43**, 1117 (1951).
198. Watanabe, S., Report of Hokkaido Synthetic Petroleum Co., (Japan), edited by R. C. Grass, Bureau of Mines Inform. Circ. 7611 (1951).
- 198a. Weil, B. H., and Lane, J. C., "Synthetic Petroleum from the Synthine Process," Brooklyn, Chemical Publishing Co., 1948.
199. Weiser, H. B., and Milligan, W. O., *J. Am. Chem. Soc.*, **57**, 238 (1935).
200. Weitkamp, A. W., Seelig, H. S., Bowman, N. J., and Cady, W. E., *Ind. Eng. Chem.*, **45**, 343 (1953).
201. Weller, S., Hofer, L. J. E., and Anderson, R. B., *J. Am. Chem. Soc.*, **70**, 799 (1948).
202. Wenzel, W., TOM Reel 134, Rept. 326.
203. Wenzell, L. P., Dressler, R. C., and Batchelder, H. R., *Ind. Eng. Chem.*, in press.
204. Wheeler, A., "Advances in Catalysis," ed. by W. G. Frankenburg, V. I. Komarewsky, and E. K. Rideal, Vol. 3, p. 250, New York, Academic Press, Inc., 1951.
205. Wilkins, E. T., and Jolley, L. J., *Coke and Gas*, **9**, 245 (1947).
206. Zorn, H., "The CO-H₂ Synthesis at I. G. Farben," PB 97,368 (1949); FIAT Final Rept. 1267 (1949).
207. Zwietering, P., Bokhoven, C., van Heerden, C., and Westrik, R., "Catalysis," Vol. III, p. 265, New York, Reinhold Publishing Corp., 1955.



CHAPTER 3

KINETICS AND REACTION MECHANISM OF THE FISCHER-TROPSCH SYNTHESIS

Robert B. Anderson

*Chief, Branch of Coal-to-Oil Research, Division of Solid Fuels Technology,
Bureau of Mines, Pittsburgh, Pa.*

This chapter assembles data pertinent to the kinetics and reaction mechanism of the Fischer-Tropsch synthesis. First, the kinetics on cobalt, nickel, iron, and ruthenium catalysts are considered, followed by a discussion of two similar reactions: the hydrogenation of carbon dioxide and the reaction of water plus carbon monoxide. Then a number of catalytic reactions that may possibly occur in some of the synthesis steps are described. The chemical and physical nature of the catalyst are discussed next and finally many of the hypotheses on reaction mechanism are assembled and evaluated. Although a few aspects of the reaction mechanism, such as chain growth, appear to be adequately interpreted, the present theories fall far short of providing a unified picture capable of explaining or predicting kinetics, promoter effects, selectivity, etc.

KINETICS OF THE FISCHER-TROPSCH SYNTHESIS

Few satisfactory, unambiguous data on the kinetics of the Fischer-Tropsch synthesis are available. The principal reason for the paucity of adequate kinetic results is the difficulty of arranging experiments amenable to simple analysis on a group of reactions of the relatively high degree of complexity of the Fischer-Tropsch synthesis. Analytical methods are usually not of sufficient accuracy to permit the use of the "differential reactor" in which the conversion in the catalyst bed is maintained sufficiently low so that the composition of the feed gas remains essentially unchanged; and the difficulties in interpreting data from so-called "integral reactors" involving sizable changes in conversion and gas composition are great. In the following paragraphs, the general methods of analyzing kinetic data and definitions regarding conversion, rate, etc., are described. For a process as complex as the Fischer-Tropsch synthesis, some of the definitions may appear arbitrary.

It is usually desirable to express conversion in terms of the fraction of

$\text{H}_2 + \text{CO}$ consumed, x , and to express the distribution of products as moles produced per moles of $\text{H}_2 + \text{CO}$ consumed. However, such data are frequently not available, and the apparent contraction or yields of liquid plus solid hydrocarbons in g/m^3 of gas passed must be used as a measure of conversion. Relative usage of hydrogen and carbon monoxide is usually expressed as the molar usage ratio, $\text{H}_2:\text{CO}$; however, the ratio of moles H_2 to moles $\text{H}_2 + \text{CO}$ consumed has better properties than the simple ratio. The differential reaction rate per unit volume of catalyst, r , is given by

$$r = dx/d(1/S) \quad (1)$$

where S is the space velocity. Frequently rate data at constant temperature

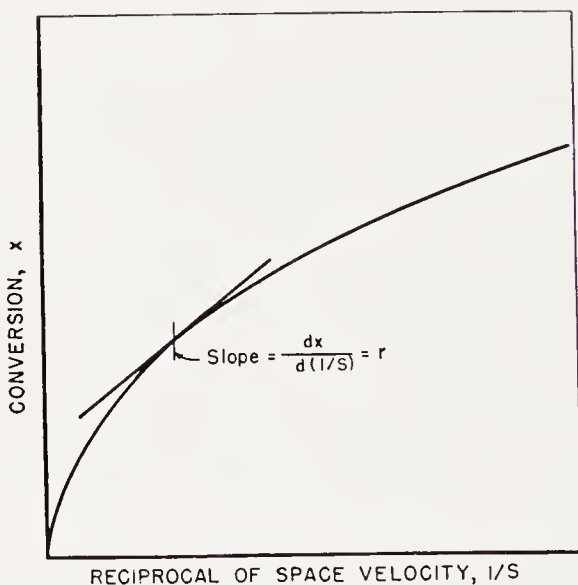


Figure 1. Kinetic plot illustrating the determination of differential reaction rate, r .

are presented graphically, as shown in Figure 1, where the slope of the curve is the differential reaction rate, r . Identical curves may usually be obtained by varying either the flow of gas over a constant volume of catalyst or varying the amount of catalyst with the flow maintained constant.

A goal of kinetics is to find a fundamental rate equation relating the differential rate to the partial pressures (or concentrations) of reactants, p_A, p_B, \dots , and of products p_R, p_S, \dots ,

$$r = dx/d(1/S) = F(p_A, p_B, \dots, p_R, p_S). \quad (2)$$

The equation may be tested by (a) differentiating the rate data, or (b) expressing the partial pressures in terms of conversion based on the stoichiometry of the reaction and integrating in the following way

$$\frac{1}{S} = \int_0^x \frac{dx}{F(p_A, p_B, \dots, p_R, p_S, \dots)} = G(x). \quad (3)$$

Method (b) is particularly difficult for the Fischer-Tropsch synthesis with iron catalysts, because the stoichiometry (especially the usage ratio) changes with conversion and feed gas composition. The validity of a given rate equation can be judged by its ability to describe rate data for widely varying reaction conditions, the reasonableness of values of the constants and their temperature dependence, and consistency of postulates of the rate equation with available information on reaction mechanism. The task of formulating and proving a fundamental rate equation that can be related to reaction mechanism is difficult, especially since the effects of diffusion in catalyst pores can produce changes in the dependency of observed rate upon concentrations of reactions and products. For the Fischer-Tropsch synthesis, only a few experiments have been arranged to afford simple, unambiguous interpretation; difficulties in obtaining sufficiently accurate, detailed analytical data and constant, reproducible catalyst behavior cause uncertainties in even the best experiments. From available data, useful empirical equations relating rate to either partial pressures of components or conversion have been obtained, together with information on pressure and temperature dependencies, selectivity, and the general course of the synthesis. The usual analysis of rate data assumes an isothermal bed of catalyst, and with the high exothermic synthesis reactions, sizable temperature differences may occur, although in liquid-jacketed reactors these differences are usually small if the conversion is limited to the order of 300 to 400 volumes of $H_2 + CO$ converted per volume of catalyst per hour, unless the reaction takes place in a very limited portion of the bed.

Useful data on the over-all dependence of rate on temperature and pressure may be obtained by comparing the space-time-yield (xS) either at constant conversions obtained by adjusting flow or at low conversions with the flow maintained constant.

The kinetics of synthesis on cobalt and nickel catalysts are similar and will be discussed first, followed by a discussion of iron and ruthenium catalysts, respectively. The kinetics of the Fischer-Tropsch synthesis as summarized by Storch, Golumbic, and Anderson¹²³, will be reviewed briefly, and the few pertinent data that have subsequently become available will be described in more detail.

Kinetics of the Fischer-Tropsch Synthesis on Cobalt and Nickel Catalysts

All published experiments with nickel catalysts were made at atmospheric pressure. Plots of conversion against reciprocal space velocity are approximately linear until moderately high conversions are attained. Tsuneoka and Fujimura¹²⁸ maintained a constant flow of synthesis gas at 200°C and varied the volume of Ni-Mn-ThO₂-kieselguhr catalyst. With both $2H_2 + 1CO$ and $1H_2 + 1CO$, the yield of "benzine" increased ap-

proximately linearly until about 80 per cent of either hydrogen or carbon monoxide were consumed, as shown in Figure 2. Similar results were obtained by Aicher, Myddleton, and Walker² with Ni-Mn-Al₂O₃-SiO₂-kieselguhr and 2H₂ + 1CO or water gas (approximately 1H₂ + 1CO), as illustrated in Figure 3. Comparison of space-time-yield for a constant conversion at different temperatures permits an estimate of the over-all activation energies, 26 to 29 kcal/mole for 2H₂ + 1CO and about 23 kcal/mole for water gas. The approximately linear plots indicate that the reaction rate

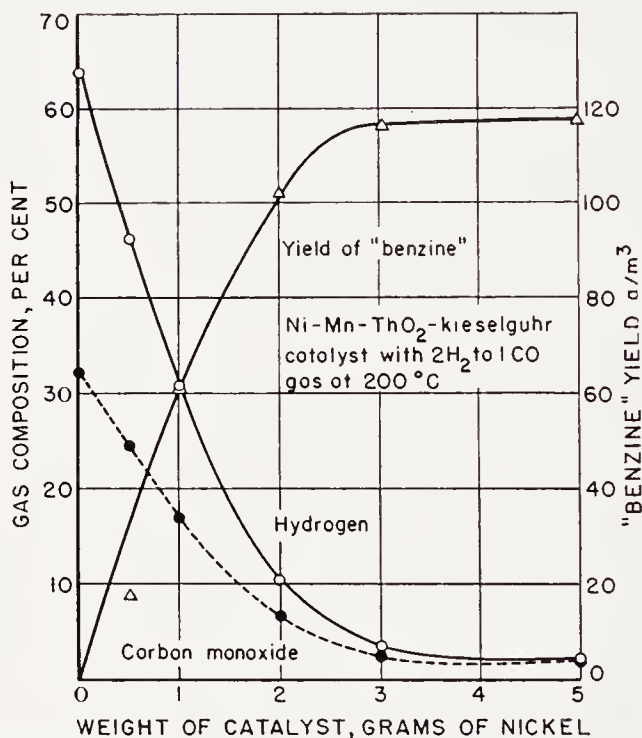


Figure 2. Variation of gas composition and yield of "benzine" with weight of catalyst charge at constant flow of synthesis gas. (Reproduced from Ref. 128)

is relatively independent of partial pressures of products and reactants, and hence the rate may be similarly independent of total operating pressure. Data are not available to show the effect of total pressure; however, at relatively low pressures the catalyst behavior is impaired by carbonyl corrosion.

In contrast to this interpretation, Aicher, Myddleton, and Walker² concluded that rate, in terms of space-time-yield of oil, increased with partial pressure of reactants and decreased with partial pressure of products. Apparently this relationship is valid only for relatively high conversion, where hydrocracking proceeds to a sufficient extent to decrease the over-all yield. Under these conditions, synthesis in stages with removal of liquid

hydrocarbons between stages should result in larger yields of liquids, and this postulate was demonstrated experimentally. Murata⁹⁶ studied the synthesis with $2\text{H}_2 + 1\text{CO}$ gas on $\text{Ni}:\text{Co}:\text{Si} = 50:50:100$ skeletal catalysts as a function of space velocity. The data in Figure 4 indicate that the yields of both water and "benzine" increased to a maximum and then decreased as the space velocity was decreased. Apparently hydrocracking and water-gas shift become important at low flow-high conversion conditions. The unsaturation of the "benzine," indicated by iodine numbers, decreased rapidly to very low values in the range of hydrocracking.

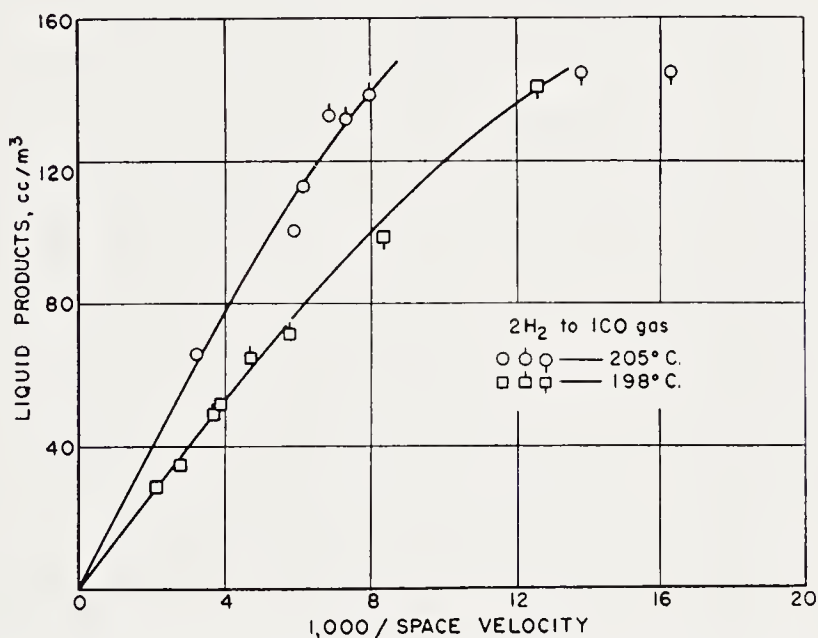


Figure 3. Yield of liquid hydrocarbons from a nickel catalyst as a function of the reciprocal of space velocity. (Reproduced with permission from Ref. 2)

The usage ratio, $\text{H}_2:\text{CO}$, usually varied from 2.1 to 2.3 for feed gas of rather widely varying $\text{H}_2:\text{CO}$ ratios. Fujimura and Tsuneoka⁵¹ investigated the influence of $\text{H}_2:\text{CO}$ feed ratio on the synthesis with a precipitated $\text{Ni-Mn-Al}_2\text{O}_3$ -kieselguhr catalyst at 190 to 200°C. Although the conversion was maintained so high that either the hydrogen or carbon monoxide was almost completely consumed, the usage ratios varied only from 1.73 to 2.38, when the feed ratio was increased from 0.932 to 4.47. Similar results were obtained by Myddleton and Walker⁹⁷ for feed ratios from 0.67 to 2.5. Water was the principal oxygenated product, and the water-gas shift does not proceed to a great extent.

With cobalt supported on kieselguhr, the rate is approximately independent of operating pressure, as shown by data of Ruhrchemie¹¹¹ (Chapter 2, Table 41, p. 103) for $\text{Co-ThO}_2\text{-MgO}$ -kieselguhr catalysts in the range of

0.2 to 1 atm. absolute. The principal change in selectivity was a slight decrease in gaseous hydrocarbons and a small increase in wax as the pressure was increased. U. S. Bureau of Mines experiments⁶ at 1 and 7.8 atm. absolute (Table 1) confirmed these trends. For granular catalysts, the yield of gaseous hydrocarbons decreased slightly with pressure, but increased for pelleted catalysts. These results are obtained in separate tests of a given

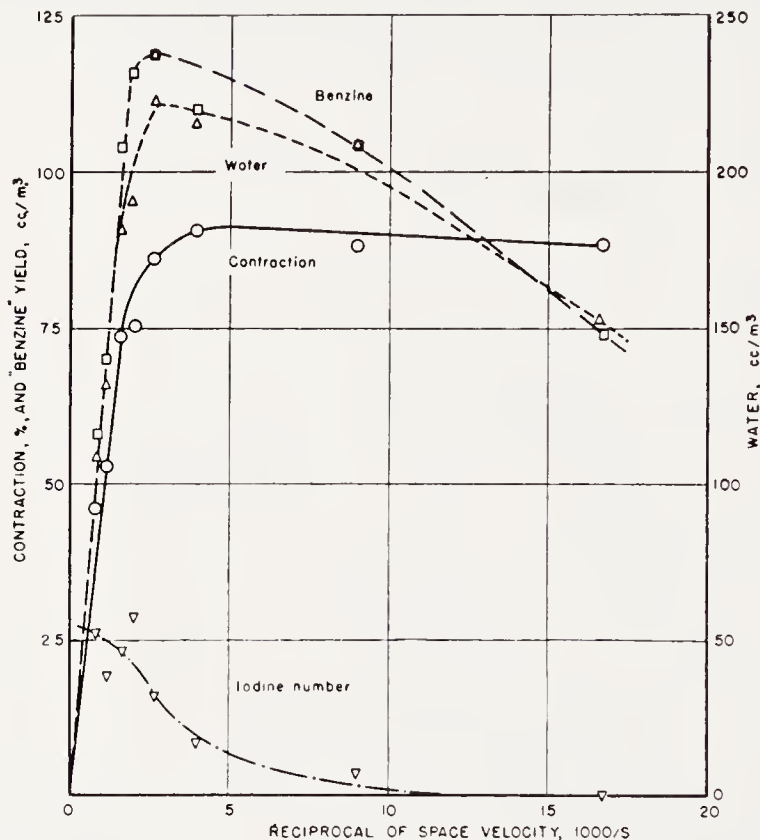


Figure 4. Variation of selectivity with reciprocal of space velocity on Ni-Co-Si catalyst with $2\text{H}_2 + 1\text{CO}$ gas at 185°C and atmospheric pressure. From data of Ref. 96)

catalyst or single tests in which the pressure was increased. If the operating pressure was decreased during the test, the activity was strongly diminished, and successive cycles of medium and atmospheric pressure synthesis, progressively decreased the activity at both pressures as shown in Table 44 Chapter 2, p. 107. These phenomena and the difficulty of reactivating catalysts used at medium-pressures are probably related to differences in the amount and chemical nature of the adsorbed material. In atmospheric synthesis, the catalyst pores are partly filled with wax, whereas at medium-pressure pores are probably entirely filled. Although the products from the medium-pressure synthesis have a greater molecular weight than

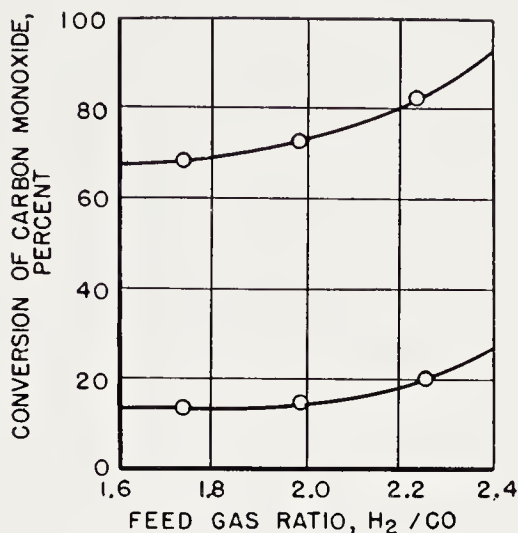


Figure 5. Variation of consumption of carbon monoxide on cobalt catalysts at atmospheric pressure as a function of feed gas ratio. (Reproduced with permission from Ref. 16)

TABLE 1. EFFECT OF OPERATING PRESSURE ON COBALT CATALYSTS^a
(Tests at space velocity per hour of 100)

Test	Operating Period (wks)	Pressure (atm.)	Average Temperature (°C) ^b	Apparent Contraction (%)	Products (%)			
					CH ₄	C ₃ + C ₄	C ₁ - C ₄	Liquids and Solids
<i>Pelleted Co-ThO₂-kieselguhr catalyst 108B</i>								
X-29	b-g	1	185 (186)	70.9	12.1	10.0	24.5	75.5
X-29	i-p	7.8	189 (186)	71.3	19.0	10.9	33.5	66.5
X-31	b-j	7.8	187	71.8	18.6	10.5	32.0	68.0
<i>Granular^c Co-ThO₂-MgO-kieselguhr catalyst 89K</i>								
X-17	b-k	1	186 (187)	74.4	13.1	10.2	25.6	74.4
X-17	v-z	7.8	188 (188)	72.0	14.0	8.6	23.2	76.8
<i>Pelleted Co-ThO₂-MgO-kieselguhr catalyst 89J</i>								
X-21	c-l	1	186 (186)	72.0	15.6	8.1	24.9	76.1
X-21	o-u	7.8	191 (188)	69.5	18.2	10.4	28.3	71.7

^a From Ref. 6.

^b The temperatures in parentheses are for the last 2 weeks of operation at 1 atm. and the first 2 weeks of operation at 7.8 atm.

^c Broken filter cake.

those from atmospheric-pressure synthesis, the average molecular weights of products adsorbed on the catalyst are in reverse order. This anomaly apparently arises from adsorption of products on catalyst from the vapor phase in atmospheric synthesis, resulting in segregation of fractions of high molecular weight, whereas at medium pressures adsorption occurs from the liquid phase (see p. 106). Thus, the apparent zero-order dependence may result from a fortuitous combination of kinetic effects and a semi-permanent poisoning or pore-blocking, as suggested by the irreversibility of activity changes upon increasing and decreasing pressure. For these reasons probably no simple rate equation involving reversible inhibition will properly express the kinetic data. Above pressures of about 30 atm., catalyst activity and life decreases. In this range, cobalt carbonyl is produced in appreciable amounts, and the deleterious effects have been attributed to carbonyl corrosion. These pressure dependencies are apparently characteristic only of synthesis on catalysts supported on kieselguhr. In early studies⁴⁵ with a precipitated catalyst supported on "Stuttgart Masse," the rate decreased with an increase in pressure above atmospheric, whereas from 0.3 to 1.0 atm. the rate was proportional to pressure.

Although some studies have been made upon the influence of gas composition, most of these data have little value for kinetics, since conversions were usually maintained as high as possible to determine maximum productivity. As the usage ratio usually did not deviate greatly from 2, maximum yields were obtained with $2\text{H}_2 + 1\text{CO}$ gas. Seligman¹¹⁷ studied the influence of $\text{H}_2:\text{CO}$ ratio on rate with Co-ThO_2 -kieselguhr at atmospheric pressure and 170° with constant flow of gas and conversions of 10 to 20 per cent. The volumes of $\text{H}_2 + \text{CO}$ consumed per hour were 23.6, 24.6, and 17.7 cc (STP) per gram of catalyst for $3\text{H}_2 + 1\text{CO}$, $2\text{H}_2 + 1\text{CO}$, and $1\text{H}_2 + 1\text{CO}$, respectively. Data of Brotz¹⁶ (Figure 5) for two experiments, one at high and another at low conversions, show that the fractional conversion of carbon monoxide increased with hydrogen content in the range $1.8\text{H}_2:1\text{CO}$ to $2.2\text{H}_2:1\text{CO}$. These curves are, however, misleading, because the concentration of carbon monoxide in the feed gas varied inversely with the fractional conversion. The fraction of $\text{H}_2 + \text{CO}$ in each of these series appears to be constant within experimental error.

In the atmospheric-pressure synthesis with gas containing $2\text{H}_2 + 1\text{CO}$ or greater concentrations of hydrogen, the activity remained relatively constant for periods of 10 to 20 days before activation was required, but the activity decreased more rapidly with gases containing less hydrogen than $2\text{H}_2 + 1\text{CO}$. In medium-pressure synthesis (10 atm.), long life and constant activity could be attained with $1.5\text{H}_2 + 1\text{CO}$ as well as $2\text{H}_2 + 1\text{CO}$ gas, and as smaller yields of gaseous hydrocarbons were produced with $1.5\text{H}_2 + 1\text{CO}$, this gas was used in the commercial synthesis in Germany.

The synthesis with cobalt catalysts has approximately the same over-all apparent activation energy as with nickel catalysts. At atmospheric pressure, Anderson, Krieg, Seligman, and O'Neill⁸ varied the space velocity of $2\text{H}_2 + 1\text{CO}$ gas and temperature to maintain constant conversion with Co-ThO₂-MgO-kieselguhr. Data for experiments in which the contraction was held at 70 per cent are shown in Figure 6. The space-time-yield, a

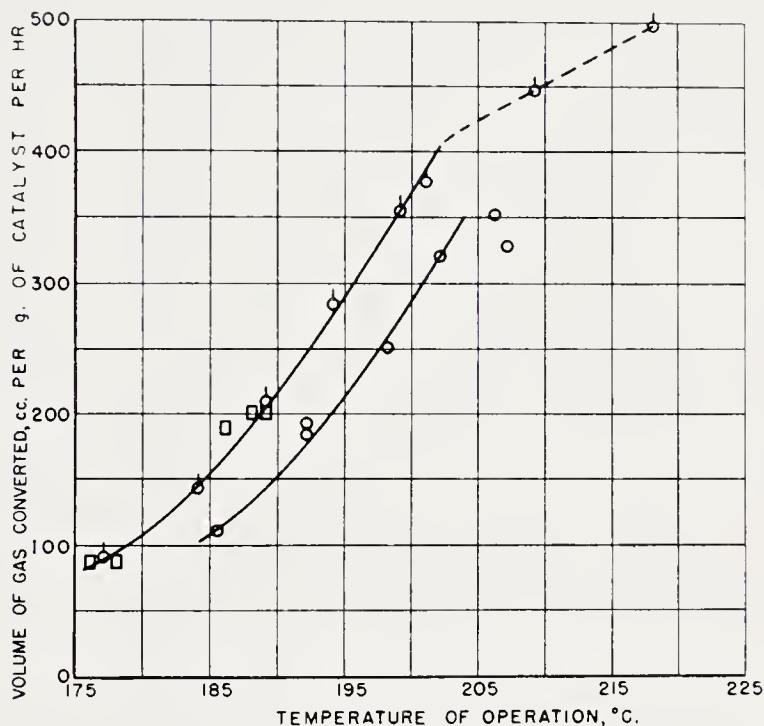


Figure 6. Conversion of synthesis gas as a function of temperature. Contractions maintained at about 70 per cent, \odot represents pelleted catalyst 89K, \square granular catalyst 89K, and \circ pelleted catalyst 89-O. (Reproduced with permission from Ref. 8)

measure of reaction rate, increased exponentially with temperature up to 200–210°C but above this temperature the rate increased less rapidly. Larger yields of gaseous hydrocarbons were produced above 205°C and extended periods of synthesis at these temperatures deactivated the catalyst. Arrhenius plots of data obtained below 205°C were straight lines with slopes corresponding to activation energies of 23.8 and 26.4 kcal/mole. Similar experiments at contractions of 15, 35, 55, and 75 per cent gave activation energies varying from 24.4 to 26.6 kcal/mole. These activation energies agree well with the value of 26.5 kcal/mole obtained by Weller¹³⁵ with Co-ThO₂-kieselguhr in a glass gas-circulation system in which the conversion per pass was maintained at 1 to 2 per cent. At 7.8 atm. of $2\text{H}_2 + 1\text{CO}$ on Co-ThO₂-MgO-kieselguhr, Seligman¹¹⁷ determined an acti-

vation energy of 20.0 kcal/mole. Anderson¹²³ obtained satisfactory Arrhenius plot from data of Fischer and Pichler⁴⁷ for the first stage of a two-stage operation with Co-ThO₂-kieselguhr catalyst at 10 atm. of 2H₂ + 1CO gas; the over-all activation energy was 24.3 kcal/mole. From data of Gibson and Hall⁵⁵ with Co-ThO₂-MgO-kieselguhr at 11 atm. of 2H₂ + 1CO gas, in which flow and temperature were varied to maintain conversion at about 80 per cent, a satisfactory Arrhenius plot (Figure 7) was obtained with a slope corresponding to an over-all activation energy of 22.9 kcal/mole. The rate for the highest temperature, 219°C, lies somewhat below the value predicted by the straight line.

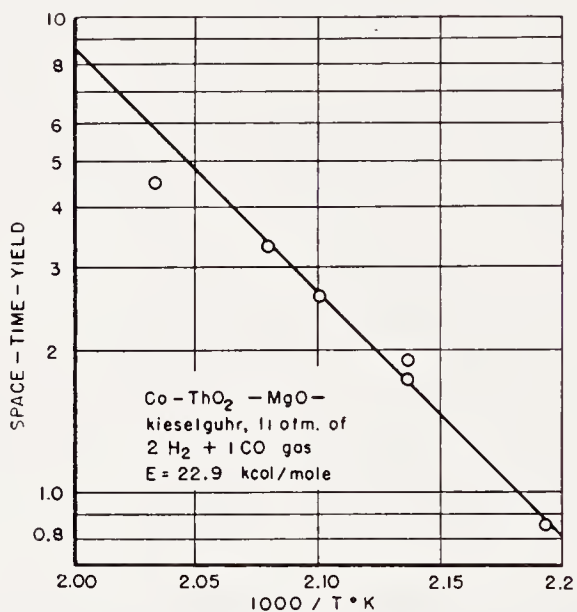


Figure 7. Arrhenius plot of kinetic data from cobalt catalysts. (From data of Ref. 55)

Russian workers³⁹ studied variation of conversion with flow of 2H₂ + 1CO on Co-ThO₂-silica gel at atmospheric pressure. For the range of conversion reported, 25 to 45 per cent, the data could be expressed by the linear equation

$$x = a + b/S \quad (4)$$

where x and S are the conversion of H₂ + CO and space velocity, respectively, and a and b are constants. A kinetic experiment at I.G. Farbenindustrie, Leuna⁶⁶, gave similar results. A plot of yield of total hydrocarbons in g/m³, against the reciprocal of space velocity had a long linear portion that could be described by Eq. (4).

U. S. Bureau of Mines workers⁷ studied the kinetics on a Co-ThO₂-

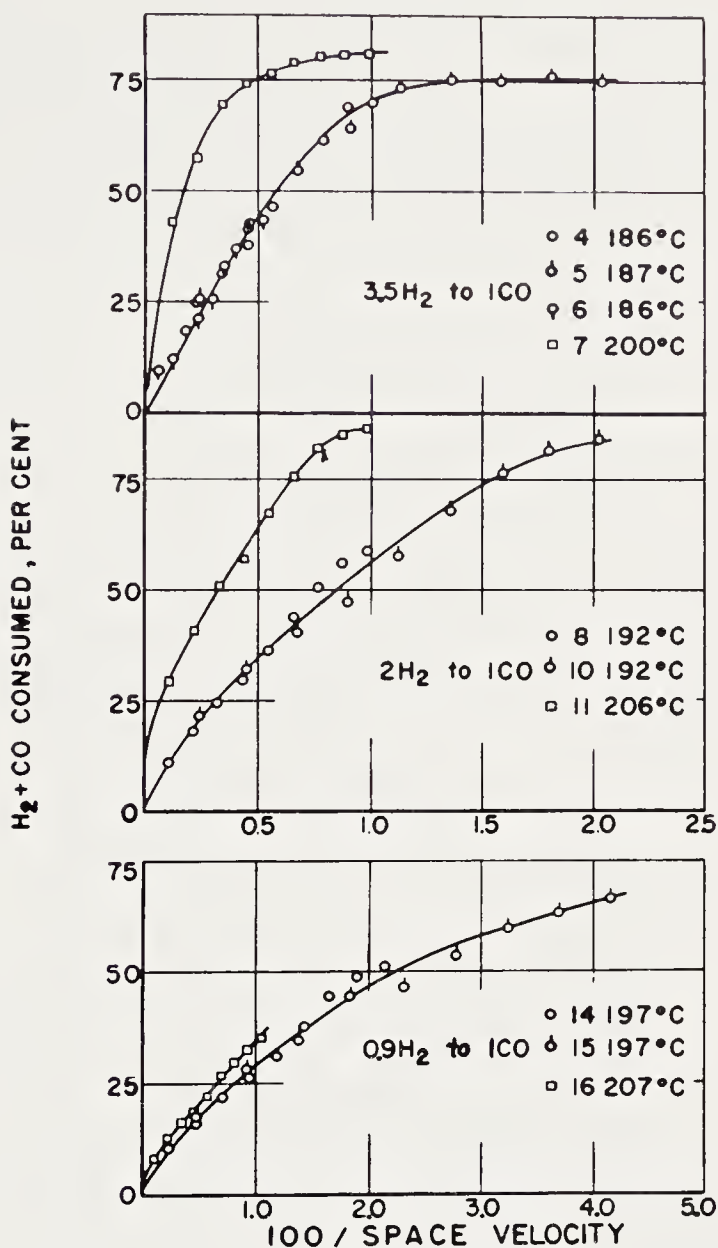


Figure 8. Variation of the extent of conversion of hydrogen plus carbon monoxide with the reciprocal of the space velocity for Co-ThO₂-kieselguhr catalyst at atmospheric pressure with synthesis gas having ratios of H₂:CO of 3.5, 2 and 0.9. (Reproduced with permission from Ref. 7)

kieselguhr at atmospheric pressure by a special technique involving analysis of reaction products at various intervals in a catalyst bed and changing space velocity. The rate data for $2H_2 + 1CO$ and $0.9H_2 + 1CO$ in Figure 8 show a rapid initial increase in conversion followed by a linear portion with a smaller slope and finally no further increase at high conversions. With

$3.5\text{H}_2 + 1\text{CO}$ the abrupt initial increase was not found and the initial parts of the curves were nearly linear. In most of the curves sizable linear portions can be selected in the same conversion range as described in the Russian experiments³⁹. Although catalytic activity remained constant during individual experiments, the activity appears to have been affected more strongly by feed gas composition and temperature than expected; these

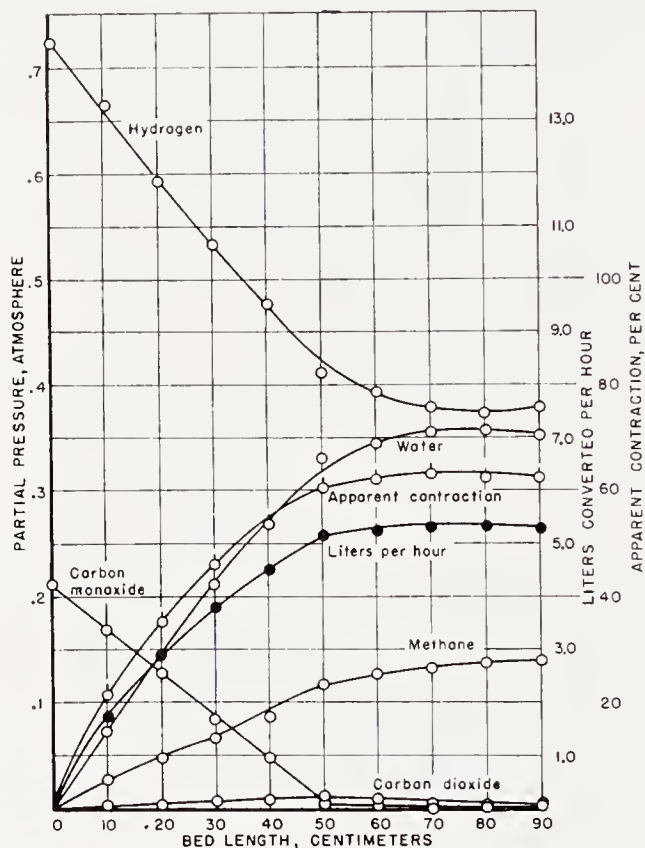


Figure 9. Test 5. A plot of partial pressures of reactants and products, apparent contractions and integral reaction rate as a function of bed length for Co:ThO₂:kieselguhr catalyst 108B with 3.5 H₂ to 1CO gas at 187°C and space velocity of 49.3 per hours. (Reproduced with permission from Ref. 7)

differences may have resulted from progressive changes in catalytic activity. For this reason the data were not analyzed in detail for the effect of feed gas composition and temperature. From mass spectrometric analysis of gas samples taken at intervals in the catalyst bed, plots of partial pressure and conversion were made as shown in Figures 9 to 11. From Figure 8 the differential rate, r , was determined by graphical differentiation; partial pressures were read from Figures 9 to 11 at corresponding positions in the bed; and a table was constructed giving r and corresponding partial pressures at various points in the bed.

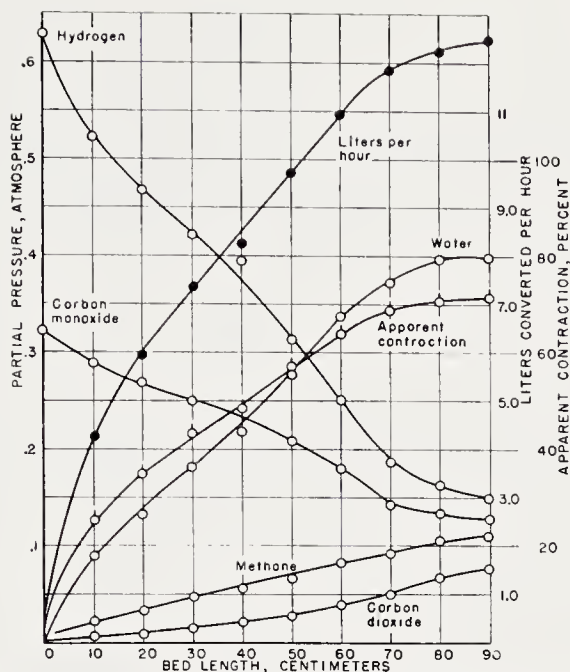


Figure 10. Test 11. A plot of partial pressures of reactants and products, apparent contractions and integral reaction rate as a function of bed length for Co:ThO₂:kieselguhr catalyst 108B with 1.96H₂ to 1CO gas at 206°C and space velocity of 102 per hour. (Reproduced with permission from Ref. 7)

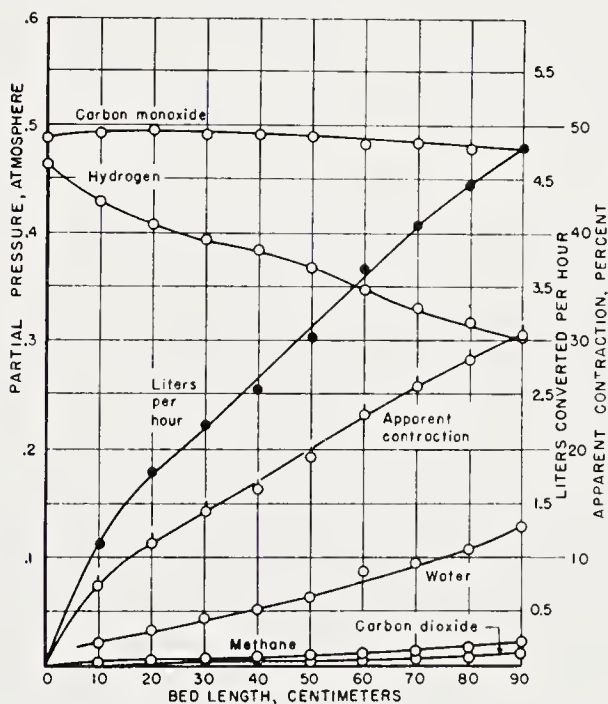


Figure 11. Test 16. A plot of partial pressures of reactants and products, apparent contractions and integral reaction rate as a function of bed length for Co:ThO₂:kieselguhr catalyst 108 B with 0.95H₂ 95.5 per hour. (Reproduced with permission from Ref. 7)

These data^{9, 123} were used to test a number of rate equations; only one was found that even approximated the rate data. This equation⁶⁴ postulates that the rate is proportional to the desorption of growing chains from catalyst surface and that the concentration of these chains is proportional to $p_{H_2}^2 p_{CO}$;

$$r = \frac{ab\beta}{1 + b\beta} \quad (5)$$

where $\beta = p_{H_2}^2 p_{CO}$, a is the product of effective surface area times the rate of desorption, and b is the equilibrium constant for the formation of chains. Plots of the rate data were moderately satisfactory, except that the observed rate at low conversions was at least twice as high as predicted by the equations that expressed the remainder of the data. The values of b were large, varying from 134 to 245 atm.⁻³. Thus, the equation predicts that the synthesis should have only a slight pressure dependence above atmospheric pressure, but a moderately large dependence at subatmospheric pressure. Further, according to the equation, a maximum rate should be expected for $2H_2 + 1CO$ gas. Although Eq. (5) properly expresses some of the kinetic phenomena, it cannot be considered a particularly successful relationship, and at best is first approximation.

Brotz¹⁶ described kinetic experiments on Co-ThO₂-MgO-kieselguhr, presumably with $2H_2 + 1CO$ at atmospheric pressure. The space-time-yield increased linearly with space velocity according to

$$xS = b + aS \quad (6)$$

when the space velocity was varied from 100 to 200 hr.⁻¹ Equation (6) reduced to Eq. (4) when divided by S , and in the range of applicability of the equation the differential reaction rate, $dx/d(1/S)$, is constant. The kinetic analysis of Brotz, however, led to the conclusion that the rate could be expressed by

$$r = kp_{H_2}^2/p_{CO} \quad (7)$$

Data of Brötz for the conversion of carbon monoxide as a function, of H₂:CO ratio in Figure 5 do not show the strong dependence of rate on H₂:CO ratio required by Eq. (7). Equation (7) apparently does not describe properly most of the kinetic data.

The activity of a series of Co-ThO₂-MgO-kieselguhr catalysts varied linearly with surface areas and volumes of carbon monoxide chemisorbed at -195°C (a measure of cobalt metal on the catalyst surface)¹²³. In addition, the data demonstrate that the synthesis is a very slow catalytic process. At 185°C only 1.9 cc (STP) of synthesis gas were converted per hour per square meter of catalyst surface, and 35.6 cc (STP) of H₂ + CO

or 11.9 cc of carbon monoxide reacted per cc of chemisorbed carbon monoxide per hour. On this basis, if chemisorption of carbon monoxide at -195°C is an effective measure of possible reaction sites, the average carbon monoxide molecule remains on the surface for about 5 minutes before reacting. The calculations indicate that, due to pore blocking by adsorbed hydrocarbons and/or poisoning by carbon monoxide, only a small fraction of the total surface is effective in the synthesis.

Apparently no data are available to demonstrate the influence of size of catalyst particles upon activity and selectivity; however, some fragmentary results have been obtained on the effect of catalyst density. Figure 6 demonstrates that Co-ThO₂-MgO-kieselguhr catalyst 89K as broken filter cake and pellets had the same activity. The surface area and volume of

TABLE 2. INFLUENCE OF PELLET SIZE AND DENSITY ON ACTIVITY AND SELECTIVITY^a
(Co-ThO₂-kieselguhr, space velocity of 2H₂ + 1CO gas = 100 hr.⁻¹, 7.8 atm.)

Catalyst pellets		
Length, mm	3.17	6.35
Diameter, mm	3.2	3.2
Mercury density, g/cc	1.13	1.51
Synthesis gas flow, liters/hr/g catalyst	0.14	0.11
Average temperature, °C	187	191
Apparent contraction, %	71.6	71.4
Hydrocarbon distribution, wt-%		
CH ₄	19.9	25.8
C ₂	3.4	4.2
C ₃ + C ₄	11.6	13.4
Liquids + solids	65.1	56.6

^a From Ref. 6.

chemisorbed carbon monoxide⁵ were only slightly changed by pelleting (Table 21, Chapter 2, p. 75), but the external volume of the particles as measured by mercury displacement was decreased from 1.900 to 0.934 cc/g of reduced catalyst, the pore volume from 1.54 to 0.63 cc/g, and the average pore diameter from 804 to 327 Å. With very large, dense pellets, however, activity and selectivity were adversely affected. A sample of standard pelleted Co-ThO₂-kieselguhr was crushed and pressed into very dense, long pellets⁶. The data in Table 2 indicate that the activity of the large pellets was lower and the production of gaseous hydrocarbon larger.

Brötz and Spengler¹⁷ examined the pore structure of a standard granular Co-ThO₂-MgO-kieselguhr by adsorption and gas flow methods. They concluded that the catalyst contained systems of micro and macro pores. The entire granule was believed to be effective in the synthesis, and a process of surface diffusion was postulated to account for this assumption in pores filled with liquid hydrocarbons.

Available data from measurements of pore volumes and surface areas (p. 70) and extraction studies (p. 94) indicate that the catalyst surface is heavily covered with adsorbed wax, so that the mechanism must involve diffusion through adsorbed films. This postulate is consistent with the slow rate of the synthesis. Furthermore, studies in reactors in which the catalyst is submerged in cooling oil, such as the internally-cooled converter, have shown that the activity of a submerged catalyst is not significantly lower than that of a dry-bed catalyst. Therefore, diffusion in pores may be an important step in the synthesis. Analysis of simple reactions by Wheeler¹³⁷

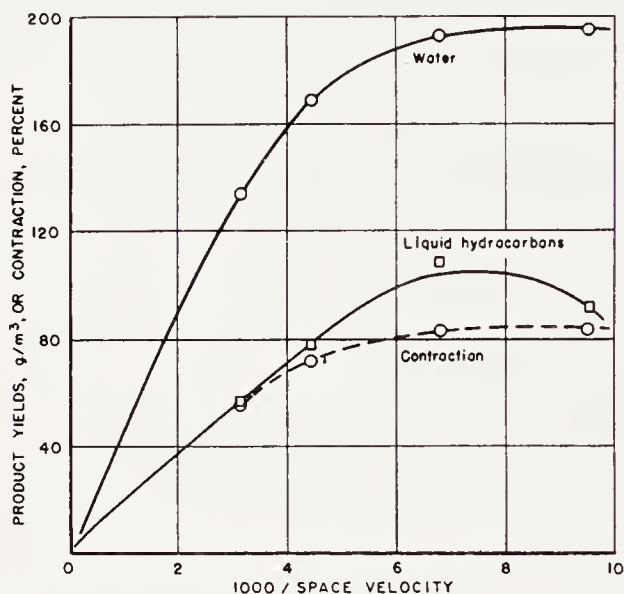


Figure 12. Kinetic experiment with cobalt catalyst $2\text{H}_2 + 1\text{CO}$ gas at atmospheric pressure and 197°C . (From data of Ref. 132)

and others indicates that, under these conditions, the observed dependence upon partial pressures may be different from that of the surface process and that the observed activation energy is only half of the activation energy that would exist on a nonporous surface.

A few studies of the influence of diluents have been reported, and these results have been summarized in a previous publication¹²³. These results are difficult to interpret and in part contradictory. The productivity does not decrease sharply with increasing concentration of diluent, a behavior which is consistent with the relative independence of rate upon partial pressures.

For $2\text{H}_2 + 1\text{CO}$ the selectivity is moderately independent of conversion until high values are reached, where the yields of gaseous hydrocarbons and carbon dioxide increase rapidly. Japanese workers¹³² found that the yield of liquid hydrocarbon from Co-Cu-ThO_2 at 197°C passed through a maximum as the flow was decreased (Figure 12). The water yield, however,

did not decrease in the range of lower flow and followed the same pattern as the contraction; hence, it may be inferred that the production of carbon dioxide did not increase sizably. Craxford²³, observed a similar maximum

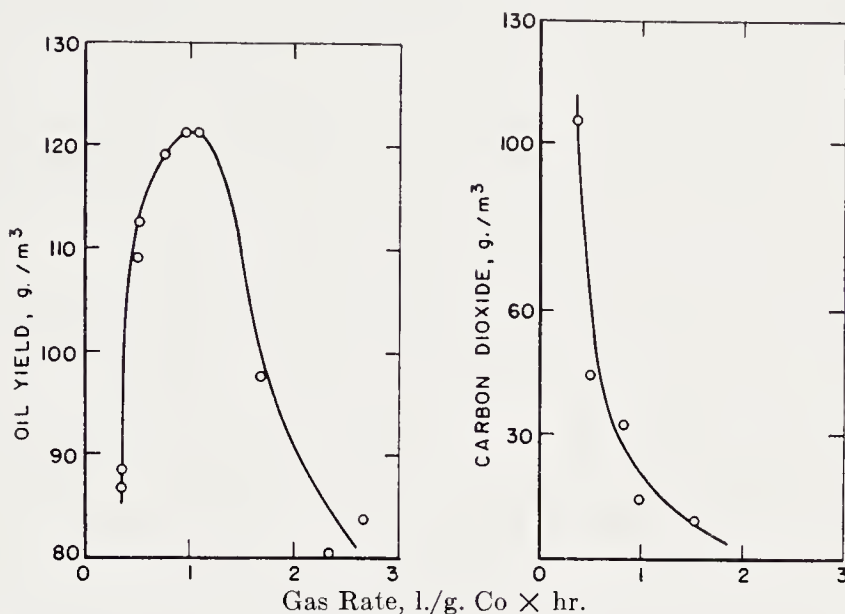


Figure 13. Formation of liquid hydrocarbon and carbon dioxide with a Co-ThO₂-MgO-kieselguhr catalyst with 2H₂ to 1CO gas at 185°C as a function of flow rate. (Reproduced with permission from Ref. 23)

TABLE 3. SELECTIVITY OF COBALT CATALYST AS FUNCTION OF CONVERSION AND FEED GAS COMPOSITION^a
(180°C and atmospheric pressure)

Test No.	Feed Gas Ratio H ₂ /CO	Space Velocity (hr ⁻¹)	Contraction (%)	Yield		CO Conversion (%)	Usage Ratio H ₂ /CO	Per cent Reaction Forming	
				Total Hydrocarbons (g/m ³)	Per cent as CH ₄			CO ₂	H ₂ O
1	2	100	70	170	12	85	2.1	1	99
2	2	10	65	170	14	100	1.8	19	81
3	1	10	74	185	13.8	100	1.1	51	49
4	0.70	10	65	185	15	89	0.8	77	23
5	0.56	10	63	187	15	100	0.6	99	1

^a From Ref. 77.

in oil yield with Co-ThO₂-MgO-kieselguhr at atmospheric pressure of 2H₂ + 1CO and 185°C, (Figure 13), and the yield of carbon dioxide increased rapidly at a somewhat lower flow than that corresponding to this maximum.

Koelbel and Engelhardt⁷⁷ studied the production of water and carbon dioxide as a function of conversion and gas composition (Table 3). Test 1

represents normal synthesis conditions for which the production of carbon dioxide was very low. In test 2, at a space velocity of 10 hr^{-1} , 19 per cent of the synthesis proceeded by reactions forming carbon dioxide, and carbon monoxide was completely consumed. In contrast to the work of Watanabe and Craxford, just described, the distribution of hydrocarbons remained about the same under all conditions. At lower space velocities or higher temperatures, the yield of gaseous hydrocarbons might have increased. At a space velocity of 10 hr^{-1} , the relative production of carbon dioxide increased as the ratio $\text{H}_2:\text{CO}$ of the feed gas decreased until reactions producing carbon dioxide accounted for 99 per cent of the synthesis with $0.56 \text{ H}_2 + 1 \text{ CO}$.

U. S. Bureau of Mines kinetic data, such as presented in Figures 8 to 11, provide information on the relative consumption of hydrogen and carbon monoxide and the formation of CO_2 and CH_4 . In the original paper⁷ the relative usage of hydrogen and the production of methane and carbon dioxide were reported as functions of bed length, and the plots showed the influence of gas composition and temperature on selectivity. The data indicated the occurrence of hydrocracking and the water-gas-shift reaction under certain synthesis conditions. The original data were recalculated by Kelly⁶⁹, and new selectivity curves are presented in Figures 14 to 18. In these curves the volumes of hydrogen consumed and the volumes of methane formed per volume of $\text{H}_2 + \text{CO}$ consumed are plotted against the fraction of $\text{H}_2 + \text{CO}$ consumed. For carbon dioxide the volume of this product per volume of CO consumed is plotted against the fraction of CO consumed.

The relative usage of hydrogen, $\text{H}_2/(\text{H}_2 + \text{CO})$, was nearly independent of feed-gas composition, conversion, and temperature, as shown in Figure 14. With $0.9\text{H}_2 + 1\text{CO}$ gas the relative usage of hydrogen was about 0.67 (corresponding to a usage ratio, $\text{H}_2:\text{CO}$, of 2) and decreased slightly with conversion. For $2\text{H}_2 + 1\text{CO}$ gas the relative usage was about 0.69 and decreased slightly with conversion, whereas with $3.5\text{H}_2 + 1\text{CO}$ gas the relative usage was 0.70 and increased slightly at high conversions.

Methane production, Figures 15 to 18, increased with temperature for all feed gases. With $2\text{H}_2 + 1\text{CO}$ gas, Figure 15, the formation of methane at the lower temperature decreased with conversion, apparently passed through a minimum at about 45 per cent conversion, and then increased. At the higher temperature methane production increased slightly in the range for which data are available. For $3.5\text{H}_2 + 1\text{CO}$ (Figure 16) methane production increased with conversion, the curve rising steeply above $x = 0.65$. For $0.9\text{H}_2 + 1\text{CO}$ (Figure 17) formation of methane decreased with increase in conversion at the lower temperature and increased slightly at the higher temperature. In tests with $0.9\text{H}_2 + 1\text{CO}$ and $3.5\text{H}_2 + 1\text{CO}$ the ratio of $\text{H}_2:\text{CO}$ in the catalyst bed decreased and increased, respectively,

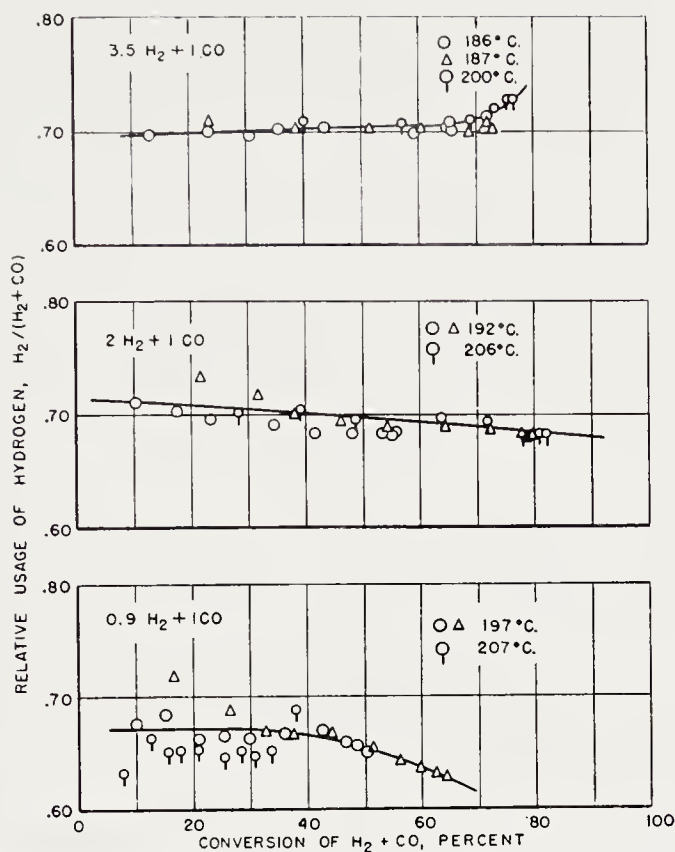


Figure 14. Relative usage of hydrogen as a function of conversion for Co-ThO₂-kieselguhr catalyst at atmospheric pressure. (From data of Ref. 7)

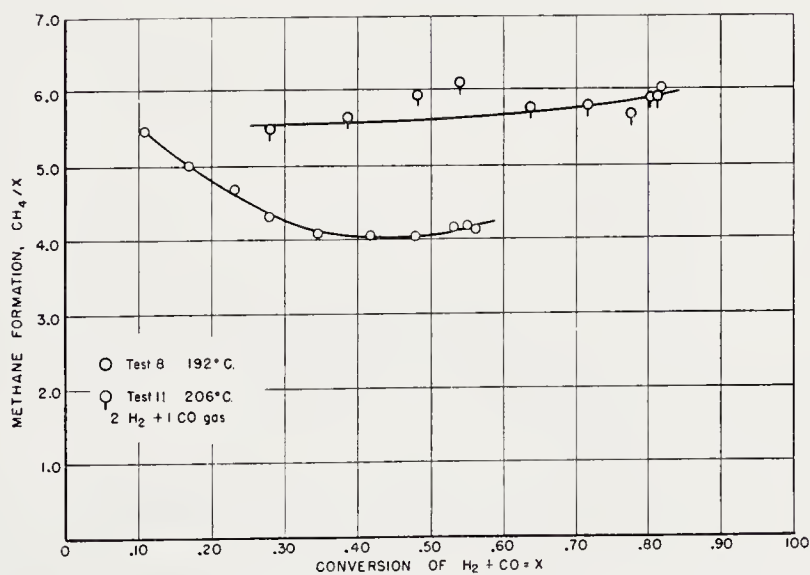


Figure 15. Production of methane on Co-ThO₂-kieselguhr catalyst at atmospheric pressure. (From data of Ref. 7)

with increase in conversion, whereas the ratio remained about constant for $2\text{H}_2 + 1\text{CO}$. The changes of methane formation with conversion (Figures

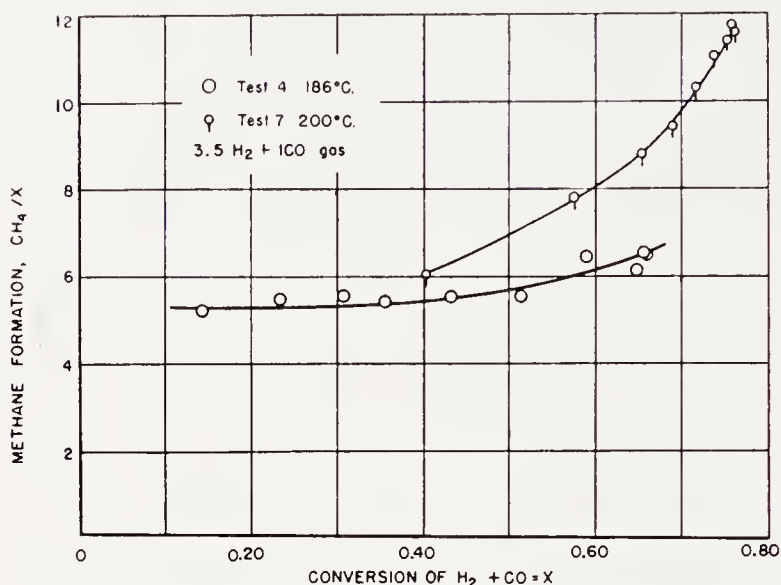


Figure 16. Production of methane on Co-ThO₂-kieselguhr catalyst at atmospheric pressure. (From data of Ref. 7)

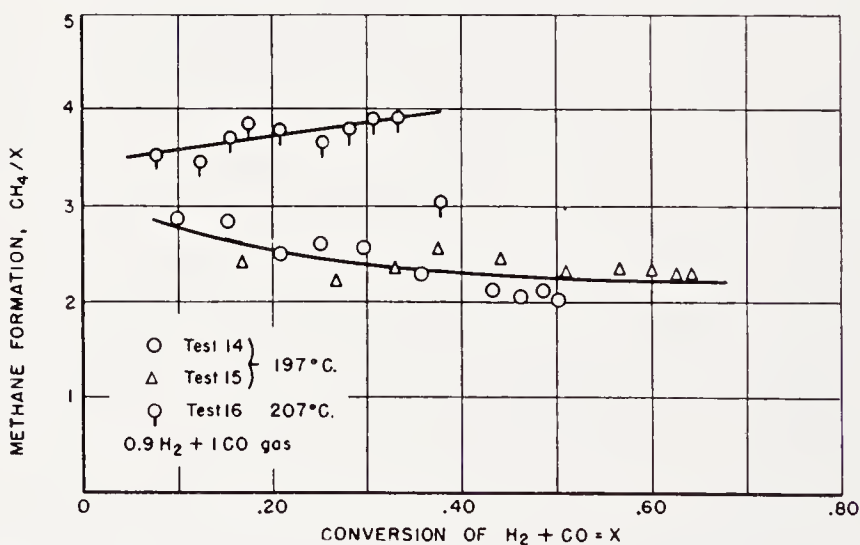


Figure 17. Production of methane on Co-ThO₂-kieselguhr catalyst at atmospheric pressure. (From data of Ref. 7)

16 and 17) as well as variations of relative usage of hydrogen (Figure 14) probably reflect the changing $\text{H}_2:\text{CO}$ ratios; however, this effect can hardly explain the decrease in methane formation with conversion at 192°C. (Figure 15), although the $\text{H}_2:\text{CO}$ ratio did decrease slightly in this test. Figure 18 illustrates the increase in methane production with increasing

H_2 :CO ratio in the feed gas. Although the temperatures are not the same in these tests, the curves were chosen so that a comparison at constant temperatures would show even greater differences.

Figures 19 to 22 show the production of carbon dioxide. Since the number of moles of $\text{H}_2 + \text{CO}$ is not affected by the water-gas-shift reaction, these data are presented as moles CO_2 produced per mole CO consumed. With $2\text{H}_2 + 1\text{CO}$ at 192°C (Figure 19) the curve was S-shaped and possibly passed through the origin. The ratio CO_2 :CO was virtually constant from 30 to 60 per cent conversion. At 207°C the CO_2 formation was about double that at the lower temperature; the data, however, do not cover a sufficient

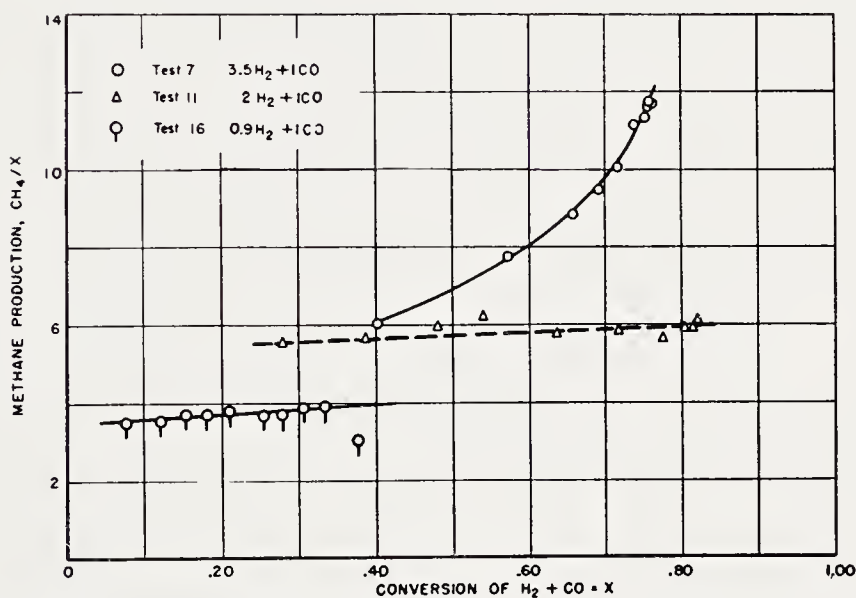


Figure 18. Production of methane on Co- ThO_2 -kieselguhr catalyst at atmospheric pressure. (From data of Ref. 7)

range of conversion to ascertain whether this curve passes through the origin. With hydrogen-rich synthesis gas (Figure 20), formation of carbon dioxide increased from zero at zero conversion until about 98 per cent of the carbon monoxide was consumed. At greater conversions of carbon monoxide, the ratio CO_2 :CO decreased abruptly and was zero at complete conversion of carbon monoxide. Increasing the temperature from 186 to 200°C doubled the production of carbon dioxide. With carbon monoxide-rich gas (Figure 21) the plots approximated an S-shaped curve possibly passing through the origin; however, the data were quite scattered. Figure 22 demonstrates that the formation of CO_2 varies considerably with H_2 :CO ratio of the feed gas.

The analyses of gas samples were not sufficiently accurate for a detailed consideration of gaseous hydrocarbons other than methane; however, it

was possible to demonstrate the production of olefins and paraffins in the C_4 fraction as a function of bed length, as shown in Figure 23. The wide variation of olefin content with bed length for $0.9H_2 + 1CO$ and $3.5H_2 + 1CO$ gases probably is influenced by the large changes in $H_2:CO$ ratio

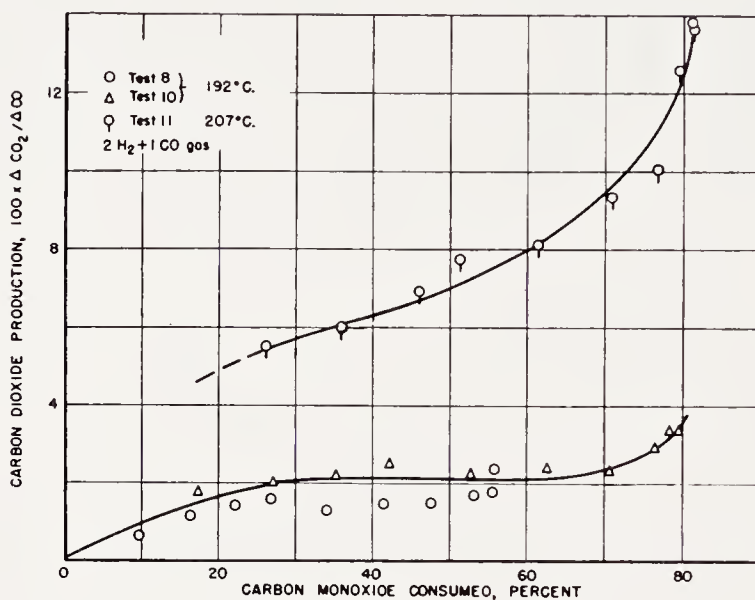


Figure 19. Production of carbon dioxide on Co-ThO₂-kieselguhr catalyst at atmospheric pressure. (From data of Ref. 7)

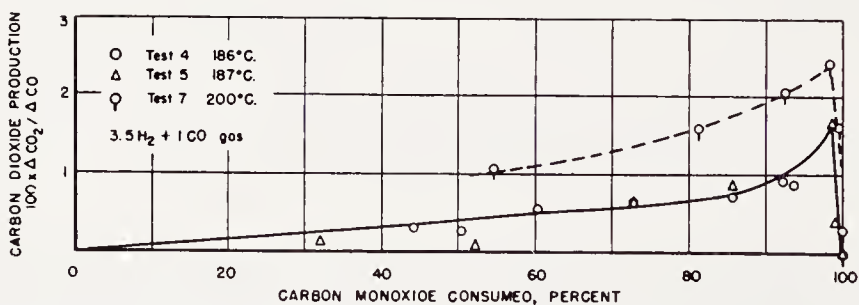


Figure 20. Production of carbon dioxide Co-ThO₂-kieselguhr catalyst at atmospheric pressure. (From data of Ref. 7)

with conversion; however, with $2H_2 + 100$ the fraction of olefins decreased with bed length or conversion.

From the data in Figures 14 to 23 and those in the original paper, certain tentative conclusions may be drawn regarding the primary synthesis products by extrapolating the selectivity curves to zero conversion or bed length. Obviously the extrapolations are moderately large and the conclusions should be accepted with the reservation that pronounced changes in the selectivity may occur at very low conversions.

1. The usage ratio, H_2/CO , of the primary reaction is slightly higher than
- 2.
2. Methane, higher paraffins, and olefins are primary products.

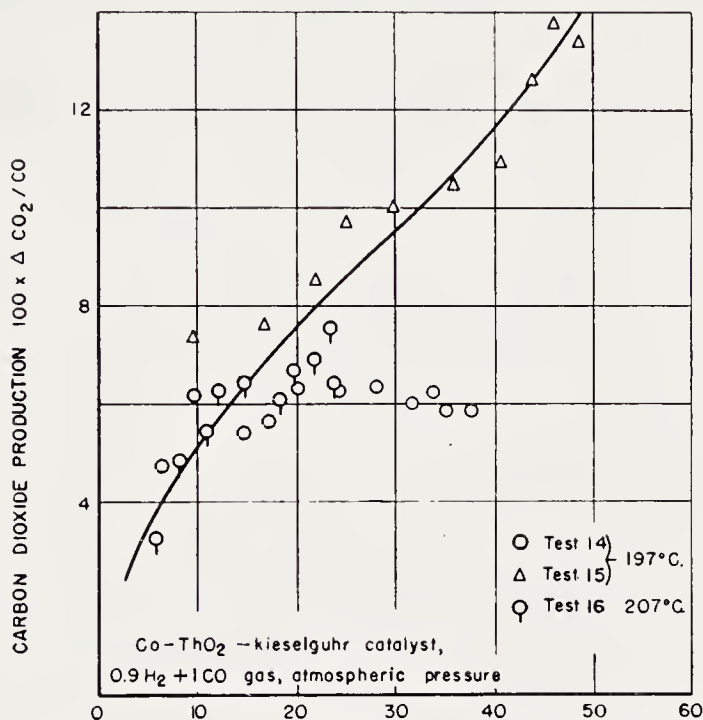


Figure 21. Production of carbon dioxide as a function of carbon monoxide consumed. (From data of Ref. 7)

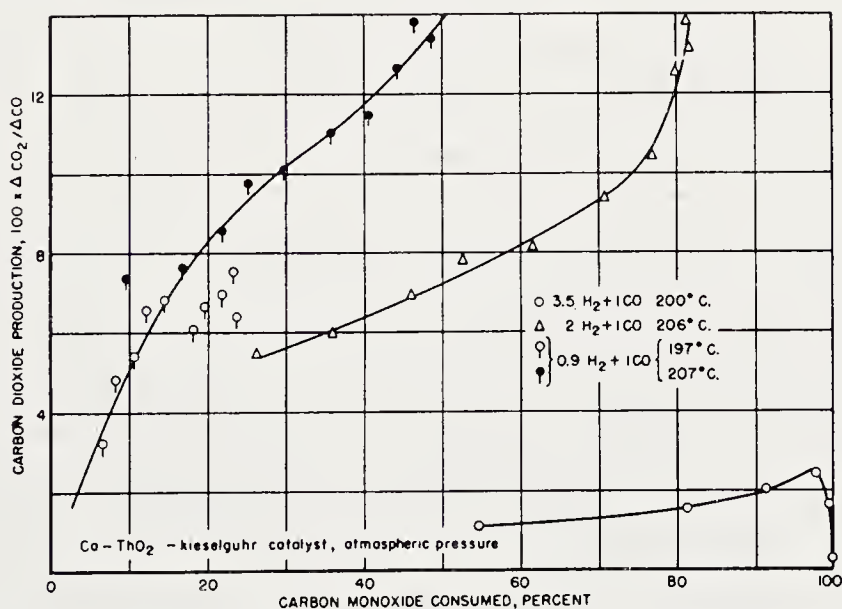


Figure 22. Production of carbon dioxide as a function of conversion and gas composition. (From data of Ref. 7)

3. Carbon dioxide is produced in only small quantities, if at all, in the primary step.

Further conclusions regarding selectivity are:

4. Methane and carbon dioxide formation increase with operating temperature.

5. Methane formation increases with increasing H_2/CO ratio. Hydrocracking of hydrocarbons probably occurs at high H_2/CO ratios.

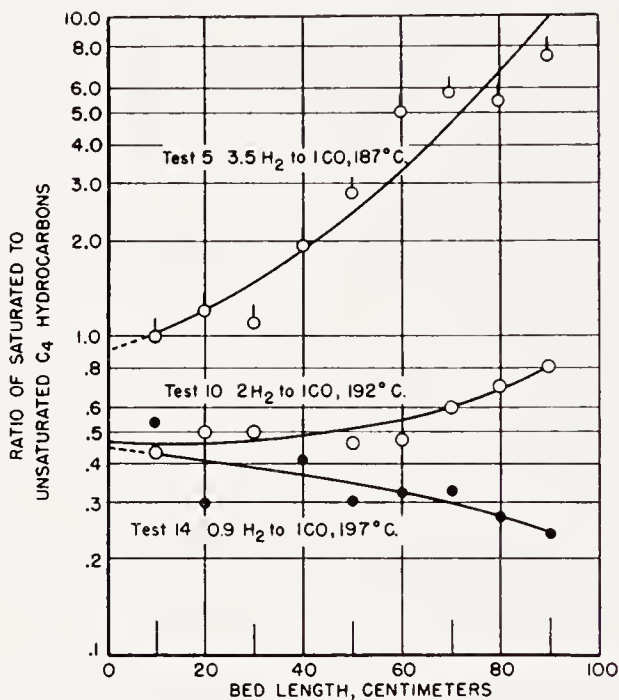


Figure 23. Change of saturation of C_4 hydrocarbons with bed length on cobalt catalyst at atmospheric pressure. (From data of Ref. 7)

6. The olefin content in the C_4 fraction decreases with increasing H_2/CO ratio; however, for constant H_2/CO ratio the olefin content decreased with conversion.

7. Carbon dioxide content increased with increasing concentrations of carbon monoxide and water vapor, suggesting that the water-gas shift reaction produces most of the carbon dioxide.

8. Carbon dioxide production increases with conversion until virtually all of the carbon monoxide was consumed. Under these circumstances carbon dioxide was consumed presumably by hydrogenation to gaseous hydrocarbons. This result is consistent with the observations of Fischer and Pichler^{46, 100} that carbon dioxide was not hydrogenated in the presence of carbon monoxide (see p. 300).

Gibson and Hall⁵⁵ studied the synthesis on Co-ThO₂-MgO-kieselguhr

catalysts under a variety of operating conditions. Products were separated into five fractions and the alcohols and olefins in the distillation fractions were determined. In addition, the average molecular weight of the product, exclusive of carbon dioxide and the aqueous phase, was reported. The influence of temperature on selectivity is given by tests of catalyst 118 at 11 atm. of $2\text{H}_2 + 1\text{CO}$ in which the temperature and flow was varied to give about 80 per cent conversion, as shown in Figure 24. (For an Arrhenius

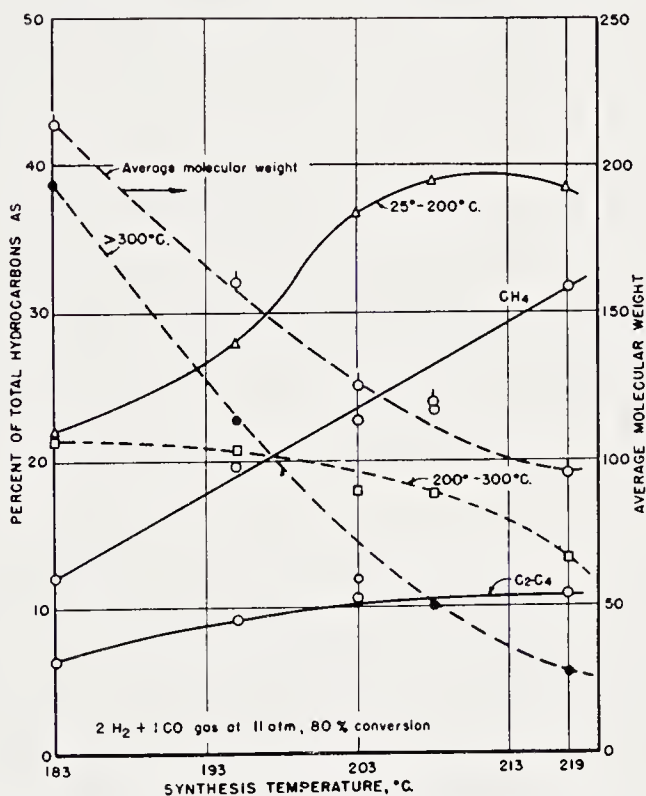


Figure 24. Selectivity of Co-ThO₂-MgO-kieselguhr catalyst as a function temperature. (From data of Ref. 55)

plot of total conversion data, see Figure 7.) Alcohol yields under these conditions were low and hence were not reported. The data are plotted as weight per cent of total hydrocarbons and *not* on a cumulative basis. In the range studied, 183 to 219°C, methane increased linearly, C₂-C₄ hydrocarbons up to about 203°C, and the liquid fraction, <200°C, increased to a maximum at about 211°C and then decreased. The 200 to 300°C fraction decreased slowly with an increase in temperature, and the >300°C cut decreased rapidly. The average molecular weight decreased monotonically from 214 at 183°C to 95 at 219°C. These data suggest a gradual shift in the entire product distribution with temperature. Data for temperature below

183°C (Table 4) are difficult to interpret, because the flow was usually maintained constant and the conversion, which varied widely as the temperature was changed, had nearly as large an effect on selectivity as tem-

TABLE 4. SELECTIVITY OF COBALT CATALYSTS^a
(Co-ThO₂-MgO-kieselguhr catalyst with 2H₂ + 1CO gas at 11 atm.)

Temp. (°C)	Flow, (l./g. Co/hr)	Conversion H ₂ + CO (%)	Product Distribution, Weight-Per cent of Total					Average Molec- ular Weight	Weight-Per cent of Liquid + Solid Hydro- carbons as	
			C ₁	C ₂ -C ₄	<200°C	200- 300°C	>300°C		Olefins	Alco- hols
160	1.03	26	21.9	18.1	36.3	17.1	6.6	104	29.3	20.2
167	1.00	50	9.3	14.0	30.9	18.1	27.7	178	11.4	13.4
173	0.97	80	8.8	9.5	25.8	18.6	37.3	208	7.1	8.3
176	0.97	91	12.5	8.3	24.0	18.7	36.5	205	6.9	6.0
182	0.93	88	14.2	5.3	21.2	21.7	37.6	211	8.2	2.1
182	6.25	28	35.8	6.4	25.3	16.4	16.1	126	14.9	4.8

^a From Ref. 55.

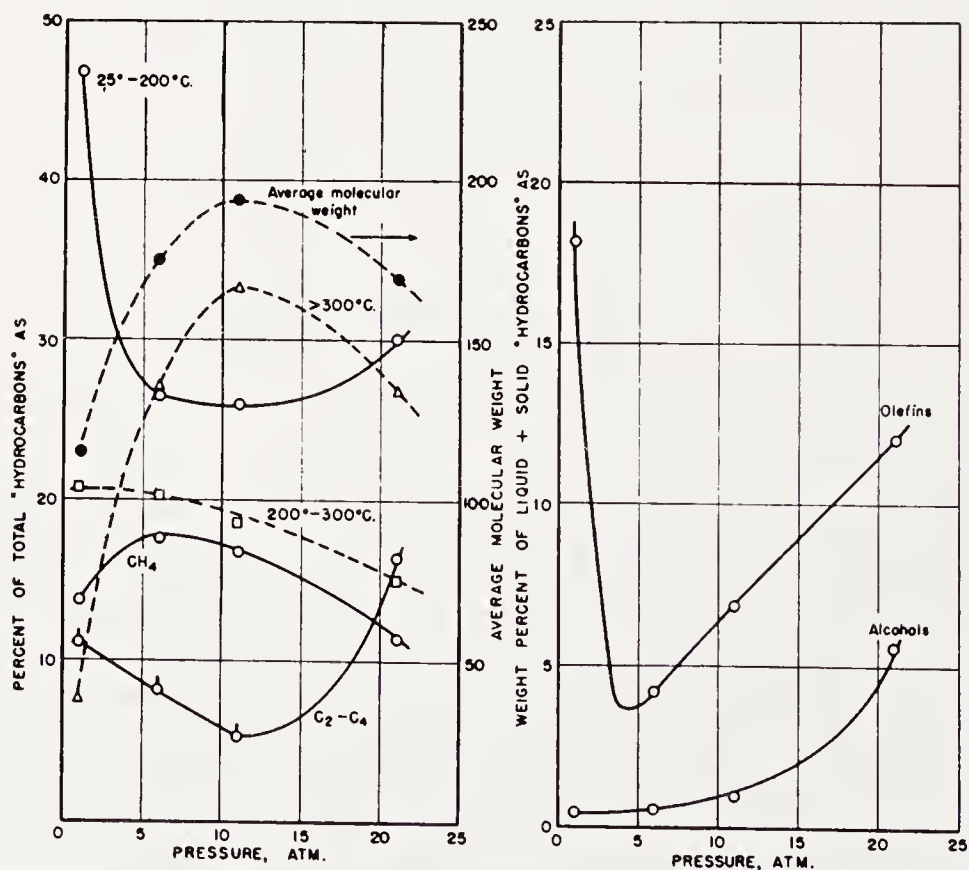


Figure 25. Selectivity of cobalt catalyst as a function of operating pressure. 2H₂ + 1CO gas at 185°C. (From data of Ref. 55)

perature. However, for tests at 160 and 182°C, in which the conversion was maintained at 26 to 28 per cent, the yields of both alcohols and olefins were greater at the lower temperature, although the average molecular weight was somewhat *higher* at the higher temperature. At 182°C the average molecular weight of the product decreased from 211 to 126 as the conversion was decreased from 88 to 28 per cent by increasing the flow, while the percentage of olefins and alcohols, respectively, increased from 8.2 to 14.9 and 2.1 to 4.8. These and other data indicate that the percentages of both alcohols and olefins increase as conversion is decreased, and both of these molecules must be regarded as primary products; however, paraffins are not excluded.

Data in Figure 25 for experiments at 185°C with a constant flow (STP) of $2\text{H}_2 + 1\text{CO}$ gas demonstrate the influence of pressure on selectivity. In these tests the conversion was maintained at approximately 90 per cent, except at the highest pressure, where the conversion was 70 per cent. The average molecular weight increased with pressure to a maximum at about 11 atm. The largest changes in selectivity were observed between 1 and 6 atm. In this range the olefin content of the oil phase decreased sharply and then increased about linearly with pressure from 6 to 21 atm. The alcohol yields increased continuously with pressure, the yield rising sharply between 11 and 21 atm.

Kinetics of the Fischer-Tropsch Synthesis on Iron Catalysts

The kinetics of the synthesis on iron catalysts are different than on cobalt and nickel in the following ways: On iron catalysts (a) the usage ratio H_2/CO is lower and usually varies widely with conversion and gas composition, (b) the rate increases approximately linearly with operating pressure, and (c) the rate is roughly proportional to the partial pressures of reactants.

Most experimental studies of cobalt and nickel catalysts were made with precipitated preparations supported on kieselguhr after reduction in hydrogen. The diversity of types and pretreatments of iron catalysts could possibly produce major differences in kinetic behavior; however, available data indicate that these factors usually do not cause large variations.

Conversion-reciprocal space velocity plots for iron catalysts show more curvature than corresponding curves for cobalt and nickel catalysts. For German data of the medium-pressure synthesis with a fused iron catalyst¹¹⁶ (Figure 26) and of the atmospheric synthesis with a precipitated iron-copper-kieselguhr catalyst⁷⁹ (Figure 27), the conversion is expressed as per cent carbon monoxide consumed, whereas in the Bureau of Mines data¹⁰ for fused iron catalysts at 7.8 atm. (Figure 28), conversion is expressed as per cent $\text{H}_2 + \text{CO}$ consumed. All of the curves have the same general shape and can be expressed satisfactorily up to conversions of 60 to 80 per cent

by the empirical equation

$$-\log(1 - x) = k/S \quad (8)$$

despite the fact that the conversion, x , was expressed in two different ways. Similar curves were obtained for nitrated fused iron catalysts at 7.8 and

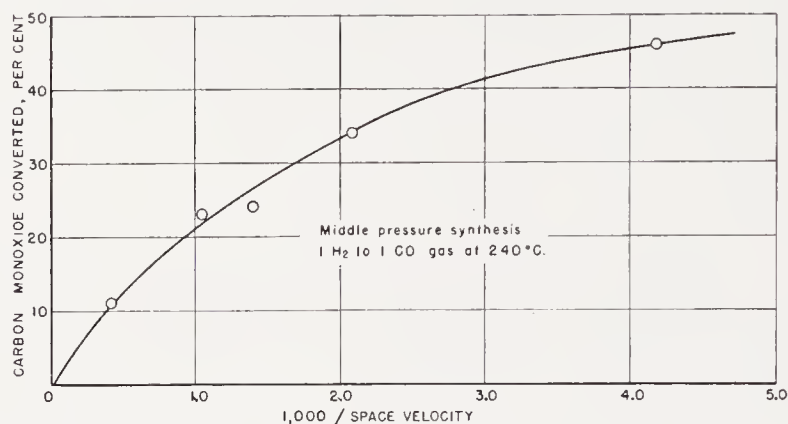


Figure 26. Variation of the conversion of carbon monoxide with the reciprocal of space velocity with a fused iron catalyst. (From data of Ref. 116)

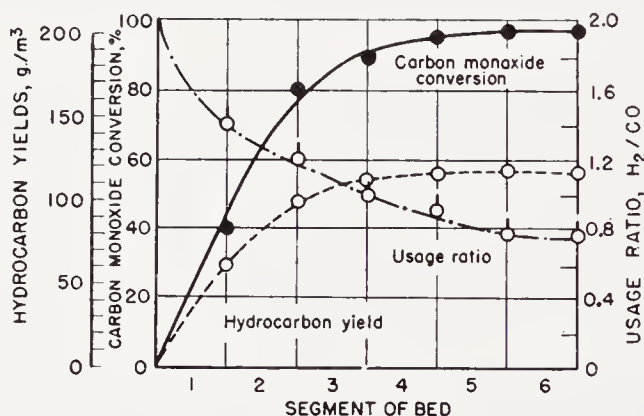


Figure 27. Variation of conversion and usage ratio with bed length on iron catalyst at 230°C and constant flow of 2H₂ + 1CO at atmospheric pressure. (Reproduced with permission from Ref. 79)

21.4 atm. In Figure 27 the abscissa are reported as bed length at constant synthesis gas flow, and under these conditions bed length is proportional to the reciprocal of space velocity.

The increase of rate with temperature is usually somewhat smaller than that found for cobalt and nickel catalysts. With two precipitated iron catalysts in the medium-pressure synthesis, Pichler¹⁰² varied gas flow and temperature, maintaining the contraction (not CO₂-free) at 50 per cent in one experiment and 15 per cent in another. Arrhenius plots (Figure 29)

are approximately linear with slopes corresponding to an over-all apparent activation energy of 20.9 kcal/mole. Similar experiments of the Bureau of Mines¹⁰ with fused and precipitated iron catalysts and $1\text{H}_2 + 1\text{CO}$ gas at

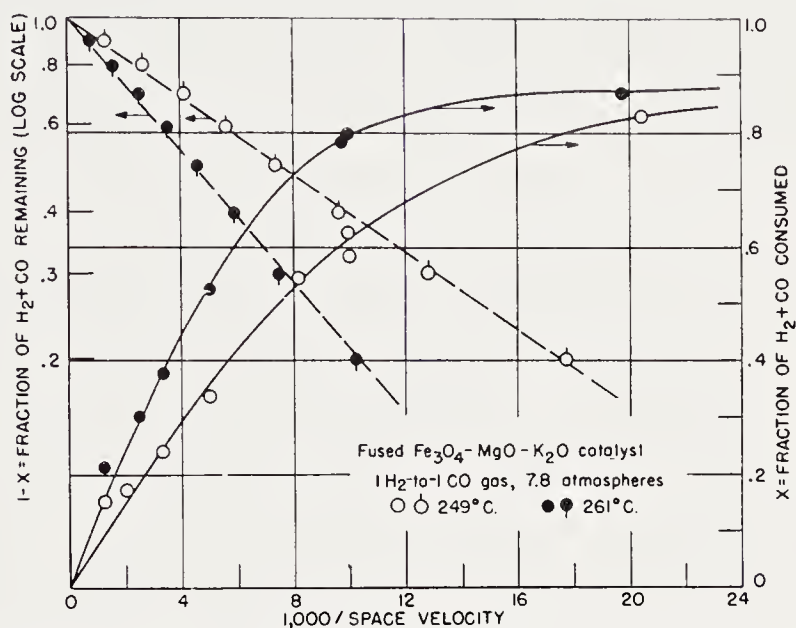


Figure 28. Variation of conversion with the reciprocal of space velocity. (Reproduced with permission from Ref. 10)

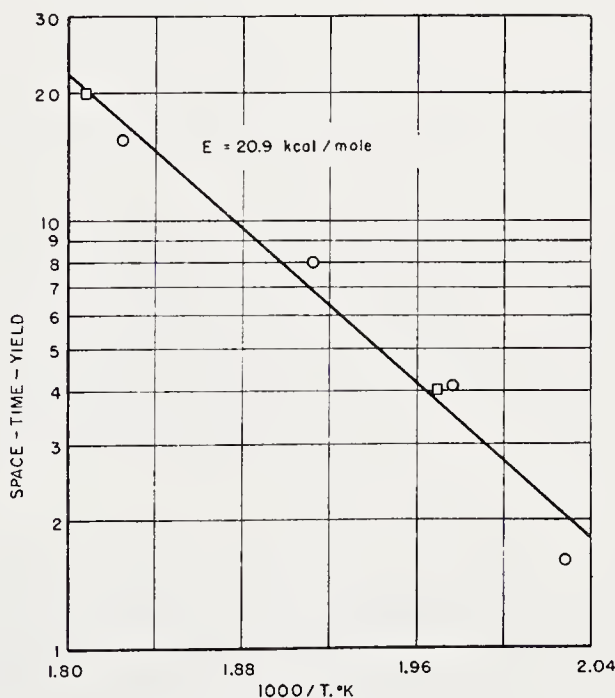


Figure 29. Arrhenius plots for medium-pressure synthesis with two precipitated iron catalysts. (From data of Ref. 102)

7.8 atm. (Figure 30) gave activation energies of 20.0 and 20.9 kcal/mole. The apparent activation energy computed from the temperature dependence of constant k of empirical Eq. (8) for data of Figure 28 was also 20 kcal/mole. At 21.4 atm. the activation energy for nitrified fused catalysts was between 19 and 21 kcal/mole.

The data of tests of iron catalysts with $1\text{H}_2 + 1\text{CO}$ gas can usually be expressed satisfactorily by the equation

$$-\log(1 - x) = \frac{A}{S} e^{-E/RT} \quad (9)$$

where A and E are, respectively, a temperature-independent rate constant

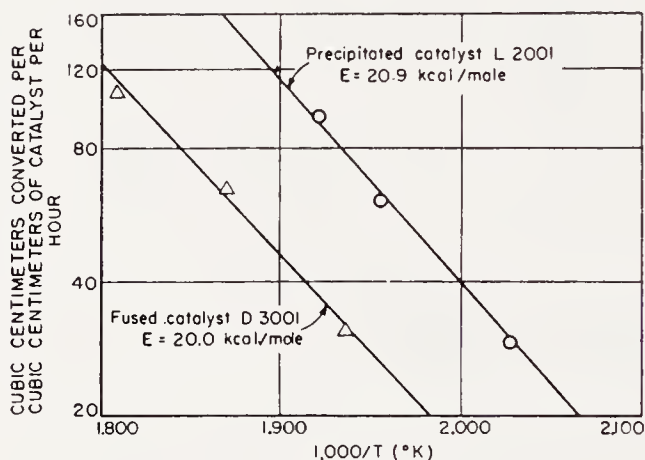


Figure 30. Arrhenius plots of space-time yield (in terms of volume of synthesis gas converted) against reciprocal of absolute temperature. Flow was varied to maintain apparent contractions of 65 per cent. (Reproduced from Ref. 10)

and the over-all activation energy. Equation (9) is useful in correlating data at different flows, temperatures, and pressures. The constant A can be used as an index of catalyst activity. Equation (9) can be modified to give the activity, A_v , expressed as cc synthesis gas converted per cc of catalyst per hour at 240° when the flow is adjusted to give a conversion of 65 per cent. The resulting equation with the activation energy taken as 19 kcal/mole is

$$A_v = 1.241 \times 10^{-8} \times S \times 10^{4130/T} \times \log_{10} \frac{1}{1 - x} \quad (10)$$

In practice the apparent contraction (CO_2 -free) is used since it differs from the real contraction by only about 2 per cent for most experiments. For some purposes activity is better expressed per gram of iron, the value, A_{Fe} , being obtained by dividing A_v by the weight of iron per cc. Figure

31 demonstrates the use of activities (computed from average values of temperature, flow, and contraction for weekly synthesis periods) for comparing the reproducibility of catalyst tests at 7.8 atm. This graph also shows the relative activity per gram of iron for different types of catalysts.

Empirical rate Eq. (9) has been thoroughly tested only for $1\text{H}_2 + 1\text{CO}$ gas. It also holds moderately well for other feed-gas compositions; however, the upper limit of conversion to which the equation applies is lower

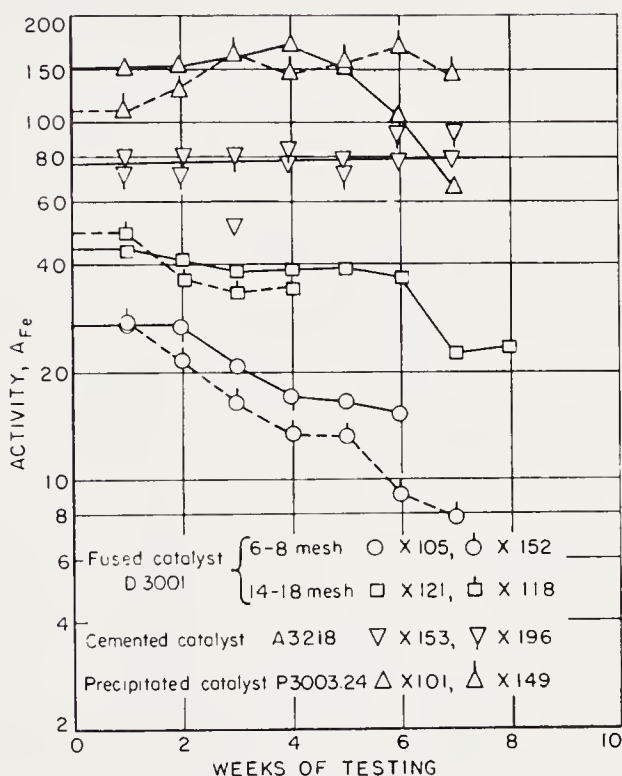


Figure 31. Reproducibility of catalysts tests at 100 psig with 1H_2 to 1CO gas. (Reproduced with permission from Ref. 10)

for gases having compositions widely different from $1\text{H}_2 + 1\text{CO}$. The rate constant k is the maximum space-time-yield obtained as the flow is increased, as shown by rewriting Eq. (8) as

$$k = -S \log (1 - x). \quad (11)$$

For small values of x , $-\log (1 - x) \cong x$ and $k \cong Sx = r$. This procedure may be used for extrapolating to the limiting space-time-yield (zero conversion) and should be especially useful for comparing data obtained with different feed-gas compositions at a constant temperature, since the rates at zero conversion can be related directly to the feed composition.

Most iron catalysts are not effective in the synthesis at atmospheric

pressure unless given special treatment, such as solvent extraction at intervals of 1 or 2 days. Pichler¹⁰¹ found that both activity and life of precipitated catalysts operated with carbon monoxide-rich gas at 235°C increased to a maximum at about 15 atm. and then decreased, the highest pressure in this study being 60 atm. Data of Scheuermann¹¹⁶ showed that the activity was greater at 12 atm. than at 50 or 200 atm. Similarly, the activities of fused iron catalysts in synthesis experiments of Linckh and Klemm⁸⁹ at 100 atm. were relatively low. Data of Pichler¹⁰² for precipitated

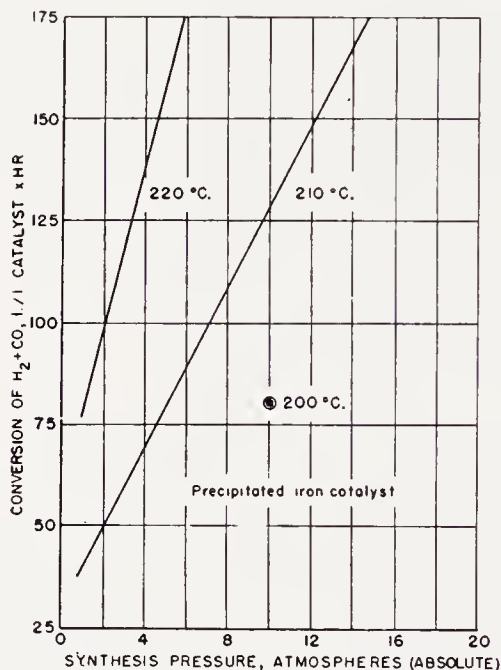


Figure 32. Variation of space-time yield with pressure and temperature. (From Ref. 102)

catalysts at constant temperatures and approximately constant conversion in Figure 32 indicate that the rate increased linearly with pressure; however, the lines do not pass through the origin. With reduced fused iron ($\text{Fe}_3\text{O}_4\text{-MgO-K}_2\text{O}$) Bureau of Mines workers¹⁰ found that activity computed by Eq. (10) was proportional to pressure, and for two temperatures the data fell on the same line as shown in Figure 33. Similar experiments with nitrified fused catalysts⁶⁸ also indicated that the rate was proportional to operating pressure. Hall, Gall, and Smith⁵⁸ studied the pressure dependence of the synthesis in the range 300 to 675 psig with mill scale and fused iron catalysts in fixed-bed, slurry, and fluid-bed reactors with $2\text{H}_2 + 1\text{CO}$ gas at relatively constant conversions and recycle ratios. The data in Figure 34 indicate that the rate (expressed as space-time yield) increased linearly up to the highest pressure, 675 psig. With catalysts containing relatively

inert forms of iron oxide that require reduction in hydrogen before synthesis, the rate increases directly with pressure up to at least 45 atm. With precipitated catalysts the optimum rate is obtained at 15 to 20 atm. In the linear rate-pressure region, the constant A of Eq. (9) can be replaced by $A'P$, where P is the operating pressure.

With iron catalysts the relative usage of hydrogen and carbon monoxide varies from nearly $2\text{H}_2 + 1\text{CO}$ to $0.5\text{H}_2 + 1\text{CO}$, and is principally a function of feed composition, the fraction of gas converted and recycle ratio. The dependence of usage ratio on temperature and pressure is usually small.

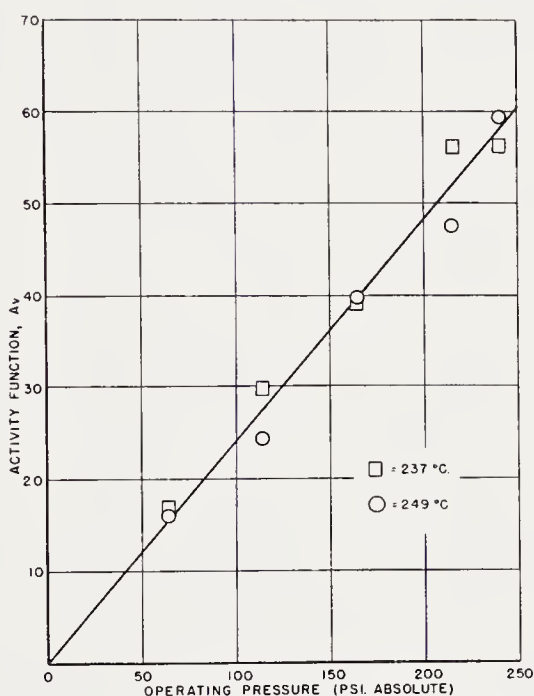


Figure 33. Variation of activity with operating pressure on fused catalyst D3001 with $1\text{H}_2 + 1\text{CO}$ gas. (Reproduced with permission from Ref. 10)

Data of Pichler¹⁰¹ for tests with precipitated catalysts, presumably at high conversions, indicate that production of water decreased with increasing carbon monoxide content, and was greater at 15 atm. (gage) than at atmospheric pressure. Similar trends have been found with other types of catalysts.

The influence of conversion and recycle on usage ratio can be explained by assuming that: (a) water is the principal primary product, and (b) carbon dioxide is produced by the water-gas-shift reaction with the rate of this reaction being proportional to the concentrations of water and carbon monoxide.

Koelbel^{79, 75} observed that usage ratios in tests at atmospheric pressure with $2\text{H}_2 + 1\text{CO}$ gas decreased with increasing conversion from 1.75 at

25 per cent conversion of CO to 0.78 at 97 per cent, as shown in Figure 27 and Table 5. At 180°C the usage ratio was 1.45, possibly somewhat larger than would be expected for the same conversion at 230°C. From these and

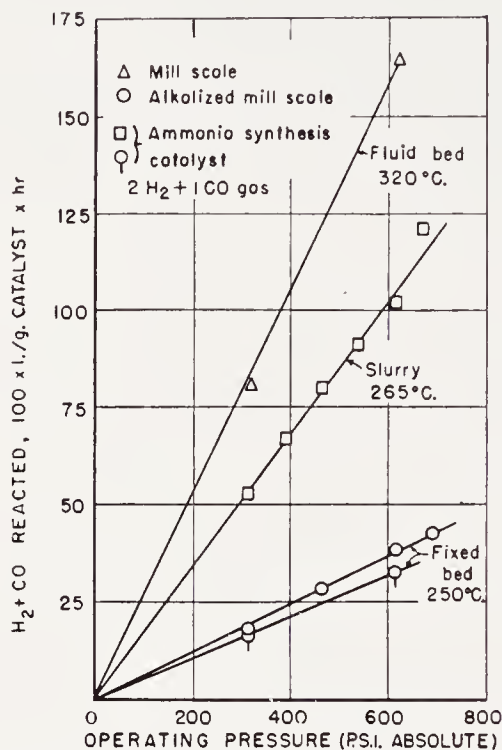


Figure 34. Variation of rate with operating pressure on iron catalysts for three types of reactors. (Reproduced with permission from Ref. 58)

TABLE 5. VARIATION OF USAGE RATIO WITH CONVERSION AND TEMPERATURE^a
($2\text{H}_2 + 1\text{CO}$ gas at atmospheric pressure)

Space Velocity (hr^{-1})	Temp. ($^{\circ}\text{C}$)	Usage Ratio, H_2/CO	Conversion of CO (%)
100	230	0.78	97.0
200	230	1.43	70.0
500	230	1.75	25.0
30	180	1.45	48.0

^a From Ref. 75.

data for the reaction of $\text{H}_2\text{O} + \text{CO}$ on iron catalysts⁷⁹ (see p. 305) at various temperatures, it may be concluded that the water-gas-shift reaction has a moderately large temperature coefficient. Koebel inferred that as the temperature was decreased, the rate of the water-gas-shift reaction decreased more rapidly than the rate of the primary synthesis reaction. However, his own data in Table 5 apparently contradict this generaliza-

tion. Work of the Bureau of Mines in Table 6 indicates that the usage ratio at 65 per cent contraction with $1\text{H}_2 + 1\text{CO}$ at 7.8 to 21.4 atm. is relatively constant over a wide range of temperature, 222 to 271°C, for catalysts pretreated in a variety of ways. At least in this range of tempera-

TABLE 6. USAGE RATIOS IN BUREAU OF MINES TESTS
($1\text{H}_2 + 1\text{CO}$ gas, conversion about 65 per cent)

Pretreatment ^a	Initial Phases ^b	Operating Conditions		Usage Ratio, H ₂ /CO
		Pressure (atm.)	Temp. (°C)	
A. Fused Fe ₃ O ₄ -MgO-K ₂ O				
R	α	7.8	226	0.78
			238	.71
			253	.79
			260	.72
R	α	21.4	258	.72
RN	ε	7.8	225	.75
	ε	21.4	238	.79
	ε, γ'	21.4	242	.77
RC	χα	7.8	229	.75
	χ	11.1	239	.83
	χ	14.5	235	.84
	χ	21.4	250	.83
B. Fused Fe ₃ O ₄ -Al ₂ O ₃ -K ₂ O				
R	α	7.8	271	.69
		21.4	250	.67
RN	ε	7.8	230	.69
		21.4	243	.73
RC	χα	21.4	233	.80
C. Precipitated Fe ₂ O ₃ -CuO-K ₂ CO ₃				
I	M ?	7.8	221	.57
R	α	7.8	229	.66
RN	ε	7.8	229	.69

^a R = reduced in H_2 , N = nitrided in NH_3 , C = carburized in CO, I = pretreated with $1\text{H}_2 + 1\text{CO}$. All pretreatments at atmospheric pressure.

^b Phases from x-ray diffraction: α = α -iron, ϵ = ϵ -nitride, γ' = γ' -nitride, χ = Hägg carbide, M = magnetite.

tures the water-gas-shift reaction must increase with temperature at about the same rate as the primary synthesis step.

The usage ratio, H_2/CO , increases with recycle ratio. For processes other than hot-gas-recycle, the exit gas is cooled to room temperature or lower before recirculation. In the medium pressure range this cooling condenses most of the water vapor; however, the water is not completely removed at atmospheric pressure. Thus, the average concentration of water vapor decreases as the recycle ratio increases, and the observed increase in usage ratio apparently results from the lower concentration of water vapor. U. S. Bureau of Mines data²⁶ (p. 236, Chapter 2) for the oil circulation process with fused iron catalysts demonstrate the increase in usage

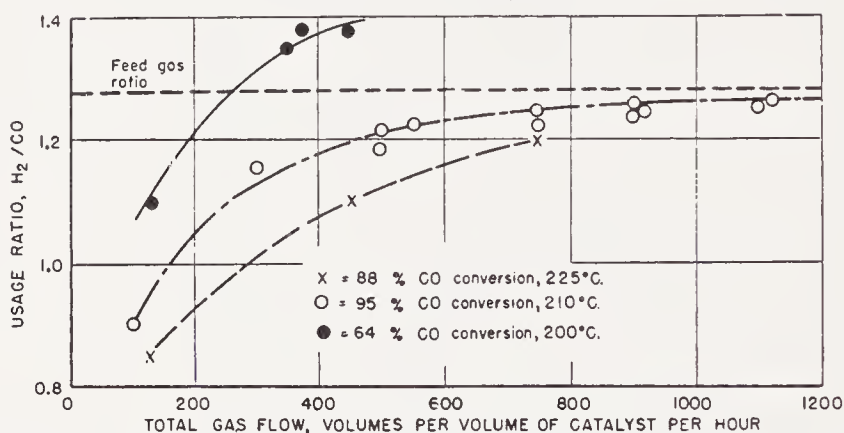


Figure 35. Variation of usage ratio with recycle ratio with iron catalysts at 10 atm. The lowest flow points represent fresh feed, and increased flow values result from recycle. (Reproduced with permission from Ref. 76)

ratio with gas recycle, and with $1H_2 + 1CO$ gas the usage ratio eventually exceeded the feed-gas ratio. Koelbel⁷⁶ observed that the usage ratio with $2H_2 + 1CO$ gas at atmospheric pressure and $222^\circ C$ increased from 0.84 to 1.8 as the recycle ratio (with special drying of recycle gas) increased from 0 to 9. Lower usage ratios at the same recycle ratios were observed when the gas was not dried. In these experiments the conversion of carbon monoxide was about 85 per cent. With $2H_2 + 1CO$ gas at 10 atm., $220^\circ C$, and carbon monoxide conversions of about 93 per cent, the usage ratio increased from 1.2 to 1.95 as the recycle ratio was increased from 0 to 14. Data for $1.28H_2 + 1CO$ at 10 atm. and several temperatures in Figure 35 show the effect of average conversion of carbon monoxide produced by varying the temperature. In this figure the usage ratio is plotted against the total gas flow, fresh plus recycle, and the points for the lowest flow (at about 100 hr^{-1}) represent the fresh feed only (no recycle). At all temperatures the usage ratio increased with recycle ratio. For an average conversion of car-

bon monoxide of 64 per cent, the usage ratio was greater than the feed-gas ratio for recycle ratios greater than about 2.

As a conclusion of this discussion, the variation of relative usage of hydrogen and carbon monoxide with conversion will be examined with respect to the results described previously. The data in Figure 36 for a test of a fused iron catalyst with $1\text{H}_2 + 1\text{CO}$ at 7.8 atm. and 249°C are plotted as volumes H_2 consumed per volume of $\text{H}_2 + \text{CO}$ consumed against frac-

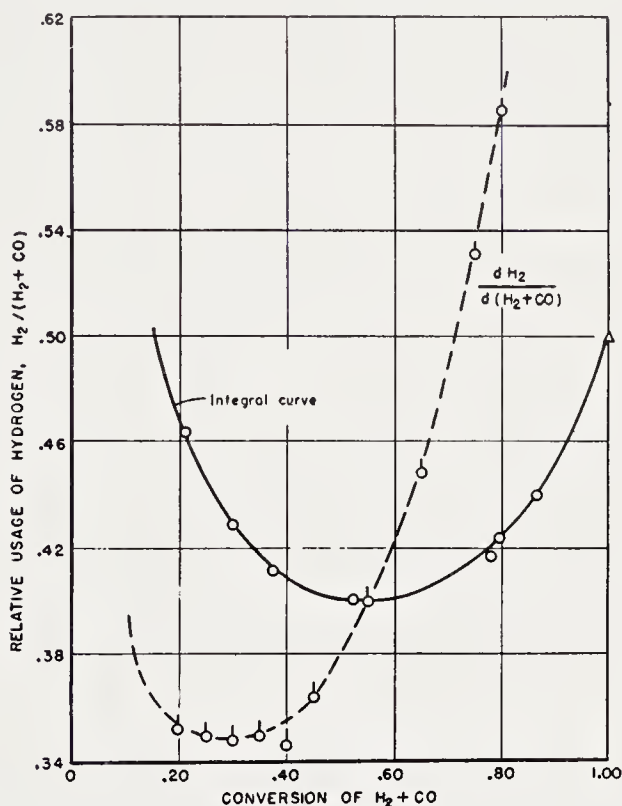


Figure 36. The integral and differential usage of hydrogen on fused iron catalyst with $1\text{H}_2 + 1\text{CO}$ gas at 7.8 atm. and 249°C .

tion of $\text{H}_2 + \text{CO}$ consumed. This plot has the advantages that the ordinates vary only from 0 to 1.0 and that the differential usage of hydrogen, $d\text{H}_2/d(\text{H}_2 + \text{CO})$, may be obtained by a simple graphical method. On the integral (solid) curve, experimental points cover conversions from 0.21 to 0.87. The triangle at a conversion of 1.0 results from the requirement that usage and feed ratios must be equal when all of the gas is consumed. Although this point may not be attainable experimentally, it appears to be a logical extrapolation of the available data. As the conversion approaches zero, the integral curve rises steeply, and its extrapolation to a utilization of 0.67 (corresponding to a usage ratio, $\text{H}_2:\text{CO}$, of 2.0) at zero conversion

seems reasonable. The differential curve falls steeply with increasing conversion to a minimum at a conversion of 0.3 and then increases continuously. The initial decrease is probably caused by the water-gas-shift reaction favored by the water vapor produced in the synthesis. As conversion is increased, the ratio of $H_2:CO$ in the exit gas increased, having the values of 1.13, 1.50, and 2.49 at conversions of 0.3, 0.5, and 0.7, respectively. The increase in $dH_2/d(H_2 + CO)$ at conversions above 0.3 is probably related to the increasing $H_2:CO$ ratio of the gas in contact with the catalyst. This effect apparently outweighs the influence of the water-gas-shift reaction. Thus, the curves in Figure 36 result from two processes: (a) the water-gas-shift reaction decreasing the utilization ratio, and (b) the increasing $H_2:CO$ ratio of the reacting gas tending to increase the usage of hydrogen.

TABLE 7. VARIATION OF RATE WITH PARTICLE SIZE^a
(Fused iron catalyst with $2H_2 + 1CO$ gas in fixed-bed reactor)

Catalyst size			Pressure (psig)	Temp. (°C)	Flow per Gram Catalyst (l./hr)	Recycle Ratio	Con- version of $H_2 + CO$ (%)	Space-time- yield Conversion × Flow
Mesh B S S	Range (mm)	Average (mm)						
7-14	2.41-1.20	1.80	300	265	0.21	2.0	89.2	0.187
25-36	0.60-0.44	0.52	300	265	.60	2.8	88.0	.528
7-14	2.41-1.20	1.80	600	305	1.02	2.3	88.0	.898
25-36	0.60-0.44	0.52	600	305	3.42	2.0	90.1	3.08

Ratio of space-time-yields at 300 psig = 2.82. Ratio of space-time-yields at 600 psig = 3.43. Ratio of average particle diameters = 1/3.46.

^a From Ref. 58.

With fused or sintered iron catalysts, the activity increases as the particle size decreases. Thus, Reisinger¹⁰⁸ observed that, at the same medium-pressure synthesis conditions, catalyst particles (presumably of fused WK 17) from 0.3-0.5 mm operated at 188°C compared with 198° for 1 to 2 mm particles. These workers concluded that the activity increased with decreasing particle size until the wax film caused the particles to adhere together to an extent that caused fluctuations of gas flow and poor gas distribution within the bed. In this range of particle size a 3- to 4-fold decrease in particle size produced approximately a 1.6-fold increase in activity (based on an activation energy of 20.0 kcal/mole). Data of Hall, Gall, and Smith⁵⁸ at 300 and 600 psig of $2H_2 + 1CO$ with mill scale and fused iron catalysts indicate that the rate, under similar synthesis conditions, varied approximately inversely with particle size, as shown in Table 7. Over the range of particle sizes studied, the rates increased by 2.8 and 3.4 when the particle size decreased by a factor of 3.5. Thus the rate increased slightly less than linearly with the external surface area per

unit weight of catalysts, the external area being inversely proportional to the particle diameter.

In the U.S. Bureau of Mines tests¹⁰ at 7.8 atm. of $2\text{H}_2 + 1\text{CO}$ with fused $\text{Fe}_3\text{O}_4\text{-MgO-K}_2\text{O}$ catalyst of sizes varying from 4–6 to 40–60 mesh, the activity increased with decreasing particle size. For the larger particles the rate increased approximately linearly with external area, but the curve flattened at high areas (small particles). The data of Figure 37 may be approximated by assuming that the active portion of the catalyst is confined to an outer shell of constant depth on spherical particles and that

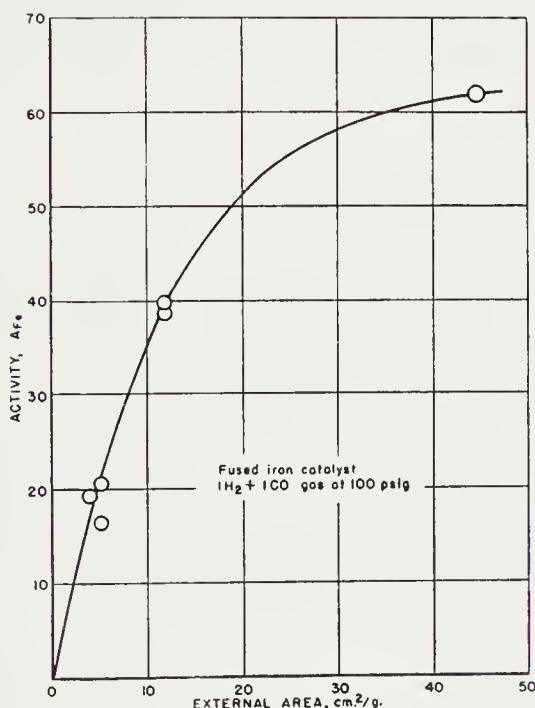


Figure 37. Variation of activity with external area. (Reproduced with permission from Ref. 10)

the rate is proportional to the volume of catalyst (per gram of catalyst) in this shell. Based on these assumptions, the depth of the active layer was about 0.1 mm. Although these postulates constitute a great oversimplification, the calculation demonstrates that only a small fraction of the total surface area is accessible and effective in the Fischer-Tropsch synthesis. These results are very different from the data on the decomposition of ammonia on similar fused iron catalysts where the rate was found to be independent of particle size³⁵. The observation of the low accessibility of the internal surface of fused catalysts in the Fischer-Tropsch synthesis is not expected, since the pores of used catalysts are nearly completely filled with wax. Furthermore, the oxidation that occurs during synthesis destroys an appreciable fraction of the pores^{59, 120}.

In synthesis studies at temperatures greater than 300°C, such as employed in the fluidized process, the deposition of carbon with subsequent catalyst deterioration is a major problem. Arnold and Keith¹¹ and Hall, Gall, and Smith⁵⁸ observed that the rate of carbon deposition decreased sharply as the partial pressure of hydrogen was increased to values above 100 to 135 psig. High partial pressures of hydrogen are obtained by using hydrogen-rich synthesis gas, about $2\text{H}_2 + 1\text{CO}$, at high conversions and high recycle ratios.

The empirical treatment of available kinetic data on the Fischer-Tropsch synthesis on iron catalysts lead to the following conclusions:

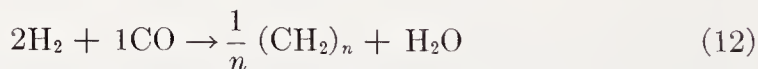
1. The over-all activation energy for the process is about 20 kcal/mole. This high value excludes diffusion to or from the catalyst particles as a rate-determining step.

2. The rate is strongly dependent upon particle size, suggesting that diffusion in the catalyst pores is slow compared with the reaction rate. Apparently only the outer portion of the catalyst is effective. The slow diffusion in pores probably results from a decrease in the pore volume by oxidation during synthesis and blocking of pores by wax. Under these conditions the observed activation energy may be only one-half of the value that would be obtained on a planar surface¹³⁷.

3. At constant temperature and conversion, the rate is proportional to the operating pressure.

4. At constant pressure and temperature, the synthesis rate appears to increase with partial pressure of hydrogen up to at least $2\text{H}_2 + 1\text{CO}$ ¹²³.

5. The principal primary reaction appears to be



with carbon dioxide produced by a subsequent water-gas-shift reaction. At temperatures above 200°C the rate of this secondary process seems to vary with temperature in about the same way as the primary reaction

6. The occurrence of the water-gas-shift reaction is primarily a function of the ratio $\text{H}_2:\text{CO}$ of the feed gas and of the conversion. The rate of this reaction increases with increasing concentrations of water vapor and carbon monoxide.

The simple empirical first-order-type rate equation (Eq. 9, p. 286) fits experimental data remarkably well over a variety of operating conditions; however, this equation has no fundamental basis. For conversions up to 60 per cent the equation

$$r = k p_{\text{H}_2} \quad (13)$$

holds fairly well. This equation appears similar to the differential form

of Eq. (9)

$$r = k(1 - x). \quad (14)$$

However, the function $(1 - x)$ decreases more rapidly than p_{H_2} as the conversion, x , increases.

A second equation, in which rate is assumed to be proportional to the partial pressure of hydrogen and to the fraction of reduced iron, (including iron as carbide or nitride) in the active zone near the external surface, θ_M , has been shown to fit experimental data over a very wide range of operating variables. The fraction of iron in the surface layers is postulated to be determined by competitive first-order reactions involving oxidation of iron with steam and reduction of oxide by carbon monoxide. Thus

$$r = k p_{\text{H}_2} \theta_M = \frac{k p_{\text{H}_2}}{1 + a \frac{p_{\text{H}_2\text{O}}}{p_{\text{CO}}}}. \quad (15)$$

In unpublished work of the U. S. Bureau of Mines⁶³, this equation has been tested for data from experiments of nitrified as well as reduced-fused iron catalysts with different feed-gas compositions at several temperatures and pressures. The equation usually fits the data of individual experiments within the limits of accuracy. Although the values were reasonable, the constants from experiments at the same temperature showed definite trends as the feed-gas composition was changed. Thus, further studies will be required to establish the validity of Eq. 15. A number of equations of the type proposed by Hougen and Watson⁶⁴ were examined, but none of these expressed the data properly. Tramm¹²⁷ proposed rate equations for the synthesis on iron catalysts. The most important term in these expressions relates rate to $p_{\text{H}_2} p_{\text{CO}}$ or $p_{\text{H}_2}^2 p_{\text{CO}}$. These equations suggest a greater dependence of rate on total pressure than is observed.

Kinetics of the Fischer-Tropsch Synthesis on Ruthenium Catalysts

Pichler and Buffleb^{103, 104} reported a detailed study of the activity and selectivity of ruthenium catalysts. The usage ratio $\text{H}_2:\text{CO}$ was about two for most synthesis conditions (pp. 240-241). The average molecular weight of the product increased with operating pressure from almost entirely methane at atmospheric pressure to virtually all wax at 1,000 atm. Fractions of the waxes from the 1,000 atm. synthesis melted as high as 134°C and had molecular weights as high as 23,000.

The conversion increased with operating pressure to the highest pressure studied, and the rate also increased with an increase in temperature, as shown in Figure 38. These experiments were not, however, designed to give the pressure or temperature coefficients. A plot of contraction against

reciprocal of flow in Figure 39 shows that the rate is also strongly dependent upon partial pressures.

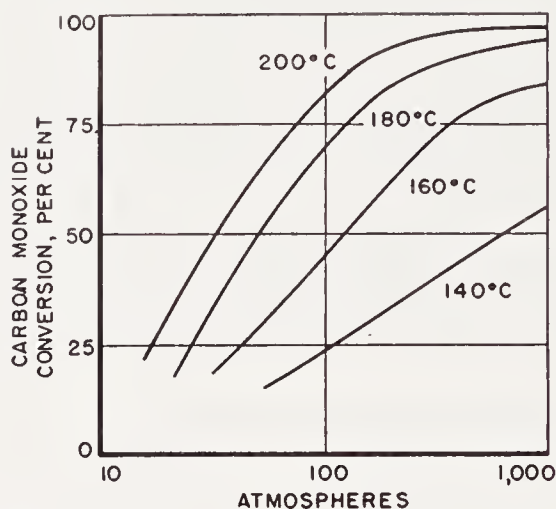
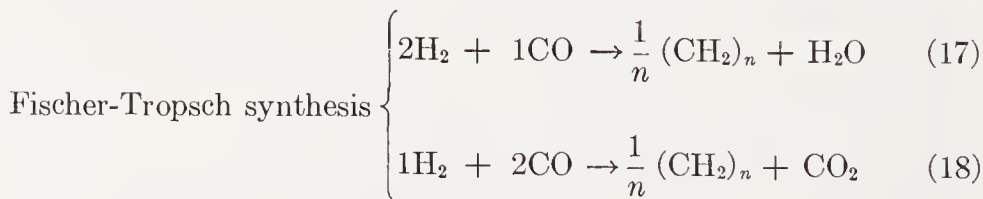


Figure 38. Variation of the extent of conversion with pressure on ruthenium catalysts. Flow of $2\text{H}_2 + 1\text{CO}$ of $\frac{1}{3}$ l/g Ru \times hr. (From Ref. 104)

VARIATIONS OF THE FISCHER-TROPSCH SYNTHESIS

The following series of equations may be obtained by the addition of the water-gas-shift reaction to the equation above it:



Each equation consumes three moles of $\text{H}_2 + \text{CO}$ per mole of CH_2 produced. In the temperature range normally considered for Fischer-Tropsch synthesis, the standard state free energy per CH_2 group becomes more negative in proceeding from Eq. (16) to (19). However, under most conditions of the Fischer-Tropsch synthesis, all of the reactions are thermodynamically possible. The following observations can be made regarding Eqs. (16) and (19):

(a) The reactants in Eqs. (16) and (19) are, respectively, the products and reactants of the water-gas-shift reaction.

(b) Formic acid under suitable experimental conditions can be produced from the reactants of Eqs. (16) and (19), and formic acid has been postulated as an intermediate in the water-gas-shift.

(c) With iron catalysts H_2 and CO_2 have, respectively, a lower tendency to reduce magnetite and to oxidize iron than CO and H_2O . Iron oxide may also be an intermediate in the water-gas-shift.

(d) In both laboratory experiments and commercial practice, it has been shown that methanol can be produced from $H_2 + CO_2$ gas on typical methanol catalysts under conditions of the synthesis of methanol from $H_2 + CO$ gas.

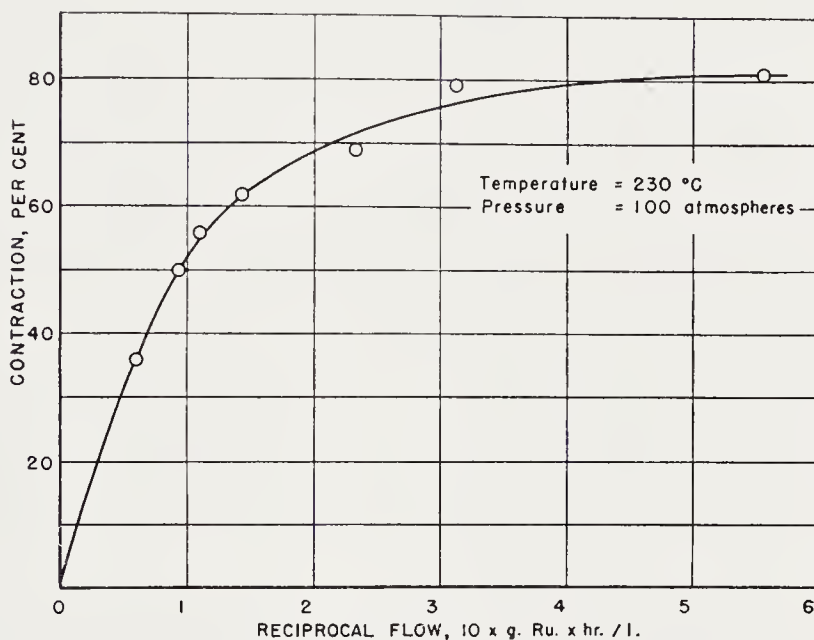


Figure 39. Conversion-reciprocal space velocity curves for synthesis on ruthenium catalysts. (From Ref. 104)

Papers of Pichler^{99, 100, 105} describe reactions of $H_2 + CO_2$, $H_2O + CO$, formic acid, and formates.

Hydrogenation of Carbon Dioxide

Studies of the catalytic hydrogenation of carbon dioxide date back to Sabatier and Senderens¹¹⁴. Koch and Kuster⁷² reviewed the literature of this reaction up to 1933. These authors studied the hydrogenation of carbon dioxide at atmospheric pressure on cobalt and nickel catalysts. With $4H_2 + 1CO_2$ gas, cobalt and nickel catalysts had appreciable activity at $150^\circ C$, and sizable conversions were attained at $200^\circ C$. The conversion increased to a maximum at $300^\circ C$ and then decreased. Methane was the only hydrocarbon found. With $1H_2 + 4CO_2$ gas on a nickel catalyst, the

hydrogen was virtually completely consumed at 175 to 300°C, and the exit gas contained about 92 per cent CO_2 , 0.1 CO , 0.0 to 0.2 H_2 , and 5.5 CH_4 . In one experiment, tests for traces of methanol and formaldehyde were obtained; however, hydrocarbons higher than methane were not found. In tests at 300 and 350°C with high flows of $\text{H}_2 + 4\text{CO}_2$ on cobalt and nickel catalysts, small quantities of carbon monoxide, 0.2 to 2.6 per cent, were found in the exit gas. Other experiments showed that hydrogen sulfide severely poisoned cobalt and nickel catalysts for the hydrogenation of carbon dioxide. The reaction was also strongly inhibited by added water vapor.

Fischer and Pichler⁴⁶ investigated the hydrogenation of carbon dioxide and mixtures of CO_2 and CO at atmospheric pressure on cobalt, nickel, and iron catalysts. With cobalt and nickel catalysts at temperatures from 150 to 200°C: (a) carbon dioxide was not hydrogenated in the presence of carbon monoxide, (b) the hydrogenation of carbon monoxide was not inhibited by the presence of carbon dioxide and the selectivity was not changed, (c) the hydrogenation of carbon monoxide yielded typical Fischer-Tropsch products, but methane was the only hydrocarbon from the hydrogenation of carbon dioxide, and (d) for gases containing H_2 , CO , and CO_2 the hydrogenation of carbon dioxide occurred only after essentially all of the carbon monoxide was consumed. These results are demonstrated by the analyses of exit gases, as shown in Figure 40. In these tests the feed gas rate was presumably held constant and the temperature was increased from 150 to 200°C. With a nickel catalyst at 215 to 275°C the same results were obtained with the exception that methane was the only hydrocarbon produced.

With an iron catalyst the same feed gases were used as shown for cobalt catalysts in Figure 40. At 250°C and atmospheric pressure, contractions of about 15 per cent were observed. From gases containing carbon monoxide, about 20 g of liquid hydrocarbons per cubic meter of feed were produced, but no liquid hydrocarbons were obtained from $\text{H}_2 + \text{CO}_2$. At 300°C small amounts of carbon monoxide were produced from $\text{H}_2 + \text{CO}_2$.

Kinetic experiments of the U. S. Bureau of Mines⁷, (p. 21) also showed that carbon dioxide produced in the synthesis with a cobalt catalyst was hydrogenated only after the carbon monoxide had been completely consumed.

Kuster⁸⁷ showed that most iron catalysts were ineffective in the hydrogenation of carbon dioxide to hydrocarbons at atmospheric pressure; however, the water-gas-shift reaction occurred. Iron catalysts containing small amounts of cobalt and copper produced small yields of liquid hydrocarbons, and the addition of one per cent of potassium carbonate to these preparations increased the yields of gasoline. The aqueous phase was acidic. With

Fe-Co and Co catalysts impregnated with copper and alkali, the yields of liquid and solid hydrocarbons varied from 56 to 164 g/m³ of carbon dioxide. Kuster⁸⁷ postulated that the hydrogenation of carbon dioxide to higher hydrocarbons followed the path:

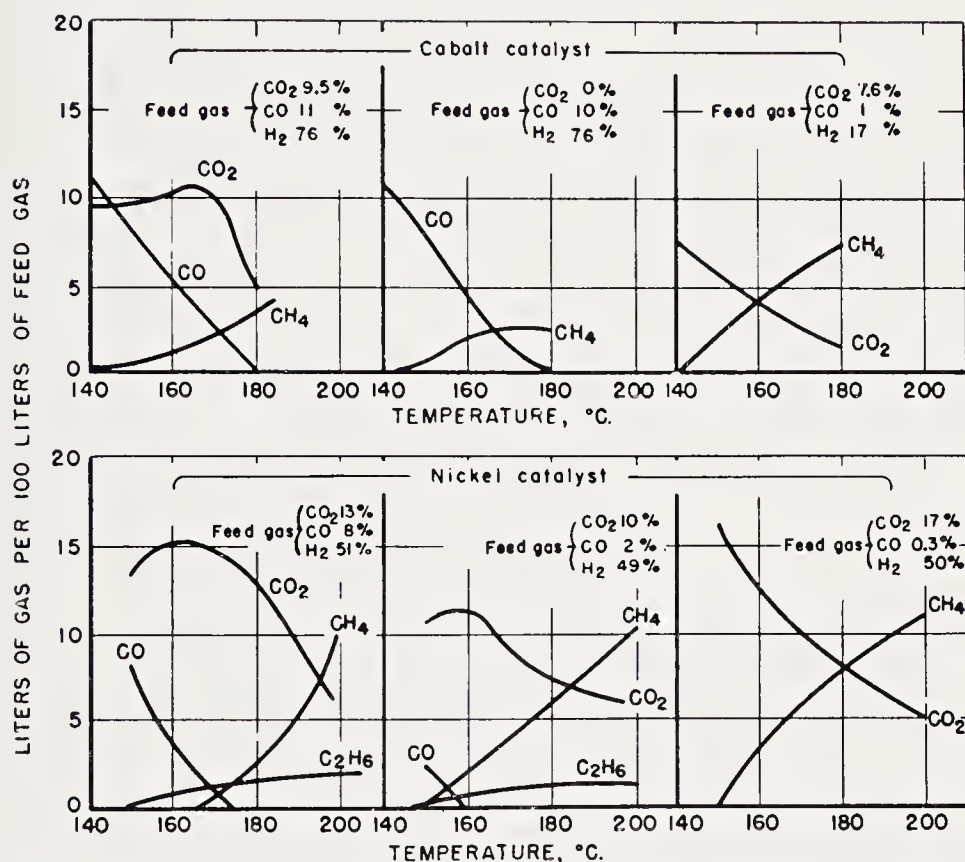
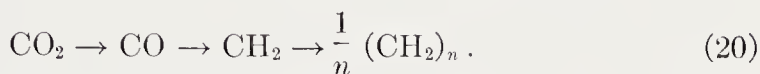


Figure 40. The influence of carbon monoxide on the hydrogenation of carbon dioxide at atmospheric pressure (From data of Ref. 46)

Russell and Miller¹¹³ studied the hydrogenation of carbon dioxide on unsupported precipitated 100Co:5Cu catalysts with or without added alkali and/or cerium oxide at atmospheric pressure. Catalysts without alkali produced no liquid hydrocarbons, although the catalysts were active at 200 and 225°C. In most cases the hydrocarbon product was entirely methane. When 2 per cent K_2CO_3 was added to the same batches of catalyst, liquid hydrocarbons and wax were produced in moderate amounts at 200 to 225°C, the highest yields being 116 g/m³ of carbon dioxide converted. Although the gas contraction decreased steadily with time, the

yields of liquid and solid hydrocarbons increased. This behavior was interpreted as a process of preferential poisoning that improved the selectivity. The activity and selectivity of catalysts containing CeO_2 and K_2CO_3 changed much less with time than catalysts promoted with K_2CO_3 , and moderately long periods of operation with relatively constant catalytic behavior were possible. The temperature dependence was determined on a $\text{Co-Cu-CeO}_2\text{-K}_2\text{CO}_3$ catalyst by varying space velocity and temperature to maintain constant conversion. Activation energies of 20.3 to 25.3 kcal/mole, averaging 23.1 kcal/mole, were found; these values are essentially the same as those found in the hydrogenation of carbon monoxide (p. 265). The largest yields of liquid and solid hydrocarbons were obtained from $2\text{H}_2 + 1\text{CO}_2$ gas, although the gases were not consumed in this ratio.

Catalysts supported on a natural kieselguhr and impregnated with alkali and cerium oxide produced only methane, but a similar preparation containing a flux-calcined kieselguhr produced moderate yields of oil. These experiments confirm previous observations that the presence of natural kieselguhr renders alkali ineffective, presumably by adsorption or reaction (p. 133).

With similar catalysts, Mulford and Russell⁹⁵ studied the effect of a water-gas-shift catalyst before the synthesis catalyst. The $\text{H}_2 + \text{CO}_2$ gas was passed over an iron water-gas catalyst at 450 to 750°C, and the gases were dried before entering the synthesis reactor. Depending on the temperature and activity of the water-gas catalyst, from 25 to 40 per cent of the carbon dioxide was converted to carbon monoxide. When the water-gas catalyst was used, the yields of liquid and solid hydrocarbons increased 5- to 35-fold, the production of methane decreased to less than half of the yields obtained when the shift catalyst was by-passed.

The authors⁹⁵ concluded that carbon monoxide is a critical intermediate in the synthesis of higher hydrocarbons and that alkali is a necessary promoter to accelerate the water-gas-shift and polymerization reactions and to poison sites responsible for methane formation.

Fischer, Bahr, and Meusel⁴² investigated the hydrogenation of carbon dioxide on a ruthenium catalyst at atmospheric pressure. On alkali-free catalysts, the hydrogenation rate was appreciable at 100°C and rapid at 150°C. The hydrocarbon product was entirely methane. Ruthenium catalysts alkalized with potassium or rubidium carbonates (2 per cent by weight) produced small yields of higher hydrocarbons in addition to methane. The reaction proceeded at a moderate rate at 170°C, and temperatures of about 200°C were required for large conversions. Preparations promoted with sodium and lithium carbonates produced only methane.

Apparently carbon monoxide effectively poisons Fischer-Tropsch catalysts for the hydrogenation of carbon dioxide, and this result seems consistent with the poisoning action of carbon monoxide on other catalytic

reactions. An explanation of the exclusive production of methane from $\text{H}_2 + \text{CO}_2$ on many typical Fischer-Tropsch catalysts is more difficult. Pichler¹⁰⁰ postulated that the hydrogenation of carbon monoxide involved molecular hydrogen and carbide, as suggested by Craxford²⁵, and that the hydrogenation of carbon dioxide involved atomic hydrogen and bare metal sites. This mechanism involves hydrogenation of carbon dioxide by successive steps to dioxymethylene, formaldehyde, methanol, and finally methane. This mechanism, however, can be subjected to many of the criticisms of Craxford's carbide hypothesis and others.

A more plausible explanation for the exclusive formation of methane from the hydrogenation of carbon dioxide on many catalysts may be based on the postulate that carbon dioxide is reduced to carbon monoxide and then to methane. The concentration of carbon monoxide in exit gas from the reaction of $4\text{H}_2 + 1\text{CO}_2$ gas was always considerably smaller than the equilibrium amounts for the water-gas-shift reactions, about 1 and 7 per cent at 227 and 327°C, respectively. Low concentrations would be expected even if the hydrogenation is stepwise, as suggested above, since carbon monoxide is preferentially hydrogenated in the presence of carbon dioxide. On this basis the ratio $\text{H}_2:\text{CO}$ of the reacting gas in the hydrogenation of carbon dioxide would be very large, perhaps about 400. This high $\text{H}_2:\text{CO}$ ratio would favor the production of methane.

Reactions of Carbon Monoxide and Water

Pages 289–290 consider the reaction of water and carbon monoxide proceeding principally according to the equation of the water-gas-shift reaction. The formation of products typical of the Fischer-Tropsch synthesis from water and carbon monoxide will now be described.

Production of carbon dioxide in the synthesis (pp. 274–283, and 289–291) was shown to result chiefly from the water-gas-shift reaction subsequent to the primary process. The velocity of the water-gas-shift reaction appears to increase with the concentrations of both water and carbon monoxide, and on iron catalysts the rate increases with temperature at approximately the same rate as the primary synthesis process. With cobalt catalysts Craxford²³ postulated that the water-gas-shift reaction as well as hydrocracking are rapid on portions of the catalyst containing metallic cobalt, whereas these reactions are slow on surfaces of cobalt carbide presumed to be the catalyst phase effective for synthesis. Bashkirov, Kryukov, and Kazan¹⁴ studied the influence of added water vapor on the synthesis with precipitated iron catalysts at atmospheric pressure. The apparent contraction and the concentration of carbon dioxide in the exit gas were determined. At 230°C with $1\text{H}_2 + 1\text{CO} + 1\text{H}_2\text{O}$ gas, the rate of the water-gas-shift reaction was shown to be 13.6 times the rate of the synthesis reaction.

Koelbel and Engelhardt⁷⁷ passed $1\text{H}_2\text{O} + 1\text{CO}$ over a standard Co-

ThO₂-MgO-kieselguhr catalyst that had been pretreated as follows:

- (a) Reduction in hydrogen at 450°C.
- (b) Treatment (a) plus carburization in carbon monoxide at 270°C for 24 hours.
- (c) Treatment (a) plus 150 hours of synthesis.

Figure 41 shows that the velocity of the water-gas-shift at 240°C was rapid approaching equilibrium with the reduced catalyst, low with carburized sample, and intermediate for the sample used in the synthesis. Koebel believed that treatment (b) produced cobalt carbide; however, with similar catalysts Hofer⁶² and Anderson⁶ have shown that carburization at 270°C usually produces chiefly elemental carbon and very little

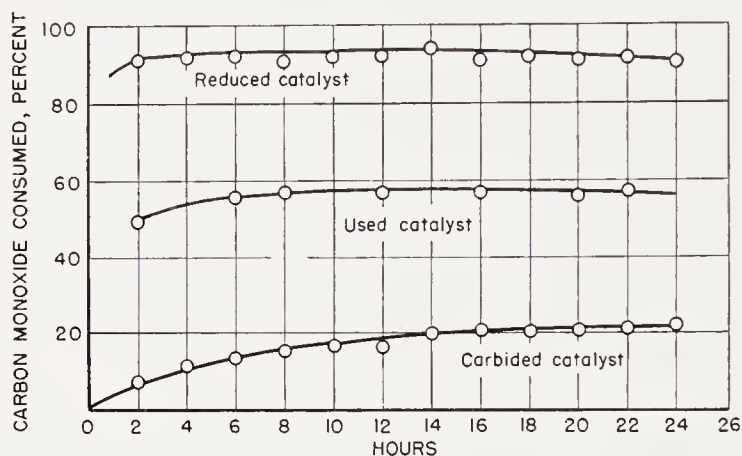


Figure 41. Reaction of carbon monoxide and water at 240°C on Co-ThO₂-MgO-kieselguhr catalyst. Space velocity of 1CO + 1H₂O of 1 hr⁻¹. (Reproduced with permission from Ref. 77)

carbide. Furthermore, the catalyst after a treatment similar to (b) was relatively inactive in the synthesis, which may also account for its low activity in the water-gas-shift.

Koebel and Engelhardt⁷⁷ studied the water-gas-shift reaction on a precipitated Fe₂O₃-CuO-K₂CO₃ catalyst after:

- (a) Treatment with carbon monoxide at 270°C for 24 hours;
- (b) treatment (a) plus hydrogenation at 270°C for 24 hours;
- (c) reduction in hydrogen at 270°C; and
- (d) synthesis for 100 hours with 2H₂ + 1CO gas at 230°C and atmospheric pressure.

Treatment (a) probably converted the catalyst to Hägg carbide, and step (b) may have removed a sizable portion of the carbide. Treatment (c) probably converted the catalyst to a mixture of iron and magnetite (termed "oxide" on Figure 42), and the synthesis step (d) possibly converted the catalyst to a mixture of magnetite and Hägg or hexagonal carbide. At

240°C the water-gas-shift (Figure 42) was slow on sample (c). The activity of the carbide (a) increased rapidly with time, and the curves for (a) and (b) appear to converge on the curve for the used catalyst (d).

Studies at different temperatures⁷⁷ in Figures 43 and 44 show that the rate of the water-gas shift increases with temperature. The curves for the cobalt catalyst were only slightly lower than the corresponding ones for iron catalysts.* However, the rate of synthesis at a given temperature is considerably greater with the cobalt catalysts than with the iron; high conversion can be attained at 185 to 190°C with the cobalt catalyst compared with about 230°C for the iron catalyst. On this basis, the cobalt

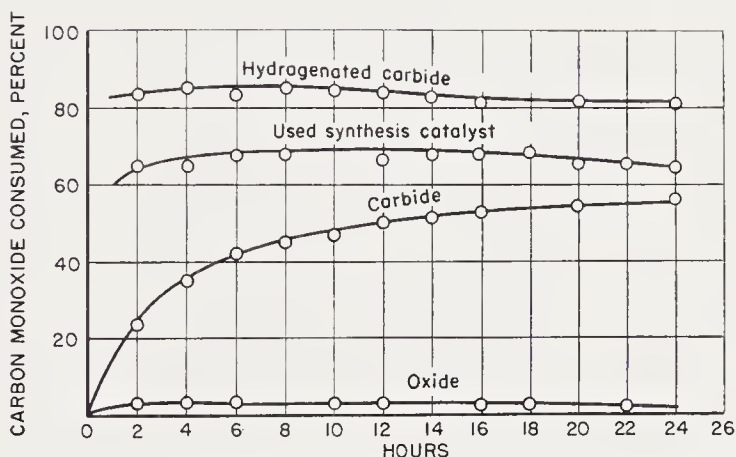


Figure 42. Reaction of carbon monoxide and water at 240° on iron catalyst. Space velocity of $1\text{CO} + 1\text{H}_2\text{O}$ of 100 hr^{-1} . (Reproduced with permission from Ref. 77)

catalyst at 185 to 190°C would be expected to produce very little carbon dioxide and the iron catalyst at 230°C large amounts.

In a second paper, Koelbel and Engelhardt⁷⁹ studied the variation of conversion of $1\text{H}_2\text{O} + 1\text{CO}$ gas as a function of space velocity at atmospheric pressure on a precipitated iron catalyst. Their data in Figure 45 are similar to those for the synthesis and can be represented by Eq. (9) up to conversions of about 65 per cent.

Cobalt and nickel catalysts are not appreciably oxidized by $\text{H}_2\text{O} + \text{CO}$ mixtures; however, iron catalysts may either be oxidized or reduced, depending upon the relative amounts of water and carbon monoxide. Koelbel and Engelhardt⁷⁹ measured the production of carbon dioxide at 240°C as a function of time and $\text{CO}:\text{H}_2\text{O}$ ratio for a pretreated, precipitated iron-copper catalyst, as shown in Figure 46. Initial carbon dioxide production was greatest with $1\text{CO} + 1\text{H}_2\text{O}$ and $4\text{CO} + 3\text{H}_2\text{O}$ gas; the rate, however,

* White and Shultz¹³⁸ have shown that fused cobalt oxide catalysts are more active in the water-gas-shift than usual iron shift catalysts.

decreased with time. With $2\text{CO} + 1\text{H}_2\text{O}$ and $4\text{CO} + 1\text{H}_2\text{O}$, the production of carbon dioxide was constant after about 20 hours. Values for the percentage of reduced iron (including $\alpha\text{-Fe}$ and carbides) in the catalysts after the pretreatment (68 per cent) and at the end of the experiment

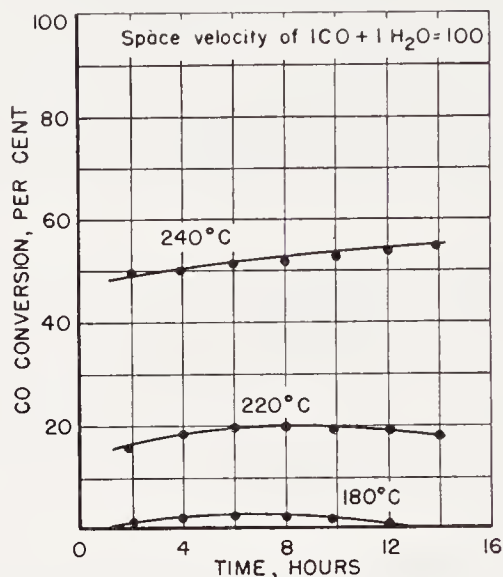


Figure 43. Conversion of carbon monoxide in a mixture of carbon monoxide and water vapor on a used cobalt catalyst as a function of temperature. (Reproduced with permission from Ref. 77)

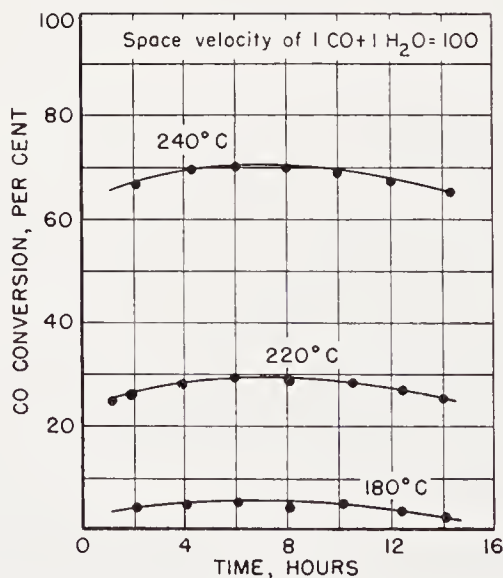


Figure 44. Conversion of carbon monoxide in a mixture of carbon monoxide and water vapor on a used iron catalyst as a function of temperature. (Reproduced with permission from Ref. 77)

(Figure 46) indicate that the reduced iron content was unchanged with $2\text{CO} + 1\text{H}_2\text{O}$ and $4\text{CO} + 1\text{H}_2\text{O}$ gas, but had decreased considerably with $4\text{CO} + 3\text{H}_2\text{O}$ and $1\text{CO} + 1\text{H}_2\text{O}$ gas. In tests with $2\text{CO} + 1\text{H}_2\text{O}$ gas at atmospheric pressure and 200 to 240°C, the catalyst, which was reduced

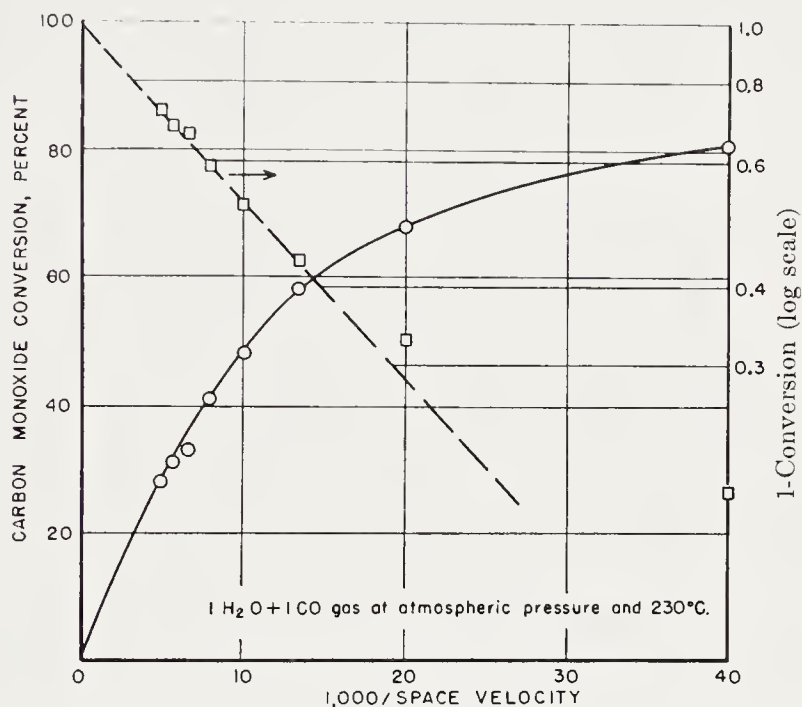


Figure 45. Variation of conversion with reciprocal space velocity for $\text{CO} + \text{H}_2\text{O}$ reaction on iron catalyst. (From data of Ref. 79)

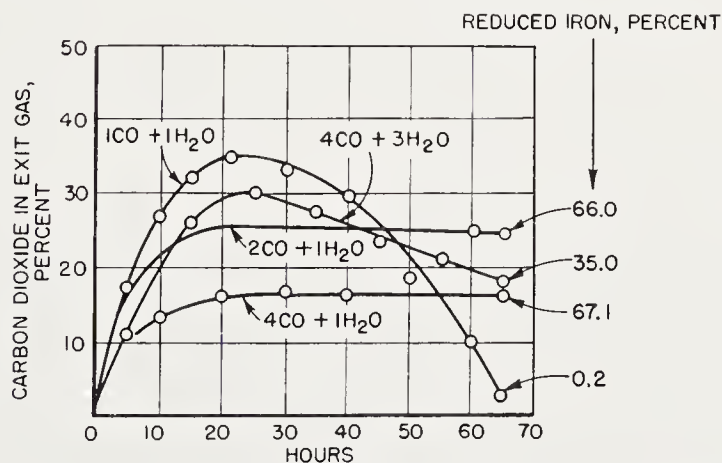


Figure 46. Oxidation of pretreated Fe-Cu catalyst by water as a function of relative amounts of carbon monoxide and water. Space velocity of 100 hr^{-1} and 240°C . (Reproduced with permission from Ref. 79)

68 per cent in the pretreatment, was not oxidized, although the carbon dioxide production increased with temperature (Figure 47).

Although the principal studies of the production of hydrocarbons from water and carbon monoxide have been made by Koebel and co-workers, this problem had been considered previously. Koch and Kuster⁷² studied the reaction of water and blast furnace gas (CO 30.2, H₂ 2.8, CO₂ 8.0, CH₄ 0.0, O₂ 0.4, and N₂ 58.6 per cent, respectively) on cobalt and nickel cata-

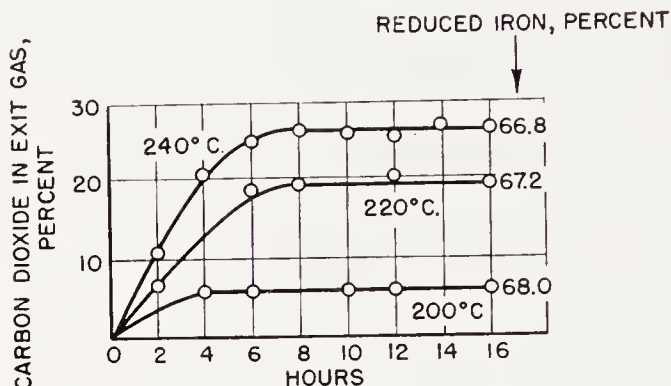


Figure 47. Reaction of water and carbon monoxide on pretreated Fe-Cu catalyst. Space velocity of $2\text{CO} + \text{H}_2\text{O}$ of 100 hr^{-1} . (Reproduced with permission from Ref. 79)

TABLE 8. FEED AND EXIT GAS ANALYSES^a
(Blast furnace gas plus water, $\text{CO}:\text{H}_2\text{O} = 3$, 235°C and 10 atm.)

	Per cent by volume						
	CO ₂	CO	H ₂	Olefins	N ₂	Paraffins	Carbon Number of Paraffins
Feed gas	0.0	29.0	1.0	0.0	70.0	0.0	—
Exit gas	17.5	1.1	2.4	0.7	76.9	1.5	1.35

^a From Ref. 80.

lysts at atmospheric pressure and 200 to 350°C . The gas was 13, 25, or 50 per cent saturated with water vapor. With the cobalt catalyst a maximum of only 1.5 per cent methane was found in the exit gas at 250°C , and apparently no higher hydrocarbons were produced. The water-gas-shift reaction proceeded slowly so that the exit gas contained 4.2 and 21.9 per cent of hydrogen at 210 and 300°C , respectively. The nickel catalyst was somewhat more active, and in some cases the percentage of methane in the exit gas was as high as 8 to 9 at 250 and 300°C . Traces of higher gaseous hydrocarbons were produced at 250°C . The extent of the water-gas-shift reaction increased with temperature; however, when high yields of methane

were produced, the hydrogen content of the exit gas was correspondingly decreased. These data demonstrate that the water-gas reaction was more rapid than reactions producing methane.

Koelbel and Engelhardt⁸⁰ described tests with precipitated iron catalysts in which typical Fischer-Tropsch products were produced from $\text{CO} + \text{H}_2\text{O}$

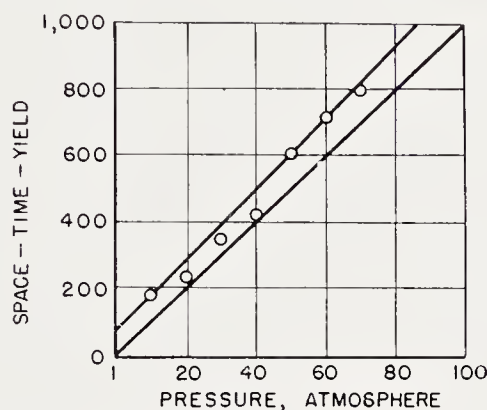


Figure 48. Variation of rate of synthesis from $\text{H}_2\text{O} + \text{CO}$ with operating pressure. (Reproduced with permission from Ref. 80)

TABLE 9. COMPOSITION OF PRODUCTS FROM $\text{H}_2\text{O} + \text{CO}$ AS A FUNCTION OF OPERATING PRESSURE^a

Pressure, atm. absolute	Composition of Liquid Plus Solid Oil Phases			
	Density (d_{20}^4)	Oxygen Content (%)	Alcohols (wt. %)	Acid number (mg KOH/g)
1	0.747	0.10	0.1	0.7
11	.744	.72	.4	3.0
31	.747	1.04	3.0	5.3
51	.762	1.00	5.2	7.2
71	.775	3.03	12.1	10.8
101	.768	7.10	29.5	30.5

^a From Ref. 80.

gas. The thermodynamics and stoichiometry of these reactions were also considered. At 235°C , 10 atm., and a space velocity of $100\text{--}200\text{ hr}^{-1}$, high conversions of blast furnace gas plus water ($\text{CO}/\text{H}_2\text{O} = 3$) were attained with yields of total hydrocarbons of 195 g/m^3 of carbon monoxide. The feed and exit gas analyses (Table 8) show increases in the concentrations of both hydrogen and carbon dioxide during synthesis and rather complete consumption of carbon monoxide.

A series of tests was made at varying pressures, presumably with a constant $\text{CO}/\text{H}_2\text{O}$ ratio and at constant temperature; however, these conditions

are not specified. The conversion of carbon monoxide was held at about 90 per cent by varying the space velocity as the pressure was changed. A plot of space-time-yield, under these conditions an index of activity, against pressure was approximately a straight line, as shown in Figure 48. The changes in the composition of reaction products are shown in Table 9. These data indicate that both the rate of synthesis and the selectivity vary with pressure in the same way as in the usual Fischer-Tropsch synthesis.

The temperature dependence of the synthesis, presumably with $3\text{CO} + 1\text{H}_2\text{O}$ gas at constant space velocity and atmospheric pressure, was studied. Tests were made at 10°C intervals from 200 to 300°C ; each test used a freshly reduced sample of supported iron catalyst and was continued for 150 hours. Yields of methane and total hydrocarbons and the conversion of

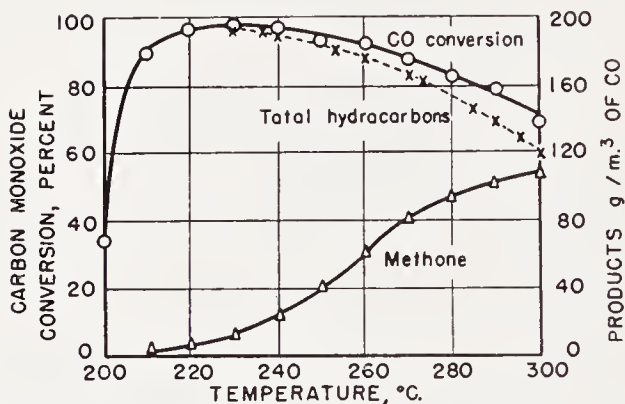


Figure 49. Influence of temperature on synthesis with $3\text{CO} + 1\text{H}_2\text{O}$ on iron catalysts. (Reproduced with permission from Ref. 80)

carbon monoxide are shown as a function of temperature in Figure 49. Only the water-gas-shift occurred at 200°C . At 210°C the carbon monoxide conversion had increased to 90 per cent and the yield of total hydrocarbons was 185 g/m^3 of carbon monoxide. The yield of methane increased with temperature. The yields of total hydrocarbons and the conversion of carbon monoxide increased to a maximum at about 230°C and then decreased. These decreasing yields and conversion were related to the change in stoichiometry due to the greater production of methane. The usage ratio, $\text{CO}/\text{H}_2\text{O}$, is 2 for methane compared with about 3 for higher hydrocarbons. Hence, if the feed gas was $3\text{CO} + 1\text{H}_2\text{O}$, complete consumption of this gas would not be possible when sizable yields of methane are produced.

SELECTED REACTIONS OF POSSIBLE IMPORTANCE TO THE FISCHER-TROPSCH MECHANISM

The mechanism of the Fischer-Tropsch synthesis probably involves a series of consecutive as well as side reactions. Before attempting to unravel

the complex synthesis mechanism, a few reactions that may be involved in the synthesis will be considered. A detailed presentation is beyond the scope of this chapter, since many of these reactions are covered in other parts of this series. The selection of reactions is somewhat arbitrary. It should be emphasized that reactions in the absence of one or more of the components of the normal synthesis may be entirely different from reactions in their presence.

Hydrocracking of Paraffins

Taylor and Taylor¹²⁵ studied the hydrocracking of ethane to methane on cobalt catalysts. The reaction was moderately slow at usual synthesis temperatures, with a Co-Cu-ThO₂-kieselguhr catalyst being somewhat less active than a cobalt catalyst supported on magnesia. Activation energies of 31 to 34 kcal/mole were reported. The authors suggested the desirability of examining synthesis catalysts in a separate reaction such as this, because only one phase of a complex process may be examined. Studies of this type may indicate the causes of ineffective catalysts. In the hydrocracking of ethane the rate increased in the following order: Co-Cu-ThO₂-kieselguhr, Co-MgO, and nickel catalysts. The tendency to produce liquid and solid hydrocarbons in the hydrogenation of carbon monoxide falls in the opposite order.

Thompson, Turkevich, and Irsa¹²⁶ studied the reaction of deuterium with paraffin hydrocarbons on a typical Co-ThO₂-MgO-kieselguhr catalyst at 183°C and atmospheric pressure. Mixtures of 6 volumes of D₂ plus 1 volume of hydrocarbon at space velocities of about 150 hr⁻¹ were used. With methane no exchange occurred under these conditions; however, when the mixture was in contact with the catalyst for 17 hours, 11 per cent exchange occurred. The principal product was CH₃D with smaller amounts of CD₄. Exchange between CH₄ and CD₄ was also very slow. Under synthesis conditions, 6 per cent of the ethane exchanged with D₂ and small amounts of deuterated methane were formed. The principal products were C₂D₆ (2.4 per cent) and C₂H₄D₂ (2.7 per cent). Under similar conditions propane yielded C₃D₈ (4.7 per cent) and C₃D₇H (1.4 per cent) and small amounts (1 to 2 per cent) of deuterated methane. With normal and isobutane under synthesis conditions, about half of the hydrocarbon exchanged. With *n*-butane only higher deuterated molecules were produced. When the space velocity was increased to 3000 hr⁻¹, the extent of exchange decreased sharply, but the only product was C₄D₁₀. Apparently this molecule is the primary product, and other species are produced by back hydrogenation. Although deuterated methane was produced, no ethane or propane was formed. With isobutane, C₄D₁₀ also appears to be the primary product of exchange.

These experimental results suggest that CH_3 and C radicals are produced from methane, C_2H_4 and C_2 from ethane, C_3 from propane, and C_4 from butanes. An alternate explanation is that alkyl radicals are produced on the surface, but their retention time is sufficiently long to permit all of the hydrogen to be exchanged. This research demonstrates clearly that gaseous paraffin hydrocarbons do not hydrocrack rapidly on a cobalt catalyst at flows and temperatures of the synthesis. Furthermore, exchange reactions are slow for C_1 to C_3 paraffins.

Haensel and Ipatieff⁵⁷ studied the hydrocracking of paraffin hydrocarbons on nickel and cobalt catalysts at temperatures from 250 to 290°C and pressures from 100 to 900 psig. The process was shown to involve a stepwise demethylation of the hydrocarbon. Methyl groups attached to secondary carbon atoms ($-\text{C}-\text{C}-\text{CH}_3$) were most readily hydrogenated,

those attached to tertiary carbons ($\text{C}-\overset{\text{C}}{\underset{\text{C}}{\text{C}}}-\text{CH}_3$) less readily, and methyl groups attached to quaternary carbon atoms ($-\text{C}-\overset{\text{C}}{\underset{\text{C}}{\overset{\text{C}}{\text{C}}}}-\text{CH}_3$) were most

resistant to hydrogenation. On this basis the hydrocarbons resulting from extensive demethylation contain a greater fraction of branched molecules than the original material. Thus the ease of demethylation of straight chain hydrocarbons parallels the ease of formation of these carbon chains in the Fischer-Tropsch synthesis. The rate of hydrocracking increased with an increase in temperature, but decreased with an increase in operating pressure and apparently with an increase in the partial pressure of hydrogen.

Koch and Titzenthaler⁷³ utilized this demethylation reaction to characterize the chain branching of high molecular weight hydrocarbons. The hydrocarbon was hydrocracked over a $\text{Co-ThO}_2\text{-MgO-kieselguhr}$ catalyst at atmospheric pressure and temperatures from 180 to 240°C. The products boiling from 25 to 175°C were analyzed by precision distillation. From the isoparaffin content of this fraction, an estimate was made of the degree of chain branching in the original high molecular weight product. In tests with a cobalt catalyst traces of ammonia very strongly inhibited the hydrocracking of hexane. At 205 to 210°C the percentage of methane in the exit gas was only 1 to 2 when ammonia was added compared with 85 to 90 in the absence of ammonia. A precipitated $\text{Fe}_2\text{O}_3\text{-CuO-K}_2\text{CO}_3$ catalyst after reduction in hydrogen at 235°C was inactive in hydrocracking of wax at 200 to 350°C; however, the catalyst was active in hydrogenation of carbon monoxide at 220°C.

Koch and Gilfert⁷¹ studied the hydrocracking of saturated hydrocarbons

over a Co-ThO₂-MgO-kieselguhr catalyst at 200°C and atmospheric pressure. The hydrocarbons were recirculated in hydrogen over the catalyst for periods of 2 to 5 days in a distillation system that separated higher boiling compounds. The hydrocarbons were extensively hydrocracked; however, a portion of product had carbon numbers greater than that of the original hydrocarbon and a small amount of isomerization had occurred. Thus, 53 per cent of *n*-hexane disappeared in 83 hours, about half appearing as methane; the product contained 1.3 per cent isohexanes, 4.2 heptanes, and 0.7 higher hydrocarbons. Similar results were obtained with *n*-heptane and *n*-octane. With 2-methylpentane, 33 per cent was transformed in 70

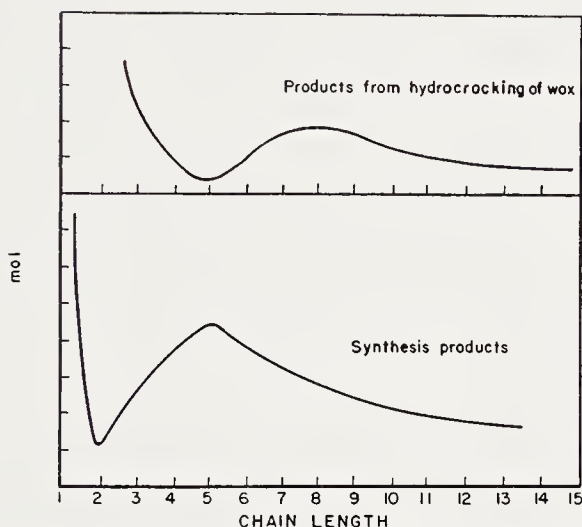


Figure 50. Comparison of the products formed by hydrogenation of a used cobalt catalyst with those formed in the synthesis. (Reproduced with permission from Ref. 24)

hours. In C₄+ fractions, branched hydrocarbons predominated, a consequence of the greater stability of branched structures. Small amounts of C₇ and higher hydrocarbons were produced. The amount of cyclohexane that disappeared in 46 hours was 27 per cent. The product contained, in addition to straight chain C₁ to C₅ hydrocarbons, 3.4 per cent cyclopentane, 15.7 benzene, 46.4 toluene, and 3.6 xylenes.

The presence of methane in the hydrogen sharply decreased the transformation of *n*-hexane, with only 13 per cent disappearing in 98 hours (compared with 53 per cent in 83 hours in pure hydrogen). Although sizable amounts of gaseous hydrocarbons were produced, the yields of C₇ and C₈+ hydrocarbons were appreciably increased by the presence of methane, 13.4 and 3.8 per cent of the transformation products, respectively. *n*-Hexane did not react in pure methane.

Craxford²⁴ presented data on the hydrocracking of wax deposited on

standard, unpelleted cobalt catalyst. In three weeks of atmospheric pressure synthesis at 185°C, 20 to 25 grams of wax were deposited upon the catalyst; the volume of this wax corresponded to about half of the pore volume. Under synthesis conditions when hydrogen rather than $2\text{H}_2 + 1\text{CO}$ gas was passed over the catalyst, about 15 grams of wax were removed in 3 hours. The rate of removal of wax (5 g/hr) was about five times faster than the usual total synthesis rate. The carbon number distribution of the products from this type of hydrocracking in Figure 50 was similar in shape to the distribution from the synthesis, with the minimum and maximum shifted to higher carbon numbers for the products from hydrocracking. There seems to be no simple explanation for the similarity of the two curves.

Craxford's results demonstrate that the rate of hydrocracking must be very slow in the presence of carbon monoxide. Apparently the saturated hydrocarbons are only weakly chemisorbed on metallic catalysts, and the presence of strongly adsorbed molecules, such as carbon monoxide, ammonia, water and olefins, will seriously decrease the rate of hydrocracking. This reaction is also inhibited by large amounts of chemisorbed hydrogen, because the rate decreases with increasing partial pressure of hydrogen.

Incorporation of Hydrocarbons in the Hydrogenation of Carbon Monoxide

In studies of the Fischer-Tropsch synthesis "incorporation" denotes the reaction of a given molecule of carbon number n with hydrogen and carbon monoxide to yield a product of carbon number greater than n . As shown in Chapter 1, it is thermodynamically possible to incorporate olefins at any ratio of olefin to carbon monoxide. The thermodynamics of incorporating paraffins are less favorable and the reactions are possible only for ratios of paraffin to carbon monoxide less than some value. For example, in the incorporation of methane to produce n -decane and water at 300°C, the equilibrium constant becomes less than 1 when the ratio of $\text{CH}_4:\text{CO}$ reacting is greater than 0.25.

Data for the incorporation of methane are contradictory in that some workers have reported incorporation and others have found none. Either the preparation and pretreatment of catalysts must be very critical in this reaction, or some of the analytical data are incorrect. With cobalt catalysts, Craxford²⁴ observed yields of liquids plus solid hydrocarbons of 96 g/m³ of synthesis gas when 20 per cent nitrogen was added compared with 113 g/m³ of synthesis gas when 16 per cent methane was added. Methane formation was entirely suppressed by the added methane. Similar results were obtained when feed gases containing 50 per cent nitrogen or 50 per cent methane were compared. Craxford postulated that methane was dis-

sociatively adsorbed and participates in a polymerization-depolymerization equilibrium at the catalyst surface. Prettre and Perrin^{98, 107} reported that sizable amounts of methane were consumed in the synthesis on $\text{Ni-Al}_2\text{O}_3$ (or MnO)-kieselguhr catalysts when the synthesis gas contained 25 or more per cent methane. Figure 51 presents the moles of methane consumed per mole of $\text{H}_2 + \text{CO}$ consumed as a function of hours of testing. With feed

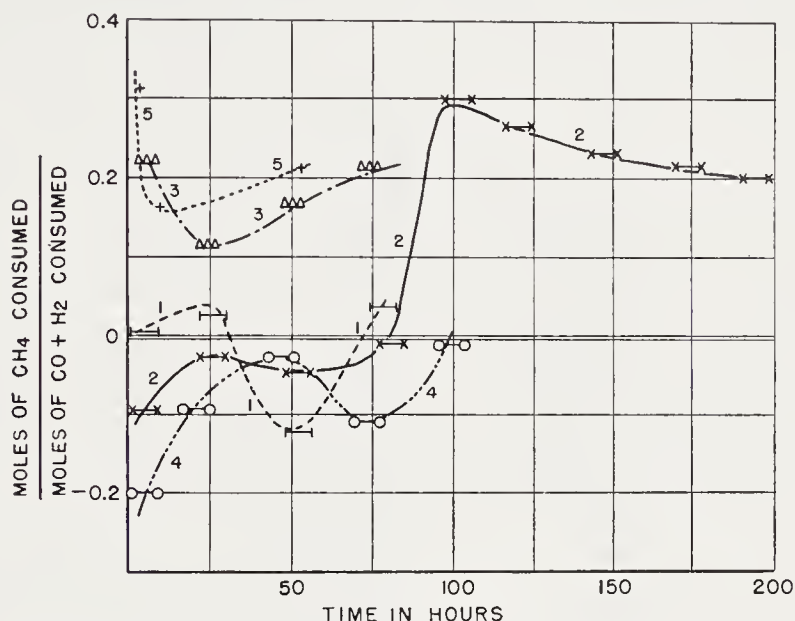


Figure 51. Utilization of methane on nickel catalysts with mixtures of methane and 2H_2 to 1CO gas.

- Curve 1, catalyst A.7 at 190°C ., 50 % CH_4
- x-x Curve 2, catalyst C.I. 1 at 190°C ., 50 % CH_4
- △△ Curve 3, catalyst C.I. 4 at 190°C ., 75 % CH_4
- Curve 4, catalyst C.I. 4 at 190°C ., 25 % CH_4
- + Curve 5, catalyst C.I. 6 at 175°C ., 50 % CH_4

The length of the lines indicate the period in which the individual determinations were made. Reproduced with permission from reference 98.

gas containing 75 per cent methane at 190°C and 50 per cent methane at 175°C , methane consumption was consistently high, approaching the ratio of 0.7CH_4 to 1CO .

On the other hand, Kummer, DeWitt, and Emmett⁸³ found that methane was not incorporated in atmospheric tests of cobalt and iron catalysts. A mixture of 50 per cent synthesis gas and 50 per cent methane containing C^{14}H_4 was circulated over the catalyst, and the higher hydrocarbon products were analyzed for radioactive C^{14} . The products in no case showed appreciable radioactivity. The reliability of the tracer technique is very much

greater than the comparison of net changes in large quantities of methane by conventional analytical methods.

Koelbel and Ackermann⁷⁴ studied the increase in molecular weight of the suspension oil of the slurry process with an iron catalyst and $1\text{H}_2 + 2\text{CO}$ gas at 10 atm. and 240°C . The cooling oil was a 270 to 330°C distillation fraction of a product from the atmospheric cobalt synthesis. The original fraction contained 11 per cent olefins, and a portion was hydrogenated until the olefin content was about 2 per cent. The two oils were used as a sus-

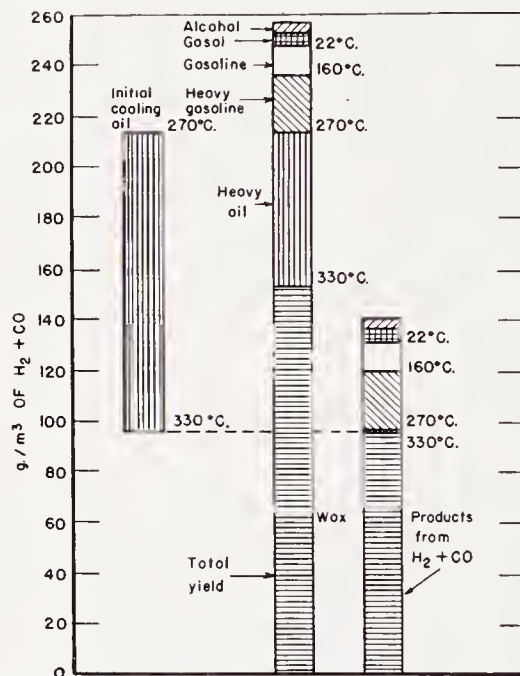


Figure 52. Comparison of products of slurry process with initial cooling oil after 390 hours of synthesis. (Reproduced with permission from Ref. 74)

pension medium in the slurry synthesis. The total products were recovered and a material balance was made on the basis of cubic meters of synthesis gas passed, as shown in Figure 52, for synthesis with the low-olefin-content oil. After 93 hours of synthesis, it was possible to recover only about 50 per cent of the 270 to 330°C fraction by distillation. Similar results were obtained with the olefinic suspension oil. Apparently the molecular weight of the oil was increased during the synthesis. The conditions for incorporation of high molecular weight hydrocarbons are very favorable, since the residence time of the suspension oil in contact with the catalyst is very long compared with conditions in a dry-bed reactor.

Smith, Hawk, and Golden¹¹⁸ studied the mechanism of the Fischer-Tropsch reaction with respect to possible reactions of hydrocarbons on

cobalt and iron catalysts at atmospheric pressure. A C_6^+ fraction of synthesis product was passed over a Co-Cu-manganese oxide catalyst in nitrogen at 206°C. The oil was recovered essentially unchanged, indicating that no cracking occurred on the catalyst in the absence of hydrogen.

Next, reactions of ethylene were investigated. Ethylene and mixtures of ethylene plus carbon monoxide were unchanged in passing over the catalyst at synthesis temperatures. Mixtures of ethylene and hydrogen produced only ethane. Ethylene in the presence of synthesis gas was, however, incorporated. Mixtures of approximately $1H_2 + 1CO + 1C_2H_4$ and $1H_2 + 1CO + 1N_2$ were compared in the synthesis. At 204°C the liquid "hydrocarbons" from the feed gas containing ethylene were 860 g/m³ of carbon monoxide compared with 300 g/m³ for the gas containing nitrogen. In addition, a sizable portion of the ethylene was hydrogenated to ethane, and a fraction of the hydrogen was consumed in this reaction. The liquid "hydrocarbons" from the ethylene experiments contained 25 to 35 per cent oxygenated molecules compared with only traces of oxygenates from the normal synthesis. The oxygenated material was shown to contain aldehydes and alcohols; however, a complete analysis was not reported. Samples of the liquid product from the ethylene experiments were passed over the catalyst at 211°C in a stream of nitrogen, hydrogen, or carbon monoxide. Water corresponding to about 15 per cent of the original oil was eliminated. From these results the authors suggested that the oxygenated molecules may be intermediates in the synthesis, but are normally converted to hydrocarbons by reactions on the catalyst, so that virtually none of this material leaves the catalyst bed. Further evidence for this hypothesis was given by experiments in which the yield of oxygenated material was shown to increase sharply as the ethylene content was increased.

Similar atmospheric pressure experiments were made with precipitated iron catalysts; however, ethylene in the presence of synthesis gas was neither incorporated nor hydrogenated.

Ruschenburg¹¹² studied the incorporation of ethylene, propylene, and butylene as well as a "gasol" fraction from the commercial cobalt synthesis on standard Co-ThO₂-kieselguhr and Co-ThO₂-MgO-kieselguhr catalysts at atmospheric pressure and 187 to 200°C. The gasol fraction contained 12 volume per cent propylene, 23 butylene, 37 propane, 22 butane, and 6 of other gases. Usually the gasol was added in amounts by volume corresponding to 4 to 14 per cent of the synthesis gas. The gasol incorporated into the synthesis products varied from 38 to 85 per cent of the olefins introduced. Butylene and ethylene were incorporated to about the same extent as the olefins of the gasol, but propylene was incorporated to a considerably smaller extent. The liquid products from the synthesis in the presence of olefins contained very little oxygen.

Eidus and co-workers studied the incorporation of ethylene in the presence of hydrogen and carbon monoxide at atmospheric pressure, presumably on a cobalt catalyst; however, the nature of the catalyst has not been disclosed. In the first paper³² $2\text{H}_2 + 1\text{CO} + 3\text{C}_2\text{H}_4$ gas was passed over the catalyst at a space velocity of 100 hr^{-1} and 190 to 200°C . The total oil yield from this gas mixture was 343 cc/m^3 compared with 123 cc/m^3 from $2\text{H}_2 + 1\text{CO}$ gas. Of the ethylene introduced, about 80 per cent was incorporated and 20 per cent hydrogenated to ethane. Each mole of carbon monoxide reacted with 2 to 3 moles of hydrogen and 3 to 4.5 moles of ethylene. The yields of oxygenated molecules, especially alcohols, were slightly greater than those produced from $2\text{H}_2 + 1\text{CO}$, and propyl alcohol was detected. The product contained, however, principally saturated and unsaturated hydrocarbons of both odd and even carbon numbers. In subsequent work^{31, 33}, equimolar mixtures of hydrogen and ethylene plus 4 to 7 per cent carbon monoxide were converted to liquids boiling below 300°C and containing over 70 per cent olefins.

Eidus³⁰ investigated the incorporation of 1-butene with hydrogen and carbon monoxide on an undisclosed catalyst. Gases containing $1\text{H}_2 + 0.08\text{CO} + 1\text{C}_4\text{H}_8$ were passed over the catalyst at atmospheric pressure, 190°C , and a space velocity of about 100 hr^{-1} . In a typical experiment, 97 per cent of the butylene reacted, 74 per cent of the hydrogen, and 100 per cent of the carbon monoxide. The yields of light plus heavy oil were 565 cc/m^3 . In another experiment, 11 per cent of the butylene was not consumed and 20 per cent was hydrogenated to butane. Precision distillation showed that the C_5 , C_6 , C_7 , C_8 , and C_9 fractions contained, respectively, 24, 15, 8, 8, and 9 volume per cent of the liquid hydrocarbon fraction. These results suggest that chain-growth may be stepwise, one carbon atom at a time, since the yield of C_8 hydrocarbons, which could be formed by dimerization, was about the same as C_7 and C_9 . One half of the C_5 fraction was isopentane, indicating the possibility that the chain growth mechanism is similar to that of the oxo synthesis with respect to chain branching. The liquid condensate was composed of aliphatic hydrocarbon containing 28 per cent olefins. In a subsequent paper^{29a}, the incorporation of isobutylene was shown to be as rapid as that of butene-1. The liquid hydrocarbons contained 12, 22, 22, and 12 per cent in the C_5 , C_6 , C_7 , C_8 fractions. These hydrocarbons were predominantly 2-methyl substituted molecules. Further incorporation studies^{29b} using 2-methyl butene-2 and 2,3-dimethyl butene-2 indicated that these molecules were incorporated to only a small extent, less than 10 per cent, whereas 30 to 50 per cent of the olefin was hydrogenated.

In unpublished experiments of the U. S. Bureau of Mines¹ on Co-ThO_2 -kieselguhr catalyst at about 190°C with gas containing $2\text{H}_2 + 1\text{CO}$ and 20 to 80 per cent ethylene at atmospheric pressure and 7.8 atm., almost all

of the ethylene was either incorporated or hydrogenated. At atmospheric pressure, the ratios of moles of ethylene incorporated to moles of carbon monoxide consumed were 0.8 and 1.7 for feed gases containing 20 and 80 per cent ethylene, respectively. At 7.8 atm. this ratio was 0.14 for the lower concentration of ethylene. In atmospheric pressure experiments, propylene was not completely consumed and was incorporated to the extent of 0.2 mole per mole of carbon monoxide consumed.

Infrared analyses of liquid "hydrocarbon" fractions indicated only a slight increase in oxygenated molecules during olefin incorporation compared with the normal synthesis products. In most instances the differences in yields of oxygenated molecules were only slightly larger than the experimental errors of the analytical method, and in all cases the yield of oxygenated molecules was very low.

These results¹ are essentially in agreement with those of Eidus and Ruschenburg in demonstrating a large incorporation of olefins without sizable yields of oxygenated molecules and differ from the results of Smith, Hawk, and Golden¹¹⁸, in which the production of oxygenates was high. The differences in selectivity probably can be related to differences in the catalyst used. Further experimentation on incorporation of olefins, especially tests at high space velocity and low conversion, may reveal whether or not oxygenated molecules are produced and subsequently converted to hydrocarbons, as suggested by Smith, Hawk, and Golden.

Catalytic Reactions of Alcohols and Their Incorporation in the Synthesis

On nickel catalysts, primary aliphatic alcohols decompose according to the following reaction path: (a) dehydrogenation to the corresponding aldehyde, (b) deformylation of the aldehyde to carbon monoxide and an olefin having one carbon atom less than the alcohol, and (c) hydrogenation of the olefin. At 230°C decanol-1 decomposed catalytically to yield 43 mole per cent of *n*-nonane, 36 of nonene, and 21 of decylaldehyde¹². Similarly, at 250°C, heptaldehyde decomposed on a nickel catalyst to hexane and hexene¹²⁴. On nickel-kieselguhr catalysts⁶⁷, the rate of decomposition of primary alcohols decreased with an increase of operating pressure. Fischer and Koch⁴⁴ passed methanol over a nickel catalyst in either hydrogen or nitrogen at atmospheric pressure and 185 to 210°C. Sizable yields of liquid hydrocarbons, apparently similar to normal synthesis products, were obtained. Higher yields of liquid hydrocarbons were produced in the presence of hydrogen. In similar experiments with formic acid, only small amounts of higher hydrocarbons were formed, the principal products being carbon dioxide and hydrogen.

Eidus²⁸ studied the decomposition of methanol and ethanol on cobalt-

thoria-kieselguhr at atmospheric pressure and 170 to 200°C. Hydrogen, carbon monoxide, and gaseous and liquid hydrocarbons were obtained from methanol. The hydrocarbons were similar to those produced in the normal synthesis; however, the rate of hydrocarbon production was lower with methanol than with synthesis gas. The rate of hydrocarbon production from methanol increased when hydrogen was added. With ethanol large yields of methane were obtained in addition to gaseous and liquid hydrocarbons. Eidus postulated that the alcohols decomposed by the scheme described above and that hydrogen and carbon monoxide combine in usual synthesis reactions.

Gall, Gibson, and Hall⁵² studied the decomposition of primary alcohols on cobalt Fischer-Tropsch catalysts in the presence of hydrogen. The rate of decomposition of ethanol was low. The decomposition of C₃ and higher alcohols was more rapid, with the rate increasing slightly with carbon number. Gibson⁵⁴ continued these studies. At 150 to 185°C, the rate of decomposition of propanol-1 expressed as space-time-yield, xS , increased approximately linearly with the flow of alcohol and could be expressed by the equation

$$xS = aS + b \quad (20)$$

or

$$x = a + b/S \quad (21)$$

Equation 21 will also express the kinetics of the synthesis on cobalt catalysts for a limited range of conversion (p. 266), and where Eq. 21 holds, the differential reaction rate, $dx/d(1/S)$, is constant. With other alcohols from methyl to *n*-decyl, the moles of alcohol decomposed also increased with flow, but data were obtained at two flows only. The variation of decomposition rate with temperature was studied for *n*-propyl and *n*-octyl alcohols in the range 150 to 185°C, and activation energies of 23 to 24 kcal/mole were obtained. These values compare favorably with activation energies of 24 to 26 kcal/mole obtained in the atmospheric synthesis⁸. When the system pressure was increased from atmospheric to 11 atm., the rate was decreased by about 25 per cent. The rate of decomposition of alcohols in hydrogen was found to be 1.5 to 2.0 times greater than in hydrogen containing 5 to 10 per cent carbon monoxide. The rate of alcohol decomposition in the presence of carbon monoxide was, however, about the same as rate of synthesis in 2H₂ + 1CO gas (here, moles of alcohol decomposed per unit time are compared with moles of carbon monoxide consumed).

The influence of chain length on the catalytic decomposition of normal primary alcohols at 150 and 180°C is shown in Figure 53. Ethanol decomposed

at the lowest rate, a fact which may explain the large yields of ethanol from the synthesis. The rate of decomposition of propanol-1 at 150°C was the most rapid of all the alcohols at 150°C, but at 185°C propanol decomposed relatively slowly. Experiments with secondary, iso-, and normal butyl alcohols showed that the rate for the secondary isomer was about twice as great as for the other two. The rate of decomposition of butanol-2 was not sufficiently large, however, to explain the absence of this isomer in synthesis products.

Gibson also examined the decomposition products. Methanol produced $2\text{H}_2 + 1\text{CO}$ and typical Fischer-Tropsch products; however, the decompo-

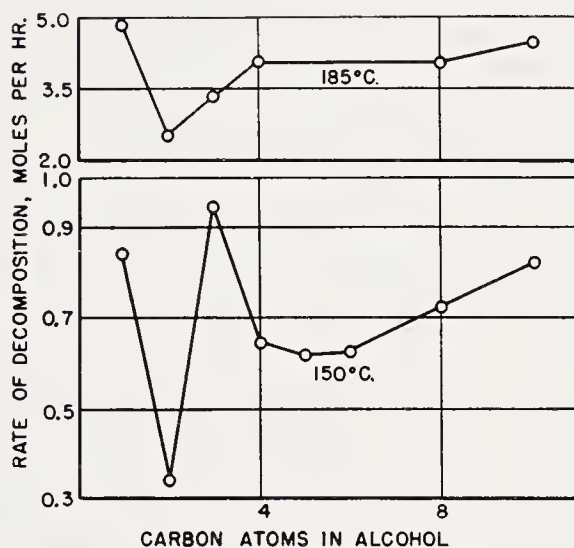


Figure 53. Rate of decomposition of primary straight-chain alcohol on a cobalt catalyst. (Reproduced with permission from Ref. 54)

sition of higher alcohols in the presence of hydrogen was more complex than the decomposition on nickel catalysts described on p. 319. For ethanol the carbon number of the gaseous product was about 1.6. Higher alcohols of carbon number n decomposed principally to hydrocarbons of carbon number n plus smaller yields of $n - 1$ hydrocarbons. Propyl and higher alcohols gave moderately high yields of ethers; however, the author concluded that ether formation has no part in the Fischer-Tropsch mechanism, because ethers, although somewhat more stable than alcohols, are not found in synthesis products. Aldehydes decomposed at a slower rate than the corresponding alcohols, and formation of ester and acid probably resulted from the reactions of aldehydes. From alcohols of carbon number n , hydrocarbons with carbon atoms equal to or greater than $n - 2$ were produced at 150°C and $n - 3$ at 185°C. Hence, hydrocracking reactions were not very important. Hydrocarbons containing more carbon atoms than the alcohols were

produced in amounts as high as 14 per cent. The mode of decomposition of alcohols on cobalt catalysts in the presence of hydrogen is different from that of alcohols on nickel catalysts described previously. The kinetics of alcohol decomposition on cobalt catalysts are similar to the Fischer-Tropsch synthesis with respect to the dependence of rate on temperature and space velocity.

Gibson⁵⁴ obtained evidence that alcohols were incorporated into the synthesis with cobalt catalysts. At 185°C with $9\text{H}_2 + 1\text{CO}$ gas about 21 per cent of the reacted ethanol was apparently found in the C_5^+ fraction, and in another experiment 7 per cent of the reacted propanol appeared to be incorporated.

In exploratory experiments, Stein¹¹⁹ passed primary alcohols over cobalt catalysts at atmospheric pressure and usual synthesis temperatures. The decomposition pattern was that described earlier for alcohols on nickel catalysts. Thus, from *n*-propyl alcohol, hydrogen, C_2 hydrocarbons, and a complex liquid mixture containing principally propylaldehyde were obtained. The only major difference between the experiments of Stein and Gibson seems to be that Gibson used hydrogen as a carrier gas and Stein introduced pure alcohol vapor.

Further exploratory tests at the Bureau of Mines¹²¹ indicate that the decomposition of C_2 to C_4 primary alcohols on fused iron catalysts at atmospheric pressure and 200 to 300°C yielded a gaseous product containing chiefly hydrogen with only minor quantities of hydrocarbons. The principal liquid product was the corresponding aldehyde.

Kummer, Emmett and co-workers^{85, 86} studied the incorporation of alcohols tagged with C^{14} in the atmospheric synthesis with fused iron catalysts. Only small concentrations of alcohols were added to the synthesis gas (about 1 mole per cent), and this alcohol was largely incorporated into the synthesis products. The products were separated into fractions of different carbon numbers and analyzed for radioactive C^{14} . For ethanol and higher primary alcohols, the radioactivity *per mole of hydrocarbon* was essentially constant, indicating that the alcohol initiated a chain which then grows by stepwise addition of carbon atoms, as has been postulated for the synthesis mechanism. Since these results are very important to the mechanism of the synthesis, they will be considered in detail later (p. 363).

Kagan^{67a} studied the reactions of primary alcohols and synthesis gas at 1 and 20 atm. and 240 to 300°C on an iron-copper Fischer-Tropsch catalyst. Amounts of alcohol approximately equivalent to the production of hydrocarbons, if no alcohol were present, were introduced. Apparently the rate of the synthesis was suppressed by the addition of alcohols in these amounts. The product contained about one-third unreacted alcohol and one-third a mixture of aldehyde, acid and esters, corresponding to the alcohol intro-

duced. The remaining material was not characterized. For *n*-butanol plus $1\text{H}_2 + 1\text{CO}$ gas at 20 atm. and 300°C , the liquid products contained, by weight, 3.3 per cent butyraldehyde, 0.4 butyric acid, 34.7 *n*-butyl *n*-butyrate, and 32.2 unreacted butanol. From these results, the authors concluded that alcohols are not important intermediates in the Fischer-Tropsch synthesis. A more valid conclusion is that alcohols in high concentrations do not incorporate to a large extent but react in other ways.

Gall, Gibson, and Hall⁵² and Morrell⁹⁴ compared the carbon number distributions of alcohols and hydrocarbons produced in the Fischer-Tropsch synthesis over cobalt and iron catalysts. The distribution curves of alcohols and hydrocarbons are qualitatively similar if alcohols with $n + 1$ carbon atoms are compared with hydrocarbons of carbon number n . Since alcohols are important primary products and possibly intermediates in the synthesis, this comparison suggests that hydrocarbons may be produced from alcohol-like intermediates by a process of deformylation, although this process apparently does not proceed to a major extent in alcohol decomposition in the presence of hydrogen or synthesis gas⁵⁴.

Warner, Derrig, and Montgomery¹³¹ passed ketene and hydrogen over cobalt-thoria-kieselguhr catalyst at atmospheric pressure and 200°C . The products contained gaseous hydrocarbons and liquids and solids in amounts typical of the Fischer-Tropsch synthesis; however, the liquids and solids contained more oxygen than usual synthesis products. A mechanism involving the formation of methylene radicals and their stepwise addition to growing carbon chains was postulated. The authors suggested that ketene may be an intermediate in the synthesis.

NATURE OF THE CATALYTIC SURFACE AND EFFECT OF PROMOTERS

The nature of catalytic surfaces is difficult to ascertain by any method. Electron diffraction gives information regarding phases near the catalyst surface; however, this technique is difficult with typical porous catalysts and has been effectively utilized only with evaporated films. Physical adsorption and chemisorption measures properties of surfaces, but the results are often difficult to interpret. Electron diffraction and chemisorption will be considered first, followed by the role of promoters in Fischer-Tropsch catalysts.

Chemisorption on Fischer-Tropsch Catalysts

Chemisorption has been reviewed by Laidler⁸⁸ in Volume I of this series. The reader is also referred to reviews of data to 1943 by Hunsmann⁶⁵ and by Beebe¹⁵. In isobars of hydrogen on iron-group metals, the volume adsorbed usually increases with increasing temperature to a maximum in temperature range 0 to 200°C ; and for some catalysts other maxima have been observed

at lower temperatures. In temperature regions in which the amount adsorbed increases with temperature, the adsorption process or the production of sites¹²⁹ must involve an activation energy limiting the amount adsorbed. Studies of the chemisorption of carbon monoxide or synthesis gas on metal catalysts must be interpreted cautiously, since the data may be complicated by carburization, synthesis, or carbonyl formation.

Matsumura⁹¹ studied the chemisorption of H_2 , CO, CO_2 on cobalt and iron catalysts. The catalysts were precipitated from solutions of nitrates with potassium carbonate, and after filtering and drying, the catalysts were reduced in hydrogen at $350^\circ C$. The hydrogen isobar on the cobalt catalyst passed through a minimum at $60^\circ C$ and increased to a maximum at $200^\circ C$. On iron a minimum in hydrogen adsorption was observed at $30^\circ C$ and a maximum at $170^\circ C$. For carbon monoxide on cobalt, the amount adsorbed increased three-fold in the temperature range 50 to $200^\circ C$, whereas the isobar for carbon monoxide on iron passed through a minimum at $150^\circ C$ and increased. The increasing adsorption of carbon monoxide at temperatures from 100 to $200^\circ C$ may be due in part to bulk carbide formation. The adsorption of carbon dioxide on cobalt was fairly independent of temperature, with indications of a slight minimum at $100^\circ C$ and a slight maximum at $150^\circ C$. On the iron catalyst the carbon dioxide isobar decreased with increasing temperature. Water adsorption, determined by a questionable experimental method, was low on both cobalt and iron catalysts. The authors related the greater production of carbon dioxide in the synthesis on iron catalysts to the differences in amounts of carbon dioxide adsorbed and the shapes of the isobars for iron and cobalt.

Ghosh, Sastri, and Kini⁵³ studied the chemisorption of hydrogen, carbon monoxide, and mixtures of $H_2 + CO$ on two precipitated cobalt catalysts. Data on preparation B, containing Co-Cu-ThO₂-CeO₂-Cr₂O₃-kieselguhr, will be used to illustrate the sorption on cobalt catalysts. The surface area of this catalysts was $131\text{ m}^2/\text{g}$ and the monolayer of physically adsorbed nitrogen, V_m , was 33.0 cc (STP)/g . Adsorption isobars for hydrogen and carbon monoxide in Figures 54 and 55, respectively, show the chemisorption from the pure gases and from $1H_2 + 1CO$ and $2H_2 + 1CO$ on 7.55 g of reduced catalyst. The physical monolayer of nitrogen for this weight of catalyst is 249 cc (STP) ; therefore, the adsorption of carbon monoxide, 7 to 16 cc (STP)/g, and hydrogen, 3 to 11 cc, correspond to only a small coverage of the total surface. The chemisorption of pure hydrogen was essentially independent of temperature (Figure 54). From $H_2 + CO$ mixtures the sorption of hydrogen at $50^\circ C$ was lower than from pure hydrogen but increased with temperature so that at $100^\circ C$, the volume of hydrogen sorbed from $H_2 + CO$ equaled or exceeded the sorption from pure hydrogen. The chemisorption of hydrogen was *greater* from $1H_2 + 1CO$ than from $2H_2 + 1CO$.

The chemisorption of pure carbon monoxide (Figure 55) decreased with increasing temperature and passed through a minimum at about 120°C. From $H_2 + CO$ mixtures the isobars of carbon monoxide had the same

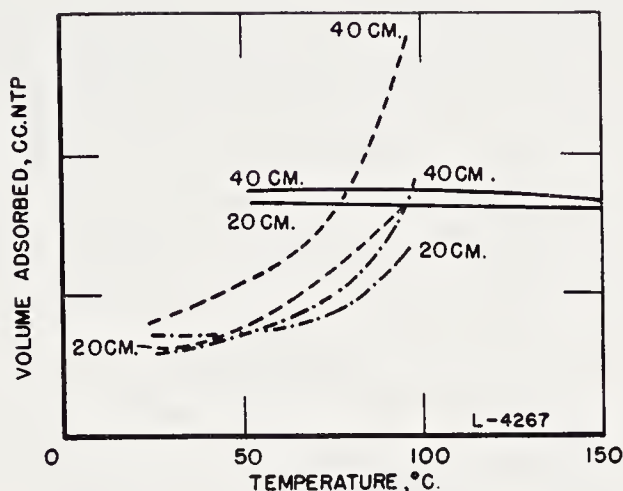


Figure 54. Adsorption isobars of hydrogen on cobalt catalyst. Pure hydrogen —, $2H_2 + 1CO$ ·····, and $1H_2 + 1CO$ ---. (Reproduced with permission from Ref. 53)

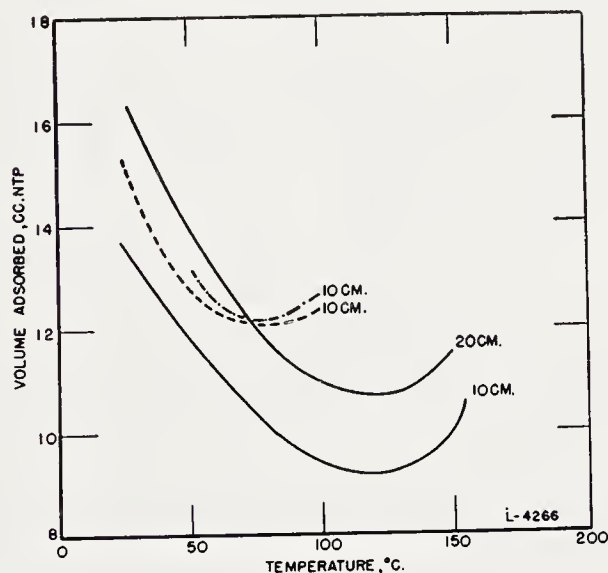


Figure 55. Adsorption isobars of carbon monoxide on cobalt catalyst. Pure CO —, $2H_2 + 1CO$ ·····, and $1H_2 + 1CO$ ---. (Reproduced with permission from Ref. 53)

shape; however, the volume adsorbed was greater than for pure carbon monoxide and the minima occurred at a lower temperature. Plots for the simultaneous adsorption (Figure 56) indicate that carbon monoxide is more strongly adsorbed than hydrogen. At 25°C the sorption of carbon monoxide increased four-fold with only a small increase in hydrogen. At 97°C the

gases were chemisorbed in the ratio $1\text{H}_2:2\text{CO}$, and the authors noted that this ratio corresponds to the composition of an enolic surface complex $-\text{COH}$. The dotted extrapolations of these curves to lower adsorptions seem to lead to a ratio of $1\text{H}_2:1\text{CO}$.

The second catalyst (A) of the same composition as (B) but without chromium oxide adsorbed relatively more hydrogen. In synthesis tests

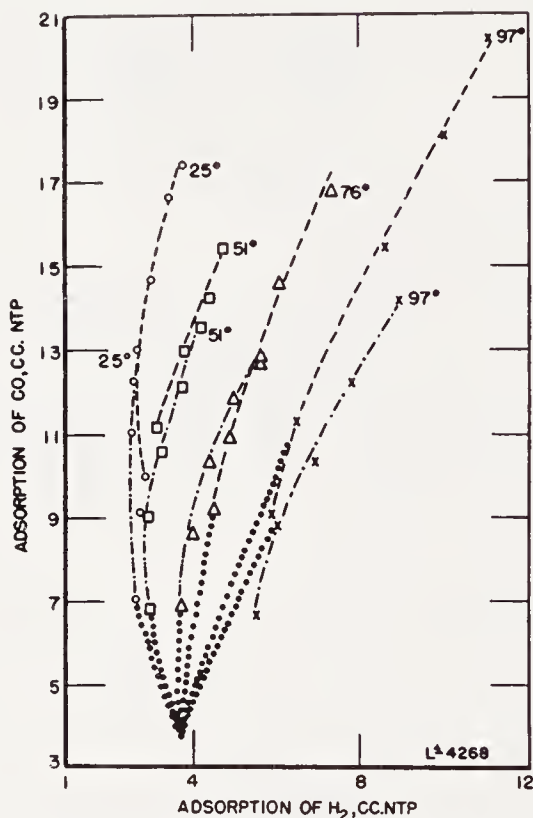


Figure 56. Adsorption of hydrogen vs. adsorption of carbon monoxide on cobalt catalyst. $2\text{H}_2 + 1\text{CO}$, and $1\text{H}_2 + 1\text{CO}$ -----. (Reproduced with permission from Ref. 53)

catalyst (A) was shown to produce smaller yields of C_2^+ hydrocarbons than catalyst (B).

Sastri and Srinivasan¹¹⁵ studied the chemisorption of carbon monoxide at -187°C on a precipitated $\text{Co-ThO}_2\text{-MnO-kieselguhr}$ catalyst after 4 hours of synthesis followed by evacuation at 200°C . The chemisorption of carbon monoxide was typical of a reduced cobalt catalyst. Nitrogen and carbon monoxide isotherms were determined on (a) the raw catalyst and (b) after reduction in hydrogen at 300°C ; (c) after 4 hours of synthesis with $2\text{H}_2 + 1\text{CO}$ gas at atmospheric pressure involving an increase of temperature from 150 to 190°C followed by 3 hours of flushing with a stream of

pure nitrogen at 200°C and an 8-hour evacuation at this temperature, (d) after re-reduction in hydrogen at 200 to 300°C, and (e) after carburization in carbon monoxide at 200 to 250°C for 32 hours. All experiments were made on the same catalyst sample, and carbon monoxide chemisorption was taken as the difference of the carbon monoxide (physical plus chemisorption) and the nitrogen isotherms plotted on a relative pressure basis. After synthesis the ratio of carbon monoxide chemisorption (V_{CO}) to the physically adsorbed monolayer of nitrogen from the BET equation (V_m) was somewhat higher than this ratio for the reduced or re-reduced catalyst, as shown in Table 10. After carburization, the chemisorption of carbon monoxide was lower than that of used catalyst, and the ratio V_{CO}/V_m was also lower. Since

TABLE 10. ADSORPTION DATA ON REDUCED, USED, AND CARBIDED CATALYSTS^a
Co-ThO₂-MnO-kieselguhr

Treatment	Evacuation Temperature (°C)	Adsorption Data ^b per Gram of Unreduced Catalyst			V_{CO}/V_m
		Surface Area (m ²)	V_m (cc)	V_{CO} (cc)	
a. Original catalyst	300	81.4	18.1	—	—
b. (a) plus reduction at 300°C	300	24.5	5.45	3.00	0.55
c. (b) plus use in synthesis	200	15.0	3.35	2.20	0.66
d. (c) plus hydrogen at 200–300°C	300	24.0	5.35	2.75	0.52
e. (d) plus carbon monoxide at 200–250°C	300	18.8	4.19	0.70	0.17

^a From Ref. 115.

^b Adsorption isotherms determined at –187°C.

the nitrogen flushing and evacuation of the used catalyst should not decompose carbide, the authors concluded that *the active catalyst in the synthesis did not contain appreciable amounts of either surface or bulk carbides*. The reduced catalyst was shown to be active in the synthesis and to produce typical products; however, after carburization the activity was very low.

Emmett and Harkness³⁸ and Kummer and Emmett⁸⁴ determined hydrogen isobars on reduced, fused-iron catalysts. These isobars show adsorption maxima at about –100°C (termed Type A chemisorption) and 100°C (Type B). Emmett and Brunauer³⁷ studied the adsorption of H₂, N₂, CO, CO₂ on a series of reduced fused catalysts. The chemisorption of carbon monoxide at –183°C was shown to be a good index of the fraction of iron at the surface, and carbon dioxide chemisorption at –78°C was an index of alkali on the surface. The alkali promoter accumulated at the surface. For a catalyst containing 1.07 per cent potassium oxide, about 70 per cent of the surface was covered by the alkali. Structural promoters such as

alumina were present in greater amounts at the surface than in the bulk of the catalyst; however, the accumulation of structural promoters was much less than observed for alkali. The influence of the chemisorption of one gas on the chemisorption of another was also investigated.²⁰ The chemisorption of hydrogen at 100°C on singly promoted Fe-Al₂O₃ catalysts was enhanced by the presence of chemisorbed nitrogen, suggesting the formation of N—H complexes on the surface.

Podgurski, Kummer, DeWitt, and Emmett¹⁰⁶ studied the adsorption of hydrogen and carbon monoxide on reduced and carbided samples of pure fused Fe₃O₄ (910) or fused Fe₃O₄-Al₂O₃-SiO₂-ZrO₂ (423) catalyst. Hägg iron

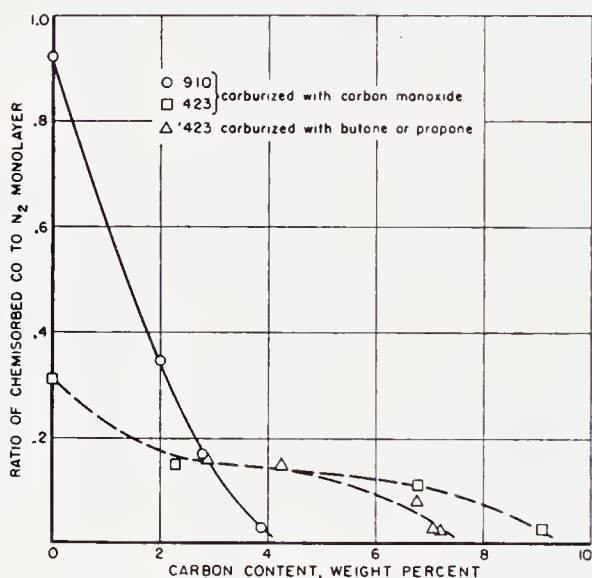


Figure 57. The decrease in carbon monoxide chemisorption at -195°C with carburization. (From data of Ref. 106)

carbide was produced by treating the catalyst with carbon monoxide, *n*-butane, or propane. On both catalysts the chemisorption of carbon monoxide at -195°C was sharply decreased by carburization, as shown in Figure 57. For pure iron catalyst 910 the ratio of chemisorbed carbon monoxide to the monolayer of physically adsorbed nitrogen decreased to a low value at about 4 per cent carbon by weight, but the ratio for the promoted catalyst (423) decreased to a similar low value at 7 and 9 per cent carbon for samples carburized in *n*-butane and carbon monoxide, respectively. Although the chemisorption of carbon monoxide was strongly decreased by the presence of carbide, the chemisorption was not zero even for samples carburized to Fe₂C. Nevertheless, the "free iron" in the catalyst surface decreased sharply with extent of carbiding. Similar decreases in the chemisorption of carbon monoxide with carbiding were found at -78

and -46°C ; however, the results suggested that a loosely-held chemisorption of carbon monoxide, which proceeds slowly, occurs at these temperatures. On carbided samples the chemisorption of carbon monoxide did not occur to an appreciable extent at 0, 100, and 200°C . With reduced catalysts, carbon monoxide chemisorption was extensive at 50 and 100°C , and carburization of the catalyst proceeded at 150°C .

Isobars for hydrogen on reduced catalyst 423 showed maxima corresponding to Type A and Type B chemisorption. Carburization with either carbon monoxide or *n*-butane practically eliminated the low-temperature Type A chemisorption, but had only a slight effect on Type B until the carbon content was increased to 7.7 to 9.1 per cent. For the catalyst containing 9.1 per cent carbon, the chemisorption of hydrogen was still about two-thirds of the value for the reduced sample. At and above 100°C the adsorption of hydrogen was greater on samples that were carburized in carbon monoxide than on those treated with *n*-butane. Samples carburized with butane and oxidized by chemisorption of small amounts of oxygen adsorbed more hydrogen than the same sample before oxidation. Possible explanations are (1) surface oxide adsorbs hydrogen more strongly than carbide, or (2) the surfaces carburized with hydrocarbons contain adsorbed hydrogen or hydrocarbon fragments which further decrease adsorption of hydrogen.

The adsorption of $1\text{H}_2 + 1\text{CO}$ gas was studied on a catalyst carburized with carbon monoxide to a carbon content of 8 per cent. At 150°C and a gas pressure of 300 mm Hg, 0.32 cc H_2 and 0.04 cc CO per gram were chemisorbed. Under similar conditions with carbon monoxide alone at a partial pressure of 150 mm 0.017 cc was adsorbed. At 200°C , 0.39 cc of H_2 and 0.11 cc of CO per gram were adsorbed. The values for chemisorption of carbon monoxide were only about 5 per cent of those observed for corresponding reduced catalysts and the adsorption of hydrogen about 50 per cent. The authors concluded that iron carbides are probably not the catalytically active phase in the synthesis, as the carbides do not strongly adsorb carbon monoxide either alone or in the presence of hydrogen at temperatures close to those employed in the synthesis.

Kini, Busak, and Lahiri⁷⁰ determined the chemisorption of hydrogen and carbon monoxide from 99 to 249°C on a precipitated $\text{Fe}_2\text{O}_3\text{-CuO-MgO-K}_2\text{CO}_3$ catalyst after reduction in hydrogen at 300°C . The chemisorption of hydrogen reached a maximum at 225°C and decreased, whereas carbon monoxide adsorption increased with temperature to the highest value investigated. The results obtained for the adsorption of carbon monoxide at temperatures above 150°C are probably complicated by carburization reactions. At 139°C and 400 mm Hg, 2.1 cc (STP) of hydrogen per gram was adsorbed, and in a similar experiment 1.9 cc (STP) of carbon monoxide.

Electron Diffraction Studies on Fischer-Tropsch Catalysts

McCartney and co-workers at the Bureau of Mines⁹² examined iron catalysts after pretreatment to form reduced iron, Hägg carbide, cementite, and ϵ -nitride, and after use in the Fischer-Tropsch synthesis. Precipitated catalysts containing $\text{Fe}_2\text{O}_3\text{-CuO-K}_2\text{CO}_3$ or $\text{Fe}_2\text{O}_3\text{-K}_2\text{CO}_3$ and a fused $\text{Fe}_3\text{O}_4\text{-MgO-K}_2\text{O}$ catalyst were used. Synthesis experiments were made with $1\text{H}_2 + 1\text{CO}$ gas, usually at 7.8 atm., but a few samples were examined after synthesis at 21.4 atm. The catalysts were ground to a fine powder before examination, and the electron patterns resulted from diffraction about the corners and edges of the particles. Samples treated with mixtures of $\text{H}_2 + \text{CO}$ or used in the synthesis gave only electron diffraction patterns of wax. Extraction of these samples with boiling toluene in a modified Soxhlet apparatus for 48 hours either greatly decreased or eliminated the pattern of wax. The experimental results were summarized as follows:

(a) For precipitated iron catalysts that were first reduced, reduced and carbided, or reduced and nitrided, electron and x-ray diffraction indicated the presence of the same phases. The electron and x-ray diffraction patterns of interstitial compounds are similar, but have some characteristic differences.

(b) After synthesis and extraction, precipitated iron catalysts usually produced electron diffraction patterns of magnetite only, even though the x-ray diffraction patterns contained lines of Hägg and/or hexagonal carbide. Only a used reduced-and-nitrided precipitated catalyst showed the presence of an interstitial phase, ϵ -carbonitride, by both electron and x-ray diffraction.

(c) After pretreatment or synthesis, the fused catalyst containing magnesia usually produced electron diffraction patterns of magnesia and/or magnetite, although x-ray diffraction indicated the presence of metallic iron, Hägg carbide, and/or cementite. Nitrides and carbonitrides were the only interstitial phases identified by electron diffraction.

(d) Catalysts converted to iron nitrides are very resistant to oxidation at both 7.8 and 21.4 atm. Hägg carbide and cementite effectively resist oxidation at 7.8 atm., but oxidize rapidly at 21.4 atm.

An interesting result of this study is the apparent absence of iron carbides in the surface layers of used Fischer-Tropsch catalysts. However, this simple interpretation of the diffraction data is complicated by several factors. First, carbides present as small or highly disordered crystallites may produce a diffraction pattern that is very different from that of the bulk carbide or an indistinct pattern. Second, unidentified diffraction lines in some electron patterns may correspond to unknown carbides. Third, with fused and sintered catalysts in which x-ray and magnetic analyses indicate Hägg carbide as the principal phase, the initial samples did not show elec-

tron diffraction patterns for known iron phases; however, after a period of synthesis the electron diffraction pattern of magnetite appeared, indicating that amorphous material containing iron was present in the surface layers at the start of the test. Fourth, when the catalyst was converted to ϵ -nitrides, electron diffraction patterns of the ϵ -phase were frequently found in used catalyst. Although the electron diffraction results must be interpreted cautiously, the presence of magnetite and the apparent absence of carbides in the surface layers of used iron catalysts do not add support to the carbide intermediate hypothesis.

Effects of Promoters

Promoters may be classified as structural and chemical. The principal function of structural promoters is the development and stabilization of structures of high surface area. Chemical promoters cause variations in the activity and/or selectivity without appreciable changes in surface area. Occasionally the product distribution may be improved by additives that decrease the over-all activity by selectively poisoning the catalyst.

Available data suggest that promoters and supports are not essential to the production of higher hydrocarbons on cobalt, iron, and ruthenium catalysts. These pure metal catalysts contained only those traces of impurities introduced in careful preparations. Most of these preparations had to be pretreated very cautiously to avoid excessive sintering. The activity of these catalysts varied from low to moderate and their life was usually short.

With cobalt and nickel catalysts, thorium, magnesia, manganese oxide, and other difficultly reducible oxides increase the surface area, and at least in the atmospheric-pressure synthesis may increase the average molecular weight of the product. In the medium-pressure synthesis, these promoters are largely ineffective in altering the molecular weight. Alkali is relatively ineffective as a chemical promoter for the usual types of cobalt and nickel catalysts that are supported on kieselguhr or active forms of silica. Presumably most of the alkali is removed by adsorption on or reaction with the silica of the support. At atmospheric pressure, alkali increases the average molecular weight of the hydrocarbons somewhat; however, the changes in selectivity are negligible in the medium-pressure synthesis.

Copper has a unique role as a promoter in cobalt, nickel, and iron catalysts. Copper often facilitates the processes of pretreatment, such as reduction and carburization. However, if the pretreatment is properly accomplished, the presence or absence of copper usually does not alter activity and selectivity. Preparations containing sizable amounts of copper sinter readily and often have shorter lives in the synthesis.

With iron catalysts, alkali is the only really important promoter. The

presence of carriers and promoters other than alkali in precipitated catalysts is neither necessary nor desirable as far as activity or selectivity is concerned; however, carriers such as kieselguhr or silica gel, and structural promoters such as magnesia or alumina may be desirable for attaining more rapid filtration during preparation or greater mechanical stability in the synthesis. When sizable amounts of silica gel or kieselguhr are used, the alkali content must be increased correspondingly to compensate for the alkali that reacts with the silica. In fused iron catalysts a variety of difficultly reducible oxides are effective as structural promoters, and the type of oxide usually has no large influence on activity or selectivity.

In the medium-pressure synthesis, the activity of fused iron catalysts increases sharply with potassium oxide content to a maximum at about $0.5\text{K}_2\text{O}$ per 100Fe , and then decreases. The average molecular weight and alcohol content of the product increases to about $1\text{K}_2\text{O}$ per 100Fe and then remains about constant.

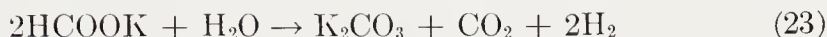
The activity of precipitated iron catalysts increased with alkali in some instances and in others remained essentially unchanged. The average molecular weight in all cases increases with alkali content to about $1\text{K}_2\text{O}$ per 100Fe and then remains constant. The usage ratio, $\text{H}_2:\text{CO}$, usually decreases sharply as the alkali content is increased from zero. The decrease in usage ratio is effected principally by a change in the rate of the water-gas-shift reaction with respect to synthesis. Under some synthesis conditions, alkali-free catalysts produce a more saturated product than corresponding alkalinized preparations. Furthermore, the rate of deposition of carbon on catalysts during synthesis, both as elemental carbon and carbide, increases with alkali content. The extent of branching of the carbon chain appears to be independent of the presence or absence of alkali.

In the atmospheric pressure synthesis the concentration of alkali required for maximum activity and life of iron catalysts is lower than in the medium pressure synthesis; the actual values vary widely with catalyst type and composition. Under these conditions moderate concentrations of alkali often have a detrimental effect on activity. The production of wax increases with concentration of alkali, and the accumulation of large quantities of wax on the catalyst causes the activity to decrease rapidly, presumably by blocking pores.

Holm and Blue⁶³ studied the influence of concentration of potassium oxide in reduced pure fused magnetite on the rate of the hydrogen-deuterium exchange reaction at 150°C , as shown in Figure 58. The rate of exchange decreased rapidly to a minimum at a concentration of 0.4 per cent potassium. Beyond this minimum, the rate increased slightly with increases in alkali content. The rate of hydrocarbon synthesis varied approximately inversely with the rate of $\text{H}_2\text{-D}_2$ exchange, and the alkali content for maxi-

imum activity occurred at about the same value as the minimum in Figure 58.

Royen and Erhard¹¹⁰ studied the reaction of carbon monoxide and water at atmospheric pressure and synthesis temperatures on potassium carbonate impregnated on activated charcoal. The water-gas-shift reaction did not occur to an appreciable extent on the charcoal support. The reaction was postulated to proceed according to



2CO + 1H₂O gas was passed over the potassium carbonate-charcoal cata-

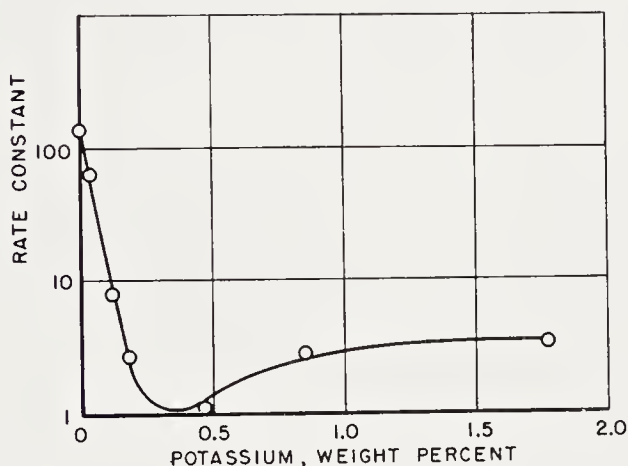


Figure 58. Effect of K₂O on the hydrogen-deuterium exchange activity of iron at 150°C. (Reproduced with permission from Ref. 63)

lyst at 200°C and a space velocity of 67 hr⁻¹. After steady conditions were attained, the exit gas contained 15 per cent CO₂, 15H₂, and 70CO. The raw catalyst contained 18.8 g of potassium carbonate, and in the steady state condition contained 19.1 g of potassium formate. It was postulated that these reactions also occur on the alkali-promoted iron catalysts.

The effectiveness of alkali promoters increases in descending order of the alkali series, i.e., Li, Na, K, Rb, Cs. Lithium and sodium compounds are relatively ineffective. Potassium compounds are satisfactory promoters, and for economic reasons are commonly used in Fischer-Tropsch catalysts. The use of rubidium or cesium compounds may be feasible for massive iron catalysts in which alkali contents of 0.05 to 0.1 per cent are sufficient. Alkaline earth hydroxides or carbonates are ineffective as alkali promoters.

At present no adequate explanation of the role of alkali in iron catalysts can be offered. If hydrocarbonyl-type intermediates are involved in the mechanism, these intermediates may be stabilized by the presence of alkali.

Other explanations may be found in consideration of the solid-state physics of catalysts, such as work function, *d*-band character, and lattice defects; however, theories relating such properties to catalytic behavior are not sufficiently developed at present to be useful in such complex systems as iron Fischer-Tropsch catalysts.

The influence of alkali promoters in the Fischer-Tropsch synthesis may be summarized as follows:

(a) Alkali promoters increase the chain growth process and in many cases increase the rate of chain initiation.

(b) Alkali increases the relative rate of some processes that may be regarded as either secondary or competitive, such as water-gas-shift and carbon deposition. The isomerization of 1-olefins to internal olefins and hydrogenation of olefins are often inhibited by alkali. Chain branching is presumably unaffected by alkali.

The Concept of Bifunctional Catalysts

In some processes the selectivity may be interpreted most simply by assuming that each of two or more catalytic components contributes its characteristic behavior to the reaction⁸¹. Thus, a platforming catalyst combines the functions of a hydrogenation catalyst and an acid isomerization catalyst. For the Fischer-Tropsch synthesis, some workers have postulated that the active metal initiates carbon chains (usually postulated to be methylene groups), and oxide promoters are required to polymerize these groups to higher hydrocarbons.

Riesz, Lister, Smith, and Komarewsky¹⁰⁹ studied a series of cobalt-alumina, nickel-alumina, and iron-alumina catalysts covering the composition ranges from low-metal content up to, in some cases, pure metal. The catalysts were precipitated from solutions of sodium aluminate and metal nitrate with sufficient sodium hydroxide or nitric acid added for precipitation. The catalysts were reduced in hydrogen before use. In synthesis tests at atmospheric pressures, maxima in the yields of liquid hydrocarbons were found at 50 per cent nickel, 75 cobalt, and 50 iron. Unfortunately, these curves show neither selectivity nor activity in an unambiguous manner, since synthesis temperatures varied considerably; for example, in the cobalt series it varied over a range of 70°C. The active metal was postulated to initiate methylene groups and the alumina to catalyze their polymerization to higher hydrocarbons.

With cobalt and nickel catalysts in the atmospheric pressure synthesis, promoters such as thoria, manganese oxides, and alkali are effective in increasing the average molecular weight of the products; however, in the medium pressure synthesis these promoters are not required for the production of high yields of wax. For iron catalysts, the alkali content largely con-

trols selectivity. These promoters alone would not be expected to catalyze polymerization reactions at or above synthesis temperatures. The author prefers to regard the promoters merely as modifiers of the active metal as the metals are capable of producing higher hydrocarbons without additives.

MECHANISM OF THE FISCHER-TROPSCH SYNTHESIS

The kinetics of synthesis have been described and the influence of various active metals and promoters summarized earlier in this chapter. A few pertinent reactions, possibly related to steps in the synthesis, were also described. Kinetic experiments have demonstrated that diffusion to or from the catalyst particle is not the rate controlling step. Diffusion in pores of the catalyst, a process intimately related to the reaction at the catalyst surface, is probably an important factor. Other than this, the kinetic data have not provided unambiguous evidence for any reaction step being the rate-controlling process.

The synthesis mechanism may be divided into a number of steps: (a) Adsorption of reactants, (b) chain initiation, (c), chain growth, (d) chain termination, (e) desorption of products, and (f) readsorption and further reaction. Provocative information on chain initiation has been gained from studies of carbided catalysts, especially carbides containing carbon-14. The chain growth process is elucidated by data on carbon number and isomer distributions as well as experiments involving the incorporation of radioactive alcohols. Studies of the incorporation of hydrocarbons and oxygenated molecules give some insight into the magnitude of readsorption and further reaction of products.

The postulate that carbides are important intermediates in the synthesis was proposed by Fischer and Tropsch in 1926⁴⁸. At that time most of the carbides of iron, cobalt, and nickel had not been investigated, and in the period 1928–1933, Bahr and Jesson^{13, 41} demonstrated the formation of carbides by carburization of these metals with carbon monoxide at synthesis temperatures. Papers of Fischer and co-workers^{40, 43, 44, 49} from 1930–32 elaborated on the carbide hypothesis. Craxford and Rideal²⁵ in 1939 formulated a detailed mechanism based on this hypothesis. This mechanism served to stimulate a vast amount of research and discussion after World War II. Following the war, Emmett, Koelbel, and workers at the Bureau of Mines demonstrated the shortcomings of the carbide theory, especially many of the details of Craxford's postulates.

Elvins and Nash³⁴ in 1926 postulated that the synthesis involved oxygenated intermediates. This proposal was extended by Storch, Golumbic, and Anderson in 1951 to a mechanism that explained many characteristics of synthesis products, such as carbon number and isomer distributions¹²³. Here the intermediate was postulated to be similar to an alcohol. The ex-

cellent researches of Kummer, Emmett and co-workers^{85, 86} on the incorporation of radioactive alcohols into the synthesis have largely confirmed these predictions. In 1953 Weitkamp and Frye¹³³ concluded that primary alcohols, aldehydes, and 1-olefins were the primary synthesis products. Apparently this conclusion demands no major revision of the concept of oxygenated intermediates in the synthesis.

Considerations of the chain-growth process by Herington in 1946 have been extended by Bureau of Mines workers and others to practical schemes of predicting carbon number and isomer distributions. Recent reviews of synthesis mechanism studies have been presented by Koelbel⁷⁸, Storch¹²³, and Weitkamp¹³³.

The Carbide-Intermediate Hypothesis

Postulates of Fischer. Fischer and Tropsch⁴⁸ postulated that (a) synthesis gas reacted with the catalyst to form a carbide, (b) the carbide was then hydrogenated to a methylene group, and (c) the methylene groups polymerized to higher hydrocarbons. It was suggested that the carbides involved were higher carbides containing at least as much carbon as M_2C . Mechanisms involving formaldehyde as an intermediate were thought to lead to production of alcohols, as observed in the methanol and higher alcohol syntheses. Later Fischer⁴⁰ suggested that carbide and oxide simultaneously may be formed according to



with the carbide being hydrogenated to methylene groups and the oxide reduced to metal. Copper was postulated to serve as an oxygen carrier



with subsequent reactions following the pattern described above. Although Fischer found traces of oxygenated material in synthesis products, he regarded them as unimportant to the synthesis mechanism.

Fischer and Tropsch⁴⁹ observed that the tendency of catalysts to produce methane varied directly with the affinity of the metal for hydrogen, i.e., increasing from iron to nickel, and they speculated on possible reactions between hydrides and carbides. To the carbide hypothesis was added the suggestion that methylene groups may be produced by hydrogenation of higher carbides, containing 3 to 4 carbon atoms per atom of metal, to leave a lower carbide, the catalyst phase varying between two carbides rather than carbide and metal. They contended that higher carbides may contain chains of carbon atoms.

Fischer and Koch⁴³ found the rate of the water-gas-shift reaction ($H_2O + CO$) to be about equal at 200°C on iron and cobalt catalysts, but at 235°C

this reaction was more rapid on the cobalt catalyst. On this basis the water-gas shift was mistakenly eliminated as a source of carbon dioxide from iron catalysts and the following equations were proposed for the carbide-forming step:



In a later paper, Fischer and Koch⁴⁴ suggested that hydrides and carbonyls were not involved in the mechanism, and, further, that higher carbides were not necessary. Carbide carbon was hydrogenated to CH , CH_2 , and CH_3 radicals, which combined in various ways to form higher hydrocarbons.

The following comments are pertinent to the early work of Fischer:

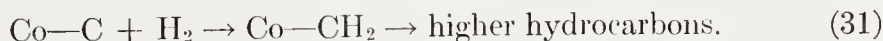
(a) The highest carbides produced in the temperature range of the Fischer-Tropsch synthesis and identified with certainty, have the formula M_2C .

(b) Although the water-gas-shift reaction was considered as a method for producing carbon dioxide from iron catalysts, this possibility was eliminated on the basis of their experimental studies of this reaction. The conclusion of Fischer and Koch was erroneous. Although the rates of the *water-gas reaction* on iron and cobalt catalysts at a given temperature are of the same order of magnitude, Fischer apparently did not consider the fact that the rate of *synthesis* on cobalt is many times greater than on iron, so that on cobalt catalysts the water-gas reaction lags far behind the primary reaction.

The Carbide Hypothesis of Craxford and Rideal. In 1939 Craxford and Rideal²⁵ presented a more detailed theory in which the following steps were postulated:



or



With cobalt catalysts step (30) must predominate over step (29) since water, the principal oxygenated product, cannot be produced in the synthesis by subsequent reactions because of thermodynamic limitations.

The reaction mechanism was studied by means of the *para*- to *ortho*-hydrogen conversion in mixtures of *para*-hydrogen and carbon monoxide.

The experimental results were summarized as follows:

"While the Fischer synthesis is proceeding at about 200°C, the *ortho-para* conversion does not occur to any marked extent, but it does occur for the following conditions under which either there is no reaction or else methane is being formed.

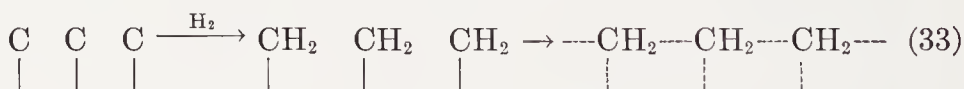
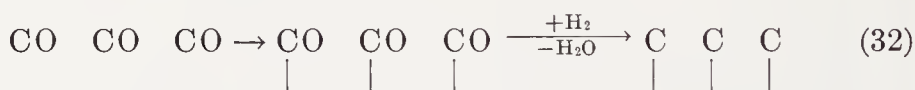
"(i) With normal synthesis, $\text{CO} + \text{H}_2$, at temperatures below 140°C, in which case there is no reaction.

"(ii) With synthesis gas at 200°C for the first hour or so, during which time methane and cobalt carbide are being produced and no oil.

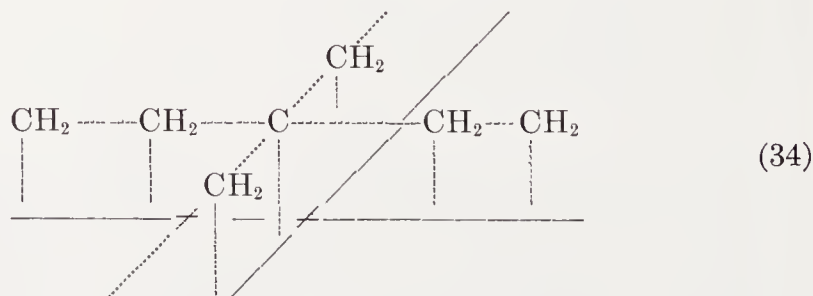
"(iii) With a mixture of $24\text{H}_2 + 1\text{CO}$ at 200°C even after 24 hours. With this gas mixture hardly any oil is formed, only methane.

"(iv) With synthesis gas above 250°C. Again methane is the product and no oil."

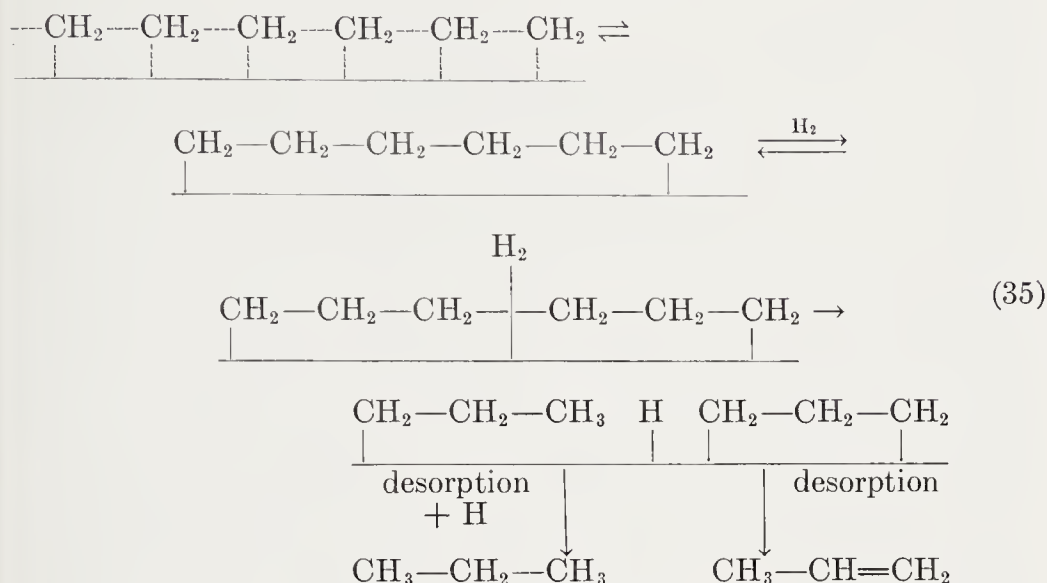
Since very little *para* to *ortho* conversion was observed during the formation of oil, Craxford and Rideal concluded that no appreciable amount of atomic hydrogen was present in normal synthesis and that the formation of methane involved atomic hydrogen in some stage of the reaction. Inhibition of the *para-ortho* conversion was related to the rather complete coverage of the surface, with cobalt carbide postulated to be the state of the catalyst surface during normal synthesis. A detailed reaction mechanism involving only molecular hydrogen was postulated for the formation of macromolecules at the catalyst surface:



These steps are similar to those postulated by Fischer and Tropsch. In Craxford's hypothesis branched macromolecules are produced by incorporation of carbon atoms into chains of methylene groups; the branched molecules contain quaternary carbon atoms according to



The macromolecules increase in size until split by hydrogen:



A pseudo-equilibrium was postulated between polymerization of methylene groups and hydrocracking, the latter reaction being favored by high concentrations of chemisorbed hydrogen. In a later paper²⁴, the hydrocracking of wax deposited on the catalyst during synthesis was considered. In the absence of carbon monoxide, this wax was hydrocracked at a more rapid rate than the synthesis reaction (pp. 313-314). From the similarity of carbon number distribution from synthesis and hydrocracking (Figure 50) Craxford concluded that hydrocracking of macromolecules was involved in the synthesis. The incorporation of methane reported by some workers was taken as evidence for dissociative adsorption of hydrocarbons on the catalyst and their participation in the polymerization-depolymerization equilibrium. In another paper, Craxford²³ postulated that carbon dioxide was produced by the water-gas-shift reaction and methane and gaseous hydrocarbons by hydrocracking. These reactions according to Craxford do not occur in the normal synthesis in which the catalyst was postulated to be covered by carbide, but they occur to a large extent on surfaces containing bare cobalt atoms and in the presence of atomic hydrogen.

The postulates of Craxford have stimulated a large amount of research and discussion on the mechanism of the synthesis. On the basis of these newer data, many aspects of the theory have been shown to be either inconsistent or incorrect. The validity of some of the details of Craxford's theory was readily evaluated; however, the basic assumption, that surface carbide is an intermediate, has been difficult to evaluate unambiguously. A number of comments follow:

1. The experimental results of Craxford and Rideal²⁵ are not as conclusive as may be desired.

2. The fact that the *ortho*- to *para*-hydrogen reaction does not proceed to a large extent does not necessarily preclude the presence of hydrogen atoms on the surface of the catalyst. In any case, hydrogen molecules converted to equilibrium concentrations of *ortho-para* forms do not escape from the surface during normal synthesis. Possible explanations are (a) the adsorption of hydrogen is the rate-determining process, and (b) the diffusion of hydrogen in long, small diameter pores—at least partly filled by wax—is an important step in synthesis. In the latter case hydrogen molecules desorbed from the surface would have to diffuse against a net gas flow in the pores caused by the gas contraction of the synthesis reaction. Hence, under certain conditions virtually all of the desorbed hydrogen would react in the pores and would not appear in the main gas stream.

3. Little if any cobalt carbide is produced in the synthesis. The use of carbon monoxide-rich gas, which should favor carbide formation, leads to a progressive decrease in activity in the atmospheric pressure synthesis. Carburized cobalt catalysts containing high concentrations of carbide have low activity in the synthesis. The deposition of free carbon on the catalyst inhibits carbide formation but does not decrease the rate of synthesis. Carburization of catalysts with carbon monoxide may, however, produce oxide as well as carbide, and these surface oxides may poison the catalyst in the synthesis. The activity of catalysts carburized with higher hydrocarbons should be investigated.

4. The chemisorption of carbon monoxide on a used cobalt catalyst after evacuation at synthesis temperatures was typical of that on a reduced catalyst and not of a carbided sample.

5. Iron catalysts containing Hägg or hexagonal (Fe_2C) carbides or cementite (Fe_3C) have activities equal to or greater than corresponding non-carburized samples. Hägg and hexagonal carbides are found in sizable amounts in some used catalysts. Although only carbides in surface layers can be effective in the synthesis, the bulk carbides may form suitable substrates for active surfaces.

6. Branched hydrocarbons produced in the synthesis contain ternary but virtually no quaternary carbon atoms that were postulated by Craxford. Alcohols appear to be an important primary product in the synthesis with iron and cobalt catalysts, and under suitable experimental conditions large yields of alcohols are obtained. The carbide theory does not predict the formation of oxygenated compounds.

7. With cobalt catalysts, reactions producing methane and carbon dioxide occur to an appreciable extent throughout the catalyst bed, and

Craxford's theory does not appear to be a satisfactory explanation of the results of Anderson⁷ and Koelbel⁷⁷.

8. The differences in the distribution curves for synthesis and hydrocracking are sufficient to make interpretation difficult.

9. When carbon monoxide is present the reaction between hydrocarbons adsorbed on the catalyst and hydrogen is very different than when it is absent; the rate of hydrocracking in pure hydrogen is greater than the rate of synthesis. Hydrocracking is inhibited by the presence of carbon monoxide or some compound or phase derived from it. The inhibition may be due to poisoning by carbide, as suggested by Craxford, chemisorbed carbon monoxide, or water. Similarly, cobalt catalysts that have been used with carbon monoxide-rich gas or precarbided have low activity. The relatively slow rate of the synthesis reaction is consistent with the concept of a partially poisoned catalyst, and the selectivity of the synthesis is probably related to selective poisoning. If this reasoning is correct, the surface phases formed in the presence of carbon monoxide should be considered as inhibitors and not the active catalyst, as postulated by Craxford.

10. Griffith⁵⁶ considered the geometry of the linear macromolecules postulated by Craxford. Due to the zig-zag structure of the hydrocarbon chain, attachment cannot occur at each carbon atom. Pairs of carbon atoms can be attached rather exactly on the 100-plane of cobalt; however, the next point of attachment must be a number of carbon atoms, apparently at least four, down the chain since only at such a distance is another pair of carbons in register with the underlying metal atoms.

Comparison of Rates of Carburization and Synthesis. A number of workers have attempted to test the carbide intermediate hypothesis by comparing the rates of carburization and synthesis. If the mechanisms of these two processes are similar and the rate-controlling process is the same, the rate of carburizing in at least the initial stage of the process should be equal to or greater than the rate of synthesis. Since the rate of carburizing decreases appreciably with extent of carburizing, it is necessary to select a rate at some definite extent of carburization. This method is not a critical procedure for testing a reaction mechanism, and strong arguments can be advanced to demonstrate that conclusions drawn from these data need not be valid. Nevertheless, the experimental results will be summarized briefly.

Eidus²⁷ compared the rates of carburizing and synthesis on cobalt, nickel, and iron catalysts after 30 minutes and 10 hours. For cobalt and nickel the rates of synthesis were 5–11 and 17–46 times the rate of carburizing at 0.5 and 10 hours, respectively. For iron catalysts at corresponding times, the rate of synthesis was 1.6–2.1 and 8 times the rate of carburizing. From these data Eidus concluded that the carbide mechanism could be valid only for

iron catalysts. In a later paper, Eidus²⁹ reported that the rate of carbiding of cobalt and nickel catalysts was also significantly slower than the rate of synthesis when the velocity of carbiding was measured at the start of the process and after 3 hours.

Weller¹³⁵ observed that the rate of carbiding of a cobalt-thoria-kieselguhr at 200°C was rapid initially, decreased to a constant value for the next 20 to 150 minutes, and then decreased further with time. The rate in the first minute was 2–4 times the rate of synthesis, but in the period from 20 to 150 minutes the rate of carbiding was about one-tenth of the synthesis rate.

Thermodynamics of Hydrogenation of Carbides. Emmett and Browning^{18, 19, 82} have determined the free energy of formation of carbides, as described in Chapter 1, 20, and noted that *only* methane and short-chain paraffin hydrocarbons can be produced by hydrogenation of bulk phase carbides. It would, nevertheless, be possible to incorporate one or more atoms of carbidic carbon into a long hydrocarbon chain. Furthermore, these data refer to bulk-phase carbides, and possibly surface carbides may have more positive free energies of formation, so that they could be hydrogenated to form the wide variety of paraffins and olefins produced in the synthesis.

Mechanism Studies with C¹⁴. Kummer, Dewitt, and Emmett⁸³ investigated the carbide intermediate hypothesis on iron and cobalt catalysts using C¹⁴ as a tracer. Only a small fraction of C¹⁴ (0.1 per cent or less) in ordinary carbon monoxide was required for accurate measurement. The radioactivity of reactants and products was determined with a Geiger counter after separation into three fractions: The first contained H₂, CO, and CH₄; the second, CO₂ and C₃ and C₄ hydrocarbons; and the third, higher hydrocarbons. The fractions were burned in oxygen to carbon dioxide and water, and the carbon dioxide was precipitated as barium carbonate for analysis in the Geiger counter. The tests were made in a glass apparatus with gases circulated by a magnetic pump. Surface areas by the nitrogen adsorption method were used to approximate the depth of the carbide layer deposited on the catalyst. Catalysts studied were (a) pure fused magnetite, (b) fused Fe₃O₄-Al₂O₃-SiO₂-ZrO₂, (c) precipitated Co-ThO₂-kieselguhr, and (d) precipitated iron oxide gel.

An experimental test of the carbide intermediate hypothesis at first consideration appears simple. A catalyst should be prepared with a surface layer of C¹⁴ carbide, and the rate of appearance of C¹⁴ in the hydrocarbon products during the synthesis should reveal the extent to which carbide participates in the reaction. However, the extent to which exchange reactions occur between radioactive carbon as carbide and carbon atoms of carbon monoxide, carbon dioxide and hydrocarbons must be established, as well as whether or not a uniform and stable surface of C¹⁴ carbide can be prepared.

In pretreating the catalyst, the reduced sample was carburized with normal carbon monoxide to 60 to 70 per cent Fe_2C or Co_2C , and then carburized an additional 10 per cent with carbon monoxide containing C^{14}O to minimize the use of radioactive carbon. The C^{14} content of the surface was determined by hydrogenating the equivalent of 25 per cent of the catalyst surface and determining the radioactivity of the methane. Although the carbide contained C^{14} equivalent to many layers, in all cases the radioactivity of the surface was lower than that of the carbon monoxide employed in the second step of the carburization. In long periods of hydrogenation, C^{14} was found in the methane until all of the carbon was removed. The authors postulated that some of the C^{14} diffused rapidly through the iron phase and deposited on the interface of crystallites of carbide at relatively large distances from the surface. During hydrogenation, both C^{14} and normal carbon diffuse to the surface. Despite a lower radioactivity than expected, the radioactivity did not change significantly over periods as long as 48 hours at 305°C .

Hydrocarbons did not exchange with C^{14} carbides in one hour. The exchange between carbon monoxide and C^{14} carbide was about 5 and 29 per cent at 250 and 322°C , respectively. A catalyst containing 65 per cent of normal Fe_2C was used in the synthesis at 253°C with $1\text{H}_2 + 1\text{CO}$ gas to which 20 per cent methane containing C^{14}H_4 had been added. The higher hydrocarbon products did not contain C^{14} , indicating that exchange between methane and higher hydrocarbons had not occurred and that *methane was not incorporated into the synthesis product*. These experiments were required because some radio-methane is produced by hydrogenation of carbide during the synthesis.

In the synthesis experiments, the C^{14} content of the surface was determined before and after synthesis by brief hydrogenations. The average radioactivity of the surface was assumed to be the mean of these two values. Typical experimental data are presented in Table 11. The radioactivity of the $\text{C}_3 + \text{C}_4$ fraction indicated that only 4.2 per cent of this fraction was produced with Fe_2C as an intermediate. Appreciable amounts of radioactive methane were produced, presumably by hydrogenation of carbide. Analysis of the gasol fraction from tests with iron catalysts at temperatures below 250°C and with cobalt at 200°C showed that on the average 10 per cent of the products were formed through a carbide intermediate. Liquid hydrocarbons had somewhat greater activity, indicating that the carbide mechanism may proceed to a greater extent in the formation of higher hydrocarbons.

Kummer, DeWitt, and Emmett⁸³ considered the influence of surface heterogeneity. The surface may exhibit true heterogeneity due to the presence of sites of different activity or superficial heterogeneity due to

blocking of pores by adsorbed hydrocarbons, see p. 95. For example, the authors pointed out that if 3 to 4 per cent of the surface synthesized 90 per cent of the hydrocarbons, the active portion of the surface would be rapidly depleted of C^{14} , and an erroneous conclusion would be made that 90 per

TABLE 11. FISCHER-TROPSCH RUN (RUN 10S) ON CATALYST B CARBIDED TO 94.7 PER CENT Fe_2C^a

(Weight of reduced sample, 1.95 g; temperature of run, $252^\circ C$; time of run, 332 min.; pressure of run, 765–580 mm; surface activity before the run, 1,410 counts per min. per cc; surface activity after the run, 745 counts per min per cc; synthesis gas contained 82.2 cc H_2 and 80.1 cc CO)

	Produced or Left ^b (cc)	Activity
CO	45.5	4.7 counts per min per cc of CO_2
H_2	22.2	
CH_4	5.1	199 counts per min per cc of CO_2
CO_2	3.02	
$C_{2.6}H_5$	3.98	45 counts per min per cc of CO_2
H_2O		

Per cent of total product formed through Fe_2C as an intermediate,

$$\frac{(45)(100)}{(1,410 + 745)/2} = 4.2 \text{ per cent.}$$

^a From Ref. 83.

^b The volumes of H_2 , O_2 , and C not accounted for were 16.7, 2.7, and 16.1 cc, respectively. The carbon being listed in terms of the equivalent of cc of a monatomic gas.

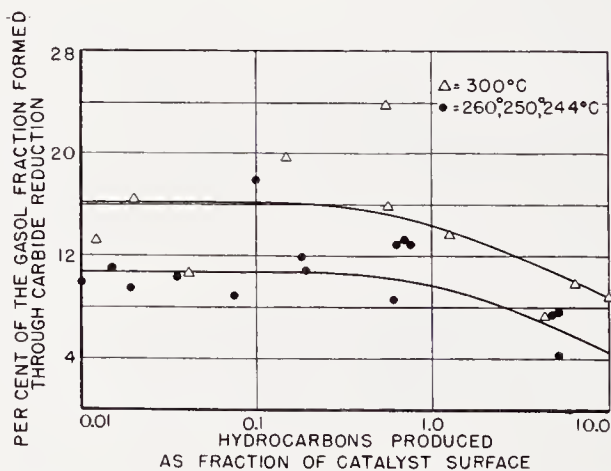


Figure 59. The per cent of the synthesis proceeding by the carbide mechanism as a function of the fraction of the surface involved in the reaction. (Reproduced with permission from Ref. 83)

cent of the reaction proceeded by a mechanism other than carbide reduction. Experiments with iron catalysts were made in which the amount of reaction, if it proceeded entirely by the carbide mechanism, would involve only a small fraction of the surface. These results in Figure 59 indicate that when as small a portion of the surface as 1 per cent was involved, only 10 and 15 per cent of the synthesis proceeded by carbide reduction at 260 and 300°C, respectively. Thus, only a small fraction of the hydrocarbons was produced from surface or bulk carbide deposited on the catalyst by a pretreatment with carbon monoxide. The authors noted that the data do not preclude the possibility that carbon atoms may exist momentarily on the catalyst surface in some step of the synthesis.

Other Mechanisms of Chain Initiation

The fact that alcohols are important primary synthesis products and are produced in high yields under certain experimental conditions is not considered in the carbide intermediate hypothesis. In the methanol and higher alcohol syntheses, formaldehyde has been postulated as an intermediate; however, the alcohol syntheses and the Fischer-Tropsch process apparently follow quite different chain-growth processes³. The small yields of formaldehyde and methanol in Fischer-Tropsch products may largely be attributed to unfavorable thermodynamics. The presence of oxygenated molecules in synthesis products is, however, not conclusive evidence against the carbide intermediate mechanism, since a number of processes, such as oxo-type reactions involving olefins produced in synthesis, can be proposed to account for their formation. The production of ethanol and methanol cannot be readily explained by an oxo-type mechanism.

The postulate of an oxygenated intermediate was first made by Elvins and Nash³⁴ in 1926. From a cobalt-manganese oxide-copper-lithium carbonate catalyst at 302°C and atmospheric pressure, a sizable yield of water-soluble oxygenated molecules, in addition to hydrocarbons, was obtained. Methanol was suggested as a possible intermediate, although none was found. The authors suggested that oxygenated molecules and hydrocarbons may be produced by the same series of consecutive reactions or that they are produced by simultaneous, independent reactions.

Pichler¹⁰² cited evidence favoring carbonyl-type intermediates:

“The possible occurrence of intermediate compounds of the carbonyl-type should not be arbitrarily disregarded . . . Optimum conditions (for the synthesis) prevail at pressures just below which (at the corresponding temperatures) the tendency toward formation of volatile carbonyls becomes so great that deterioration of the catalyst results. In other words, conditions must be chosen in such a way that the rate of formation of volatile carbonyl

remains somewhat less than that for the supposed intermediate carbon monoxide compounds with hydrogen."

Table 12 compares the optimum synthesis pressures with minimum pressure at which deleterious carbonyl erosion begins. The hypothesis of Pichler is not a unique explanation, since any reaction mechanism in which the rate increases with pressure may lead to this relationship. The carbonyl-type intermediate can, however, be the starting point for either the carbide or oxygenated intermediate mechanism.

The oxygenated intermediate hypothesis of Storch, Golumbic, and Anderson¹²³ will be considered after a discussion of mechanisms of chain growth (pp. 359-367).

TABLE 12. COMPARISON OF OPTIMUM SYNTHESIS PRESSURES WITH PRESSURES AT WHICH UNDESIRABLE FORMATION OF CARBONYLS OCCURS AT SYNTHESIS TEMPERATURES^a

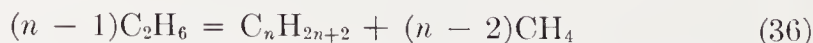
Active Component	Synthesis Gas Pressure (atm)			
	Ni	Co	Fe	Ru
Optimum for synthesis	1	5-30	10-30	100-1,000
Undesirable carbonyl formation	>1	>30	>30	Carbonyls may form on the surface of the catalyst under these conditions of temperature and pressure

^a H. Pichler; from Ref. 102.

Hypotheses Regarding the Growth of the Carbon Chain

Consideration will now be given to postulated mechanisms of chain growth that provide an explanation of the carbon number and isomer distribution of hydrocarbons. These hypotheses in general do not require a detailed description of the chemical nature of the intermediate or its attachment to the surface.

The Polymerization-Depolymerization Hypothesis. Montgomery and Weinberger⁹³ investigated the explanation of carbon number distributions on the basis of a polymerization-depolymerization mechanism, as postulated by Craxford (p. 339). Calculations were made assuming thermodynamic equilibrium between normal paraffin hydrocarbons according to equations of the type



with the ratio $\text{CH}_4:\text{C}_2\text{H}_6$, over-all ratio of hydrogen to carbon atoms, and temperature being the variables determining the carbon number distribu-

tion. At 200°C qualitative agreement with carbon number distribution from cobalt catalysts was obtained with $\text{CH}_4:\text{C}_2\text{H}_6 = 11.5$ and $\text{H}:\text{C} = 2.67$. Both of these ratios, required to fit the experimental distribution, are, however, larger than those usually found in the synthesis. The observed ratio $\text{CH}_4:\text{C}_2\text{H}_6$ usually varies from 5 to 8, and an over-all $\text{H}:\text{C}$ ratio of 2.67 requires a usage ratio $\text{H}_2:\text{CO}$ of 2.33. More satisfactory agreement was obtained if the temperature was taken as 327°C and $\text{CH}_4:\text{C}_2\text{H}_6$ and $\text{H}:\text{C}$ ratios as 7.0 and 2.59, respectively. The authors suggested that possibly the temperature of the catalyst surface was considerably higher than the measured bed temperature.

This procedure yields satisfactory approximations of carbon number distributions for products from cobalt catalysts; however, the specification of the ratios $\text{CH}_4:\text{C}_2\text{H}_6$ and $\text{H}:\text{C}$ places strong limitations on the distribution curve. Apparently the method is not valid for reproducing product distributions containing sizable amounts of olefins or oxygenated molecules, because such molecules should not be found in appreciable quantities if equilibrium is attained.

Volmer¹³⁰ presented a unique interpretation of carbon-number distribution curves. The groups on the catalytic surface were assumed to combine in a random manner so that the distribution could be expressed as a Gaussian curve. By dimerization, trimerization, etc., of olefinic molecules from the first process, other Gaussian curves with maxima at multiples of the carbon number of the maximum of the first distribution would be obtained. The observed distribution curve was assumed to be the sum of the Gaussian curves. Maxima were assigned at carbon numbers of 5.3, 10.6, 15.9, etc., the maxima at 5.3 corresponding to the maximum of the observed carbon number curve (on a weight basis), and the experimental curve was thus resolved into a number of Gaussian curves. Many of the assumptions of this hypothesis appear very difficult to justify.

Stepwise Addition to Growing Chain. Herington⁶¹ postulated that the carbon chain grows one carbon atom at a time until the chain is terminated, and that hydrocracking processes leading to degradation of the carbon chain do not occur. For a growing chain of n carbon atoms, we may define a probability α_n that the chain will grow and another $1 - \alpha_n$ that the chain will terminate. The ratio of these probabilities, β_n , was given as

$$\beta_n = \frac{1 - \alpha_n}{\alpha_n} = \frac{\phi_n}{\sum_{n+1}^{\infty} \phi_i} \quad (37)$$

where ϕ_n is the number of moles of product of carbon number n . Herington found values of β_n for products from granular cobalt catalyst to be approximately constant at 0.30. For products from pelleted cobalt catalyst, Friedel and Anderson⁶⁰ obtained values of β_n increasing from 0.1 at C_2 to 0.35 at

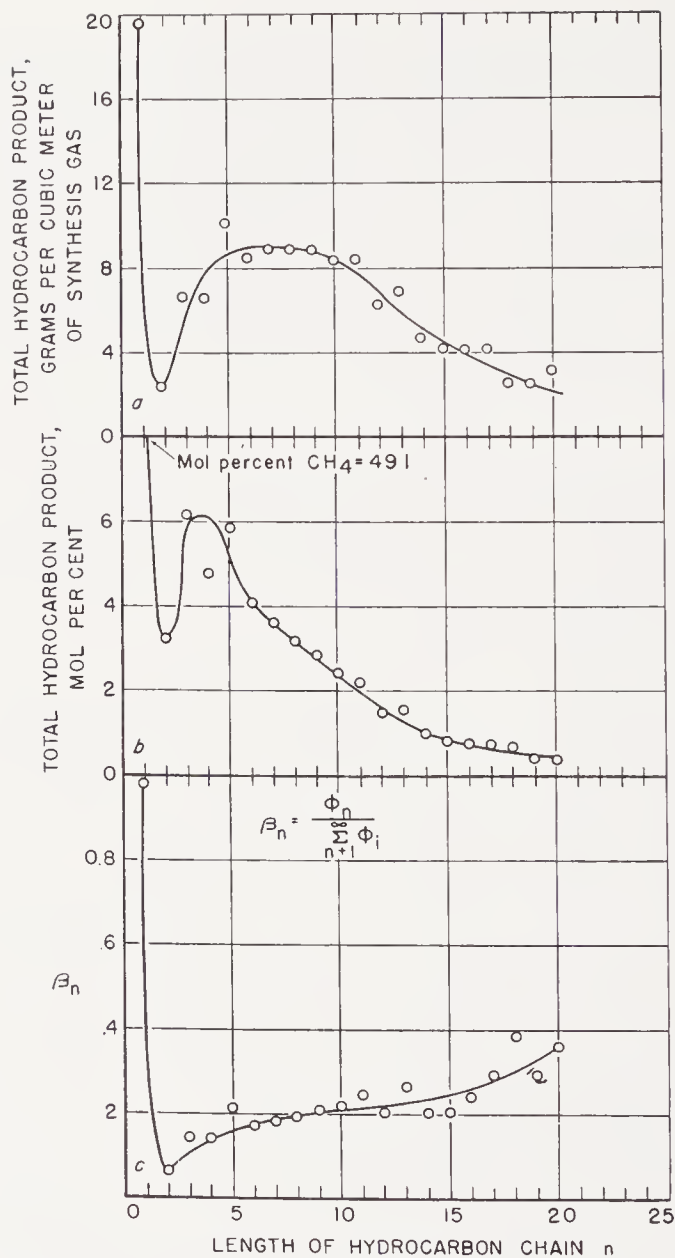


Figure 60. Parts *a* and *b* present the distribution of total hydrocarbon products from atmospheric tests of cobalt catalysts at 190°C in terms of grams per cubic meter of synthesis gas and mol per cent. Part *c* is a plot of Herington's probability term β_n . (Reproduced with permission from Ref. 123)

C_{20} , as shown in Figure 60. From C_5 to C_{15} , β_n was approximately 0.20 with a slight upward trend.

By rewriting Eq. (37), α_n can be evaluated directly

$$\alpha_n = \sum_{i=n+1}^{\infty} \phi_i / \sum_{i=1}^{\infty} \phi_i \quad (38)$$

In any range in which α_n or β_n is constant, it can be demonstrated that

$$\alpha = \phi_{n+1}/\phi_n \quad (39)$$

and

$$\phi_n = \phi_x \alpha^{n-x} \quad (40)$$

Also

$$W_n \cong 14 n \phi_x \alpha^{n-x} \quad (41)$$

where W_n is the weight of hydrocarbon of carbon number n . The weight distribution (Eq. 41) has a maximum at $n = -1/\log_e \alpha$, but the mole distribution (Eq. 40) decreases monotonically. A plot of $\log \phi_n$ against n should be linear. The value of α derived from this type of plot, however, cannot be identified with Herington's constant α (Eqs. 37 or 38) unless, on the basis of these equations, α is shown to be constant. Weitkamp¹³⁴, for example, incorrectly identified the constant of Eq. 40 with Herington's α , although the values of α of Eqs. (37) and (38) were not constant.

A number of plots of Eq. (40) are presented in Chapter 2, pp. 110, 208, 209.

For the one complete carbon number distribution available for products from cobalt catalysts, the linear plot approximated the data moderately well up to high carbon numbers. For products from iron catalysts, the data are approximately linear in the range of carbon numbers 3 to 9 or 10, but fall above the linear curve at higher carbon numbers. The region of higher carbon number can be approximated by a second straight line having a smaller slope. Distribution data of this type do not give a constant value for α_n in Eqs. (37) and (38). For products from iron catalysts the values of α from Eq. (40) for the initial linear portion are not a good index of average molecular weight. The values of α from Eq. (40) for products from iron and cobalt catalysts are summarized in Table 13.

Carbon number distributions are determined infrequently because of the time and effort involved in the precision separation, and thus Eqs. (37) to (41) are not generally useful in evaluating selectivity in catalyst testing or process development experiments. Manes⁹⁰ transformed Eq. (40) into a form that can be applied to the relatively crude fractionations into gasoline, diesel oil, and wax that are usually made on synthesis products. From Eq. (41) the weight of product with carbon number greater than $r - 1$, W_{r+} , is given by

$$W_{r+} \cong 14 \phi_x \sum_{n=r}^{\infty} n \alpha^{n-x} = 14 \phi_x \alpha^{r-x} \{r - \alpha(r - 1)\} / (1 - \alpha)^2 \quad (42)$$

and

$$W_{r+}/W_{x+} \cong \alpha^{r-x} \{r - \alpha(r - 1)\} / \{x - \alpha(x - 1)\} \quad (43)$$

For data of Herington⁶¹ with $\alpha = 0.77$, W_{12+}/W_{5+} was calculated to be 0.295 compared with 0.311 from the observed carbon number distribution, and for data of Friedel and Anderson⁵⁰ with $\alpha = 0.83$, W_{21+}/W_{5+} was computed as 0.133 compared with 0.13 observed.

From Eq. (43) with $r = 12$ and 18 and $x = 5$, cumulative distribution curves can be plotted for gasoline ($C_5 - C_{11}$), diesel oil ($C_{12} - C_{18}$), and wax (C_{19+}) as a function of α . Figures 61 and 62 demonstrate the tendency of diverse experimental data for cobalt and iron catalysts to follow the pre-

TABLE 13. VALUES OF α OF EQUATION 40 FROM CARBON NUMBER DISTRIBUTIONS

Source of Data	Range Separated, Carbon Number	Linear Portion, Carbon Number	α
A. Cobalt catalysts ^a			
Ward, <i>et al.</i>	14-18	14-18	0.76
Herington	5-11	5-11	.76
Gibson, Gall, Hall			
Hydrocarbons	6-11	6-11	.75
Alcohols	4-8	4-8	.73
Ruhrchemie			
Atm.	5-10	4-10	.75
Medium pressure	5-9	5-8	.75
Friedel and Anderson	1-20	3-20	.85
B. Iron catalysts ^b			
Ruhrchemie	1-17	3-9	.66
Rheinpreussen	1-17	3-10	.67
Kaiser Wilhelm Institut	1-17	3-9	.68
Lurgi	1-17	2-11	.69
I.G. Farbenindustrie	1-17	1-9	.66
Brabag	1-17	1-9	.69
Standard Oil	1-16	3-11	.66

^a See Figure 27, Chapter 2.

^b See Figure 76, Chapter 2.

dicted curves. From the position at which the experimental points most closely fit the calculated curves, the value of α may be estimated. According to these curves the fraction diesel oil is relatively insensitive to changes of α , and this fraction has been frequently observed to remain approximately constant despite changes of catalyst composition or operating variables. Although, as described above, Eq. (41) usually fails to represent the distribution curve for iron catalysts in the diesel oil and wax range, the plots of Manes apparently provide approximately the value of α that corresponds to the slope of the best straight line that can be passed through the data above C_4 . On this basis the values of α predicted from the charts of Manes

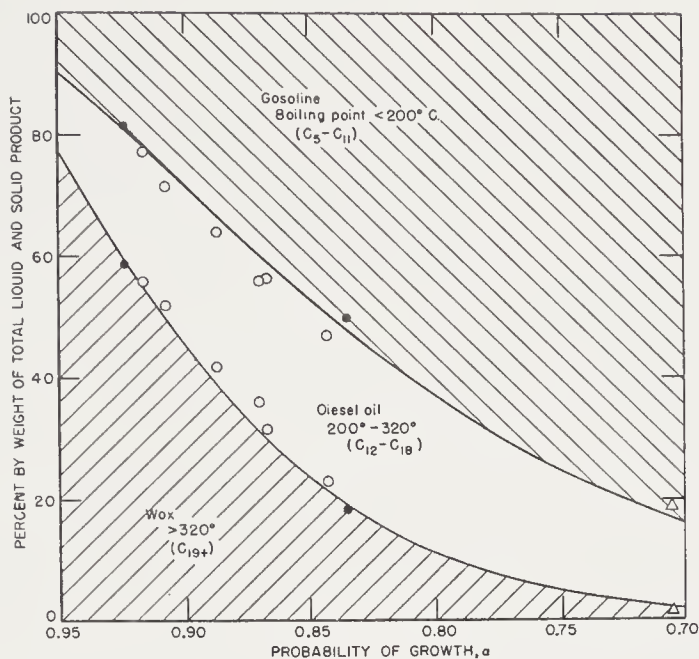


Figure 61. Observed product distributions of liquid and solid Fischer-Tropsch hydrocarbons (cobalt catalysts), fitted to Equation 43. (Reproduced with permission from Ref. 90)

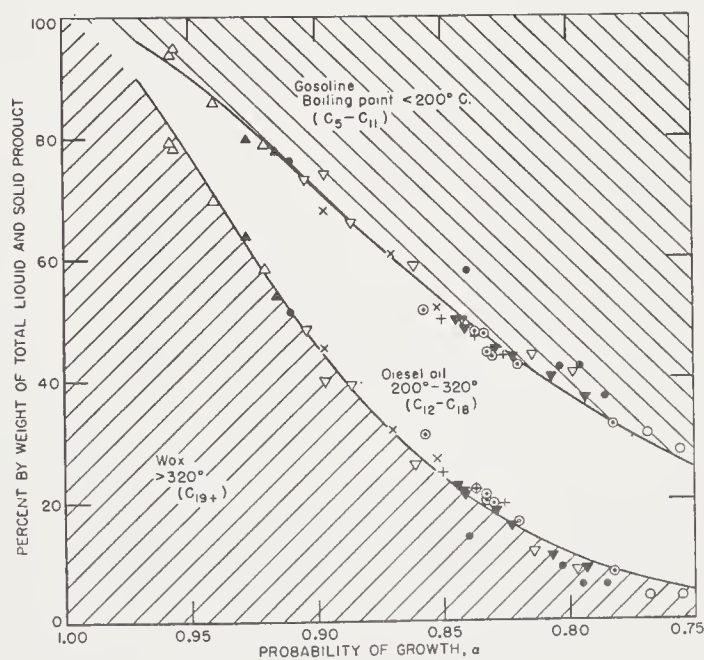


Figure 62. Observed product distributions of liquid and solid Fischer-Tropsch hydrocarbons (iron catalysts), fitted to Equation 43. (Reproduced with permission from Ref. 90).

are useful in characterizing the distribution of C_{5+} products with a single constant.

Accurate determinations of isomer distributions by mass-spectrometric methods led to more detailed considerations of the mechanism of chain growth. In general, for an adequate prediction of observed data, it is required that addition occurs stepwise at only terminal or penultimate carbon atoms with the further restriction that addition does not occur at penultimate carbons that are already attached to three carbon atoms.

Weller and Friedel¹³⁶ postulated a scheme for stepwise addition of carbon atoms that was able to reproduce successfully the isomer distribution of products from cobalt catalysts. The following assumptions were made:

(1) "The carbon skeleton is built up by successive one-step additions to the carbon chain of groups containing a single carbon atom.

(2) "Addition occurs at any terminal or next to terminal (penultimate) carbon atom, with two restrictions: (a) addition to tertiary carbon atoms does not occur, (b) addition to a side chain occurs only if the side chain is attached to a penultimate carbon.

(3) "The probability of addition to a terminal carbon is intrinsically different from that for addition to a penultimate one." This *a priori* probability of addition to a terminal carbon atom may be designated a , that of addition to a penultimate carbon, b , and " $a + b = 1$." The probability constants are independent of chain length.

(4) "The distribution of isomers in the final product is identical with the distribution on the catalyst surface."

Thus, the probability of forming the normal C_4 chain from the C_3 group is $2a$ and of the iso chain, b , and the fractions of n - C_4 and iso- C_4 in the C_4 cut are $2a/(a + 1)$ and $b/(a + 1)$, respectively. The probability of producing n - C_5 from n - C_4 is $2a/(a + 1)$, whereas iso- C_5 can be formed from n - C_4 with a probability of $2ab/(a + 1)$ and from iso- C_4 with a chance of $b/(a + 1)$. This process is continued in a similar fashion to give the predicted isomer concentration in higher fractions in terms of a and b . Values of a and b are chosen to give the best agreement between predicted and observed isomer data. For the isomer data of paraffins from cobalt catalysts (Table 14), the predicted distribution with $a = 0.961$ and $b = 0.039$ agrees with the observed data to within the experimental error of the analyses. For products from iron catalysts (Table 15), the agreement is less exact, with a major discrepancy between predicted and observed values for the C_4 -fraction.

Anderson, Friedel, and Storch⁴ considered the chain growth problem with respect to both isomer and carbon number distribution, assuming a stepwise addition of carbon atoms. It was postulated that addition occurs only at end or adjacent-to-end carbon atoms of the longest carbon chain and does

not occur on an adjacent-to-end carbon already attached to three carbon atoms. Three cases were considered: one involving addition to both ends of the growing chain, which is similar to the postulates of Weller and Friedel¹³⁶, and the other two, addition at only one end. Although in general the agree-

TABLE 14. CALCULATED CHAIN STRUCTURES OF HYDROCARBONS FROM COBALT CATALYSTS

Carbon Chain		Mole Per cent in Fraction		
		Observed ^a	Weller and Friedel ^b	Anderson, Friedel, and Storch ^c
C ₄	<i>n</i> -C ₄	^d	$a = 0.961$ $b = 0.039$	$f = 0.035$
	2-methyl-C ₃	^d	98.0 2.0	96.6 3.4
C ₅	<i>n</i> -C ₅	95.0	94.2	93.4
	2-methyl-C ₄	5.0	5.8	6.6
C ₆	<i>n</i> -C ₆	89.6	90.5	90.2
	2-methyl-C ₅	5.7	5.6	6.4
	3-methyl-C ₅	4.7	3.8	3.2
	2,3-dimethyl-C ₄	0	0.1	0.2
C ₇	<i>n</i> -C ₇	87.7	87.0	87.3
	2-methyl-C ₆	4.6	5.4	6.2
	3-methyl-C ₆	7.7	7.3	6.2
	Other C ₇ 's	0	0.3	0.3
C ₈	<i>n</i> -C ₈	84.5	83.6	84.4
	2-methyl-C ₇	3.9	5.2	6.0
	3-methyl-C ₇	7.2	7.1	6.0
	4-methyl-C ₇	4.4	3.5	3.0
	Other C ₈ 's	0	0.6	0.6

^a From Ref. 50.

^b From Ref. 136.

^c From Ref. 4.

^d Not determined.

ment between predicted and observed results for all three cases was satisfactory in view of simplifying assumptions of the development and uncertainties of the experimental results, the case for addition at both ends of the growing chain showed serious discrepancies in the prediction of C₄ isomers, as also observed in the method of Weller and Friedel¹³⁶.

Only scheme A of this paper⁴ will be considered, since this scheme is consistent with the detailed mechanism postulated by Storch, Golumbic, and

Anderson¹²³. Addition may occur at *only one end* of the growing chain on *only one end carbon* atom if two are present or on the adjacent-to-end carbon. Addition to adjacent-to-end carbon atoms is subject to the restriction that this addition does not occur if the carbon atom is already attached

TABLE 15. CALCULATED CHAIN STRUCTURES OF HYDROCARBONS FROM IRON CATALYSTS

Carbon Chain		Mole Per cent in Fraction		
		Observed ^a	Weller and Friedel ^b	Anderson, Friedel, and Storch ^c
C ₄	<i>n</i> -C ₄	89.4	$a = 0.890$ $b = 0.110$ 94.2	$f = 0.115$ 89.7
	2-methyl-C ₃	10.6	5.8	10.3
C ₅	<i>n</i> -C ₅	81.2	83.8	81.3
	2-methyl-C ₄	18.8	16.2	18.7
C ₆	<i>n</i> -C ₆	78.8	74.7	73.5
	2-methyl-C ₅	11.2	14.4	16.9
	3-methyl-C ₅	9.5	10.3	8.5
	2,3-dimethyl-C ₄	0.4	0.6	0.9
C ₇	<i>n</i> -C ₇	66.0	66.4	66.0
	2-methyl-C ₆	13.1	12.8	15.4
	3-methyl-C ₆	19.1	18.4	15.4
	2,3-dimethyl-C ₅	1.6	1.8	1.7
	2,4-dimethyl-C ₅	0.3	0.6	0.8
C ₈	<i>n</i> -C ₈	61.0 ^d	59.2	60.5
	monomethyl isomers	36.4	36.0	34.7
	dimethyl isomers	2.6	4.8	4.8

^a From Ref. 21.

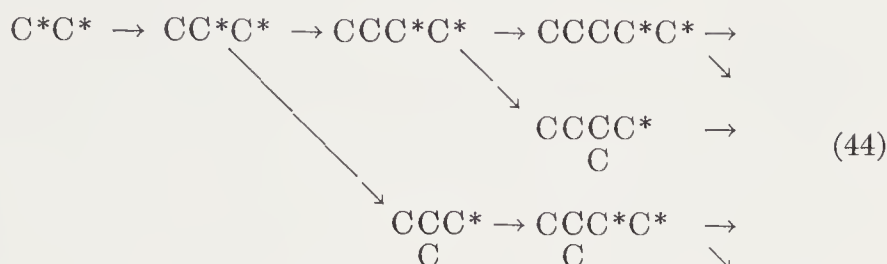
^b From Ref. 136.

^c From Ref. 4.

^d Data available for only these chain structure types.

to three carbons. The reactivity of these groups may result from the presence of reactive structures such as an olefin bond, or groups such as hydroxyl attached to the carbon atom. On addition of carbon monoxide, the growing group passes through intermediate structures and finally forms an intermediate similar to the first but containing an additional carbon. From these intermediates, molecules such as aldehydes, alcohols, olefins, or paraffins may desorb and appear as products. For scheme A the growth pattern

may be represented by



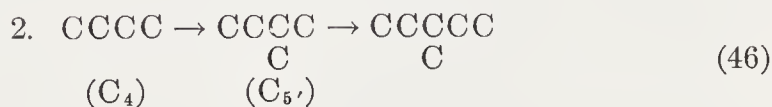
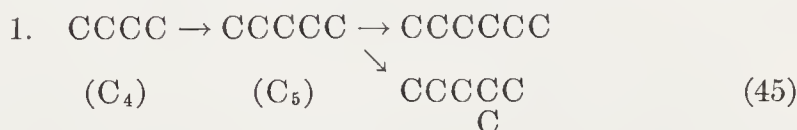
The following assumptions are made: (a) upon addition to an end carbon the rate of growth through the intermediates may be represented by a first-order rate constant, α , with respect to the concentration of the growing chain on the surface.

(b) For addition to an adjacent-to-end carbon, the rate of growth is represented by a similar first-order constant, β .

(c) The rate of desorption is characterized by a first-order rate constant, γ , with respect to the concentration of growing chains at the surface.

(d) For chain species n , the rates of chain growth at end and adjacent-to-end carbons and the rate of desorption may be represented by αC_n , βC_n , and γC_n , and C_n is the molar concentration of chain n at the catalyst surface.

For steady-state conditions, the concentration of any growing intermediate remains constant, and hence its rate of formation must equal its rate of growth and desorption. Two typical reaction sequences are considered.



For sequence 1

$$C_4\alpha = C_5(\alpha + \beta + \gamma) \quad (47)$$

$$C_5/C_4 = \alpha/(\alpha + \beta + \gamma) = R_5/R_4 = a \quad (48)$$

and for sequence 2

$$C_4\beta = C_{5'}(\alpha + \gamma) \quad (49)$$

$$C_{5'}/C_4 = \beta/(\alpha + \gamma) = R_{5'}/R_4 = b \quad (50)$$

where R_n is the rate of appearance of species n , in moles per unit time and

a and b are constants. A new constant, $f = b/a$, is introduced at this point. This constant is an index of the extent of branching of the carbon chain. For addition to an end carbon $R_{n+1}/R_n = a$ and for adjacent-to-end carbons $R'_{n+1}/R_n = af$. Thus, beginning with C_2 and accounting for all possi-

TABLE 16. ISOMER AND CARBON NUMBER DISTRIBUTIONS IN TERMS OF a AND f .

Carbon Chain		Relative Isomer Composition	Relative Carbon Number, Distribution, Moles
C_2		1	1
C_3		1	$2a$
C_4	$n-C_4$	1	$2a^2(1 + f)$
	2-methyl- C_3	f	
C_5	$n-C_5$	1	$2a^3(1 + 2f)$
	2-methyl- C_4	$2f$	
C_6	$n-C_6$	1	$2a^4(1 + 3f + f^2)$
	2-methyl- C_5	$2f$	
	3-methyl- C_5	f	
	2,3-dimethyl- C_4	f^2	
C_7	$n-C_7$	1	$2a^5(1 + 4f + 3f^2)$
	2-methyl- C_6	$2f$	
	3-methyl- C_6	$2f$	
	2,3-dimethyl- C_5	$2f^2$	
	2,4-dimethyl- C_5	f^2	
C_8	$n-C_8$	1	$2a^6(1 + 5f + 6f^2 + f^3)$
	2-methyl- C_7	$2f$	
	3-methyl- C_7	$2f$	
	4-methyl- C_7	f	
	2,3-dimethyl- C_6	$2f^2$	
	2,4-dimethyl- C_6	$2f^2$	
	3,4-dimethyl- C_5	f^2	
	2,5-dimethyl- C_6	f^2	
	2,3,4-trimethyl- C_5	f^3	

ble addition steps, the carbon number and isomer distribution may be evaluated relative to C_2 in terms of a and f , as shown in Table 16. In this development both carbons of the C_2 chain are regarded as end carbons. Although this assumption leads to good agreement between predicted and observed C_3/C_2 ratios, it is not consistent with some of the mechanisms that have been postulated. Values of f were selected to give the best fit to observed isomer data, as shown in Tables 14 and 15.

For carbon number distributions, $\phi_n = 2\phi_2 F_n a^{n-2}$ and

$$\log (\phi_n / F_n) = n \log a + \log (2\phi_2 / a^2) \quad (51)$$

where ϕ_n is the number of moles in the fraction containing n carbon atoms and F_n is the function in parentheses in Table 16. The values of f used in evaluating F_n were those obtained from isomer data in Tables 14 and 15, $f = 0.035$ for cobalt and $f = 0.115$ for iron. For products from cobalt catalysts⁵⁰ (Figure 63), the straight line fits the data, probably within the experimental error, from C_2 to C_{20} . Since the value of f was low, this plot is not greatly different from that of Eq. (40). The linear plot represented satisfactorily Weitkamp's carbon-number distribution data from iron catalysts in the range C_2 to C_{14} , but deviated at higher carbon numbers, (Fig-

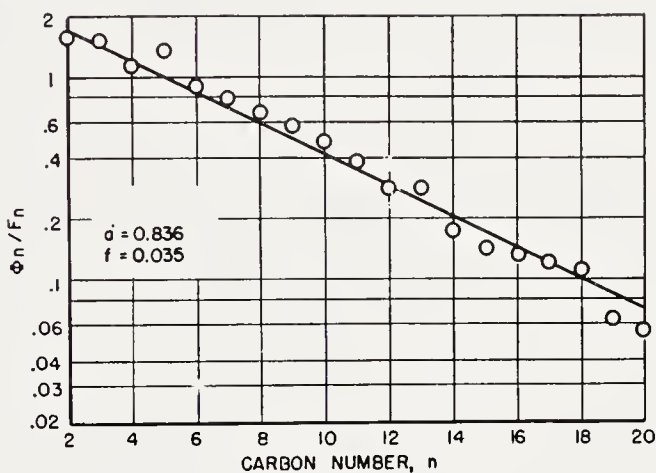


Figure 63. Plot of Equation 51 for data from cobalt catalyst. (From Ref. 4)

ure 64). Figure 65 represents typical data from the Schwärzheide tests, using the value of f of 0.115 found in Table 15. A straight line only approximates portions of the data, such as from C_3 to C_9 , since the experimental points describe a curve.

Weitkamp, Seelig, Bowman, and Cady¹³⁴ devised a scheme for predicting isomer distributions that followed essentially the mathematical development of Weller and Friedel with, however, the addition of carbon atoms limited to the end and penultimate carbons at one end of the growing chain and addition not permitted on carbon atoms already attached to three carbons. This scheme was said to be capable of predicting the isomer distributions of products from cobalt and iron catalysts.

Cady, Launer, and Weitkamp²² considered that aromatic hydrocarbons are formed by cyclization of the same growing chains that produce aliphatic hydrocarbons and devised a scheme involving formation of a bond between an end or adjacent-to-end carbon atoms and another carbon five atoms down the chain. Cyclization involving tertiary carbon atoms was not per-

mitted, as aromatic rings can not be produced from the resulting structure. Thus, from the normal C_8 chain, $C-7-6-C-C-C-2-1$, ethylbenzene is formed by 1-6 bonding and *o*-xylene from 2-7. For the 2-methyl C_8 chain, $C-6-C-C-C-C-1$, only 1-6 bonding is possible. The growing chains were assumed to be present in amounts proportional to the carbon chain isomers in C_8 hydrocarbons, and where bonding was possible between both end and adjacent-to-end carbons, 68 per cent was assumed to occur with

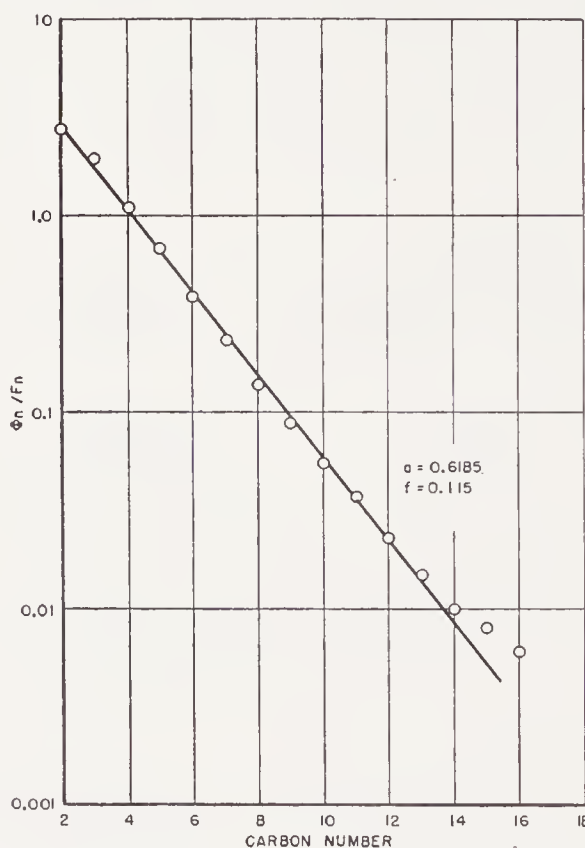


Figure 64. Plot of Equation 51 for data from synthesis with fluidized iron catalyst (Standard Oil). (Distribution data from Ref. 134)

end and 32 per cent with adjacent-to-end carbons. On this basis satisfactory agreement between predicted and experimental distributions was obtained for C_8 aromatics, as shown in Table 17, and similar but less exact agreement was found for the C_9 aromatics.

At present insufficient data on chain branching are available to correlate this factor with catalyst composition and type or operating conditions. Iron catalysts operated at 325 to 350°C produce a greater fraction of branched hydrocarbons than cobalt catalysts at 180 to 200°C; however, it is not known whether the difference results from the catalyst or the conditions of operation, especially the high temperature used in fluidized iron

tests. According to schemes for predicting isomer distribution, the ratio of iso- to *n*-hydrocarbons in the C₄ fraction should be sufficient for characterizing chain branching. Weitkamp¹³⁴ (p. 122) found that this ratio was the same for iron catalysts with or without alkali, although the olefin contents and presumably the over-all distributions were considerably different. Apparently other data of this type are not available. The relative simplicity

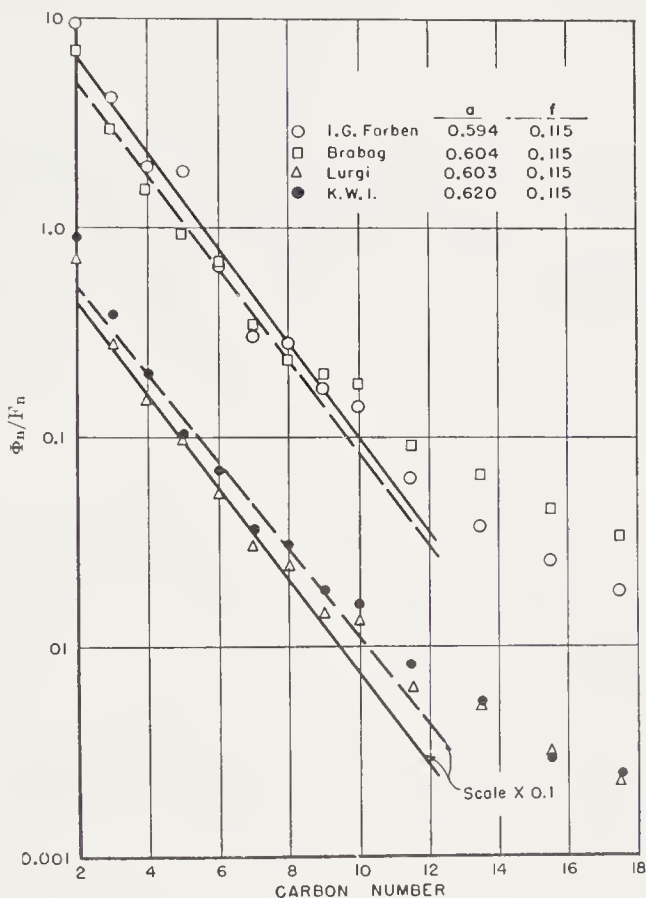


Figure 65. Plots of Equation 51 for data from Schwarzheide tests of iron catalysts.

of detailed analysis of the C₄ fraction by modern methods should make investigations of this type attractive.

Mechanisms Involving Oxygenated Intermediates

Storch, Golumbic, and Anderson¹²³ proposed a detailed set of equations that explain many of the characteristics of synthesis products. Although most of these postulates were made without significant experimental evidence, except analytical data on synthesis products, the postulates have been essentially substantiated by the mechanism experiments of Emmett and Kummer, which will be discussed subsequently. The following as-

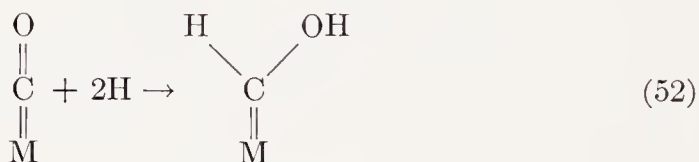
TABLE 17. COMPARISON BETWEEN PREDICTED AND OBSERVED YIELDS OF C₈ AROMATICS^a

	Predicted	Observed
Ethylbenzene	46.0	46
<i>o</i> -xylene	31.3	29
<i>m</i> -xylene	14.1	18
<i>p</i> -xylene	8.6	7

^a From Ref. 22.

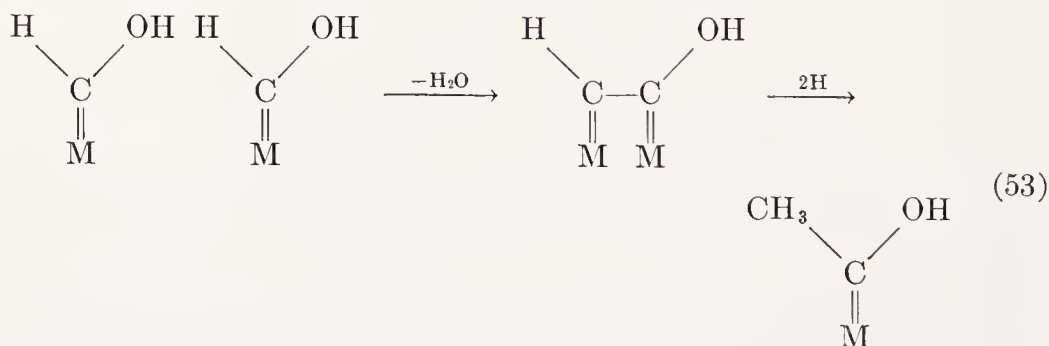
sumptions were made: (a) hydrogen is adsorbed as atoms on surface metal atoms, (b) chemisorption of carbon monoxide occurs on metal atoms with the formation of bonds similar to those in metal carbonyls, (c) the adsorbed carbon monoxide is partially hydrogenated according to Eq. (52). Chain building may occur in two ways: at the end carbon (Eqs. 53 and 54) and at the adjacent-to-end carbon (Eqs. 55 and 56). In these steps the double

Initiation of chains

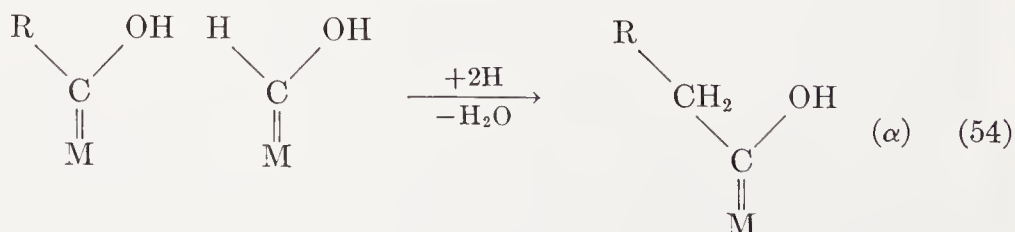


Growth of chains

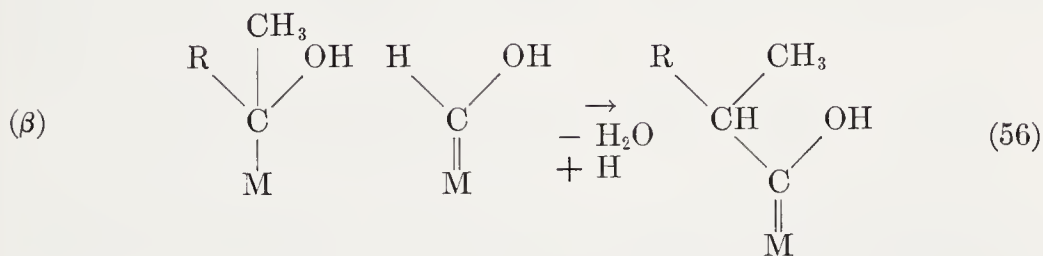
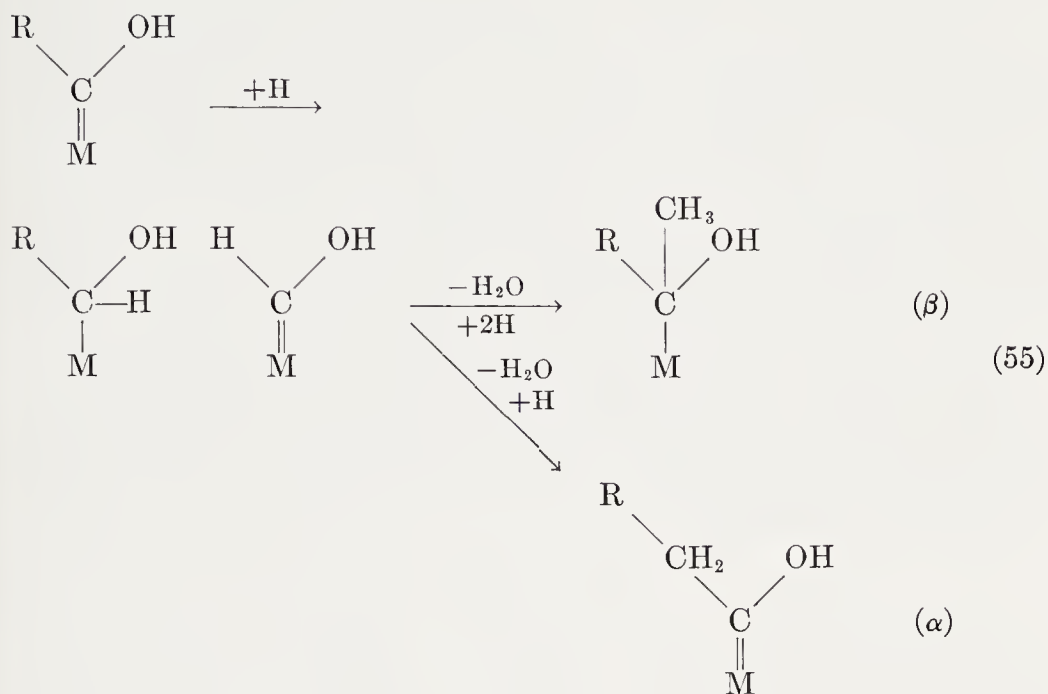
(a) At end carbon



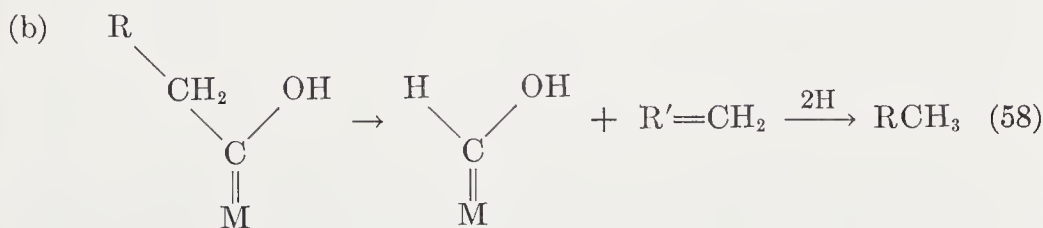
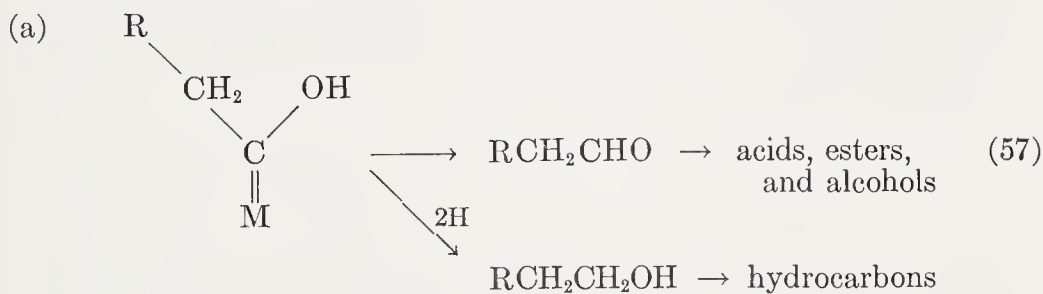
and



(b) At penultimate carbon

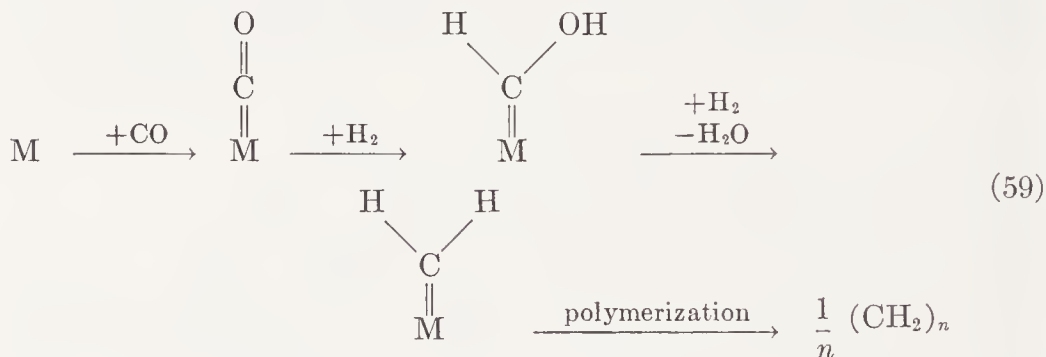


Termination of chain

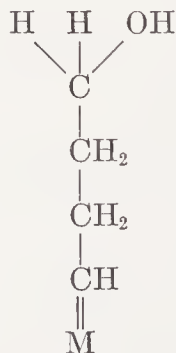


bonds between carbon and metal atoms are assumed to be more resistant to hydrogenation if the carbon atom is also attached to a hydroxyl group. Growth processes leading eventually to chain branching involve partial hydrogenation of the carbon-metal bond, according to Eqs. (55) and (56). Intermediate α is the same as in Eq. (54), but intermediate β may produce a chain with a methyl branch according to Eq. (56). Various equations (Eqs. 57 and 58) were proposed for terminating the growing chain to give aldehydes, alcohols, olefins, and paraffins. Acids and esters may result from Cannizarro reactions of aldehyde-like intermediates or by side reactions. This reaction scheme, with the exception of the $C_3:C_2$ ratio, conforms with the stepwise growth pattern of Anderson, Friedel, and Storch⁴.

Other workers have proposed intermediates similar to those of Eqs. (52) to (58). Hamai⁶⁰ and workers at I. G. Farbenindustrie⁶⁶ proposed the following sequence which, however, reverts to the methylene polymerization concept in the fourth step:



This proposal does not account for the presence of oxygenated molecules or chain branching. Gall, Gibson, and Hall⁵² postulated an oxygenated complex which was, however, attached to the catalyst at the opposite end of the chain from the hydroxyl group, such as the following structure for a straight C_4 chain,



Chain growth was postulated to proceed by addition of methylene groups at the end attached to the catalyst. The experiments of Kummer and Em-

mett^{85, 86}, described in the next several paragraphs, demonstrate that this growth mechanism is probably incorrect.

The experiments of Kummer and Emmett^{85, 86}, involving the incorporation of alcohols containing C¹⁴ in the Fischer-Tropsch synthesis with iron catalysts provide important information regarding the mechanism of chain growth. This work is an excellent example of well-planned research involving new and difficult experimental techniques. In the synthesis at atmospheric pressure alcohols were incorporated without altering the course of the reaction greatly. The tagged alcohols served as intermediates, and from analyses of resulting hydrocarbon fractions for radioactivity the pattern of chain growth can be delineated.

Alkali-free synthetic ammonia catalysts, the first containing 1.6 per cent Al₂O₃ and 0.6 ZrO₂ and the second 2.8 Al₂O₃ and 1.4 ThO₂, were used in a fixed-bed glass reaction system at atmospheric pressure and 235°C. Synthesis gas containing 1H₂ + 1CO was bubbled through the alcohol, maintained at appropriate temperatures, so that the alcohol vapor in the inlet gas was about 1.5 per cent by volume. Gaseous hydrocarbons were fractionated with a Podbielniak column and liquid products in a small glass column of negligible holdup. More detailed separations were made in a small adsorption fractionator, and dehydrated chabazite was used to separate *n*-butane from isobutane.

The incorporation of alcohols into hydrocarbon fractions of different carbon number will be considered first. For ethanol, *n*-propanol, isobutanol, the radioactivity of the hydrocarbons indicated that at least one-third of the hydrocarbon chains were produced from the alcohol. The radioactivity of the hydrocarbons *per mole* was approximately constant for fractions having a higher carbon number than the alcohol, as shown in Figure 66. With isopropanol the incorporation in the C₄ fraction was smaller, and the radioactivity *per mole* decreased rapidly with carbon number. The incorporation was still lower for methanol, but the radioactivity per mole of hydrocarbon increased linearly with carbon number (Figure 67). The incorporation of *t*-butyl alcohol was studied with non-radioactive alcohol. The hydrocarbons were fractionated into a narrow cut and examined for neopentane. None was found.

The conclusions that can be drawn from these data will be summarized briefly before considering detailed analyses of product fractions. Primary and secondary alcohols are incorporated in the synthesis. Ethanol, *n*-propanol, and isobutanol serve as intermediates in the synthesis. Apparently these alcohols initiate growing chains that eventually desorb as hydrocarbons, and only one alcohol molecule is incorporated per chain. For the secondary alcohol, isopropanol, the extent of incorporation was smaller and decreased steadily with increasing carbon number. Methanol was in-

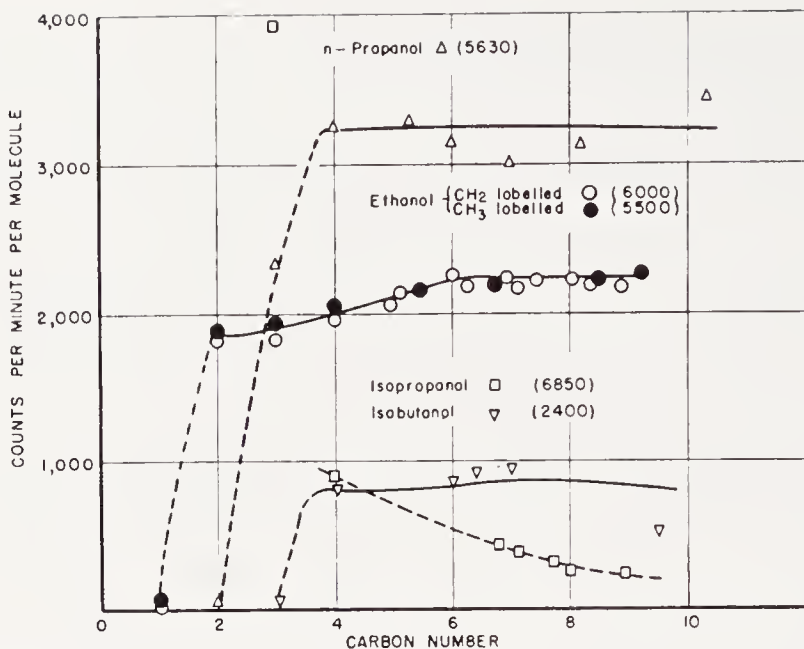


Figure 66. Incorporation of radioactive alcohols in synthesis on iron catalysts. The radioactivity of the alcohol is shown in parentheses. (From data of Refs. 85 and 86)

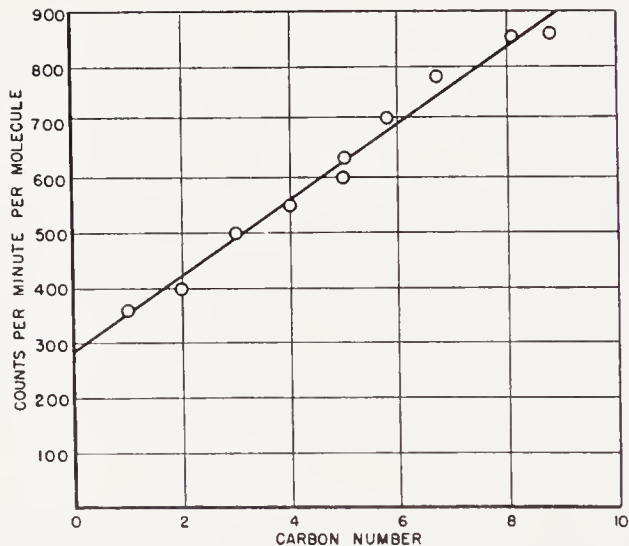


Figure 67. Incorporation of radioactive methanol in the synthesis on iron catalysts. Counts per minute for methanol = 5000. (From data of Ref. 85)

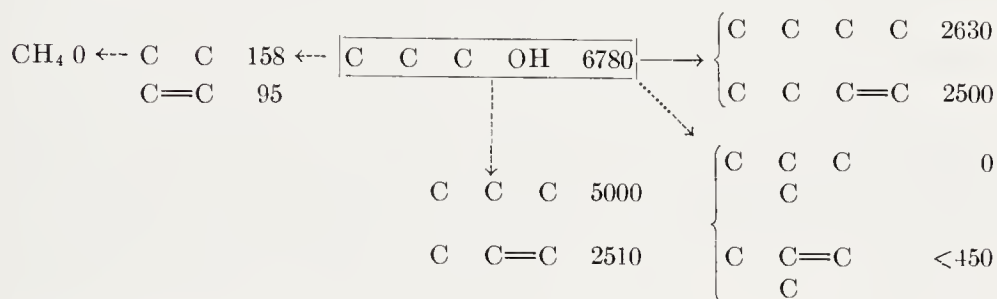
incorporated only to a small extent, and the degree of incorporation increased with carbon number apparently resulting from the incorporation of two or more alcohol carbons into the growing chain. Although the results with primary alcohols higher than methanol are consistent with a stepwise

growth of the carbon chain, these data do not limit the growth process to this pattern.

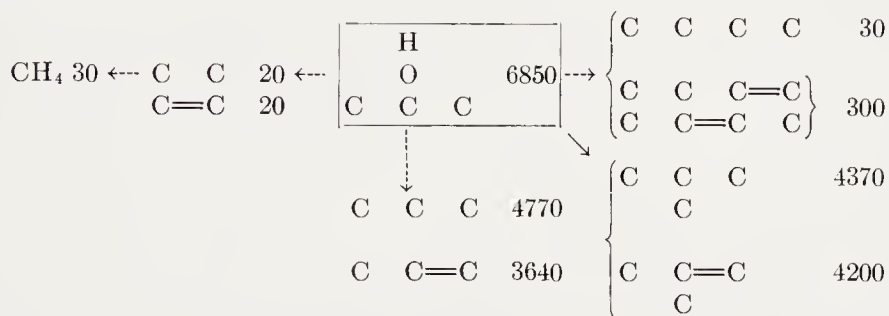
The gaseous products from tests with ethyl and propyl alcohols were given detailed analyses. Table 18 presents the radioactivity of gaseous products from the incorporation of normal and isopropanol. The data indicate that the hydroxyl group defines the point of attachment of the next

TABLE 18. RADIOACTIVITY OF GASEOUS HYDROCARBONS FROM THE INCORPORATION OF NORMAL AND ISOPROPANOL ON IRON CATALYSTS

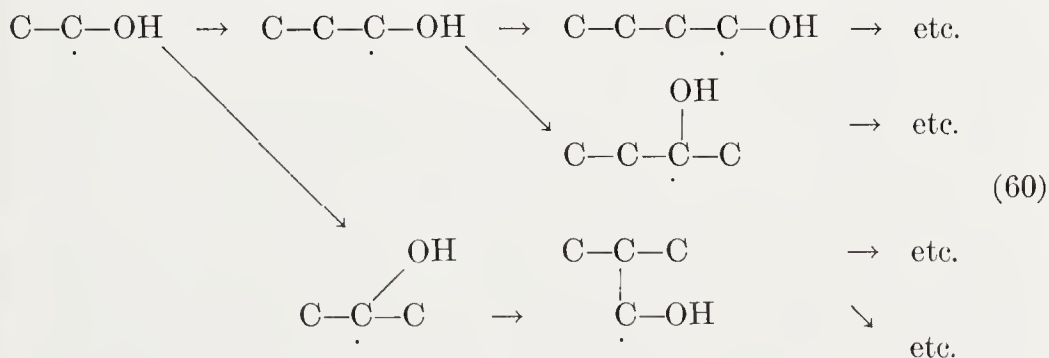
(a) *n*-propanol



(b) isopropanol

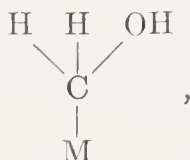


carbon atom; thus normal C₄ is formed almost exclusively from *n* propanol and iso-C₄ from isopropanol. Thus the chain growth pattern is

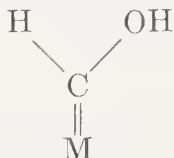


and not the pattern shown on p. 355. This reaction scheme is the same as

that of Storch, Golumbic, and Anderson¹²³ shown on p. 360. Kummer and Emmett suggested that the complex produced from methanol may be



which differs from initial complex postulated for the normal synthesis,



This difference may account for the lower incorporation of methanol. Nevertheless, methanol must to some extent produce the normal complex or the elements of synthesis gas at the surface, since the degree of incorporation increased with carbon number. If carbon monoxide is produced from dissociation of methanol, it does not escape the surface in sizable quantities, as the radioactivity of carbon monoxide was low.

The C₄ hydrocarbons produced during the incorporation of CH₃C¹⁴H₂CH₂OH were analyzed by thermal cracking to determine the radioactivity of the end carbon atoms, none was radioactive. In the synthesis experiments, the propyl alcohols were not appreciably degraded to C₁ and C₂ hydrocarbons, but sizable amounts of radioactive C₃ hydrocarbons were produced.

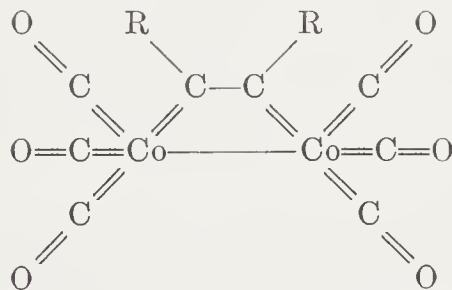
Detailed degradation experiments on C₃ hydrocarbons from the incorporation of ethanol, in one case methyl-labeled and in the other methylene-labeled, indicated that about 90 per cent of the addition occurred at the carbon attached to the hydroxyl group and 10 per cent on the second carbon. This result apparently contradicts the growth pattern illustrated on p. 365, as chain growth occurs at both carbons. Recent results from Dr. Emmett's laboratory³⁶ suggest that this apparent anomaly may have resulted from partial dehydration of ethanol to ethylene and subsequent incorporation of the ethylene.

The possibility that chain extension in Fischer-Tropsch synthesis may involve oxo-type reactions will be considered briefly. The oxo process and the chemistry of metal carbonyls may lead to valuable clues regarding the mechanism of the Fischer-Tropsch synthesis. The oxo reactions, hydroformylation of olefins or homologation of alcohols, are homogeneous processes involving cobalt hydrocarbonyl as either a catalyst or reactant. Possibly the inability of iron and nickel to accomplish these reactions is related to the relative instability of their hydrocarbonyls. The oxo catalyst appears to be unable to initiate carbon chains from H₂ + CO; how-

ever, chain extension in the Fischer-Tropsch synthesis could occur by the reaction of olefins or alcohols produced in a primary step with hydrogen and carbon monoxide (a) involving a carbonyl-type surface intermediate or (b) involving a carbonyl intermediate not attached to the catalyst surface.

Possibility (b), that chain growth occurs homogeneously in the oil phase, for example, in pores of the catalyst at some distance from the surface, appears unlikely because oxo-addition to olefins leads to more highly branched molecules than those obtained in the Fischer-Tropsch synthesis.

Some aspects of possibility (a) have been considered previously in this discussion. Since the surface intermediates may be expected to have different catalytic properties from normal metal carbonyls, this possibility cannot be eliminated on the basis of available data. Surface complexes of a hydrocarbonyl-type would be stabilized by the presence of alkali, and this suggestion should be scrutinized as a means of explaining the effects of alkali on the synthesis. Furthermore, recent studies of Sternberg and co-workers¹²² have demonstrated the existence of stable complexes formed from dicobalt octacarbonyl and acetylenic compounds. The suggested structure



resembles in some respects surface complexes that have been considered in the mechanism of the Fischer-Tropsch synthesis.

Acknowledgment

The author is pleased to acknowledge the assistance of Professor P. H. Emmett, Dr. H. H. Storch, Dr. L. J. E. Hofer, E. M. Cohn, J. F. Shultz, R. E. Kelly, Sophie Radosevich, and E. C. Ralston in the preparation and review of this and the two preceding chapters.

Bibliography

1. Abelson, M., Seligman, B., and Shultz, J. F., unpublished data of the Bureau of Mines.
2. Aicher, A., Myddleton, W. W., and Walker, J., *J. Soc. Chem. Ind. (London)*, **54**, 313T (1935).
3. Anderson, R. B., Feldman, J., and Storch, H. H., *Ind. Eng. Chem.*, **44**, 2418 (1952).

4. Anderson, R. B., Friedel, R. A., and Storch, H. H., *J. Chem. Phys.*, **19**, 313 (1951).
5. Anderson, R. B., Hall, W. K., and Hofer, L. J. E., *J. Am. Chem. Soc.*, **70**, 2465 (1948).
6. Anderson, R. B., Hall, W. K., Krieg, A., and Seligman, B., *J. Am. Chem. Soc.*, **71**, 183 (1949).
7. Anderson, R. B., Krieg, A., Friedel, R. A., and Mason, L. S., *Ind. Eng. Chem.*, **41**, 2189 (1949).
8. Anderson, R. B., Krieg, A., Seligman, B., and O'Neill, W. E., *Ind. Eng. Chem.*, **39**, 1548 (1947).
9. Anderson, R. B., and Lecky, J., unpublished work of the Bureau of Mines.
10. Anderson, R. B., Seligman, B., Shultz, J. F., Kelly, R. E., and Elliott, M. A. *Ind. Eng. Chem.*, **44**, 391 (1952).
11. Arnold, J. H., and Keith, P. C., in *Am. Chem. Soc. Advances in Chemistry Series, No. 5, Progress in Petroleum Chemistry*, 1951, p. 120.
12. Badin, E. J., *J. Am. Chem. Soc.*, **65**, 1809 (1943).
13. Bahr, H. A., and Jessen, V., *Ber.*, **61**, 2177 (1928); **63**, 2226 (1930); **66**, 1238 (1933).
14. Bashkirov, A. N., Kryukov, Y. B., and Kazan, Y. B., *Compt. rend. acad. sci. U.R.S.S.*, **67**, 1029 (1949).
15. Beebe, R. A., in "Heterogene Katalyse," I, edited by G. M. Schwab, p. 473, Vienna, Springer-Verlag, 1943, also Edward Brothers, Ann Arbor, Mich.
16. Brötz, W., *Z. Elektrochem.*, **53**, 301 (1949).
17. Brötz, W., and Spengler, H., *Brennstoff-Chem.*, **31**, 97 (1950).
18. Browning, L. C., DeWitt, T. W., and Emmett, P. H., *J. Am. Chem. Soc.*, **72**, 4211 (1950).
19. Browning, L. C., and Emmett, P. H., *J. Am. Chem. Soc.*, **74**, 1680 (1952).
20. Brunauer, S., and Emmett, P. H., *J. Am. Chem. Soc.*, **62**, 1732 (1940).
21. Bruner, F. H., *Ind. Eng. Chem.*, **41**, 2511 (1949).
22. Cady, W. E., Launer, P. J., and Weitkamp, A. W., *Ind. Eng. Chem.*, **45**, 350 (1953).
23. Craxford, S. R., *Trans. Faraday Soc.*, **42**, 576 (1946).
24. Craxford, S. R., *Fuel*, **26**, 119 (1947).
25. Craxford, S. R., and Rideal, E. K., *J. Chem. Soc.*, **1939**, 1604.
26. Crowell, J. H., Benson, H. E., Field, J. H., and Storch, H. H., *Ind. Eng. Chem.*, **42**, 2376 (1950).
27. Eidus, Y. T., *Bull. acad. sci. U. R. S. S., Classe sci. chim.*, **1942**, 190.
28. Eidus, Y. T., *ibid.*, **1943**, 65.
29. Eidus, Y. T., *ibid.*, **1946**, 447.
- 29a. Eidus, Y. T., Puzitski, K. V., and Batuev, M. I., *Izvest. Acad. Nauk. S.S.S.R., Otdel. Khim. Nauk*, **1952**, 978; *Bull. acad. sci. U.S.S.R., Classe sci. chim.*, **1952**, 859.
- 29b. Eidus, Y. T., Puzitski, K. V., and Meshcheryakov, A. P., *ibid.* **1954**, 123.
30. Eidus, Y. T., Ershov, N. I., Batuev, M. I., and Zelinskii, N. D., *ibid.* **1951**, 722.
31. Eidus, Y. T., Zelinskii, N. D., Ershov, N. I., and Batuev, M. I., *ibid.*, **1950**, 377.
32. Eidus, Y. T., Zelinskii, N. D., and Puzitski, K. V., *ibid.*, **1949**, 110.
33. Eidus, Y. T., Zelinskii, N. D., and Puzitski, K. V., *ibid.*, **1950**, 98.
34. Elvins, O. C., and Nash, A. W., *Nature*, **118**, 154 (1926).
35. Emmett, P. H., in *Twelfth Report of the Committee on Catalysis*, p. 64, New York, John Wiley & Sons, Inc. 1940.
36. Emmett, P. H., private communication.
37. Emmett, P. H., and Brunauer, S., *J. Am. Chem. Soc.*, **59**, 310, 1553, 2682 (1937).
38. Emmett, P. H., and Harkness, R. W., *J. Am. Chem. Soc.*, **57**, 1631 (1935).

39. Eroseev, B. V., Runtso, A. P., and Volkova, A. A., *Acta Physicochim. U.R.S.S.*, **13**, 111 (1940).
40. Fischer, F., *Brennstoff-Chem.*, **24**, 489 (1930).
41. Fischer, F., and Bahr, T., *Ges. Abh. Kenntnis Kohle*, **8**, 255 (1929).
42. Fischer, F., Bahr, T., and Meusel, A., *Brennstoff-Chem.*, **16**, 466 (1935).
43. Fischer, F., and Koch, H., *Ges. Abhandl. Kenntnis Kohle*, **10**, 574 (1930).
44. Fischer, F., and Koch, H., *Brennstoff-Chem.*, **13**, 428 (1932).
45. Fischer, F., and Pichler, H., *Brennstoff-Chem.*, **12**, 365 (1931).
46. Fischer, F., and Pichler, H., *ibid.*, **14**, 306 (1933).
47. Fischer, F., and Pichler, H., *ibid.*, **20**, 41 (1939).
48. Fischer, F., and Tropsch, H., *Brennstoff-Chem.*, **7**, 97 (1926).
49. Fischer, F., and Tropsch, H., *Ges. Abhandl. Kenntnis Kohle*, **10**, 494 (1930).
50. Friedel, R. A., and Anderson, R. B., *J. Am. Chem. Soc.*, **72**, 1212, 2307 (1950).
51. Fujimura, K., and Tsuneoka, S., *Sci. Papers Inst. Phys. Chem. Research (Tokyo)*, **25**, 137 (1934).
52. Gall, D., Gibson, E. J., and Hall, C. C., *J. Appl. Chem.*, **2**, 371 (1952).
53. Ghosh, J. C., Sastri, M. V. C., and Kini, K. A., *Ind. Eng. Chem.*, **44**, 2463 (1952).
54. Gibson, E. J., *J. Appl. Chem.*, **3**, 375 (1953).
55. Gibson, E. J., and Hall, C. C., *J. Appl. Chem.*, **4**, 49 (1954).
56. Griffith, R. H., in "Advances in Catalysis," Vol. I, p. 97, ed by N. G. Frankenburg, V. I. Komarewsky, and E. K. Rideal, New York, Academic Press, 1948.
57. Haensel, V., and Ipatieff, V. N., *Ind. Eng. Chem.*, **39**, 853 (1947).
58. Hall, C. C., Gall, D., and Smith, S. L., *J. Inst. Petroleum*, **38**, 845 (1952).
59. Hall, W. K., Tarn, W. H., and Anderson, R. B., *J. Phys. Chem.*, **56**, 688 (1952).
60. Hamai, S., *J. Chem. Soc. Japan*, **62**, 576 (1941); *Bull. Chem. Soc. Japan*, **16**, 213 (1941).
61. Herington, E. F. G., *Chemistry & Industry*, **1946**, 347.
62. Hofer, L. J. E., Peebles, W. C., and Bean, E. H., *J. Am. Chem. Soc.*, **72**, 2698 (1950).
63. Holm, V. C. F., and Blue, R. W., *Ind. Eng. Chem.*, **44**, 107 (1952).
64. Hougen, O. A., and Watson, K. M., *Ind. Eng. Chem.*, **35**, 529 (1943).
65. Hunsmann, W., in "Heterogene Katalyse I", p. 405, ed. by G. M. Schwab, Vienna, Springer-Verlag, 1943; also Edward Brothers, Ann Arbor.
66. I. G. Farben, T. O. M. Reel 134, Section 1a, Item 8.
67. Ipatieff, V. N., Monroe, G. S., Fischer, L. E., and Meisinger, E. E., *Ind. Eng. Chem.*, **41**, 1802 (1949).
- 67a. Kagan, Y. B., Kryukov, Y. B., Kamzolkina, E. V., and Bashkirov, A. N., *Izvest. Akad. Nauk. S.S.S.R., Otdel. Khim. Nauk.*, **1952**, 649.
68. Karn, F. S., Shultz, J. F., and Anderson, R. B., unpublished work of the Bureau of Mines.
69. Kelly, R. E., unpublished data of the Bureau of Mines.
70. Kini, K. A., Basak, N. G., and Lahiri, A., *J. Sci. Ind. Research*, **10B**, 243 (1951).
71. Koch, H., and Gilfert, W., *Brennstoff-Chem.* **30**, 213 (1949).
72. Koch, H., and Kuster, H., *Brennstoff-Chem.*, **14**, 245 (1933).
73. Koch, H., and Titzenthaler, E., *Brennstoff-Chem.*, **31**, 212 (1950).
74. Koelbel, H., and Ackermann, P., *Brennstoff-Chem.*, **31**, 10 (1950).
75. Koelbel, H., Ackermann, P., Ruschenburg, E., Langheim, R., and Engelhardt, F., *Chem. Ing. Tech.*, **23**, 153 (1951).
76. Koelbel, H., Ackermann, P., Ruschenburg, E., Langheim, R., and Engelhardt, F., *ibid.*, **23**, 183 (1951).
77. Koelbel, H., and Engelhardt, F., *Erdöl u Kohle*, **2**, 52 (1949).

78. Koelbel, H., and Engelhardt, F., *Chem. Ing. Tech.*, **22**, 97 (1950).
79. Koelbel, H., and Engelhardt, F., *Erdöl u Kohle*, **3**, 529 (1950).
80. Koelbel, H., and Engelhardt, F., *ibid.*, **5**, 1 (1952); *Angew. Chem.*, **64**, 54 (1952).
81. Komarewsky, V. I., Riesz, C. H., and Thodos, G., *J. Am. Chem. Soc.*, **61**, 2525 (1939).
82. Kummer, J. T., Browning, L. C., and Emmett, P. H., *J. Chem. Phys.*, **16**, 740 (1948).
83. Kummer, J. T., DeWitt, T. W., and Emmett, P. H., *J. Am. Chem. Soc.*, **70**, 3632 (1948).
84. Kummer, J. T., and Emmett, P. H., *J. Phys. Chem.*, **56**, 258 (1952).
85. Kummer, J. T., and Emmett, P. H., *J. Am. Chem. Soc.*, **75**, 5177 (1953).
86. Kummer, J. T., Podgurski, H. H., Spencer, W. D., and Emmett, P. H., *J. Am. Chem. Soc.*, **73**, 564 (1951).
87. Kuster, H., *Brennstoff-Chem.*, **17**, 203, 221 (1936).
88. Laidler, K. J., in "Catalysis," Vol. I, p. 75, ed. by P. H. Emmett, New York, Reinhold Publishing Corp., 1954.
89. Linckh, E., and Klemm, R., in "The CO-H₂ Synthesis" ed. by H. Zorn, *F.I.A.T. Final Report* 1267, PB 97, 368.
90. Manes, M., *J. Am. Chem. Soc.*, **74**, 3148 (1952).
91. Matsumura, S., Tarama, K., and Kodama, S., *J. Soc. Chem. Ind. Japan*, **43**, Suppl. binding, 175B (1940).
92. McCartney, J. T., Hofer, L. J. E., Seligman, B., Lecky, J. A., Peebles, W. C., and Anderson, R. B., *J. Phys. Chem.*, **57**, 730 (1953).
93. Montgomery, C. W., and Weinberger, E. B., *J. Chem. Phys.*, **16**, 424 (1948).
94. Morrell, C. E., Carlson, C. S., McAteer, J. H., Robey, R. F., and Smith, P. V., *Ind. Eng. Chem.*, **44**, 2839 (1952).
95. Mulford, R. M. R., and Russell, W. W., *J. Am. Chem. Soc.*, **74**, 1969 (1952).
96. Murata, Y., Ishikawa, S., and Tsuneoka, S., *J. Soc. Chem. Ind. Japan*, **39**, Suppl. binding, 329 (1936).
97. Myddleton, W. W., and Walker, J., *J. Soc. Chem. Ind. (London)*, **54**, 313T (1935).
98. Perrin, M., "Recherches sur les synthèses d'hydrocarbures aliphatiques a l'aide des melange d'oxide de carbone et d'hydrogene," doctoral dissertation under Prof. M. Prettre, University of Lyon, 1948.
99. Pichler, H., *Brennstoff-Chem.*, **24**, 27 (1943).
100. Pichler, H., *ibid.*, **24**, 39 (1943).
101. Pichler, H., T.O.M. Reel 101, Documents PG 21,559-NID and PG 21,574-NID; translated in U. S. Bureau of Mines Special Rept. by M. Leva, 1-67, 1946, Pittsburgh, Pa.
102. Pichler, H., "Synthesis of Hydrocarbons from Carbon Monoxide and Hydrogen," U. S. Bureau of Mines Special Rept. (1947), 158 pp. Reproduced in T.O.M. Reel 259, Frames 467-654.
103. Pichler, H., "Advances in Catalysis," Vol. IV, p. 271, ed. by W. C. Frankenburg, V. I. Komarewsky, and E. K. Rideal, New York, Academic Press, 1952.
104. Pichler, H., and Buffleb, H., *Brennstoff-Chem.*, **21**, 257, 273, 285 (1940).
105. Pichler, H., and Buffleb, H., *ibid.*, **23**, 73 (1942).
106. Podgurski, H. H., Kummer, J. T., DeWitt, T. W., and Emmett, P. H., *J. Am. Chem. Soc.*, **72**, 5382 (1950).
107. Prettre, M., Eichner, C., and Perrin, M., *Compt. rend.*, **224**, 278 (1947).
108. Reisinger, Breywisch, and Geiseler, T.O.M. Reel 55, Bag 2523, Documents 86 (1943) and 87 (1942).

109. Riesz, C. H., Lister, F., Smith, L. G., and Komarewsky, V. I., *Ind. Eng. Chem.*, **40**, 718 (1948).
110. Royen, P., and Erhard, F., *Erdöl u Kohle*, **6**, 195 (1953).
111. Ruhrchemie, T.O.M. Reel 33, Bag 3,440, Target 30/5.01, Item 24; T.O.M. Reel 36, Bag 3,451, Item 13.
112. Ruschenburg, E., Doctoral dissertation, Technischen Hochschule, Dresden, F.I. A.T. Reel 115X, Frames 700-783. Recently published, Koelbel, H., and Ruschenburg, E., *Brennstoff-Chem.*, **35**, 161 (1954).
113. Russell, W. W., and Miller, G. H., *J. Am. Chem. Soc.*, **72**, 2446 (1950).
114. Sabatier, P., and Senderens, J. B., *Compt. rend.* **134**, 689 (1902).
115. Sastri, M. V. C., and Srinivasan, S. R., *J. Am. Chem. Soc.*, **75**, 2898 (1953).
116. Scheuermann, A., in report of H. Zorn, PB 97,368; F.I.A.T. Final Rept. 1,267 (1949).
117. Seligman, B., unpublished data of Bureau of Mines.
118. Smith, D. F., Hawk, C. O., and Golden, P. L., *J. Am. Chem. Soc.*, **52**, 3221 (1930).
119. Stein, K. C., unpublished data of the Bureau of Mines.
120. Stein, K. C., and Hall, W. K., unpublished data of the Bureau of Mines.
121. Stein, K. C., and Karn, F. S., unpublished experiments of the Bureau of Mines.
122. Sternberg, H. W., Greenfield, H., Friedel, R. A., Wotiz, J., Markby, R., and Wender, I., *J. Am. Chem. Soc.*, **76**, 1457 (1954).
123. Storch, H. H., Golumbic, N., and Anderson, R. B., "The Fischer-Tropsch and Related Syntheses," New York, John Wiley & Sons, Inc., 1951.
124. Suen, T. J., and Fan, S., *J. Am. Chem. Soc.*, **65**, 1243 (1943).
125. Taylor, E. H., and Taylor, H. S., *J. Am. Chem. Soc.*, **61**, 503 (1939).
126. Thompson, S. O., Turkevich, J., and Irsa, A. P., *J. Am. Chem. Soc.*, **73**, 5213 (1951).
127. Tramm, H., *Brennstoff-Chem.*, **33**, 21 (1952).
128. Tsuneoka, S., and Fujimura, K., *J. Soc. Chem. Ind. Japan*, **37**, Suppl. binding, 463 (1934).
129. Vol'kenshtein, F. F., *J. Phys. Chem. (U.S.S.R.)*, **23**, 917 (1949).
130. Volmer, W., *Z. Elektrochem.*, **54**, 252 (1950).
131. Warner, B. R., Derrig, M. J., and Montgomery, C. W., *J. Am. Chem. Soc.*, **68**, 1615 (1946).
132. Watanabe, S., Morikawa, K., and Igawa, S., *J. Soc. Chem. Ind. Japan*, **38**, Suppl. binding 70 (1935).
133. Weitkamp, A. W., and Frye, C. G., *Ind. Eng. Chem.*, **45**, 363 (1953).
134. Weitkamp, A. W., Seelig, H. S., Bowman, N. J., and Cady, W. E., *Ind. Eng. Chem.*, **45**, 343 (1953).
135. Weller, S., *J. Am. Chem. Soc.*, **69**, 2432 (1947).
136. Weller, S., and Friedel, R. A., *J. Chem. Phys.*, **17**, 801 (1949); **18**, 157 (1950).
137. Wheeler, A., "Advances in Catalysis," Vol. III, p. 250, ed by. N. G. Frankenburg, V. I. Komarewsky, and E. K. Rideal, New York, Academic Press, 1951.
138. White, E. C., and Shultz, J. F., *Ind. Eng. Chem.*, **26**, 95 (1934).

CHAPTER 4

CRYSTALLINE PHASES AND THEIR RELATION TO FISCHER-TROPSCH CATALYSTS

L. J. E. Hofer

Physical Chemist, Synthetic Fuels Research Branch, Bureau of Mines, Bruceton, Pa.

INTRODUCTION

Basic Characteristics

Fischer-Tropsch catalysts are remarkable for the number of inorganic compounds or crystalline phases which are involved in their formation, activation, and deactivation. Fischer^{64, 65, 66} early focused attention on the carbides of iron, cobalt, and nickel by his statement that these were intermediates in the Fischer-Tropsch synthesis. Although Fischer's hypothesis in its original form is no longer tenable^{5, 138, 139, 140, 143, 255}, it has served to focus attention and to stimulate experimentation on the relation of various crystalline phases to catalytic activity^{69, 70, 71, 98}. A study of all the crystalline phases involved in the Fischer-Tropsch synthesis may lead to new basic information concerning catalyst activity.

The elements iron, cobalt, nickel, ruthenium, rhodium, palladium, osmium, iridium, and/or platinum are found in almost all catalysts showing any trace of Fischer-Tropsch activity. (For the purposes of this discussion, Fischer-Tropsch reaction is defined as the reaction of carbon monoxide and hydrogen to form hydrocarbons containing more than one carbon atom.) Possibly this list is not complete. In other cases, the right combination of conditions may not have been used. However, two properties of the elements in this list are very striking: (1) They are all transition elements, i.e., they represent elements in which the "d" shell is not complete. (2) Their oxides are easily reducible with hydrogen or carbon monoxide at temperatures in the range where the Fischer-Tropsch synthesis proceeds.

Publications which consider the Fischer-Tropsch reaction in relation to the crystalline phases in the catalyst have been written by Storch and co-workers^{227, 229, 229a}, Kölbel¹³⁷, and Anderson².

Crystalline Phases Found in Fischer-Tropsch Catalysts

The present chapter, for reasons of brevity, is confined to crystalline compounds of known active elements as defined in the preceding para-

graphs. Promoters and supports which do not contain these elements will therefore not be considered. The phases involved in the Fischer-Tropsch reaction may be classified according to their function under the following headings:

1. Active phases on the surface of which the reaction is known to proceed at a reasonable rate under suitable conditions of temperature, pressure, synthesis gas composition, and surface area. These active phases include: α -iron^{6, 143}, α -cobalt⁶⁴, disordered cobalt⁴, nickel⁶⁴, ruthenium⁶⁴, platinum⁶⁷, magnetite⁹⁹, ϵ -iron nitride^{2, 3, 8, 224}, ϵ -iron carbide¹⁸⁹, ϵ -iron carbonitride^{2, 3, 8, 224}, ζ -iron nitride², ζ -iron carbonitride^{2, 8}, cementite²²³, rhodium¹⁸⁸, palladium¹⁸⁸, osmium, iridium¹⁸⁸, and Hägg iron carbide⁶. The importance of surface area in determining activity or nonactivity must be emphasized. For example, the magnetite of unreduced fused synthetic ammonia catalyst has a low specific surface and its activity is therefore scarcely detectable, whereas precipitated magnetite has a high specific surface and its activity is readily detectable.

2. Inactive phases on the surface of which the reaction proceeds at a much slower rate than on similar closely related phases. Striking examples are cobalt carbide, Co_2C ^{5, 255}, and nickel carbide, Ni_3C ¹⁴⁶.

3. Phases from which active phases are formed by reduction with hydrogen, carbon monoxide, hydrocarbons, etc. Such phases may themselves be active, although in most cases their activity or nonactivity is difficult to establish because they are not stable under conditions where activity may be observed. An exception to this rule is magnetite, which is relatively active and yet is quite persistent under the conditions of synthesis. Examples of phases in this category are: $\alpha\text{-Fe}_2\text{O}_3 \cdot \text{H}_2\text{O}$, $\beta\text{-Fe}_2\text{O}_3 \cdot \text{H}_2\text{O}$, $\gamma\text{-Fe}_2\text{O}_3 \cdot \text{H}_2\text{O}$, $\alpha\text{-Fe}_2\text{O}_3$, $\gamma\text{-Fe}_2\text{O}_3$, Fe_3O_4 , FeO , $\text{Co}(\text{OH})_2$, Co_3O_4 , CoO , $\text{Ni}(\text{OH})_2$, and NiO . Carbon monoxide or hydrogen readily reduces these compounds.

4. Phases which may be formed in the catalyst during reaction, although not present in the original catalyst. Some of these phases are active, others possibly not. They include ϵ -iron carbonitride², ζ -iron carbonitride², γ' -iron carbonitride⁸⁹, ϵ -iron carbide⁶, Hägg carbide⁶, cementite²²³, magnetite⁶, and siderite⁹⁹.

The physical constants of all these phases are assembled in Tables 1 to 5. General reference books dealing especially with the oxides and oxide hydrates have been written by Fricke and Huttig⁷³, and Weiser²⁵⁰.

The "d" Shell and Catalytic Activity

As has been pointed out, the elements catalytically active for the Fischer-Tropsch reaction are transition elements, i.e., they contain uncompleted electronic "d" shells. Dowden^{44, 45}, states that certain types of catalytic reactions, such as the hydrogenation of double bonds, are specifically af-

fects by catalysts containing elements (or compounds) with incompleated "d" shells. It is therefore tempting to classify the Fischer-Tropsch reaction as one which requires a transition-element-type catalyst. To establish this point, a correlation between catalytic activity in the Fischer-Tropsch synthesis and incompleated "d" bond character should be shown. Unfortunately, there is no sound general experimental method to determine whether an element or compound possesses an unfinished "d" shell; this information

TABLE 1. FISCHER-TROPSCH METALS

Name	Crystal Class ^{159a}	Lattice Parameters ^{159a} (Å)	Atoms per Unit Cell	Density (g/cm ³) calc.	Curie Point (°C)	Specific Magnetization	Fischer-Tropsch Activity
Iron (α)	Cubic (b.c.c.)	$a_0 = 2.8664$	2	7.82	770	218	Excellent ⁶⁴
Cobalt (α)	Hexagonal (h.c.p.)	$a_0 = 2.5070$ $c_0 = 4.069$	2	8.85		160	Excellent ⁶⁴
Cobalt (β)	Cubic (f.c.c.)	$a_0 = 3.552$	4	8.75	1115		
Cobalt (disordered)							Excellent ²⁵⁵
Nickel	Cubic (f.c.c.)	$a_0 = 3.524$	4	8.93	353	54.6	Good ⁶⁴
Ruthenium	Hexagonal (h.c.p.)	$a_0 = 2.7038$ $c_0 = 4.2815$	2	12.43	Paramagnetic ²⁴	—	Excellent ^{188, 67}
Rhodium	Cubic (f.c.c.)	$a_0 = 3.8032$	4	12.45	Paramagnetic ²⁴	—	Poor ^{188, 67}
Palladium	Cubic (f.c.c.)	$a_0 = 3.8902$	4	12.02	Paramagnetic ²⁴	—	Poor ^{188, 67}
Osmium	Hexagonal (h.c.p.)	$a_0 = 2.7353$ $c_0 = 4.0691$	2	22.15	Paramagnetic ²⁴	—	Poor ^{188, 67}
Iridium	Cubic (f.c.c.)	$a_0 = 3.8389$	4	22.75	Paramagnetic ²⁴	—	Poor ^{188, 67}
Platinum	Cubic (f.c.c.)	$a_0 = 3.9226$	4	21.48	Paramagnetic ²⁴	—	Detectable ^{188, 67}

can be deduced only from theory¹¹⁶; but while theory is reliable in the case of elements, it does not suffice to give information concerning compounds.

Certain information can be obtained from ferromagnetism. An uncompleted "d" shell is a necessary but not sufficient condition for ferromagnetism. Thus, if a compound or element is ferromagnetic, its unfinished "d" shell character is assured. On the other hand, the converse is not necessarily true. Thus antiferromagnetic compounds such as hematite, which is not ferromagnetic in the usual sense, do possess an unfinished "d" shell.

Iron, cobalt, and nickel are the only elements which are particularly prone to develop their ferromagnetic potentialities both as elements and

compounds, and the restrictions referred to above may not be too restrictive. Examination of the ferromagnetic properties of the carbides, nitrides, and borides of iron, cobalt, and nickel (see Tables 1 to 5) suggest that the specific magnetization of these compounds is a function mainly of the magnetic moment of the unfinished "d" shell of the metal and the degree to

TABLE 2. OXIDES AND OXIDE HYDRATES OF IRON, COBALT, AND NICKEL

Name	Formula	Crystal ⁷³ Class	Lattice Parameters ⁷³ (Å)	Formula Weights per Unit Cell	Density (g/cm ³) calc.	Curie Point (°C)
Wustite Magnetite ^a	Fe(OH) ₂	Hexagonal	$a_0 = 3.25$ $c_0 = 4.48$	1	3.63	Paramagnetic ⁷³
	FeO	Cubic	$a_0 = 4.30$	4	5.98	Paramagnetic
	Fe ₃ O ₄	Cubic	$a_0 = 8.39$	8	5.19	570 ⁷³
	α -Fe ₂ O ₃	Rhombohedral	$a_0 = 5.424$ $= 55.17$	2	5.30	Paramagnetic ⁷³
Maghemite	γ -Fe ₂ O ₃	Cubic	$a_0 = 8.33$		3.66	650 ¹⁶⁹
Goethite	α -Fe ₂ O ₃ ·H ₂ O	Orthorhombic	$a_0 = 4.65$ $b_0 = 10.02$ $c_0 = 3.04$	2	4.17	Paramagnetic ⁷³
	β -Fe ₂ O ₃ ·H ₂ O	Orthorhombic	$a_0 = 5.29$ $b_0 = 10.26$ $c_0 = 3.35$	2	3.24	Paramagnetic ⁷³
Lepidocrocite	γ -Fe ₂ O ₃ ·H ₂ O	Orthorhombic	$a_0 = 3.88$ $b_0 = 12.52$ $c_0 = 3.07$	2	3.95	Paramagnetic ⁷³
	Co(OH) ₂	Hexagonal	$a_0 = 3.20$ $c_0 = 4.67$	1	3.70	Paramagnetic ⁷³
	CoO	Cubic	$a_0 = 4.25$	4	6.48	Paramagnetic ⁷³
	Co ₃ O ₄	Cubic	$a_0 = 8.39$	8	5.41	Paramagnetic ⁷³
	Ni(OH) ₂	Hexagonal	$a_0 = 3.12$ $c_0 = 4.18$	1	4.36	Paramagnetic ⁷³
	NiO	Cubic	$a_0 = 4.17$	4	6.87	Paramagnetic ⁷³

^a Catalytic activity good.

which that "d" shell has been completed by electrons donated by the interstitial metalloid atoms. That electrons are donated to the metal atoms by the interstitial metalloid atoms has been indicated by Jack^{120, 36}, and by Kiessling¹³⁴. Examples of the electron donating effect of interstitial elements on the ferromagnetism are indicated below: (1) Nickel, lacking one electron of completing the "d" shell of 10 electrons, is ferromagnetic, but hexagonal nickel carbide, which contains electron-donating carbon, is non-ferromagnetic. (2) Similarly, cobalt is ferromagnetic, but orthorhombic

TABLE 3. CARBIDES OF IRON, COBALT, AND NICKEL

Name	Formula	Crystal Class	Lattice Parameters (Å)	Formula Weights per Unit Cell	Density (g/cm ³) calc.	Curie Point (°C)	Specific Magnetization	Catalytic Activity
Cementite	Fe ₃ C	Orthorhombic	$a_0 = 4.52^{257}$ $b_0 = 5.09$ $c_0 = 6.74$	4	7.692 7.74 ^a	210 ¹⁰⁴	139 ¹⁰⁴	Excellent ²²³
Hexagonal	Fe ₂ C (ε)	Hexagonal (h.c.p.)	$a_0 = 2.754^{104}$ $c_0 = 4.349$	1	7.20	380 ¹⁰⁴	140 ¹⁰⁴	Excellent ¹⁸⁹
Percarbide	Fe ₂ C (χ)	Orthorhombic ¹²⁵	$a_0 = 9.06 (?)^{125}$ $b_0 = 15.69 (?)$ $c_0 = 7.94 (?)$	—	—	247 ¹⁰⁴	140 ¹⁰⁴	Excellent ¹⁸⁹
Eckstrom and Adcock Carbide	FeC?	—	—	—	—	250 ⁵⁰	—	Excellent ⁵⁰
Martensite	Variable composition Co ₂ C	Tetragonal (f.c.t.)	$a_0 = 2.86-2.85^{189}$ $c_0 = 2.86-3.10$	2	—	Ferromagnetic	—	—
Cementite homolog	Co ₃ C	Orthorhombic	$a_0 = 2.897^{36}$ $b_0 = 4.446$ $c_0 = 4.371$ _b	2	7.64	Paramagnetic ¹⁰⁷	—	Inert ²⁵⁵
Cementite homolog	Ni ₃ C	Hexagonal (h.c.p.)	$a_0 = 2.650^{130}$ $c_0 = 4.339$ _b	$\frac{2}{3}$	7.91	Paramagnetic ¹⁴⁷	—	Inert ¹⁴⁶
Limit of terminal solid solution of carbon	Ni ₄ C	Cubic (f.c.c.)	$a_0 = 3.520^{20}$	1	9.3	220 ²⁰	—	Active ²⁴⁰

^a Experimental, see Ref. 19.^b Nearly same as cementite.

cobalt carbide is nonferromagnetic. (3) In the case of α -iron, which lacks three electrons of filling the "d" shell, the carbon present in all four of the known carbides is insufficient for donating enough electrons to complete the "d" shell, and they are all ferromagnetic, i.e., Fe_3C (cementite), Fe_2C (Hägg carbide), Fe_2C (hexagonal close-packed carbide), and Eckstrom and Adcock's carbide. However, the specific magnetization in these compounds is reduced from 218 for α -iron to *ca.* 140 for the first three of the carbides mentioned above, indicating at least partial completion of the "d" shell by electron donation. (4) Less reliable data on the nitrides and borides of iron, cobalt, and nickel show similar relationships. The above conclusions

TABLE 4. NITRIDES OF ELEMENTS CATALYTICALLY ACTIVE IN THE FISCHER-TROPSCH REACTION

Name	Composition, Per cent Nitrogen	Crystal Class	Lattice Parameters (Å)	Formula Weights per Unit Cell	Density (g/cm ³) calc.	Curie Point (°C)	Catalytic Activity
γ' - Fe_4N	5.75-5.95	Cubic (f.c.c.)	$a_0 = 3.8026\text{--}3.8076^{124}$	1	7.16	480 to 500 ¹⁵⁰	Probably excellent ²
ϵ - Fe_3N	7.2-11.0	Hexagonal (h.c.p.)	$a_0 = 2.64\text{--}2.78^{124}$ $c_0 = 4.348\text{--}4.45$	$\frac{3}{2}$	7.65	375 to -200^{27a}	Excellent ²
ζ - Fe_2N	11.1-11.3	Orthorhombic	$a_0 = 2.763\text{--}2.761^{124}$ $b_0 = 4.828\text{--}4.830$ $c_0 = 4.424$	2	7.02	—	Probably good ²
γ - Co_3N	7.6-8.0	Hexagonal (h.c.p.)	$a_0 = 2.671^{131}$ $c_0 = 4.367$	$\frac{3}{2}$	7.82	—	—
ζ - Co_2N	10.6	Orthorhombic	$a_0 = 2.848^{131}$ $b_0 = 2.632$ $c_0 = 4.339$	1	6.73	—	—
Ni_3N	7.4	Hexagonal (h.c.p.)	$a_0 = 2.670^{133}$ $c_0 = 4.307$	$\frac{3}{2}$	7.91	—	—

are uncertain to the extent that it is not known whether the nonferromagnetic compounds are diamagnetic.

The most useful measure of incomplete "d" shell and the one used here is the number of additional electrons necessary to bring the electronic structure to that of copper, silver, gold, etc., as the case may be, depending on whether we are considering the "3d," "4d," "5d," etc., shell. There are other measures—for example the one based on the electronic structure of the ground term. On this scheme, nickel lacks two electrons of a complete "d" shell, cobalt three electrons, and iron, four electrons. This system presupposes isolated gaseous atoms. A third system is based on the band theory of metals. In this theory, cognizance is taken of the fact that s electrons contribute to the filling of the "d" shell. The results are normally presented in the form of the Slater-Condon curve which is a plot of magnetic moment in Bohr magnetons against atomic number. The data here indicate nickel—0.6 electrons, cobalt—1.6 electrons, and iron—2.2 electrons. This type of data

also is somewhat irrelevant since in going from one phase to another, neither the band structure nor electronic alignments remain comparable.

The details of the catalytic activity of the various phases of iron, cobalt, and nickel are discussed below. The over-all results may be summarized by the statement that a remarkable relationship exists between catalytic activity in the Fischer-Tropsch reaction and incompleteness of the "d" shell. This relationship may be useful in surveying new possibilities for catalysts.

In addition to the other members of the first transition series of elements (with unfinished "3d" shells), there are other transition series of elements with unfinished "4d" and "5d" shells. If the unfinished "d" shell is impor-

TABLE 5. BORIDES OF IRON, COBALT, AND NICKEL

Name	Crystal Class	Lattice Parameters (Å)	Formula Weights per Unit Cell	Density (g/cm ³) calc.	Curie Point (°C)
Fe ₂ B	Tetragonal (f.c.t.)	$a_0 = 5.109^{21}$ $b_0 = 4.323$	4	7.20	Ferromagnetic ²⁴
FeB	Orthorhombic	$a_0 = 4.061^{21}$ $b_0 = 5.506$ $c_0 = 2.952$	4	6.69	—
Co ₂ B	Tetragonal	$a_0 = 5.016^{21}$ $b_0 = 4.220$	4	8.08	510 ¹⁴¹
CoB	Orthorhombic	$a_0 = 3.956^{21}$ $b_0 = 5.253$ $c_0 = 3.043$	4	7.42	Nonmagnetic ¹⁴¹
Ni ₂ B	Tetragonal	$a_0 = 4.990^{21}$ $b_0 = 4.244$	4	8.06	Nonmagnetic ¹⁴¹

tant in determining activity, the reason must be sought for the inactivity of these other elements. The obvious reason is that except for group VIII elements, they are too sensitive to oxidation under the conditions of the Fischer-Tropsch synthesis to be useful catalysts. Tungsten, molybdenum, manganum, and rhenium are possible exceptions which can be maintained in the reduced state. The unfinished "d" shell may affect catalytic activity in the Fischer-Tropsch reaction by making possible the adsorption of carbon monoxide as surface carbonyls. It is known that copper chemisorbs carbon monoxide strongly, but that such adsorption leads to surface carbonyls is questionable since copper forms no carbonyls of any sort.

The Structure and Properties of Interstitial Compounds

Because interstitial compounds are important catalysts in the Fischer-Tropsch synthesis^{2, 189, 196}, their properties will be considered in some detail. They are nonionic, intermetallic compounds having electrical con-

ductivities near those of metals. All known interstitial compounds are formed with transition metals—this point becomes significant in view of the belief of Jack¹²⁰ and Kiessling¹³⁴ that the metalloid-metal bond is formed in part by the donation of electrons from the metalloid to the metal, where it contributes to the saturation of the unfinished “*d*” shell of the transition metal. The term “interstitial” denotes that the metalloid element, i.e., carbon, nitrogen, boron, or hydrogen, fits into the interstices of the metal lattice. In most cases, interstitial atoms are isolated, but in Cr_3C_2 , some borides, particularly those with a concentration of boron equal to or exceeding the composition MB, zig-zag chains or nets of metalloid are interspersed through the metal lattice. In addition, a series of compounds exists in which two carbon atoms fit into one interstice. Known compounds of this nature are YC_2 , LaC_2 , CeC_2 , PrC_2 , NdC_2 , SnC_2 , ThC_2 , and UC_2 . Structurally they are similar to the well-known calcium carbide, but they are not nearly as polar⁹⁸. These interstitial compounds with chain and net formations of interstitial elements have not so far proved useful for catalysts and will be disregarded in the present discussion.

Interstitial compounds containing isolated metalloid atoms will be referred to simply as “interstitial compounds.” They may be divided into two categories, stable and unstable. The stable class of interstitial compounds exhibit remarkable properties; they are highly refractory. TaC has the highest known melting point, *ca.* $4,150^\circ\text{C}$ ¹¹⁶; they are extremely hard, being used in the manufacture of high-speed cutting tools; they are very resistant to the action of acids. An examination of their crystal structures shows that they have, with few exceptions, just two basic structures—a face-centered cubic arrangement of the metal atoms and a hexagonal close-packed arrangement of the metal atoms. (The position of the interstitial atoms is very difficult to determine by conventional x-ray diffraction methods, because the interstitial elements, boron, carbon, and nitrogen, have such low-scattering power compared with that of the metal atoms that they do not readily reveal their position. An interesting relationship between the crystal structure and the stoichiometry of these compounds exists. The face-centered cubic structures have either the composition MX or M_4X , where X is the metalloid and M the metal. Exceptions to this rule are the carbides MoC and WC, which have structures of hexagonal symmetry. The hexagonal close-packed structures have the composition range of approximately M_2X – M_3X ^{82, 83, 84}. The hardness, high melting point, and chemical inertness suggest that these compounds are not held together by the intermetallic bonds found in metals, but by some bond similar to the covalent bonding which holds the diamond together. Furthermore, the close relation between stoichiometry and structure suggests that this bond must have directional properties. There are not enough electrons to postu-

late covalent bonds, but Rundle^{199, 200} has shown that under certain conditions electron deficient bonds can be postulated which have properties somewhat similar to covalent bonds. Unfortunately these bonds can only be used to account for the MX face-centered cubic interstitial alloys. Any really satisfactory theory must account for the curious face-centered cubic: hexagonal close-packed: face-centered cubic sequence as the interstitial atom concentration increases from M_4X to M_2X to MX. Hume-Rothery^{116, 117} has developed a theory of the structure of the MX type of interstitial compound, which indicates that the main reason for the face-centered cubic structure is that this structure provides the metal atoms with mutually perpendicular bonds to six neighbors.

The unstable interstitial compounds are relatively soft compared with stable ones. They decompose thermally well below 1000°C, and they invariably react with acids to form hydrides (ammonia and hydrocarbons). Chemical reactivity is also shown by the ease with which the carbides react with hydrogen at temperatures well below that at which even the most reactive elemental carbon is capable of reacting. These unstable interstitial alloys have rather complex crystal structures in many cases. Hägg⁸⁴ showed that the transition from simple to complex structure occurs when the ratio of metalloid atom radius to that of the metal atom (r_x/r_m) exceeds 0.59. Since the time of Hägg's paper, compounds having a simple structure and a value of r_x/r_m greater than 0.59 have been found. Those compounds are hexagonal close-packed iron carbide (ϵ) Fe_2C ^{104, 216} and the hexagonal close-packed Ni_3C ¹³⁰. The significance of 0.59 is therefore not as a point of transition from one type of structure to another but as the measure of the relative stability of the interstitial compound of similar crystal structure. Thus, when a high ratio indicates that a simple compound is unlikely, that compound may exist, although more stable structures of greater complexity are more likely to be formed. Such a case is illustrated by the iron carbides where the highly unstable hexagonal close-packed iron carbide of simple structure is metastable to the more complex structures of cementite and Hägg carbide.

This instability suggests a possible property of the unstable interstitial compounds in catalysis. Since the positions of the metal atoms are such a precarious compromise between the bond tending to hold them in one of the simple structures assumed by stable interstitial compounds and the dislocating forces exerted by oversize interstitial atoms, the surface atoms may be rather easily pulled around by the forces exerted by adsorbed molecules. This means that the "geometric factor" is not so important for these surfaces, because the "geometric factor" on these surfaces will be determined not only by the crystal structure and crystal habit (exposed planes) of the compound but also by the adsorbed phases and the catalytic reaction

proceeding on the surface. Such compounds may have some especially useful properties as catalysts.

In common with many intermetallic compounds, the carbides, nitrides, borides, hydrides, and even the oxides of transition elements do not obey Dalton's Law of Constant Composition. For example, the ϵ -Fe₂N has compositions ranging from Fe₃N to nearly Fe₂N. The ϵ -Fe₂N case is well worked out, but the compositions of some of the other compounds reported in this chapter are not nearly so well known. The formulas given are therefore only approximate.

Information concerning the magnetic properties of iron Fischer-Tropsch active phases is to be found in summarizing papers by Pichler and Merkel^{189, 190, 191}, Hofer, Cohn, and Peebles¹⁰⁴, Selwood^{219, 220}, Lehrer¹⁵⁰, and Bozorth²⁴. In the following portion of this chapter, the behavior of iron, cobalt, and nickel systems will be treated in detail as far as the oxides, carbides, nitrides, borides, and elements are concerned. Other systems such as those of ruthenium, rhodium, osmium, iridium, palladium, platinum, molybdenum, tungsten, etc., have not been treated because of an almost complete lack of data.

It should be mentioned that molybdenum disulfide alkalized with the hydroxides or carbonates of sodium or potassium have been reported active as Fischer-Tropsch catalysts in temperature and pressure ranges close to those of the classical reaction^{226a}. According to the views presented here, Fischer-Tropsch activity may well be sought among the sulfides, selenides, tellurides, phosphides, arsenides, stibides, and bismuthides of most of the transition elements. The possibility of tailoring catalysts is greatly enhanced by the use of mixed catalysts, thus, for example, in the ϵ -Fe₂C phase of iron, a portion of the iron could in principle be replaced by nickel. This would probably change the catalytic behavior, the stability of the phase, as well as modifying side reactions such as carbon deposition and oxidation.

THE NICKEL SYSTEM OF CATALYSTS

Oxides and Oxide Hydrates of Nickel

A voluminous, pastel green precipitate is formed on the addition of base to a solution of nickelous salt. In the case of the preparation of Fischer-Tropsch catalysts, the nickelous salt is usually the nitrate and precipitation is carried out in a slurry of kieselguhr. The pure precipitate has a formula of about Ni(OH)₂ and has an easily recognizable x-ray diffraction pattern. Cairns and Ott³⁵ have worked out the crystal structure from powder patterns and the compound seems to be isomorphous with Co(OH)₂, Fe(OH)₂, Mg(OH)₂, Mn(OH)₂, Zn(OH)₂, Cd(OH)₂, and Ca(OH)₂⁷³. These com-

pounds suggest many possibilities for promotion by coprecipitation. Le-Blanc and Möbius¹⁴⁴ are not in thorough agreement with the findings of Cairns and Ott, and more work may well be done on this system.

DeLange and Visser⁴³ have studied nickel kieselguhr-type catalysts in detail and showed that they have a structure homologous to the magnesium hydrosilicate, antigorite. Feitknecht and Berger⁶² had previously studied the nickel and cobalt silicates by x-ray diffraction in considerable detail. DeLange and others for a while believed that, upon reduction of such a catalyst, the antigorite structure remained, but that the nickel was reduced from a valence of plus two to zero. This point of view is quite untenable from structure theory. However, the incipient formation of hydrosilicates may account for the promoting effect of kieselguhr in both nickel and cobalt catalysts. The difference in promoting effect between an amorphous kieselguhr ("Filter Cel") and a kieselguhr flux calcined to cristobalite ("Hyflo Super Cel") may well lie in the inability of the latter to form readily hydrosilicates with cobalt ions⁷.

The only other oxide commonly identified in nickel catalysts is NiO. This can be formed from $\text{Ni}(\text{OH})_2$ by dehydration at relatively low temperatures. Higher oxides and oxide hydrates have been reported by employing oxidizing conditions.

Trambouze^{231, 232, 233, 234} has made a special study of the oxide, carbonate, metal, hydrosilicate, and hydroaluminate phases in Fischer-Tropsch catalysts.

Reduction of Nickel Oxides

The pure nickel oxides and oxide hydrates are readily reduced at 275°C and 85 hours to virtually constant weight¹⁴. If the nickel is in the form of a hydrosilicate, temperatures near 500°C must be employed, and the reduction is by no means quantitative. Nickel, when in the form of very small crystallites, as found in the reduced nickel-kieselguhr and nickel-alumina catalysts, possesses an anomalous Curie point which is lower than that of massive nickel (see Figure 1)¹⁶³. Selwood²²¹ postulates that the Curie point is related to the coordination number z by the relation

$$C_p/631^\circ\text{K} = z/12, \quad (1)$$

where C_p is the observed Curie point, 631°K is the normal Curie point, z is the effective coordination number, and 12 is the normal one. A form of nickel so finely divided that a large fraction does not possess the normal coordination number should show the effect of electron donation by adsorbed gases through a decrease in the specific magnetization. Such an effect has been reported in the case of the system of hydrogen adsorbed on nickel²²¹.

Carburization of Nickel

The following discussions describing carbide formation and free carbon deposition on nickel, as well as on cobalt and iron, will be most readily understood in terms of the basic concepts outlined in Figure 2. The scheme will be referred to in various subsequent sections.

The carburization of pure nickel, reduced with hydrogen from the oxide, by carbon monoxide has been studied by many authors. The general behavior of the reaction is illustrated well by the data of Bahr and Bahr¹⁴

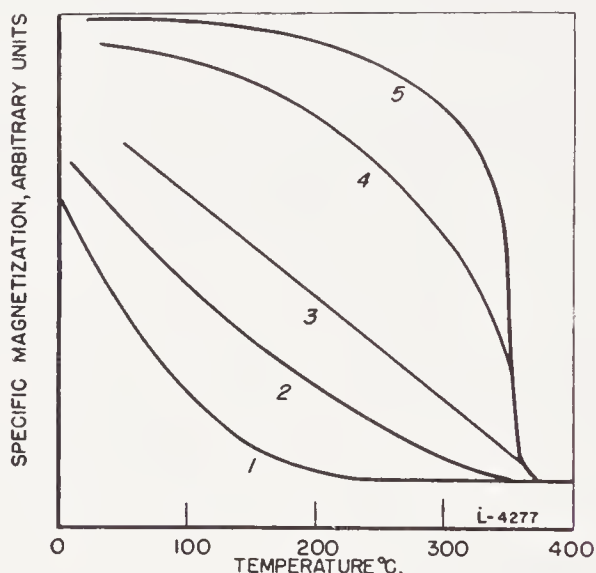


Figure 1. Thermomagnetic curves of freshly reduced nickel thoria kieselguhr catalysts showing the effect of crystallite size on the thermomagnetic curve. The crystallite size increases from 1 to 5. Catalysts of optimum activity produce curves similar to 2. Above this the crystallite size operation in Fisher-Tropsch synthesis produces deactivation through the formation of the hep nickel carbide Ni_3C . Below this crystallite size the surface does not have the proper character.

(Figure 3). There is general agreement that below *ca.* 270°C almost pure carbide is formed and that the carbon content of the solid phase increases rapidly initially and then approaches asymptotically a value which corresponds closely to the composition¹⁴ Ni_3C . Above 285°C, the carbon content also increases rapidly at first, but although the rate of increase becomes less, it remains easily measurable even after the carbon content has exceeded the value Ni_3C . Samples of nickel, carburized below 270°C until no more carbon monoxide reacts, give up carbon nearly quantitatively as methane when treated with oxygen-free hydrogen at 180°C. If instead of treating the specimen with hydrogen, one treats the specimen with hydrochloric acid, higher hydrocarbons are also formed and no trace of free carbon can be detected according to Bahr and Bahr. The quantitative conversion

of nickel carbide to hydrocarbons and nickel chloride by means of hydrochloric acid is questioned by Schmidt and Osswald²¹⁸. Carburization with carbon monoxide at 285°C and above until the rate of carburization is essentially constant leads to a product which contains just enough carbide carbon as determined by treatment with hydrogen at 180°C to correspond to Ni_3C . Treatment with hydrochloric acid forms hydrocarbons and a black residue. Thus, there seems no doubt that a carbide of formula near

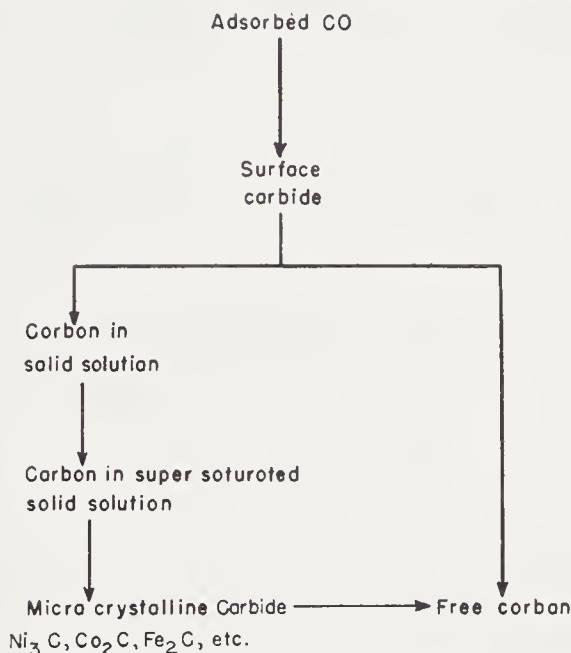
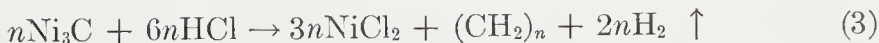


Figure 2. General reaction scheme of the formation of free carbon and cobalt carbide.

Ni_3C is formed and that the carbide readily reacts with hydrogen according to the equation



and with hydrochloric acid according to



Schmidt and Osswald²¹⁸ report the use of acetylene at 180 to 200°C for the preparation of Ni_3C . Acetylene, however, forms considerable free carbon in addition to the carbide even at these low temperatures.

Tutiya's²⁴⁵ carburizing technique is unusual in that he carburized the oxide NiO directly with carbon monoxide in the temperature range 250 to 270°C. His results are described in terms of an Ni_3C and an Ni_xC which are identified by means of their x-ray diffraction patterns.

Nickel Carbides

X-ray diffraction studies have in general amply justified the interpretation placed on the carburization experiments. The nickel carbide Ni_3C has a close-packed hexagonal arrangement of the nickel atoms. The carbon atoms, due to their relatively low atomic number, do not reveal themselves readily by their effect on the diffraction pattern. As a result, the diffraction pattern of Ni_3C is nearly the same as the one which could be expected from the hexagonal close-packed allotrope of nickel metal^{27, 147}. This mistake in

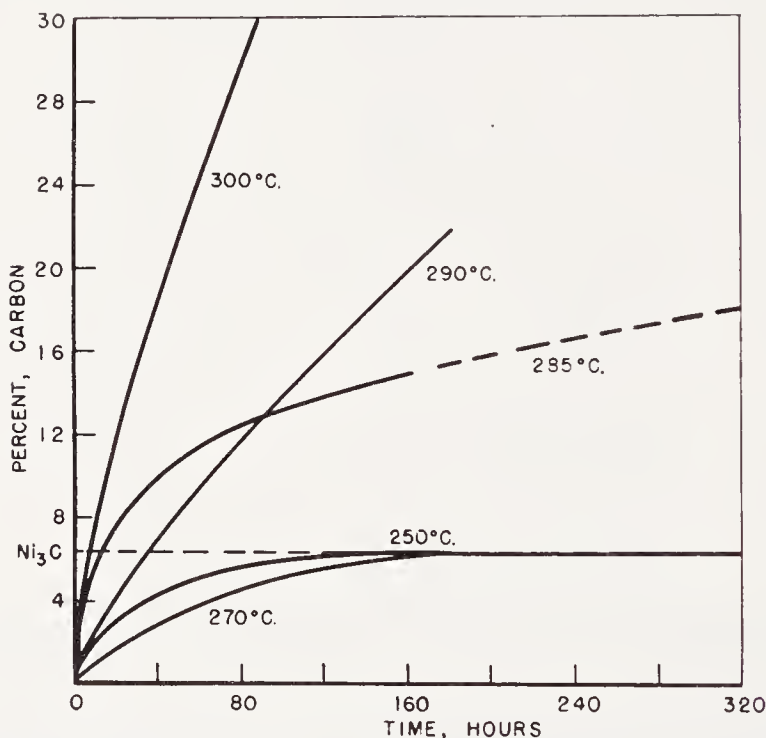


Figure 3. Carburization of nickel according to Bahr and Bahr. (See Ref. 14.)

identification has actually been made in two otherwise very useful papers^{146, 147}. The lattice parameters of Ni_3C are slightly larger than those expected in the allotrope of nickel.

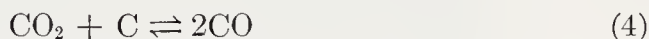
Other carbides of nickel have been reported. A phase corresponding approximately to Ni_6C has been postulated by Tebboth²³⁰, and a face-centered cubic structure with a lattice parameter slightly larger than that of the normal metallic nickel has been reported²¹⁷. Michel, Bernier, and LeClerc¹⁶⁸, have found evidence that under the carburizing conditions of the synthesis, reduced nickel thoria kieselguhr type catalysts develop a solid solution of carbon in cubic nickel. This results in a change of the Curie point to about 210°C and in a new lattice parameter of about $a_0 = 3.529 \text{ \AA}$.

Tutiya²⁴⁵ has reported the presence of unknown x-ray diffraction lines

in his powder patterns and ascribed them to an unknown nickel carbide Ni_xC .

Kohlhass and Meyer¹³⁶ have reported preparing a nickel carbide under conditions very similar to those used by Jacobsen and Westgren¹³⁰, Schmidt and Osswald²¹⁸, LeClerc and Michel¹¹⁷, Browning and Emmett³³, and Hofer, Cohn, and Peebles¹⁰⁵. All the above authors with the exception of Kohlhass and Meyer concur, in that the structure of nickel carbide is close-packed hexagonal, but Kohlhass and Meyer are positive that the carbide really is a homolog of cementite Fe_3C . Kohlhass and Meyer¹³⁶ even published a halftone of the diffraction pattern which bears a resemblance to that of cementite; however, their numerical " d " values bear a much closer resemblance to the unreliable " d " values of the early work of Westgren and Phragmen^{258, 259} than to the more recent and reliable data of Westgren²⁵⁷. Until Kohlhass and Meyer's work can be confirmed, it should be regarded with reserve.

According to Fricke and Weitbrecht⁷⁴, small amounts of carbon dissolved in nickel gave misleading information concerning the Boudouard²³ equilibrium



on nickel catalysts. Such a solid solution seems similar to the one postulated by Tebboth.

Meyer and Scheffer^{161, 162, 163, 164, 165} and Scheffer, Dokkum, and Al²⁰² carbided nickel with carbon monoxide by methods similar to those of Bahr and Bahr¹⁴. They have also determined the equilibrium of hydrogen and methane over nickel carbide. Their equilibrium values lead to a distinctly different free energy of formation of nickel carbide than that found by Browning and Emmett³³. In the absence of supporting x-ray diffraction data for the Meyer and Scheffer study, it is tempting to assign their equilibrium results to the solid solution of carbon in face centered nickel. The Browning and Emmett hydrogen-methane equilibrium studies must be assigned to Ni_3C since this compound was actually identified by x-ray diffraction in their substrate.

The Hydrogenation of Carbides of Nickel

Bahr and Bahr¹⁴, Osswald and Schmidt²¹⁸, as well as Hofer, Cohn, and Peebles¹⁰⁵ have studied the hydrogenation of nickel carbide, Ni_3C , which proceeds rapidly at 250°C and is essentially complete, according to the first author, in about 26 hours. The rate is probably a function of particle size and other factors. There is evidence that the carbon combined as nickel carbide reacts considerably more readily than free carbon, but better data are needed for the nickel-carbon system. The off-gas formed by passing

hydrogen at 250°C at atmospheric pressure has been analyzed as follows: 0.3 CO₂, 28.6 CH₄, 32 C₂H₆, 0.2 CO, 0.2 higher hydrocarbons, 2.4 H₂, and 65.1 per cent N₂ (flushing gas)¹⁵.

Carbon Deposition on Nickel

The study by Bahr and Bahr¹⁴ shows that at 285°C free carbon is deposited at a noticeable rate. This reaction has not been studied in detail, although it is probably very similar in nature to carbon deposition as it proceeds on iron and cobalt. An electron micrographic study¹¹¹ shows that

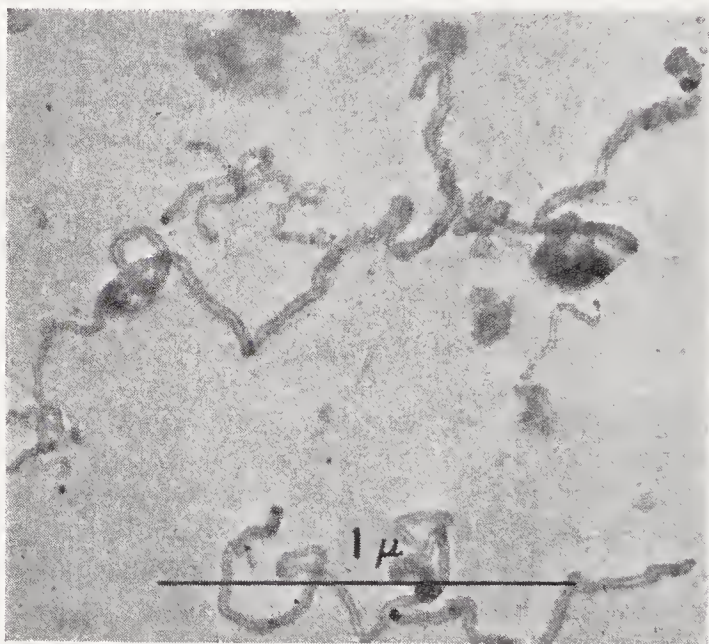


Figure 4a. Carbon deposited on nickel reduced from Ni(OH)₂ as prepared by Hofer, Cohn, and Peebles¹⁰⁵. Note well-developed tubular structure.

the free carbon consists of long tubular filaments with dense nuclei of nickel or nickel carbide at one end (Figure 4).

Leidheiser and Gwathmey¹⁵¹ have shown that free carbon deposition proceeds preferentially on the 111 planes of cubic nickel.

Other Reactions of Nickel Carbide

Schmidt and Osswald²¹⁸ state that dilute hydrochloric acid reacts with Ni₃C to form methane, ethane, unsaturated hydrocarbons, hydrogen, and in some cases free carbon. The latter was invariably found when the nickel had been carburized to within 5 per cent of the composition Ni₃C. (Bahr and Bahr's¹⁴ earlier work claimed complete solution of the carbide and no carbon residue.) No traces of oil, such as had been reported by Bahr and Bahr, were found by Schmidt and Osswald.

Bahr and Bahr¹⁵ studied the action of other reagents. Water vapor at 250°C produced 22.0 CO₂, 63.5 H₂, and 13.6 CH₄ per cent. Hydrogen sulfide at 200 to 240°C produced only an oil and no CH₄. Hydrogen chloride at 290 to 300°C formed only a yellow oil which solidified on cooling.

In some of the older literature, Ni₃C is said to be stable below 400°C. This statement, based on misinterpreted thermodynamic studies¹⁶¹⁻¹⁶⁵, is obviously incorrect. Hofer, Cohn, and Peebles¹⁰⁵ have investigated the decomposition in the temperature range 320 to 355°C. The products of the reaction were metallic nickel and free carbon. The reaction started after an

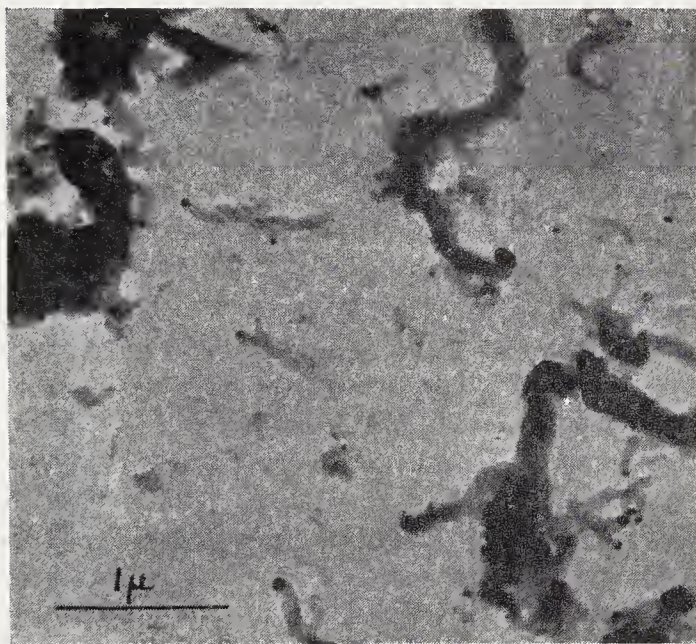


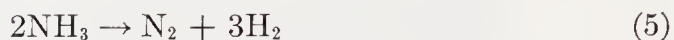
Figure 4b. Carbon deposited on nickel reduced from NiO. Note nuclei at the end of the filaments.

induction period, and followed a complex rate law. Over about 60 per cent of the reaction, the rate may be approximated by a quasi zero order law whose rate constant k may be represented for a fully carburized specimen of nickel by the equation, $k = 10^{16} \exp - 61/RT$. The induction period τ may be represented by a similar law, $1/\tau = 3 \times 10^{15} \exp - 55/RT$. In the above equations, R in kcal per mole per °K is the gas constant and T the absolute temperature. Partially carburized specimens of nickel carbide behave qualitatively similarly but quantitatively differently.

Nitriding of Nickel

Nitriding of nickel has been investigated by Beilby and Henderson¹⁸, Hägg⁸¹, Granadam⁷⁸, and Juza and Sachse¹³². Of these investigators, Hägg found that at 300°C ammonia would react with nickel to form a product

containing only 0.89 per cent nitrogen. Beilby and Henderson¹⁸, however, found 7.5 per cent nitrogen in nickel nitrided at 500°C, Granadam found 9 per cent nitrogen in some of his ammonia nitrided specimens of nickel, and Juza and Sachse found 7.37 per cent nitrogen in their most fully nitrided nickel samples. All these authors are in substantial agreement that nickel cannot be nitrided with nitrogen gas. The divergence of results by the various authors suggests that formation of the nitride requires critical conditions, high space velocity, turbulence, and intimate contact of the nitriding agent with the nickel. It is possible that the nickel must be partly poisoned to the reaction,



to prevent excessive concentrations of hydrogen from reversing the nitriding reaction. Juza and Sachse give the following directions for preparing nickel nitride of the theoretical composition 7.37 per cent N. (Ten to 20 mg of finely divided nickel prepared by the thermal decomposition of nickel carbonyl are placed in a corundum boat in a quartz tube and treated with a stream of ammonia at 22 cm/sec for 3 hours at 445°C.) Juza and Sachse also give two sets of directions for the preparation of nickel nitride from halides, as follows: ($\text{NiF}_2 \cdot 2\text{NH}_4\text{F}$ are treated in an ammonia stream for 20 hours at 390 to 410°C, NiBr_2 is heated at 80 to 120°C in an ammonia stream to form an ammoniate which then decomposes on further treatment in the ammonia stream to form a very finely divided NiBr_2 preparation. This preparation can be readily converted to Ni_3N at 420°C in 4 hours using an ammonia stream.)

Like Ni_3C , the nickel atoms in Ni_3N assume the positions of hexagonal closest packing. The lattice parameters are slightly larger than one would expect if there were no nitrogen in interstitial positions. The metal phase of partially nitrided nickel shows an expanded lattice, $a_0 = 3.519_2 \pm 0.001_6$ as compared with the literature value of 3.516_7 . This change in lattice parameter, by analogy to the change in lattice parameter of γ iron with nitrogen content, corresponds to about 0.083 per cent N.

According to Juza and Sachse Ni_3N decomposes thermally as low as 360°C.

Borides of Nickel

Borides have been suggested as catalysts for the Fischer-Tropsch reaction. The boranes are logical boriding agents. Paul, Buisson and Joseph¹⁸¹ have developed a way of preparing Ni_2B from nickel chloride solution and sodium borohydride. Whether the product so formed has the same crystal structure as the Ni_2B reported by Bjurstrom²¹ is not known.

Catalytic Activity in the Nickel System

The only nickel phase which is known to have catalytic activity for the Fischer-Tropsch synthesis is nickel metal in the face-centered cubic form. Nickel carbide Ni_3C in the hexagonal close-packed form shows such greatly reduced activity as to be considered inactive^{146, 168}. An interesting study on the methanizing reaction was conducted by Bahr and Bahr. Their results indicate that the oxygenated product is CO_2 over Ni_3C and H_2O over nickel. This suggests that Ni_3C catalyzes the water-gas shift while nickel metal does not. Troesch²⁴⁰ found that the presence of nickel carbide did not aid the efficiency of Fischer-Tropsch catalysts. Whether this data indicated that it was detrimental is not certain.

The solid solution of carbon in face-centered cubic nickel is also active in catalyzing the Fischer-Tropsch synthesis¹⁶⁸.

THE COBALT SYSTEM

Oxides and Oxide Hydrates of Cobalt

The oxides, oxide hydrates, and hydroxides involved in the cobalt system of Fischer-Tropsch catalysts are CoO , $\text{CoO} \cdot \text{H}_2\text{O}$ ^{73, 173, 174} both rose and blue, and Co_3O_4 . Other compounds may be involved, such as the $\text{Co}_2\text{O}_3 \cdot \text{H}_2\text{O}$ ¹⁷⁵ and Co_2O_3 ¹⁷⁵ which are produced by precipitation under oxidizing conditions, but such compounds probably were not formed under the conditions given for the preparation of cobalt catalysts in the literature.

By precipitation of cobaltous salts with alkali, a voluminous blue precipitate of $\text{CoO} \cdot \text{H}_2\text{O}$ is formed²⁵¹. This has a definite diffraction pattern. It is unstable and gradually reverts to the rose form of $\text{CoO} \cdot \text{H}_2\text{O}$. The process is accelerated by alkali and inhibited by sugar. The rose-colored form also has a characteristic diffraction pattern and its crystal structure is homologous to $\text{Ni}(\text{OH})_2$ and $\text{Fe}(\text{OH})_2$ ⁷³. The rose form of $\text{Co}(\text{OH})_2$ is a very satisfactory starting material for the preparation of finely-divided cobalt by reduction with hydrogen.

CoO is readily formed by dehydration of $\text{Co}(\text{OH})_2$. It has a cubic sodium chloride structure and is isomorphous with NiO and FeO .

Both $\text{Co}(\text{OH})_2$ and CoO oxidize readily in the atmosphere at 100°C to form Co_3O_4 . This compound has the spinel structure of magnetite. It is frequently found in cobalt catalysts which inadvertently have been oxidized.

The frequent occurrence of kieselguhr in cobalt catalyst formulations suggests that a cobalt hydrosilicate is formed in the catalyst preparation. The author has never observed in the examination of numerous cobalt kieselguhr catalysts such a hydrosilicate; furthermore, the exposure of the kieselguhr to the precipitating solution must be kept brief or else the ac-

tivity of the resultant catalyst will suffer. This latter observation suggests that cobalt hydrosilicate formation is detrimental. On the other hand, the fact that amorphous raw kieselguhr ("Filter Cell") makes a better catalyst than flux-calcined kieselguhr ("Hyflo Super Cel") suggests that there is incipient formation of cobalt hydrosilicates⁷ in active catalysts.

Reduction of Cobalt Oxides and Oxide Hydrates

Pure cobalt oxide or cobalt oxide hydrate can be reduced in hydrogen very readily at temperatures at least as low as 300°C. However, the cobalt thoria kieselguhr (100:18:100) catalyst, as it is usually prepared, requires 400°C for reduction; this may mean that cobalt is combined with the kieselguhr in an incipient cobalt hydrosilicate, but x-ray diffraction patterns do not show the existence of such an incipient cobalt hydrosilicate¹⁰⁸. The diffraction pattern of a freshly prepared unreduced catalyst shows almost no structure of any kind, and such structure as can be detected is traceable to the kieselguhr support¹⁰⁸. Upon reduction at 400°C, three new, relatively strong reflections are found. Attempts to index these lines showed that they might be due to face-centered cubic cobalt which is stable above 400°C²⁰¹, but such an interpretation fails to explain the absence of the 200 and 222 reflections. The lines can also be indexed as the hexagonal close-packed reflections 002, 110, and 112 of α -cobalt stable below 400°C. In this case, the absence of the 100, 101, 102, 103, 200, 201, and 004 reflections must be explained. The reflections observed are common in both methods of indexing, while with the possible exception of the 222 cubic (004 hexagonal) reflection, the missing reflections are not common (Figure 5).

Clues to this phenomenon are found in the work of Hendricks, Jefferson, and Schultz⁹⁴, Edwards, Lipson and Wilson⁵¹, and Nowotny and Juza¹⁷⁶. Hendricks, Jefferson, and Schultz previously had found that diffraction patterns of α -cobalt contained both sharp and diffuse reflections. This variation of line width was not a simple function of the angle of reflection, as would be the case for small crystallite size. Further, certain classes of reflections are not involved, as would be the case for small crystallites which are relatively large in certain crystallographic directions and small in others (platelets, needles, etc.). Edwards, Lipson and Wilson⁵¹, have partially explained these results. They show that the hexagonal close-packed structure may be visualized as the laying of successive close-packed layers of atoms one upon another so that the corresponding atoms of every second layer are directly over each other. The formula for the layering is then represented as ABABA The face-centered cubic structure may be visualized as the laying of successive close-packed layers of atoms, so that the corresponding atoms of every third layer are directly over each other as ABCABCA They postulate a close-packed hexagonal

structure in which a fault occasionally occurs and the sequence is ABAB-ABCBCBCBABA ···, etc. The diffraction pattern of such a structure, with one fault in every 14 planes, was shown to give a pattern similar to the one observed for massive cobalt. Wilson²⁶² has also developed a theoretical treatment of this effect.

With increasing imperfections, a pure hexagonal close-packed structure acquires face-centered cubic character, although if these imperfections are completely random this process will not go beyond the formation of a sort of hybrid face-centered cubic-hexagonal close-packed structure. Conversely,

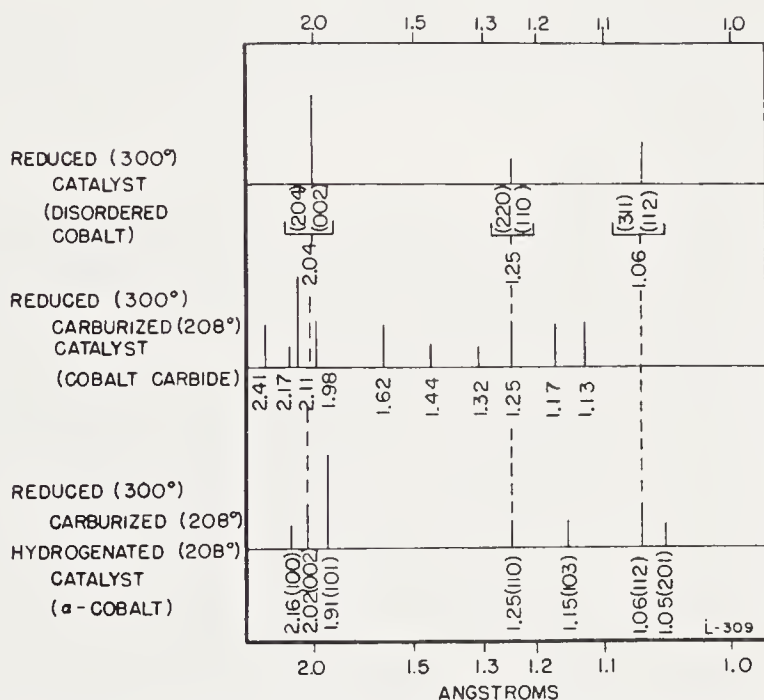


Figure 5. X-ray diffraction patterns of catalyst 89K 100:6:12:200 cobalt-thoria-magnesia-kieselguhr taken at various stages of treatment with carbon monoxide and hydrogen (See Ref. 108).

a pure face-centered cubic structure should, with increase in imperfections, acquire some hexagonal-close-packed character until it also reaches the hybrid state of completely random imperfections.

The experimental facts suggest, therefore, that the cobalt-thoria-kieselguhr catalyst does possess this hybrid structure, since the only reflections observed are those which may be considered common to both the hexagonal close-packed and face-centered cubic structures.

Nowotny and Juza¹⁷⁶ studied the structure of pure cobalt reduced with hydrogen at the transition temperature. They consider their cobalt to be essentially a mixture of face-centered cubic structure and a disordered hexagonal close-packed structure. However, since they did not use pro-

motors and supports (thoria and kieselguhr), they did not obtain as high a degree of disorder as in the promoted and reduced cobalt catalysts. The present author has also examined cobalt reduced at various temperatures from pure oxide and has found the disordering effect much less developed in such specimens. The formulators of the standard cobalt-thoria-kieselguhr catalysts may have been led by empirical studies to those conditions and compositions which maximized the disorder in the catalyst. This disorder, as will be discussed later, improves the yield of solid and liquid hydrocarbons by not more than 10 per cent when the catalyst is operating at optimal conditions²⁵⁵.

Initially, in reporting the above phenomena, Hofer and co-workers understandably considered this disordered cobalt to be the face-centered cubic form of cobalt^{108, 109}.

Carburization of Cobalt

The carbon monoxide-cobalt reaction is very similar to the carbon monoxide-nickel reaction. The first studies were made by Fischer and Bahr⁶³ and Bahr and Jessen¹⁶. At temperatures below 225°C, finely-divided cobalt produced by the action of hydrogen on cobalt oxide reacts readily with carbon monoxide. The reaction slows down with time and virtually stops when the cobalt has gained weight corresponding to the formula, approximately Co_2C . This formula is in contrast to the formula for nickel carbide, Ni_3C . The weight increase is due to carbon only, as is shown by the fact that it can be recovered as methane by treating the carbide with hydrogen at 300°C. Above 225°C, carbon monoxide reacts even more readily with cobalt, but the reaction, although it slows up in later stages, never stops. Instead, it slows down to a nearly constant rate. When the carbon has been laid down at temperatures above 225°C, it cannot be quantitatively removed by treatment with hydrogen at 300°C. Bahr and Jessen's¹⁶ data show a qualitative distinction between the carbon which can be hydrogenated below 300°C and that which can be hydrogenated above this temperature. They termed the former carbidic carbon and the latter free carbon in analogy to the nickel case. Typical carburization curves of Bahr and Jessen are shown in Figure 6. Later x-ray diffraction studies¹⁰⁷ have shown that this carbidic carbon corresponds to a definite crystalline phase structurally different from either free carbon or cobalt metal.

Carburization of the standard cobalt-thoria-kieselguhr or cobalt-thoria-magnesia-kieselguhr catalyst has been studied in greater detail than that of pure cobalt powder. As already mentioned, the cobalt metal in these catalysts possesses a disordered structure that cannot be considered either face-centered cubic or hexagonal close-packed. Carburization of these catalysts to completion is much more rapid than carburization of the pure powder.

This is probably the result of the finer crystallite size (about 50–100 m²/g for cobalt in catalyst as compared with 3.2 m²/g for reduced pure oxide). Direct estimates of the crystallite size by Debye Scherrer line-broadening give 100–300 Å for the catalysts and 800 Å for the reduced pure oxide. On the whole, the findings of Bahr and Jessen¹⁶ and Hofer and Peebles¹⁰⁷ on cobalt produced by reducing finely-divided cobalt oxide are also duplicated with standard cobalt-thoria-kieselguhr catalyst to a surprising extent¹⁰⁸. Free carbon formation becomes noticeable at about 225°C; above

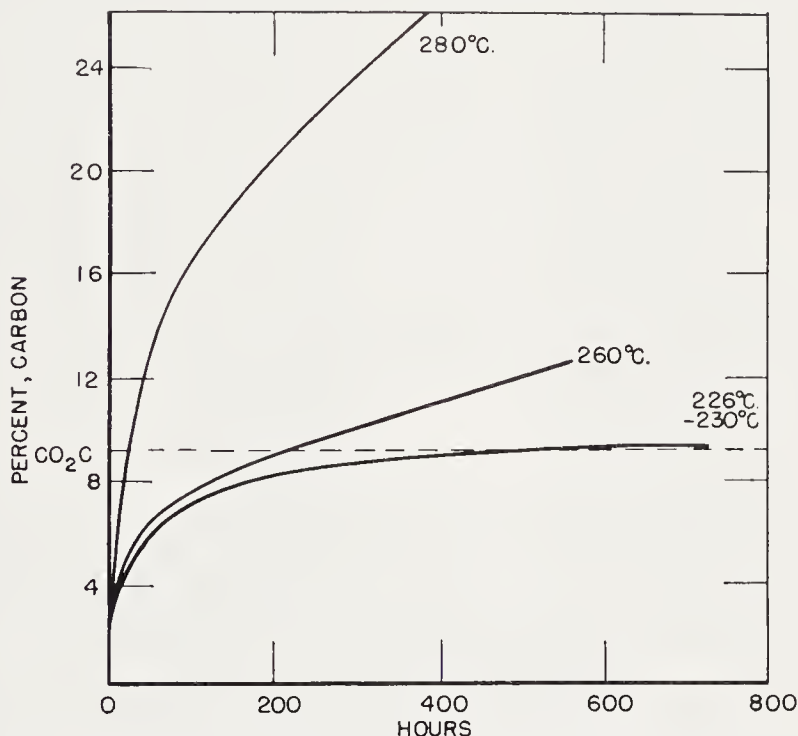


Figure 6. The carburization of cobalt with carbon monoxide according to Bahr and Jessen. (See Ref. 108)

this temperature, free carbon formation becomes increasingly important, until at 298°C very little carbide and large quantities of free carbon are found in the carburized product. The carbide has the same diffraction pattern as that found for the carbide formed in pure cobalt, although the weak and diffuse reflections are hard to detect. The carbide can be hydrogenated at temperatures well below 208°C. A clear distinction between free carbon and carbidic carbon by the relative ease of hydrogenation is possible, but the distinction is not as clear as in the case of carburized pure cobalt powder (see Figure 7). Both formation of the carbide and hydrogenation of the carbide seem to be more rapid because of the smaller crystallite size.

The carbiding process has an activation energy of 31 kcal/mole according

to Weller²⁵⁴. The pressure dependence of the reaction is small, so that the exponent in the equation $r = kp^n$, where r = rate of reaction, p = pressure, and k is a constant, is of the order of 0.20 to 0.26. It has been found that carbon monoxide will react with cobalt in a circulating system, where the carbon dioxide is constantly being removed by condensation until the pressure has been reduced to 10^{-3} mm of Hg. Weller also concluded that

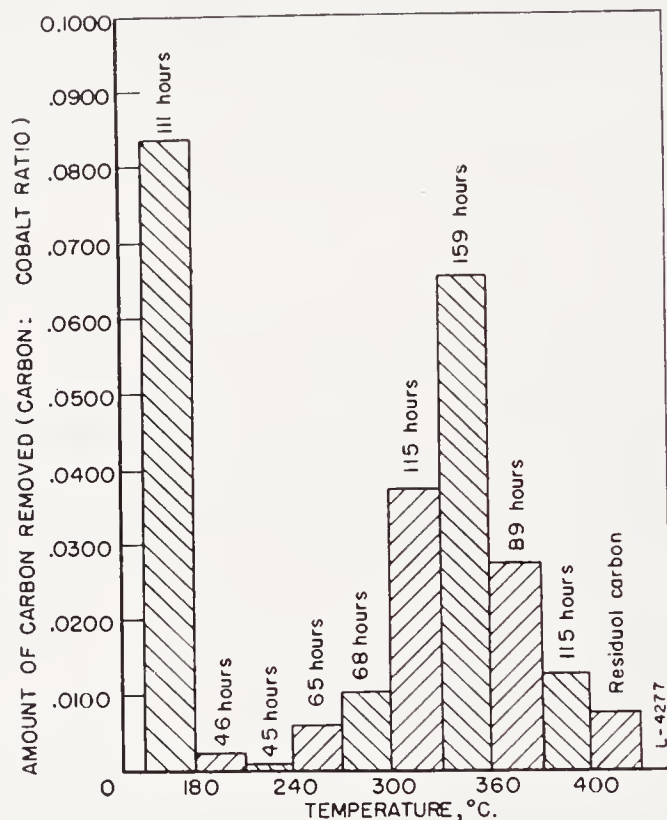


Figure 7. Carbon removed by hydrogenation at increasing temperatures showing the distribution between free carbon and carbidic carbon as deposited at 298°C from carbon monoxide on a cobalt thoria kieselguhr catalyst reduced at 400°C.¹⁰⁹

the earbiding process was too slow to permit bulk carbide to be considered an intermediate in the Fischer-Tropsch reaction. Eidus and co-workers^{54, 55, 58} obtained similar results, but because of their confusion as to the concepts of bulk carbide and surface carbide, they concluded that carbides in general were not intermediates in the Fischer-Tropsch synthesis.

Bahr and Jessen¹⁶ have published the results of a large number of runs on the earburization of pure cobalt and on the hydrogenation of the resulting products. Particularly interesting experiments were made by earburizing first at about 225°C where no detectable free carbon was formed and then earburizing at a somewhat higher temperature. The results of these two-

stage carburizing experiments, together with comparable one-stage experiments, are summarized in Table 6. The experiments lead to a number of interesting conclusions.

1. While in the initial stages, treatment with carbon monoxide increases the carbide content, the amount of carbide decreases under prolonged carburization, especially at temperatures above about 225°C. Thus

TABLE 6. SINGLE-STAGE AND DOUBLE-STAGE CARBURIZING OF COBALT METAL

Sample	1st Stage of Carbon Monoxide Treatment			2nd Stage of Carbon Monoxide Treatment			Analysis, Hydrogen Treatment		
	Temp. (°C)	Time (hr)	Carbon (%)	Temp. (°C)	Time (hr)	Carbon (%)	Temp. (°C)	Carbon from Weight Loss (%)	Carbon from Methane Determination (%)
XXXVI-B	226-230	731	9.53	—	—	—	260	9.22	9.07
LIV-B	224-226	452	9.69	—	—	—	243	8.83	9.34
XXXV-M	245-250	182	9.87	—	—	—	241	9.07	8.68
XVIII-M	250-255	345	11.10	—	—	—	262	8.43	7.31
XXXI-M	225	606	7.73	250-258	200	9.13	244	8.92	9.00
IX-M	255	243	12.12	—	—	—	250	9.09	8.80
XXVI-I	260	531	12.47	—	—	—	255	7.67	6.46
LXV-B	276	94	13.84	—	—	—	247	9.04	9.08
XXIV-I	280	349	25.7	—	—	—	255	5.90	5.99
LI-B	226	45	3.17	280	64	20.7	243	7.83	8.38
XXXVIII-B	225	140	7.38	283	133	16.25	246	9.12	9.28
LXIII-B	287	45	25.47	—	—	—	246	6.29	6.00
XXXVII-B	290	62	27.9	—	—	—	241	3.77	3.44
LXII-B	290	46	37.67	—	—	—	245	2.68	2.40
IL-B	226.5	47	5.59	294	46	14.85	244	8.80	9.03
LV-B	225	203	7.92	300	45	16.52	243	8.82	9.33
XXIX-M	305-335	41	76.5	—	—	—	252	.81	.00
XXXIX-B	227	936	8.12	315.5	45	34.96	246	.36	.23
LX-B	227	276	~9	328	43	ca. 51.7	245	.32	.29
XXIII-I	340	195	63.5	—	—	—	245	1.11	.31
XXXXI-B	226	381	7.87	520	10-20	37.0	245	.2	.2

one may compare runs LXV-B and XXIV-I or runs IX-N and XXVI-I. In each case the two runs, although carried out at nearly the same temperature, have widely different carbide content; that run which was operated longest also produced the lowest carbide content. This suggests that the carbide content reaches a maximum and then decreases thermally with time.

2. If a sample of cobalt is first carbided at around 225°C and is then carburized at higher temperatures up to 300°C, the formation of carbide is promoted even when the temperature is such that the corresponding iso-

thermal carburizing experiments indicate a decreasing amount of carbide due to thermal decomposition. Furthermore, much less free carbon is formed than one would expect from the single-stage carburizing data. These general conclusions are illustrated by the following examples: Sample XXXI-M was carburized first for 606 hours at 225°C, taking up 7.73 per cent carbon. This carbon must be almost quantitatively in the form of carbide if one judges by sample XXXVI-B. Further treatment with carbon monoxide at 250 to 258°C for 200 hours raised the total carbon content to 9.13 per cent. Analysis by treating the sample with hydrogen found it to contain 8.92 per cent carbon in the form of carbide. This agrees well with the percentages of carbon as carbide found in samples XVIII-M and IX-M. This behavior is therefore essentially as expected. Now, however, consider sample LV-B which was treated with carbon monoxide at 225°C for 203 hours. This resulted in an uptake of 7.92 per cent carbon, which again may be considered as essentially pure carbidic carbon. By treating this pre-carbided sample with carbon monoxide at 300°C for an additional 45 hours, a total carbon percentage of 16.52 was reached. Treatment with hydrogen shows the specimen to contain 8.82 per cent carbon as carbide. Measurement of the amount of methane generated gives the carbide content as 9.33 per cent. Thus in 45 hours, the carbidic carbon content increases from 7.92 to 8.82 per cent (or 9.33 per cent, depending on which method of analysis is chosen). This result must be compared with the result on LXII-B, which was treated with carbon monoxide at around 290°C for 46 hours. At the end of this period, LXII-B contained only 2.68 per cent carbidic carbon by weight loss during hydrogen treatment, or 2.40 per cent carbidic carbon by methane determination and 37.67 per cent total carbon. One would expect both of these specimens to decrease slowly in carbide content by thermal decomposition, as has been discussed above, but actually LV-B increases in carbide content. Not only that, but LV-B is increasing in carbidic carbon content in a range where inhibition of the process due to the approach to the stoichiometric composition Co_2C should be an important factor. Another important difference in behavior between LXII-B and LV-B lies in the total free carbon content of the two samples; LXII-B has $37.67 - 2.68 = 34.99$ per cent carbon, whereas LV-B has only $16.52 - 8.82 = 7.70$ per cent free carbon. These differences are summarized in Figure 8.

Carbon Deposition and Thermal Decomposition of Co_2C

One of the most difficult problems catalytic chemists must deal with is the suppression of carbon formation in Fischer-Tropsch catalysts during synthesis. As has been noted in the discussion on carburization, carbide and free carbon formation go on side by side above 225°C on cobalt; above

300°C free carbon formation proceeds to the practical exclusion of carbide formation. 225°C is the high temperature limit for practical operation of the Fischer-Tropsch process on cobalt catalysts, and one suspects that this limit may be set by carbon deposition.

Cobalt carbide is subject to thermal decomposition. This reaction has been studied under very restricted conditions when the cobalt carbide existed as a portion of a standard cobalt-thoria-kieselguhr catalyst¹⁰⁶. Pure

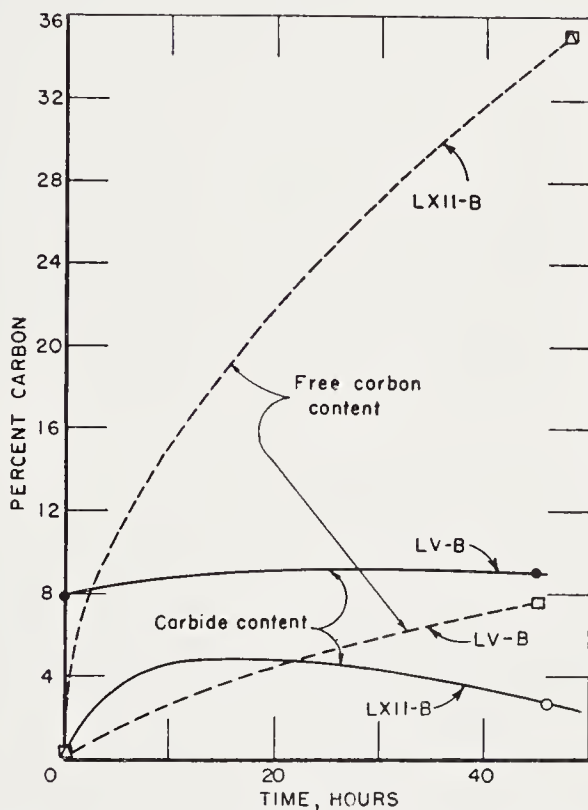


Figure 8. Comparison of carbon deposition and carbide formation as it proceeds on a prescribed specimen of cobalt LV-B and on a simple reduced specimen LXII-B.

cobalt carbide probably does not behave in the manner of the cobalt carbide studied. Thermal decomposition sets in at an appreciable rate at 300°C and increases with temperature. The reaction in the range 80 to 25 per cent carbide was quasi zero order, and the reaction rate constant, assuming that order was $k = 4 \times 10^{15} \exp. - 54/RT \text{ sec}^{-1}$, where R is in kcal mole⁻¹ °K⁻¹, and T , is the absolute temperature in °K.

The product of the decomposition between 300 and 400°C is the thermally stable hexagonal close-packed allotrope α -cobalt, and free carbon. This free carbon is apparently just as nonreactive as the free carbon formed by the carbon monoxide-cobalt reaction above 225°C. Two possibilities exist

for the mechanism of formation of free carbon by decomposition of the carbide. One possibility is that the carbon forms in intercrystalline spaces or on surfaces. The other is that the carbon forms within the crystallite itself and that its formation results in splitting of the crystallite. Both processes may be envisioned as nucleated reactions. In the former case, the nuclei form or already exist in intercrystalline spaces or on the crystal surfaces. In the latter case, the nuclei form or already exist in the interior of crystallites. No conclusive experimental data are available bearing on this point, although in the case of carbon deposition in iron catalysts a number of experiments have been conducted²⁴⁸. Thermal decomposition of cobalt carbide as it exists in the standard cobalt-thoria-kieselguhr catalyst shows no induction period in marked contrast to thermal decomposition of nickel carbide, Ni_3C . This means that the nuclei must be formed before decomposition can occur in the case of nickel carbide, but the decomposition nuclei are already present in cobalt carbide. This distinction between cobalt carbide and nickel carbide may be more apparent than real, because the cobalt carbide being present in a matrix of promoter and support may have in its structure nuclei which would not be present in pure cobalt carbide. The thermal decomposition reaction may be written:



Fischer and Bahr have suggested that the formation of free carbon by the action of carbon monoxide on cobalt may proceed simply by the formation and decomposition of bulk phase cobalt carbide, Co_2C . To check this point the following experiment was made (see Figure 9). Two specimens of cobalt-thoria-kieselguhr were used. The catalysts were identical in all respects except that the cobalt in one had been converted to Co_2C ¹⁰⁹ by carburization with carbon monoxide, whereas cobalt in the other remained in the reduced disordered cobalt phase. These two specimens were then carburized with carbon monoxide at 285°C for 22 hours, with the results shown in Figure 9. Carbon deposition initially is 20 times faster on the metallic catalyst than on the carbided catalyst. During the carburization process at 285°C, the rate of carbon deposition on the metallic specimen decreased greatly, whereas the rate on the carbided specimen remained constant. X-ray diffraction analysis showed that the precarbided specimen contained only Co_2C , showing that no net change in carbide content had occurred. The x-ray diffraction analysis of the initially metallic specimen showed the presence of the initial disordered cobalt and a small amount of Co_2C . The results show that precarbided cobalt is distinctly inferior to metallic cobalt as a catalyst for the carbon deposition reaction. This difference in activity may be ascribed either to the chemical and structural difference between the cobalt surfaces or to the presence of traces of oxygen in the carbided sur-

face. Traces of oxygen in iron catalysts are known to exert enormous influence on the activity of iron carbides¹⁴³. The rate of carbon deposition on the precarbided catalyst was 0.0064 g carbon/g cobalt/hr and the rate of carbide decomposition as calculated from the frequency factors and energies of activation previously determined on similar catalyst was 0.0015 g carbon/g cobalt/hr. The two values are sufficiently close together to suggest the possibility that all carbon in the precarburized specimen could have been formed by the alternate steps of carbide formation and carbide decomposition. There can be no doubt, however, that this mechanism is not

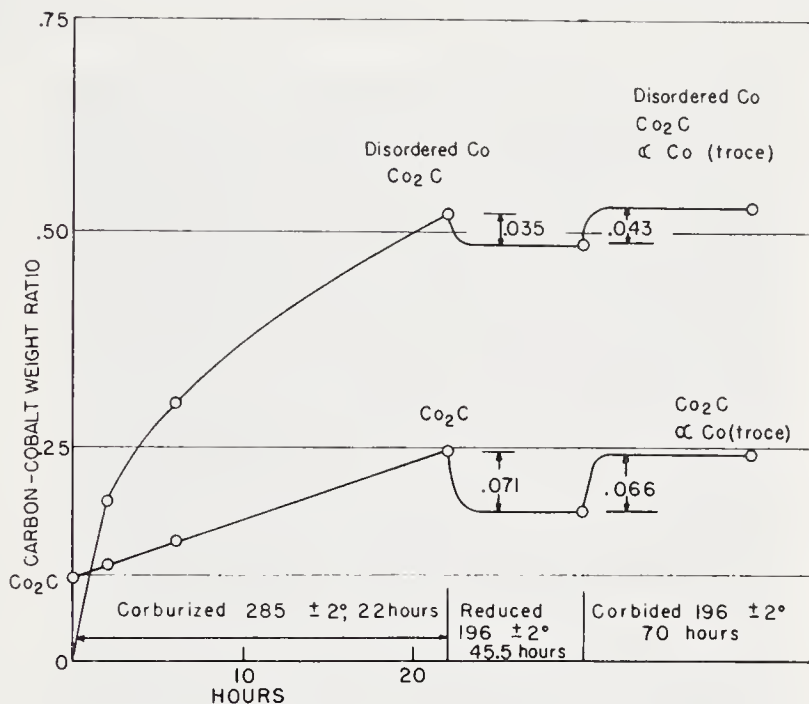


Figure 9. Comparison of carbon deposition on a carbided catalyst with carbon deposition on an uncarbided one. (See Ref. 109)

followed for the formation of free carbon from carbon monoxide on the metallic cobalt, since carbide decomposition is entirely too slow to fit into this reaction scheme.

Kehrer and Leidheiser¹⁵¹ have found that carbon deposition occurs preferentially on the 111 and associated faces (211, 311, 411) of face-centered cubic cobalt but not on the 0001 face of hexagonal close-packed cobalt. This is an amazing result when one considers that the arrangements of atoms in both these faces are exactly the same. Indeed if only the first two layers of atoms are considered, the arrangement of the face-centered cubic 111 and hexagonal close-packed 0001 are still indistinguishable. Only in the third layer is there a difference. On the hexagonal close-packed cobalt, carbon deposition occurs preferentially on the 0113 and 1124 planes.

An electron microscope study¹¹¹ of carbon deposited on cobalt reveals that it consists of filaments 0.1 to 0.01 μ in diameter (see Figures 10a and 10b). The larger filaments contain a dense nucleus near the middle. This nucleus appears on the electron micrograph as a tiny diamond-shaped area, which may be interpreted as the projection of an octahedron one of whose [001] axes coincides with the axis of the fiber. If the formation of free carbon results in the removal of cobalt atoms from single crystals, and since this process proceeds preferentially on the 111 faces of cubic cobalt as it does on cubic nickel, then the carbon-forming reaction will form just such octahedra as are observed. This electron microscope study suggests a rela-

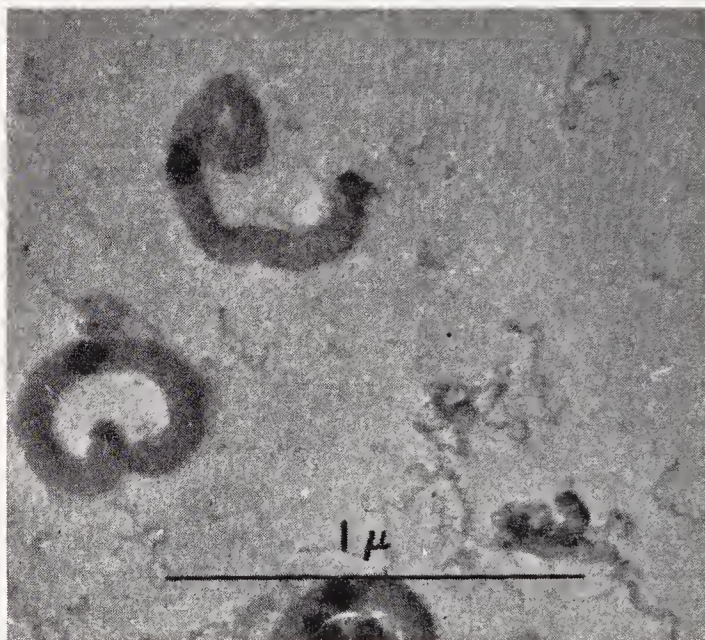


Figure 10a. Formation of carbon filaments by the action of carbon monoxide on cobalt.

tionship between the independence of the carbon deposition rate on the amount of carbon laid down and the filamentous structure of the carbon. Any mechanism producing filaments will continue to extend those filaments at a uniform rate as long as reagents are supplied to the reaction site. Interference of the filaments with the supply of carbon monoxide is not likely, since the filaments generally grow into open space. Attrition may gradually destroy the reaction sites, but this is probably a slow process.

The Carbides of Cobalt

Although the work of Bahr and Jessen demonstrated that cobalt and carbon would combine to the extent of 9.2 per cent carbon, they did not show how the carbon was combined with the cobalt. Since the Hägg rule⁸⁴

favors a hexagonal close-packed structure for metal atoms for the compounds having the formulas $M_2X - M_3X$, and since the metallic cobalt already has this hexagonal close-packed arrangement, one might expect carbon to enter into the cobalt lattice with no structural change other than a gradual increase in lattice parameter until carbiding is complete. Such a situation would simply correspond to a high solubility of carbon in cobalt.

Meyer¹⁶⁶ examined cobalt carburized with illuminating gas at a range of temperatures by means of x-ray diffraction powder patterns. He concluded that the carbon produced by carburization in the 225 to 300°C range and capable of hydrogenation below 300°C was held in solid solution in the

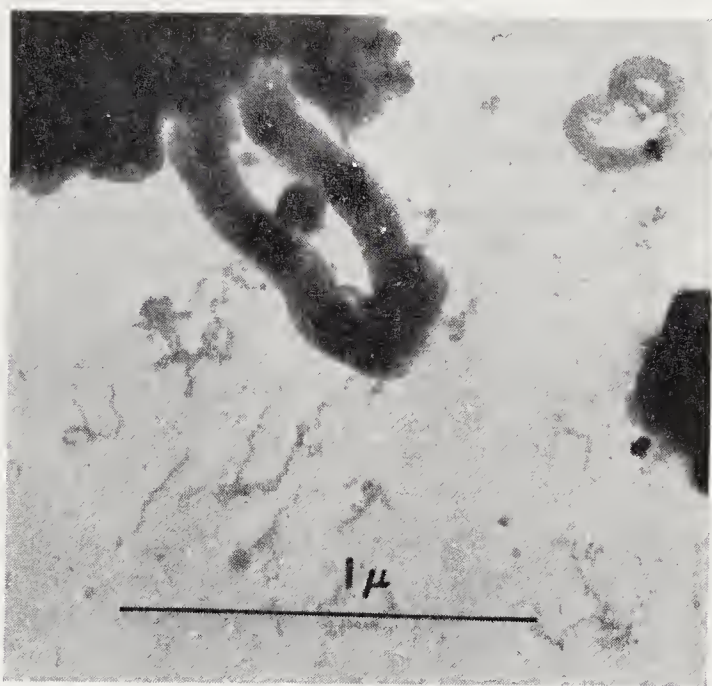


Figure 10b. Another view of specimen shown in Figure 10a.

lattice of α -cobalt. Experimentally this meant that his x-ray powder patterns for specimens carburized in the 225 to 300°C range were indistinguishable from the uncarburized cobalt. As we shall see, this is in direct contradiction to the findings of other workers. By carburization in the 450 to 600°C range, Meyer produced a product whose diffraction pattern was nearly identical with that of cementite, Fe_3C . This would indicate a carbide of the same structure and nearly the same lattice parameter as cementite. The writer has had occasion to perform experiments rather similar to those of Meyer, but neither he nor his associates have ever found a cementite-like cobalt carbide. Drain also questioned this carbide⁴⁶ recently. Nevertheless, Meyer's carbide continues to be referred to in the literature⁷⁶.

Hofer and Peebles¹⁰⁷ readily duplicated the essential features of Bahr and

Jessen's carburization experiments on cobalt, and by x-ray powder diffraction patterns demonstrated the presence of a hitherto unreported phase in those carburized specimens which contained an easily hydrogenated fraction of carbon (carbide carbon). There was a one-to-one relationship between the amount of the new phase and the amount of the carbide carbon. Thus the new phase was definitely identified as a carbide with an approximate formula of Co_2C . Upon complete removal of the carbide carbon by treatment with hydrogen, cobalt reverts to its original hexagonal close-packed form. At no stage either in carburization or hydrogenation did the lattice parameters increase above those of the pure metal. The possibility of any extensive amount of carbon in the form of a terminal solid solution of carbon in cobalt is small. It must be remembered that the lattice parameter is rather insensitive to composition. The carbide itself always had the same diffraction pattern in which the interplanar spacings were constant within the precision of measurement. The carbide, therefore, has a narrow

TABLE 7. THE LATTICE PARAMETERS (Å) OF COBALT CARBIDE AS DETERMINED BY VARIOUS INVESTIGATORS

	a_0	b_0	c_0
Clark and Jack ³⁶	2.8969 ± 0.0005	4.4465 ± 0.0010	4.3707 ± 0.0010
Drain and Michel ⁴⁷	2.904	4.465	4.368
Juza and Puff ¹³¹	2.891	4.463	4.369
Fitzwilliam ⁶⁸	2.898	4.452	4.360

range of composition. Comparison of the diffraction pattern with that of cementite showed no resemblance.

In 1951, three authors independently determined the crystal structure of this cobalt carbide, Co_2C . Clarke and Jack³⁶ and Fitzwilliam⁶⁸ agree that the space group is D_{2h}^{12} -Pnnm, while Juza and Puff¹³¹ find D_{2h}^{14} . All three groups of investigators agreed that the structure is orthorhombic with lattice parameters, shown in Table 7. In addition, Drain and Michel^{46, 47} determined the structure by comparison of its powder pattern with those of Co_2N evaluated by Juza and Sachse¹³³.

Jack placed the cobalt atoms in sites (g) at $0\ y\ z; 0\ \bar{y}\ \bar{z}; \frac{1}{2}, \frac{1}{2} + y, \frac{1}{2} - z; \frac{1}{2}, \frac{1}{2} - y, \frac{1}{2} + z$ and the carbon atoms in sites (a) at 000 , and $\frac{1}{2}, \frac{1}{2}, \frac{1}{2}$. The values of y and z are 0.347 ± 0.001 and 0.258 ± 0.002 , respectively. The cobalt positions in the Fitzwilliam structure are essentially the same, but this author places the carbons in the $2(c)$ positions. Juza and Puff place their 4 cobalt atoms in the $4(c)$ $0, y, \frac{1}{4}$ positions with $y = 0.158$.

Nitrides of Cobalt

Cobalt preparations containing combined nitrogen were prepared by Vournasos²⁴⁹ from cobalt cyanide and cobalt oxide at 2000°C . Beilby and

Henderson¹⁸ have shown that cobalt metal absorbs up to 10.33 per cent nitrogen from an ammonia stream at 470°C. By contrast, Hägg⁸¹ found no structural modification of cobalt by the action of ammonia in the range 300 to 1000°C. Juza and Sachse¹³³ prepared Co_3N by the reduction of Co_3O_4 in hydrogen for 2 hours at 350°C and for 3 hours at 380°C. The metal was then nitrided for a total of 6 hours at 380°C. Only milligram quantities of the nitride could be prepared in this fashion. This same compound could be prepared by directly nitriding $\text{CoF}_2 \cdot 2\text{NH}_4\text{F} \cdot 2\text{H}_2\text{O}$ with ammonia at 360°C. It could also be formed from CoBr_2 by direct nitriding. Juza and Sachse emphasize the difficulty of forming Co_3N . Above optimum nitriding temperatures, the presence of appreciable amounts of hydrogen in the nitriding gas favored the formation of Co_3N . Clark and Jack³⁶ found

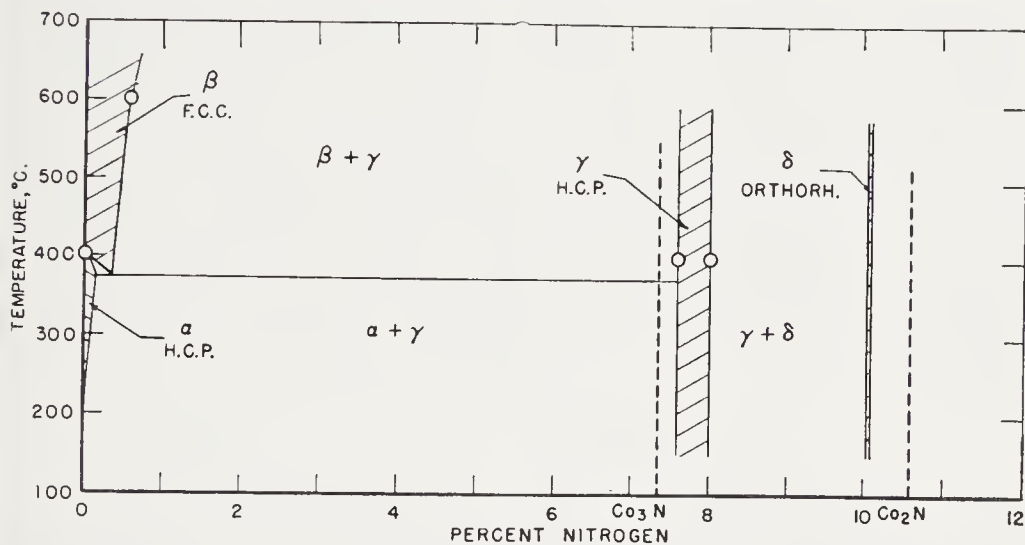


Figure 11. Cobalt-nitrogen system based on data of Juza and Sachse¹³³.

no trouble in preparing quantities of Co_2N up to one gram. The widely varying success of investigators in preparing the nitrides of cobalt points to a variable in preparation which has not been adequately controlled. Possibly the presence of an impurity in either the nitriding gas or in the metal itself may serve to poison the ammonia cracking reaction. In some cases the hydrogen partial pressure is kept sufficiently low so that the nitriding reaction can proceed.

The low-temperature existence diagram of the cobalt-nitrogen system as deduced from the data of Juza and Sachse¹³³ is given in Figure 11. Co_3N is isomorphous with Ni_3C , Fe_2C h.c.p., and $\epsilon\text{-Fe}_2\text{N}$; Co_2N is isomorphous with Co_2C .

The Borides of Cobalt

DuJassonneix⁴⁸ first demonstrated the existence of phases Co_2B , CoB , and CoB_2 . Bjurström²¹ prepared the phases Co_2B and CoB by melting the

elements together. The crystal structures were determined from powder patterns and are reproduced in this chapter. See Table V.

Catalytic Activity in the Cobalt System

The α -Co, disordered cobalt, and probably β -Co phases are all active as Fischer-Tropsch catalysts. All the active catalysts which have been investigated by x-ray diffraction contain one of these phases. Co_2C catalysts²⁵⁵ show a greatly depressed activity compared with α -Co, or disordered cobalt. Such activity as they retain may be due to traces of metal which tend to form due to the reducing action of synthesis gas. The oxides and oxide hydrates appear to be quite inactive; otherwise less emphasis would be placed on the reduction of cobalt catalysts with hydrogen. The nitrides of cobalt are too unstable with respect to thermal decomposition to the elements to permit easy investigation. This difficulty is underlined by the preparatory difficulties. The carburizing action of synthesis gas should tend to form a carbonitride which will probably be intermediate in properties between Co_2N and the isomorphous and catalytically inactive Co_2C . The borides of cobalt have hitherto been prepared only by melting together the elements. Such products have almost no surface area, and therefore are useless as catalysts. The boriding with boranes of finely-divided cobalt produced by the reduction of cobalt oxide or oxide hydrates, on the other hand, seems quite feasible, however, and since Co_2B is ferromagnetic, it may well be an active catalyst.

THE IRON SYSTEM

Oxides, Oxide Hydrates, and Hydrous Oxides of Iron

A voluminous literature exists on the oxides, oxide hydrates, and hydrous oxides of iron. To treat this literature in detail would be out of place. The excellent reviews of Weiser²⁵⁰, and Welo and Baudisch²⁵⁶ should be referred to for details. The interrelations of the various oxidic phases are summarized in Figure 12, adapted from Welo and Baudisch.

Iron oxides are crystalline phases consisting of iron and oxygen. They may contain adsorbed water, but such water is not essential to their crystal structure, as it may be removed without altering the diffraction pattern. In general, the oxides contain relatively little water. The hydrous oxides are usually not well crystallized—the diffraction pattern in many cases is quite structureless. These amorphous masses may contain surprising quantities of water. As the water is removed by evacuation, heating, aging, or coagulation, the diffraction pattern tends to sharpen. The ease with which water is removed is a function of the amount of water remaining—thus the first fractions are removed very readily and the last water comes off with difficulty, while in between lies a complete intermediate spectrum of ease

of removability. In a sense, the hydrous oxide is only the oxide in an exceedingly fine state of subdivision (about 10 Å diameter crystallites) and holding a near maximum amount of water by adsorption. The oxide hydrates are definite compounds of oxide and water with definite crystal structures of their own. The water which they contain is given up in a rather narrow temperature range. In general, the oxides and hydrous oxides of iron in the ferric state are brown or red, while the oxide hydrates of ferric iron are yellow.

The familiar, highly gelatinous, voluminous precipitate formed when a soluble base is added to a solution of a ferric salt in water is generally called ferric hydroxide, with the formula $\text{Fe}(\text{OH})_3$. By analogy to the aluminum

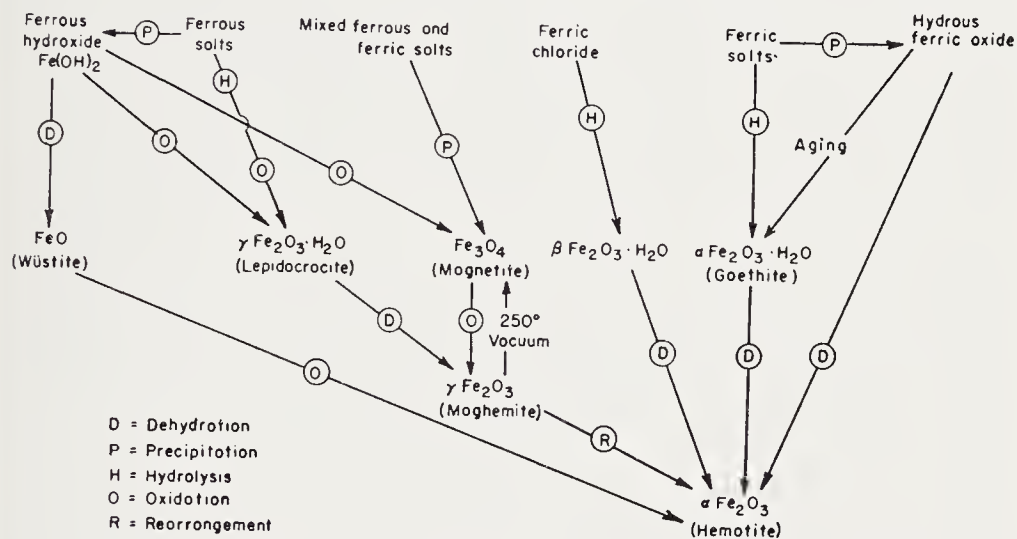


Figure 12. Important reactions of iron oxides and oxide hydrates.

system, this compound might be isomorphous with gibbsite, but actually it has no discernible structure—it is a typical hydrous oxide. As it ages under water at room temperature, the precipitate loses water—becomes more dense—and slowly, in the course of several months, the diffraction pattern sharpens into that of $\alpha\text{-Fe}_2\text{O}_3$, hematite. This suggests that hematite is related to the brown hydrous ferric oxide and differs from it largely by the increased crystallite size and decreased amount of adsorbed water.

Hematite, $\alpha\text{-Fe}_2\text{O}_3$, is generally red, although in large natural crystals it often has a metallic gray luster. It can be formed by dehydration of brown gel, as mentioned above. Dehydration of $\alpha\text{-Fe}_2\text{O}_3 \cdot \text{H}_2\text{O}$ and $\beta\text{-Fe}_2\text{O}_3 \cdot \text{H}_2\text{O}$, which occurs around 200 to 300°C, yields $\alpha\text{-Fe}_2\text{O}_3$. It is also formed by rearrangement of $\gamma\text{-Fe}_2\text{O}_3$, which occurs at 100 to 400°C, and by calcination of $\text{Fe}(\text{NO}_3)_3$ at 300°C. The structure of hematite has been determined by Pauling and Hendricks¹⁸³.

Maghemite, $\gamma\text{-Fe}_2\text{O}_3$ or magnetic ferric oxide, can be formed by dehydration of $\gamma\text{-Fe}_2\text{O}_3 \cdot \text{H}_2\text{O}$ at about 200°C or by oxidation of magnetite at 220°C with air. The compound is closely related to magnetite. The diffraction patterns are nearly the same, but the larger lattice parameter of magnetite results in a perceptible shift of the reflections to smaller Bragg angles. Maghemite, like hematite, is red, whereas magnetite is black. The crystal structure has been studied in detail by Hägg⁸⁷, Verwey²⁴⁶, and others. $\gamma\text{-Fe}_2\text{O}_3$ has been reported as a normal constituent of iron Fischer-Tropsch catalyst¹⁴⁹, but this identification was based on an erroneous interpretation of thermomagnetic data. (See material on Hägg carbide (pp. 418–427); also the resumé by Hofer¹⁸⁹).

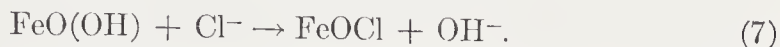
Goethite, nadeleisenerz, or $\alpha\text{-Fe}_2\text{O}_3 \cdot \text{H}_2\text{O}$ is a relatively common mineral that has also been produced synthetically in a number of ways. Following are the methods which have been used to make Fischer-Tropsch catalysts. Meyer¹⁶⁰ has made an extensive study of such an $\alpha\text{-Fe}_2\text{O}_3 \cdot \text{H}_2\text{O}$ catalyst, produced essentially by the method of Fricke and Ackermann⁷², as follows:

A solution of one mole of iron nitrate in one liter of water was added, with violent agitation, to a solution containing $3\frac{1}{2}$ moles of ammonia per liter of water. The precipitate was washed seven times, each time with 4 liters of water. Separation of wash water from precipitate was accomplished with decantation and subsequent filtration. All operations were carried out at room temperature. Before drying, the amorphous precipitate was mixed with twice its volume of 2*N* KOH solution. Then the mixture was heated 2 hours at 140 to 160°C in a silver-lined autoclave. The product was bright yellow. Meyer modified¹⁶⁰ the method of Fricke and Ackermann as he found extensive washing unnecessary after precipitation with ammonia. Precipitation may be carried out with KOH or K_2CO_3 instead of ammonia. The digestion, however, must be carried out with potassium hydroxide. Sodium hydroxide does not produce $\alpha\text{-Fe}_2\text{O}_3 \cdot \text{H}_2\text{O}$. The silver lining of the autoclave is a catalyst; no $\alpha\text{-Fe}_2\text{O}_3 \cdot \text{H}_2\text{O}$ is obtained in iron- or copper-lined autoclaves.

Pressure is not essential in forming a goethite catalyst. Bureau of Mines catalyst 80-A²²⁸ was made by precipitating 0.6*M* $\text{Fe}(\text{NO}_3)_3$ with 9*M* KOH at 83°C in a simple borosilicate glass jar. The precipitate, while not containing pure $\alpha\text{-Fe}_2\text{O}_3 \cdot \text{H}_2\text{O}$, contains a large percentage of it. The main crystalline phase is $\alpha\text{-Fe}_2\text{O}_3$. Both the $\alpha\text{-Fe}_2\text{O}_3$ and $\alpha\text{-Fe}_2\text{O}_3 \cdot \text{H}_2\text{O}$ were well crystallized. Weiser and Milligan have reported a method of synthesizing $\alpha\text{-Fe}_2\text{O}_3 \cdot \text{H}_2\text{O}$ which differs from ours, largely in the greatly extended period of time (16 hours) during which the precipitate was digested in boiling KOH solution.

The $\beta\text{-Fe}_2\text{O}_3 \cdot \text{H}_2\text{O}$ is formed by slow hydrolysis of ferric chloride solutions. It has a distinct diffraction pattern different from those of $\alpha\text{-Fe}_2\text{O}_3 \cdot$

H₂O and $\gamma\text{-Fe}_2\text{O}_3 \cdot \text{H}_2\text{O}$. Bohm believed this compound to be a basic chloride²². Weiser and Milligan²⁵² were able to show that the compound held one molecule of water per formula weight of Fe₂O₃. They found the Fe:Cl ratio varied from 4.8 to 45 in samples prepared in various ways and suggested that the chloride stabilized $\beta\text{-Fe}_2\text{O}_3 \cdot \text{H}_2\text{O}$. The $\beta\text{-Fe}_2\text{O}_3 \cdot \text{H}_2\text{O}$, when relatively chloride-free, acts as an ion exchange agent when placed in dilute hydrochloric acid according to the reaction



When ferric ion is precipitated in the presence of chloride ion at about 70°C with a K₂CO₃ solution, $\beta\text{-Fe}_2\text{O}_3 \cdot \text{H}_2\text{O}$ is the main product. If any appreciable amount of ferrous ion is present, Fe₃O₄ is formed instead. These relationships have important implications in the preparation of Fischer-Tropsch catalysts. The chloride that is retained in the catalyst by $\beta\text{-Fe}_2\text{O}_3 \cdot \text{H}_2\text{O}$ is particularly troublesome in that the catalytic activity of the catalysts so formed is greatly reduced. Chloride does not appear to inhibit reduction, but seems to operate directly on the reaction sites in the reduced catalyst^{100, 110}.

A third ferric oxide hydrate is $\gamma\text{-Fe}_2\text{O}_3 \cdot \text{H}_2\text{O}$ or lepidocrocite. It occurs as a rare natural mineral. The methods of preparing it are few and involve oxidation of ferrous ion in aqueous solution under conditions which favor formation of a complex ion. Hahn and Hertrich⁸⁸ showed that the oxidation of ferrous salt solutions with iodate in the presence of sodium thiosulfate yields a granular precipitate, which Albrecht¹ found to be $\gamma\text{-Fe}_2\text{O}_3 \cdot \text{H}_2\text{O}$. The obstacles of preparation seem to have discouraged investigators from using this hydrate as a catalyst. The crystal structure has been determined by Ewing⁶¹.

Magnetite is an exceedingly well-known crystalline phase. As lodestone, its history goes back to mythology. It can be prepared by direct precipitation of ferrous and ferric ion with most of the common water soluble bases. Magnetite is also readily prepared by melting iron powder in a stream of oxygen or with an electric current. There are, of course, many other ways of preparing magnetite, but these methods are illustrative of those important in catalyst preparation.

Magnetite is one of a large number of compounds known as spinels¹⁶⁷, mixed oxides of bivalent and trivalent elements of the formula $\text{M}^{++}\text{M}_2^{+++}\text{O}_4$. It will be recognized that magnetite is a spinel with a ferrous-to-ferric ratio of 1 to 2. Other bivalent elements which may be substituted in the structure are Mg⁺⁺, Co⁺⁺, Ni⁺⁺, Cu⁺⁺, Zn⁺⁺, Mn⁺⁺; trivalent elements are Al⁺⁺⁺, Fe⁺⁺⁺, Co⁺⁺⁺. This ability of spinel structure of magnetite to incorporate various other elements increases the possibilities of promoting the catalysts containing magnetite. Incorporation of these bivalent and

trivalent ions results in modification of the Curie point and the specific magnetization¹⁵⁷, which are normally about 570°C and 80 c.g.s. units per gram.

Some spinels can be made by coprecipitation of nitrates. CuFe_2O_4 is an important spinel because of the usefulness of copper in aiding reduction of iron oxide¹⁴⁹. Coprecipitation of copper and ferric nitrates with alkali yields a precipitate with a structureless diffraction pattern under most conditions¹⁷⁰. Only when the nitrates are precipitated with great rapidity is the spinel formed as can be shown by its ferromagnetism and its diffraction pattern¹⁵⁵.

Ferrous hydroxide, $\text{Fe}(\text{OH})_2$, is commonly obtained by precipitation of ferrous ion with alkali. Its color in the unoxidized state is white, although only a very slight amount of oxidation converts it to green. It is thought to be an intermediate in the corrosion of metallic iron and steel. Because of the difficulty of preparation, little has been done to make use of it as a catalyst. The compound is isomorphous with $\text{Co}(\text{OH})_2$, $\text{Mg}(\text{OH})_2$, $\text{Ca}(\text{OH})_2$, $\text{Cd}(\text{OH})_2$, $\text{Ni}(\text{OH})_2$, $\alpha\text{-Zn}(\text{OH})_2$, and $\text{Mn}(\text{OH})_2$ ⁷³.

Reduction of Iron Oxide and Oxide Hydrates

Iron oxide catalysts in the raw unreduced state exist generally as a nearly amorphous gel-like material closely related to hematite, magnetite (Fe_3O_4), or maghemite ($\gamma\text{-Fe}_2\text{O}_3$) which is closely related in structure to Fe_3O_4 . Wustite (FeO) probably because of its instability is rarely found in the raw catalysts. The iron oxide hydrates, goethite ($\alpha\text{-Fe}_2\text{O}_3 \cdot \text{H}_2\text{O}$), lepidocrocite ($\gamma\text{-Fe}_2\text{O}_3 \cdot \text{H}_2\text{O}$), and $\beta\text{-Fe}_2\text{O}_3 \cdot \text{H}_2\text{O}$ are also found in raw catalysts. The latter is, however, present only in poor catalysts.

Several processes take place when these oxides and oxide hydrates are subjected to reducing conditions with hydrogen at the normal reducing temperature of 250 to 500°C. The oxide hydrates, on the basis of purely thermal decomposition, will be expected to dehydrate to form $\alpha\text{-Fe}_2\text{O}_3$ in the case of $\alpha\text{-Fe}_2\text{O}_3 \cdot \text{H}_2\text{O}$ and $\beta\text{-Fe}_2\text{O}_3 \cdot \text{H}_2\text{O}$ and $\gamma\text{-Fe}_2\text{O}_3$ in the case of $\gamma\text{-Fe}_2\text{O}_3 \cdot \text{H}_2\text{O}$. The hematite ($\alpha\text{-Fe}_2\text{O}_3$) so formed, as well as the hematite and gel-type catalysts, reacts rapidly with pure hydrogen to form magnetite. When the catalyst approximates the composition Fe_3O_4 , the reduction rate decreases sharply. Further reduction produces metallic $\alpha\text{-Fe}$. This sharp difference in reaction rate between the reduction of hematite and magnetite with hydrogen is most pronounced with unpromoted catalysts^{19a}. Promoters tend to smear out this difference. By saturating the hydrogen with water vapor at room temperature, the reduction of hematite can be made to stop at magnetite. It can be shown that thermodynamically such a mixture of hydrogen and water is not capable of reducing iron oxide beyond magnetite.

Reduction data of promoted magnetite D3001 at 450°C and 1000 space velocity are given in Figure 53 (Chapter 2). It shows that the reduction slows down as complete reduction is approached. Unpublished data from the Bureau of Mines show that the rate of reduction of promoted magnetite type catalysts at any given temperature decreases as the surface area of the reduced catalyst increases. In general, such increase in surface area is achieved by an increase in the amount of structural promoters. It is known

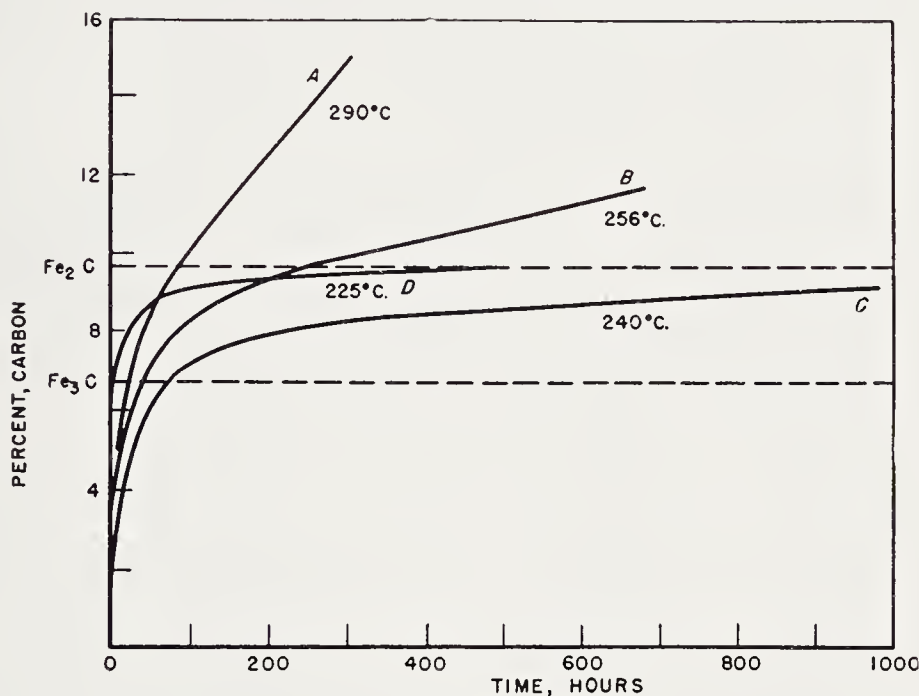


Figure 13. Carburization of iron according to Bahr and Jessen at various temperatures as indicated. Samples A, B, and C were reduced at about 300°C. Sample D was reduced at 225°C. (See Ref. 17)

that such magnetite catalysts containing structural promoters are thermodynamically more stable toward reduction than unpromoted magnetites.

The Carburization of Iron and Iron Oxide

As in the case of cobalt and nickel, treatment of iron with carbon monoxide results in two products—free carbon and iron carbides. Carburization of metallic iron below about 225°C leads to the formation of nearly pure iron carbide; above this temperature, free carbon and iron carbide are formed. The magnetite is thermodynamically more stable than the oxides of cobalt and nickel and conditions are often favorable to the formation of magnetite during carburization². Bahr and Jessen¹⁷ have presented the data shown in Table 8 and in Figure 13. It is representative of the results obtained by other authors, such as Pichler and Merkel^{189, 190, 191}, Kummer,

DeWitt, and Emmett¹⁴³. Bahr and Jessen¹⁷ analyzed their products by treating them with hydrogen at about 290°C. Hydrogenation at this temperature appeared to discriminate well between carbon in the form of carbide and free carbon.

The reaction of carbon monoxide with iron oxide is more obscure, because it is more difficult to follow by the usual analytical methods. Gluud, Otto, and Ritter⁷⁵, in carburizing the oxide, found evidence for the formula Fe_2C for the compound formed. By carbiding iron oxide with carbon monoxide

TABLE 8. CARBIDE FORMATION ON REDUCED IRON

Reduction		Carbon Monoxide Treatment				Analysis, Per cent					
						Iron as Fe_3O_4 from—		Temp. (°C)	Carbon from—		Residue (mg C)
Time (hr)	Temp. (°C)	Time (hr)	Temp. (°C)	Liters (per hr)	Composition	Weight Loss Minus Carbon	Water		Methane Evolved ^a	Weight Loss Minus Oxygen ^a	
497	292	994	240	0.8	1.4235 g Fe .1440 g C	0		291 322 446	7.43 7.62 9.17		5.6
486	290	350	273	.8	1.5181 g Fe .1993 g C	0		291 318 401	7.75 7.92 11.66		4.1
190	290	65	324	.8	.9550 g Fe .2288 g C	0		291 322 446	7.65 8.08 19.44		.4
200	291	93	333	.5	1.5682 g Fe .6338 g C + O	4.45	2.04	287 316 483	8.23 8.23 29.6	8.02 8.10 29.0	5.5
143	291	1.6	354	1.5	1.458 g Fe .1234 g C + O	.68	1.22	280 317 483	7.12 7.12 8.05	7.07 7.15 7.92	.9
206	290	41	362	.8	1.8080 g Fe 1.1017 g C + O	7.36	7.39	291 322 450	7.75 7.72 38.7	7.40 ? 38.7	3.1

^a Values are cumulative.

at 275 to 320°C, Hofmann¹¹² and co-workers produced a substance whose x-ray powder diffraction pattern contained, in addition to the reflections of Fe_3O_4 and cementite those of a phase which had previously been formed by Brill and Mark³¹ from the decomposition of $\text{Fe}(\text{CN})_2$. That these reflections may be due to a carbide is made rather probable by Hilpert and Dieckmann's⁹⁷ observation that if $\text{K}_4\text{Fe}(\text{CN})_6$ is thermally decomposed and the resultant potassium cyanide leached out, the product will react with hydrochloric acid to form hydrocarbons. As this latter reaction is characteristic of carbides²¹⁵, the product is probably a carbide.

Bahr and Jessen¹⁷ have studied the carburization process in great detail from a chemical point of view. Their data on the carburization of oxides

are summarized in Table 9. They determined the weight loss of the reaction vessel during hydrogen treatment, weight of water evolved, and quantity of methane formed. From these, they determined the amount of iron oxide present (a) by the water formed and (b) by the weight loss minus the carbon converted to methane. Similarly, the carbide was measured (a) by the quantity of methane formed and (b) by the weight loss minus the oxygen con-

TABLE 9. CARBIDE FORMATION ON IRON OXIDE

Carbon Monoxide Treatment				Analysis by Hydrogen treatment, Per cent					
				Iron as Fe_2O_3 from—		Temp. ($^{\circ}\text{C}$)	Carbon from—		Residue (mg C)
				Weight Loss Minus Carbon	Water		Methane Evolved ^a	Weight Loss Minus Oxygen ^a	
1036	234	0.8	1.4361 g Fe .4252 g C + O	3.28	4.41	276	10.53	10.00	1.7
						305	12.14	11.68	
						401	23.1	23.0	
405	226	.8	1.9353 g Fe .9143 g C + O		3.87	257		9.64	3.9
						282		11.61	
						317		17.91	
						481		32.2	
576	238	.8	1.3619 g Fe		3.57	257		9.17	2.7
138	276		.6579 g C + O			282		10.67	
						318		15.40	
						478		33.0	
216	276	1.5	1.7168 g Fe .5890 g C + O	5.42	2.90	259	8.67	8.80	1.0
						274	8.61	9.03	
						324	13.99	14.42	
						403	25.02	25.73	4.2
57	275	1.5	1.8402 g Fe	7.97	9.19	257	9.35	9.47	
			.3933 g C + O			274	9.44	9.57	
						298	11.22	10.87	
						356	16.73	16.53	

^a Values are cumulative for each sample.

verted to water. One of the striking results of the experiments on iron oxide, as compared with those on metallic iron, is the much higher rate of free carbon formation. For example, the carburization of iron oxide at 234°C for 1034 hours produced some 13 per cent free carbon, whereas a similar experiment on metallic iron at 240°C for 994 hours produced only 2 per cent. This situation also holds at higher temperatures. For example, carburization of the oxide at 275°C for 57 hours produced 7.4 per cent free carbon, whereas carburization of metallic iron at 273°C for 350 hours yielded only 3.9 per cent free carbon. The iron oxide used by Bahr and

Jessen was prepared by calcination of ferric nitrate. This method of preparation does not form a high surface area oxide so that it is questionable whether the high rate of free carbon deposition is attributable to the high surface area of the oxide. Analysis by hydrogenation for carbidic carbon laid down in iron oxide is not as reliable as it is for carbidic carbon laid down in metallic iron. Olmer¹⁷⁸ studied the decomposition of carbon monoxide on iron to see whether the Curie point affected the reaction in any way but with negative results.

Hydrocarbons can apparently also be used for preparing iron carbides. This reaction can be achieved by passing such hydrocarbons as propane, butane, or pentane over the thoroughly reduced iron catalyst at 250 to 350°C¹⁹³.

A number of advantages accrue from the use of hydrocarbons as carbiding agents. First, the reaction involves no appreciable temperature rise at 275 to 325°C. Carbon monoxide on the other hand reacts with iron under these same conditions with temperature gradients of nearly 20°. As a possible corollary to this effect, little or no free carbon is formed under these conditions. A second advantage is that the carbide resulting from carburization with hydrocarbons is entirely free of oxygen. Some 0.3 per cent oxygen is taken up during carburization to carbon contents ranging from 2 to 9.1 per cent. This corresponded to about 2 layers of iron oxide on the particular catalyst studied. Carburization with hydrocarbons never leads to the incorporation of more than 7.5 per cent carbon as carbide. This should be compared with the 9.1 per cent carbidic carbon which can be combined with iron by means of carbon monoxide. This difference is apparently not caused by a difference in composition of the carbide formed because the x-ray reflections of metallic iron in the diffraction pattern of the hydrocarbon carburized material (7.5 per cent carbon) are considerably more intense than the same reflections in the diffraction pattern of carbon monoxide carburized material. No satisfactory reason can be advanced to explain why the carbiding process should stop short of complete conversion to Hägg iron carbide. As will be indicated later the thermal reactions of the carbides of iron formed by hydrocarbons are quite different from those formed by carbon monoxide.

Tutiya^{241, 244} studied the carburization of iron catalysts with carbon monoxide, but his work, being prior to the establishment of the Hägg iron carbide, was not satisfactorily interpreted.

Carburization studies of Eidus and co-workers^{52, 53, 56, 57, 59} on various iron catalysts, such as Fe:Cu, Fe:Cu:K₂O, Fe:Cu:ThO₂:K₂O, and Fe:Cu:ThO₂:K₂O:kieselguhr showed essentially that the more highly promoted catalysts carbide more rapidly, as might be expected from their greater surface area. Kodama *et al.* also studied the initial stages of the

carburization of iron without identification of the solid phases¹³⁵. Carbiding of iron catalysts, unlike those of cobalt and nickel, can readily be achieved by synthesis gas of composition $\text{CO} + 2\text{H}_2$ ^{6, 26, 135, 137, 255}.

The carbiding of iron must go through the same series of steps discussed in the case of the carbiding of cobalt and nickel (Figure 2), namely (a) chemisorbed carbon monoxide, (b) surface carbide, (c) solid solution of carbon in iron, (d) supersaturated solid solution of carbon in iron, (e) iron carbide (hexagonal close-packed)¹⁵⁶. The supersaturated solution (d), which decomposes into carbide, is probably very similar in structure and thermodynamic stability to martensite (see pp. 418–427, the Carbides of Iron). It may differ from martensite in being cubic rather than tetragonal, but this is minor. By using special x-ray diffraction techniques, Roberts, Averbach, and Cohen¹⁹⁸ and Lement, Averbach, and Cohen¹⁵² were able to determine the concentration of carbon in the martensite, 0.25 per cent, which is in equilibrium with the hexagonal close-packed iron carbide. This value should be compared with 0.03 per cent²²⁶, which is the concentration of carbon in α -iron in equilibrium with cementite. The concentration¹⁹⁵ of carbon in α -iron which must be exceeded to produce Hägg iron carbide must lie at an intermediate concentration, since its free energy lies between those of cementite and the ϵ -iron carbide^{2, 32, 101, 142}.

Kummer, DeWitt, and Emmett¹⁴³ have shown by C^{14} tracer experiments that carbon was not removed by hydrogenation in exactly the reverse order in which it was laid down. They suggested, therefore, that the carbide was laid down on nuclei throughout the mass of the iron crystallites. Mitchel¹⁷¹ amplified and corroborated these studies.

The equilibria of various gases with each other over iron group elements have been extensively studied by Schenck and his co-workers²⁰³⁻²¹⁵. Such equilibria involve carbides in many cases, and the thermodynamic properties of these carbides can be determined by the position of the equilibria. Unfortunately, the equilibria have been studied at too high temperatures to be of direct use in the conventional Fischer-Tropsch reaction.

Trillat and Oketani²³⁵⁻²³⁹ have studied the carbiding of thin films of uni- and polycrystalline iron by electron diffraction transmission patterns. Carburization with carbon monoxide leads only to magnetite, cementite, and graphite, the relative amounts depending on temperature of treatment. Carburization with synthesis gas yielded varying amounts of Hägg carbide and cementite, depending on time and temperature. Hydrogen accelerated the rate of carburization. Unicrystalline films of iron were made by evaporating iron onto a hot sodium chloride crystal and annealing it in a hydrogen atmosphere at 600 to 700°C after the salt had been dissolved. Treatment with $4\text{CO} + \text{H}_2$ synthesis gas at 500°C for one hour produced a small amount of cementite crystals, the (111) plane of which was parallel to the

(001) plane of iron (film surface) and the $(1\bar{2}1)$ plane of cementite was parallel to the (110) plane of iron.

Free Carbon Deposition on Iron

The reaction of carbon monoxide with iron to form free carbon and carbon dioxide proceeds between 240 and 900°C. Von Wangenheim^{247, 248} has made a detailed study of the behavior of the reaction between 350 and 500°, with special attention to the carbon phase produced. The carbon could never be produced free of iron regardless of the form in which the iron catalyst was introduced. The reaction ceased when the carbon iron ratio became approximately 100 to 1 by weight. Fischer and Bahr⁶³ were able to show that an iron-copper catalyst, when heated with carbon monoxide at 500°C, forms a carbon which contains copper as well as iron, well separated from the mass of the catalyst. If the iron were carried into the carbon phase as volatile carbonyls of iron, the copper, which forms no carbonyl, would be left behind. The copper and presumably the iron must therefore be carried into the carbon phase by some other method, probably mechanical. Hofer⁹⁸ suggested that this mechanical action might come from the formation of deposits of carbon within the catalyst which grow until fragments of the catalyst are split off. The electron microscopy of these carbon deposits, as described below, is enlightening in this connection.

The structure of carbon formed by decomposition of carbon monoxide on an iron catalyst was described by Radushkevich and Luk'yanovich in 1952¹⁹⁴. They reported that carbon particles formed at 600°C had elongated, thread-like shapes. They postulated that thread-like nuclei, apparently consisting of iron carbides, were formed first and that these grew transversely by deposition of carbon. They also noted the presence of twisted multiple threads.

Davis, Slawson, and Rigby⁴² published electron micrographs of filamentous carbon growths formed by the interaction of carbon monoxide and iron oxide in blast furnace brickwork. They observed that these structures were formed at temperatures of 450°C on different forms of iron oxide. X-ray examination showed the presence of amorphous carbon, cementite (Fe_3C), and an iron percarbide (Fe_{20}C_9) (referred to here as Hägg carbide). They postulated that the catalyst for the reaction, either iron or iron carbide, formed on the surface of the oxide as a speck, which in turn gave rise to a thread of carbon. Threads from a collection of specks became twisted together and probably coalesced to form the characteristic vermicle. They suggested that, after carbon deposition began, the catalyst particles were located on the growing ends of the threads.

Hofer, Sterling, and McCartney¹¹¹ essentially corroborated these findings, but in addition found nuclei in the middle (see Figure 14; also the discussion of the carbon deposits on cobalt and nickel.)

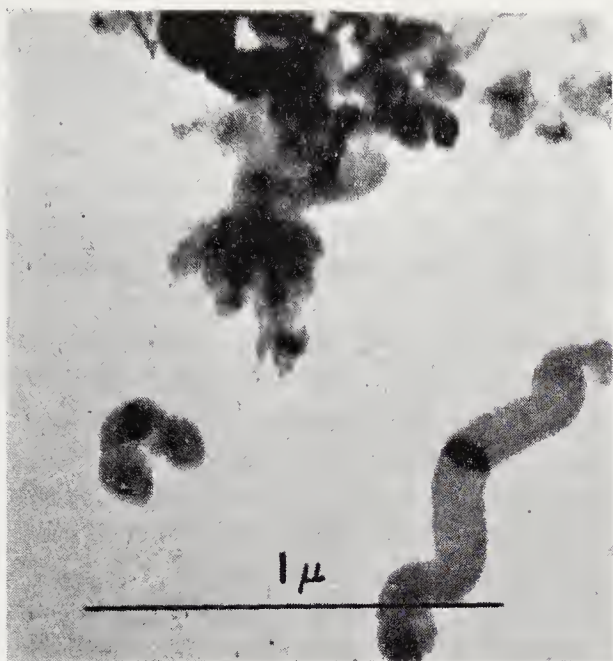


Figure 14a. Carbon deposited on iron reduced from an oxide prepared by precipitation from the nitrate with ammonia. Note filaments extending in two directions from central nuclei.

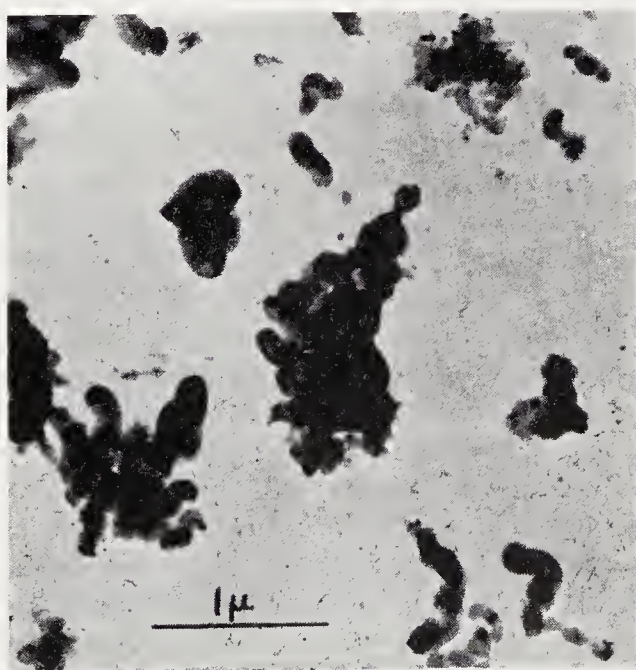


Figure 14b. Another view of specimen shown in Figure 14a.

The Carbides of Iron

Cementite is the best known and most stable carbide of iron. It occurs in steels as a component of pearlite (0.9 per cent carbon), the eutectoid mixture of α -iron and cementite; as a component of ledeburite (4.2 per cent carbon), the eutectic mixture of γ -iron and cementite; and as primary and secondary cementite. Pure cementite is difficult to form by quenching a stoichiometric melt of iron and carbon because of the high rate of graphitization.

Mixtures of cementite and α -iron are also formed by carburizing iron at above the eutectoid temperatures (723°C) and cooling the resultant solid solution of carbon in γ -iron to room temperature. When cooling is rapid, retained austenite or martensite or both may be formed. Martensite may be regarded as a deformed, supersaturated solid solution of carbon in α -iron in which the carbon atoms occupy preferred positions^{85, 119, 153}.

Cementite may also be formed by the action of Hägg carbide on α -iron at 300°C and above. Hägg carbide, in relatively pure form, does not decompose at appreciable rates to form cementite and free carbon below 450°C. Pingault¹⁹² has prepared pure massive cementite.

The crystal structure of cementite has been thoroughly established by numerous authors^{93, 118, 154, 182, 185, 186, 222, 257, 258, 259, 260}.

Like many other transition elements, iron also forms a carbide in which the metal occupies hexagonal close-packed positions and the carbon atoms occupy the interstices. Heidenreich, Sturkey, and Woods^{91, 92} probably found this carbide by electron diffraction methods in a specimen of tempered steel, but they interpreted their diffraction patterns as those of ϵ -iron nitride. The formula is roughly Fe_2C . This phase was first found in used Fischer-Tropsch catalysts by Herbst and Halle^{95, 96} and Scheuermann²¹⁶. This carbide was later shown by Hofer, Cohn, and Peebles¹⁰⁴ to have a Curie point at 380°C and to be identical with one of the carbides previously found by Merkel¹⁵⁹ and Pichler and Merkel¹⁸⁹. At one time, the presence of copper was thought to be essential to the formation of this carbide by carburization of iron with carbon monoxide. It has, however, since been formed in iron preparations containing no copper¹⁵⁶. The function of the copper appears to be a lowering of the reduction temperature of the iron oxide resulting in finer crystallite size of the reduced iron, which in turn permits carburization at lower temperatures¹¹⁵. (Carburization at these low temperatures of larger crystallite sizes of iron takes too much time to be practical.) Carburization at higher temperatures results in products appreciably contaminated with Hägg carbide or even cementite^{114, 156}. To obtain a product 99 per cent pure, the iron specimen must be carburized at 170°C or below (see Figure 15). It is conceivable that stabilizers or catalytic agents of various sorts may change the stability of the hexagonal close-packed carbide so that it may vary considerably.

The hexagonal close-packed iron carbide decomposes into Hägg carbide at about 250°C and Hägg carbide, in turn, reacts with α -iron to form cementite in the range 300 to 400°C^{37, 103, 193}. This suggests that the h.c.p. carbide may be a precursor of Hägg carbide in the carburizing process and that both h.c.p. and Hägg carbide are precursors of cementite, where cementite is the final product. In order to check this possibility, specimens of reduced iron synthetic ammonia catalysts were carburized for very short periods of time at temperatures up to 325°C, and in every case significant amounts of h.c.p. carbide were found¹⁵⁶. Carburization carried out on similar catalysts for longer periods of time in this same temperature range gave no

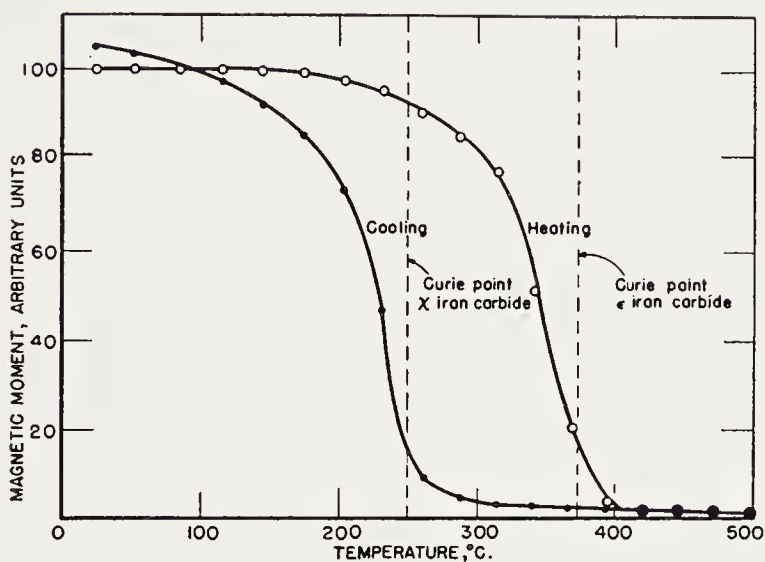


Figure 15. Thermomagnetic curve of iron catalyst carburized at 170°C.

evidence of this carbide. Therefore, h.c.p. carbide is an intermediate in the carburization process. The data are summarized in Table 10.

The diffraction pattern of Hägg carbide was first reported by Gunnar Hägg—hence the name⁸⁶. The powder pattern is quite complex. Jack¹²⁵ has attempted to index the pattern, but since the indexing involves an orthorhombic unit cell and relatively large lattice parameters, there is a serious question concerning this indexing. The powder diffraction pattern, however, remains as a trustworthy method of identifying this carbide.

This diffraction pattern has been found for used Fischer-Tropsch catalysts, in specimens of metallic iron carburized with carbon monoxide, and hydrocarbons between about 200 and 300°C. Above this temperature range, cementite becomes an important constituent and below this temperature range h.c.p. carbide becomes important. The studies of Hägg⁸⁶, Jack^{125, 127}, Kummer, DeWitt, and Emmett¹⁴³, and Hofer, Cohn and Peebles¹⁰⁴ have well established the conditions under which this carbide forms. The

experiments of Bahr and Jessen¹⁷ and Fischer and Bahr⁶³ must have led to the formation of this carbide, even though they did not identify it.

The Curie point of Hägg carbide is 247°C as compared with 210°C for cementite and 380°C for h.c.p. carbide. The difference between the Curie points of cementite and Hägg carbide is sufficient that they may be readily separated. The so-called stabilized cubic iron oxide of LeFebvre and LeClerc^{145, 148, 149}, with its Curie point at 250°C, appears to be Hägg car-

TABLE 10. HIGHER IRON CARBIDES IN CARBIDED IRON CATALYSTS

Carbiding		Subsequent Tempering		Magnetic Analysis (%) ^a	
Temp. (°C)	Duration (min.)	Temp. (°C)	Duration (min.)	ε-carbide	χ-carbide
Catalyst A-1008					
250	15	None		25	0
		250	300	16	11
275	6	None		21	7
		275	30	12	14
300	3	None		9	9
325	1¾	None		8	13
350	½	None		<i>b</i>	<i>b</i>
Catalyst D-3001					
190	60	None		25	0
250	3	None		34	0
275	1	None		26	6

^a Carbide + iron = 100 per cent.

^b Hägg carbide and cementite present.

bide. Unfortunately these authors did not examine their product by x-ray diffraction.

Brill and Mark³¹ found evidence of a new diffraction pattern in the thermal decomposition products of iron cyanides. Previously, this thermal decomposition had been investigated by Mittasch, Kuss, and Emert¹⁷². Brill and Mark interpreted the strange pattern as that of an unknown carbide.

The carbides of Brill and Mark³¹, Hofmann¹¹² and Groll¹¹³, and Tutiya^{241, 242, 243, 244} all produce diffraction patterns which bear a superficial resemblance to the h.c.p. carbide. They are all formed by direct carburization of the iron oxide in the temperature range 200 to 400°C. In this group, the carbides produced by Pichler and Merkel¹⁸⁹, with a Curie point of 265°, and the carbide of Bahr and Jessen¹⁷, produced by direct carburization of

oxide, may also be mentioned. Preliminary data at the Bureau of Mines suggest that these carbides are related to but differ from the Hägg carbide in some as yet undetermined way.

The results obtained by Antheaume⁹ suggests the presence of Hägg carbide in his used catalysts.

The carbide of Durand⁴⁹, produced by the action of acetylene on ferrous chloride solutions, might be related to the well-known copper acetylide. Its preparation though attempted at the Bureau of Mines has never been duplicated.

Eckstrom and Adcock⁵⁰ have reported a carbide phase formed in Fischer-Tropsch catalysts operated in fluidized bed converters. A period of several months appears to be necessary to develop this phase. Efforts to make this crystalline phase by direct carburization with carbon monoxide have so far failed.

Steel shot, iron turnings, steel wool, recently proposed as Fischer-Tropsch catalysts, have introduced the possibility of finding martensite and austenite in catalysts. Since such catalysts must first be oxidized, reduced, and carburized or inducted before they have sufficient activity and because martensite and austenite are generally labile during this treatment, the phases present in the activated portion of such catalysts are probably the same as found in those prepared from precipitated or fused oxide, namely, h.c.p. carbide, Hägg carbide, cementite, magnetite, and α -iron. Austenite and martensite, if present at all, will be confined to the nonporous portions of the catalyst.

Austenite¹⁸⁷ is a solid solution of carbon in the face-centered cubic form of iron, which can contain as much as 1.7 per cent carbon at 1,150°C. With proper cooling, austenite can be retained at room temperature, especially when stabilized by traces of chromium or nickel.

In a certain temperature range, austenite undergoes a diffusionless transition in which the face-centered iron lattice is distorted into a body-centered cubic martensite lattice similar to that of α -iron, but differing from it by the fact that one of the axes of the unit cell is longer than the others. It is thus tetragonal. The axial ratio is a function of carbon content^{177, 180, 195}. Martensite may therefore be regarded as a deformed supersaturated solid solution of carbon in α -iron.

McCartney *et al.* have found that the electron diffraction patterns of the interstitial compounds of iron frequently are atypical in that they do not possess all the reflections found in the x-ray diffraction pattern¹⁵⁸.

Podgurski *et al.*¹⁹³ and Anderson and co-workers⁶ have reported on the stability and adsorptive properties of various carbides of iron in catalytic preparations. Such studies are essential to intelligent use of carbide catalysts and also to the interpretation of results.

The Thermal Reactions of Iron Carbides

The carbides of iron found in Fischer-Tropsch catalysts are all metastable with respect to the elements. The most unstable carbide is ϵ -Fe₂C. Its thermal decomposition into Hägg iron carbide has been studied thermomagnetically^{39, 102, 104}. The reaction can be studied in the temperature range 200 to 350°C (see Figure 16-a and 16-b). The apparent order of the reaction is 5/3 in the amount of remaining ϵ -iron carbide. The energy of activa-

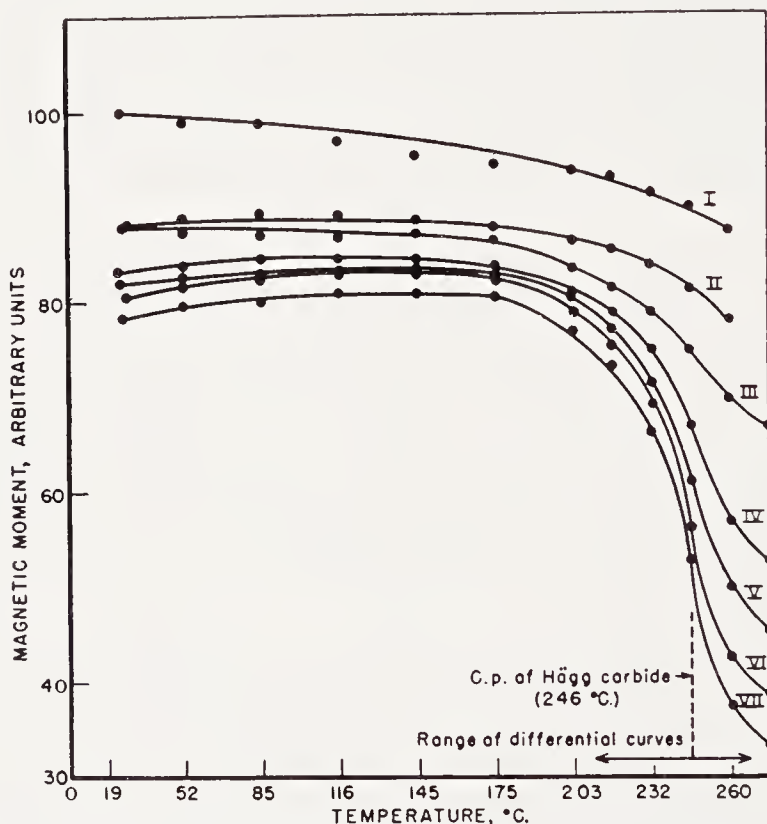


Figure 16a. Thermomagnetic curves showing the rearrangement from hexagonal to Hägg iron carbide upon heating.

tion obtained by using this law is 50 kcal/mole, and the pre-exponential factor is 1×10^{15} (sec.)⁻¹ (per cent ϵ -Fe₂C)^{-2/3}. No detectable change in the composition of either ϵ -Fe₂C or χ -Fe₂C as indicated by a shift in Curie point occurs as the reaction proceeds.

Hägg carbide (χ -carbide) reacts with α -iron to form cementite if the mixture is formed by partly carburizing a reduced iron catalyst^{37, 103, 193}. The reaction becomes measurable at 300°C, and is completed in about an hour at 450°C. It lends itself to the preparation of finely-divided cementite of high surface area and devoid of free carbon. The kinetics are difficult to analyze, and the order of the reaction could not be established. The energy of activation appears to be about 80 kcal./mole.

Hägg carbide in the absence of α -iron does not undergo any reactions up to about 440°C, at which temperature it decomposes to form cementite and free carbon⁸⁸. The reaction is discontinuous, that is, no detectable changes in composition of either the Hägg carbide or of the cementite, as revealed by changes in the Curie point, take place during the reaction (see Figures 17-a and 17-b). This reaction does not lend itself to a ready determination of the kinetics. Some preliminary results indicate an activation energy of

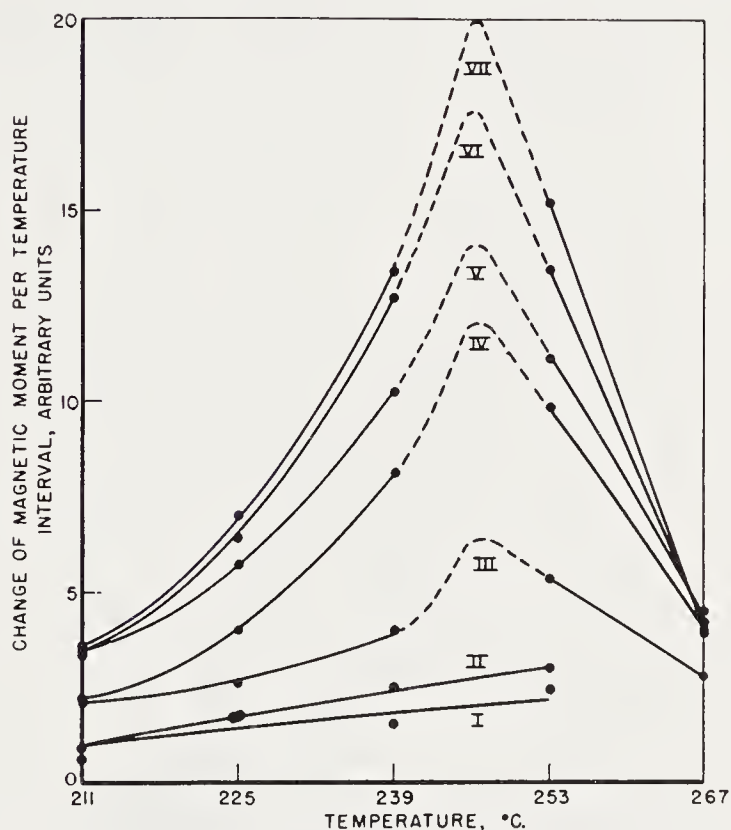
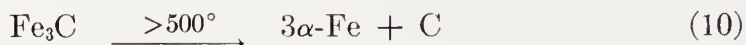
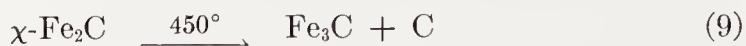


Figure 16b. Differential thermomagnetic curves showing the discontinuous transition from hexagonal to Hägg iron carbide.

325 kcal/mole, and an order which varies from 0.8 at 473° to 6.4 at 506°C.

The decomposition of cementite to form free carbon and α -iron has been reported over a wide range of temperatures. Podgurski, Kummer, DeWitt, and Emmett¹⁹³ found that Hägg carbide formed by carburization with butane at 275 to 325°C yielded an unusually unstable cementite when heated to 400 or 450°C. Cementite so formed decomposed readily in a few hours at 500°C. On the other hand, cementite from Hägg carbide produced from carbon monoxide will not decompose until higher temperatures are employed. Drain¹⁶ showed that normal cementite decomposes in vacuum at 645°C. Pingault¹⁹² describing a pure cementite of very large particle size found that it decomposed only after long periods of time at 760°C.

If a specimen of $\epsilon\text{-Fe}_2\text{C}$ containing no α -iron is slowly heated, one may expect the following reactions to proceed in the order indicated.



If, on the other hand, the specimen of $\epsilon\text{-Fe}_2\text{C}$ contains α -iron, the reac-

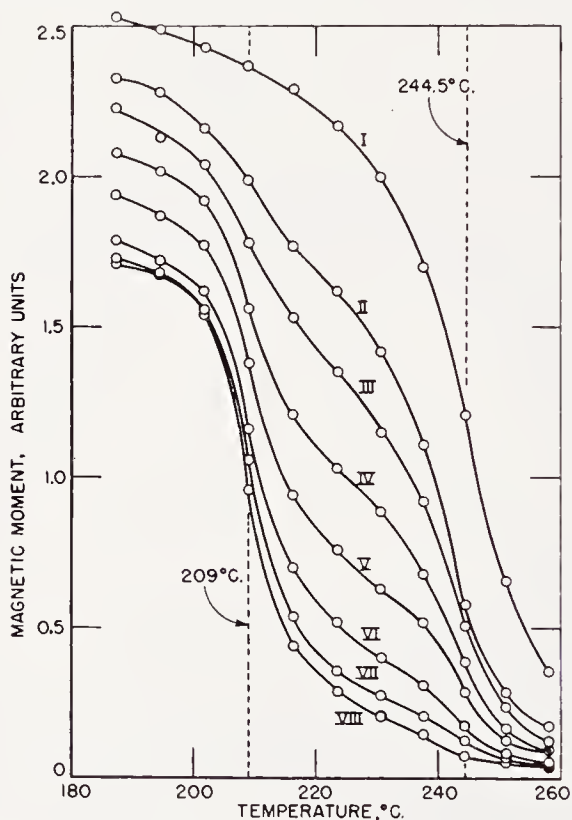
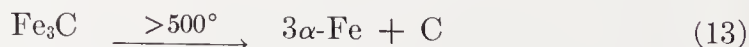


Figure 17a. Thermomagnetic curve showing discontinuous transition from x iron carbide to cementite. The Roman numerals refer to tempering for 0, 10, 20, 40, 70, 130, 250 and 490 minutes at 525°C , respectively.

tions will proceed



It should be noted that reactions (10) and (13) are identical.

The series of reactions indicated here is very similar to the reactions involved in the tempering of carbon steel^{10, 11, 12, 13, 101} with one difference. Up to the present, there have been indications^{40, 177a, 177b, 197}, but no definite evidence, that Hägg carbide is involved in the tempering of steel. Diffraction patterns of tempered steel have often contained reflections which have been attributed to unknown carbides¹¹⁶. The fact that most of these transi-

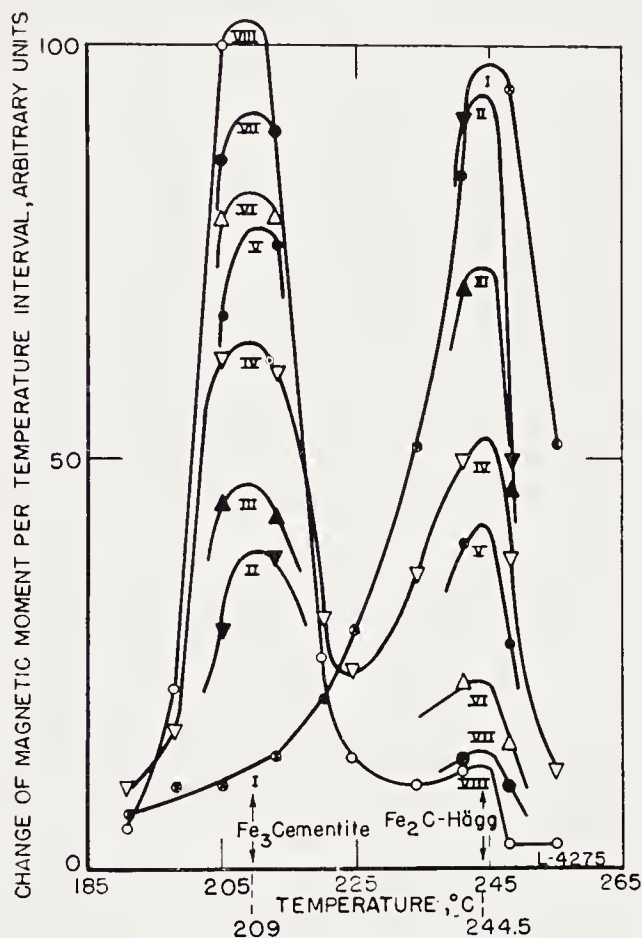


Figure 17b. Differential curve derived from Figure 18.

tions are discontinuous indicated that they proceed by a mechanism of nucleation and growth. The reactions indicated above may require modification as more precise stoichiometric information is obtained.

Impurities affect the stability and probably the kinetics of the reactions. In all likelihood, other factors, such as the state of subdivision and previous history, affect the kinetics, but no evidence on this point has yet been collected.

The effect of sulfur is of special interest because of the well-known poisoning action of sulfur on iron, cobalt, and nickel catalysts used in

Fischer-Tropsch and related reactions. Sulfur can be introduced into cementite by directly sulfiding the pure cementite with sulfur in a vacuum at 450°C or by the simultaneous carburization and sulfiding of iron oxide at 550°C with synthesis gas ($2\text{H}_2 + 1\text{CO}$) and H_2S . Sulfided cementite prepared by these methods has a Curie point about 10°C higher than normal. The outstanding effect, however, is the increase in stability produced by very small quantities (0.1 to 1 per cent) of sulfur. Sulfur-bearing cementite in some cases did not decompose in vacuum up to 900°C. Decomposition at 900 to 1050°C led to austenite stabilized by sulfur. Such austenite was readily retained on cooling^{47a}.

By carburization of sulfided cementite at 550°C, a phase was obtained whose x-ray diffraction pattern corresponded to that of the Hägg carbide. Its Curie point was 260°C, about 10°C higher than the Curie point of pure Hägg carbide. While ordinary Hägg carbide begins to decompose at 450°C and decomposes rapidly at 550°C, the sulfided Hägg carbide did not decompose up to 700°C, and complete transformation was attained only by heating to 900°C. The very fact that it was produced by carburization at 550°C is an indication of its stability. An interesting technique of desulfurizing the sulfocarbides by heating with powdered magnesium was mentioned. This treatment restored the properties of the carbides to their original state^{47a}.

It has been said that copper promoters stabilize the h.c.p. carbide of iron. Copper facilitates its formation by increasing the ease of reduction of the oxide¹⁴⁹, but no definite proof exists to indicate that copper stabilizes the h.c.p. carbide.

Bernier²⁰, in addition to studying the nickel and iron carbides themselves, has endeavored to produce mixed iron-nickel carbides. In this he may have been partly successful.

Hydrogenation of Iron Carbides

Bahr and Jessen¹⁷ have shown that the iron carbide reacts readily with hydrogen at 300°C to form methane and metallic iron. Kummer, DeWitt, and Emmett¹⁴³ have published data on the stepwise hydrogenation of iron catalyst previously carbided to 66.1 per cent conversion to Fe_2C . The reaction of hydrogen with a fully carbided specimen of iron accelerates with time in the initial stages of the reaction. Unpublished data at the Bureau of Mines show similar characteristics, although the self-accelerating feature is not as marked. Eidus^{52, 53, 54, 56, 57, 59} and his co-workers have accumulated a large amount of data on the hydrogenation of iron carbide and have used the data to support the theory that iron carbide is an intermediate in the reaction. However, they did not discriminate adequately between surface carbide and bulk carbide. Thus they mistook the kinetics of converting

the massive catalyst to crystalline carbides for the rate of activated adsorption; Craxford and Rideal have probably made a similar mistake⁴¹. Their work would have had much greater utility had they accompanied their studies with x-ray powder diffraction analysis or thermomagnetic analysis.

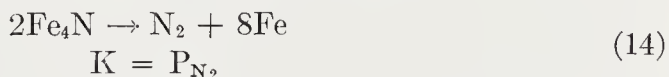
Reactions of Iron Carbides with Acids

Carbides of iron react readily with acids to form hydrocarbons, free carbon, and ferrous iron in solution. The reaction has been used for analyzing carbides in iron catalysts. Also, iron catalysts in operation are exposed to acidic conditions which may result in catalyst deterioration. Unlike the carbides of strongly electropositive elements, the carbides of iron, cobalt, and nickel are nearly nonionic. The hydrolysis of these carbides probably proceeds by forming a highly reactive form of a surface carbide, which then may or may not be attacked by chemisorbed hydrogen, depending on such factors as acidity of the solution, inhibition by reaction products, and effectiveness of the metal for hydrogenation. Thus cementite, a carbide of iron, a weak hydrogenation catalyst, produces free carbon when hydrolyzed in the presence of the reaction product, ferrous iron. A high hydrogen ion concentration, on the other hand, favors nearly quantitative formation of methane and higher hydrocarbons²¹⁵. In contrast to iron the carbide of nickel, a strong hydrogenation catalyst, yields almost exclusively methane on hydrolysis¹⁵. Numerous studies of these reactions have been made, especially by Schenck and Stenkhoff²¹⁵ and Stamme²²⁵.

The Nitriding of Iron and the Iron Nitrides

Nitriding with ammonia is carried out on metallic iron. Attempts to nitride the oxides directly have yielded only magnetite. The nitrides so far have been prepared using anhydrous ammonia without further purification. High space velocities must be employed so that hydrogen does not build up within the bed. Similarly, to retard the catalytic decomposition of ammonia, relatively low temperatures are preferred. Thus, for nitriding the reduced, fused catalyst (Bureau of Mines No. 3001, $\text{Fe}_3\text{O}_4\text{-MgO-K}_2\text{O}$), hourly space velocities between 750 and 5000 and temperatures between 250 and 450°C were employed.

At atmospheric pressure, the nitrides of iron are metastable. Hendricks, Brunauer and Emmett^{93a} have investigated the dissociation pressure of Fe_4N indirectly by a study of the ammonia-hydrogen-nitrogen equilibrium over this phase. The equilibrium constant for the reaction



varies from 4,250 atmospheres at 420°C to 5,600 atmospheres at 525°C.

Nitrogen austenite, γ -phase (see below) was prepared by treating pure iron powder, 300 mesh, with ammonia at 700 to 750°C and rapidly quenching to room temperature in a nitriding atmosphere. However, decomposition to the nitrogen martensite α' -phase could only be completely inhibited by using a 15 per cent manganese iron alloy¹²⁹.

Since the iron nitrides are metastable at atmospheric pressure^{34, 93a, 184} phase diagrams which have been published are in reality existence diagrams which show the crystalline phases which can be prepared at various compositions and temperatures. Discrepancies in the various diagrams^{60, 150, 159a} which have been proposed cannot, at present, be resolved. However, since the differences are minor, we have selected the diagram of Jack¹²¹ because

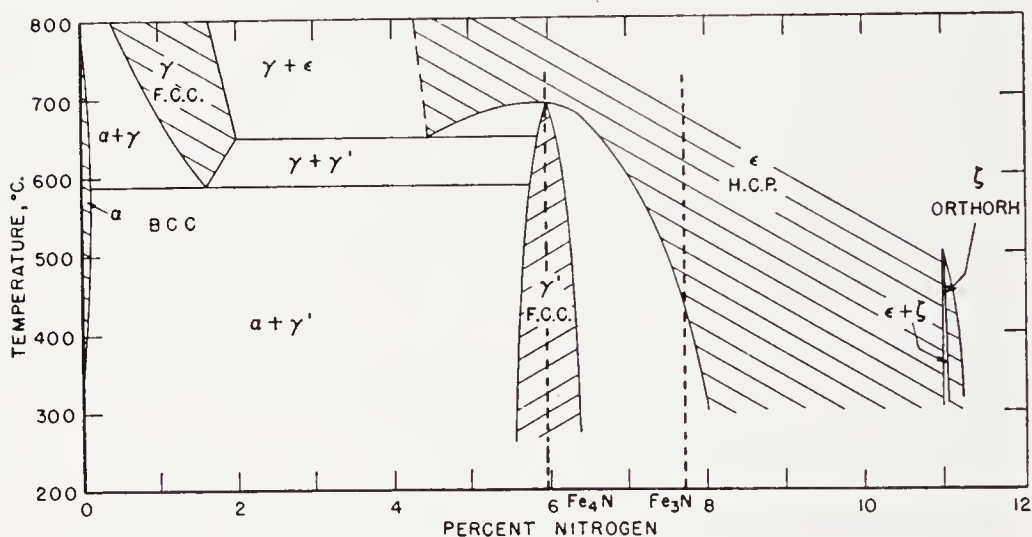


Figure 18. Iron nitrogen phase diagram according to Jack. (See Ref. 25)

his methods of preparation and analysis most closely approximate those used in catalytic preparations (Figure 18).

Five phases are indicated in Jack's¹²¹ diagram and studies, the α -, the γ -, the γ' -, the ϵ -, and ζ -phases. Lehrer¹⁵⁰, Eisenhut and Kaupp⁶⁰, and Hägg^{79, 80, 82} also find these phases. The α -phase is simply the solid solution of nitrogen in α -iron. As in the case of carbon, the solubility of nitrogen is very low. The γ -phase represents the solubility range of nitrogen in the face-centered cubic γ -iron. The existence of this phase makes possible the formation of a nitrogen martensite analog α' -phase, which cannot be represented in the iron-nitrogen diagram, just as martensite cannot be represented in the iron carbon diagram^{126, 128, 129}. By tempering the α' -phase, the nitrogen in the phase becomes completely ordered so that the nitrogen atoms achieve maximum separation and the tetragonality of the unit cell becomes increased. This phase has been designated the α'' -phase. It also

has no place in the standard phase diagram. Tempering the α'' -phase at 160°C leads eventually to α -iron and γ' -iron nitride.

The γ' -iron nitride has a face-centered cubic close-packing of iron atoms, with the nitrogen atoms equidistant from each other and occupying one-fourth of the octahedral interstices in a completely ordered way^{29, 30, 93a, 123}. It differs from the γ -phase or nitrogen austenite only in that the latter has a random arrangement of nitrogen atoms, while the former has an ordered arrangement (Jack has found eight superlattice reflections). Since the γ' -phase can be formed from the γ -phase by tempering at 160°C, it is obviously less stable than the γ -phase under these conditions. The γ' -phase can also be formed by the direct nitriding of iron. The homogeneity range at 450°C lies between 5.7 and 6.1 per cent N.

In the ϵ -iron nitride, the iron atoms have a hexagonal close-packed arrangement, and the nitrogen atoms are believed to be in the octahedral interstices^{122, 123, 179}. This structure is therefore isomorphous with the h.c.p. iron carbide. The homogeneity range is wide, extending from 7.3 to 11.1 per cent N. It thus includes the composition Fe_3N , but not quite the composition Fe_2N . This phase is by far the most important under Fischer-Tropsch conditions, since the catalysts tend to approach and remain in this structure and the closely-related ϵ -carbonitride structure.

The ζ -phase is an orthorhombic structure closely related to the ϵ -phase, crystallographically. By nitriding below 450°C and using very high space velocities, this nitride which has a narrow range of composition is formed.

The Carbonitrides of Iron

Carbon monoxide (and possibly other carburizing agents) reacts with the nitrides of iron in three ways. First, carbidic carbon may replace nitrogen with carbon; the crystal structure of the original nitride is maintained, with only a possible modification of the lattice parameters. This substitution reaction occurs in the case of the γ' -, ϵ -, and ζ -nitrides. Secondly, carbidic carbon may be added to (instead of replacing) the interstitial nitrogen in the nitride crystals without modification of the crystal structure, other than a change in lattice parameter. This can occur only if the nitride phase has a wide range of composition, which is usually not the case. Thus the only phase for which this completion reaction is important is the ϵ -nitride, with a composition (see above) ranging from Fe_3N to Fe_2N . Both of these reactions result in iron carbonitrides that are crystals composed of three elements: iron, carbon, and nitrogen. Finally, the substitution reaction may proceed so far and the carbon-nitrogen ratio may become so large that the carbonitride phase becomes unstable and a phase change reaction takes place. Jack has studied these reactions on pure iron¹²⁴, while Hall, Dieter, Hofer, and Anderson⁸⁹ have studied them in reduced synthetic ammonia catalysts.

The completion reaction is relatively rapid and is completed in 5 to 10 hours at 300°C. On the other hand, the substitution reaction is considerably slower, becoming appreciable in 5 to 10 hours at 400°C. Jack¹²⁴ and Goodeve and Jack⁷⁷ proposed the hypothesis that the rate of the substitution reaction in the completely nitrified ϵ -nitride was dependent on the rate of removal of nitrogen, and to support this hypothesis, they were able to demonstrate that the rate of elimination of nitrogen was the same in carbon monoxide, nitrogen, and in vacuo. They also showed that the substitution reaction was proportional to the square of the nitrogen concentration, which suggests that the formation of nitrogen molecules is the rate-determining step. Thus the substitution reaction may essentially be regarded as a slow nitrogen elimination step, producing vacant positions, followed by the fast completion step as a result of which those positions are occupied. According to this mechanism, elimination of nitrogen becomes slower as the nitrogen concentration drops. This is in accordance with the facts observed by Emmett and Love^{51a}. The presence of hydrogen with carbon monoxide accelerates the elimination of nitrogen, probably by a new mechanism, namely, formation of ammonia, which deposits from the gaseous products as ammonium carbonate. When the synthesis gas mixture contains less than 50 per cent hydrogen, the completion reaction can keep pace with the nitrogen elimination. However, at higher hydrogen concentrations, the ratio of combined nitrogen and carbon to iron drops below the value 0.5 in the steady state. Although elimination of nitrogen in the presence of synthesis gas is more rapid than in the presence of pure carbon monoxide, it is slower than the elimination of nitrogen by pure hydrogen. This inhibiting effect of carbon monoxide may be attributed to its strong chemisorption and is the reason why nitrides can be used in the Fischer-Tropsch reaction.

As ϵ -iron nitride and ϵ -iron carbide are isomorphous, they might be expected to form a continuous series of solid solutions or ϵ -iron carbonitrides. This may indeed be the case, but efforts to prepare the series through the carburization of ϵ -iron nitride have failed, because the temperature at which substitution takes place, about 350°C is well above the temperature at which pure ϵ -iron carbide decomposes, about 200°C. Thus, as the substitution reaction proceeds at any given temperature above the upper limit of metastability of ϵ -iron carbide, a composition of the ϵ -iron carbonitride eventually is reached which is unstable. At 350°C this occurs when the nitrogen iron ratio becomes less than 0.14. The product which is then formed depends approximately on the kinetics of the decomposition of pure ϵ -iron carbide³⁹ into Hägg carbide (Fe_2C) and cementite. All that is required is a knowledge of the carbidic carbon-iron ratio and the temperature. If the carbidic carbon-iron ratio is about 0.5, which will be true if the phase decomposition takes place under carburizing conditions, Hägg carbide will

be found from 200 to about 500°C (see Table 11). Above this temperature, Hägg carbide decomposes thermally to produce free carbon and cementite. If, conversely, the decomposition of the ϵ -carbonitride takes place under decarburizing conditions, then free iron will be formed. Since free iron

TABLE 11. CARBURIZATION OF ϵ -IRON NITRIDE WITH CARBON MONOXIDE^a

Temp. (°C)	Time (hr)	$\frac{C}{Fe}$	$\frac{N}{Fe}$	$\frac{C+N}{Fe}$	Phases ^b
Space velocity = 80 hr ⁻¹					
Original nitride	0	0.00	0.46	0.46	ϵ
250	1	.02	.47	.49	ϵ
	5	.02	.46	.48	ϵ
	10	.03	.45	.48	ϵ
350	1	.04	.45	.49	ϵ
	5	.06	.44	.50	ϵ
	10	.08	.43	.51	ϵ
400	1	.03	.46	.49	ϵ
	5	.14	.36	.50	ϵ
	10	.30	.18	.48	ζ
450	1	.18	.20	.38	ϵ , M
	5	.41	.02	.43	χ , M, α ?
	10	.46	.01	.47	χ , α ?, M?
Space velocity 2500 hr ⁻¹					
450	1	.32	.27	.59	ϵ
	5	.42	.16	.58	ϵ
	10	.53	.08	.61	ϵ , χ

^a See Ref. 89.

^b ϵ = ϵ -iron nitride or carbonitride, ζ = ζ -iron nitride or carbonitride, M = magnetite, χ = Hägg iron carbide, α = α -iron.

reacts with Hägg carbide to form cementite at about 300°C, cementite will be found in carbonitride specimens decomposed under decarburizing conditions above 300°C, and Hägg carbide in carbonitride specimens decomposed under decarburizing conditions below this temperature. Table 12 shows diffraction analyses and chemical compositions of ϵ -carbonitrides treated with pure hydrogen for varying periods of time.

Carburization of a mixture of γ' -iron nitride plus α -iron indicated in Table 13 shows that γ' -iron nitride can undergo the substitution reaction.

TABLE 12. HYDROGENATION OF ϵ -CARBONITRIDES^a

Temp. (°C)	Time (hr)	$\frac{C}{Fe}$	$\frac{N}{Fe}$	$\frac{N + C}{Fe}$	Phases ^b
Carbonitride formed by nitriding followed by carburizing	0	0.36	0.14	0.50	ϵ, χ
	1	.35	.15	.50	ϵ, χ
	10	.36	.13	.49	ϵ, χ
	1	.35	.14	.49	
	5	.34	.07	.41	α, χ, C
	10	.35	.02	.37	α, C, χ
	1	.36	.07	.43	χ, ϵ
	5.3	.35	.02	.37	$\alpha, \chi, C?$
	10	.28	.004	.28	$\alpha, \chi, C?$
	1	.36	.01	.37	$\chi, \alpha, C?$

^a See Ref. 89.^b ϵ = ϵ -iron nitride or carbonitride, χ = Hägg iron carbide, C = cementite, α = α -iron.TABLE 13. CARBURIZATION OF α -IRON AND γ' -NITRIDE^aSpace velocity = 80 hr⁻¹

Temp. (°C)	Time (hr)	$\frac{C}{Fe}$	$\frac{N}{Fe}$	$\frac{N + C}{Fe}$	Phases ^b
Original nitride	0	0.00	0.08	0.08	α, γ'
250	1	.07	.06	.13	α, γ'
	4	.19	.06	.25	α, γ'
	5	.25	.04	.29	α, γ'
300	1	.11	.07	.18	α, γ'
	5	.27	.05	.32	α, γ'
	10	.29	.08	.37	γ', α
350	1	.24	.07	.31	α, γ', M
	5	.33	.07	.40	$\epsilon, \chi, M, \alpha$
	10	.36	.08	.44	χ, α

^a See Ref. 89.^b α = α -iron, γ' = γ' -iron nitride-nitrogen austenite, M = magnetite, χ = Hägg carbide.

Furthermore, since the amount of γ' -phase can be increased by carburization after 10 hours at 300°C, γ' is the primary phase.

Another way of preparing carbonitrides is by nitriding the carbides. This has been studied in the case of cementite and Hägg iron carbide, but not with ϵ -iron carbide. In every case, the final product was ϵ -iron carbonitride. Results of such nitriding are illustrated in Table 14.

Bridelle and Michel²⁸ made additional studies on the carbonitrides of

TABLE 14. AMMONIA TREATMENT OF CEMENTITE AND HÄGG CARBIDE^a
Space velocity = 1000 hr⁻¹

Temp. (°C)	Time (hr)	$\frac{C}{Fe}$	$\frac{N}{Fe}$	$\frac{N + C}{Fe}$	Phases ^b
Cementite	0.00	0.35	0.00	0.35	C
	300				
	1	.30	.07	.37	C, ϵ
	6.25	.31	.09	.40	C, ϵ
	9	.30	.10	.40	C, ϵ
350	15	.27	.20	.47	ϵ
Mixture of α -iron and Hägg carbide	0.00	.48	0.00	.48	χ , α
	350				
	8	.46	.06	.52	χ , ϵ
	24.2	.44	.12	.56	χ , ϵ
	48.2	.37	.21	.58	χ , ϵ
	72.2	.33	.25	.58	χ , ϵ
	120.2	.26	.34	.60	χ , ϵ
	158.2	.18	.42	.60	ϵ

^a See Ref. 89.

^b C = cementite, ϵ = ϵ -iron nitride or carbonitride, χ = Hägg iron carbide, α = α -iron.

iron. In particular they followed the thermal evolution of nitrogen from a high nitrogen ϵ -iron carbonitride with a Curie point of -90°C and lattice parameters $a_0 = 2.762$ and $c_0 = 4.414$. Loss of nitrogen with heat treatment eventually produced a high carbon carbonitride with a Curie point of 388°C and lattice parameters $a_0 = 2.693$ and $c_0 = 4.370$. These physical changes with composition suggest the possibility of chemical analysis by Curie point determination or lattice parameter measurement.

The Borides of Iron

Beyond the basic phase rule studies of Wever and Muller²⁶¹, and Bjurström²¹ determined that Fe_2B and FeB are isomorphous with corresponding

cobalt and nickel compounds. Du Jassoneix⁴⁸ and Weiss and Forrer²⁵³ found Fe_2B to be ferromagnetic, but the ferromagnetism of FeB is uncertain. No methods have been described for producing the borides with sufficient surface area to be useful as catalysts.

Borocarbides of Iron

Recently a borocarbide of iron has been reported by Carrol, Darkin, Filer, and Zwell^{34a}. This compound seems to be isomorphous with the complex cubic chromium carbide, Cr_{23}C_6 , reported by Westgren^{256a} and to have nearly the same lattice parameter 10.62 Å. The composition of the borocarbide ranges from 1½ to 2½ per cent boron and from 2½ to 4½ per cent carbon. The compound was prepared by heating -100 mesh powders of an iron carbon alloy (4.4 per cent carbon) and an iron boron alloy (5.7 or 8.9 per cent boron) or elemental boron in vacuo at 850° for several days. This method of preparation will probably yield a material with insufficient surface area to be useful as a catalyst.

Catalytic Activity of the Iron System

The iron system is endowed with a much greater number of catalytically active phases than either the nickel or the cobalt system. This is understandable in terms of the electronic structure of iron metal, which lacks three electrons of a completed "3d" shell. It can therefore form compounds involving donation of electrons into its "3d" shell without completely filling that shell, and as a result many iron compounds are catalytically active. On the other hand, iron because it lies to the left of most of the other Fischer-Tropsch catalysts in the periodic table, is particularly sensitive to oxidation. Fortunately, the oxide generally formed, magnetite, is catalytically active and reducible with either hydrogen or carbon monoxide, and therefore oxidation is not too serious a matter.

Iron phases, the surfaces of which are catalytically active, are the metal $\alpha\text{-Fe}^6$, the carbides, $\epsilon\text{-Fe}_2\text{C}^{189}$, $\chi\text{-Fe}_2\text{C}^{189}$, $\text{Fe}_3\text{C}^{223}$, FeC^{50} , the nitrides $\epsilon\text{-Fe}_2\text{N}^2$, $\gamma\text{-Fe}_4\text{N}$, the carbonitrides, $\epsilon\text{-Fe}_2\text{X}^2$, $\gamma\text{-Fe}_4\text{X}^2$, and the oxide, Fe_3O_4^6 . The well-known operational flexibility of iron Fischer-Tropsch catalysts must be attributed to these relationships. The possibilities of this system are far from explored. Other phases, such as $\gamma\text{-Fe}$ and FeO (wustite), are so unstable thermally at Fischer-Tropsch temperatures that it is doubtful whether adequate activity data on these phases will ever be obtained using the present methods. The borides of iron have so far not been investigated.

Ternary and quaternary compounds such as the sulfocarbides, the borocarbides, compounds with mixed metallic elements, present many opportunities for tailoring catalysts.

Almost as important as the specific activity of the catalyst surface is the

manner in which the formation of crystalline phases affects the accessibility of the catalyst. This is a function of the specific volume or density of the pertinent phases and the manner in which they develop from their matrix. These relations are particularly important in synthetic ammonia catalysts. Thus in these catalysts, oxidation chokes the pores of the catalyst while carbiding does not^{90, 90a}.

Bibliography

1. Albrecht, W. H., *Ber.*, **62**, 1475 (1929).
2. Anderson, R. B., "Advances in Catalysis," Vol. V., New York, Academic Press, Inc., 1953.
3. Anderson, R. B., Feldman, J., and Storch, H. H., *Ind. Eng. Chem.*, **44**, 2418 (1952).
4. Anderson, R. B., Hall, W. K., and Hofer, L. J. E., *J. Am. Chem. Soc.*, **70**, 2465 (1948).
5. Anderson, R. B., Hall, W. K., Krieg, A., and Seligman, B., *J. Am. Chem. Soc.*, **71**, 183 (1949).
6. Anderson, R. B., Hofer, L. J. E., Cohn, E. M., and Seligman, B., *J. Am. Chem. Soc.*, **73**, 944 (1951).
7. Anderson, R. B., McCartney, J. T., Hall, W. K., and Hofer, L. J. E., *Ind. Eng. Chem.*, **39**, 1618 (1947).
8. Anderson, R. B., Shultz, J. F., Seligman, B., Hall, W. K., and Storch, H. H., *J. Am. Chem. Soc.*, **72**, 3502 (1950).
9. Antheaume, J., Thesis, Univ. of Lille, 1934.
10. Antia, D. P., Fletcher, S. G., and Cohen, M., *Trans. Am. Soc. Metals*, **32**, 290 (1944).
11. Arnold, J. O., and Read, A. A., *J. Chem. Soc.*, **65**, 788 (1894).
12. Averbach, B. L., and Cohen, M., *Trans. Am. Soc. Metals*, **41**, 1024 (1949).
13. Averbach, B. L., Cohen, M., and Fletcher, S. G., *Trans. Am. Soc. Metals*, **40**, 728 (1948).
14. Bahr, H. A., and Bahr, Th., *Ber.*, **61**, 1277 (1928).
15. Bahr, H. A., and Bahr, Th., *ibid.*, **63**, 99 (1930).
16. Bahr, H. A., and Jessen, V., *Ber.*, **63**, 2226 (1930).
17. Bahr, H. A., and Jessen, V., *ibid.*, **66**, 1238 (1933).
18. Beilby, G. T., and Henderson, G. G., *J. Chem. Soc.*, **79**, 1251 (1901).
19. Benedicks, G., Doctoral dissertation, Univ. of Upsala, Sweden, 1904.
- 19a. Benton, A. F., and Emmett, P. H., *J. Am. Chem. Soc.*, **46**, 2728 (1924).
20. Bernier, R., *Ann. Chim. (Paris)*, [12], **6**, 194 (1951).
21. Bjurström, T., *Arkiv. Kemi. Mineral Geol.*, **11A**, No. 5 (1933).
22. Böhm, J., *Z. anorg. allgem. Chem.*, **149**, 203 (1925).
23. Boudouard, O., *Compt. rend.* **128**, 98, 307 (1899).
24. Bozorth, R. M., "Ferromagnetism," New York, D. van Nostrand Co., Inc., 1951.
25. Braude, G., and Bruns, B., *J. Phys. Chem. U.S.S.R.*, **22**, 487 (1948).
26. Braude, G., Shurmovskaya, N., and Bruns, B., *J. Phys. Chem., U.S.S.R.*, **22**, 483 (1948).
27. Bredig, G., and Schwarz von Bergkampff, E., *Z. physik. Chem. Bodenstein Festband*, 172 (1931).
- 27a. Bridelle, R., *Ann. Chim. (Paris)*, [12] **10**, 824 (1955).
28. Bridelle, R., and Michel, A., *Rev. met.*, **51**, 278 (1954).

29. Brill, R., *Z. Krist.*, **68**, 379 (1928).
30. Brill, R., *Naturwissenschaften*, **16**, 593 (1928).
31. Brill, R., and Mark, H., *Z. physik. Chem.*, **133**, 443 (1928).
32. Browning, L. C., DeWitt, T. W., and Emmett, P. H., *J. Am. Chem. Soc.*, **72**, 4211 (1950).
33. Browning, L. C., and Emmett, P. H., *J. Am. Chem. Soc.*, **74**, 1680 (1952).
34. Brunauer, S., Jefferson, M. E., Emmett, P. H., and Hendricks, S., *J. Am. Chem. Soc.*, **53**, 1778 (1931).
- 34a. Carrol, K. G., Darkin, L. S., Filer, E. W., and Zwell, L., *Nature*, **174**, 978 (1954).
35. Cairns, R. W., and Ott, E., *J. Am. Chem. Soc.*, **55**, 534 (1933).
36. Clark, J., and Jack, K. H., *Chemistry & Industry*, 1004 (1951).
37. Cohn, E. M., and Hofer, L. J. E., U. S. Patent 2,535,042, Dec. 26, 1950.
38. Cohn, E. M., and Hofer, L. J. E., *J. Am. Chem. Soc.*, **72**, 4662 (1950).
39. Cohn, E. M., and Hofer, L. J. E., *J. Chem. Phys.*, **21**, 354 (1953).
40. Crangle, J., and Sucksmith, W., *J. Iron Steel Inst. (London)*, **168**, 141 (1951).
41. Craxford, S. R., and Rideal, E. K., *J. Chem. Soc.*, **1939**, 1604.
42. Davis, W. R., Slawson, R. J., and Rigby, G. R., *Nature*, **171**, 756 (1953).
43. DeLange, J. J., and Visser, G. H., *Ingenieur Utrecht*, **58**, No. 26 (July 5, 1946).
44. Dowden, D. A., *J. Chem. Soc.*, **1950**, 242.
45. Dowden, D. A., *Research (London)*, **1**, 239 (1948).
46. Drain, J., *Ann. Chim. (Paris)*, [12] **8**, 900 (1953).
47. Drain, J., and Michel, A., *Bull. Soc. Chim. France*, Jan.-Feb. 1951, p. 23.
- 47a. Drain, J., and Michel, A., *Rev. met.*, **49**, 585 (1952).
48. DuJassoneix, B., "8th International Congress Applied Chemistry," Vol. **2**, p. 165 (1912).
49. Durand, J. F., *Compt. rend.*, **177**, 693 (1923).
50. Eckstrom, H. C., and Adcock, W. A., *J. Am. Chem. Soc.*, **72**, 1042 (1950).
51. Edwards, O. S., Lipson, H., and Wilson, A. J. C., *Proc. Roy. Soc. (London)*, **180**, 268 (1942).
- 51a. Emmett, P. H., and Love, K. S., *J. Am. Chem. Soc.*, **55**, 4043 (1933).
52. Eidus, Y. T., *Bull. acad. sci. U.R.S.S. Classe sci. chim.* 1944, 255.
53. Eidus, Y. T., *Bull. acad. sci. U.R.S.S. Classe sci. chim.*, 1945, 62.
54. Eidus, Y. T., *Bull. acad. sci. U.R.S.S. Classe sci. chim.*, 1946, 447.
55. Eidus, Y. T., and Altshuller, S. B., *Bull. acad. sci. U.R.S.S. Classe sci. chim.*, 1944, 349.
56. Eidus, Y. T., and Elagina, N. V., *Bull. acad. sci. U.R.S.S. Classe sci. chim.*, 1943, 303.
57. Eidus, Y. T., Epifanskii, P. F., Petrova, L. V., and Elagina, N. V., *Bull. acad. sci. U.R.S.S. Classe sci. chim.*, 1943, 145.
58. Eidus, Y. T., and Zelinskii, N. D., *Bull. acad. sci. U.R.S.S. Classe sci. chim.* 1942, 45.
59. Eidus, Y. T., and Zelinskii, N. D., *Bull. acad. sci. U.R.S.S. Classe sci. chim.* 1942, 190.
60. Eisenhut, O., and Kaupp, E., *Z. Elektrochem.*, **36**, 392 (1930).
61. Ewing, F. J., *J. Chem. Phys.*, **3**, 420 (1935).
62. Feitknecht, W., and Berger, A., *Helv. Chim. Acta.*, **25**, 1543 (1942).
63. Fischer, F., and Bahr, H. A., *Ges. Abhandl. Kenntnis Kohle*, **8**, 225 (1928).
64. Fischer, F., and Tropsch, H., *Ges. Abhandl. Kenntnis Kohle*, **10**, 313 (1937).
65. Fischer, F., and Tropsch, H., *Ber.*, **59B**, 830 (1926).
66. Fischer, F., and Tropsch, H., *Brennstoff-Chem.*, **7**, 299 (1926).
67. Fischer, F., Tropsch, H., and Dilthey, P., *Ges. Abhandl. Kenntnis Kohle*, **8**, 175 (1924).

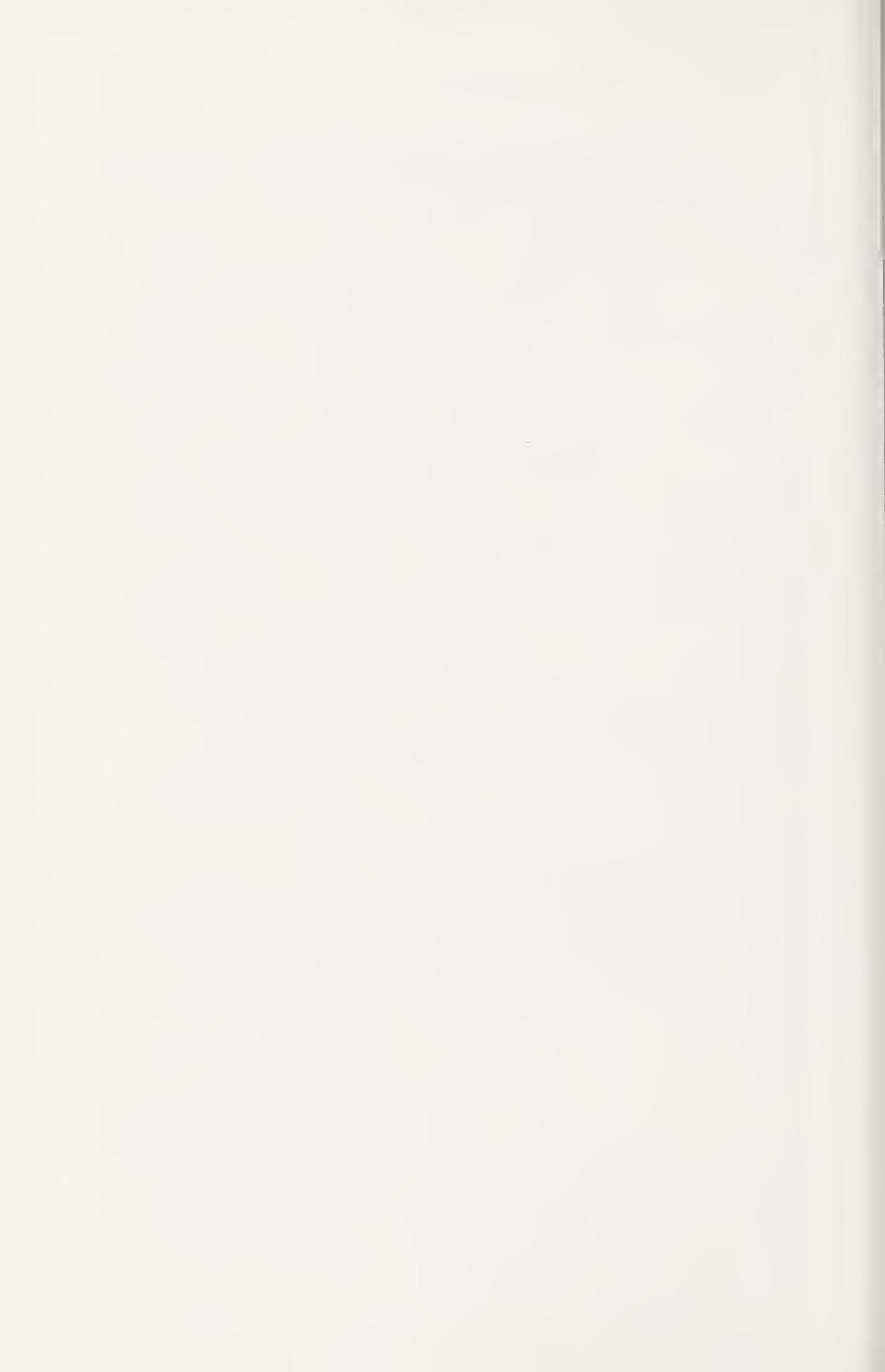
68. Fitzwilliam, J. W., 9th Annual Pittsburgh Diffraction Conference, Abstracts, 1951.
69. Frankenburg, W. G., U. S. Patent 2,507,510, May 16, 1950.
70. Frankenburg, W. G., U. S. Patent 2,539,414, Jan. 30, 1951.
71. Frankenburg, W. G., U. S. Patent 2,531,420, Nov. 28, 1950.
72. Fricke, R., and Ackermann, P., *Z. Elektrochem.*, **40**, 630 (1934).
73. Fricke, R., and Hüttig, G. F., "Hydroxyde und Oxydhydrate," Vol. IX, "Handbuch der Allgemeine Chemie," Leipzig, Akademische Verlagsgesellschaft, 1937.
74. Fricke, R., and Weitbrecht, G., *Z. Elektrochem.*, **48**, 106 (1942).
75. Glud, W., Otto, H., and Ritter, H., *Ber.*, **62**, 2483 (1929).
76. Goldschmidt, H. J., *J. Iron Steel Inst. (London)*, **170**, 187 (1952).
77. Goodeve, C., and Jack, K. H., *Discussions Faraday Soc.*, No. 4, 82 (1948).
78. Granadam, P., *Ann. Chim. (Paris)* [11], **4**, 83 (1935).
79. Hägg, G., *Nature*, **121**, 826 (1928).
80. Hägg, G., *ibid.*, **122**, 314 (1928).
81. Hägg, G., *Z. physik. Chem.*, **B4**, 346 (1929).
82. Hägg, G., *Nova Acta Regiae Soc. Sci. Upsaliensis* [4] No. 1, 7 (1929).
83. Hägg, G., *Z. physik. Chem.*, **B8**, 455 (1930).
84. Hägg, G., *ibid.*, **B12**, 33 (1931).
85. Hägg, G., *Jernkontorets Ann.*, **118**, 173 (1934).
86. Hägg, G., *Z. Krist.*, **89**, 92 (1934).
87. Hägg, G., *Z. physik. Chem.*, **B29**, 95 (1935).
88. Hahn, F., and Hertrich, F., *Ber.*, **56**, 1729 (1923).
89. Hall, W. K., Dieter, W. E., Hofer, L. J. E., and Anderson, R. B., *J. Am. Chem. Soc.*, **75**, 1442 (1953).
90. Hall, W. K., Tarn, W. H., and Anderson, R. B., *J. Phys. Chem.*, **56**, 688 (1952).
- 90a. Hall, W. K., Tarn, W. H., and Anderson, R. B., *J. Am. Chem. Soc.*, **72**, 5436 (1950).
91. Heidenreich, R. D., Sturkey, L., and Woods, H. L., *J. Appl. Phys.*, **17**, 127 (1946).
92. Heidenreich, R. D., Sturkey, L., and Woods, H. L., *Nature*, **157**, 518 (1946).
93. Hendricks, S. B., *Z. Krist.*, **74**, 534 (1930).
- 93a. Hendricks, S. B., Brunauer, S., and Emmett, P. H., *J. Am. Chem. Soc.*, **52**, 1456 (1930).
94. Hendricks, S. B., Jefferson, M. E., and Schultz, J. F., *Z. Krist.*, **73**, 376 (1930).
95. Herbst, M., F.I.A.T. Reel R19, 7136, Jan. 13, 1942.
96. Herbst, M., and Halle, T.O.M. Reel 26, Bag 2463, Frames 900,000,232, Mar. 31, 1943.
97. Hilpert, S., and Dieckmann, T., *Ber.*, **48**, 1281 (1915).
98. Hofer, L. J. E., U. S. Bureau of Mines Rept. Investigations 3770 (1944).
99. Hofer, L. J. E., Unpublished data of the Bureau of Mines.
100. Hofer, L. J. E., Anderson, R. B., Peebles, W. C., and Stein, K. C., *J. Phys. & Colloid Chem.*, **55**, 1201 (1951).
101. Hofer, L. J. E., and Cohn, E. M., *Nature*, **167**, 977 (1951).
102. Hofer, L. J. E., and Cohn, E. M., *Anal. Chem.*, **22**, 907 (1950).
103. Hofer, L. J. E., and Cohn, E. M., *J. Chem. Phys.*, **18**, 766 (1950).
104. Hofer, L. J. E., Cohn, E. M., and Peebles, W. C., *J. Am. Chem. Soc.*, **71**, 189 (1949).
105. Hofer, L. J. E., Cohn, E. M., and Peebles, W. C., *J. Phys. & Colloid Chem.*, **54**, 1161 (1950).
106. Hofer, L. J. E., Cohn, E. M., and Peebles, W. C., *ibid.*, **53**, 661 (1951).
107. Hofer, L. J. E., and Peebles, W. C., *J. Am. Chem. Soc.*, **69**, 893 (1947).

108. Hofer, L. J. E., and Peebles, W. C., *ibid.*, **69**, 2497 (1947).
109. Hofer, L. J. E., Peebles, W. C., and Bean, E. H., *J. Am. Chem. Soc.*, **72**, 2698 (1950).
110. Hofer, L. J. E., Peebles, W. C., and Dieter, W. E., *J. Am. Chem. Soc.*, **68**, 1953 (1946).
111. Hofer, L. J. E., Sterling, E., and McCartney, J. T., *J. Phys. Chem.*, **59**, 1153 (1955).
112. Hofmann, U., *Ber.*, **61B**, 1180 (1928).
113. Hofmann, U. and Groll, E., *Z. anorg. allgem. Chem.*, **191**, 414 (1930).
114. Honda, K., and Murakami, T., *Science Repts. Tohoku Imp. Univ.*, **6**, 23 (1917).
115. Hoog, H., Dutch Report on Additional Information on Various Catalytic Processes in Western Germany, II, B.I.O.S. Misc. Rept. 113, 1947.
116. Hume-Rothery, W., *Phil. Mag.* [7], **44**, 1053 (1953).
117. Hume-Rothery, W., *Phil. Mag. Suppl.*, **3**, 149 (1954).
118. Hume-Rothery, W., Raynor, G. V., and Little, A. T., *J. Iron Steel Inst. (London)*, **145**, 143 (1942).
119. Isaichev, I. V., *Zhur. Tekh. Fiz.*, **17**, 839 (1947).
120. Jack, K. H., 9th Annual Pittsburgh Diffraction Conference Abstracts, 1951.
121. Jack, K. H., *Acta. Cryst.*, **3**, 392 (1950).
122. Jack, K. H., *ibid.*, **5**, 404 (1952).
123. Jack, K. H., *Proc. Roy. Soc. London*, **A195**, 34 (1948).
124. Jack, K. H., *ibid.*, **A195**, 41 (1948).
125. Jack, K. H., *ibid.*, **A195**, 56 (1948).
126. Jack, K. H., *Nature*, **158**, 60 (1946).
127. Jack, K. H., *J. Iron Steel Inst. London*, **169**, 26 (1951).
128. Jack, K. H., *Proc. Roy. Soc. London*, **208A**, 200-216 (1951).
129. Jack, K. H., *ibid.*, **208A**, 216 (1951).
130. Jacobsen, B., and Westgren, A., *Z. physik. Chem.*, **B20**, 360 (1933).
131. Juza, R., and Puff, H., *Naturwissenschaften*, **38**, 331 (1951).
132. Juza, R., and Sachse, W., *Z. anorg. allgem. Chem.*, **251**, 201 (1943).
133. Juza, R., and Sachse, W., *ibid.*, **253**, 95 (1945).
134. Kiessling, R., *J. Electrochem. Soc.*, **98**, 166 (1951).
135. Kodama, S., Matsumura, S., Tarama, K., Ando, T., and Yoshimori, K., *J. Soc. Chem. Ind. Japan*, **47**, 1 (1944).
136. Kohlhass, R., and Meyer, W. Fr., *Metalwirtschaft*, **17**, 786 (1938).
137. Kölbel, H., *Chem.-Ing.-Tech.*, 153 (1951).
138. Kölbel, H., Ackermann, P., Juza, R., and Tentschert, H., *Erdöl u. Kohle*, **2**, 278 (1949).
139. Kölbel, H., and Engelhardt, F., *Zeit. Chem.-Ing.-Tech.*, 97 (1950).
140. Kölbel, H., and Engelhardt, F., *Erdöl u. Kohle*, **2**, 52 (1949).
141. Koster, W., and Mulfinger, W., *Z. Metalkunde*, **30**, 348 (1938).
142. Kummer, J. T., Browning, L. C., and Emmett, P. H., *J. Chem. Phys.*, **16**, 739 (1948).
143. Kummer, J. T., DeWitt, T. W., and Emmett, P. H., *J. Am. Chem. Soc.*, **70**, 3632 (1948).
144. LeBlanc, M., and Mobius, E., *Z. Elektrochem.*, **39**, 753 (1933).
145. LeClere, G., *Compt. rend.*, **207**, 1099 (1938).
146. LeClere, G., and LeFebvre, H., *Compt. rend.*, **208**, 1650 (1939).
147. LeClere, G., and Michel, A., *Compt. rend.*, **208**, 1583 (1939).
148. LeFebvre, H., and LeClere, G., *Compt. rend.*, **203**, 1378 (1936).
149. LeFebvre, H., and LeClere, G., *Congr. chim. ind. Compt. rend. 18th Congr. Nancy*, Sept.-Oct. 1938, 725.

150. Lehrer, E., *Z. Elektrochem.*, **36**, 383, 460 (1930).
151. Leidheiser, H., Jr., and Gwathmey, A. T., *J. Am. Chem. Soc.*, **70**, 1206 (1948).
See also Kehrner, V. J., Jr., and Leidheiser, H., Jr., *J. Phys. Chem.*, **58**, 550 (1954).
152. Lement, B. S., Averbach, B. L., and Cohen, M., *A.S.M. Preprint No. 25* (1953).
153. Lipson, H., and Parker, A. M. B., *J. Iron Steel Inst. (London)*, **149**, 123 (1944).
154. Lipson, H., and Petch, N. J., *J. Iron Steel Inst. (London)*, **142**, 95 (1940).
155. Longuet, Mlle, J., *thesis, Univ. of Strasbourg, France, Series E*, No. 72 (1943).
156. Manes, M., Damick, A. D., Mentser, M., Cohn, E. M., and Hofer, L. J. E., *J. Am. Chem. Soc.*, **74**, 6207 (1952).
157. Maxwell, L. R., Smart, J. S., and Brunauer, S., *J. Chem. Phys.*, **19**, 303 (1951).
158. McCartney, J. T., Hofer, L. J. E., Seligman, B., Lecky, J. A., Peebles, W. C., and Anderson, R. B., *J. Phys. Chem.*, **57**, 730 (1953).
159. Merkel, H., *Brennstoff-Chem.*, **31**, 208 (1950).
- 159a. "Metals Handbook," American Society for Metals, New York, 1948.
160. Meyer, Reel 101, Doc. PG 21,581, N.I.D. Vide., Leva, M. Translations of German Documents on the Development of Iron Catalysts for the Fischer-Tropsch Synthesis, 1946.
161. Meyer, G., and Scheffer, F. E. C., *J. Am. Chem. Soc.*, **75**, 486 (1953).
162. Meyer, G., and Scheffer, F. E. C., *Rec. Trav. Chim.*, **46**, 359 (1927).
163. Meyer, G., and Scheffer, F. E. C., *ibid.*, **46**, 754 (1927).
164. Meyer, G., and Scheffer, F. E. C., *ibid.*, **47**, 401 (1928).
165. Meyer, G., and Scheffer, F. E. C., *ibid.*, **46**, 1 (1927).
166. Meyer, W. F., *Z. Krist.*, **97**, 145 (1937).
167. Michel, A., *Ann. Chim. (Paris)* [11], **8**, 317 (1937).
168. Michel, A., Bernier, R., and LeClerc, G., *J. chim. phys.*, **47**, 269 (1950).
169. Michel, A., and Chaudron, G., *Compt. rend.*, **201**, 1191 (1935).
170. Milligan, W. O., and Holmes, J., *J. Am. Chem. Soc.*, **63**, 149 (1941).
171. Mitchell, J. J., *J. Chem. Phys.*, **21**, 1153 (1953).
172. Mittasch, A., Kuss, E., and Emert, O., *Z. anorg. allgem. Chem.*, **170**, 193 (1928).
173. Natta, G., *Gazz. chim. ital.*, **58**, 344 (1928).
174. Natta, G., and Passerini, L., *Gazz. chim. ital.*, **58**, 597 (1928).
175. Natta, G., and Strada, M., *Gazz. chim. ital.*, **58**, 427 (1928).
176. Nowotny, H., and Juza, R., *Z. anorg. Chem.*, **253**, 109 (1945).
177. Ohman, E., *J. Iron Steel Inst. London*, **123**, 445 (1931).
- 177a. Okada, M., and Arata, Y., *Technol. Repts. Osaka Univ.* **2**, 224 (1952).
- 177b. Okada, M., and Arata, Y., *Technol. Repts. Osaka Univ.* **3**, 311 (1953).
178. Olmer, F., *J. Phys. Chem.*, **46**, 405 (1942).
179. Osawa, A., and Iwaizumi, S., *Z. Krist.*, **69**, 26 (1928).
180. Paranjpe, V. G., Cohen, M., Bever, M. B., and Floe, C. F., *Trans. Am. Inst. Mining & Met. Eng.*, **188**, 261 (1950).
181. Paul, R., Buisson, P., and Joseph, N., *Compt. rend.*, **232**, 627 (1951).
182. Pauling, L., *J. Am. Chem. Soc.*, **69**, 542 (1947).
183. Pauling, L., and Hendricks, S. B., *J. Am. Chem. Soc.*, **47**, 781 (1925).
184. Pearson, J., and Ende, U. J. C., *J. Iron. & Steel Inst. London*, **175**, 52 (1953).
185. Petch, N. J., *J. Iron & Steel Inst. London*, **147**, 221 (1943).
186. Petch, N. J., *J. Iron & Steel Inst. London*, **149**, 143 (1944).
187. Petch, N. J., *J. Iron & Steel Inst. London*, **145**, 111 (1942).
188. Pichler, H., "Advances in Catalysis," Vol. IV, New York, Academic Press, Inc., 1953.
189. Pichler, H., and Merkel, H., U. S. Bur. of Mines Tech. Paper 718 (1949). This paper also contains a review by Hofer, L. J. E.

190. Pichler, H., and Merkel, H., *Brennstoff-Chem.*, **31**, 1 (1950).
191. Pichler, H., and Merkel, H., *Brennstoff-Chem.*, **31**, 33 (1950).
192. Pingault, P., *Ann. Chim. (Paris)* [10], **20**, 371 (1933).
193. Podgurski, H. H., Kummer, J. T., DeWitt, T. W., and Emmett, P. H., *J. Am. Chem. Soc.*, **72**, 5382 (1950).
194. Radushkevich, L. V., and Luk'yanovich, V. M., *Zhur. Fiz. Khim.*, **26**, 88 (1952).
195. Richardson, F. D., *J. Iron Steel Inst. London*, **175**, 33 (1953).
196. Riley, H. L., *Quart. Revs. London*, **3**, 160 (1949).
197. Roberts, E. C., *J. Metals*, **188**, 1210 (1950).
198. Roberts, C. S., Averbach, B. L., and Cohen, M., *A.S.M. Preprint*, **11** (1952).
199. Rundle, R. E., *Acta Cryst.*, **1**, 180 (1948).
200. Rundle, R. E., *J. Am. Chem. Soc.*, **69**, 1327 (1947).
201. Sage, M., *Compt. rend.*, **230**, 1354 (1950).
202. Scheffer, F. E. C., Dokkum, T., and Al, J., *Rec. Trav. Chim.*, **45**, 803 (1926).
203. Schenck, R., *Z. anorg. allgem. Chem.*, **164**, 145 (1927).
204. Schenck, R., *Z. anorg. allgem. Chem.*, **167**, 254 (1927).
205. Schenck, R., *Z. anorg. allgem. Chem.*, **167**, 315 (1927).
206. Schenck, R., and Dingmann, Th., *Z. anorg. allgem. Chem.*, **166**, 146 (1927).
207. Schenck, R., and Dingmann, Th., *Z. anorg. allgem. Chem.*, **171**, 239 (1928).
208. Schenck, R., and Dingmann, Th., *Z. anorg. allgem. Chem.*, **209**, 1 (1932).
209. Schenck, R., Dingmann, Th., Kirscht, P. H., and Kortengraber, A., *Z. anorg. allgem. Chem.*, **206**, 73 (1932).
210. Schenck, R., Dingmann, Th., Kirscht, P. H., and Weselcock, H., *Z. anorg. allgem. Chem.*, **182**, 97 (1929).
211. Schenck, R., Franz, H., and Laymann, A., *Z. anorg. allgem. Chem.*, **206**, 129 (1932).
212. Schenck, R., Franz, H., and Willeke, H., *Z. anorg. allgem. Chem.*, **184**, 1 (1929).
213. Schenck, R., and Klas, H., *Z. anorg. allgem. Chem.*, **178**, 146 (1929).
214. Schenck, R., Krageloh, F., and Eisenstecken, F., *Z. anorg. allgem. Chem.*, **164**, 313 (1927).
215. Schenck, R., and Stenkhoff, R., *Z. anorg. allgem. Chem.*, **161**, 287 (1927).
216. Scheuermann, A., *Z. angew. Chem.*, **60**, 211 (1948).
217. Schirmacher, H., Dissertation, Westphalian Wilhelms Univ., Munster, 1936.
218. Schmidt, J., and Osswald, E., *Z. anorg. allgem. Chem.*, **216**, 85 (1933).
219. Selwood, P. W., "Advances in Catalysis," Vol. III, New York, Academic Press, Inc., 1951.
220. Selwood, P. W., "Catalysis," Vol. I, "Fundamental Principles," P. H. Emmett, ed., New York, Reinhold Publishing Corp., 1954.
221. Selwood, P. W., Phillips, T. R., and Adler, S., *J. Am. Chem. Soc.*, **76**, 2281 (1954).
222. Shimura, S., *Proc. Imp. Acad. (Tokyo)*, **6**, 269 (1930).
223. Schultz, J. F., Hall, W. K., Thompson, G. P., and Anderson, R. B., unpublished data of Bureau of Mines.
224. Shultz, J. F., Seligman, B., Lecky, J., and Anderson, R. B., *J. Am. Chem. Soc.*, **74**, 637 (1952).
225. Stamme, K., *Poggendorf Annalen*, **82**, 136 (1851).
226. Stanley, J. K., *J. Metals*, **1**, 752 (1949).
- 226a. Stewart, S. G., U. S. Patent 2,490,488, Dec. 6, 1949.
227. Storch, H. H., "Advances in Catalysis," Vol. I, New York, Academic Press, Inc., 1948.
228. Storch, H. H., Anderson, R. B., Hofer, L. J. E., Hawk, C. O., Anderson, H. C., and Golumbic, N., *Bureau of Mines Tech. Paper*, **709**, 1948.

- 229. Storch, H. H., Golumbic, N., and Anderson, R. B., "The Fischer-Tropsch and Related Syntheses," New York, John Wiley & Sons, Inc., 1951.
- 229a. Synthetic Liquid Fuels Annual Report of the Secretary of the Interior, 1954.
- 230. Tebbboth, J. A., *J. Chem. Ind.*, **67**, 62 (1948).
- 231. Trambouze, Y., *Compt. rend.*, **227**, 971 (1948).
- 232. Trambouze, Y., *J. chim. phys.*, **47**, 258 (1950).
- 233. Trambouze, Y., *Compt. rend.*, **228**, 1432 (1949).
- 234. Trambouze, Y., and Perrin, M., *Compt. rend.*, **228**, 1015 (1949).
- 235. Trillat, J. J., and Oketani, S., *Compt. rend.*, **230**, 2203 (1950).
- 236. Trillat, J. J., and Oketani, S., *Metaux & Corrosion*, **25**, 263 (1950).
- 237. Trillat, J. J., and Oketani, S., *Rev. met.*, **4**, 489 (1951).
- 238. Trillat, J. J., and Oketani, S., *Compt. rend.*, **232**, 1116 (1951).
- 239. Trillat, J. J., and Oketani, S., *Acta Cryst.*, **5**, 469 (1952).
- 240. Troesch, A., *J. chim. phys.*, **47**, 274 (1950).
- 241. Tutiya, H., *Sci. Papers Inst. Phys. Chem. Research (Tokyo)*, **10**, 69 (1929).
- 242. Tutiya, H., *Bull. Inst. Phys. Chem. Research (Tokyo)*, **10**, 556 (1931).
- 243. Tutiya, H., *Bull. Inst. Phys. Chem. Research (Tokyo)*, **8**, 609 (1929).
- 244. Tutiya, H., *Bull. Inst. Phys. Chem. Research (Tokyo)*, **8**, 206 (1929).
- 245. Tutiya, H., *Bull. Inst. Phys. Chem. Research (Tokyo)*, **10**, 951 (1930).
- 246. Verwey, E. J. W., *J. Chem. Phys.*, **3**, 592 (1953).
- 247. Von Wangenheim, *Brennstoff-Chem.*, **8**, 385 (1927).
- 248. Von Wangenheim and Winkelmann, Thesis, Cologne, Germany, quoted by Fischer, F., and Dilthey, P., *Ges. Abhandl. Kenntnis Kohle*, **8**, 235 (1924-27).
- 249. Vournasos, A. C., *Compt. rend.*, **168**, 889 (1919).
- 250. Weiser, H. B., "Inorganic Colloid Chemistry," Vol. II, "The Hydrous Oxides and Hydroxides," New York, John Wiley & Sons, Inc., 1935.
- 251. Weiser, H. B., and Milligan, W. O., *J. Phys. Chem.*, **36**, 722 (1932).
- 252. Weiser, H. B., and Milligan, W. O., *J. Am. Chem. Soc.*, **57**, 238 (1935).
- 253. Weiss, P., and Forrer, R., *Ann. Phys. (Paris)* [10], **12**, 279 (1929).
- 254. Weller, S., *J. Am. Chem. Soc.*, **69**, 2432 (1947).
- 255. Weller, S., Hofer, L. J. E., and Anderson, R. B., *J. Am. Chem. Soc.*, **70**, 799 (1948).
- 256. Welo, L. A., and Baudisch, O., *Chem. Rev.*, **15**, 45 (1935).
- 256a. Westgren, A., *Nature*, **132**, 480 (1933).
- 257. Westgren, A., *Jernkontorets Ann.*, **116**, 457 (1937).
- 258. Westgren, A., and Phragmen, G., *Z. physik. Chem.*, **102**, 1 (1922).
- 259. Westgren, A., and Phragmen, G., *J. Iron Steel Inst. (London)*, **105**, 241 (1922).
- 260. Wever, F., *Mitt. Kaiser-Wilhelm Inst. Eisenforsch. Dusseldorf*, **4**, 67 (1922).
- 261. Wever, F., and Muller, A., *Z. anorg. allgem. Chem.*, **192**, 317 (1930).
- 262. Wilson, A. J. C., "X-ray Optics," Methuen & Co., Ltd., London, 1949.



CHAPTER 5

THE ISOSYNTHESIS

Ernst M. Cohn

*Physical Chemist, Synthetic Fuels Research Branch, Bureau of
Mines, Bruceton, Pa.*

PURPOSE AND HISTORY OF THE SYNTHESIS

The isosynthesis was developed during World War II at the Kaiser Wilhelm Institut für Kohlenforschung in Mülheim, Ruhr, Germany, by H. Pichler and K. H. Ziesecke in collaboration with F. Fischer and other members of the Institut. Details of the project, which was first suggested by Fischer in 1940⁹ and was actually begun in October 1941⁶, were kept secret because its primary goal was the catalytic production of isobutane and isobutene, raw materials for high-octane gasoline. Allied technical missions to Germany made the main results available in 1945^{3, 6}; detailed papers were later published in German^{9, 10, 12, 13} and English¹¹. That development of the isosynthesis was rapid is shown by the fact that four German patent applications had already been made in November and December of 1942⁴. The only other original papers on the subject appear to be notes of a meeting, held in June of 1943, in which Fischer and Pichler of the K. W. I. and Martin, Roelen, and Neweling of Ruhrchemie participated¹⁷. Large-scale utilization of the synthesis was considered at that time; as far as is known, it has never been in commercial use, although at least two American firms have obtained patents on modifications of it^{2, 5, 14}.

DESCRIPTION OF THE SYNTHESIS

The passage of synthesis gas, a mixture of hydrogen and carbon monoxide, over certain difficultly reducible oxide catalysts under given operating conditions results in products consisting predominantly of saturated, branched-chain, aliphatic hydrocarbons containing four to eight carbon atoms. Best results were obtained at K. W. I. with a durable catalyst consisting of 100 parts thoria promoted by 20 parts alumina and, in certain cases, 1 part alkali, operated at 300 to 600 atmospheres, 400 to 450°C, and with a synthesis gas the composition of which corresponded to its usage ratio. Figure 1 shows the temperature and pressure ranges as given in the basic German patent application St 61,125. A cheaper alumina-zinc oxide

catalyst was reasonably satisfactory. To avoid undesirable products, such as methane and free carbon, the walls of the reactor had to be inert and traces of iron carbonyl had to be eliminated. The presence of sulfur was not deleterious to the catalyst, and temperature control did not have to be as rigorous as for the Fischer-Tropsch synthesis. The conditions and mechanism of the reaction were more closely related to those for the synthesis of higher alcohols than those for the Fischer-Tropsch reaction^{15, 16}.

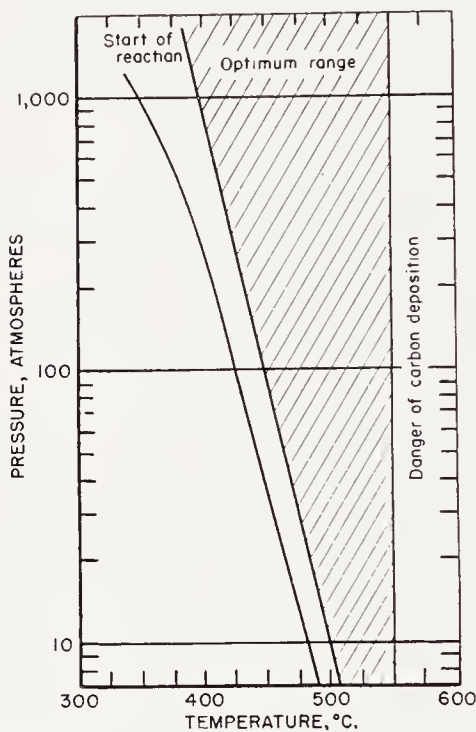


Figure 1. Temperature and pressure ranges of the isosynthesis (adapted from German Patent application St 61,125).

PREPARATION AND REACTIVATION OF CATALYSTS

All catalysts were prepared by precipitation from aqueous solution, usually by quickly adding boiling sodium carbonate solution to boiling metal nitrate solution (Table 1). Variation of the conditions of preparation resulted in large changes of the properties of the catalysts; for example, the bulk density of thoria ranged from 0.7 to 2.3. Typical preparations were as follows:

(a) "Normal" thoria catalysts were made by quickly adding boiling sodium carbonate solution to boiling thorium nitrate solution. When 2 liters of water containing 240 grams of thorium nitrate and 2 liters of water containing a slight excess of sodium carbonate were used, the bulk density of the hard granular catalyst was 1.3 after it had been washed free of alkali and dried at 110°C. More concentrated solutions yielded lower bulk densi-

TABLE 1. CATALYSTS PREPARED FOR ISOSYNTHESIS AT K.-W.-I.

Catalyst	Remarks
<i>A. One-component catalysts</i>	
ThO ₂	"Normal" method used, also precipitation from cold solutions and addition of hot nitrate to hot Na ₂ CO ₃ solution, usually washed free of alkali, dried at 110° and then at 300°C in stream of air; NH ₄ OH also used as precipitant.
Al ₂ O ₃	Precipitated by H ₂ SO ₄ or CO ₂ from solution of NaAlO ₂ , or prepared from Al(NO ₃) ₃ + Na ₂ CO ₃ , washed, sintered in air at 300°C.
W ₂ O ₅	Precipitated by HNO ₃ from Na ₂ WO ₄ solution.
UO ₂	Precipitated by H ₂ O ₂ from UO ₂ (NO ₃) ₂ solution.
ZnO	Precipitated by addition of alkali to nitrate and vice versa. Other catalysts included Cr ₂ O ₃ , TiO ₂ , BeO, ZrO ₂ , CeO ₂ , MnO, MgO, La, Pr, and Nd. They were usually prepared from nitrates.
<i>B. Multi-component catalysts</i>	
ThO ₂ + H ₃ PO ₄	To 100 g ThO ₂ , dried at 300°C and powdered, 27 cc of cold 89% H ₃ PO ₄ was added and the paste dried at 250°C.
ThO ₂ + K ₂ CO ₃	To a slurry of washed ThO ₂ , sufficient aqueous K ₂ CO ₃ was added to yield preparations containing 0.6, 1, 5, and 25% K ₂ CO ₃ . The mixture was dried on a steam bath at 110° and then at 300°C.
ThO ₂ + Al ₂ O ₃	(a) Slowly coprecipitated (5, 10, or 20% Al ₂ O ₃) from boiling solutions, slurry boiled briefly, filtered, washed, dried at 110° and 300°C in stream of air. (b) Separate layers of ThO ₂ and Al ₂ O ₃ (29% of weight of first layer) used in this order. (c) Separately precipitated, hot slurries mixed (20% Al ₂ O ₃), dried on steam bath, then at 110 and at 300°C in air. In (b) and (c) H ₂ SO ₄ was used with solution of NaAlO ₂ .
ThO ₂ + Al ₂ O ₃ + K ₂ CO ₃	(a) Oxides precipitated separately (see above), K ₂ CO ₃ (1 or 3% based on Al ₂ O ₃) added to washed Al ₂ O ₃ , then mixed (ThO ₂ :Al ₂ O ₃ = 100:20). (b) As (a) but K ₂ CO ₃ (0.6% based on ThO ₂) added to washed ThO ₂ , then mixed (ThO ₂ :Al ₂ O ₃ = 100:20).
ThO ₂ + Al ₂ O ₃ + kguhr.	Oxides precipitated separately, mixed wet with kieselguhr (ThO ₂ :Al ₂ O ₃ :kguhr. = 100:20:10).
ThO ₂ + ZnO	Coprecipitated from boiling solutions by adding Na ₂ CO ₃ to nitrate solution or preferably <i>vice versa</i> , washed, dried at 110 and 300°C. (ThO ₂ :ZnO = 75:25 or 87:13).
ThO ₂ + ZnO + Al ₂ O ₃	ThO ₂ and ZnO coprecipitated, slurried with Al ₂ O ₃ precipitate, and dried (ThO ₂ :ZnO:Al ₂ O ₃ = 2:1:0.4).
ThO ₂ + Cr ₂ O ₃	Coprecipitated, dried at 110 and 300°C.
ThO ₂ + Fe	Coprecipitated (ThO ₂ :Fe = 100:0.25 or 100:1.25).
ThO ₂ + Cu	ThO ₂ :Cu = 100:0.25 or 1:1.

TABLE 1 (CONTINUED)

Catalyst	Remarks
Al ₂ O ₃ + K ₂ CO ₃	Precipitated with H ₂ SO ₄ from NaAlO ₂ (Al ₂ O ₃ :K ₂ CO ₃ = 100:3).
Al ₂ O ₃ + Cr ₂ O ₃	Al ₂ O ₃ :Cr ₂ O ₃ = 100:10.
ZnO + Al ₂ O ₃	Coprecipitated (bulk density 0.84) or precipitated separately (bulk density 0.32), washed, dried at 110 and 300°C.; also used in separate layers in order ZnO-Al ₂ O ₃ (ZnO:Al ₂ O ₃ = 61:39 or 44:56).
	Other catalysts used were ThSiO ₄ , Th ₃ (BO ₃) ₄ , Th ₃ (PO ₄) ₄ , and Al ₂ O ₃ + MoO ₃ .

ties; for example, a three-fold increase in concentration resulted in a bulk density of 0.76 and a crumbly, soft preparation. Slow precipitation (say, one hour) gave especially dense, glass-like catalysts (bulk density 2.3); sodium hydroxide or ammonia precipitants gave dense catalysts upon rapid precipitation similar to those from sodium carbonate with slow precipitation. Sintering of the dried catalysts in a stream of air at 300°C increased their bulk density. Thus, the density of the "normal" thoria was increased from 1.3 to 2.0, while the dull, hard appearance persisted. The original precipitate, ThO(CO₃)·2H₂O, was transformed at 240°C to 3ThO₂·ThO(CO₃)·H₂O and at 300°C to 4ThO₂·H₂O. At still higher temperatures, especially above 400°C, ThO₂ was formed. The loss of carbonate resulted in shrinkage of the catalyst. Since such reactions also occurred during synthesis, pretreatment at 300°C made possible the use of maximum amounts of catalyst in the reactors. Pretreatment at temperatures up to 1000°C further increased the activity of thoria but also shifted its selectivity so that more methane was formed; hence, pretreatment at 300°C was usually used.

(b) A 100ThO₂:20Al₂O₃ coprecipitated catalyst was made by slowly adding boiling carbonate solution (167 grams Na₂CO₃ in 2 liters H₂O) to boiling nitrate solution (240 grams thorium nitrate and 169 grams aluminum nitrate in 2 liters H₂O), briefly boiling the precipitate, filtering, washing 15 times each with 400 cc boiling distilled water, drying at 110° and then at 300°C in streaming air.

(c) A similar catalyst, the components of which were precipitated separately, however, was made as follows: To boiling thorium nitrate solution (240 grams in 2 liters H₂O), boiling carbonate solution (95 grams Na₂CO₃ in 2 liters H₂O) was added. The precipitate was filtered and washed as above. In a separate operation, 169 grams of aluminum nitrate in 1 liter of boiling water was treated with 77 grams of sodium hydroxide in 500 cc of water; aluminum hydroxide was first precipitated and then almost completely dissolved again. The boiling solution of sodium aluminate was

then treated with a solution of 17.2 cc of concentrated sulfuric acid in 350 cc of distilled water, and the precipitated aluminum hydroxide was slurried and washed by decantation 12 times each with 1 liter of water. After being filtered with suction, it was washed 3 times each with 400 cc of boiling water. Finally, both precipitates were slurried in hot water, mixed, evaporated on a water bath with constant stirring, dried at 110° and at 300°C in a current of air.

(d) A coprecipitated $3\text{ThO}_2:1\text{ZnO}$ catalyst was made by inverse precipitation as follows: The boiling nitrate solution (120 grams $\text{Th}(\text{NO}_3)_4 \cdot 4\text{H}_2\text{O}$ and 74 grams $\text{Zn}(\text{NO}_3)_2 \cdot 6\text{H}_2\text{O}$ in 2 liters H_2O) was added to boiling carbonate (86 grams Na_2CO_3 in 1 liter H_2O) with stirring; the precipitate was filtered under suction, washed 15 times each with 400 cc water, and dried at 110°C. The granules were 2 to 4 mm in diameter and had a bulk density of 0.75 before and 1.15 after drying in air at 300°C.

(e) A coprecipitated $1\text{ZnO}:1\text{Al}_2\text{O}_3$ catalyst was made by combining boiling carbonate (117 grams Na_2CO_3 in 2 liters H_2O) with boiling nitrate (187.5 grams $\text{Al}(\text{NO}_3)_3 \cdot 9\text{H}_2\text{O}$ and 74.5 grams $\text{Zn}(\text{NO}_3)_2 \cdot 6\text{H}_2\text{O}$ in 2 liters H_2O) while stirring, boiling the slurry, filtering it with suction, washing the filter cake 13 times each with 400 cc of boiling water, and drying it at 110° and then for 3 hours at 300°C in flowing air. The bulk density of the 48-gram yield of 2- to 4-mm granules was 0.84. A catalyst that was similar, except for being prepared by separate precipitation, had a density of only 0.32.

Unlike catalysts of the iron group, thoria was not poisoned by sulfur compounds. Thoria pretreated with hydrogen sulfide or carbon disulfide and thoria precipitated with ammonium sulfide showed particularly good activity, a fact which is not yet explained¹⁷.

Carbon that was deposited on thoria during synthesis reduced the activity of the catalyst. Used thoria containing excessive amounts of carbon was reactivated by passing air over it at synthesis temperature until no more carbon dioxide was detected in the exit gas. This method of reactivation was possible because thoria did not lose its activity even after having been heated to red heat. Longer periods of constant activity and higher yields of liquid hydrocarbons were realized with thoria-zinc oxide catalysts. No carbon was deposited on these mixed catalysts; they retained their white or light gray color even after prolonged use.

APPARATUS FOR ACTIVITY TESTS

The basic assembly for synthesis experiments, partly shown in Figure 2, contained a 1000-atmosphere reservoir (1); a high-pressure charcoal trap (2); a high-pressure converter tube (12 mm I.D.) inside an aluminum block furnace (3); a high-pressure receiver (4), kept at 31°C to avoid condensation

of carbon dioxide, for collecting most of the liquid product; a low-pressure charcoal trap (5) for removing the remaining C_3 products; and a flow

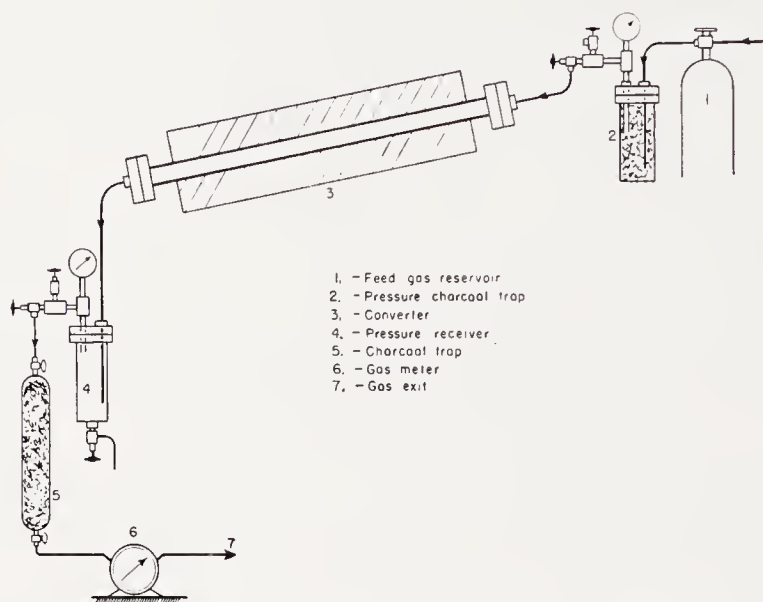


Figure 2. Schematic diagram of isosynthesis apparatus.

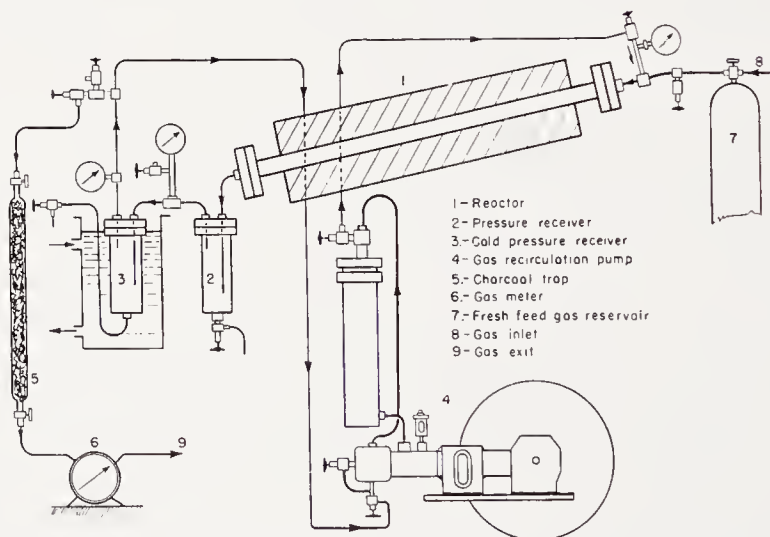


Figure 3. Pressure apparatus for recycling experiments.

meter (6). The modified apparatus, used for recycling experiments, is shown in Figure 3.

In preliminary experiments, the passage of water gas at 30 atmospheres and 450°C through an ordinary steel tube of 12 mm I.D. yielded largely free carbon, carbon dioxide, and methane—all undesirable products. To avoid their formation, inert reactor walls had to be chosen. An aluminum lining

was unsuitable, especially above 150 atmospheres, since it was destroyed by oxygenated reaction products. Copper-clad high-pressure pipes and pipes made of, or lined with, highly alloyed steel (at least 17.5 per cent chromium) were satisfactory. A detailed study of this subject has been published by Ziesecke¹⁸.

SYNTHESIS EXPERIMENTS

Most of the experiments were carried out on a small scale with about 25 cc of catalyst spread in a layer 30 cm long. Gas flows ranged from 0.3 to (usually) 10 liters (S.T.P.) of exit gas per hour per amount of catalyst (expressed either as 25 cc or as 28 grams of thoria), temperatures from 375 to 500°C, pressures from 1 to 1000 atmospheres (usually 30, 150, and 300), and input ratios of hydrogen to carbon monoxide from about 0.77 to 1.3 with small admixtures of nitrogen and carbon dioxide. The total gas input was determined by metering the depressurized exit gas and correcting for the contraction that was calculated from the difference of concentrations of nitrogen in the feed and exit gases.

The usage ratio of hydrogen-carbon monoxide in a single-pass operation usually was 0.85 to 0.90 at 450°C and about 1 at 475°C. Thus, at 450°C higher conversion was obtained with gas rich in carbon monoxide than with normal water gas. Generally, carbon monoxide-rich gas led to more carbon deposition, while hydrogen-rich gas yielded more gaseous hydrocarbons.

Of the products that were removed from the exit gas by cooling or sorption on activated carbon, the C₃-C₄ fraction ("gasol") was analyzed by low-temperature distillation. In certain cases fractional distillation, sometimes after hydrogenation over nickel, served to separate the liquid hydrocarbons into their components which were identified by their physical constants. In other instances, the products in the aqueous layer were fractionated and identified. Motor octane ratings of some gasolines also were determined.

Survey of One-Component Catalysts

Table 2 contains a summary of the results obtained with various one-component catalysts and some quantitative data for the best of these, which were, in order of their effectiveness, thoria, zirconia, ceria, and alumina. The relatively high carbon number (2.5-2.8) of the hydrocarbon gases obtained with thoria is remarkable; the "gasol" hydrocarbons (mainly C₃ and C₄) included large amounts of isobutane.

Alumina used at 30 and 150 atmospheres produced principally methane and carbon, together with small amounts of "gasol" and liquid compounds. Only traces of *iso*-C₄ hydrocarbons were present in the "gasol" formed at 30 atmospheres, while somewhat larger amounts were found in the product obtained at 150 atmospheres. Alumina prepared from the nitrate and used at 300 atmospheres showed little activity.

Zinc oxide produced no liquid hydrocarbons but chiefly methane and alcohols at 300 atmospheres and 450°C.

TABLE 2. RESULTS OBTAINED WITH ONE-COMPONENT CATALYSTS IN THE ISOSYNTHESIS

(450°C, 25 cc catalyst, 10 liter exit gas/hour)

Catalyst	Starting Material	Water Gas Conversion at			Hydrocarbons in End Gas (%)	C-No.	Oil	<i>i</i> -C ₄ , Per cent of C ₄ Fraction	G/M ³ Inert-Free Gas (S.T.P.)	
		30 atm.	150 atm.	300 atm.					<i>i</i> -C ₄	C ₅ + Hydrocarbons
		(vol.-per cent)								
ThO ₂	Nitrate	19	—	—	2.1	2.5	+	88	16	40
ThO ₂	Nitrate	—	46	—	5.1	2.6	+			
ThO ₂	Nitrate	—	—	66	6.4	2.8	+			
Al ₂ O ₃	Na aluminate	54	—	—	11.0	1.4	+	59	2.8	5
Al ₂ O ₃	Na aluminate	—	53	—	10.5	1.5	+			
Al ₂ O ₃	Al nitrate	—	—	21	3.1	2.0	+			
W ₂ O ₅	Na tungstate + HNO ₃	58	—	—	12.9	1.3	+			
Cr ₂ O ₃	Nitrate	19	—	—	3.0	1.5	Traces			
TiO ₂	—	0	—	—	—	—	0			
BeO	—	0	—	—	—	—	0	82	9	—
ZrO ₂	Nitrate	9	—	—	1.0	—	+			
ZrO ₂	Nitrate	—	31	—	3.5	2.1	+			
ZrO ₂	Nitrate	—	—	36	3.5	2.3	+			
UO ₂	Nitrate and H ₂ O ₂ ^a	—	—	—	3.7	1.4	+			
ZnO	Nitrate	10	—	—	1.2	1.3	Traces			
ZnO	Nitrate ^b	—	—	44	10.0	1.1	+			
MnO	Nitrate	15	—	—	0.8	1.2	Little			
MgO	Nitrate	12	—	—	3.0	1.3	Traces			
CeO ₂	Nitrate	7	—	—	0.5	2.0	+	81	1.3	—
CeO ₂	Nitrate	—	10	—	1.0	2.4	Traces			
La	—	3	—	—	—	—	—			
Pr	—	—	—	12	1.3	2.0	+			
Nd	—	—	—	8	0.8	1.9	Traces			

^a 21 per cent at 75 atmospheres.

^b Inverse precipitation; Nitrate added to sodium carbonate solution.

Effect of Operating Variables on Products from Thoria

Temperature. Figure 4 shows the effect of temperature on the types of reaction products obtained by passing water gas over thoria at 150 atmospheres. Alcohol formation predominated below 375°C; methane, ethane, and propane were the principal products above 475°C. The temperature region for the isosynthesis lies between these two limits.

Pressure. Figure 5 shows the effect of pressure (at an hourly flow rate of 10 liters of exit gas per 28 grams of thoria) upon the liquid and "gasol"

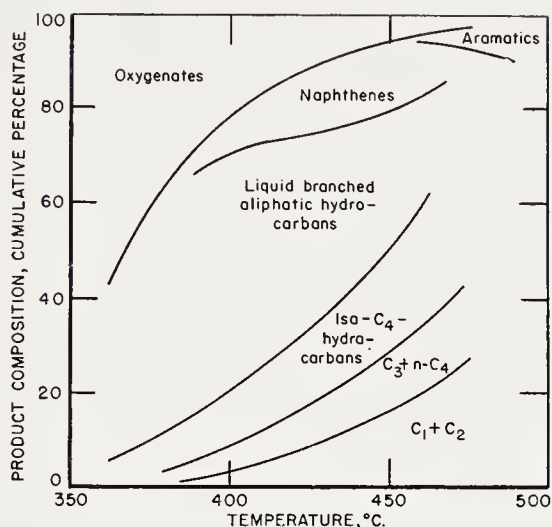


Figure 4. Effect of temperature upon product distribution in the isosynthesis (ThO_2 catalyst, 150 atmospheres).

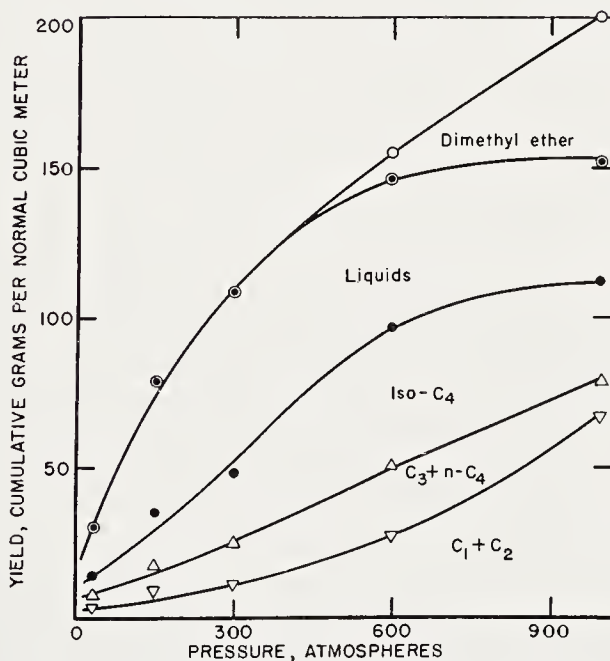


Figure 5. Effect of pressure upon product distribution in the isosynthesis (ThO_2 catalyst, 450°C).

yields at 450°C in a single-pass operation. Best results were obtained between 300 to 600 atmospheres. Below 300 atmospheres gas conversion was relatively small. Above 600 atmospheres methane and dimethyl ether were

the principal products. At 1000 atmospheres the yield of isobutane decreased and that of dimethyl ether increased greatly. Pressures of 1000 atmospheres and above were too high for this catalyst, even at other temperatures. At 400°C, for example, 200 grams of dimethyl ether were formed per cubic meter of gas; at 450°C production of methane was excessive. The yields, including methane and ethane, per unit volume of synthesis gas increased with increasing pressure. Between 30 and 600 atmospheres, the relative distribution of the reaction products did not change radically, but at 1000 atmospheres 60 per cent of the total yield consisted of C₁ and C₂ hydrocarbons and dimethyl ether.

Rate of Flow of Gas. To separate the effect of gas flow from that of pressure on conversion, two series of experiments were made. In the first series at 150 atmospheres, the rate of flow was varied. In the second series, the flow was constant while the pressure was increased. The results, given

TABLE 3. EFFECTS OF PRESSURE AND RATE OF FLOW OF GAS ON THE ISOSYNTHESIS

	Pressure, (atm)	Calculated Flow of Feed Gas, (l/hr)	Flow of Exit Gas (l/hr)	Contraction (%)	CO Conversion (%)
1	150	13.4	10	25	46
2	150	7.0	5	28	53
3	150	3.6	2.5	30	58
4	300	15.9	10	37	65
5	600	20.4	10	51	83

in Table 3, indicate that the effect of pressure was much greater than that of the rate of flow: Experiments 3 and 5 show that a fourfold increase in pressure was eight times as effective as a fourfold reduction of gas flow in increasing the conversion of carbon monoxide. The conclusions are further substantiated by the fact that almost no gas was converted at atmospheric pressure, even when the throughput of synthesis gas was only $\frac{1}{30}$ of the usual rate.

Two-Stage and Recycling Operations. Figure 6 shows the results obtained when two converters were operated in a single stage with standard thoria catalyst at 150 atmospheres and 450°C (columns 1 and 2) and when the two converters were operated in series (column 3). Comparison of the data in columns 1 and 2 with row 1 of Table 3 shows that the catalysts used for the two-stage experiments were somewhat more active under similar conditions.

In the two-stage operation, liquid products were removed between stages I and II at a pressure of 150 atmospheres and at -25°C. Conversion of carbon monoxide in this and other two-stage experiments was consider-

ably higher than in otherwise comparable single-pass experiments. As was to be expected from the increased hydrogen consumption, formation of hydrocarbon gases was somewhat higher in the two-stage than in the single-stage operation. For approximately the same contact time, operation in two stages at 150 atmospheres produced about the same total yield as

	1 Reactor I	2 Reactor II	3 Reactor I + II (2-stage operation)	4 No recycling	5 Recycling
Temperature, °C.	450	450	450	475	475
Pressure, atmos.	150	150	150	30	30
Space velocity, l. in-gas/28 g. ThO ₂ /hr.	11.4	13.7	6.0	11.4	12.4
Fresh gas ratio, H ₂ :CO	1.13	1.13	1.13	1.11	1.11
Usage ratio, H ₂ :CO	0.78	0.83	0.95	0.88	1.50
Recycle gas/fresh gas	0	0	0	0	6
CO conversion, %	55	50	75	40	32

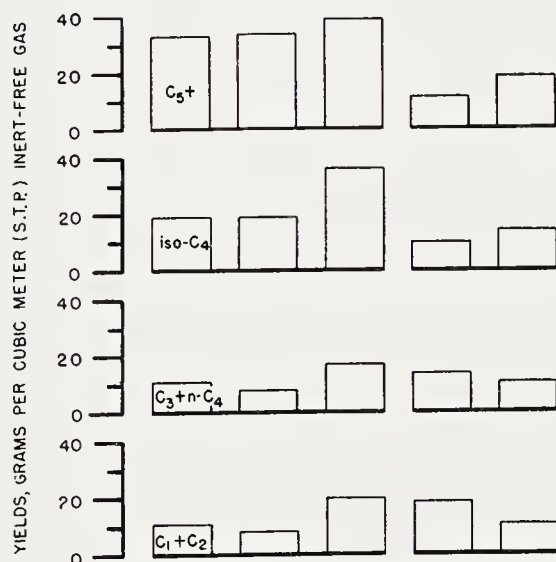


Figure 6. Effect of mode of operation with ThO₂ on product distribution from isosynthesis.

operation in a single stage at 300 atmospheres. However, the space velocity of synthesis gas at 150 atmospheres was half that used at 300 atmospheres. When, in a similar experiment, the temperature of stage I was adjusted to 430°C and that of stage II to 470°C, conversion was distributed more equally between the reactors, and the yield of hydrocarbons was increased to 125.7 grams (37.6 per cent liquids, 26.8 per cent *iso*-C₄ hydrocarbons) per cubic meter of inert-free feed gas.

In recycle experiments (for apparatus see Figure 3), the liquid products

and less volatile hydrocarbons were removed after each pass in a pressure separator at -25°C . Fresh gas was continuously added and a portion of the total gas removed at the hourly rate of 10 liters per 28 grams of thoria. The ratio of fresh to recycled gas was 1:6. The results from a single-pass and a recycle test are compared in columns 4 and 5 of Figure 6. Recycling decreased the consumption of carbon monoxide and increased that of hydrogen. More water and liquid hydrocarbons were obtained, although the total hydrocarbon yields were approximately the same for both methods of operation. Recycling thus offered a means of varying the usage ratio over a relatively wide range.

Multicomponent Catalysts

Experiments with catalysts consisting of more than one component were made to determine which compounds were suitable promoters for thoria and whether multicomponent catalysts could be substituted for thoria.

Phosphoric Acid-, Iron-, and Copper-Thoria. Thorium phosphate (like silicate and borate) was inactive, but powdered thoria impregnated with phosphoric acid gave a small yield of liquid hydrocarbons. Methane production was high.

Yields of liquid hydrocarbons and alcohols decreased with increasing iron contents of thoria. The amounts of C_3 and C_4 hydrocarbons remained unchanged, whereas formation of C_1 and C_2 hydrocarbons (principally methane) increased. Thus, even small amounts of iron were undesirable.

Results obtained with $100\text{ThO}_2\text{-}0.25\text{Cu}$ at 75 atmospheres and 450 or 475°C were essentially the same as those obtained in the absence of copper. Experiments with $1\text{ThO}_2\text{-}1\text{Cu}$ at 30 atmospheres and the same temperatures produced hydrocarbon mixtures of low molecular weight, higher yields of water-soluble products, and free carbon.

Thoria- and Alumina-Chromia. A chromia-thoria catalyst, operated at 450°C and 300 atmospheres, yielded more *iso*- C_4 hydrocarbons (34.2 g/m^3 of inert-free feed gas) than a straight thoria catalyst (22.7), but considerably less than a $100\text{ThO}_2\text{-}20\text{Al}_2\text{O}_3$ catalyst (47.2).

A temperature of 500°C was apparently *necessary* for synthesis at 30 atmospheres with a chromia-alumina catalyst because of its low activity, and *possible* because of the slow rate of formation of carbon. The yields of liquid hydrocarbons were small (5 to 10 g/m^3 of inert-free synthesis gas), but these hydrocarbons were almost entirely aromatic, containing benzene, toluene, xylene, and probably mesitylene. The aromaticity may be due in part to the high temperature.

Thoria-Alumina. The first ten columns of Figure 7 show the results obtained with coprecipitated thoria-alumina catalysts. The presence of up to 40 per cent of alumina had no appreciable effect on the conversion of

carbon monoxide, yields of water-soluble alcohols (chiefly methanol), and amount of branching of the C_4 fraction at a given temperature. Alumina did, however, increase the usage ratio because of the higher conversion of hydrogen. Higher yields of methane and C_4 -hydrocarbons and decreased yields of C_2 , C_3 , and liquid hydrocarbons and of oil-soluble alcohols were observed. More unsaturates were produced at lower temperatures: The isobutene content of the C_4 fraction was 6 per cent at 475°C , 18 per cent

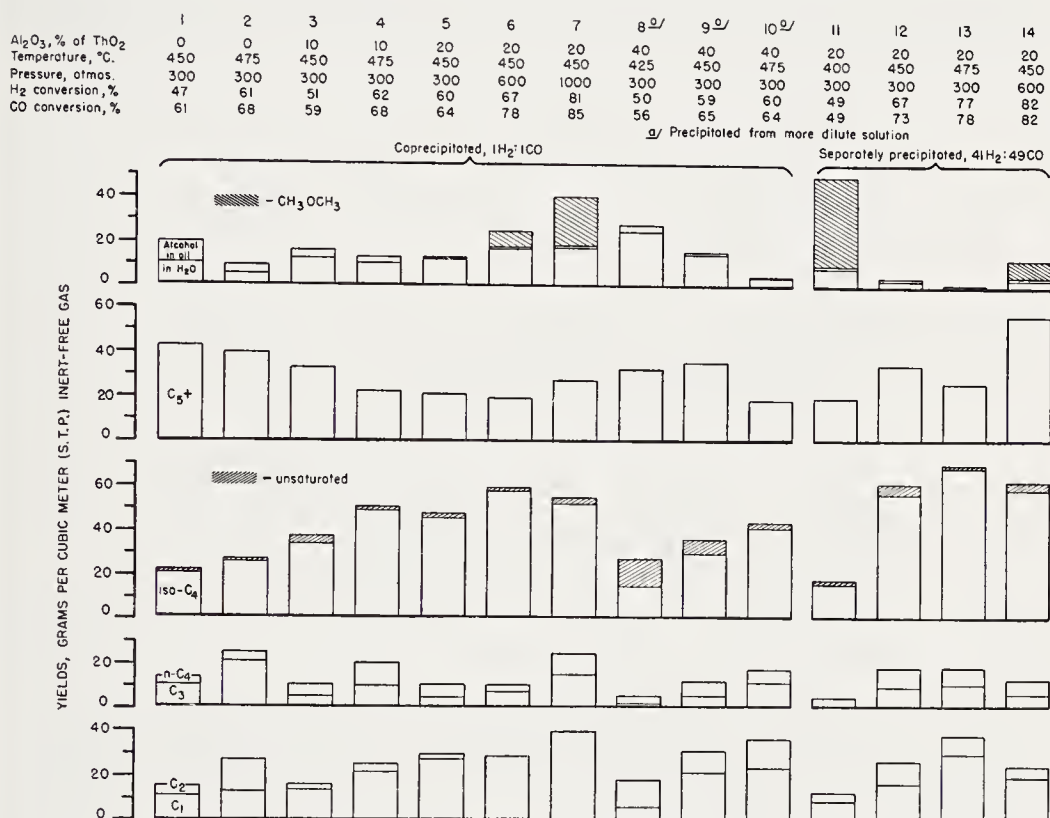


Figure 7. Effect of alumina on thoria in isosynthesis (catalyst sintered in air at 300°C ; 10 liters of outlet gas per 28 grams of ThO_2 per hour).

at 450°C , and 46 per cent at 425°C . Increased temperature and pressure increased the conversion of carbon monoxide and (up to 600 atmospheres) the $iso\text{-}C_4$ yield. The optimum pressures ranged between 300 and 600 atmospheres and optimum temperatures between 450 and 475°C . Under otherwise identical conditions, addition of up to 20 per cent of alumina (the optimum amount for maximum formation of $iso\text{-}C_4$) more than doubled the yield of $iso\text{-}C_4$ hydrocarbons.

An experiment made with a separate layer of alumina, which was placed immediately after a layer of thoria, gave total yields of $iso\text{-}C_4$ and liquid hydrocarbons similar to those obtained with an alumina-free thoria cata-

lyst; the alcohol yield was small and methane yield large. Thus, no advantage was gained from using successive layers of thoria and alumina.

A catalyst containing 100 parts of thoria, 20 alumina, and 10 kieselguhr formed excessive amounts of methane at 300 atmospheres and 425°C; little liquid and "gasol" product was formed, and about one-third of the total C_4 hydrocarbon fraction was straight-chain product. Kieselguhr is therefore not a desirable catalyst constituent for the isosynthesis.

Catalysts in which the separate thoria and alumina precipitates were mixed while wet produced exceptionally good yields of *iso*- C_4 hydrocarbons

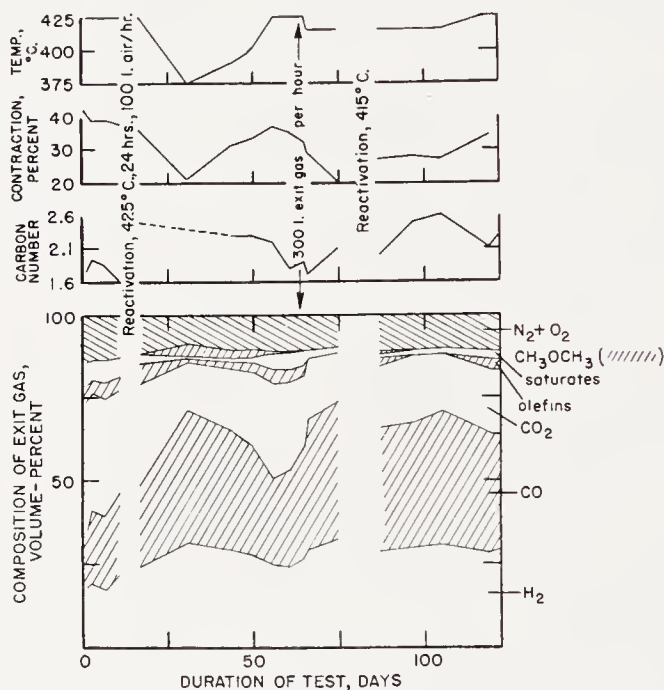


Figure 8. Life test of $100\text{ThO}_2\text{-}20\text{Al}_2\text{O}_3$ at 300 atmospheres with $1\text{H}_2\text{:}1\text{CO}$ (205 liters of exit gas per hour except as shown).

and only very small amounts of alcohols when operated at 450 to 475°C and 300 to 600 atmospheres (Figure 7, columns 11–14), proving that simultaneous precipitation of the oxides was not necessary.

A durability test with $1\text{H}_2\text{:}1\text{CO}$, at 300 atmospheres and various temperatures was made with 684 grams of 100:20 thoria-alumina, prepared by separate precipitation and mixing. The converter was 165 cm long and 2.2 cm in diameter. The usual gas throughput was 205 liters of outlet gas per hour. The recorded temperatures are those of the aluminum furnace surrounding the converter tube. Allowing for the difference in heat removal, the initial temperature of 425°C corresponded to 450–475°C in the small-scale experiments. The results are summarized in Figure 8; detailed analyses are given later.

During the first 13 days the activity was high. Relatively large amounts

of hydrocarbon gas were formed but no dimethyl ether. By the 14th day the conversion of carbon monoxide had dropped from 82 to 70 per cent and hydrogen from 74 to 65 per cent. The increased pressure drop across the catalyst bed indicated that reactivation was necessary. 100 liters of air per hour were passed over the catalyst at 425°C for 24 hours, until no more carbon dioxide was in the exit air. After treatment the pressure drop across the bed was again small. When operation was resumed at 425°C, conversion of carbon monoxide was approximately the same as initially. However, little hydrocarbon gas was being formed, and the conversion of hydrogen showed a corresponding drop from 65 to 60 per cent. On the

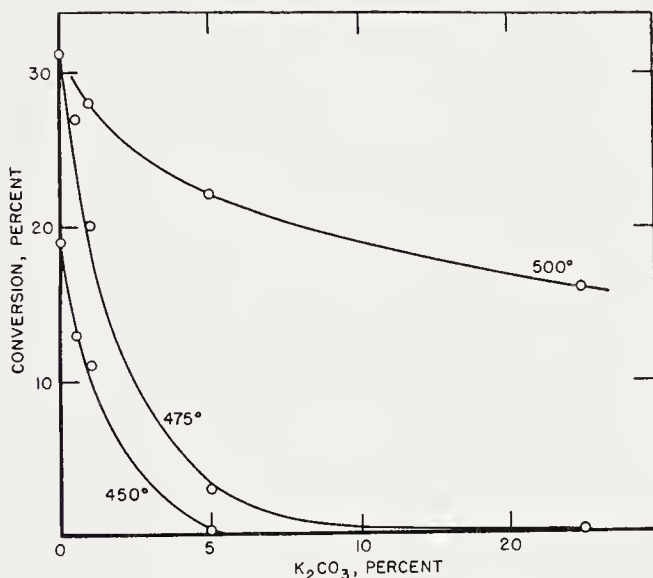


Figure 9. Effect of alkali in thoria on the isosynthesis (30 atmospheres, 10 liters of exit gas per hour per 28 grams of ThO₂, various temperatures).

17th day the temperature was decreased to 375°C to obtain sufficient liquid product at that temperature for detailed characterization. Conversion of both hydrogen and carbon monoxide was 38 per cent. Beginning with the 42nd day, the temperature was gradually increased to 425°C again. Simultaneously, contraction increased and the dimethyl ether content decreased. At 425°C conversion was approximately the same as that observed on the 18th day. The gas throughput was temporarily increased from 205 to 300 liters from the 63rd to the 65th day. The 55 per cent conversion of hydrogen and carbon monoxide during that period indicated that the gas throughput can be increased considerably when heat removal is good. The experiment was terminated after 122 days.

Thoria-(Alumina)-Alkali. A series of experiments with thoria containing potassium carbonate showed that the activity decreased with increasing alkali content, especially at lower temperatures (Figure 9; the

abscissa of this figure^{10, 11} appears to be in error). The yields of low-boiling liquid and gaseous hydrocarbons decreased more rapidly than those of higher hydrocarbons. This finding was probably the basis for patent application St 62,438 which indicates that formation of gas can be greatly diminished by operating at temperatures lower by as much as 50 to 100°C than those given in application St 61,125. The increased activity necessary for this modification of the process may have been gained by (1) thorough removal of alkali by washing of the thoria with boiling water and (2) drying the catalyst in air at 300°C before use.

On the other hand, the presence of alkali may be desirable for shifting the product distribution. In the presence of 1 per cent of alkali, the activity was lower but synthesis at 30 atmospheres and 500°C became possible without excessive formation of methane. The liquid hydrocarbons from one such test contained 42 per cent naphthenes, 8 aromatics (principally toluene), and 3 phenols, i.e., more than 50 per cent of cyclic compounds. Again, the high temperature may have had a considerable effect on the aromaticity of the product.

The first two columns of Figure 10 indicate that addition of only 0.6 per cent of potassium carbonate increased the yields of liquid hydrocarbons and higher alcohols (principally isobutanol), while decreasing the yields of lower hydrocarbons (C_1 - C_4) and methanol. The effect of small amounts of alkali was thus similar to that obtained in the Fischer-Tropsch synthesis.

Columns, 3, 4, 5 and 6 of Figure 10 summarize the experiments conducted with thoria-alumina catalysts containing potassium carbonate. Column 5 shows the highest *iso*- C_4 hydrocarbon yield; 2-methylbutane comprised 30 to 50 per cent of the liquid reaction products. Thus, about 100 grams of *iso*- C_4 and $-C_5$ hydrocarbons were produced per cubic meter of inert-free synthesis gas. When the alkali was added to thoria (column 6), higher liquid and much lower gas yields were observed. Thoria-free alumina with and without alkali (columns 7 and 8) was a very poor catalyst.

Thoria- and Alumina-Zinc Oxide. Columns 1 to 4 of Figure 11 show that raising the temperature from 425 to 450°C and the pressure from 150 to 300 atmospheres increased the conversion of synthesis gas by inversely coprecipitated thoria-zinc oxide catalysts (see p. 460). Experiments 3 and 4, run with duplicate catalysts and about 0.9H₂:1CO, permit an estimate of the reproducibility of the activity tests. In an otherwise identical experiment with 1.25H₂:1CO, i.e., a hydrogen-rich gas, less hydrogen was used and less liquid product and saturated *iso*- C_4 were produced. A catalyst made by normal coprecipitation (test 5) also gave poor liquid yields. Similar results were obtained with a preparation that was inversely precipitated from more dilute alkali solution (86 grams Na₂CO₃ in 2 instead of 1 liter of H₂O); the durability of this catalyst was poor.

Important advantages of the thoria-zinc oxide catalysts were their tendency to form liquid products and lack of carbon deposits. Even after prolonged operation, their color remained white or pale grey. Catalysts

	1	2	3	4	5	6	7	8
ThO ₂ , weight-%	100	100	100	100	100	100	0	0
Al ₂ O ₃ , weight-%	0	0	20	20	20	20	100	100
K ₂ CO ₃ , weight-% of ThO ₂	0	0.6	0	0.2	0.6	0.6 (added to ThO ₂)	0	3 (based on Al ₂ O ₃)
H ₂ conversion, %	—	—	67	68	75	—	—	—
CO conversion, %	62	62	73	72	78	70	24	25

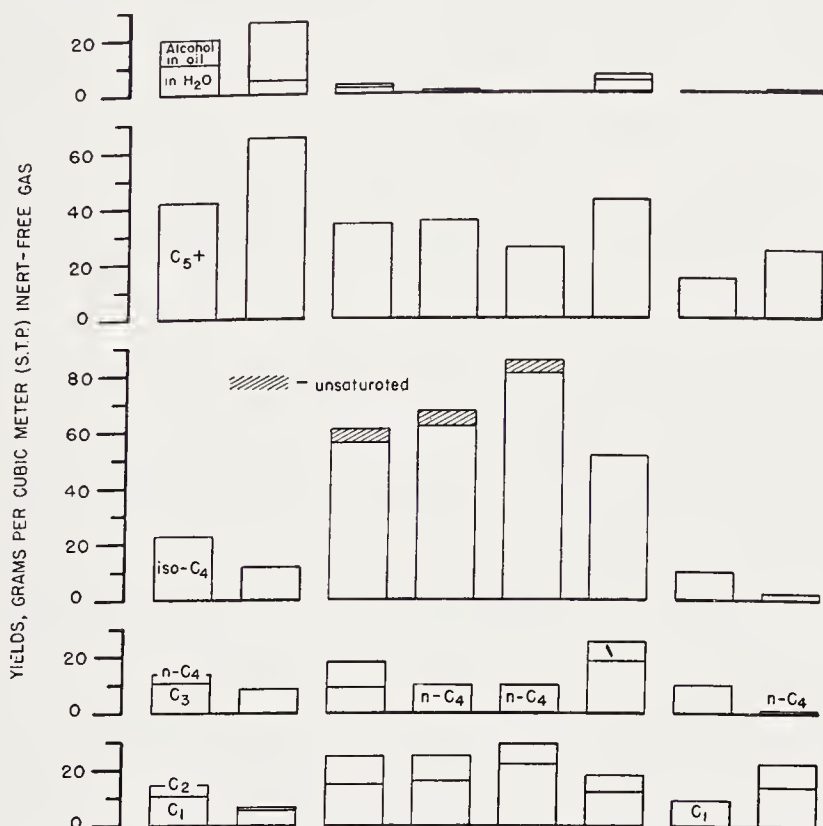


Figure 10. Effect of alkali on ThO₂, Al₂O₃, and ThO₂-Al₂O₃ in isosynthesis with 41H₂:49CO at 300 atmospheres and 450°C (10 liters of outlet gas per 28 grams of ThO₂ or 25 cubic centimeters of catalyst per hour).

prepared by inverse coprecipitation (nitrate added to precipitant) produced exceptionally high yields of liquid hydrocarbons.

Although neither alumina nor zinc oxide alone was satisfactory for the isosynthesis, each was a promoter for thoria. Alumina increased the production of gases (particularly isobutane) and zinc oxide increased liquid hydrocarbons. Hence alumina-zinc oxide preparations were thought to be possible substitutes for thoria. Tests 6 to 9 of Figure 11 contain data on experiments with such inversely precipitated catalysts, the space-time yields of which were inferior to those of thoria preparations. The specific

yield at 150 atmospheres was increased by reducing the hourly gas throughput by 50 per cent, but this lowered the space-time yield still further. Comparison of experiments 8 and 9 shows that a fairly high alumina content

	1	2	3	4	5 (Normal pptn.)	6	7	8	9	10 ThO ₂ and ZnO from nitrates, Al ₂ O ₃ from aluminate
ThO ₂ , weight-%	75	75	75	75	75	0	0	0	0	59
Al ₂ O ₃ , weight-%	0	0	0	0	0	39	39	39	56	11
ZnO, weight-%	25	25	25	25	25	61	61	61	44	30
Temperature, °C.	425	450	450	450	450	425	450	450	450	450
Pressure, atmos.	150	150	300	300	300	150	150	300	300	300
H ₂ conversion, %	49	65	69	69	67	31	34	50	51	—
CO conversion, %	49	64	77	73	70	36	42	58	63	—

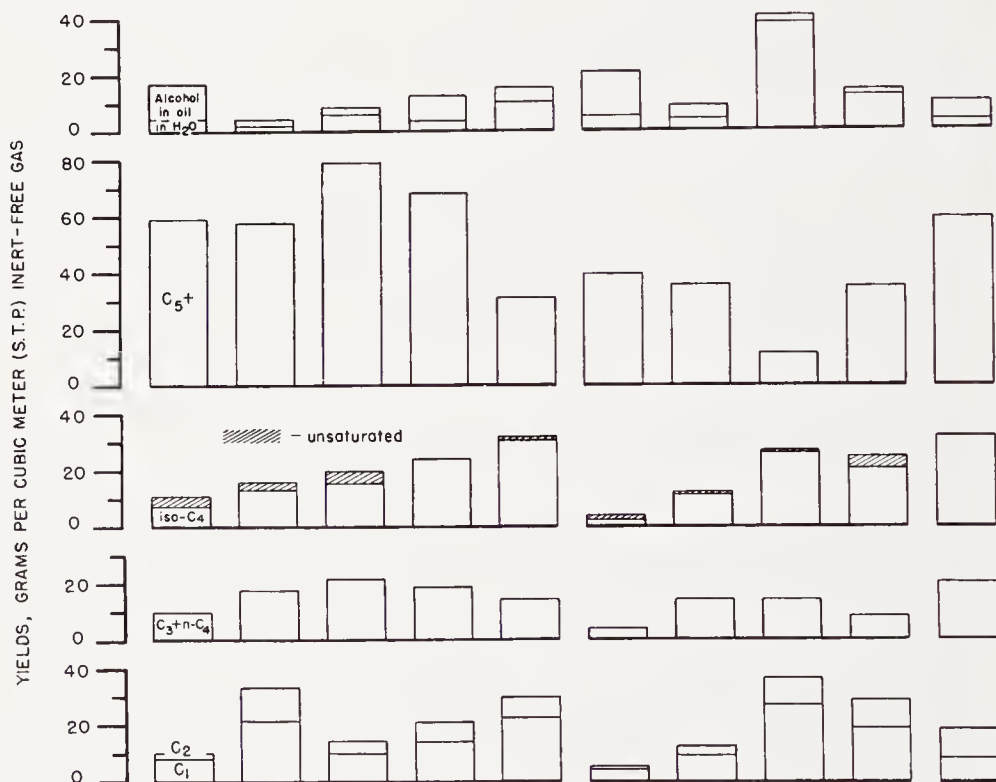


Figure 11. Effect of zinc oxide on thorium, alumina, and thorium-alumina in isosynthesis (10 liters of outlet gas per 28 grams of ThO₂ or 25 cubic centimeters of catalyst per hour).

was necessary to lower the production of alcohol. Alumina-zinc oxide (mole-ratio 1:1), prepared by separate precipitation of the oxides with sodium carbonate, had a very low bulk density and would probably have given even lower space-time yields. However, availability and low cost of these catalytic materials might make them attractive for a large-scale process, even though the specific yields of *iso*-C₄ plus liquid hydrocarbons

were only one-third to one-half of those obtained with thoria-alumina-(alkali) catalysts. Patent application St 62,589 mentions that part or all of the thoria may be replaced by oxides of elements from groups III to VI of the periodic table to which a smaller amount of zinc oxide should be added; the only example given is an experiment with an alumina-zinc oxide preparation. Separate, successive layers of zinc oxide and alumina produced principally methane.

A catalyst containing thoria, alumina, and zinc oxide, tested at 300 atmospheres and 450°C, produced 59.2 grams of C_5+ and 31.7 grams of *iso*- C_4 hydrocarbons per cubic meter of inert-free feed gas (test 10, Figure 11). These yields were similar to those obtained with thoria-zinc oxide catalysts (test 4). The C_5+ yield was larger and the *iso*- C_4 yield smaller than in most tests of thoria-alumina catalysts (see Figure 7).

Conversion of Dimethyl Ether

The amounts of dimethyl ether obtained in the isosynthesis were quite small below 300 atmospheres but increased with pressure, until, in some cases, dimethyl ether was the principal product at 1000 atmospheres. At high temperatures, or in the presence of particularly active catalysts, the yield of dimethyl ether decreased and that of hydrocarbons increased. Since dimethyl ether was believed to be a possible intermediate product of the isosynthesis, some experiments were made at 450°C to determine the nature of the compounds obtained by passing dimethyl ether over thoria. In all cases, the carrier gas—nitrogen or hydrogen—was saturated with dimethyl ether at various temperatures by passing it through liquid dimethyl ether under pressure. The results are summarized in Figure 12.

With dimethyl ether and nitrogen, no *iso*- C_4 hydrocarbons were produced at 1 atmosphere. At 30 atmospheres, *iso*- C_4 hydrocarbons were obtained in the first few hours of the test, but none could be detected subsequently. Furthermore, the carbon number of the products decreased with time, and the activity of the catalyst diminished rapidly. Pichler stated that insufficient hydrogenation of the products led to clogging of the catalyst and loss of activity¹⁷. The decrease of conversion with time is compared in Figure 13 with the constant conversion obtained when nitrogen was replaced by hydrogen. Under these conditions, the fraction of *iso*- C_4 produced remained constant throughout the duration of the runs.

With zirconium oxide, 19.3 per cent of dimethyl ether was converted to *iso*- C_4 hydrocarbons at 150 atmospheres and 450°C. Under the same conditions, the reaction over cerium oxide produced 6.5 per cent conversion. No *iso*- C_4 hydrocarbons were obtained with zinc oxide or alumina. With diethyl ether and hydrogen, C_2 , C_3 , and liquid hydrocarbons but neither isobutane nor isobutene were obtained over thoria.

Thus, in the presence of hydrogen under pressure, the catalytic decomposition of dimethyl ether but not of diethyl ether results in products obtained in the isosynthesis. Patent application St 62,439 covers this process which offers a potential saving in the cost of the catalyst. Cheaper

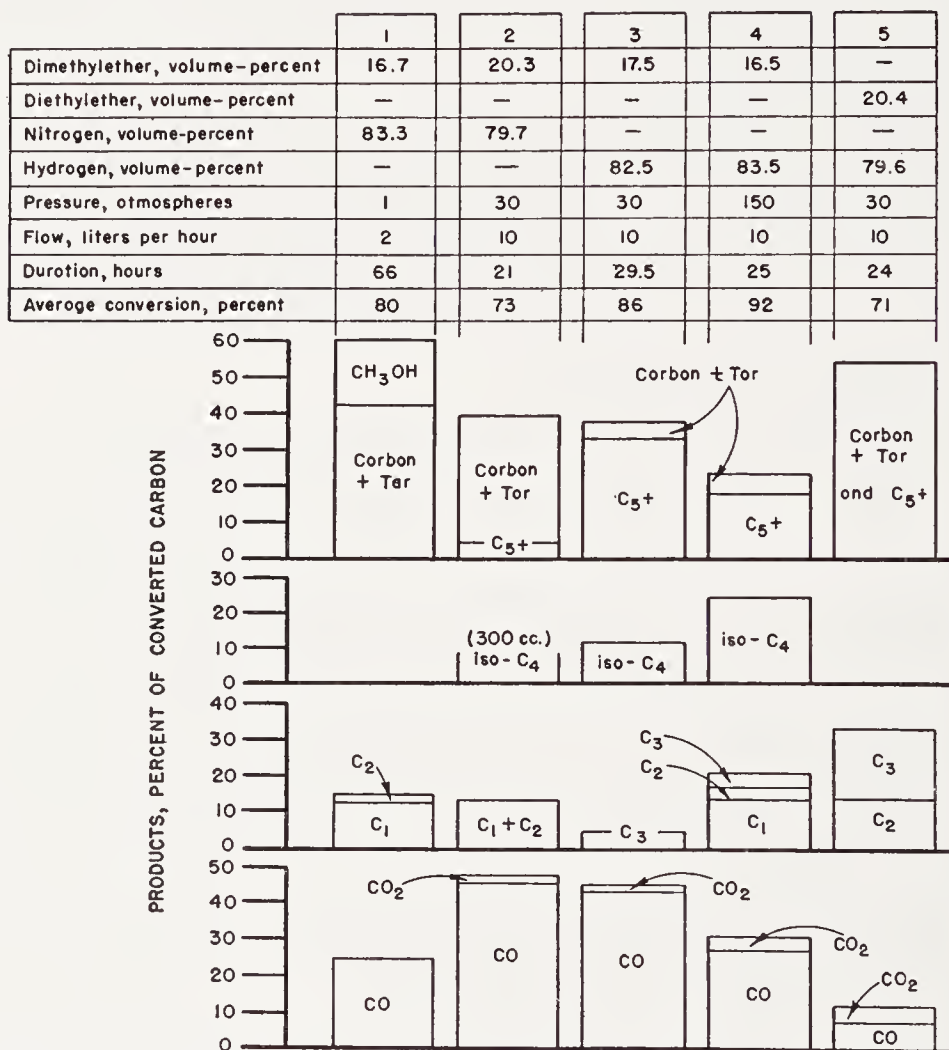


Figure 12. Products from conversion of ethers over thoria at 450°C (C₁ through C₅+ are hydrocarbons).

catalysts may be used to prepare methanol and dimethyl ether, thus relieving the load on the expensive thoria. An experiment with a 1:5 mixture of ether and hydrogen at 450°C and 300 atmospheres is cited, in which 35 per cent ether was converted to *iso*-C₄ and 25 per cent to liquid hydrocarbons.

DETAILED CHARACTERIZATION OF PRODUCTS

In addition to the summary analyses already reported, detailed analyses of gases and liquids were made in a number of tests where sufficient product

was collected for this purpose. The liquids generally, though not always, formed an oil and an aqueous layer. The former contained virtually all of the hydrocarbons; the oxygenates were distributed between the two layers according to their solubilities. Only the final analytical results are given

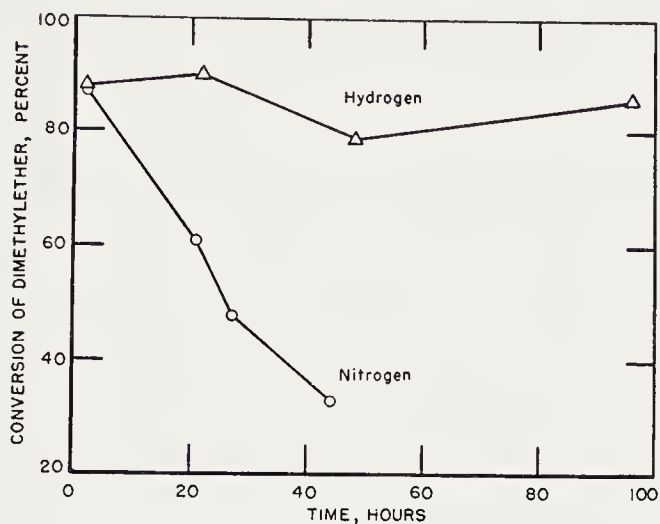


Figure 13. Effect of carrier gas on conversion of dimethylether at 30 atmospheres.

TABLE 4. ANALYSIS OF PRODUCT FROM DURABILITY TEST

Synthesis Temp. (°C)	425	375
Yields, g/m ³ of inert-free feed gas		
Methane	19.5	0.7
Ethylene	1.0	0.5
Ethane	6.2	0.3
Propene	1.3	0
Propane	5.5	0
<i>i</i> -Butene	7.8	5.2
<i>i</i> -Butane	60.7	4.5
<i>n</i> -Butene	3.5	1.0
<i>n</i> -Butane	6.7	0.3
C ₅ + hydrocarbons	20.0	11.6
Alcohols (mainly methanol)	2.5	6.7
Dimethyl ether		65.7

here; particulars of the techniques may be found in References 11, 12 and 13.

Hydrocarbons

An analysis of light hydrocarbons is shown in Table 4. These were collected at 425°C during the first 13 days and at 375°C from the 18th to the 42nd day of the durability test described on pp. 464 and 465. Particularly

noteworthy is the fact that almost fifteen times as much isobutane was obtained at 425° as at 375°C.

The olefinic and aromatic contents of the same products were determined by distillation of the unhydrogenated liquids. No attempt was made to isolate individual hydrocarbons. Table 5 indicates that the average olefin content of the 425°C product was 39 per cent; calculated for an average carbon number, it was 34 per cent. The total olefin content of the 425°C product was lower than that of the 375°C product (76 per cent). This temperature effect is the opposite of that observed in the Fischer-Tropsch synthesis. Except for the lowest-boiling fraction, the olefinic and aromatic contents increased with increasing boiling points of the fractions. The

TABLE 5. OLEFINS AND AROMATICS IN LIQUID PRODUCTS FROM DURABILITY TEST

Boiling range (°C)	Product Collected at:					
	425°C				375°C	
	Vol.-per cent	Average C-No.	Olefins	Aromatics	Olefins	Aromatics
			(wt-per cent)		(wt-per cent)	
21-65	46.0	5.33	39	0	—	—
65-95	15.2	6.87	25	0	51	0
95-125	10.9	7.72	31	0	89	0
125-150	10.9	8.89	50	5	91	0
150-175	5.4	~9.9	55	3	—	—
175-195	5.0	~11	62	31	—	—

trend of the olefin content is also opposed to that in the Fischer-Tropsch process.

Results obtained with the hydrogenated liquid products of four experiments are summarized in Figure 14; product C is probably from the durability test¹¹, although it is stated to have been obtained with 100ThO₂:10Al₂O₃¹². In all cases, the extent of branching of paraffins and naphthenes increased with increasing molecular weight. A similar effect, though not as great, has been observed in Fischer-Tropsch products. Furthermore, alumina appeared to favor multiple branching and formation of products containing quaternary carbon atoms. The abundance of such compounds also increased with higher molecular weight.

The thoria-containing catalysts, especially the one with alkali, produced more naphthenes than the others, probably from branched paraffins by secondary reactions. The naphthenic content increased with increasing boiling points of the distillate fractions: While the low-boiling fractions

of product C contained no naphthenes, the 64–86°C fraction contained about 13 volume-per cent, the 86–103°C fraction 46 per cent, and the 103–140°C fraction 74 per cent. More precise fractionation showed the fraction boiling at 104–106°C to be 100 per cent naphthenic; between 108 and 114°C the naphthene content dropped to 30 per cent, then rose again to 100 per cent at 134°C. The low naphthene content in the middle of this temperature region was caused by the presence of octanes.

The 150 to 200°C fraction of the 375°C product from the life test had a

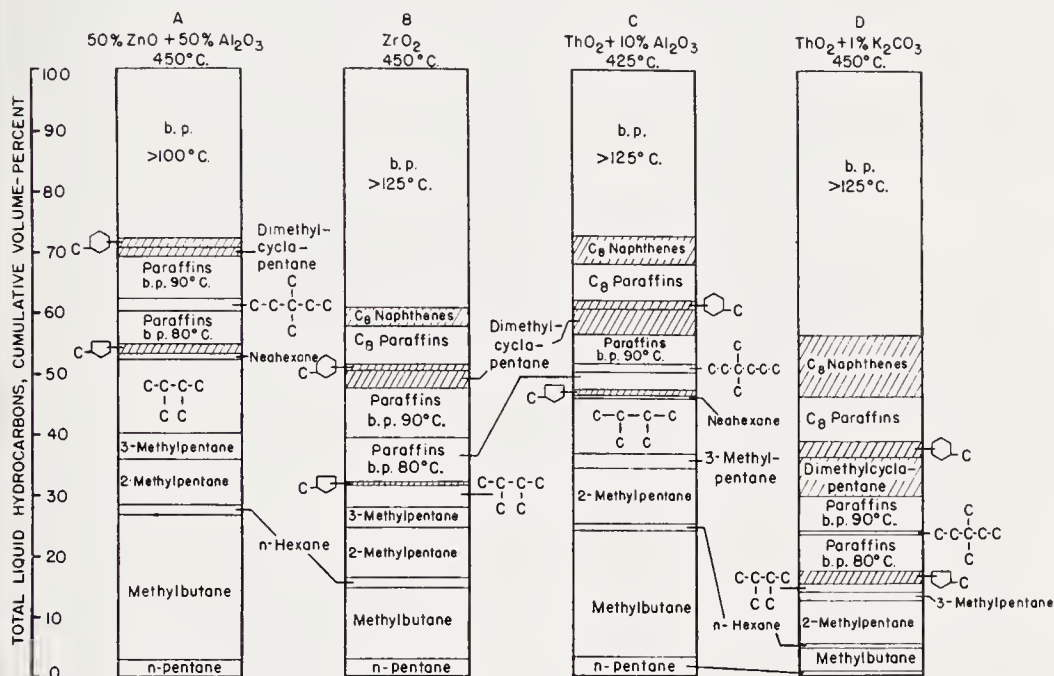


Figure 14. Distribution of hydrogenated liquid hydrocarbon products from several isosynthesis experiments at 300 atmospheres (Naphthenic compounds are indicated by /////).

strong terpene odor and reacted violently with bromine. Six grams of hexamethylbenzene were recovered from the 200–275°C fraction of the same product.

Oxygenated Products

Ten analyses of oxygenated products are given in Figure 15. Traces of isopropanol, 2-methylpropanol-2, and tertiary butanol were also found in some of these samples. The C_5 group contained mostly 2-methylbutanol-1, C_6 mostly 2-methylpentanol-1, and C_7 mostly 2,4-dimethylpentanol-1; the ethers were methylisobutyl and some di-isobutyl ether. Aldehydes plus ketones were calculated as isobutyraldehyde, esters as isobutyric-isobutyl ester, and acids as isobutyric acid. Comparison of Columns A,

E, and C indicates that up to 1 per cent of potassium carbonate in these, as in alcohol catalysts, increased the yield of higher alcohols. However,

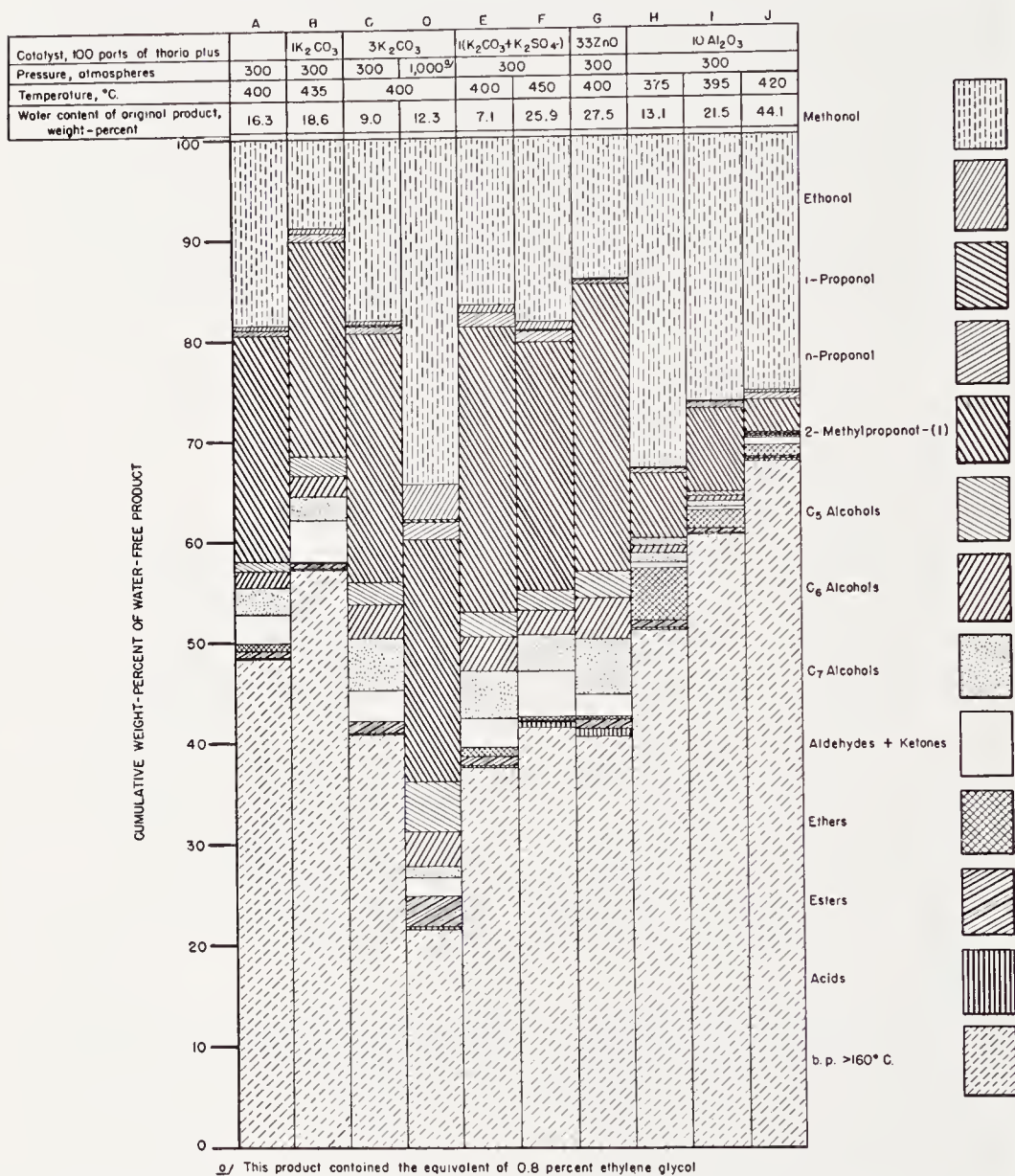


Figure 15. Oxygenated products from various isosynthesis experiments with 1.2H₂:1CO.

the same effect was also obtained by adding zinc oxide to thorio (G), even though zinc oxide by itself is a catalyst for the synthesis of methanol; in this experiment, the methanol content was actually smaller than in that with a pure thorio catalyst (A). Alumina performed according to expectation: Although the methanol content of the product from experiment (I)

was high compared with that of experiment (A), most of the higher alcohols were dehydrated, and the amounts of water and ethers had been increased accordingly.

Higher temperatures caused decreases in the alcohol yields and corresponding increases in water yields, probably because of greater dehydrogenation activity of the catalysts (compare E and B; H, I, and J). The ether contents also decreased with increasing temperature. A pressure increase from 300 to 1000 atmospheres (C and D) effected a large increase in the relative yields of methanol, ethanol, and propanol, virtually no change in isobutanol, and a decrease of alcohol yield with increasing carbon number from C_5 on. At 300 atmospheres, the C_5 to C_7 alcohol yield either increased or at least did not change with increasing carbon number.

DETERMINATION OF MOTOR OCTANE NUMBER

The most abundant constituents of hydrocarbon product C (Figure 14), 2-methylbutane, 2-methylpentane, and 2,3-dimethylbutane had motor octane numbers of 89, 73, and 95. Simple calculation—disregarding deviations due to mixing—showed octane numbers of about 80 for the 72 per cent of total liquid boiling below 130°C , 82.5 for the 62 per cent below 100°C , and 84 for the 47 per cent below 75°C . Actual tests made on mixtures obtained with thoria and thoria-alumina catalysts gave motor octane numbers of 77.3 to 80.5 before and (in one case) 89.9 after addition of 0.08 per cent of TEL. Addition of the same amount of TEL to a mixture, containing 6 parts of alkylation gasoline as commercially available and 1 part of primary product boiling below 180°C , should result in a calculated octane number of 99.2.

MECHANISM OF SYNTHESIS AND FUNCTION OF CATALYST

During the time of the laboratory-scale development of the isosynthesis in Germany, large-scale industrial expansion of catalytic cracking of petroleum took place in the United States, the primary purpose of both processes being the production of aviation gasoline⁷. About the mechanism of the latter process, Oblad, Milliken, and Mills⁸ said that:

“For the most part, the suggestions concerning the gross aspects of the mechanisms involved in catalytic cracking have been deduced from the distribution of the products obtained. The cracking of pure compounds has shown that many of the secondary reactions occur very rapidly. The primary reactions are, therefore, obscure and any conclusions regarding the nature of the primary products obtained in catalytic cracking which are based on extrapolation of the product composition to zero time are, therefore, highly uncertain. . . . Catalytically cracked products . . . contain hydrocarbons with a high ratio of isoparaffins to normal paraffins (exceeding

vestigated. . . . The equilibrium constants of Eqs. (1) and (2) decrease rapidly with increasing temperature, and the temperatures at which the equilibrium constants equal 1 may be taken as the upper limits at which sizable yields of alcohols may be obtained at low operating pressures. For reactions (1) and (2), respectively, these temperatures are 238 and 318°C for ethyl alcohol, 316 and 358°C for 1-propanol, and 330 and 378°C for 1-butanol. For methanol, Eqs. (1) and (2) are identical and the equilibrium constant is unity at 146°C. Thus, at any given temperature, reactions of the second type are thermodynamically favored over corresponding reactions of the first type and the synthesis of alcohols of higher molecular weight is more likely thermodynamically than alcohols of lower molecular weight in both cases. However, the production of paraffins and olefins is thermodynamically favored over that of alcohols under synthesis conditions. In addition, dehydration of alcohols to olefins and their subsequent hydrogenation to paraffins are thermodynamically possible under most synthesis conditions. Hence, the production of alcohols depends upon the selectivity of the catalyst as well as upon thermodynamics."

At higher temperatures, catalytic dehydration of alcohols led to the formation of ethers and, under more severe conditions, of hydrocarbons and water. Similarly, reaction of dimethyl ether with two moles of formaldehyde to yield isobutanol and two moles of water, or dehydration of dimethyl ether to ethylene and water, and reaction of ethylene with another molecule of dimethyl ether to yield isobutene and water have been assumed to account for the product distribution obtained in the experiments with dimethyl ether¹¹. The tendency of alcohols toward dehydration increased with molecular weight and extent of branching. The occurrence of cyclic hydrocarbons and lack of cyclic alcohols indicate that ring formation took place during or after dehydration of the alcohols. Paraffins were presumably produced by hydrogenation of olefins.

Concerning the higher (presumably C₅+) olefins, Pichler and Ziesecke stated that their formation by dehydration of higher alcohols over thoria is accompanied by equilibration of isomers. Whether synthesis gas might inhibit isomerization during the synthesis appears not to be known, however. They suggested that lack of isomeric equilibrium of olefins produced in the isosynthesis and the virtual absence of C₅+ alcohols below 300 atmospheres indicate that the bulk of the olefins was not formed by direct dehydration of the corresponding alcohols¹¹. Instead, these olefins were probably formed by dehydration of alcohols of lower molecular weight and polymerization of the resulting olefins. Since thoria promotes isomerization of olefins more than their hydrogenation at the temperatures of the isosynthesis, isomerization may have proceeded faster than hydrogenation in some cases. If, furthermore, isomerization of paraffins over thoria

is assumed to be negligible, their composition must correspond to that of the olefins.

A mechanism of growth of straight chains and subsequent isomerization of paraffins is ruled out from consideration of Figure 17, which shows the isomerization equilibrium of butane as a function of temperature. While the Fischer-Tropsch reaction at atmospheric pressure resulted in less than 10 per cent of isobutane at 190°C, indicating that growth of straight chains predominated, the isosynthesis yielded less than 10 per cent of normal butane at 450°C, an isomer ratio that would have been impossible to attain by isomerization of *n*-butane in the whole range of temperatures shown in this figure. The same reasoning applies to the pentane and hexane fractions.

Since by far the largest portion of the higher hydrocarbons could not have been formed by isomerization of normal paraffins nor by dehydration

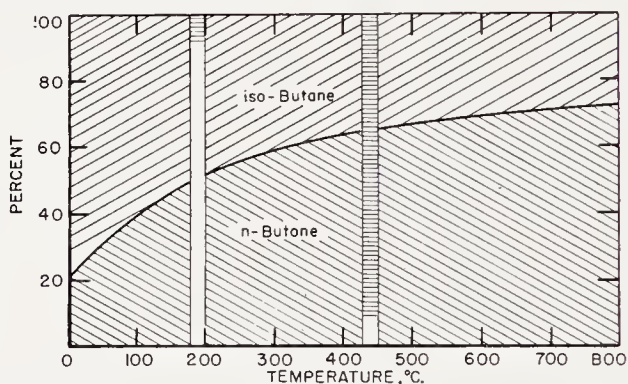


Figure 17. Isomerization equilibrium of butane (columns indicate distribution of product from Fischer-Tropsch synthesis at 190°C and from isosynthesis at 450°C).

of the corresponding alcohols, they must have resulted from polymerization, alkylation, and cyclization, mainly of C_2 to C_4 hydrocarbons. Also, because of the low concentration of olefins, alkylation probably occurred more rapidly than polymerization. Chromia, a dehydrogenation catalyst, was most active in cyclization; thoria was intermediate; and alumina, a dehydration catalyst, was poorest. Equilibrium between paraffinic and cyclic compounds and between naphthenes and aromatics appears to have been closely approached in the isosynthesis, at least at the higher temperatures. Below 400°C high-boiling, viscous polymers were formed.

Aldehydes and acids may have been formed as primary products, or the former by dehydration of the alcohols and the latter by addition of carbon monoxide to aldehyde. The large amounts of esters (formed from the acids) present at high pressure may indicate that high pressure favors their formation or—if they are formed at high temperatures and low pressures—that they can be dehydrated to yield ketones and unsaturated hydrocarbons.

Thus, the isosynthesis process appears to involve the formation of alcohols (primarily methanol and isobutanol) and their dehydration, followed by or concurrent with hydrogenation, polymerization, and alkylation. Although the functions of the catalyst are reasonably well established, the choice of the best catalytic components is still an empirical one.

Thorium, aluminum, and tungsten oxides are known to be very effective in dehydrating ethyl alcohol. These are the same oxides that were most active in the isosynthesis. However, aluminum and tungsten oxides *per se* were undesirable because of their tendency to form carbon and methane. The oxides from chromium to vanadium are not suitable catalysts for dehydration and showed little activity in the isosynthesis. The oxides from zinc to copper (the latter prepared at low temperatures) were suitable neither as catalysts for dehydration of ethanol nor as one-component catalysts for isosynthesis. In thoria-alumina catalysts, which are best for the isosynthesis, the dehydrating action of thoria is promoted by alumina. Under conditions of the synthesis, thoria is far more active than the other oxides in hydrogenating carbon monoxide to alcohol and in dehydrating the alcohol. That thoria has two primary functions in the isosynthesis is proved by the fact that it can be replaced by a two-component catalyst, zinc oxide-alumina, in which one component is a hydrogenating and the other a dehydrating agent. To obtain increased isomerization and cracking activity, Bloch and Schaad², as well as Grahame⁵ have added silica to the catalyst.

Acknowledgments

Helpful suggestions by R. B. Anderson and M. Wolfson are gratefully acknowledged.

Bibliography

1. Anderson, R. B., Feldman, J., and Storch, H. H., *Ind. Eng. Chem.*, **44**, 2418 (1952).
2. Bloch, H. S., and Schaad, R. E. (to Universal Oil Products Co.), U. S. Patent 2,389,406 (Nov. 20, 1945); *C.A.*, **40**, P1532⁹; also U.O.P. Co., British Patent 626,071 (July 8, 1949); *C.A.*, **44**, P2205f.
3. Dewey, D. R., CIOS Rept. XXV-27 (1945); PB 289; *Oil Gas J.*, **44**, No. 37, 86, 89 (1946).
4. Fischer, F., Pichler, H., and Ziesecke, K.-H. (to Studien- & Verwertungsgesellschaft m.b.H., Muelheim, Ruhr), German Patent Applications St 61,125, 62,438, 62,439, and 62,589, Class IVd/12o (1942); TOM Reels 100 and 134.
5. Grahame, J. H. (to Texas Co.), U. S. Patents 2,464,501 (March 15, 1949); *C.A.*, **43**, P4447h; and 2,503,724 (April 11, 1950); *C.A.*, **44**, P7516d.
6. Haensel, V., CIOS Rept. XXV-1 (1945); PB 284; *Natl. Petroleum News, Tech. Sect.* **37**, 955 (1945).
7. Hansford, R. C., "Advances in Catalysis," Vol. IV, Chemical Concepts of Catalytic Cracking, p. 3, New York, Academic Press, Inc., 1952.
8. Oblad, A. G., Milliken, T. H. Jr., and Mills, G. A., "Advances in Catalysis,"

- Vol. III, Chemical Characteristics and Structure of Cracking Catalysts, p. 239, New York, Academic Press, Inc., 1951.
9. Pichler, H., and Ziesecke, K.-H., *Brennstoff-Chem.* **30**, 13 (1949).
 10. Pichler, H., and Ziesecke, K.-H., *ibid.*, **30**, 60, 81 (1949).
 11. Pichler, H., and Ziesecke, K.-H., *Bur. Mines Bull.* **488** (1950).
 12. Pichler, H., Ziesecke, K.-H., and Titzenthaler, E., *Brennstoff-Chem.* **30**, 333 (1949).
 13. Pichler, H., Ziesecke, K.-H., and Traeger, B., *Brennstoff-Chem.* **31**, 361 (1950).
 14. Sellers, F. B. (to Texas Co.), U. S. Patent 2,464,532; *C.A.*, **43**, P4448a.
 15. Storch, H. H., "Advances in Catalysis," Vol. I, The Fischer-Tropsch and Related Processes, pp. 136, 454, New York, Academic Press, Inc., 1948.
 16. Storch, H. H., Golumbic, N., and Anderson, R. B., "The Fischer-Tropsch and Related Syntheses," 96, New York, John Wiley & Sons, Inc., 1951.
 17. TOM Reel 45, Bag 3441, Item 80, Frames 90-95.
 18. Ziesecke, K.-H., *Chem. Tech. & Chem-Ingenieurwesen*, **21**, 15 (1949).

CHAPTER 6

METHANATION

Murray Greyson

Physical Chemist, Bureau of Mines, Pittsburgh, Pa.

INTRODUCTION

Since 1902, when Sabatier and Senderens^{1, 2} first produced methane by passing mixtures of carbon monoxide, carbon dioxide, and hydrogen over finely divided metals, the catalytic synthesis of methane has been the subject of a large amount of experimental work. In many geographical areas where natural gas reserves are small or nonexistent, the catalytic synthesis of methane is looked upon as a possible method for obtaining large supplies of high-heating value fuel gases from coal. Methanation reactions have also been used for purifying hydrogen of undesired oxides of carbon. Another field of study has been the investigation of techniques that will prevent the methanation reactions from occurring; an experimental direction that is illustrated by the work in Fischer-Tropsch syntheses, in which methane and other low molecular-weight saturated hydrocarbons are undesirable products of the reactions of hydrogen and carbon monoxide.

Although the catalytic hydrogenation of the oxides of carbon is actually a part of the more generalized reaction systems associated with the Fischer-Tropsch syntheses, and is normally treated as such, the growing industrial interest in methanation in the United States suggests that this subject be treated as a separate and distinct entity. This chapter will, therefore, attempt to bring together some important facts concerning the reactions of hydrogen and the oxides of carbon that produce methane, the catalysts that are used to bring about these reactions, and the conditions of synthesis that appear to be best for the production of methane.

Most of the chapter emphasizes work done in the hydrogenation of carbon monoxide, and very little of the material deals with the reactions of carbon dioxide; a situation that has arisen because of the meager amount of information that is available on the latter system. This is not too serious a problem, however, since it is generally found that the catalysts which are active for the former system are also active for the latter one.

Since the subject has been actively studied for a period exceeding fifty years, the reference material is somewhat voluminous, and a selection of

references had to be made. Enough reference material is included, however, to allow detailed literature searches to be made by individuals who are interested.

CHEMISTRY AND THERMODYNAMICS OF METHANATION

Chemistry of Methanation

The catalytic production of methane from carbon monoxide and carbon dioxide can be described by the following reactions:



For all practical purposes, it can be assumed that reaction (2) is a combination of reaction (1) and the water-gas-shift reaction,



Some credence is lent to this assumption by the fact that the carbon dioxide concentrations of a product gas are observed to fall off rapidly with increases in hydrogen-carbon monoxide ratio of the synthesis gas in reaction systems that are not at equilibrium^{3, 4, 5, 6}, a phenomenon that is illustrated in Figure 1. If reaction (2) were a primary reaction, it would be necessary to postulate some mechanism by which the carbon dioxide is removed from the product gas. Only two reactions in the system can possibly serve as vehicles for the removal of carbon dioxide. The first reaction is the hydrogenation of carbon dioxide via reaction (3). Experimental evidence has shown, however, that carbon dioxide will not hydrogenate in the presence of carbon monoxide^{6, 7, 8}. The second way in which this component can be removed from the system is through the reverse of reaction (4). Examination of the free energy changes for this reaction, which are shown in Figure 2, reveals that it is extremely unlikely that carbon dioxide would be consumed in the temperature range from 200 to 400°C, the temperature range in which most previous experimental work has been done. These, plus the additional observations that the water-gas-shift equilibrium is easily satisfied over nickel catalysts⁹, a phenomenon that would make the carbon dioxide concentration extremely sensitive to the concentration of carbon monoxide in the system, indicate that reaction (2) is not a primary reaction.

Another reaction that occurs to a varying extent during the catalytic synthesis of methane is a decomposition of carbon monoxide to carbon and carbon dioxide,



This reaction is of interest because it tends to reduce the efficiency of a process by consuming carbon monoxide, and because the deposition of

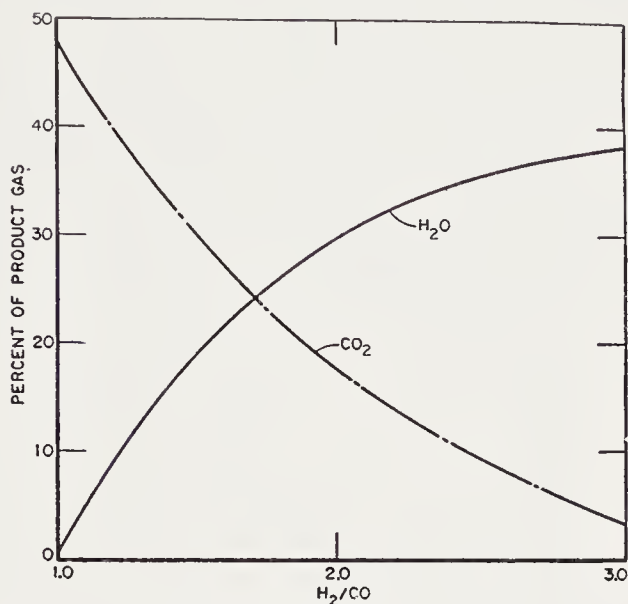


Figure 1. Water vapor and carbon dioxide as function of H_2/CO ratio at $350^\circ C$ and 1 atmosphere. (From Ref. 6)

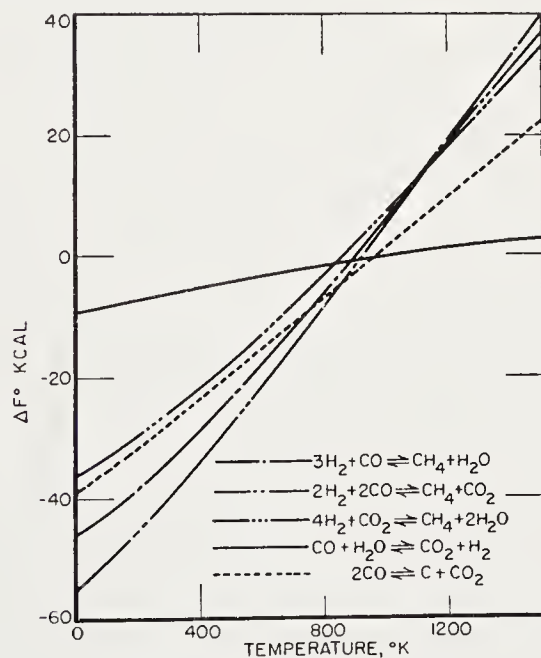


Figure 2. Free energy changes as functions of temperature. (From Ref. 10)

carbon can plug a reactor and prevent the free passage of reactant gases through the reactor tube. The problem of carbon deposition is one that

appears in a great deal of the published experimental work and is, perhaps, one of the most serious problems that must be dealt with in both small- and large-scale experimental work.

Thermodynamics

One of the most important thermodynamic factors in this type of reaction system, with respect to catalyst life and process design, is the heats of reaction, which are shown as functions of temperature from 0 to 1500°K in Figure 3, and tabular form from 0 to 726.8°C (Table 1¹⁰). All of the reactions are exothermic and, except for reaction (4), the heats of reactions are very high and only slightly dependent on temperature. These high heats of re-

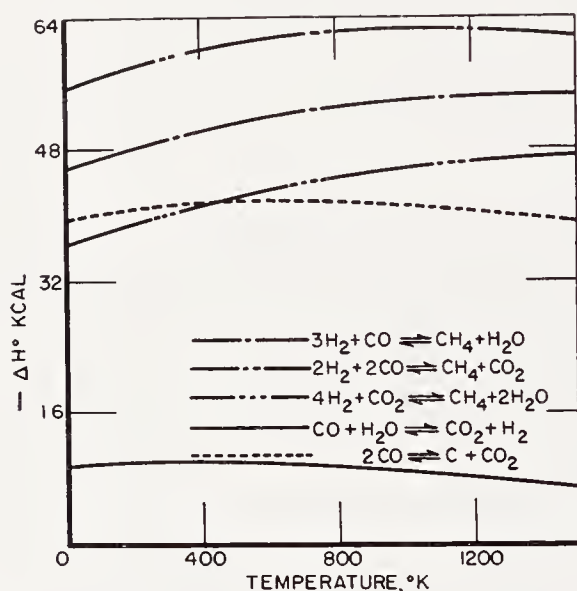


Figure 3. Heats of reactions as functions of temperature. (From Ref. 10)

action, although creating few serious operating problems in small laboratory experiments, have proved to be the source of severe operating difficulties in large-scale process equipment because of the problem of removing large quantities of heat from large catalyst beds. Unless the heat is successfully removed from the catalyst bed, high feed-gas throughputs can produce excessive catalyst-bed temperatures that can, in addition to destroying the activity of the catalyst, cause poor methane yields. An idea of the effect of temperature on the reaction system may be obtained from Figure 4, which shows the equilibrium constants for the various reactions associated with the methanation system as functions of temperature.

Calculations of the theoretical equilibrium compositions of the hydrogen-carbon monoxide system have been made by Dent *et al.*⁴ of the British Gas Research Board. However, since the equilibrium constant used in these

calculations differed appreciably from those published by the United States Bureau of Standards¹⁰, the compositions of the system were recalculated by Greyson *et al.*⁵, who used the data published by the Bureau of Standards. Compositions were determined for the temperature range 500–900°K, which range is of most practical interest for industrial processing, for pres-

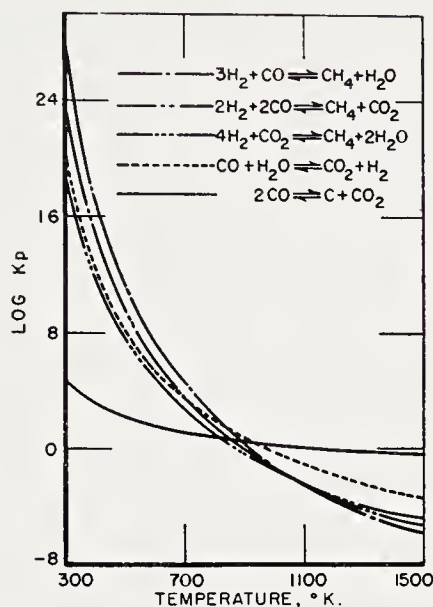


Figure 4. Equilibrium constants as functions of temperature. (From Ref. 10)

TABLE 1. HEATS OF REACTION¹⁰

Reaction	ΔH° (Kcal)							
	0°C	126.8°C	226.8°C	326.8°C	426.8°C	526.8°C	626.8°C	726.8°C
1	-49.271	-50.353	-51.283	-52.062	-52.703	-53.214	-53.610	-53.903
2	-59.109	-60.063	-60.803	-61.356	-61.754	-62.016	-62.162	-62.214
3	-39.433	-40.643	-41.763	-42.768	-43.652	-44.412	-45.058	-45.592
4	-9.838	-9.710	-9.520	-9.294	-9.051	-8.802	-8.552	-8.331
5	-41.220	-41.226	-41.435	-41.501	-41.463	-41.353	-41.193	-40.997

ures of 1, 10, and 25 atmospheres, and for hydrogen-carbon monoxide ratios from 0.5 to the limiting ratio above which carbon deposition does not occur, assuming that complete equilibrium is realized for reaction (1), (4) and (5), simultaneously. The results of these calculations are summarized in Figures 5, 6, and 7.

Methane yields, which are summarized in Figure 5, are most critically affected by temperature and synthesis-gas ratio, the methane yields being highest at the lower temperatures and higher synthesis-gas ratios. Owing

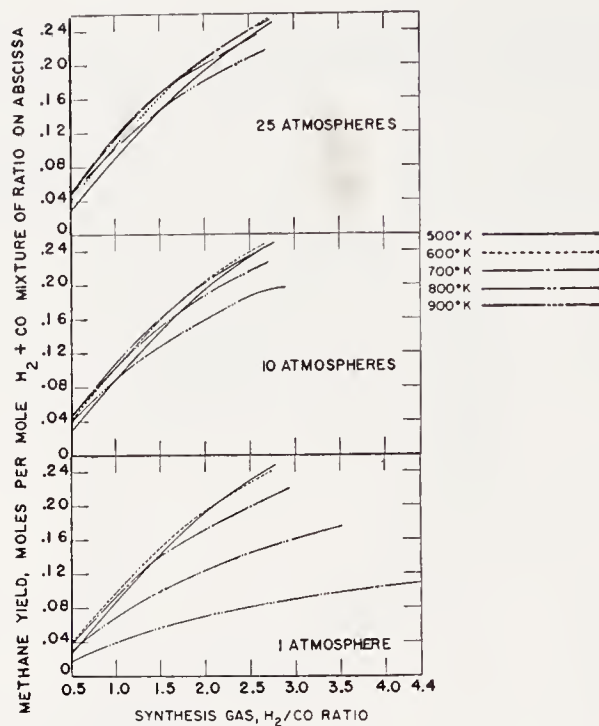


Figure 5. Equilibrium methane yields. (From Ref. 5)

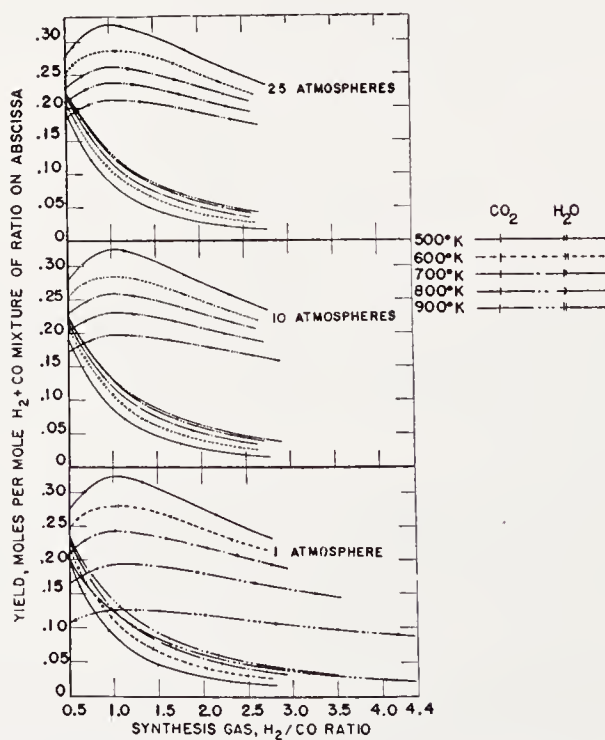


Figure 6. Equilibrium carbon dioxide and water yields. (From Ref. 5)

to the high conversion of synthesis gas at the lower temperatures, pressure does not appreciably affect methane yields until temperatures of approximately 700°K are exceeded. Above this temperature, increases in pressure produce increased methane yields.

Water-vapor yields, which are shown in Figure 6, respond to variations in temperature in a manner similar to that of methane, except that the pressure effect is not as pronounced. The effects of synthesis-gas ratio are not as great, and a peak yield is reached at all pressures at a ratio of ap-

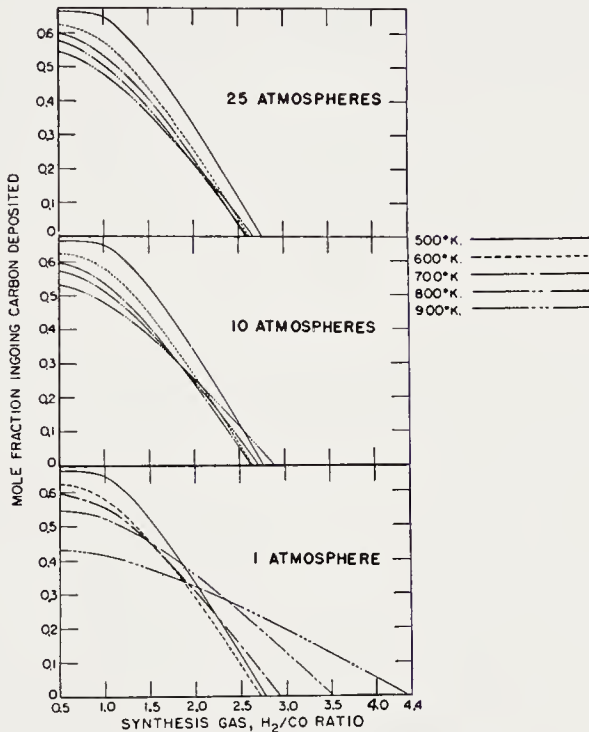


FIGURE 7 — DEGREE OF CARBON DEPOSITION
FROM REFERENCE 5

Figure 7. Degree of carbon deposition. (From Ref. 5)

proximately 1.0. Pressure increases, although tending to increase the yields of water, do not have appreciable effects on the system and, except at the highest temperatures, may be ignored.

Figure 6 also summarizes the theoretical yields of carbon dioxide. The yield of this particular component appears to be, primarily, a function of synthesis-gas ratio. A very small temperature effect can be observed, but in general, it, as well as the pressure effects, may be ignored.

The effects of temperature, pressure, and synthesis-gas ratio on the degree of carbon deposition are shown in Figure 7. Below ratios of 1.5 to 2.0, temperature increases tend to favor decreased carbon deposition; however,

above these ratios, temperature increases above approximately 600°K tend to favor increased deposition. Despite these temperature effects, the degree of carbon deposition is, primarily, a function of synthesis-gas ratio. As with other components of the system, pressure exerts a maximum influence at the highest temperatures, and may, for all practical purposes, be ignored at the lower temperatures.

The carbon deposition boundaries, or limiting synthesis-gas ratios above which carbon will not deposit, are shown in Figure 8 for the temperature range 500 to 1400°K, and for pressures of 1, 10, and 25 atmospheres. The largest effect of pressure is exerted on this characteristic of the reaction system, increases in pressure tending to decrease the minimum ratio re-

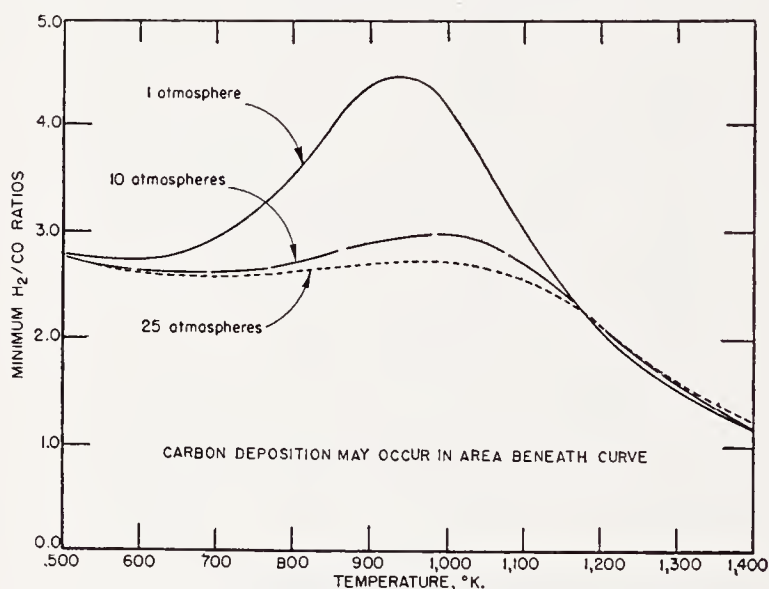


Figure 8. Carbon deposition boundaries. (From Ref. 5)

quired for the prevention of carbon deposition. Maximum pressure effects are observed, as with system components, in the temperature range 800 to 1000°K.

It can be concluded from the preceding data that catalyst beds should be operated at the lowest temperatures that are consistent with catalyst activity, and with synthesis gases having hydrogen-carbon monoxide ratios at or above the limiting boundary ratio. Pressure conditions are, as a general rule, not too important under these conditions. If, however, synthesis gases having ratios appreciably less than the boundary values are used, the reactions should be carried out at elevated pressures of the order of 10 to 25 atmospheres. This method of operation would tend to reduce the quantity of carbon that is deposited on the catalyst particles. Unfortunately, operation of reaction equipment at elevated pressures, and/or

high feed-gas throughputs produces excessive quantities of heat, which, unless adequate means for removal are available, tend to increase catalyst-bed temperatures and decrease methane yields. High catalyst-bed temperatures also require higher boundary synthesis-gas ratios and can result in excessive carbon deposition on the catalyst.

A problem that has arisen in connection with heat transfer in catalyst beds is the interpretation of much of the experimental data that has been published in connection with methanation. In most instances, either initial feed-gas temperatures, or final exit-gas temperatures, or both, are reported. In very few instances have actual catalyst-bed temperatures been reported. As a result, it is extremely difficult to determine temperature effects on yields of components and carbon deposition. Owing to this lack of information, the reader is cautioned about attempting to interpret the temperatures reported here until a full evaluation of the experimental techniques and the heat-transfer limitations of the equipment have been made.

CATALYSTS

Work Prior to 1940

Some of the materials that were tested for methanation activity during the years between the initial discovery of the synthesis in 1902 and 1939 are listed in Tables 2 and 3. Most of these studies have been well summarized by Berkman, Morell, and Egloff⁴⁵, and by Lazier⁴⁶, and need not be repeated here. Some of these experiments, however, give insight into some of the more recent studies, and a brief discussion of these works is in order. It must be recognized, however, that much of the early work was limited by a lack of understanding of the effects of sulfur poisoning, and, as has been discussed previously, by an ignorance of operating temperatures.

Sabatier and Senderens², extending their work on synthesis, found that copper, iron, palladium, and platinum were not active methanation catalysts. Vignon¹¹, on the other hand, found that methane could be produced by passing mixtures of carbon monoxide and steam over iron at 950°C. These observations, in contrast with those of Sabatier and Senderens, and later to those of Tropsch and Schellenberg⁴⁷, could only be explained on the basis of a water-gas-shift reaction followed by the hydrogenation of carbon monoxide to methane. This situation, involving what appeared to be contradictory data, was clarified some months later when Fischer and Tropsch¹⁵, working with iron catalysts at elevated pressures, found that, although negligible quantities of methane formed at 400 to 430°C and atmospheric pressure, considerable quantities of the gas formed in the same temperature range at pressures of 40 to 45 atmospheres.

In general, most of the very early work on methanation catalysts was done with metallic nickel catalysts. In 1914, Jochum¹² described the metha-

nation of mixtures of hydrogen and carbon monoxide with hydrogen-carbon monoxide ratios ranging from 1 to 5 over nickel supported on unglazed

TABLE 2. CATALYSTS FOR THE METHANATION OF CARBON MONOXIDE AND HYDROGEN

Catalyst	Ref.	Catalyst	Ref.
Ag	18, 37	Ni ₃ C	27
Co	2, 9, 18, 33	Ni with alkali	20
Cu	11	Ni with ceria	44
Fe	11, 15, 18	Ni with chromium acetate	44
Fe from Fe(CO) ₅	35	Ni with ammonium vanadate	44
Ir	18	Raney alloy	34
Mo	18, 37, 42	SiO ₂	11
Ni	1, 2, 7, 9, 11, 16, 18, 20, 33, 36, 42	Co + Zn + Mn + clay + alkali	30
Ni-Mn	36	Fe + Ni + Cr on activated carbon	32
Os	18	Ni on Al ₂ O ₃	32
Pd	18	Ni-Mn with Al ₂ O ₃	36
Pd sponge	13	Ni with Al and Mn on kieselguhr	38
Pt	18	Ni on activated carbon	38
Rh	18	Ni on activated C with 18% ThO ₂	28
Ru	18	Ni + FeCO ₃ with Al and Mg on kieselguhr	38
Al ₂ O ₃	11	Ni + MgO	29
Fe activated by Al ₂ O ₃	35	Ni, Mn, Mg, Zn, V, Cr, Al, Pb	
Fe activated by MeOH	35	as hydroxides, molybdates	23
Fe activated by NH ₄ OH	35	Vanadates on asbestos—together or alone	
Fe oxide	35	Ni on granules of MgO	17
MgCO ₃	37	Ni on porcelain	12, 26
MgO	11	Ni on pumice	19
MoS ₂	42	Ni + promoters on pumice	14
Ni—sugar charcoal—pumice	22	Ni on sugar charcoal	21
Ni with silica gel	42	Ni with thorium and ceria on carbon	43
Mo with silica gel	42	MoS ₂ with silica gel	42

porcelain, and in 1923, Medsforth¹⁴ reported that the activity of supported nickel catalysts could be enhanced if dehydrating agents such as alumina were incorporated into the catalysts. An interesting sidelight of the effects

of promoters is illustrated by the work of Küster⁴¹ who observed that the addition of copper and cobalt to nickel catalysts decreased the activity of these catalysts, whereas the addition of these same materials enhanced the activity of iron catalysts, an effect that can be partially explained by the fact that copper, when added to iron catalysts, reduces the temperature that is required for the reduction of the oxides of iron⁶³.

Materials other than nickel were tested for methanation characteristics, but in most instances the work was extremely limited. Ruthenium was found to produce large quantities of methane^{18, 39}, but the scarcity of the metal did not appear to encourage a great deal of experimental work. Sebastian⁴², in 1936, reported that molybdenum sulfide catalysts supported

TABLE 3. CATALYSTS FOR THE METHANATION OF CARBON DIOXIDE AND HYDROGEN

Catalyst	Ref.
Co	2, 23
Fe	41
Fe with Cu and Co	41
Ni	1, 2, 33, 7
CoSO ₄ with CuO and MnO	40
Ni on MgO granules	17
Ni on porcelain	12, 24, 25
Ni on porcelain with ceria	25
Ni on pumice	31
Ni + promoters on pumice	14
Ni with thoria and ceria on C	43
Ru on asbestos	39
Ru-Th on asbestos	39

on silica gel, although less active than nickel catalysts, were resistant to the poisoning effects of sulfur. Some aspects of this work were repeated by the British Fuel Research Board⁴⁸ in 1938, and it was observed that, in addition to activities that were appreciably lower than nickel catalysts, molybdenum sulfide catalysts produced excessive quantities of carbon deposition.

Work of British Fuel Research Board. Major developments in methanation technology actually began with the work of the British Fuel Research Board⁴⁹ on supported-nickel and cobalt catalysts in 1939. This work initiated a six-year program on the development of catalysts and processes for the industrial production of methane. The catalysts used in this work were prepared by precipitating the metals and promoters onto acid-extracted kieselguhr from solutions of the nitrate salts of these elements. Catalysts were then reduced with hydrogen, and tested under various con-

ditions of synthesis, which included tests to determine the sulfur resistivity of catalysts.

The composition of the catalysts materially affected both the relative ease of reducing the catalysts, which is illustrated in Table 4, and the sulfur resistance of these materials. The later effect of composition of three of the catalysts is shown in Figure 9. The activity of the four catalysts, however, was reported to be approximately the same, although the thorium-pro-

TABLE 4. CONDITIONS OF REDUCTION, FUEL RESEARCH BOARD CATALYSTS⁴⁹

Catalyst		Conditions of Reduction	
No.	Composition (pts. by wt.)	Duration (hrs.)	Temp. (°C)
I	100 Co:18ThO ₂ :100 Kieselguhr	24	375
II	100 Ni:18ThO ₂ :100 Kieselguhr	3	450
III	90 Ni:10Cu:18ThO ₂ :100 Kieselguhr	3	350
IV	90 Ni:10Cr ₂ O ₃ :18ThO ₂ :100 Kieselguhr	3	450

Curve	Catalyst	Temperature °C.	Sulfur g/m ³	H ₂ /CO
1	I	350	625	3.4
2	II	350	265	3.6
3	III	450	265	3.6

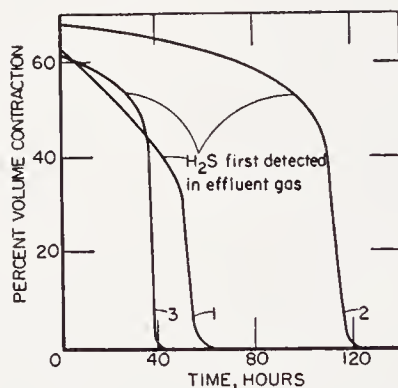


Figure 9. Effects of sulfur on catalyst activity. (From Ref. 49)

moted-nickel catalyst, catalyst II, appeared to have a slightly higher initial activity than the rest.

At 350°C, the temperature at which most of these tests were reported to have been performed, increases in hydrogen-carbon monoxide ratios of the reactant gas resulted in decreased concentrations of carbon dioxide in the effluent gas. Space-velocity effects were more complex, however, and could not be defined as clearly as the effects of hydrogen-carbon monoxide ratio. It was found, however, that the carbon dioxide-methane ratios in the effluent gas increased, whereas the concentration of saturated hydrocarbons in the effluent gas decreased with increases in space velocity.

One observation that was made during these tests appears to throw a little more light on the question of which reactions occur during the synthesis of methane. Figure 10 shows both the volume contraction and the carbon dioxide concentration of the effluent gas as functions of time after initiation of synthesis with a sulfur-containing reactant gas. The increase in carbon dioxide concentration that is shown here, as contrasted with the decrease in volume contraction, would indicate that, although the methanation centers in the catalysts are poisoned by sulfur, the sites upon which the water-gas-shift reaction occurs are not materially affected. A conclusion

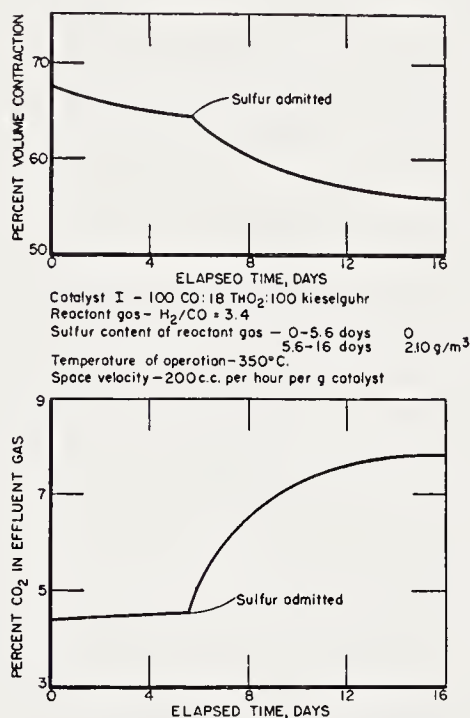


Figure 10. Effect of sulfur on catalyst activity. (From Ref. 49)

that might be drawn from these results is that the water-gas-shift reaction takes place on catalyst sites that are independent and of a different nature than those on which the methanation reactions occur. Another conclusion is that the same sites are utilized for both reactions, but that the relative rates of reaction are so affected that the chance of an adsorbed carbon monoxide molecule undergoing a shift reaction is greater than the chance of it undergoing a hydrogenation.

Work Since 1940

The work after 1940 can be considered to have been done in two phases. The first phase was the continuation of the work of the British Fuel Research Board that was done by the Fuel Research Station⁶ in conjunction

with the British Gas Research Board^{4, 50, 51} and which was completed in 1945. The second phase was initiated by the United States Bureau of Mines with the work of Coopperman *et al.*⁵² in 1951, and has continued to the present with the work of Wainwright *et al.*⁵³ and Greyson *et al.*⁵. In general, both phases of work have been concerned with finding catalysts and developing processes for the industrial production of methane, and as a result, the more academic aspects of the catalyst studies have been ignored or neglected. However, sufficient data exists to present a fairly clear picture of the problems that exist and the advances that have been made in methane technology.

Since most of the work has been directed toward practical development, rather than fundamental catalyst research, it would be best to describe, briefly, the aspects of catalyst studies that have been emphasized, and the underlying motivation for these studies. The discussion is extremely important, since no study has led to the successful solution of any of the problems that have proved to be obstacles in the development of a successful commercial-scale operation.

Although many of the materials studied for use as methanation catalysts have been found to be of limited initial methanation activity, and/or of poor methane specificity, most nickel and supported-nickel catalysts initially produce relatively high yields of methane, and little or no yields of higher molecular-weight hydrocarbons. All methanation catalysts, however, including nickel, suffer from slow losses of activity during synthesis, and these activity losses can prove to be more critical than the initial activity and specificity of the catalysts, with respect to catalyst cost and equipment maintenance time. Losses in activity can result from high operating temperatures, which appear to cause destruction of the active structure of the catalyst, from normal operating temperatures, for which no good explanation can be given, and from exposure to sulfur compounds, which produce permanent losses of activity in the catalyst.

In addition to loss of activity, most catalysts that have been tested appear to be subject to some degree of carbon deposition, the extent of which is determined by the synthesis-gas ratio, the conditions of synthesis, and the particular catalyst that is used. Carbon deposition, in any appreciable degree, although appearing to have no effect on catalyst activity, results in poor process efficiency, and unit operating difficulties, which arise from the plugging of reaction tubes with carbon.

Catalyst-Testing Equipment. Most equipment used for fixed-bed catalyst testing is similar in design. Figure 11 shows a type of unit used by the British Gas Research Board⁴. The unit consists of a vertical silica tube, $\frac{3}{16}$ -inch in diameter and 8-inches long, enclosed in a steel shell, which serves to reinforce the reactor tube during operations at elevated pressures. The reaction tube is heated by an electrically heated furnace.

Similar equipment was used by the United States Bureau of Mines⁵, and diagrams of the reactor tube and gas-flow system are shown in Figures 12 and 13. This unit consists of a vertical seamless steel reaction tube, $\frac{1}{2}$ -inch in diameter, surrounded by a steel jacket containing a boiling liquid coolant. The unit is heated by electrical coils wound around the coolant-jacket wall.

In addition to the fixed-bed equipment, the Bureau of Mines also conducted catalyst-evaluation studies in bench-scale fluidized-catalyst equipment, a type of which is shown, together with the gas-flow system, in Figures 14 and 15. The unit shown in Figure 14, which utilizes a multiple-feed

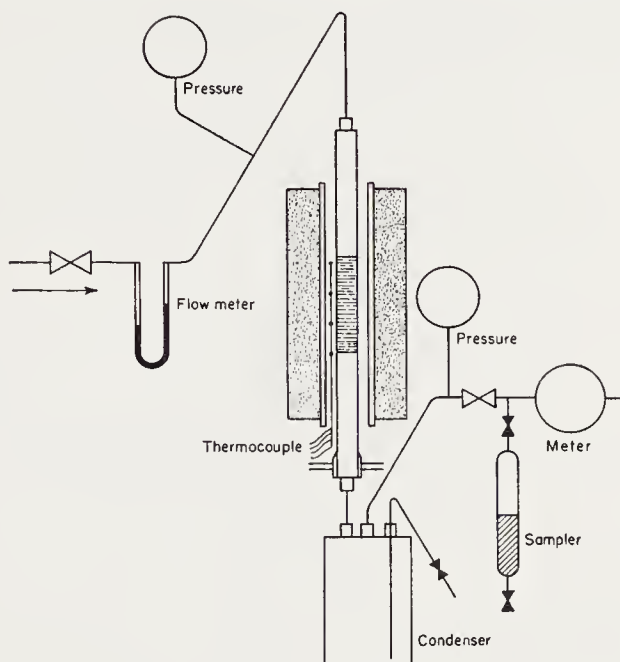


Figure 11. Typical catalyst-testing apparatus used by British Gas Research Board. (From Ref. 4)

type of gas-inlet arrangement, is fabricated from a 1-inch diameter seamless steel tube, 6-feet high, enclosed in a 3-inch diameter heat-exchange jacket containing a boiling liquid coolant. The gas-flow system, which is shown in Figure 15, allows the reactant gas, with or without the addition of recycled product gases, to be fed into the bottom of the tube. Product gases are taken off the top of the unit after the gas passes through two stainless steel porous filters. The unit was heated by electrical coils wound around the outside wall of the heat-exchange jacket.

The additional feed-gas inlet points that are placed in the sides of the reaction tube allow for better temperature control of the catalyst bed by providing means for distributing reactant- and recycle-gas flows over the length of the catalyst bed.

Catalysts. The Group VIII transition elements, mainly iron, nickel, and cobalt, appear to be the most suitable for use as methanation catalysts; although other materials, in raw or modified forms, have been used to catalyze the methanation reactions. Some idea of the variety of materials that have been tested may be obtained from the qualitative catalyst-activity tests performed by the British Gas Research Board⁴. Working with a sulfur-free reactant gas having a synthesis-gas ratio of 2.5 at a pressure of 50 atmospheres, in the temperature range from 600 to 1000°C, and at a space velocity* of 10,000 hr⁻¹, they found that calcium oxide, porous pot

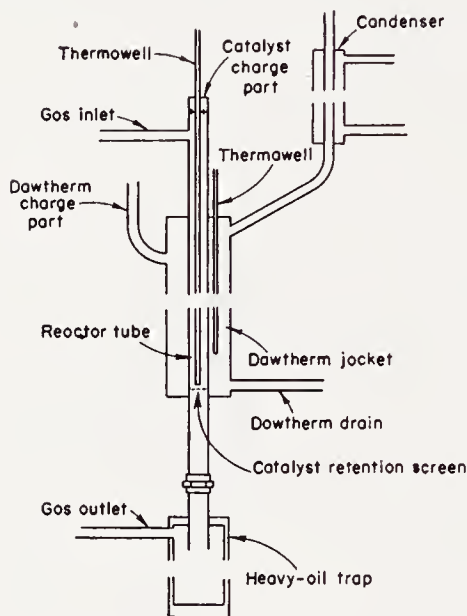


Figure 12. Fixed-bed catalyst reactor. (From Ref. 5)

(a type of sintered clay), and porous pot with added alkali all produced excessive quantities of carbon and very little methane. Iron and molybdenum, although also subject to heavy carbon deposition, produced considerable quantities of methane; nickel and cobalt, in contrast to iron and molybdenum, produced high yields of methane and very little carbon.

It is of interest to note here, as well as throughout this chapter, that any one of the reactions in this system can take place preferentially. In this instance, there is evidence that reaction (5) occurred preferentially in a synthesis-gas ratio region, in which the equilibrium formation of carbon would have been negligible.

Materials, such as molybdenum sulfide⁴, stainless steel⁵⁴, and thorium-promoted copper⁵⁵ have also been studied. The molybdenum-sulfide studies,

* Space velocity—volumes of reactant gas per hour (N.T.P.) per catalyst-bed volume.

which were, in effect, repeated studies of the work of Sebastian⁴², and the Fuel Research Board⁴⁸ were made at 50 atmospheres of pressure, and at

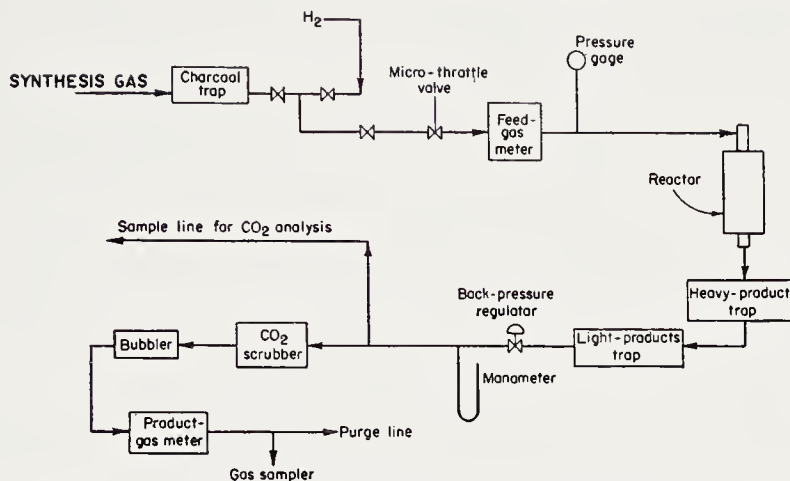


Figure 13. Flow diagram of fixed-bed catalyst testing apparatus. (From Ref. 5)

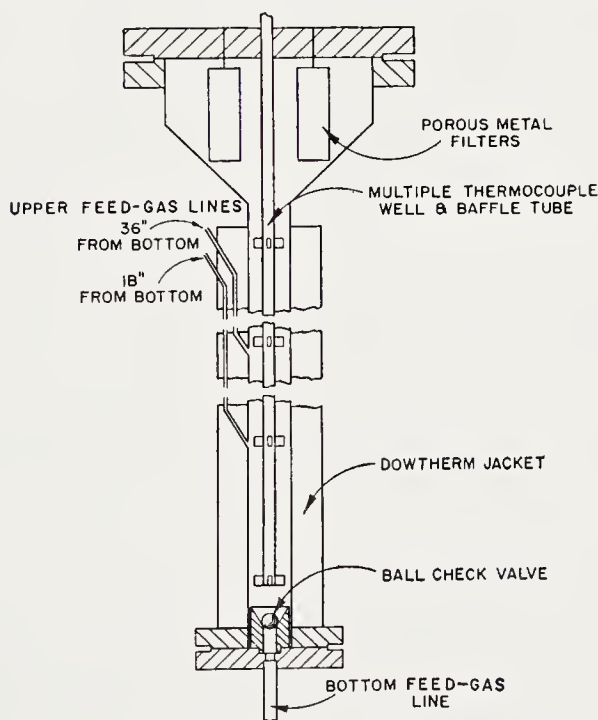


Figure 14. Multiple-feed fluidized-catalyst reactor. (From Ref. 5)

temperatures of 500, 600, and 700°C, with reactant gases having hydrogen-carbon monoxide ratios of 3.0, and containing from 200 to 2000 grains of sulfur, as carbon disulfide, per thousand cubic feet. This catalyst proved to be resistant to the effects of sulfur but was much less active than nickel,

a conclusion that had been arrived at by the previous investigators. It was also observed that the resistance of this catalyst to thermal effects was very poor, the activity of the material at 600°C being greatly reduced after a short period of synthesis at 700°C.

Limited studies of the effects of the various promoters and supports used with various catalysts have also been made. Alkali materials when used as catalyst promoters were found to poison the ability of a catalyst to produce methane^{56, 57}, although the types of alkali used to precipitate the catalysts from solution had little effect on the initial activity of these materials⁵⁶. Russell and Miller⁵⁷ also found that cerium-promoted cobalt catalysts supported on natural kieselguhr produced only methane from carbon

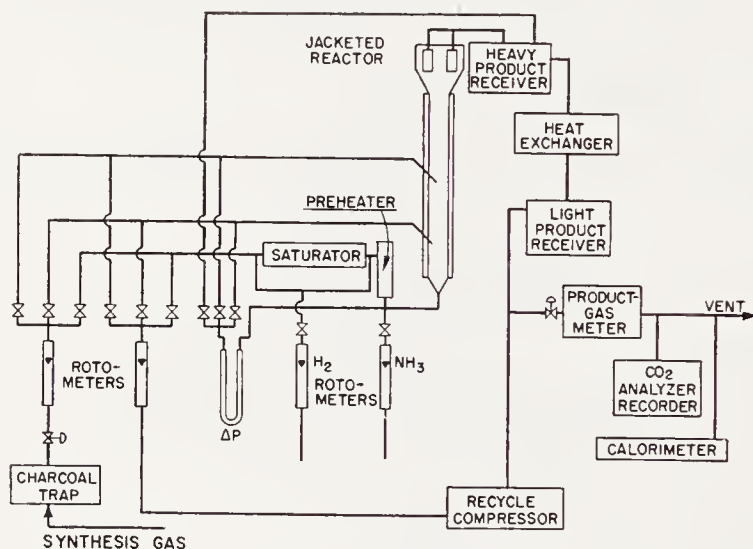


Figure 15. Multiple-feed fluidized-catalyst reactor flow diagram. (From Ref. 5)

dioxide and hydrogen, in contrast to the same catalyst supported on a flux-calcined kieselguhr, which produced high yields of liquid hydrocarbons. A further discussion of the effects on catalysts of calcining kieselguhr appears on pages 498–499⁶³.

Despite the variety of materials that have been studied, the most informative work to date has been done on iron and nickel catalysts of various compositions, and as a result, the discussion of catalyst and process variables, which follows, must be limited, primarily, to these materials.

Iron Catalysts. Iron catalysts, in general, produce small yields of methane, and are subject to heavy carbon deposition even at high hydrogen-carbon monoxide ratios. The over-all synthesis characteristics of a number of iron catalysts tested by the United States Bureau of Mines have been summarized in Table 5⁵.

The United States Bureau of Mines, in particular, made a fairly com-

plete variable study of a reduced and nitrided steel-shot catalyst, which contained, in the raw state, approximately 69 per cent iron, 6.58 per cent silicon, 0.47 per cent carbon, and 0.23 per cent sulfur; the remainder of the catalyst probably consisted of oxygen, the concentration of which was not determined analytically.

The effects of temperature on the activity and specificity of this catalyst in a fluidized catalyst-bed type of reactor, which are shown in Figure 16, are typical of those observed with other iron catalysts in the same type of

TABLE 5. BUREAU OF MINES FIXED-BED IRON-CATALYST TESTS⁵

No.	Material	Pretreatment ^a	H ₂ /CO	Temp. (°C)	Pressure (psig)	Space Velocity (hr ⁻¹)	Per cent ^b CH ₄	Life (hrs.)
1	Cuban iron ore	Reduced	1.0	250-320	0-300	100-300	4-37	942 ^c
2	Cuban iron ore	Reduced	2.0	320-380	300	300	13-36	750+
3	Fused iron	Reduced and ni- trided	2.0	240-400	300	100-300	4-31	1012 ^c
4	Fused iron and ball clay	Reduced and ni- trided	2.0	240-312	0-300	100-300	4-28	726 ^c
5	Iron and alu- mina precipi- tated on kaolin	Reduced	2.5	340-360	300	300	12	245 ^c
6	Iron, nickel, magnesia, and silica	Reduced and ni- trided	1.0	240-270	300	300	27-40	1460 ^d

^a Reduction with hydrogen, 375-400°C, 100 psig.

Nitrided with anhydrous ammonia, 375°C, 0 psig, until ϵ -phase iron nitride was obtained.

^b Based on product gas that is free of water and carbon dioxide.

^c Reaction tube blocked with carbon.

^d Some carbon deposition.

equipment. It would appear from these data, that temperatures must be increased above 335°C to increase the yields of methane and reduce the yields of hydrocarbons with chain lengths having more than 3 carbon atoms. At these high temperatures, however, the degree of carbon deposition on the catalyst, which is not shown in the figure, becomes excessive. Although the addition of steam to the reactant gas inhibits the formation of carbon, the activity of the catalyst is materially reduced by this technique, as is shown in Table 6, and increased recycle ratios are required to obtain conversions of reactant gas equivalent to those obtained without the addition of steam.

Space-velocity effects on methane yields, which are shown in Figure 17,

are much greater than the temperature effects. The increase in methane concentration, is also accompanied by initial increases in the yields of C^{3+} hydrocarbons and carbon dioxide; the C^{3+} hydrocarbon yield reaches

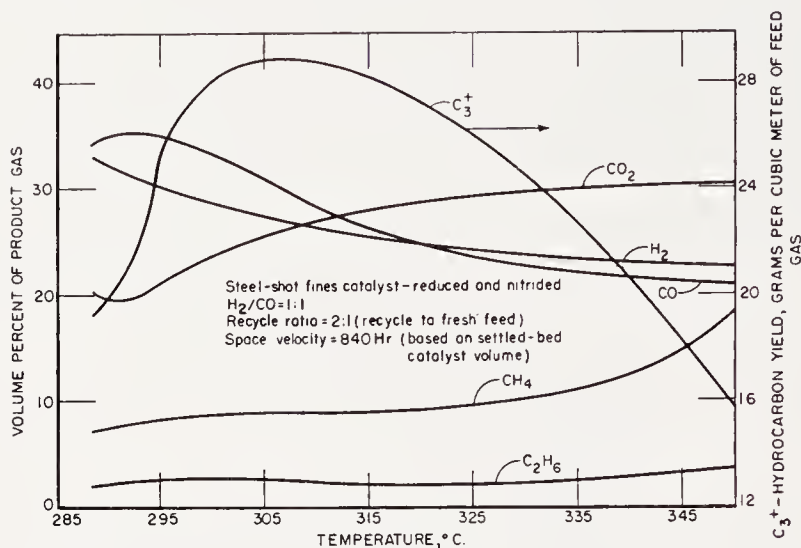


Figure 16. Effect of temperature on products; 100 psig. (From Ref. 5)

TABLE 6. EFFECT OF STEAM ADDITION ON IRON CATALYSTS⁵

Catalyst: steel-shot fines; reduced and nitrified

H_2/CO : 2.5

Total space velocity (reactant gas plus recycled product gas): 7200 hr^{-1}

Temperature, 340°C

Pressure, 300 psig

Steam addition, % reactant gas

Recycle ratio (product gas: reactant gas)

Conversion of $CO + H_2$

Product gas analysis, % by vol.

CH_4

C_2H_6

CO_2

H_2

CO

C_4 and higher hydrocarbon yield, grams
per cubic meter reactant gas

0	0	0	2.6	2.6
1:1	2:1	3:1	3:1	4:1
57.3	67.9	74.7	69.1	79.5
12.7	18.2	24.1	19.6	26.7
2.92	3.85	4.67	3.75	5.49
9.70	10.6	11.0	11.8	12.1
61.3	55.8	50.1	55.2	48.6
11.4	9.14	7.66	7.59	3.97
12.3	8.97	12.0	8.06	9.03

a peak, however, and the rate of increase of the carbon dioxide yield falls below that of methane.

Conversions of synthesis gas over iron catalysts are typified by the curves in Figure 18, which show the effects of space velocity and temperature on the conversion of synthesis gas over a nitrified steel-shot catalyst. These conversions generally are not high and usually lie in the range between 40 and 50 per cent.

As a result of low conversion, excessive carbon deposition, and high yields of C_3^+ hydrocarbons, iron catalysts cannot be considered as good methanation catalysts; unless one thinks in terms of processes producing both liquid and gaseous hydrocarbons, in which case, iron may prove to be a more suitable catalyst than the more active nickel and cobalt materials. In a combined process, however, the high temperatures required for the production of appreciable quantities of methane would probably also result in a large amount of carbon deposition. The addition of steam to the reactant gas, although limited by the activity effects, might be a partial solution

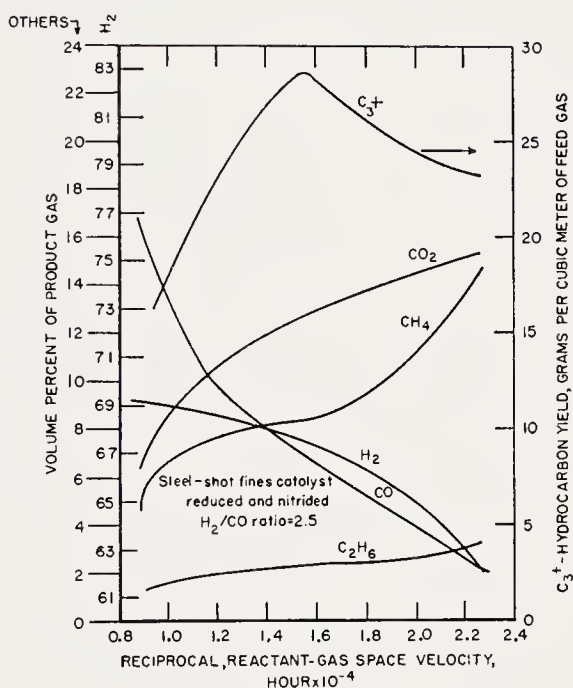


Figure 17. Effect of space velocity on products; 340°C., 300 psig. (From Ref. 5)

to the problem. A more practical one, however, would be to develop iron catalysts that are less subject to carbon deposition.

The resistance of iron catalysts to sulfur poisoning appears to be much greater than nickel materials. The Bureau of Mines⁵, as well as other groups^{4, 53}, found that sulfur in concentrations ranging from 0.1 to 1.0 grain per thousand cubic feet did not appear to materially affect the activity of these iron materials, whereas the same amount of sulfur appeared to reduce the activity of nickel catalysts very rapidly. These conclusions are not based on very reliable data, however, and much more work must be done before they can be considered valid.

Nickel Catalysts. Reduced nickel catalysts are, in general, more active than iron catalysts, more specific than iron catalysts in that they produce only small yields of higher molecular-weight hydrocarbons, and are less

subject to carbon deposition than iron catalysts⁵. In particular, it has been observed that the better types of nickel catalysts are those in which the nickel is supported on a carrier with or without a promoter. A number of these materials are illustrated in Table 7, together with the best methanation operating conditions for each catalyst.

Supported-nickel catalysts have been studied by a number of individuals with a view toward improving certain of the operating characteristics of the catalysts^{4, 5, 6}, the most important of which are the carbon-deposition characteristics of these catalysts with low-ratio synthesis gases, the loss of

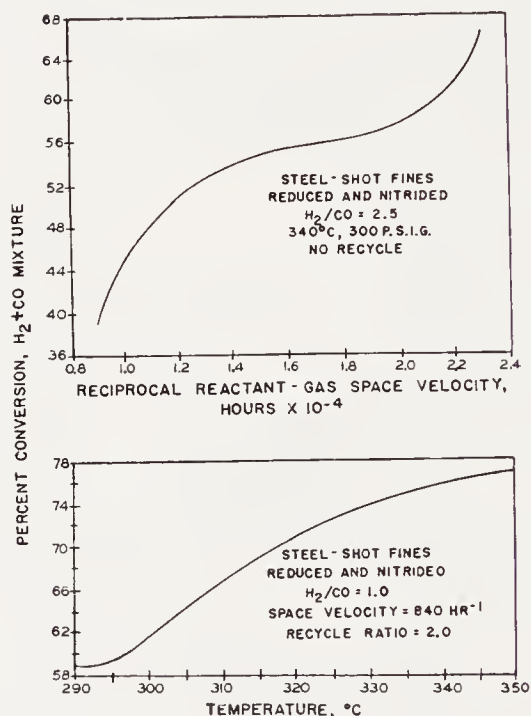


Figure 18. Effects of temperature and space velocity on conversion.

catalyst activity with use, and the poor resistance of these materials to thermal sintering, which usually results in a loss of catalyst activity.

Carbon Deposition. The carbon-deposition characteristics of the thorium-promoted supported-nickel catalyst that was reported by the British Fuel Research Board⁴⁹, may be appreciably improved by replacing a portion of the thoria in the catalyst with magnesia⁶. The improvement in the deposition characteristics of the catalyst, which is illustrated by the data in Table 8, is extremely difficult to explain on a structural basis because the magnesia is added to the catalyst in the form of a water-suspension during the precipitation of the nickel and thorium with potassium carbonate solution, whereas the thorium, in both the initial and modified forms of the catalyst is coprecipitated with the nickel onto the kieselguhr support. If the mag-

nesia does not act as a structural promoter and plays the role of additional carrier for the nickel and thorium, it is possible to explain the effects of

TABLE 7. FIXED-BED NICKEL-CATALYST TESTS—U. S. BUREAU OF MINES⁵

Variable Range Studied ^a			Best Operating Conditions		
Catalyst Composition and Treatment	Feed Gas H ₂ /CO	Operating Temp. Range (°C)	Temp. (°C)	Space Velocity (hr ⁻¹)	CH ₄ ^b (%)
5% Ni ppt. on cracking-catalyst base with alkali, reduced	2.5	390-406	400	300	61.5
10% Ni ppt. on silica, reduced	1	319-379	355	100	48.3
NiO-Al ₂ O ₃ ppt. on kaolin, reduced	2.5	213-410	351	300	96.9
NiO-MgO ppt. on kaolin, reduced	2.5	209-350	264	300	97.3
NiO-Al ₂ O ₃ -MnO ₂ ppt. on kaolin, reduced	2.5	274-332	274	300	94.4
NiO-Al ₂ O ₃ impregnated on Norton cylinders	2.5	298-354	346	500	96.7
NiO-MnO ₂ -Al ₂ O ₃ ppt. and slurried with Na ₂ CO ₃ and zirconia cement, reduced	2.5	300-324	300	300	94.8

^a All tests conducted at 300 psig.

^b Based on H₂O- and CO₂-free product gas.

TABLE 8. EFFECTS OF CATALYST COMPOSITION ON CARBON DEPOSITION⁶

Catalyst charge: 8 cc, 6-8 mesh (B.S.S.) catalyst particles

H₂/CO: 1.5

Space velocity: 3700 hr⁻¹

Exit gas temperature: 350°C

Pressure: 1 atm.

(Duration of test not known)

Composition (pts. by wt.)				Per cent of Ingoing Carbon Deposited
Ni	ThO ₂	MgO	Kieselguhr	
100	—	—	100	0.688
100	—	18	100	0.028
100	18	—	100	0.317
100	6	12	100	0.0072

magnesia on carbon deposition in terms of the distance between active sites on the catalyst surface.

It has been argued by the British Gas Research Board⁴ that the deposition of carbon on a catalyst is, in part, controlled by the ability of adsorbed carbon atoms to form interatomic linkages, and that any technique that

increases the distances between active catalyst sites, such as the dilution of the catalyst with additional carrier, or the poisoning of a fraction of the available sites by sulfur impregnation, would tend to reduce the quantity of carbon that is deposited. Experimental data to support this argument are illustrated in Figures 19 and 20 which show the back pressure of the reaction tube, or more precisely, the pressure drop along the reaction tube as a function of time and hydrogen-carbon monoxide ratio for manganese- and alumina-promoted catalysts containing various concentrations of alumina support and nickel sulfate, which was added to the catalyst by impregnat-

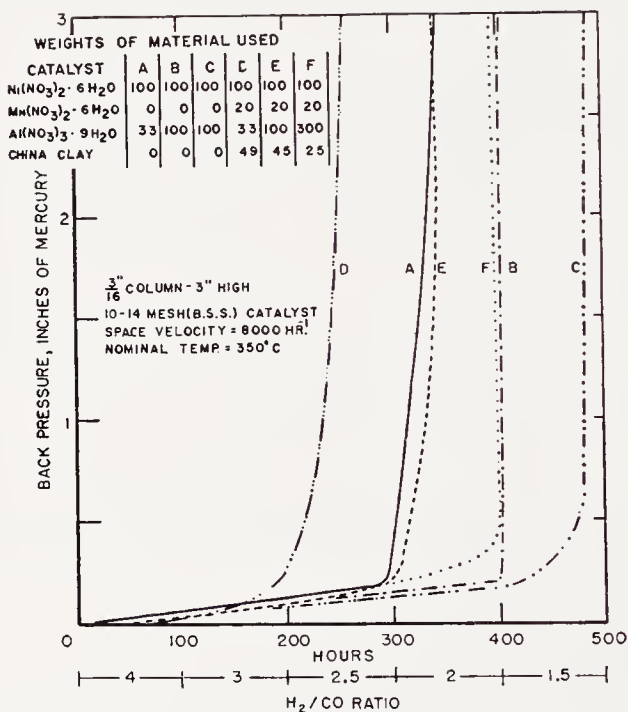


Figure 19. Effect of composition on carbon deposition. (From Ref. 5)

ing the precipitated filter cake of the catalyst with a solution of nickel sulfate. It is assumed, in interpreting these data, that the pressure drop along the reaction tube is a function of the quantity of carbon that has deposited in the tube.

Some question arises as to the interpretation of these data, however, if a study of the data that were reported by the Fuel Research Station⁶ is examined. These data, some of which are summarized in Table 9, indicate that, although increases in the concentration of support tend to decrease the tendency for a reaction tube to plug with carbon, no systematic decrease in the quantity of carbon that is deposited on a thorium-promoted nickel catalyst results from increasing the proportion of kieselguhr in the catalyst. The decreases in the tendency for the reaction tube to block are

explained by the fact that the dilution of the catalyst and the poisoning of the catalyst surface effectively act to decrease the number of active sites in

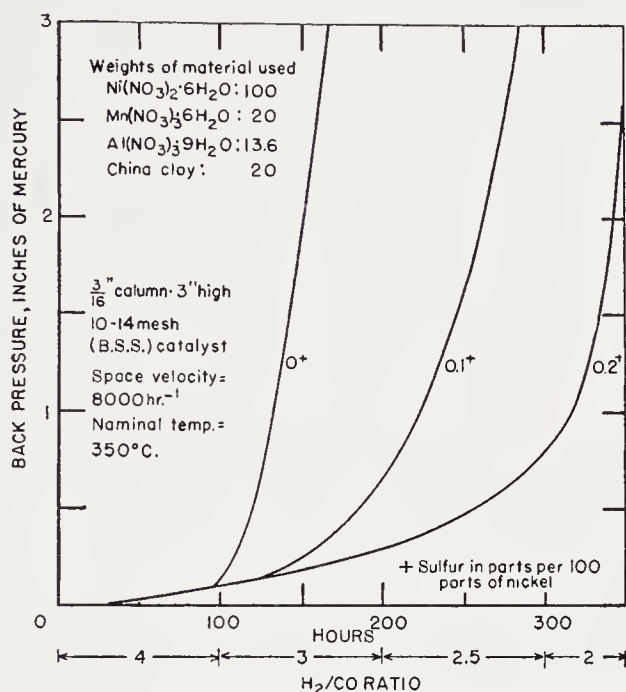


Figure 20. The effect of sulfur on carbon deposition with a nickel catalyst. (From Ref. 4)

TABLE 9. EFFECTS OF SUPPORT CONCENTRATION

Catalyst charge: 8 cc, 6-8 mesh (B.S.S.) catalyst particles

H_2/CO : 1.5

Space velocity: 3700 hr^{-1}

Exit gas temp.: 350°C

Pressure: 1 atm.

Catalyst Composition (pts. by wt.)				Maximum Bed Temp. ($^\circ\text{C}$)	Initial CO Conversion (%)	Life (hrs.)	Per cent of Ingoing Carbon Deposited
Ni	ThO ₂	MgO	Kieselguhr				
100	6	12	100	540	99.9	—	0.0072 ^a
100	6	12	200	540	99.2	—	0.0310 ^b
100	6	12	400	545	99.6	960	0.0143
100	6	12	800	550	98.9	560	0.0280
100	6	12	1600	505	97.7	312	0.0159

^a Blocked with carbon 600 hours.

^b Blocked with carbon 480 hours.

a fixed volume of catalyst. As a result of the decreased number of catalyst sites, carbon, which deposits at approximately the same rate per active

site as in the initial catalyst, tends to deposit more evenly through the catalyst bed.

Another explanation of the data of the British Gas Board can be made from observations of the United States Bureau of Mines⁵, which show that during synthesis operations in fluidized beds, supported-nickel catalysts tended to shatter into smaller particles. In a fixed bed, these small particles would tend to fill spaces and channels within the catalyst bed and would result in increases in pressure drop along the bed. All of the data, however, are insufficient in quantity and scope to permit valid descriptions of either the effects or the causes of increased pressure drop.

The carbon-deposition characteristics of nickel catalysts are also materially affected by the types of carrier materials used to prepare the cata-

TABLE 10. EFFECT OF KIESELGUHR CALCINATION TEMPERATURES⁶

Catalyst charge: 8 cc, 6-8 mesh (B.S.S.) catalyst particles

H₂/CO: 1.5

Space velocity: 3700 hr⁻¹

Exit gas temp.: 350°C

Pressure: 1 atm.

(Duration of tests unknown)

Treatment of Raw Kieselguhr	Per cent of Ingoing Carbon Deposited
1 hr. at 500°C	0.054
24 hr. at 600°C	0.113
24 hr. at 700°C	0.011
24 hr. at 800°C	0.011
24 hr. at 900°C	0.417
24 hr. at 1000°C	1.228

lysts, both thorium-promoted and manganese-promoted catalysts showing increases in carbon deposition upon substitution of china clay for kieselguhr in the catalysts^{4, 6}. The pretreatment of support materials also appears to be a factor in determining the deposition characteristics of the catalyst. An example of the effects of heat-treating a kieselguhr support prior to the catalyst preparation is shown in Table 10. Although no surface-area measurements were made on these particular supports, it has been demonstrated by others that the heat treatment of kieselguhr can result in sintering of the particle structure, with a resulting decrease in the surface area of the particle^{5,8}.

The presence of impurities in catalysts, such as iron and alumina, do not appear to affect the deposition characteristics of the catalysts⁶. Other types of impurities, however, particularly phosphates, materially reduce the quantity of carbon that deposits on a catalyst surface. Table 11, which sum-

marizes data from the work of the Fuel Research Station⁶, shows the results of including various phosphate compounds with the catalyst.

Two other factors which are critical in determining the deposition characteristics of a catalyst are the manner in which it is prepared and the

TABLE 11. EFFECT OF PHOSPHATE ADDITION ON PROCESS LIFE AND DEPOSITION OF CARBON⁶

Catalyst: 100 Ni:22 ThO₂:100 kieselguhr

Catalyst charge: 8 cc, 6-8 mesh (B.S.S.) catalyst particles

H₂/CO: 1.5

Space velocity: 3700 hr⁻¹

Exit gas temp.: 350°C

Pressure: 1 atm.

Phosphate Added % of K ₂ CO ₃	Per cent of Ingoing Carbon Deposited	Life (hrs.)
None	0.477	Blocked with carbon prior to activity loss
K ₂ HPO ₃		
0.25	0.361	Blocked with carbon prior to activity loss
0.50	0.192	Blocked with carbon prior to activity loss
0.75	0.046	300
0.80	0.029	300
0.90	0.027	180
1.00	0.024	141
1.25	0.019	119
1.50	0.011	No activity
K ₄ P ₂ O ₇		
0.5	0.155	Blocked with carbon prior to activity loss
0.8	0.051	69
1.0	0.055	16
NaPO ₃		
0.25	0.235	Blocked with carbon prior to activity loss
0.50	0.110	Blocked with carbon prior to activity loss
0.60	0.043	260
0.80	0.036	90

treatment to which it is subjected prior to synthesis. Precipitated catalysts, for example, are generally less subject to carbon deposition than corresponding impregnated catalysts⁶. However, if the precipitation and subsequent preparation techniques are not carried out in exactly the same manner each time a catalyst is prepared, large variations in deposition characteristics can result. Examples of this phenomenon are shown in Table 12, which gives the deposition characteristics of a group of identical catalysts, each

of which was boiled at a different temperature immediately after precipitation, and in Table 13, which shows the carbon-deposition characteristics of a group of catalysts that were subjected to different heat treatments, presumably in a hydrogen atmosphere, immediately after being reduced with hydrogen at 400°C.

TABLE 12. EFFECTS OF CATALYST-PREPARATION CONDITIONS⁵¹
Catalyst: 100 Ni:6ThO₂:12 MgO:100 Kieselguhr

Catalyst Heated for 2 Minutes at: Temp. (°C)	Bulk Density of Granules (lbs/ft ³)	Per cent of Ingoing Carbon Deposited	
		Jacket Temp. 204°C	Exit Gas Temp., 350°C
95.0	35.6	0.0156	0.1489
100.0	45.0	0.0087	0.111
103.6	48.7	0.0113	0.0082
108.4	50.6	0.0275	0.0066
115.2	56.2	0.0210	0.0045

TABLE 13. EFFECTS OF THERMAL TREATMENT OF CATALYSTS⁶

Catalyst: 100 Ni:6ThO₂:12MgO:100 kieselguhr
Catalyst charge: 8 cc, 6-8 mesh (B.S.S.) catalyst particles
H₂/CO: 3.00
Space velocity: 3700 hr⁻¹
Exit gas temp.: 350°C
Pressure: 1 atm.

Catalyst Reduced for 2 hrs. at 400°C Followed by:	Initial CO Conversion (%)	Final CO Conversion, (% at hrs.)	Per cent of Ingoing Carbon Deposited
No treatment	98.3	90.8 at 1750 (97.5 at 1070)	0.0051
100 hr. at 500°C	99.3	97.5 at 1000	0.0054
100 hr. at 600°C	99.4	95.8 at 670	0.0103
100 hr. at 700°C	99.1	93.7 at 480	0.0211
1000 hr. at 700°C	97.9	88.9 at 290	0.0294
100 hr. at 800°C	95.3	85.7 at 120	0.0370
100 hr. at 900°C	Low activity		Not determined

It is interesting to note in Table 12 that systematic changes in carbon-deposition characteristics were obtained only when the tests were run at a constant exit-gas temperature. This phenomenon is more clearly explained by the data that are shown in Figure 21, in which the catalyst-bed temperature profiles of a reaction unit that was operated at a constant coolant-bath temperature of approximately 300°C are plotted. It is obvious from these data that jacket temperatures are not necessarily representative of the synthesis temperatures within a catalyst bed.

Catalyst Life. The activity of most methanation catalysts is not constant and usually decreases with time. The relative lengths of time during which catalysts maintain an activity level above a specific value, normally referred to as the process life of a catalyst, become an important factor in the evaluation of the catalysts, and much effort has been directed at improving this characteristic of supported-nickel catalysts.

The problem of determining the process life of a catalyst is a complex one and is not simply a matter of determining the number of hours that a particular catalyst will run under a specified set of conditions. As shown in Table 14, which is a summary of the process lives of a number of catalysts of different compositions, catalysts vary in nickel, promoter, and support

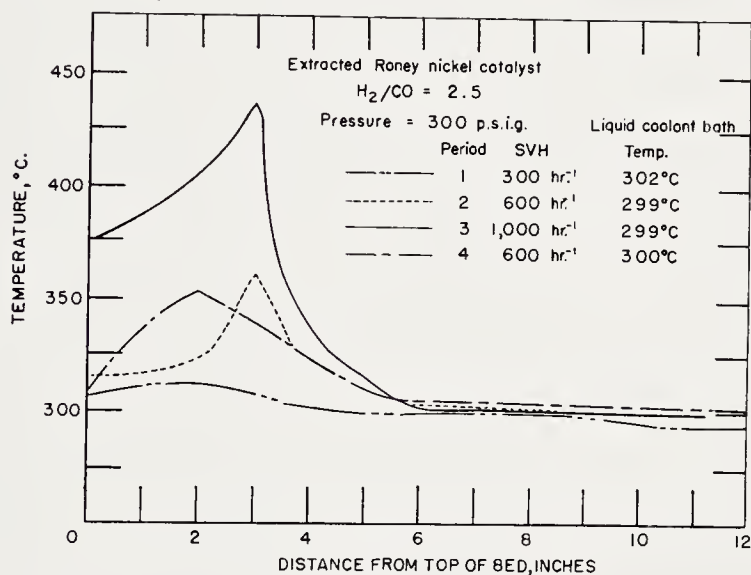


Figure 21. Effect of space velocity on temperature profile. (From Ref. 5)

concentrations, and if process lives are considered only in terms of total catalyst charge, a variable involving the concentration of the active material in the catalyst, nickel, is lost. This fact can be illustrated by conclusions drawn by the Fuel Research Station from the data given in Table 9, which show a progressive loss in catalyst life with increases in the concentration of support material. These tests were run, however, with a constant 8-cc volume of catalyst, each catalyst volume containing a quantity of nickel, thorium, and magnesia that was inversely related to the concentrations of support in the catalyst. In view of the fact that these materials, and not the carrier, are the active components of the catalyst, and the fact that we are primarily interested in knowing what effects the support concentrations have on a particular characteristic of active material, it would appear that the more correct way of reporting catalyst life would be on the basis of the

quantity of active materials in the catalyst. If the data in Table 9 are referred to the relative weights of nickel, thorium, and magnesia in each catalyst, and are based on the life of the catalyst containing 400 parts of kieselguhr, the relative lives of the last three catalysts would be 960, 990, and 1030 hours, respectively. Although this calculation is based on the assumption that the densities of the various catalyst compositions are approximately equal and is, admittedly, approximate, the evidence indicates that

TABLE 14. FLUIDIZED-BED CATALYST TESTS—U. S. BUREAU OF MINES⁵

Pressure: 300 psig

Recycle ratio, recycle: fresh feed: 1

Catalyst Composition		Supports	Feed Gas H ₂ /CO	Avg. Temp. (°C)	Reactant Gas Space Velocity (hr ⁻¹)	Life ^a (hrs.)	lb CH ₄ ^b lb Ni
Nickel (%)	Promoters						
16.6	Al ₂ O ₃	Kaolin	2.5	350	7100	45	ND
26.0	5.5% Mn, 2.4% Al	Kaolin	2.5	330	2800-10,000	220	ND
31.7	5.5% Mn, 4.7% Al	Kaolin	2.5	350	7500	150	750
28.4	6.3% Mn, Al	Alumina	2.5	360	7500	171	500
5.6	1.7% Mn	Alumina	2.5	345	7500	6	ND
21.9	4.5% Mn, Al	Cracking cat.	2.5	345	7000	60	ND
15.0	Mn, Al	Silica	2.5	350	7000	14	ND
11.8	1.6% Mn, Al	Alumina	2.5	380	7500	8	ND
29.0	8.3% Mn, 4.2% Al	Kaolin	3.0	345	7500	132	1200
14.3	13.1% Mn, Al	Alumina	3.0	340	3600	78	ND
21.3	Mn, Al	"Filtrol-S"	3.0	350	7500	237	2500
13.6	2.3% Th, Al	Alumina	3.0	368	7000	550	6500
33.3	2.9% Th	Kieselguhr	3.0	370	7000	380	4000
11.8	2.9% Th, Al	Alumina	3.0	361	7000	425	5500
15.3	3.4% Th, Al	Alumina	3.0	361	7000	336	3700

^a Duration of time for which the carbon dioxide- and water-free volume contraction of the reactant gas was equal to or greater than 70 per cent.

^b ND—not determined.

the process life is increased, rather than decreased by the increases in support concentration. This small increase in operating life, if true, however, might be offset by the decreased initial activities of the more dilute catalysts, and a more precise way of reporting the life would be in terms of the yield of methane per unit weight of nickel, etc., in the catalyst, as is done with the catalysts in Table 14.

The presence of trace quantities of sulfur, which have been added to some catalysts to reduce carbon deposition, can reduce the process life of a catalyst by as much as one-half⁶. Phosphates also tend to reduce the active life of a catalyst, as is shown in Table 11. However, materials that are detri-

mental to the process life of a catalyst can normally be eliminated by careful selection of the raw materials that are used to prepare the catalysts.

More important to the life of the catalysts, and a factor that can overshadow the effects of both composition and impurities, are the techniques that are used to prepare the catalysts. It has been found, for example, that precipitated catalysts are generally more long-lived than corresponding impregnated catalysts^{4, 6}. Table 15, taken from data reported by the British Gas Research Board⁴, shows the respective activities, under identical synthesis conditions, of nickel, manganese, and alumina precipitated on porous pot, and impregnated in china clay. Both the initial activity and

TABLE 15. EFFECTS OF PREPARATION TECHNIQUES ON THE LIFE OF MANGANESE-PROMOTED-NICKEL CATALYSTS⁴

Catalyst composition:

Impregnated: 160 $\text{Ni}(\text{NO}_3)_2 \cdot 6\text{H}_2\text{O}$, 20 $\text{Mn}(\text{NO}_3)_2 \cdot 6\text{H}_2\text{O}$, and 13.6 $\text{Al}(\text{NO}_3)_3 \cdot 9\text{H}_2\text{O}$ impregnated on 160 parts porous pot

Precipitated: 100 $\text{Ni}(\text{NO}_3)_2 \cdot 6\text{H}_2\text{O}$, 20 $\text{Mn}(\text{NO}_3)_2 \cdot 6\text{H}_2\text{O}$, and 13.6 $\text{Al}(\text{NO}_3)_3 \cdot 9\text{H}_2\text{O}$ precipitated on 25 parts china clay by a solution containing 97 parts K_2CO_3 .

H_2/CO : 3.05–3.25:

Space velocity: 10,000 hr^{-1}

Exit gas temp.: 350°C

Pressure: 20 atm.

Product gas analysis, % by volume

	Impregnated Catalysts			Precipitated Catalyst					
	3.5	12.5	16.0	2	150	300	400	500	600
Hours of Syntheses.....									
CH ₄	77.0	59.4	23.0	86.8	73.3	56.3	54.7	48.6	42.1
H ₂	18.5	32.2	79.9	12.2	23.5	35.7	35.5	42.6	45.4
CO	0.2	1.4	23.6	0.1	0.0	0.2	0.6	1.2	3.8
CO ₂	3.7	6.5	0.4	0.2	2.8	7.5	6.8	7.2	8.1

change in activity with time are quite different from the two forms of catalyst. These differences were assumed to be due to the difference in preparation techniques used by the Gas Board and not to the quantity or type of support.

One preparation factor that appears to have influence on the process lives of thorium-promoted catalysts is the temperature at which the catalyst mass is dried after precipitation⁵. Table 16, which summarizes the drying temperatures, densities of catalyst, operating temperatures, and life of a single type of thorium-promoted catalyst, shows that an optimum life is obtained from a catalyst that is dried at 180°C. The reason that this drying temperature is critical is not known, and as can be seen from the table, large variations in life can result even at the optimum temperature.

Thermal Stability of Catalyst. Because of the high exothermic heats of the reactions that produce methane, most methanation catalysts can, in the course of the synthesis operations, be subjected to extremely high temperatures, and it would be extremely advantageous to know the effects of catalyst variables on the sintering and activity characteristics of these catalysts. Very few data, other than knowing that sulfur reduces and alumina increases the resistance of a catalyst to thermal sintering⁴, are

TABLE 16. EFFECT OF DRYING TEMPERATURE ON CATALYST LIFE⁵

Approximate catalyst analyses; pts. by weight: 12Ni:2ThO₂:86Al₂O₃

Catalyst charge: 450 cc, minus 80 mesh (U.S.S.) catalyst particles

H₂/CO: 3.0

Space velocity: 7000 hr⁻¹

Recycle ratio, recycle: fresh feed: 1:1

Operating pressure: 300 psig.

Drying Temperature, Approx. 12 hrs. at °C	Catalyst Density, Settled Bed (g/cc)	Initial ^a Activity Temp. (°C)	Operating Temp. Range (°C)	Life (hrs.)	Approx. Yield ($\frac{\text{lbs CH}_4}{\text{lb Ni}}$)
120	0.72	351	350-374	28	330
120	0.70	345	350	150	2200
120 (redried 180)	0.70	364	355-370	185	2700
150	0.74	369	363-372	82	970
170	0.70	363	360-372	156	1800
180	0.73	370	360-377	550	6500
180	0.81	374	361	425	5500
180	0.74	360	365	336	3700
180	0.74	373	370-375	406	4800
190	0.78	365	363-372	110	1300
210	0.74	380	373-380	112	1300
222	0.76	377	375-380	256	3000
250	0.68	380	364-375	207	2400

^a The initial activity temperature was that temperature at which self-sustained reaction was first observed.

available on this particular subject, however, and little can be said about thermal resistance of catalysts.

Sulfur Poisoning. As has been previously mentioned, the sulfur resistance of nickel catalysts is extremely poor, and a permanent loss of activity normally results from exposure of the catalyst to sulfur compounds. An example of the resistance to sulfur poisoning of a thoria- and magnesia-promoted nickel catalyst is shown in Table 17, which shows the conversion changes that occur when a synthesis gas containing trace amounts of sulfur is used with this catalyst. Poor sulfur resistance is not limited to this particular catalyst, and similar losses of activity of manganese-promoted catalysts have been reported by the British Gas Research Board⁴, and by

TABLE 17. EFFECT OF SULFUR ON CATALYST ACTIVITY⁶Catalyst: 100 Ni:6ThO₂:12MgO:400 Kieselguhr

Catalyst charge: 8 cc, 6-8 mesh (B.S.S.) catalyst particles (1.8 inch bed height)

H₂/CO: 3.0Space velocity: 3700 hr⁻¹

Exit gas temp.: 350°C

Pressure: 1 atm.

Sulfur added as CS₂

0.02 Grains S, 100 c.f.

Hours from start	20	240	400	575	740	910	1080	1250	1420
Total gas passed (NTP)	22	269	458	618	780	950	1132	1310	1490
CO conversion, %	98.3	98.9	98.8	98.2	98.3	98.0	97.5	96.8	95.6
H ₂ conversion, %	84.6	79.8	75.3	75.6	72.4	72.5	72.4	70.4	70.1
Distance of max. temp. from exit, in.	1.4	1.4	1.2	1.1	0.9	0.8	0.7	0.5	0.4

0.004 Grains S, 100 c.f.

Hours from start	20	190	360	500	680	840	1000	1200	1370
Total gas passed (NTP)	20	206	381	554	730	899	1076	1270	1450
CO conversion, %	99.7	99.4	99.3	99.1	99.3	99.2	99.1	98.9	98.9
H ₂ conversion, %	86.6	86.0	83.1	80.6	81.1	81.8	82.0	78.6	79.6
Distance of max. temp. from exit, in.	1.4	1.3	1.3	1.3	1.2	1.1	1.1	1.0	1.0

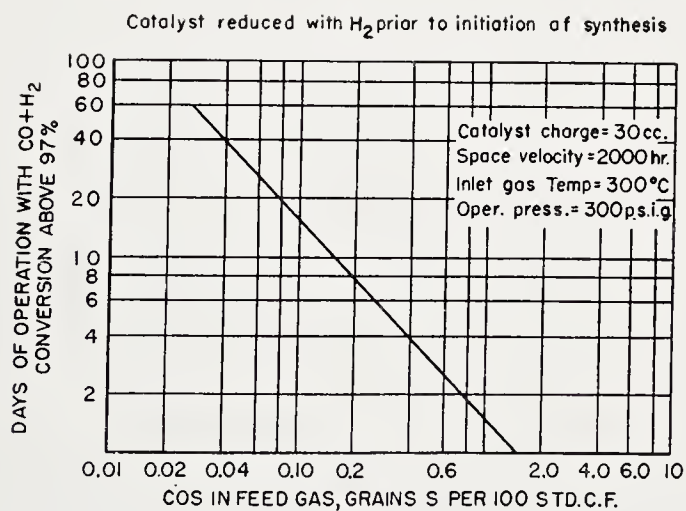


Figure 22. Effect of sulfur content of feed gas on catalyst activity. (From Ref. 53)

Wainwright *et al.*⁵³, who postulated the relationship between operating time and sulfur concentration that is shown in Figure 22. Wainwright concluded that the activity of the manganese-promoted nickel-alumina catalyst started to decrease rapidly after a quantity of sulfur approximately equal to 0.58 per cent of the weight of the nickel in the catalyst had been adsorbed.

It can be concluded from these data, as well as from data reported prior to 1940, that nickel catalysts, in contrast to iron, are extremely susceptible to sulfur poisoning, which is a permanent type of poisoning. To date, no method of operation or formula for catalyst composition has been suggested that will allow a nickel catalyst to be used in synthesis operations for any extended period of time with reactant gases containing more than about 0.005 grains of sulfur per thousand cubic feet. This limitation means that any synthesis gas that is used with nickel catalysts must be freed of almost all sulfur compounds, a process that can be very costly.

INDUSTRIAL TECHNIQUES

The development of commercial methanation procedures is normally undertaken on the assumption that means exist, or will exist, for the conversion of coal to mixtures of hydrogen and carbon monoxide. The Lurgi Gasification Process, for example, would be an excellent gasification procedure for methanation processes, since a product gas containing approximately 15 per cent methane and having a hydrogen-carbon monoxide ratio of approximately 2.5 is produced by this process. American coals, however, are not well suited for this process because of their caking qualities and, other types of gasifier designs, which produce gases having hydrogen-carbon monoxide ratios closer to unity, must be considered.

In general, methanation is considered, primarily, as a technique for producing high heating-value fuel gas, and in this sense, commercial methanation plants should be capable of very high rates of gas production, a point that is well illustrated by the fact that a plant producing approximately 6,000,000 cubic feet of methane per day that is operated at fresh feed space velocities of 1000 hr^{-1} would require catalyst volumes of the order of 1,000 cubic feet. Unless high space velocities are used, the catalyst volume and reactor design requirements might become excessive. Although this assumed value for the capacity of a methane plant may appear high, cities in the United States with populations of from 300,000 to 500,000 people would be expected to use no less than about 100,000,000 cubic feet of fuel gas per day during winter months.

At high space velocities, specific problems of commercial-scale operation are: the control of catalyst-bed temperatures, the prevention of carbon deposition with low ratio synthesis gases, and the prevention of rapid losses

of catalyst activity during synthesis. Some of the methods that have been suggested are discussed below.

Temperature Control

A number of methods have been suggested to achieve temperature control in methanation reactors^{4, 5, 6}. One of the suggested methods involves a separation of the feed-gas stream by means of multiple inlet points, or a perforated feed-gas tube running the length of the reactor tube. By this technique, reaction gases are distributed throughout the length of the bed, and as a result, the heats of the reactions are distributed over the whole bed. A technique for use with fluidized-bed systems has been described previously and is illustrated in Figure 14.

Another method of controlling catalyst-bed temperatures consists of recycling a portion of the product gases through the reactor^{4, 5, 6, 51}. These recycled product gases reduce the pressure of the reacting components and tend to distribute the reaction and the resulting heat over the whole catalyst bed. A recycle system has been incorporated into the fluidized-catalyst reactor design previously described and is shown in Figure 15.

A modification of this type of temperature control is the "hot-gas" recycle system, which involves the recycling of gases through the catalyst bed at ratios ranging from 30:1 to 100:1. Temperature control of the catalyst bed depends on the ability of the gases to carry the heats of the reactions out of the reactor as sensible heat. Little application of this type of recycle design has been made in the past because of the large and costly pressure drops that result in fixed catalyst beds from the very high gas velocities that must be used. If bulk catalyst beds having high void volumes are used, however, this objection is no longer completely valid.

Carbon-Deposition Control

Two techniques are presently available for the prevention of carbon deposition. The first, which has been suggested by a number of individuals, is the use of reactant gases having high hydrogen-carbon monoxide ratios^{1, 2, 4, 5, 59}. This increase in hydrogen-carbon monoxide ratio can be achieved by treating the low-ratio gases with steam over a water-gas shift reaction catalyst. If this step proves to be too expensive, or, as in the case of iron catalysts, not particularly effective in decreasing the amount of carbon that is deposited, steam may be added to the reactant gas. Table 18 shows the results obtained with a nickel catalyst when both steam and recycled product gases were added to the reactant gas⁴.

Maintenance of Catalyst Life

The factors affecting catalyst life are not completely understood. It is known that sulfur is a permanent poison and tends to reduce catalyst ac-

tivity very rapidly after being admitted into the reaction system. It is also known that high operating temperatures usually result in a rapid loss of catalyst activity. The problem of catalyst life is extremely complex, however, and much more work in fundamental catalyst studies must be done before concrete suggestions for maintaining and increasing catalyst life may be made.

KINETICS AND MECHANISMS OF REACTION

As is prevalent with most reaction systems that have immediate industrial application, studies of the kinetics and mechanisms of the methana-

TABLE 18. GAS BOARD CATALYST TEST WITH STEAM AND RECYCLE GAS⁴

Inlet gas temp. 300–330°C

Exit gas temp.: 500°C

Pressure: 1 atm.

Recycle: fresh feed ratio: 5

H₂/CO: 1.07

Steam added: 20 vols. per 100 vols. reactant gas

N₂ in feed gas: 4.0%

Product Gas Composition Corrected to 3% CO₂, % by Vol.

	Hours of Syntheses				
	250	1000	1700	2000	3000
CO ₂	3.0	3.0	3.0	3.0	3.0
CO	9.1	5.1	10.9	11.3	12.6
H ₂	38.4	44.0	38.9	38.5	39.9
CH ₄	38.0	36.5	34.0	34.8	34.0
N ₂	11.5	11.4	13.2	12.4	10.5

Heating value based on CO₂- and N₂-free gas at N.T.P. approximately equal to 990 Btu/cf.

tion reactions have lagged behind the practical development studies. Some data are available, but in most instances, these data have been obtained over limited ranges for very specific catalyst materials, which in most cases have not proved to be the best methanation catalysts, and are frequently ambiguous because of poor temperature control of reaction systems.

Aikers and White³, Binder and White⁶⁰, and Gilkeson *et al.*⁶⁴ have demonstrated that the over-all rates of reaction of hydrogen with both carbon monoxide and carbon dioxide are controlled by surface processes and not by the rates of diffusion of gas molecules to and from the catalyst particle. R. F. Strickland-Constable⁶¹ has shown that the reaction of hydrogen and carbon monoxide over supported-nickel catalysts has a small temperature coefficient and an activation energy for the reaction of the order of 10 kcal, as determined by low-pressure static kinetic techniques.

Both the Bureau of Mines⁵ and the British Fuel Research Station⁶ have shown that the reaction rates over supported-nickel catalysts are extremely high, the latter group demonstrating that increases in space velocity from 3225 to 5965 hr⁻¹ at an observed nominal temperature of 350°C and a pressure of 50 atmospheres, resulted in a decrease in carbon monoxide conversion from 99.3 to 98.5 per cent. Similar relationships have also been observed at 400°C. At 550°C, the reactor tube blocked with carbon before sufficient conversion data could be obtained. It was observed, however, that increases in space velocity from 3740 to 13,950 hr⁻¹ at this temperature resulted in a decrease in carbon-monoxide conversion from 94.6 to 67.2 per cent. It is questionable whether the decrease in conversion was due to a space velocity effect, or to the fact that the temperature control was so poor at the high space velocity that the temperatures of the system were of sufficient magnitude to affect the equilibrium compositions of the product gases. It has been shown in both theoretical and experimental discussions by the British Gas Board⁴ that the temperature of the reaction system is somewhat self-controlling and rarely exceeds 700°C. This controlling effect is due, primarily, to equilibrium-composition effects. It has also been shown that approximately 100 per cent conversion of carbon monoxide occurs in fluidized-beds at space velocities in excess of 10,000 hr⁻¹ when the temperature is carefully controlled⁵. Few other kinetic data exist that are capable of interpretation, and it would appear to be advisable to delay any kinetic discussions until unambiguous kinetic data become available.

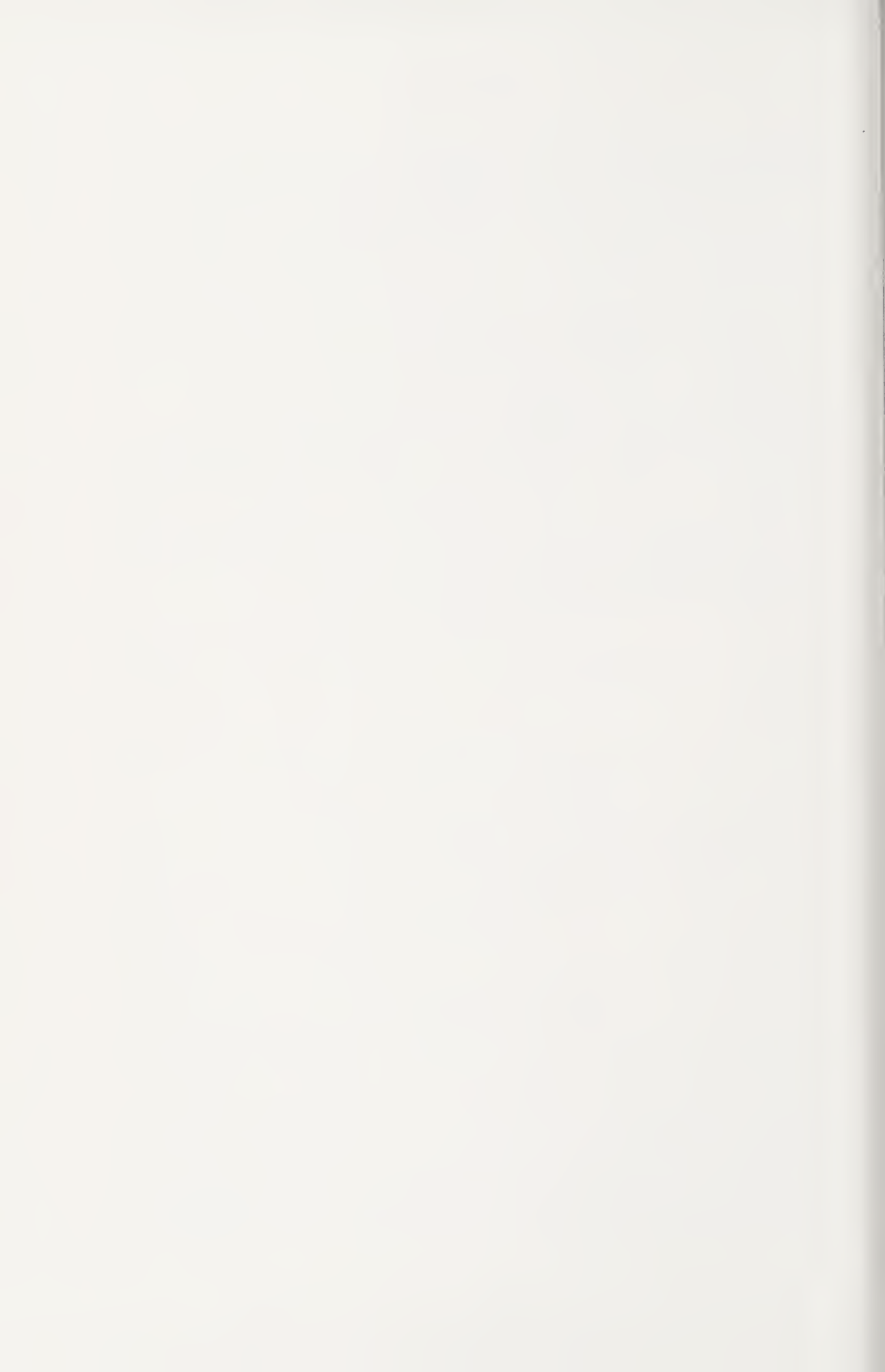
Mechanisms for the reactions have been postulated by Craxford⁶², Medsforth¹⁴, Dent *et al.*⁴, and Strickland-Constable⁶¹. The various mechanistic theories that have been proposed will not be discussed here, since R. B. Anderson will discuss Fischer-Tropsch reaction mechanisms and other relationships to methanation reaction mechanisms in his Chapter on Fischer-Tropsch Catalysts⁶³. It is, therefore, recommended that the reader who is interested in this phase of the problem refer to that Chapter.

Bibliography

1. Sabatier, P., and Senderens, J. B., *Compt. rend.*, **134**, 514 (1902).
2. Sabatier, P., and Senderens, J. B., *J. Chem. Soc.*, **88**, 333, 401 (1905).
3. Aikers, W. W., and White, R. R., *Chem. Eng. Progr.*, **44**, 553 (1948).
4. Dent, F. J., Moignard, L. A., Eastwood, A. H., Blackburn, W. H., and Hebden, D., British Gas Research Board, Communication GRB 20, 1945.
5. Greyson, M., Demeter, J. J., Schlesinger, M. D., Johnson, G. E., Jonakin, J., and Myers, J. W., United States Bureau of Mines, Report of Investigations No. 5137, July 1955.
6. Booth, N., Wilkins, E. T., Jolley, L. J., and Tebboth, J. A., British Gas Research Board, Communication GRB 21, 1945.
7. Schuster, P., Panning, G., and Buelow, H., *Brennstoff-Chem.*, **16**, 368 (1935).
8. Nicolai, J., d'Hont, M., and Jungers, J. C., *Bull. soc. chim. Belg.*, **55**, 160 (1946).
9. Armstrong, E. F., and Hilditch, T. P., *Proc. Roy. Soc.*, **103A**, 25 (1923).

10. Rossini, F. D., Pitzer, K. S., Taylor, W. J., Ebert, J. P., Kilpatrick, J. E., Beckett, C. W., Williams, M. G., and Werner, H. G., Selected Values of Properties of Hydrocarbons, United States Bureau of Standards, Circular C-461, 1947.
11. Vignon, L., *Compt. rend.*, **157**, 131 (1913).
12. Jochum, P., *J. Gasbeleucht.*, **57**, 73, 103, 124, 149 (1914).
13. Sabatier, P., "Catalysis in Organic Chemistry," p. 186, New York, D. Van Nostrand Co., Inc., 1922.
14. Medsforth, S., *J. Chem. Soc.*, **123**, 1452 (1923).
15. Fischer, F., and Tropsch, H., *Brennstoff-Chem.*, **4**, 193 (1923).
16. Haslam, R. T., and Forest, H. O., *Gas Age-Record*, **52**, 615, 620 (1923).
17. Neumann, B., and Jacob, K., *Z. Electrochem.*, **30**, 557 (1924).
18. Fischer, F., Tropsch, H., and Dilthey, P., *Brennstoff-Chem.*, **6**, 265, (1925).
19. Jaeger, A., and Winkelmann, H., *Ges. Abhandl. Kenntnis Kohle*, **7**, 55 (1925).
20. Tropsch, H., Schellenberg, A., and von Philippovitch, A., *Ges. Abhandl. Kenntnis Kohle*, **7**, 63 (1925).
21. Chakravorty, K. M., and Ghosh, J. C., *Quart. J. Ind. Chem. Soc.*, **2**, 150 (1925).
22. *Ibid.*, **2**, 157 (1925).
23. *Ibid.*, **4**, 431 (1925).
24. Pease, R. N., and Chesebro, P. R., *J. Am. Chem. Soc.*, **50**, 1464 (1928).
25. Randall, M., and Gerard, F. W., *Ind. Eng. Chem.*, **20**, 1335 (1928).
26. Hightower, F. W., and White, A. H., *Ind. Eng. Chem.*, **20**, 10 (1928).
27. Bahr, H. A., and Bahr, T., *Ber. deut. chem. Ges.*, **61B**, 2465 (1928).
28. Kemmer, H., *Gas u. Wasserfach*, **72**, 744 (1929).
29. Pascal, P., and Botalfsen, E., *Compt. rend.*, **191**, 186 (1930).
30. Morgan, G. T., and Taylor, R., *Proc. Roy. Soc.*, **131**, 533 (1931).
31. Ghosh, J. C., Chakravorty, K. M., and Bakshi, J. B., *Z. Electrochem.*, **37**, 775 (1931).
32. Kemmer, H., *Gas u. Wasserfach*, **75**, 269 (1932).
33. Koch, H., and Küster, H., *Brennstoff-Chem.*, **14**, 245 (1933).
34. Fischer, F., and Meyer, K., *Brennstoff-Chem.*, **15**, 84, 107 (1934).
35. Klemenc, A., and Rupp, J., *Angew. Chem.*, **47**, 182 (1934).
36. Rapoport, I. B., and Blyudov, A. P., *Khim. Tverdogo Topliva*, **5**, 625 (1934).
37. Fischer, F., and Pichler, H., *Ges. Abhandl. Kenntnis Kohle*, **11**, 386 (1934).
38. Dovani, C., and Franchetti, P., *Acquae gas.*, **24**, 57 (1935).
39. Fischer, F., Bahr, T., and Meusel, A., *Brennstoff-Chem.*, **16**, 466 (1935).
40. Morgan, G. T., *Bull. soc. chim. Belg.* **45**, 287 (1936).
41. Küster, H., *Brennstoff-Chem.*, **17**, 203 (1936).
42. Sebastian, J. J. S., Carnegie Institute of Technology, Coal Research Laboratory, Contribution No. 35, 1936.
43. Chakravorty, K. M., *Science and Culture*, **3**, 396 (1938).
44. Chakravorty, K. M., *J. Ind. Chem. Soc.*, **15**, 245 (1938).
45. Berkman, S., Morrell, J. C., and Egloff, G., "Catalysis," New York, Reinhold Publishing Corp., 1940.
46. Lazier, W. A., 12th Report, Committee on Catalysis, National Research Council, 1940, p. 120.
47. Tropsch, H., and Schellenberg, A., *Ges. Abhandl. Kenntnis Kohle*, **6**, 317 (1921); *Ibid.*, **3**, 33 (1922).
48. Report of Director, Year ending March 31, 1938, British Fuel Research Board, p. 135.
49. Report of Director, Year ending March 31, 1939, British Fuel Research Board, p. 118.

50. Dent, F. J., and Hebden, D., British Gas Research Board, Communication GRB 51, 1950.
51. Catalytic Enrichment of Industrial Gases by the Synthesis of Methane, Department of Scientific and Industrial Research, Fuel Research, Technical Paper No. 57, 1953.
52. Cooperman, J., Davis, J. J., Seymour, W., Ruckes, W. L., United States Bureau of Mines, Bulletin No. 498, 1951.
53. Wainwright, H. W., Egleson, G. C., and Brock, C. M., United States Bureau of Mines, Report of Investigations 5046, 1954.
54. Gilkeson, M. M., White, R. R., and Sliepcevich, C. M., *Ind. Eng. Chem.*, **45**, 460 (1953).
55. Von Itterbeek, A., and Von Dingen, W., *Physica*, **8**, 810 (1941).
56. Chakravorty, K. M., and Sarker, J. M., *Current Sci.*, **13**, 127 (1944).
57. Russell, W. W., and Miller, G. H., *J. Am. Chem. Soc.*, **72**, 2446 (1950).
58. Storch, H. H., Golumbie, N., and Anderson, R. B., "The Fischer-Tropsch and Related Syntheses," pp. 163-184, New York, John Wiley & Sons, Inc., 1951.
59. "Cedford Gas Process," *Gas World*, **55**, 195 (1911).
60. Binder, G. G., and White, R. R., *Chem. Eng. Progr.*, **46**, 563 (1950).
61. Strickland-Constable, R. F., British Gas Research Board, Communication GRB 46, 1949.
62. Craxford, S. R., *Trans. Faraday Soc.*, **35**, 946 (1939).
63. Anderson, R. B., (See Chapt. 2, this volume).



CHAPTER 7

CATALYSIS IN THE LIQUID-PHASE HYDROGENATION OF COAL AND TAR

S. W. Weller

*Houdry Process Corporation, Research and Development Laboratories,
Linwood, Pennsylvania*

INTRODUCTION

Commercially, the conversion of coal and coal tar to gasoline by hydrogenation is carried out in two stages, both catalyzed. In the first stage, the principal product, of which is a distillable oil, the finely divided catalyst passes with the coal or tar through the reaction system. In the second stage, the middle oil product from the first stage passes over a fixed bed catalyst and is converted primarily to gasoline. This chapter will be concerned almost exclusively with the first, or "liquid phase," stage, so-called because it is normally carried out in the liquid phase. The processes occurring during the second stage are discussed elsewhere, along with other hydrocracking reactions.

The liquefaction of coal by direct hydrogenation was discovered by Friedrich Bergius in 1911 as a by-product of his experiments on the formation of coal. The metals commonly used at that time as hydrogenation catalysts—nickel, platinum, palladium—were known to be poisoned by even small amounts of sulfur in the feed. Since large quantities of hydrogen sulfide are evolved during coal hydrogenation, Bergius maintained that this reaction could not be specifically catalyzed. He did incorporate in his reaction mixture Luxmasse, an alkaline iron oxide by-product of the aluminum industry, to assist in the removal of sulfur from the products. Ironically, not only has Bergius' Luxmasse been shown to be a specific catalyst for coal hydrogenation, but the whole commercial development of the process has been possible only since the vital importance of catalysis in this reaction was appreciated.

Although numerous studies of coal hydrogenation catalysts have been made, most of these are of the nature of empirical testing. As a result, very little knowledge is available on the mode of action of these catalysts

or even on their active form during the reaction. The system is an unusually difficult one to study, not only by reason of the complexity of the reactant, coal, and the reaction products, but also because of the high pressure and high temperature necessary for reaction. Some progress has been made, however, in understanding the effects of certain variables, and one may expect that, in time, the mechanism of the reaction will be much more clear than it is today.

WALL EFFECTS

In any but the most gross tests of coal hydrogenation catalysts in autoclaves, it is essential that the autoclave be equipped with a glass liner that can be thoroughly cleaned. If this is not done, there is always a possibility that results may be vitiated by the retention on the converter walls of cat-

TABLE 1. WALL EFFECT IN ABSENCE OF A GLASS LINER

Catalyst Added	CHCl ₃ Insoluble Residue (% m.a.f. coal)
None	17.6
None	16.2
None	18.5
None	16.9
0.1% Sn(OH) ₂	8.6
2.5% Sn(OH) ₂	8.0
0.1% Sn(OH) ₂	9.3
None	8.1
None	10.2
None	12.1

alysts previously used. This precaution has not always been observed, and as a result many literature data on coal hydrogenation catalysts may have value only for qualitative purposes. The "memory effect" of converter walls has been vividly demonstrated by experiments of the British Fuel Research Board¹. In one case a series of experiments was performed on the hydrogenation of Beamshaw coal in the presence of tar vehicle, each experiment immediately following the preceding one in the same autoclave. The autoclave was cleaned with emery cloth and paraffin between successive experiments. The results, summarized in Table 1, show that, after a stannous hydroxide catalyst had been used, the proper value of coal conversion for a noncatalyzed run was approached only very slowly. Similar results, showing the catalytic effect of (presumably contaminated) converter walls, are given in Table 2. In this case the walls are at least as effective as 0.1 per cent of stannous hydroxide.

This wall effect is probably less important in large reactors, used in

continuous plants, where the surface-to-volume ratio is small. However, the results of the experiments of Morgan and Veryard², which showed an effect of turbulence on reaction rate, have been interpreted by Storch³ as being possibly caused in part by a catalytic effect of the tube walls in the small-diameter reactor used.

INFLUENCE OF VEHICLE AND CATALYST DISTRIBUTION

Presence of an oil vehicle during coal hydrogenation may or may not have a favorable effect; evidence on this point is contradictory^{4, 5, 6}. Regardless of the influence of a vehicle when it is used without catalyst, it is quite cer-

TABLE 2. INFLUENCE OF GLASS LINER ON COAL CONVERSION
Beamshaw coal, low temperature tar vehicle, 2 hours at 450°C

Liner Fitted	Catalyst	Insoluble Residue (% m.a.f. coal)
No	None	12.0
Yes	None	45.2
No	0.1% Sn(OH) ₂	9.8
Yes	0.1% Sn(OH) ₂	14.5
No	50% "Pyrex" glass	15.3

TABLE 3. EFFECT OF VEHICLE AND CATALYST ON OIL PRODUCTION

Converter Charge	Total Dry Oil (%)
Coal alone	42.4
Coal + vehicle	54.4*
Coal + 0.1% Sn(OH) ₂	64.4
Coal + vehicle + 0.1% Sn(OH) ₂	70.3*

* Vehicle netted out.

tain that use of a vehicle appreciably enhances the effect of powdered catalysts, especially at low catalyst concentrations. Table 3, based on experiments of the Fuel Research Board⁵, illustrates this. A mechanically-stirred converter was used which permitted continuous removal of volatile products. The vehicle, when used, was low-temperature tar topped to 230°C. A significantly higher yield of dry oil was obtained in the presence of a vehicle than in its absence.

The effect of a vehicle in enhancing the effects of powdered catalysts is probably due to its ability to improve the physical distribution of the catalysts rather than to any specific chemical interaction between vehicle and catalyst. It is known, for example, that tin compounds are able to achieve better distribution than other coal hydrogenation catalysts, when

the catalysts are employed as powdered solids (see below). This is consistent with various findings that a vehicle has a greater effect in promoting the action of molybdenum catalysts than in that of tin catalysts. The Fuel Research Board has reported that, although 2.5 per cent MoO_3 plus 2.5 per cent S in the presence of a low-temperature tar vehicle gives the same total yield of oil from Beams Shaw coal as does 2.5 per cent $\text{Sn}(\text{OH})_2$, in the

TABLE 4. COMPARISON OF TIN AND MOLYBDENUM CATALYSTS IN PRESENCE AND ABSENCE OF VEHICLE

Amount of Catalyst, % of Charge	Yield of Volatile Products, Per Cent of Moisture- and Ash-free Coal	
	No Vehicle	Vehicle
SnO		
0.0096	63.7	73.4
.0951	69.3	79.5
.899	75.7	82.3
4.56	80.6	83.5
9.51	80.5	84.0
SnC ₂ O ₄		
0.0104	60.1	70.9
.0955	65.7	78.3
.773	73.3	80.2
5.09	78.5	82.8
10.24	80.4	82.9
Amm. molybdate		
0.0145	56.7	76.6
.121	57.2	80.1
.817	58.3	83.9
4.91	63.2	84.4
9.06	66.4	84.2

absence of a vehicle somewhat poorer results are obtained with 2.5 per cent MoO_3 plus 2.5 per cent S than with 0.1 per cent $\text{Sn}(\text{OH})_2$ ⁷. There was, accordingly, less difference in the value of tin and molybdenum catalysts in the presence of a vehicle than in its absence.

More detailed experiments bearing on the same point have been reported by Warren, Bowles, and Gilmore⁸. In Table 4 are summarized some of their results on the hydrogenation of a high-volatile A bituminous coal. The vehicle, when used, was a heavy, distillable oil produced by coal hydrogenation. In the absence of a vehicle, ammonium molybdate was

quite ineffective as a catalyst; in the presence of a vehicle, however, it became at least as good as tin oxide or oxalate. Even the tin catalysts were improved by the addition of a vehicle, but it is noteworthy that the greatest effect of the vehicle was at low catalyst concentration, where one may anticipate that the greatest difficulty will occur in achieving good catalyst distribution.

Recent studies have emphasized the vital role which the physical distribution of a catalyst may play in determining its effectiveness⁹. Almost all published autoclave tests of solid catalysts for coal hydrogenation have involved addition of the powdered catalyst to dry coal or coal-oil paste. Although major differences between catalysts are observed when catalyst addition is made in this way, the results may be very deceptive. Apparent

TABLE 5. STUDIES OF CATALYST DISTRIBUTION IN THE ABSENCE OF VEHICLE

Catalyst	Mode of Catalyst Distribution	Per Cent of Moisture- and Ash-free Coal			
		Conversion	Asphaltene	Oil	Gaseous Hydrocarbon
No catalyst	—	33.4	2.8	10.4	9.0
SnCl ₂ (1% Sn)	Powder added	82.3	26.5	29.2	14.5
SnCl ₂ (1% Sn)	Impregnated	88.3	19.9	41.4	15.5
NiCl ₂ (1% Ni)	Powder added	44.2	6.8	13.2	13.4
NiCl ₂ (1% Ni)	Ball-milled	56.9	17.2	19.3	10.4
NiCl ₂ (1% Ni)	Impregnated	88.3	15.5	45.3	18.0
FeSO ₄ (1% Fe)	Powder added	38.9	6.9	8.1	13.1
FeSO ₄ (1% Fe)	Ball-milled	66.2	24.1	21.2	11.4
FeSO ₄ (1% Fe)	Impregnated	84.9	38.9	21.7	15.0
(NH ₄) ₂ MoO ₄ (1% Mo)	Powder added	33.7	1.0	13.8	8.1
(NH ₄) ₂ MoO ₄ (1% Mo)	Impregnated	92.7	27.2	41.1	13.6

differences in intrinsic ability of substances to catalyze the hydrogenation seem, in some cases, to be related simply to the ability of the catalysts to achieve good physical distribution. This has been shown to be the case in experiments with a high-volatile C bituminous coal, from Rock Springs, Wyoming, data for which are given in Table 5⁹. No added vehicle was used in these experiments. The catalysts were added by impregnation from aqueous solution or as powdered solids; in some cases the mixture of powdered catalyst and powdered coal was given an extended ball-milling prior to the hydrogenation test. In Table 5 the column headed "conversion" shows the per cent of coal converted to gaseous products, water, and liquid products soluble in benzene; "asphaltene" represents liquid products soluble in benzene but insoluble in *n*-hexane; and "oil" includes liquid products soluble in *n*-hexane.

When the catalysts are added as powders, stannous chloride appears to

be outstanding and the others to be almost valueless. This evaluation is drastically changed when catalyst addition is accomplished by impregnation. In this case nickelous chloride becomes quite as effective as stannous chloride, ferrous sulfate almost as good for coal conversion though poor in accomplishing asphaltene reduction, while ammonium molybdate is superior to any of the other catalysts. Other experiments (not included in Table 5), carried out at a concentration level of 0.1 per cent metal, confirm the superiority of impregnated ammonium molybdate. The activity even of stannous chloride is increased by impregnation. Ball-milling, in the cases investigated, is of intermediate effectiveness.

These results, originally obtained in autoclave experiments, have been confirmed in Bureau of Mines pilot plant operations^{10, 11}. In a study of the conversion of Rock Springs coal to fuel oil using impregnated catalysts, these same catalysts were found to be decreasingly effective for coal liquefaction in the following order: ammonium molybdate > stannous chloride > nickelous chloride > ferrous sulfate. The same order of effectiveness obtained for asphaltene removal, except that nickelous chloride was at least equal to stannous chloride.

In the light of these results, it is clear that particular care should be paid to obtaining optimum catalyst distribution in all fundamental studies of the intrinsic value of coal hydrogenation catalysts. This has not often been done, and, as a result, many literature data on catalyst comparisons have only qualitative value.

The question of catalyst distribution may be associated with a recent observation made on the hydrogenation of bituminous (Bruceton) coal¹². Whole coal was found to have, on hydrogenation, a conversion (to liquid and solid products) of 50 to 60 per cent under a specified set of experimental conditions. Hand-picked anthraxylon from the same mine showed a conversion of only 30 per cent under the same conditions. This is surprising, since anthraxylon is considered to be the petrographic constituent of coal which is most easily hydrogenated. Ultimate analyses of the two materials showed significant differences only in the ash content, which was 7.2 per cent for the whole coal and only 1.4 per cent for the anthraxylon. The results suggested that some ash constituent, present in whole coal but not in anthraxylon, was acting as a moderately active catalyst for the hydrogenation. By spectrographic analyses of the ash it was learned that the only elements present in appreciably larger amounts in the whole coal were aluminum, calcium, iron, and silicon. However, numerous attempts to achieve the conversion shown by whole coal by adding various compounds of these elements (as powdered solids) to anthraxylon were unsuccessful. Makh¹³, in a somewhat similar study, had also found that although poorer conversions were obtained with coal from which ash had been extracted by

mineral acids than with untreated coal, addition of identifiable ash constituents to the extracted coal did not increase the conversion to its original value.

When the importance of catalyst distribution was realized, however, a sample of anthraxylon was tested which had been impregnated with ferrous sulfate (1 per cent Fe). Under the same conditions of hydrogenation, this sample showed a conversion of 80 per cent, considerably greater than that of the whole coal. Although the iron in the ash is probably not present as ferrous sulfate, it was considered probable that the iron, in whatever form it occurs, is intimately distributed in the coal substance. Impregnating with ferrous sulfate is simply a means of approximating a catalyst distribution comparable to that in whole coal.

COMPARATIVE CATALYST TESTS

A number of comparative catalyst studies of varying scope have been published¹⁴⁻²⁴. It is possible to make only a few generalizations on the basis of the results. In some cases a catalyst reported poor by one investigator is ranked as good by another; this is true for ferric oxide, for example. Such variations are probably due in part to differences in the nature of the coal hydrogenated, but the effects of catalyst distribution discussed above may also be partly responsible.

Tin in various forms has been reported to be the most active catalyst for the hydrogenation of higher rank coals (however, see effect of catalyst distribution, above). Good results have also been obtained with compounds of molybdenum, zinc, and lead, among others. For a number of metals, the chlorides are more active than the oxides or sulfides. Tungsten compounds are reported to be very poor, an interesting result in view of their outstanding effectiveness in catalyzing the vapor phase (fixed bed) hydrogenation of middle oil to gasoline. Several standard hydrogenation catalysts such as nickel-kieselguhr and copper chromite, which are very useful with many organic compounds, are quite poor for coal hydrogenation.

Similar results have been obtained in studies of catalysts for the hydrogenation of tars. In this case, however, molybdenum compounds are apparently superior to tin, and excellent results are also obtained with hydriodic acid and compounds, such as iodoform, which can liberate hydriodic acid under reaction conditions.

Two interesting cases of synergism have been reported for coal hydrogenation catalysts. Luxmasse, a crude iron oxide obtained as a by-product of the aluminum industry, was used extensively in German commercial coal hydrogenation practice. Titania is an important minor constituent of Luxmasse. As the British Fuel Research Board and others have shown, neither iron oxide nor titania is a very effective coal hydrogenation catalyst.

The data of Table 6 (taken from Ref. 17) demonstrate, however, that a mixture of the two oxides is much more active than either used separately and gives essentially the same results as whole Luxmasse. The reason for this effect is not known.

Similar behavior has been observed for the combination of tin and those materials which can give rise to a halogen acid under reaction conditions. Table 7²⁴ illustrates this for a Wyoming, high-volatile C bituminous coal. In the absence of a catalyst and for an arbitrary set of conditions, the conversion of moisture- and ash-free coal to gas, water, and liquid products

TABLE 6. CATALYTIC EFFECT OF LUXMASSE, FERRIC OXIDE, AND TITANIA

Catalyst	Concentration, % m.a.f. Coal	Products, % m.a.f. Coal			
		CHCl ₃ Insoluble	CHCl ₃ Soluble	Water	Gas
None	—	49.2	27.6	7.1	10.7
Luxmasse	2.5	10.0	66.1	5.9	8.2
Fe ₂ O ₃	2.5	27.3	52.4	2.0	8.8
TiO ₂	2.5	36.9	38.4	7.2	10.8
{ Fe ₂ O ₃ TiO ₂	{ 2.29 0.21 }	12.0	65.7	6.9	6.5

TABLE 7. CATALYTIC EFFECT OF TIN AND AMMONIUM CHLORIDE

Catalyst	Coal Conversion (%)	Gas Production (%)
None	30.9	13.3
1% Sn	44.2	13.6
0.5% NH ₄ Cl	33.5	—
1% Sn + 0.5% NH ₄ Cl	88.6	15.3

soluble in benzene was only 31 per cent, of which 13 per cent was gas. Powdered tin by itself increased the conversion to 44 per cent. Ammonium chloride, which is equivalent to hydrochloric acid in these experiments, was essentially without catalytic effect; with some other coals, use of ammonium chloride results even in *decreased* conversions (see below). The combination of tin and ammonium chloride was far superior to either used separately; a coal conversion of almost 89 per cent was observed, most of the increase occurring in the liquid products. Rather similar results have been obtained by the Fuel Research Board for tin hydroxide with either iodine or bromine, as well as with hydrochloric acid¹⁷.

A related case may be that of the ammonium molybdate-sulfuric acid combination. It was first discovered by I. G. Fardenindustrie at Leuna

that the amount of ammonium molybdate required to catalyze the hydrogenation of brown coal could be greatly reduced if 50 to 90 per cent of the alkalinity of the coal was first neutralized with sulfuric acid. This effect has been confirmed in recent experiments at the Bureau of Mines¹². Table 8 contains data obtained with Rock Springs coal and with Beulah lignite. With both coals the use of impregnated ammonium molybdate as catalyst resulted in a great improvement in conversion of the coal. When, in addition, 90 per cent of the alkalinity was neutralized with sulfuric acid, not only was the coal conversion still further increased, but also a marked increase in the asphaltene-to-oil reaction occurred. The effect of sulfuric acid was not one of simple neutralization, however, since the use of hydrochloric,

TABLE 8. INFLUENCE OF SULFURIC ACID ON EFFECTIVENESS OF AMMONIUM MOLYBDATE

Coal	Catalyst	Per Cent of m.a.f. Coal			
		Con- version	Asphal- tene	Oil	Gaseous Hydro- carbons
Rock Springs (bituminous)	None	33.4	2.8	10.4	9.0
	Imp. $(\text{NH}_4)_2\text{MoO}_4$ (1% Mo), not neut.	92.7	27.2	41.1	13.6
	Imp. $(\text{NH}_4)_2\text{MoO}_4$ (1% Mo), 90% neut.*	94.7	10.0	62.6	13.9
Beulah (lig- nitic)	None	48.9	8.1	11.2	11.2
	Imp. $(\text{NH}_4)_2\text{MoO}_4$ (1% Mo), not neut.	75.2	14.5	22.6	19.6
	Imp $(\text{NH}_4)_2\text{MoO}_4$ (1% Mo), 90% neut.*	82.7	10.0	44.0	14.1

* 90% of alkalinity of coal neutralized with dilute H_2SO_4 .

acetic, or phosphoric acid for neutralization (in conjunction with impregnated ammonium molybdate) was reported to result in lower conversions than when no acid at all was used.

The Bureau of Mines has also reported an interesting anion effect in studies of iron, cobalt, nickel, and tin salts (impregnated) as catalysts for the conversion of Rock Springs coal¹². Table 9, which summarizes the results, illustrates the peculiar change in the relative effectiveness of the sulfate and chloride salts as one proceeds through this series of metals. Impregnated ferrous sulfate is an excellent conversion catalyst, ferrous chloride a very poor one. Cobaltous sulfate is as active as ferrous sulfate, and cobaltous chloride is still a poor catalyst, though somewhat better than ferrous chloride. With nickel, the situation is already reversed; nickelous chloride is an exceptionally good catalyst, and nickelous sulfate is less

active, though still good. Stannous chloride again is an excellent catalyst, while stannous sulfate is as poor as ferrous chloride. The reason for this change in relative behavior of the sulfate and chloride salts is obscure, especially since in all cases the metal is probably converted to the sulfide under reaction conditions (see below). For ferrous sulfate, at least, acidic chloride appears to be a negative catalyst. Impregnation of Rock Springs coal with ammonium chloride (0.5 per cent) along with ferrous sulfate (1 per cent iron) caused a decrease in coal conversion from 85 (no ammonium chloride) to 52 per cent.

It is significant that, although ferrous sulfate and cobaltous sulfate were almost as effective coal conversion catalysts as were nickelous chloride and stannous chloride, much superior conversions of asphaltene to oil were

TABLE 9. COMPARISON OF METAL SULFATES AND CHLORIDES
(Rock Springs Coal)

Catalyst	Per Cent of m.a.f. Coal			
	Conversion	Asphaltene	Oil	Gaseous Hydrocarbons
Imp. FeSO_4 (1% Fe)	84.9	38.9	21.7	15.0
Imp. FeCl_2 (1% Fe)	44.8	4.8	12.2	15.2
Imp. CoSO_4 (1% Co)	83.6	36.5	22.5	14.9
Imp. CoCl_2 (1% Co)	58.0	11.2	16.3	8.3
Imp. NiSO_4 (1% Ni)	78.9	33.0	14.8	10.0
Imp. NiCl_2 (1% Ni)	88.3	15.5	45.3	18.0
Imp. SnSO_4 (1% Sn)	46.3	7.9	12.3	12.9
Imp. SnCl_2 (1% Sn)	88.3	19.9	41.4	15.5

achieved with the latter catalysts. This fact is relevant to the discussion below of the mechanism of coal hydrogenation.

STABILITY OF CATALYSTS

In connection with the mode of action of catalysts, it is of interest to inquire in what chemical form the catalyst is present during the hydrogenation. This question has been studied to some extent with tin catalysts, though without shedding much light on the nature of the catalytic action.

The effectiveness of tin is greatly enhanced by the addition of a halogen acid or ammonium halide. Moreover, in the presence of ammonium chloride, approximately equal activity is shown by metallic tin, stannous sulfide, or stannic oxide, while stannous chloride by itself is as effective as tin plus an equivalent amount of ammonium chloride. These results would be explicable if stannous chloride were the most active tin compound, and if the other materials were converted to stannous chloride under reaction conditions.

Stannous chloride also has a relatively high vapor pressure of about 40 mm Hg at 450°C, a fact which could account for the unusually good physical distribution achieved by tin catalysts.

Unfortunately, this hypothesis is made less cogent by the fact that, under reaction conditions (ca. 450°C, $p_{H_2} = 200\text{--}700$ atm., $p_{H_2S} = 1$ atm.), stannous chloride becomes thermodynamically somewhat less stable than stannous sulfide, and, in fact, stannous sulfide becomes the most stable tin compound. In this connection, autoclave experiments have been reported¹² which show that both stannous chloride and stannic oxide are largely converted to stannous sulfide in 1 hour at 450°C, under partial pressures of H_2 and H_2S comparable with those occurring in coal hydrogenation. The conversion of stannous sulfide to the chloride is, therefore, not to be expected during coal hydrogenation. Presumably, the two constituents of the synergistic combination, tin compound-halogen acid, exercise their functions separately rather than by formation of a tin halide. This concept of separate action of tin and halogen acid has also been employed in some discussions of the mechanism of coal hydrogenation (see below).

Calculations also indicate that, in the case of nickel and iron, nickel sulfide and ferrous sulfide are the stable forms when compounds of these metals are employed. It is important to note that reduction of the metal sulfates to sulfides is strongly favored for these metals under reaction conditions.

It may seem odd to the casual observer that nickel catalysts, usually considered so susceptible to sulfur poisoning, should be very effective for the hydrogenation of coal. Perhaps even more surprising is the fact that platinum, impregnated on coal from a solution of chloroplatinic acid, shows an activity comparable with that of stannous chloride²⁵. In the case of platinum, the activity in the presence of H_2S may be due to the instability of platinum sulfide under reaction conditions. Thermodynamic data²⁶ indicate that, for example, at 423°C and a hydrogen partial pressure of 150 atm., the partial pressure of hydrogen sulfide must equal at least 3.6 atm. in order to prevent the reduction of PtS to Pt . The case of nickel is different in that the hydrogen sulfide pressure during coal hydrogenation is always sufficient to make either NiS or Ni_3S_2 the stable phase. These sulfides have been reported to be hydrogenation catalysts in other systems²⁷. They are normally used at elevated temperatures, however, and they probably have a lower intrinsic activity than do metallic nickel catalysts.

CATALYSIS AND THE MECHANISM OF HYDROGENATION

Catalysts furnish a useful tool for the study of coal and tar hydrogenation. A full understanding of the ways in which catalysts work will lead not

only to an understanding of the mechanism of hydrogenation, but also to some insight into the structure of coal itself. Progress in this direction has been slow, but some attempts have been made to relate the effects of individual catalysts to the mechanism of the reactions occurring.

One such attempt involved the study of catalysts for the hydrogenation of coal-hydrogenation asphaltene²⁸. The crude asphaltene used contained 1.4 per cent benzene insolubles, 93.8 per cent asphaltene (benzene soluble, hexane insoluble material), 4.4 per cent oil (hexane soluble material), and

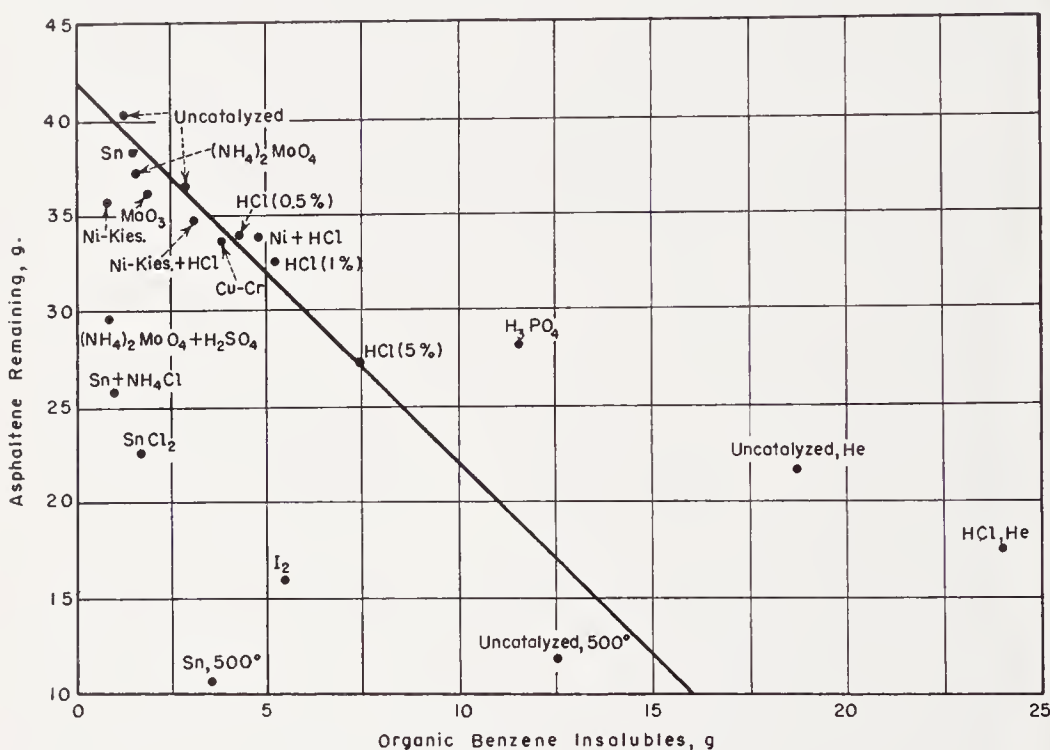
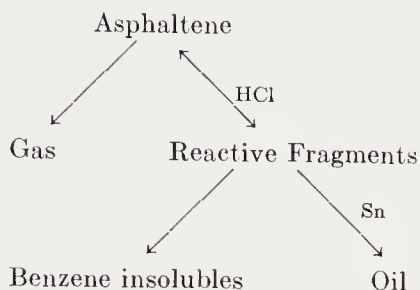


Figure 1. Hydrogenation of asphaltene.²⁸

0.1 per cent H₂O. This material is a convenient substrate for study; it is also a reasonable one in view of the fact that asphaltene is probably an intermediate product in the over-all conversion of coal to oil^{29, 30}.

In most of these experiments the reaction temperature was 450°C. During the hydrogenation, a small fraction of the asphaltene (4 to 9 per cent) was converted to gas. Most of the asphaltene converted appeared as hexane-soluble oil, but with most catalysts, an appreciable amount of benzene insoluble material was also formed. The relation observed between asphaltene remaining and organic benzene insolubles is shown in Figure 1. These results were interpreted on the basis of the following scheme for the hydrogenation:



Asphaltene is assumed to be split with the formation either of gas, by a noncatalytic reaction, or of reactive fragments of some kind. The reactive fragments may (1) recombine to form asphaltene, (2) polymerize further to produce benzene-insoluble material, or (3) be stabilized with the addition of H_2 to form oil. (It may be noted that similar ideas, applied to the hydrogenation of coal, have been expressed by Graham and Skinner³¹ and by Cawley³².) According to this scheme, the relative proportions of insolubles, asphaltene, and oil in the product depend on the relative rates of splitting, hydrogenation-stabilization of fragments, and polymerization of fragments. The product distribution should correspondingly depend on the presence of splitting catalysts, hydrogenation catalysts, and high pressure H_2 . The points clustered about the straight line in Figure 1 represent catalysts which are considered either to have no catalytic effect or, like HCl, to catalyze the splitting of asphaltene but not the hydrogenation of fragments. Tin is assumed to catalyze only the hydrogenation-stabilization; in the absence of a splitting catalyst, tin is unable to catalyze the over-all conversion of asphaltene. Points lying to the right of the line are for materials or conditions which favor the polymerization by fragments over their hydrogenation; H_3PO_4 and an inert atmosphere (He) come in this category. Points lying to the left of the line represent materials which catalyze both the splitting and the hydrogenation of fragments. In this group are the Sn-HCl and $(NH_4)_2MoO_4$ - H_2SO_4 combinations and I_2 , which is converted to HI, a dual-function catalyst. The two experiments carried out at $500^\circ C$ are also interpretable on this basis. The rates of all the reactions are increased by the rise in temperature, which leads both to increased asphaltene conversion and increased insolubles production in the absence of added catalyst. In the presence of Sn, however, hydrogenation to oil occurs preferentially to polymerization to insolubles.

The detailed results of this study must be qualified because the solid catalysts were added as powders. For some of the catalysts, such as ammonium molybdate and nickelous chloride, a greater activity would probably have been observed had it been possible to achieve better physical distribution.

Additional experiments were carried out on the hydrogenation of the

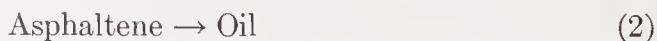
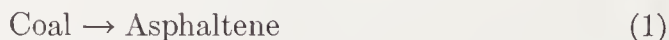
anthraxylon fraction of Bruceton (Pittsburgh seam) coal²⁶. The dependence of coal conversion on catalyst used is summarized in Table 10. These results were interpreted on the basis of a reaction scheme similar to that outlined above. It was assumed that primary fragment formation occurs relatively readily with anthraxylon, even in the absence of a catalyst. When no hydrogenation catalyst is present, a large fraction of the fragments re-polymerizes to form benzene insolubles; in the presence of Sn, however, most of the fragments are hydrogenated to form benzene soluble products. The rate of splitting, already too high in the absence of a hydrogenation catalyst, is increased by the addition of NH_4Cl ; as a result, NH_4Cl acts as a "negative catalyst."* This action of NH_4Cl , or of HCl , which behaves identically, in decreasing coal conversion when used alone has also been noted by the Fuel Research Board³³. This group observed that the addition of HCl to Beamshaw coal in excess of the amount required to combine with the alkalis in the inorganic constituents resulted in the production of more

TABLE 10. INFLUENCE OF TIN AND AMMONIUM CHLORIDE ON HYDROGENATION OF BRUCETON ANTHRAXYLON

Catalyst	Conversion (%)
None	29.5
1% Sn	85.3
0.5% NH_4Cl	22.6
1% Sn + 0.5% NH_4Cl	92.9

solid residue on hydrogenation than when no acid was used. A less marked effect occurred with H_2SO_4 , while HCOOH was without influence.

As mentioned above, evidence has been accumulating that asphaltene is an intermediate product in the conversion of coal to distillable oil. This may be represented schematically by the consecutive reactions:



There is a marked difference in the rates of these reactions; normally, reaction (2) is much more difficult to accomplish than is (1)²⁸. Much of the oxygen in coal is liberated as water and carbon dioxide during (1)³⁴. One is led to conjecture that, to a large extent, the molecular weight reduction represented by (1) is associated with breaking weak carbon-oxygen bonds, while reaction (2) involves breaking carbon-carbon bonds³⁵. The validity

* The assumption here, that an increased rate of splitting causes a higher ratio of fragments polymerized to fragments hydrogenated, can be valid only if the polymerization reaction is of a higher kinetic order in fragment concentration than is the hydrogenation reaction. This is reasonable, however.

of such a conjecture will be more easily tested when a better understanding has been achieved of the relationship between the coal hydrogenation reactions and those of pure "model" compounds. Orlov³⁶, Prokopets³⁷, Hall^{38, 39} and Charmbury⁴⁰ and their coworkers have already published interesting information on the products of hydrogenation of certain polycyclic compounds at elevated temperatures. An extension of these investigations with pure compounds to a comparative study of different catalysts would be very helpful in establishing the detailed function of individual catalysts.

It is certainly known now that the relative effectiveness of certain catalysts is quite different for reactions (1) and (2). Impregnated ferrous sulfate, for example, is almost as good as impregnated nickelous chloride in catalyzing the conversion of coal, but is much less effective in catalyzing the asphaltene-to-oil conversion (Table 9). For the present, it remains dangerous to over-simplify the action of an individual catalyst. Ammonium chloride, whose function has been interpreted as that of a splitting catalyst, acts as a promoter for tin catalysts but as an antagonist for ferrous sulfate. Until more detailed information has been collected concerning the mode of action of each material, it will be difficult to treat these interrelations on a unitary basis. Significant progress has been made, however, and continuous intelligent research will lead to a much fuller understanding of the role of catalysis in the hydrogenation of coal and tar.

References

1. Dept. Sci. Ind. Research (Brit.), Fuel Research, "Rept. for Period Ended March 31, 1936," p. 151. "Rept. for Period Ended March 31, 1937," p. 151.
2. Morgan, G. T., and Veryard, J. T., *J. Soc. Chem. Ind.*, **57**, 152 (1938).
3. Storch, H. H., "Hydrogenation of Coal and Tar," in Lowry, "Chemistry of Coal Utilization," Vol. II, pp. 1750-1796, New York, John Wiley & Sons, Inc., 1945.
4. Horton, L., King, J. G., and Williams, F. A., *J. Inst. Fuel*, **7**, 85 (1933).
5. Dept. Sci. Ind. Research (Brit.), Fuel Research, "Rept. for Period Ended March 31, 1934," p. 98.
6. Pelipetz, M., Kuhn, E. M., Friedman, S., and Storch, H. H., *Ind. Eng. Chem.*, **40**, 1259 (1948).
7. Dept. Sci. Ind. Research (Brit.), Fuel Research, "Rept. for Period Ended March 31, 1936," p. 151.
8. Warren, T. E., Bowles, K. W., and Gilmore, R. E., *Ind. Eng. Chem., Anal. Ed.*, **11**, 415 (1939).
9. Weller, S., and Pelipetz, M. G., *Ind. Eng. Chem.*, **43**, 1243 (1951).
10. Kandiner, H. J., Hiteshue, R. W., and Clark, E. L., *Chem. Eng. Progr.*, **47**, 392 (1951).
11. Clark, E. L., Hiteshue, R. W., and Kandiner, H. J., *ibid.*, **48**, 15 (1952).
12. Weller, S., and Pelipetz, M. G., World Petroleum Congress, Hague, 1951, Sect. 4.
13. Makh, G. M., *J. Applied Chem. (U.S.S.R.)*, **12**, 457 (1939).
14. Abe, R., Huzikawa, S., Kakutani, T., and Okamura, T., *J. Soc. Chem. Ind. Japan*, **41**, supplementary binding, 417 (1938).
15. Ando, S., *J. Soc. Chem. Ind. Japan*, **38**, supplementary binding, 567 (1935).

16. Cawley, C. M., and Kingman, F. E. T., *Fuel*, **22**, 15 (1943).
17. Dept. Sci. Ind. Research (Brit.), Fuel Research, "Rept. for Period Ended March 31, 1930," p. 103; "Rept. for Period Ended March 31, 1932," p. 52; "Rept. for Period Ended March 31, 1933," p. 94; "Rept. for Period Ended March 31, 1938," p. 206.
18. Graham, J. I., and Skinner, D. G., *Proc. Intern. Conf. Bituminous Coal, 3rd Conf.*, **1931**, Vol. 2, p. 17.
19. Kosaka, Y., Yamanouchi, A., and Tanaka, K., *J. Soc. Chem. Ind. Japan*, **40**, supplementary binding, 3 (1937).
20. Kurokawa, M., Hurota, W., Fujiwara, K., and Asaoka, N., *J. Fuel Soc. Japan*, **18**, 31A (1939).
21. Kurokawa, M., *J. Soc. Chem. Ind. Japan*, **46**, supplementary binding, 535 (1943).
22. Rapoport, I. B., and Sudzilovskaya, M. S., *Khim. Tverdogo Topliva*, **6**, 40 (1935).
23. Storch, H. H., Hirst, L. L., Fisher, C. H., Work, H. K., and Wagner, F. W., *Ind. Eng. Chem.*, **33**, 264 (1941).
24. Weller, S., Pelipetz, M. G., Friedman, S., and Storch, H. H., *Ind. Eng. Chem.*, **42**, 330 (1950).
25. Unpublished results, U. S. Bureau of Mines.
26. Kelley, K. K., U. S. Bur. Mines Bull. 406 (1937).
27. Kirkpatrick, W. J., "Nickel Sulfide Catalysts," in "Advances in Catalysis," Vol. III, pp. 329-338, New York, Academic Press, 1951.
28. Weller, S., Pelipetz, M. G., and Clark, E. L., *Ind. Eng. Chem.*, **42**, 334 (1950).
29. Morikawa, K., Okamura, T., and Abe, R., *J. Soc. Chem. Ind. Japan*, **41**, suppl. binding, 431 (1938).
30. Weller, S., Pelipetz, M. G., and Friedman, S., *Ind. Eng. Chem.*, **43**, 1575 (1951).
31. Graham, J. I., and Skinner, D. G., *J. Soc. Chem. Ind.*, **48**, 129T (1929).
32. Cawley, C. M., *Research*, **1**, 553 (1948).
33. Dept. Sci. Research (Brit.). Fuel Research, "Rept. for Period Ended March 31, 1935," p. 125.
34. Pelipetz, M. G., Weller, S., and Clark, E. L., *Fuel*, **29**, 208 (1950).
35. Storch, H. H., Fisher, C. H., Hawk, C. O., and Eisner, A., U. S. Bur. Mines Tech. Paper 654 (1943), p. 18.
36. Orlov, N. A., *et al.*, *Ber. Gesell. Kohlentechn.*, **64B**, 2361 (1936).
37. Prokopets, E. I., *et al.*, *Ukrain. Khim. Zhur.*, **6**, 244 (1931); *Coal and Chem. (U.S.S.R.)*, **1**, 35 (1932); *J. Appl. Chem. (U.S.S.R.)*, **10**, 126 (1937); **11**, 823 (1938).
38. Hall, C. C., *Fuel*, **12**, 76, 419 (1933); *J. Soc. Chem. Ind.*, **54**, 208T (1935).
39. Hall, C. C., and Cawley, C. M., *J. Soc. Chem. Ind.*, **58**, 7 (1939).
40. Charmbury, H. B., *et al.*, *J. Am. Chem. Soc.*, **66**, 526 (1944); **72**, 4478 (1950).

CHAPTER 8

CATALYTIC CYCLIZATION AND AROMATIZATION OF HYDROCARBONS

H. Steiner

Petroleum Limited, Manchester, England

INTRODUCTION

The reaction leading from paraffins and olefins by ring closure to aromatic compounds was first discovered in 1936 by Moldavski and Kamusher¹. These authors passed *n*-heptane vapors over a chromium oxide catalyst and obtained considerable quantities of toluene. Negligible cracking took place, and apart from unconverted heptane and an olefinic by-product only toluene was found among the reaction products. The only related reaction known previously to this discovery was the isomerizing dehydrogenation of methylindene to give naphthalene². It is clear that in this reaction the five ring is opened and closure to a six ring takes place, with simultaneous dehydrogenation to naphthalene.

Soon after Moldavski's and Kamusher's discovery, and independently of it, a patent was taken out by Grosse and Morrell³ to cover the catalytic cyclization of *n*-heptane and similar *n*-paraffins to the corresponding aromatic compounds. This patent covered as catalysts, generally, oxides of the metals belonging to the 5th and 6th subgroup of the periodic system.

At about the same time Kazanski and Plate⁴ discovered that at 350°C platinum catalysts are able to cyclize paraffins to aromatic compounds, though the yields were considerably lower than those obtained with oxide catalysts in the higher temperature range of 450 to 500°C.

In the years following its original discovery this reaction was thoroughly investigated by the Russian workers themselves, but soon American, Dutch and British chemists contributed to the further development of this field. Particularly notable contributions were made by Taylor and collaborators⁵; by Hoog, Verheus and Zuiderweg⁶; and by Herington and Rideal⁷. It was found that a group of related reactions existed by which various paraffins, olefins and five-ring naphthenes could be transformed into aromatics without degradation of the carbon chain into lower molecular

weight compounds. It was clear that not only cyclization and dehydrogenation reactions were involved, but in many cases isomerization took place as well. Naturally, the well-known dehydrogenation of six-ring naphthenes to aromatics is also closely related.

Apart from the scientific interest of this new group of hydrocarbon reactions, the important industrial aspects, particularly for the petroleum industry, were soon realized: first, as a means to upgrade motor fuels because of the conversion of straight or slightly branched chain hydrocarbons of low octane rating into aromatics of high octane rating; secondly, because of the possible synthesis of certain individual aromatic compounds from petroleum or petroleum fractions. The most notable example of the latter application of the reaction is the production of toluene, which was synthesized from petroleum fractions in enormous quantities during the last war. The production of *o*-xylene from C_8 hydrocarbons and benzene from C_6 hydrocarbons are more recent examples of applications of this reaction.

GENERAL CHEMISTRY OF THE REACTION

In the laboratory the cyclization reaction is usually carried out by leading the vapors of the hydrocarbon charge at or near atmospheric pressure over the catalyst. In technical applications, pressure is applied and the reaction is carried out in the presence of substantial amounts of hydrogen. This method of operation will be discussed later.

The useful temperature range for reaction over oxide catalysts is from 450 to 550°C. Below 450°C the activity of these catalysts is small, and above 550°C cracking reactions become prominent. Contact times under these conditions range from a few seconds up to one minute. At about 475°C conversions of 80 to 90 per cent can be achieved, depending on the activity of the catalyst and on the reactivity of the hydrocarbon used.

Cyclizations which do not require simultaneous isomerization can be achieved over reasonably active catalysts from 450°C upward; if, on the other hand, an isomerization step is involved, temperatures above 500°C are required for sufficiently fast reaction rates.

Oxides of the 5th and 6th subgroup of the periodic table are employed as catalysts. Chromium oxide and molybdenum oxide are most generally used. These catalysts must be prepared in a state of fine subdivision such as, for instance, by precipitation as gels and subsequent calcination, or by precipitation on certain supports such as activated alumina, which exhibit large surface areas. The activity of all oxide catalysts declines in the course of several hours, due to the formation of polymer deposits on the catalytic surface. These surface polymers can be burned off, as a result of which the original activity of the catalyst can be restored. The question of catalysts for the cyclization reaction will be discussed in detail later.

It was, of course, of great interest to see which classes of hydrocarbons were amenable to the cyclization reaction, and many individual compounds were tested. A reasonably complete summary is given in Tables 1 and 2, where the various compounds which have been cyclized and the resulting products are listed. Table 1 lists compounds which can be aromatized by

TABLE 1. CYCLIZATION OF PARAFFINS AND RESULTING AROMATIC PRODUCTS

Base Material	Aromatics Found	Per cent Observed	Per cent Calculated Assuming Direct Ring Closure ^a	Experimental Conditions*	Ref.
<i>n</i> -Hexane	Benzene	~100	100	I	6
<i>n</i> -Heptane	Toluene	>95	100	II	7
2-Methyl hexane	Toluene	~100	100	I	6
<i>n</i> -Octane	Ethylbenzene	23	66	II	7
	<i>o</i> -Xylene	33	33		
	<i>m</i> -Xylene	27	0		
	<i>p</i> -Xylene	7	0		
2-Methyl heptane	<i>m</i> -Xylene	100	100	II	7
3-Methyl heptane	Ethyl benzene	15	33	II	7
	<i>o</i> -Xylene	25	33		
	<i>p</i> -Xylene	60	33		
2,5-Dimethyl hexane	<i>p</i> -Xylene	80	100	I	6
2,3-Dimethyl hexane	<i>o</i> -Xylene	90	100	II	7
	<i>p</i> -Xylene	10	0		
3-Ethyl hexane	Ethyl benzene	100	100	II	7
Nonane	<i>n</i> -Propyl benzene	25-29		II	7
	<i>o</i> -Methyl ethyl benzene	75-71			
	Traces of indene				
Decane	Naphthalene	One of several components		II	7
Tetradecane	Anthracene and phenanthrene	Two of many products		II	7

* Experimental conditions. I. 465°C, 18-24 sec. contact time, specially prepared Cr₂O₃ catalyst. II. 475°C, Catalyst Cr₂O₃ on alumina.

^a See page 538 for details of this calculation.

straight cyclization and dehydrogenation; Table 2 deals with compounds where, in addition, isomerization must be a step in the reaction sequence.

Based on these experiments one can define the following classes of hydrocarbons which can be converted into aromatic compounds by cyclization and dehydrogenation.

1. Straight-chain paraffins or olefins from C₆ hydrocarbons upward (e.g., *n*-heptane to toluene—see Figure 1a).

2. Branched-chain paraffins or olefins having a chain of at least six carbon atoms within their molecular structure (e.g., 2-methylhexane to toluene, see Figure 1b).

3. At higher temperatures, C_6 and higher hydrocarbons having a straight chain of only five carbon atoms within their molecular structure can also be cyclized to six-ring aromatic compounds; it is evident that an isomeriza-

TABLE 2. ISOMERIZING CYCLIZATION AND RESULTING AROMATIC PRODUCT⁷

Hydrocarbon	Aromatic Formed, % of Liquid Product	Aromatic Compound Formed	Per Cent of Total Aromatic	
			Observed ^b	Calculated ^a
2,3-Dimethylpentane	30	Toluene	100	100
2,2,3-Trimethylpentane	—	<i>m</i> -Xylene	100	100
2,2,4-Trimethylpentane	50	<i>p</i> -Xylene	100	100
2,3,3-Trimethylpentane	—	<i>m</i> -Xylene	100	100
2,3,4-Trimethylpentane	—	<i>o</i> -Xylene	60	50
		<i>p</i> -Xylene	40	50
		Ethylbenzene	12.5	12.5
		Toluene	12.5	12.5
2-Methyl-3-ethylpentane	—	<i>o</i> -Xylene	25	25
		<i>m</i> -Xylene	50	50
		Ethylbenzene	24	25
		Toluene	24	25
3-Methyl-3-ethylpentane	—	<i>o</i> -Xylene	48	50
		<i>m</i> -Xylene	4	
		Toluene	100?	
		Toluene	100?	
		Ethylbenzene	10	10
		Toluene	10	10
Ethylcyclopentane	20	<i>o</i> -Xylene	40	40
<i>trans</i> -1:2-dimethylcyclopentane	27	<i>m</i> -Xylene	20	20
3:3-Dimethylcyclohexane	50	<i>p</i> -Xylene	20	20
2:2-Dimethylcyclohexane	50	<i>m</i> -Xylene	100	100

^a See pages 538-544 for significance of calculated results.

^b Experimental conditions: 550°C; catalyst— Cr_2O_3 on alumina.

tion step must be involved in this reaction (e.g., 2,2,4-trimethylpentane—see Figure 1c).

4. Under similar conditions, C_6 and higher hydrocarbons having a five ring within their molecular structure, can also be isomerized and dehydrogenated to six-ring aromatic structures (e.g., ethylcyclopentane to toluene, see Figure 1d).

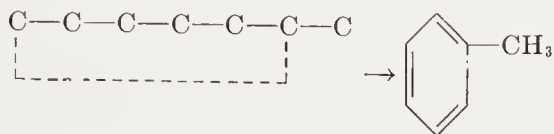
5. Formation of condensed polycyclic compounds such as naphthalene is possible from paraffins of sufficient chain length (e.g., *n*-decane, or from an appropriate alkylbenzene compound, such as butylbenzene⁸).

6. In addition to hydrocarbons it has been shown that alcohols are capable of undergoing this reaction in a manner essentially similar to that of hydrocarbons⁹.

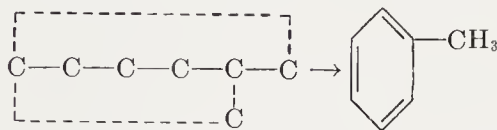
In cases (1) and (2) the resulting aromatic compound is usually the one to be expected from the simple mechanism indicated in Figure 1. Thus hexane gives benzene, heptane or the methylhexanes, toluene, etc.

If the chain length is further increased several methods of reaction become possible; thus cyclization of 3-methylheptane can produce ethylbenzene,

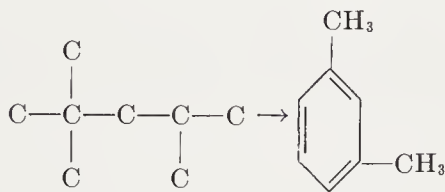
(a) cyclization of a *n*-paraffin (*n*-heptane)



(b) cyclization of a branched paraffin type A (2-methylhexane)



(c) cyclization of a branched paraffin type B (2,2,4-trimethylpentane)



(d) cyclization of an alkylcyclopentane (ethylcyclopentane)

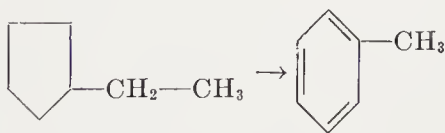


Figure 1. Modes of cyclization of various types of hydrocarbon

o- and *p*-xylene. In fact, all three compounds can be found among the reaction products. (Figure 2.)

However, there are cases where these simple rules do not apply. For example, *n*-octane gives ethylbenzene and *o*-xylene, both of which are to be expected according to the simple cyclization scheme, but in addition *m*- and *p*-xylene are found among the products. These must have been produced as a result of an isomerization mechanism (Figure 3).

Olefins can be cyclized in an analogous way to the paraffins. As far as the resulting products have been investigated they are identical with those obtained from the structurally related paraffin. In general, the rates of cycliza-

tion are increased as compared with those of paraffins, but so are the poisoning effects of the catalyst, limiting their useful life to even shorter periods than when paraffins are cyclized.

In the case of compounds requiring isomerization, such as those in groups

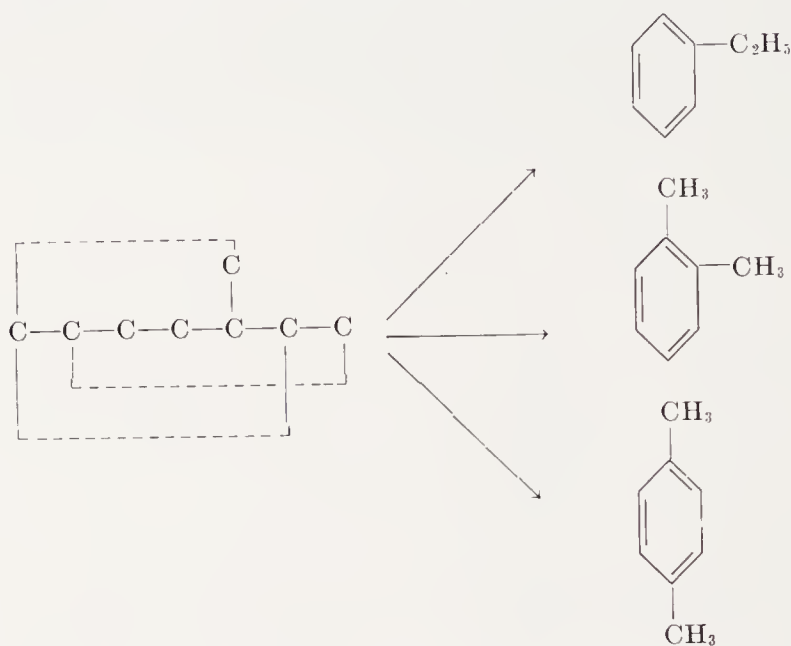


Figure 2. Various methods of cyclization of 3-methylheptane⁷

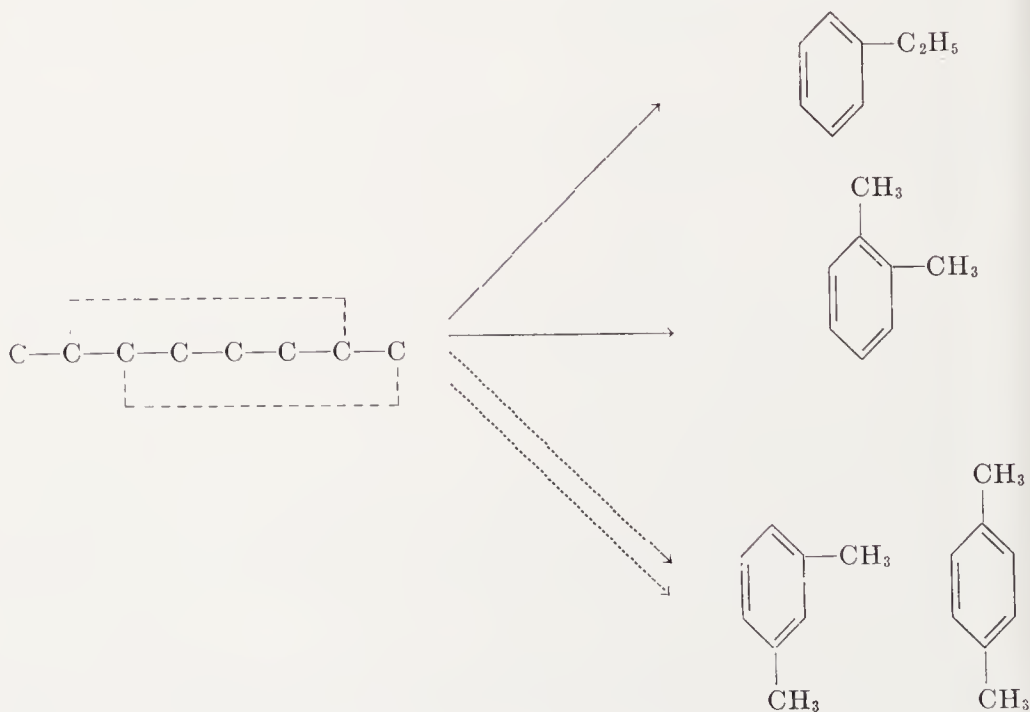
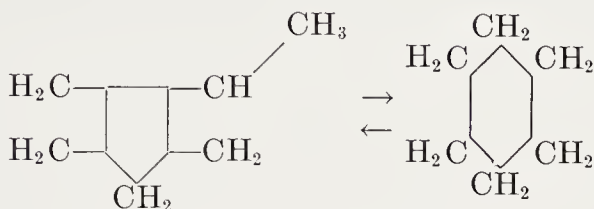


Figure 3. Various methods of cyclization of *n*-octane

(3) and (4), it is not easy to predict the aromatic compound which will be formed on cyclization. It is possible however to establish certain rules and these will be discussed later. It is fairly certain that the isomerization step proceeds via the well-known interconversion between five- and six-ring naphthenes:



THERMODYNAMIC CONSIDERATIONS

Sufficiently accurate data¹⁰ are available for an appraisal of the thermodynamic factors governing the cyclization reaction. These conditions are illustrated in Figure 4, which gives the free energy changes for the following reactions:

- (a) Paraffins to naphthenes.
- (b) Paraffins to olefins.
- (c) Naphthenes to olefins.
- (d) Naphthenes to aromatics.

The well-known fact that above a certain temperature range aromatics are by far the most stable of all hydrocarbons is confirmed. The critical temperature range is around 250°C. Above 250°C it is possible to dehydrogenate naphthenes or cyclize paraffins or olefins; above about 400°C the equilibria are displaced to such an extent to the side of the aromatics that even considerable pressures of hydrogen cannot repress the dehydrogenation reactions to any degree.

One important factor is the equilibrium between paraffins and olefins. This equilibrium is displaced to the olefin side at much higher temperatures than the dehydrogenation of naphthenes to aromatics. In fact, a 20 per cent dehydrogenation at atmospheric pressure is reached at temperatures of 550 to 600°C only, and substantial dehydrogenation occurs at temperatures of 700 to 800°C, where most hydrocarbons are already very unstable.

As for isomerizations of paraffins or olefins into naphthenes, and of five rings into six rings, the data show that all these equilibria are favorable over the entire range of temperature, which is of interest. In this range, appreciable quantities of all reacting partners are present at equilibrium, and interconversion of paraffins and olefins into naphthenes, and of five into six ring compounds, and vice-versa, is possible.

MECHANISM OF THE REACTION

The mechanism of the cyclization reaction has aroused considerable interest and has been investigated extensively. A good part of the informa-

tion was derived from a study of the kinetics of the reaction, particularly of the system *n*-heptane-toluene. The very careful and detailed investigation of the products from the cyclization of various specific hydrocarbons and the determination of the relative rates of formation of the resulting aromatic compounds led to a better understanding of the reaction. As a

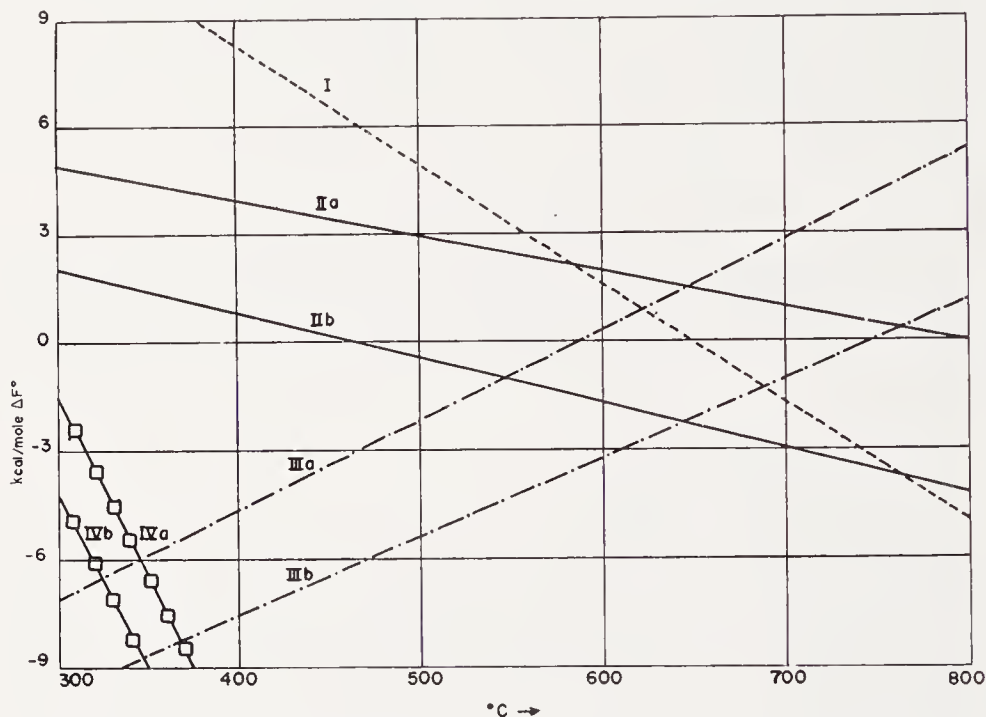


Figure 4. Standard free energy changes for reaction steps involved in cyclization.¹⁰

- I $\left\{ \begin{array}{l} n\text{-Hexane} \rightarrow n\text{-Hexene (1)} \\ n\text{-Nonane} \rightarrow n\text{-Nonene (1)} \end{array} \right.$
- IIa $n\text{-Hexane} \rightarrow \text{Cyclohexane}$
- IIb $n\text{-Nonane} \rightarrow \text{Propylcyclohexane}$
- IIIa $n\text{-Hexene (1)} \rightarrow \text{Cyclohexane}$
- IIIb $n\text{-Nonene (1)} \rightarrow \text{Propylcyclohexane}$
- IVa $\text{Cyclohexane} \rightarrow \text{Benzene}$
- IVb $\text{Propylcyclohexane} \rightarrow \text{Propylbenzene}$

result we now have a fairly comprehensive understanding of the mechanism of cyclization.

If, for instance, *n*-heptane is cyclized over a chromium oxide catalyst, the product, apart from unconverted heptane, consists of toluene and a comparatively small amount of an olefin, identified as *n*-heptene⁶. Products resulting from a degradation of the hydrocarbon chain are formed in small quantities (below about 5 per cent), and compounds such as heptadiene, methylcyclohexane, methylcyclohexene, and methylcyclohexadiene, which could be anticipated as intermediates in the cyclization reaction, have not

been detected. Traces of unsaturated bodies of the fulvene type are present among the reaction products, but while they were shown to be an important cause of the progressive poisoning of the catalysts they do not appear to be of interest in connection with the main reaction mechanism.

The question arises whether the olefin (*n*-heptene) found in the reaction products is formed as a by-product or as an intermediate in the reaction sequence.

It has been shown by Pitkethly and Steiner¹¹ that the concentration of *n*-heptene in the reaction product does not correspond to the hydrogenation—dehydrogenation equilibrium with the paraffinic starting material. The evidence is based on two facts:

(1) Thermodynamic data show that the olefin concentration is much too low to be at or near equilibrium under the conditions of reaction.

TABLE 3. CONVERSION OF *n*-HEPTANE INTO TOLUENE AT VARIOUS PARTIAL PRESSURES OF *n*-HEPTANE (CARRIER GAS—NITROGEN)

H ₂	C ₇ H ₁₆	C ₇ H ₁₄	C ₇ H ₈	N ₂	$\frac{H_2 \times C_7H_{14}}{C_7H_{16}}$	$\frac{C_7H_{14}}{C_7H_{16}}$	C ₇ H ₁₄ theor.
222	160	21	34	208	29	0.13	190
185	125	22	36	320	32	0.17	180
295	260	30	40	25	25	0.12	234
120	78	10	28	379	16	0.13	170
495*	99	14	25	—	67	0.14	53

All exp. at 475°C ant 20 ± 4 sec. contact time; all pressures mm Hg. Catalyst: Cr₂O₃ on alumina.

* Exp. 41 hydrogen used as carrier gas. For data: see Ref. 11).

(2) Addition of hydrogen does not reduce the concentration of olefins in the products, which would be the case if a dehydrogenation equilibrium were established.

This is clearly demonstrated in Table 3, where data on the conversion of *n*-heptane to toluene at various partial pressures of *n*-heptane are given. These data show that the equilibrium expression (column 6) is far from constant. Moreover, assuming a value of 0.07 atmospheres for the equilibrium constant, values for the partial pressure of *n*-heptene (column 8) in equilibrium with the measured partial pressure of *n*-heptane and hydrogen were calculated. Comparison with the actually determined partial pressures of heptene (column 3) demonstrates the wide discrepancy in the calculated and observed values.

Variation of contact time showed (Figure 5) that at very short times the concentration of olefins rises much more rapidly than the concentration of aromatics; after reaching a maximum, the olefin concentration falls slowly

with increasing contact time, whereas the concentration of aromatics continues to rise. Moreover, there is evidence that at very short contact times the rate of formation of aromatics approaches zero. All these facts point to the olefins as intermediate products in the cyclization reaction. Thus, after building up the olefin concentration a stationary state is reached where the olefin is formed as rapidly as it is cyclized to the aromatic product.

Assuming the *n*-heptene adsorbed on the catalyst to be in equilibrium with the *n*-heptene in the vapor phase, and assuming the reaction on the surface to follow first order kinetics, we have, under stationary state condi-

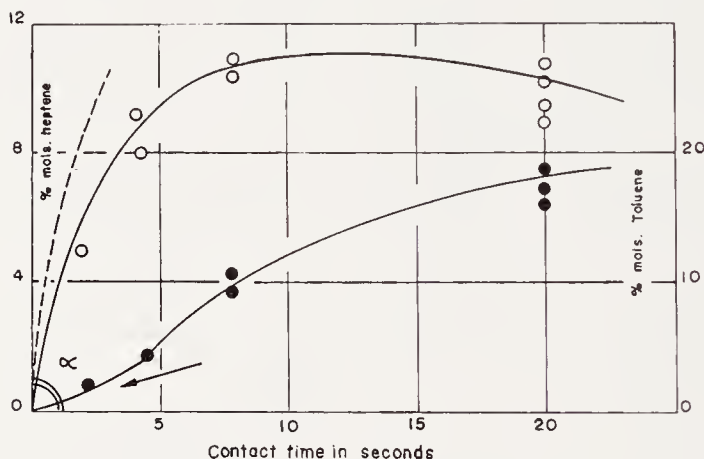


Figure 5. Conversion of *n*-heptane to toluene.¹¹

tions (after build-up of the olefin concentration):

$$\frac{dp_0}{dt} = K_D p_p = \frac{-dp_0}{dt} = k_c p_0$$

$$\frac{p_0}{p_p} = \frac{k_D}{k_c} \quad (1)$$

where p_p and p_0 stand for the partial pressures of *n*-heptane and *n*-heptene, respectively, and k_D and k_c for the rate constants for dehydrogenation and cyclization, respectively. The latter constants include factors governing the adsorption equilibria of the compounds referred to.

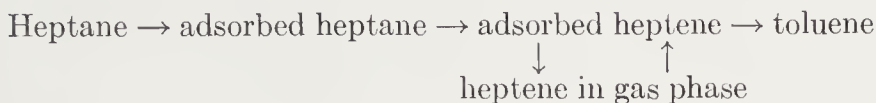
Thus, under these conditions, the ratio:

$$\frac{p_0}{p_p} = \text{const.}$$

should be approximately constant and independent of the initial partial pressure of heptane. As the data of Table 3 show, this is the case.

These experiments lead to the conclusion that the reaction proceeds ac-

according to the following scheme:



From the data in Table 3 it is clear that under the particular experimental conditions the stationary state has been largely established. Using Eq. (1) we can therefore relate the rate of formation of toluene to the mean concentration of heptane as follows:

$$\frac{\Delta p_a}{\Delta t} = k_c \bar{p}_0 = k_D \bar{p}_p \quad (2)$$

where Δp_a stands for the rate of formation of toluene and \bar{p}_0 and \bar{p}_p are the mean partial pressures of heptene and heptane, respectively. Thus, according to Eq. (2) the formation of toluene should be proportional to the mean partial pressure of heptane. However, as the data of Table 3 show, the reaction rate is dependent on pressure to a power much lower than the first, approximately 0.6, indicating partial saturation of the surface⁵.

The simple mechanism given above does not take this fact into account, but it can easily be shown that a more elaborate treatment leads to the same final result⁵⁻¹². Assuming that heptane and heptene compete for identical catalytic centers, and that heptene is strongly adsorbed and can displace the weakly adsorbed heptane from the catalyst, we have for the fraction of the catalytic surface covered by heptene and heptane, respectively:

$$\begin{aligned} S_0 &= \frac{A_0 p_0}{1 + A_0 p_0} \\ S_p &= A_p p_p (1 - S_0) = \frac{A_p p_p}{1 + A_0 p_0} \end{aligned}$$

A Langmuir adsorption isotherm is assumed and A_0 and A_p stand for the adsorption coefficients of heptane and heptene, respectively.

For the rates of dehydrogenation and cyclization, respectively, we then find:

$$\begin{aligned} + \frac{dp_0}{dt} &= k_d \frac{A_p p_p}{1 + A_0 p_0} \\ - \frac{dp_0}{dt} &= k_c \frac{A_0 p_0}{1 + A_0 p_0} \end{aligned}$$

Equalizing these equations for the stationary state condition we end up with an equation equal in form to Eq. (1).

The rate of formation of toluene is given as follows:

$$\frac{\Delta p_0}{\Delta t} = k_c \frac{A_0 p_0}{1 + A_0 p_0} = \frac{k_d A_p p_p}{1 + \frac{k_d}{k_c} A_p p_p}$$

It is seen that the relation between rate of formation of toluene and partial pressure of heptane need no longer be of the first order in accordance with the experimental results.

The numerical value for the ratio of the two constants in Eq. (1) is about 0.25, indicating that the over-all rate of cyclization of the olefin is much more rapid than the dehydrogenation of the paraffin to the olefin. This is supported by the fact that some, though not all, olefins cyclize much more

TABLE 4. CYCLIZATION OF OLEFINS

	Mole % Aromatics in Product	Aromatic Compound Formed	Catalyst, Temp. (°C), Approx. L.s.v.*	Ref. No.
			<i>cc/cc/hr</i>	
<i>n</i> -Hexene-1	31	Benzene	Cr ₂ O ₃ , 465°C, s.v. 0.2	6
<i>n</i> -Hexene-2	18	Benzene		6
<i>n</i> -Heptane	45	Toluene		6
<i>n</i> -Heptene-1	69	Toluene		6
<i>n</i> -Heptene-2	65	Toluene		6
<i>n</i> -Heptene-1	19.8	Toluene	V ₂ O ₅ , 480°C, s.v. 0.5	13
<i>n</i> -Heptene-3	13.7			13
<i>n</i> -Octene-2	57	Mixed xylenes	Cr ₂ O ₃ , 465°C, s.v. 0.2	6

* L.s.v. = Liquid hourly space velocity.

rapidly than the corresponding paraffins (see Table 4). However, this is not true in all cases, as the rate of cyclization of olefins depends on the position of the double bond within the molecule.

This leads to another interesting feature of this mechanism:

It has been shown by Hoog, Verheus and Zuidervog⁶ that hexene-1 cyclizes at about double the rate of hexene-2, whereas heptene-1 cyclizes at about the same rate as heptene-2. These results were further extended by Plate and Tarasova¹³, who showed that heptene-3 cyclizes at a much reduced rate as compared with heptene-1 or -2.

We have, therefore, the position that the olefin is an essential intermediate in the reaction, but that olefins with a double bond located in the center of the molecule, hexene-2 in the case of the *n*-hexenes, or heptene-3 in the case of the *n*-heptenes, are less reactive than those with the double bond toward the end of the molecule. These results can be explained by assuming the following mechanism for the actual cyclization step on the catalyst.

The olefin molecule, e.g., *n*-heptene, is assumed to be adsorbed by a two point contact with simultaneous opening of the double bond (Figure 6). Cyclization then proceeds between atoms 1 and 6 as follows: a bond is formed between these two atoms, and simultaneously a hydrogen atom is split off from carbon atom 6.

This mechanism was first proposed by Twigg¹⁴ in analogy to the mechanism introduced for exchange reactions between deuterium and olefins by Horiuti and Polanyi¹⁵, and by Twigg and Rideal*¹⁶. If the further assumption is made that cyclization must involve a carbon atom linked to the catalyst,

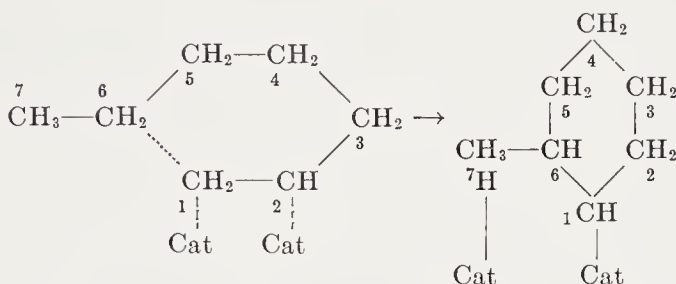


Figure 6. Twigg's mechanism for cyclization¹⁴

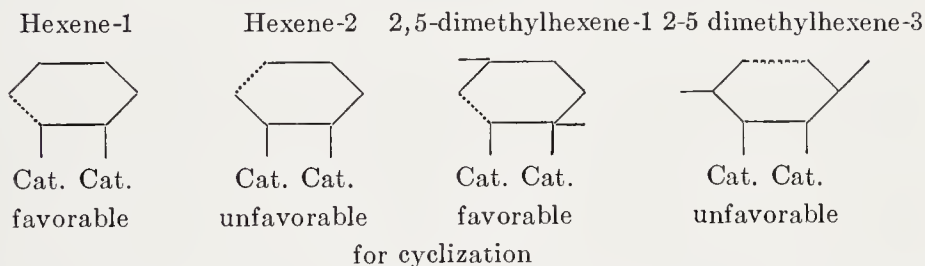
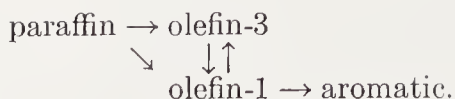


Figure 7. Methods of adsorption for cyclization of hexene and 2,5-dimethylhexene

then in the case of *n*-heptane it is clear that cyclization can take place only if the intermediate olefin is adsorbed on the 1-2 or 2-3 position corresponding to adsorption of a heptene-1 or a heptene-2 molecule, whereas heptene-3 has to be isomerized first to the -1 or -2 olefin before cyclization can take place. This is compatible with the fact that heptene-1 and -2 cyclize at approximately double the rate of heptene-3. The difference in the cyclization rate of *n*-hexene-1 and -2 equally fits into this picture, because *n*-hexene-1 can be cyclized directly, whereas *n*-hexene-2 can be cyclized only after isomerization to hexene-1. We have, therefore, to extend our mechanism

* Twigg's mechanism implicitly assumes that identical catalytic centers are involved in cyclization and dehydrogenation; also, as will be seen later, in isomerization. This assumption will be justified later (see page 553).

as follows:

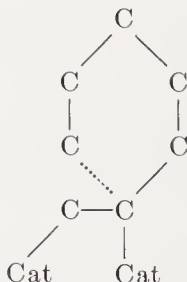


The isomerization of the olefins to the olefin with the double bond in a suitable position for cyclization is, therefore, an important step in the reaction sequence. This step may take place by a mechanism analogous to the one proposed by Twigg for the migration of a double bond in the conversion of butene-1 into butene-2 over nickel catalysts.

That isomerization of the double bond does actually take place under conditions of cyclization is clearly shown by experiments of Hoog and collaborators, and of Plate and Tarasova^{6, 13}. These authors used the pure isomeric heptenes-1, -2, and -3, respectively, as feed to the cyclization reaction, but invariably the heptenes isolated from the reaction products consisted of a mixture of all three isomers, with the -3 isomer present in greatest proportion (see Table 4, page 540).

Further support for this mechanism of the cyclization reaction comes from calculations of Herington and Rideal⁷, which are based on experiments carried out by Hoog, Verheus and Zuiderweg⁶ (see Table 1, p. 531). Herington and Rideal calculated the probability for cyclization of certain paraffins based on the assumption that a two-point contact between catalyst and the intermediate olefin is necessary, and that only certain positions are favorable, depending on whether cyclization can be achieved according to the scheme proposed in Figure 6. This is further illustrated in Figure 7 for *n*-hexane and 2,5-dimethylhexane, respectively. Thus, in the case of *n*-hexane five two-point contacts are possible; but only two can lead to cyclization according to the above mechanism. The relative cyclization probability, therefore, is 2/5. Another example is 2,5-dimethylhexane; here seven two-point contacts are possible, four of which are favorable, but each of these four has two possibilities for reaction; the relative probability for cyclization, therefore, is 8/7*.

* This calculation assumes that the following method of cyclization, illustrated for the case of *n*-heptane, does not contribute to the reaction:



This assumption seems justified, because the resulting product would not lead directly to an aromatic hydrocarbon. While this method of cyclization may not be excluded it will probably be considerably slower, and therefore may be neglected.

The cyclization rate of various aromatics will be proportional to these probabilities, i.e.,

$$k_c = \text{constant } p \quad (3)$$

where p stands for the cyclization probabilities as derived above and k_c is the rate constant for cyclization, which, assuming an exponential decline of the cyclization rate, is related to the fraction (α) converted to aromatics as follows:

$$k_{c1} = \log_{10} \frac{1}{1 - \alpha} \quad (4)$$

Taking the constant in Eq. (3) as equal to 0.28, the values in Table 4,

TABLE 5. RELATIVE CYCLIZATION RATES OF VARIOUS HYDROCARBONS AT 465°C, CONTACT TIME 18-24 SECONDS, Cr_2O_3 CATALYST⁷

Paraffin	P	Conversion to Aromatic	
		% Observed	% Calculated
Pentane	0.00	3	0
<i>n</i> -Hexane	0.40	20	23
2-Methylpentane	0.00	5	0
<i>n</i> -Heptane	0.66	36	35
2-Methylhexane	0.66	31	35
<i>n</i> -Octane	0.84	46	42
3-Methylheptane	0.84	35	42
2,5-Dimethylhexane	1.14	52	52
2,2,4-Trimethylpentane	0.00	3	0
<i>n</i> -Nonane	1.00	58	48

were calculated and compared with those obtained experimentally by Hoog, Verheus and Zuiderweg. The agreement seems satisfactory.

The mechanism and the probability considerations just discussed should also lead to the correct ratio of aromatic isomers which can be formed from a given paraffin. These experimental and calculated ratios are compared in Table 1 (page 531). While these data are largely in agreement with the prediction of the theory there are discrepancies. The most notable occur in the case of *n*-octane, which should form ethyl benzene and *o*-xylene only, but *m*-xylene and *p*-xylene are formed in addition, mainly at the expense of ethyl benzene. It is clear in this case that an isomerization step is involved. An important point to establish was at what stage in the reaction sequence the isomerization step occurred. The following experiments of Herington and Rideal were designed to give the answer:

It was shown that no isomerization occurs if the following hydrocarbons are passed over the catalyst, *o*- and *p*-xylene, ethyl benzene, mesitylene,

trans-1-2- and *trans*-1,4-dimethylcyclohexane, ethylcyclohexane, and *trans*-1,3,5-trimethylbenzene, although dehydrogenation of the naphthene takes place.

These experiments show that no isomerization occurs after ring closure.

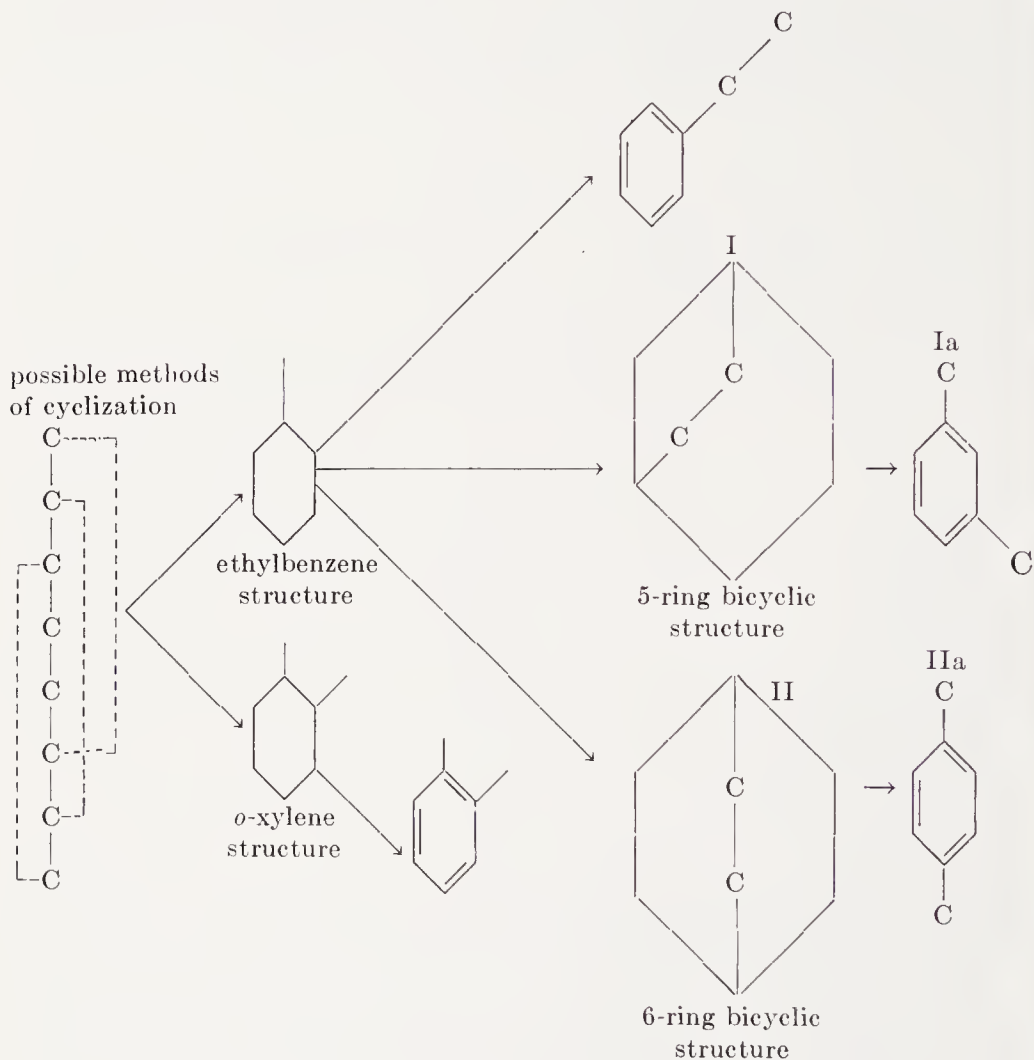


Figure 8. Isomerization in the cyclization of *n*-octane⁷

On the other hand, it was shown in further experiments that identical aromatics are formed from the paraffin and the corresponding olefin (*n*-octane-*n*-octene); therefore isomerization does not precede the dehydrogenation step. The only remaining possibility, therefore, is that isomerization occurs simultaneously with ring closure.

In order to explain the isomerization in the cyclization of *n*-octane, Herington and Rideal⁷ assume that the ethyl group, after cyclization of the

main ring, can form an additional five or six ring according to the scheme of Figure 8.

On further dehydrogenation the bicyclic naphthenic ring (structures I and II), which are nonplanar, are transformed into the planar aromatic structures Ia and IIa, respectively. The resulting strain breaks the secondary five and six rings with simultaneous formation of *m*- and *p*-xylene, respectively.

Other paraffins which are cyclized to ethyl benzene type structures, such as 3-methylheptane or 2-ethylhexane, fail to show isomerization to other aromatic structures. According to Herington and Rideal⁷ this must be due to a unique method of adsorption of all C₈ hydrocarbons only open to *n*-octane, and shown in Figure 9a. In this configuration the ethyl group is linked to the chemisorbed carbon atom undergoing cyclization, and it is postulated that simultaneous ring closure of the ethyl group to form the secondary five or six ring can take place only under these conditions.

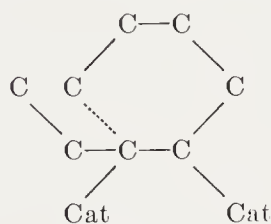


Figure 9a⁷

Since simultaneous ring closure of both the primary and the secondary ring is postulated, closure of the secondary ring must take place at some distance from the catalytic center. Since interaction of the catalytic centers with the cyclizing atoms is most probably an essential condition for reaction, it is difficult to see how, under these circumstances, cyclization of the secondary ring can take place.

A different anomaly is found in the case of 3-methylheptane. Here the expected isomers, namely, ethyl benzene, *p*-xylene, and *o*-xylene, are formed on cyclization, *m*-xylene being absent, but the proportion of the isomers is quite different from that calculated. It will be seen from the data of Table 6 that *p*-xylene has been formed at the expense of *o*-xylene and ethyl benzene. According to Herington and Rideal⁷ the explanation lies in the suppression of certain configurations in the transition state prior to ring closure because of steric hindrance. This is illustrated in Fig. 9, where the various possible configurations of the substrate on the catalyst are demonstrated. Configurations h and i are suppressed because of the steric hindrance of one ethyl group or two methyl groups linked to the chemisorbed carbon atoms. These are the configurations which lead to ethyl ben-

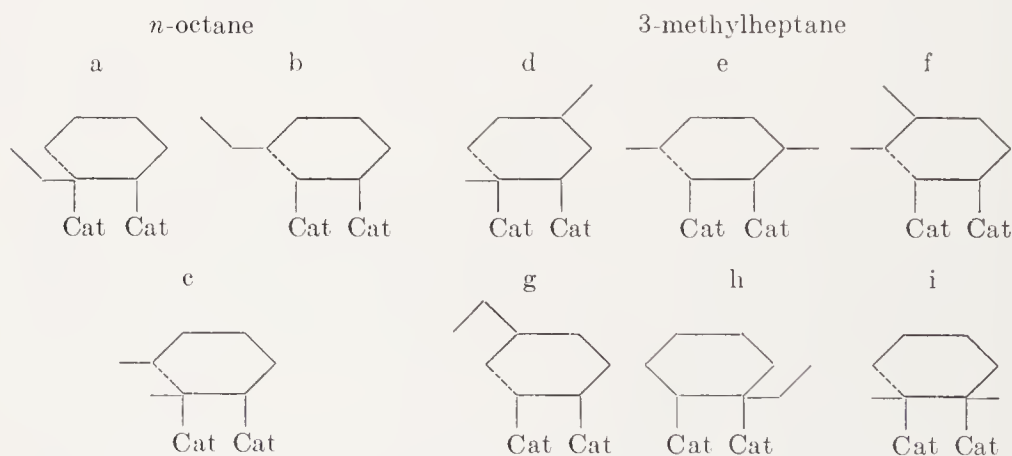
zene and *o*-xylene, respectively. Assuming that these configurations are suppressed, the calculated ratio for the various isomers becomes that shown in Table 6, which is in reasonable agreement with experiments.

As far as the ring closure of compounds which can cyclize only after isomerization has taken place is concerned, these reactions require tempera-

TABLE 6. ISOMERIZATION OF 3-METHYLHEPTANE⁷

Isomers	3-Methylheptane		
	Found	Calculated	Calculated, Assuming Configurations h and i are absent. (Fig. 9)
	(% of Total Aromatics in Product)		
Ethylbenzene	15	33	20
<i>o</i> -Xylene	25	33	20
<i>p</i> -Xylene	60	33	60
Total cyclization*	35		42

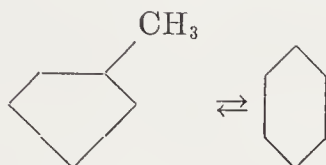
* % total aromatics in product.

Figure 9.⁷ Methods of adsorption of *n*-octane and 3-methylheptane

tures which are considerably higher than those in the case of simple ring closure⁷. It is necessary to raise the temperature some 60 to 80° to achieve conversions comparable with those when only a simple cyclization takes place in the reaction. The results of such isomerizing cyclizations, particularly the starting materials and the end products, are summarized in Table 2 (p. 532).

Although 2,3-dimethylbutane and 2,2,3,3-tetramethylbutane contain sufficient carbon atoms to form a six-numbered ring, they do not give aromatic products when passed over a chromium-oxide catalyst. The former

gave 2,3-dimethylbutadiene, while the latter passed through unchanged. It can be concluded, therefore, that only pentane and cyclopentane structures can be aromatized by this isomerizing cyclization reaction, and the view that isomerization takes place by way of the well-known interconversion of five- and six-ring naphthenes seems very plausible.



It is known that this reaction proceeds over oxide catalysts at temperatures of about 500 to 600°C.

Further evidence for this mechanism comes from the relative rates of aromatization of the various compounds listed in Table 2. All these compounds, including the cyclopentane derivatives, and the cyclohexane de-

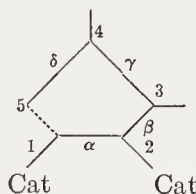


Figure 10. Ring closure of C_5 hydrocarbons

derivatives with geminal methyl groups, aromatize at about the same rate, showing that the same elementary step must be rate determining in all reactions. It is suggested that this step is the breaking of the five-membered ring and the simultaneous formation of the six ring⁷.

Certain rules can be formulated which allow one to predict the aromatic compound formed on isomerization⁷. Assuming that the substrate is first dehydrogenated to the corresponding olefin and the latter is adsorbed by a two-point contact on the catalyst (Figure 10) on carbon atoms 1 and 2, ring closure should take place between carbon atoms 1 and 5:

In general, on subsequent ring enlargement bond γ breaks unless carbon atom 3 carries an ethyl group or carbon atoms 2 and 3 both carry methyl groups. On remaking the six ring the probability for participation in the ring enlargement is equal for all alkyl groups adjacent to the broken bond unless there is a quaternary carbon present, in which case ring enlargement takes place using one of the alkyl groups attached to this atom.

The rules governing the breaking of the γ and β bonds, respectively, are related to the anomalies in ring closure of six rings which were discussed earlier. It was shown in the case of 3-methylheptane that certain methods of adsorption were excluded because of steric hindrance due to the presence

of ethyl and methyl groups. In the case of 5-ring isomerization, similar factors govern the breaking of bonds in the β and γ position, respectively. The mechanism as proposed by Herington and Rideal is illustrated in Figure 11 for the two typical methyl cyclopentanes, 2,3-dimethyl- and 2,3,4-trimethylpentane.

In I(a) cyclization to a five ring takes place; in I(b) shift of the adsorbed linkages into a favorable position according to the double bond shift scheme has occurred; in I(c) ring enlargement is demonstrated (breaking of γ bond).

In case certain critical adsorption configurations are prevented by steric hindrance the mechanism represented in Figure 11 (scheme II) is proposed. In this case double bond shift to configuration (b) of scheme I is not possible

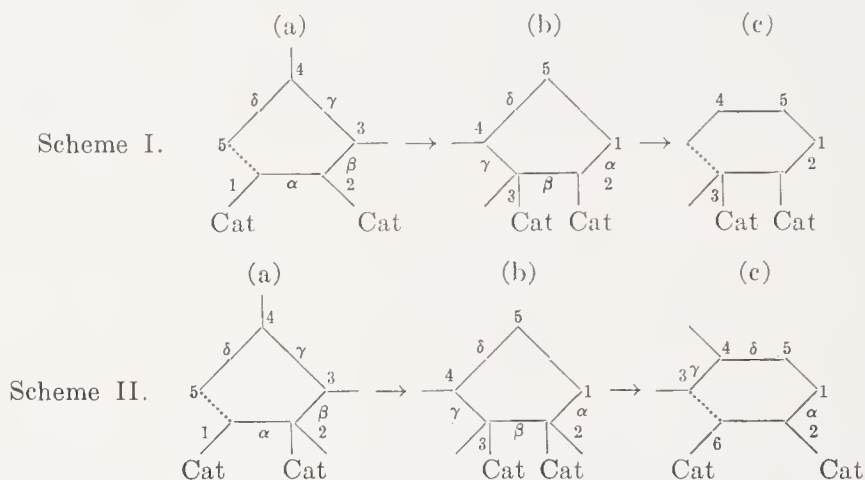


Figure 11.⁷ Cyclization of 2,3 di- and 2,3,4 trimethylpentane

because the analogous method of adsorption is prohibited, due to the steric hindrance of the methyl groups on carbon atoms 2 and 3; instead the bond β breaks and ring enlargement takes place in this position, as illustrated in II(c).

Justification of these rules lies in the quantitative prediction of the products of isomerizing cyclization. The results of these calculations are given in Table 2 (page 532), where they are compared with experiments. The agreement seems satisfactory.

We have thus a fairly complete, and remarkably consistent picture of the molecular mechanism of cyclization and isomerization on oxide catalysts. This picture was obtained with only a few plausible postulates, such as that of a two-point contact on the catalyst and the mechanism for cyclization as first proposed by Twigg¹⁴. Our state of knowledge is less satisfactory if we turn our attention to the question of the catalyst, the seat of the catalytic activity, its structure, and the reason for the catalytic action.

CYCLIZATION CATALYSTS

Composition of Catalysts

A survey of the published information on the oxide catalysts used in the cyclization reaction (Table 7) reveals that they belong almost exclusively

TABLE 7. OXIDE CATALYST USED IN CYCLIZATION REACTIONS

Composition	Feed	Reaction Temp. (°C)	Approx. Contact Time (Sec.)	Activity, Amount in Products		Ref. No
				% Aromatics	% Olefins	
Cr ₂ O ₃ gel	Heptane	475	20	15	15	5
Cr ₂ O ₃ gel	Heptane	475	—	41.5	13.5	
10% Cr ₂ O ₃ on alumina	Heptane	475	120	27	15	
10% Cr ₂ O ₃ on alumina	Heptane	510	120	60.8	12.3	
10% V ₂ O ₅ on alumina	Heptane	510	120	29.1	12.7	
10% ThO ₂ on alumina	Heptane	555	120	16.3	11.7	7
CeO ₂ gel	Heptane	510	120	12.8	5.4	
ZrO ₂	Heptane	475	20	8	12	
10% MoO ₂ on alumina	50% heptane	475	12	24	?	
MoS ₂	Heptane	475	—	Activity comparable with that of Cr ₂ O ₃		
10% UO ₃ on alumina	Synthine* fraction boiling 83–138°C	500	—	11.4	11.2	Kazanski, B. A., Ser-gienko, S. R. and Zelinski, N. D. Compt. rend., acad. sci. U.S.S.R., 27, 664, (1940).

* Synthine, synthetic gasoline fraction, containing mainly paraffins (octane rating 10).

to those of the metals of the 4th, 5th, and 6th subgroups of the periodic table¹⁷. The exception is cerium oxide, which does not belong to these groups, and molybdenum sulfide, the only non-oxide which has shown catalytic activity for cyclization.

Various promoters and catalyst stabilizers not belonging to these groups

of the periodic table have been tried, but invariably they have been associated with one or the other of the oxides mentioned in Table 7.

In a lower temperature range (*ca.* 300°C) platinum on charcoal was also shown to promote cyclization to a certain extent⁴. Lately, a catalyst of a similar type has become of practical importance in a hydro-reforming process¹⁸. In this process a catalyst consisting of platinum supported on alumina or silica alumina is used for dehydrogenation and isomerization of petroleum naphthas. The reactions taking place are dehydrogenation of six-ring naphthene, but equally important is the isomerizing-dehydrogenation of five-ring naphthenes. Cyclization of paraffins takes place to a lesser extent. The literature on this reaction is mainly concerned with the technical process, and little has been published on the catalyst and the mechanism of the reaction.

Alumina in the γ modification is preferred as a carrier for most of the oxide catalysts, but by itself it has no catalytic activity. It is noticeable from the preparation of all active catalysts that they must be present either in an amorphous or at least microcrystalline state. Typical examples are the chromium oxide gel catalysts. On the other hand, crystalline Cr_2O_3 , for instance, was shown to be inactive⁵. Alternatively, active catalysts can be prepared by precipitation on or impregnation of supports like activated alumina. Oxides in the gel or microcrystalline form usually have a large surface area. The same is true of supports like activated alumina.

In some cases the alumina, in addition to acting as a suitable support of large surface area, has additional functions. Thus, MoO_2 by itself is inactive, but supported on Al_2O_3 it is one of the most active and stable catalysts. It is likely that this is due to the reduction of MoO_2 under the reaction conditions to the inactive molybdenum, metal. Alumina retards this reduction to such an extent that the supported catalyst shows activities for sufficiently long periods⁷.

The most active catalysts have been prepared by precipitating chromium oxide on activated alumina, preferably in the presence of small amounts of promoters such as K_2O or CaO .

For technical applications catalysts consisting of MoO_2 precipitated on alumina are preferred. These catalysts are more active than the Cr_2O_3 catalysts under the conditions of high hydrogen partial pressure which are employed in the technical process.

It will be noted that all the active oxides belong to transition elements with incompleated inner electron shells. Oxides of these elements in most cases can be present in several states of valency, and it has been suggested that the active oxide is obtained by reduction under reaction conditions from a higher to a lower valent oxide⁵. The metallic ions of the reduced oxide would contain unpaired electrons, and it would be plausible if these were to interact with the electrons of the double bonds of the olefins which,

as has been stated, play a key role in cyclization. However, the fact that ThO_2 and ZrO_2 show cyclization activity does not fit into this picture. There is practically no evidence for the existence of oxides of these elements in a lower state of valency; particularly, there is no reason to believe that either ThO_2 or ZrO_2 could be reduced by hydrogen or hydrocarbons under the reaction conditions (450 to 550°C). On the other hand, the quadrivalent ions of Th and Zr have rare gas electron shells, and an interaction of unpaired electrons with those of the double bond of olefins is not possible in these cases. It could be argued that the activity of ThO_2 is considerably below that of chromium oxide or molybdenum oxide (reaction temperature, 550°C, as compared with 475°C, see Table 7), but ZrO_2 , though less active than Cr_2O_3 , compares, at least as to order of magnitude, with the latter.

The view described, which assumes the metallic cation to be the main active center of the catalyst, ignores a possible role of the oxygen anions. A possible function of these may be their conversion into a hydroxyl ion by interaction with a hydrogen of a hydrocarbon; the residual alkyl radical may then interact with the metallic cation to form a bond, as suggested previously. Such a reaction may possibly take place on the surface of the catalyst, even if it is not possible that such a reduction could take place in the bulk phase.

Recent work suggests that the electronic interaction of substrate and catalyst is in many cases a very important factor in catalytic reactions¹⁹. A typical class of catalysts where such interaction could be demonstrated is that of oxide catalysts, which show properties of electrical semiconductors. In this connection, experimental work by Weisz, Prater and Ritterhouse²⁰ on a typical cyclization catalyst is of great interest. These workers were able to demonstrate that a chromium-oxide alumina-oxide gel, when heated in an oxygen atmosphere, shows the typical behavior of a P-type semi-conductor. On replacing the oxygen with hydrogen or butane, the polarity of the conductivity changes and the behavior of the catalyst becomes that of an N-type semi-conductor. This change of polarity was particularly rapid and pronounced when cyclohexane was passed over the catalyst under conditions which occurred when dehydrogenation to benzene took place.

No precise interpretation of such experiments appears possible at present, but the result shows clearly the importance of electronic factors in the behavior of such catalysts.

Poisoning Effects

The activity of all cyclization catalysts decreases with time, the active lifetime ranging from 5 to 40 hours. A typical course of a cyclization experiment showing progressive poisoning of the catalyst is given in Table 8.

It is seen that in this particular case the activity as measured by the con-

centration of toluene in the product decreases fourfold within two hours. This decrease in activity is due to polymers which accumulate on the surface, and eventually cover it entirely. These polymers can be burned off with air diluted with nitrogen, when both CO_2 and H_2O are formed, showing that the surface deposits consist of hydrocarbons. After this air treatment the catalyst activity is restored. The poisoning effects are much more pronounced when olefins are cyclized, and from experiments of Herington it is likely that diolefinic compounds, such as the fulvenes which are formed in small amounts as by-products in the cyclization reaction, also contribute strongly to the poisoning effects observed.

As has been shown previously, olefinic compounds are strongly adsorbed on the catalyst and it is likely that the probability of a link-up with another adsorbed olefinic or diolefinic molecule before desorption takes place is quite high. Eventually the greater part of the active surface will be covered by

TABLE 8.⁵ PROGRESSIVE POISONING OF CYCLIZATION CATALYST ($\text{Cr}_2\text{O}_3 + 10\% \text{ZrO}_2$)

Reaction Period	Mole % of Liquid Product			$\frac{\text{Heptene}}{\text{Heptane}}$
	Heptane	Heptene	Toluene	
1st half-hour	48	12	40	0.25
2nd half-hour	59	14	27	0.24
3rd half-hour	68.5	14.5	17	0.21
4th half-hour	74	15	11	0.20

such adsorbed polymers, reducing the cyclization activity of the catalysts to a fraction of what it was initially. On the other hand, if a six-ring cycloparaffin such as, for instance, methylcyclohexane, is dehydrogenated over a cyclization catalyst, the poisoning effects are greatly reduced, if not entirely absent.

If a link-up of olefinic or diolefinic compounds is the decisive factor in the poisoning of a catalyst, then a catalyst where the active centers are separated from each other by dilution with a catalytically inactive substance should show a decrease in the poisoning effects. Such experiments were carried out by Herington and Rideal⁷ with chromium oxide as the active substance and alumina as the diluent, both components being coprecipitated. The results show that, under comparable conditions, the more dilute the active catalyst the longer the lifetime and the slower the decay of activity.

The activity of the catalyst can be prolonged considerably if the reaction is carried out under conditions of a substantial partial pressure of hydrogen. Under these conditions a proportion of the surface polymer is removed continuously as methane by a hydrogenating cracking reaction, and the

accumulation of surface polymer is thus retarded. This method of operation will be covered later.

Apart from the temporary poisoning effects, which are due to the accumulation of polymers, there is a permanent loss of activity which takes place over a period of many regeneration cycles. For technical application, where periodic regeneration is carried out every few hours, this is a matter equally as serious as the temporary inactivation. Much effort was devoted to improving the stability of the catalysts to repeated regeneration treatment. By incorporation of various additions, particularly of alkali, the lifetime of these catalysts could be prolonged considerably.

Identity of Catalytic Centers for Dehydrogenation Cyclization and Isomerization

From the results of the studies of the kinetics of the reaction some interesting conclusions regarding the active centers of the catalyst can be drawn. It has been shown that the intermediate olefins repress the dehydrogenation of the paraffins, by displacing the latter from the catalytic surface due to the stronger adsorption on the catalyst. This suggests that identical catalytic centers must be involved in the dehydrogenation and cyclization step of the reaction.

A stronger support for this view can be obtained from an analysis of the poisoning effects using Eq. (1) (p. 538). This equation allows one to calculate the ratio of cyclization to dehydrogenation rates from the ratio of the partial pressures of heptane and heptene^{11, 21}. This has been done for the experiments reported in Table 8, where this ratio is given for the catalyst at various stages of poisoning in the course of a run⁵. For the same experiments the decline of the yield of toluene is a measure of the decline of the cyclization activity itself. It will be seen that while the cyclization rate declines by a factor of four, the ratio of the rates of cyclization and of dehydrogenation does not alter by more than 20 per cent. One must conclude, therefore, that the poisoning effects reduce both rates to very nearly the same degree, and that identical centers are involved in both reactions.

The experiments concerned with the mechanism of the reaction lead to similar conclusions with regard to the isomerization step occurring in the aromatization of pentanes and cyclopentanes. It has been shown in the experiments described on page 546 that this step takes place simultaneously with the cyclization itself, and the conclusion is therefore justified that here, too, identical catalytic centers are involved in cyclization and isomerization.

These results taken together are strong evidence for the view that in this whole complex of reactions, namely, dehydrogenation, cyclization, and isomerization, identical catalytic centers are involved. This evidence also justifies the mechanism of the dehydrogenation, cyclization and isomeriza-

tion reactions as proposed by Twigg and elaborated by Herington, as outlined in the previous pages. Twigg's mechanism implicitly assumes identical catalytic centers for dehydrogenation and cyclization, and Herington extended this assumption to isomerization.

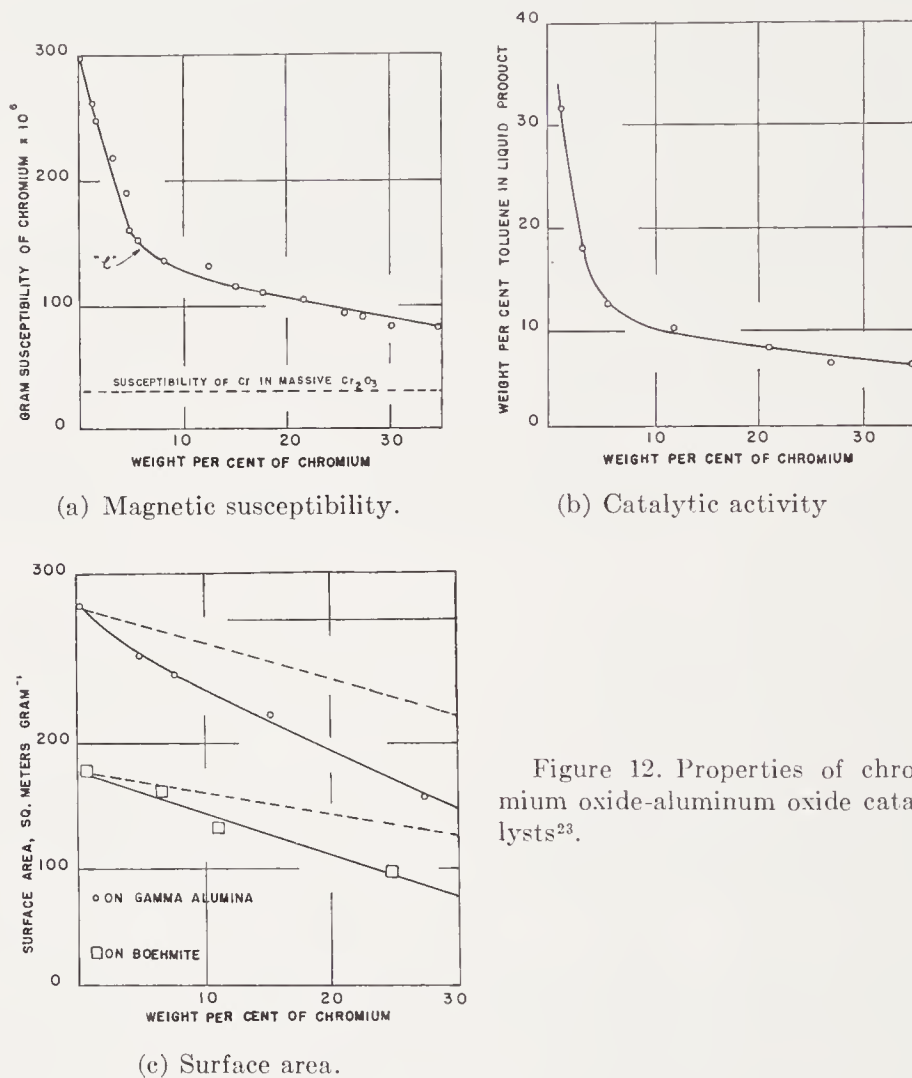


Figure 12. Properties of chromium oxide-aluminum oxide catalysts²³.

Structure of Supported Oxide Catalysts

Many of the most active catalysts for cyclization are obtained by supporting an active oxide like chromium-oxide, or molybdenum-oxide, on alumina, which by itself is not active. The alumina used has to have a large internal surface, as measured by nitrogen adsorption, and for highest catalytic activity has to be present in the γ -form²².

Considerable insight into the structure of these catalysts has been obtained by Selwood and Eischens²³. They found that catalysts consisting of

a number of oxides of the transition elements either deposited or precipitated on various types of alumina show a magnetic susceptibility (calculated per gram of active oxide) considerably in excess of that of the pure crystalline oxides themselves. Using this phenomenon they compared the magnetic susceptibility, internal surface and catalytic activity of various catalysts consisting of chromium oxide, either impregnated or precipitated on alumina.

The most important of their results are reproduced in Figure 12, a, b and c. It can be seen that there is a marked parallelism between catalytic activity and magnetic susceptibility when both are determined as functions of the chromium content of the catalyst. In both cases a marked change in the slope of the graph occurs at point *l*, almost at the same concentration of chromium on the catalyst. On the other hand, no such feature is noticeable on the graph (Figure 12c) relating chromium content to total surface area.

For a fuller interpretation of these results use is made of the Curie-Weiss formula:

$$\chi = \frac{C}{T + \Delta}$$

where χ is the magnetic susceptibility; C = Curie constant; Δ = Weiss constant; and T the absolute temperature.

It is found that the changes in susceptibility with increasing Cr_2O_3 concentration are due mainly to a change in the Weiss constant, whereas the changes in the Curie constant are relatively small. The Curie constant is a measure of the oxidation state of the compound under investigation, whereas the Weiss constant in this particular case is most probably a measure of the electronic interaction of the nearest paramagnetic neighbors. Calculation shows that the number of nearest Cr-Cr neighbors increases rapidly with increasing chromium oxide concentration until about three successive layers of chromium oxide are built up; after this state has been reached the number of further nearest neighbors increases at a much smaller rate. Applying this result to the experimental results reproduced in Figure 12, it is concluded that at point *l* of graphs (a) and (b) a thickness of about three molecular layers has been reached for the chromium oxide. However, at this point the Cr_2O_3 concentration of the catalyst has only reached 6 per cent, and from the surface area data (Figure 12c) it can be calculated that under these conditions only one-tenth to one-fifth of the surface of the activated alumina is covered by chromium oxide. This, therefore, pictures chromium oxide particles of average molecular thickness of three layers covering not more than a fraction of the total available surface of the alumina.

An alternative picture, that only part of the surface is accessible to the chromium oxide molecules, is shown to be in contradiction to the experimental facts. This is further confirmed by the fact that the Weiss constant approaches zero with increasing dilution of the chromium oxide on the alumina, showing that with increasing dilution the catalyst is more and more dispersed, but reaches complete dispersion only at infinite dilution. The conclusion is clear that magnetic susceptibility is a measure of the dispersion of the chromium oxide over the alumina support, and it is a significant result of these investigations that the catalytic activity is closely paralleled by the dispersion of the chromium on the alumina support.

Other oxides of the transition elements, such as uranium oxide, thorium oxide, titanium oxide, which are active cyclization catalysts, also show the magnetic susceptibility effect when dispersed on alumina, though these cases have not been studied in such detail as that of chromium oxide. A significant exception, however, is molybdenum oxide. This oxide fails to show the magnetic susceptibility effect. A satisfactory explanation for this anomaly is lacking, but it may be connected with the partly nonpolar character of the Mo-O bond.

The X-ray diffraction patterns of $\text{Cr}_2\text{O}_3\text{—Al}_2\text{O}_3$ and $\text{MoO}_2\text{—Al}_2\text{O}_3$ have been studied²³. In the case of Cr_2O_3 it was found that Cr_2O_3 lines could only be detected at Cr_2O_3 concentrations considerably greater than those used for the actual catalysts. An interesting result is that the more dispersed the chromium oxide over the catalyst, according to the magnetic data, the higher is the chromium oxide concentration at which the X-ray pattern appears first. Since the intensity of X-ray diffraction patterns is a function of the size of the crystallites, this fact further confirms the evidence from the magnetic investigations that greater activity is associated with greater dispersion of the active oxide on the carrier. It has not been possible to obtain X-ray diffraction diagrams of $\text{MoO}_2\text{—Al}_2\text{O}_3$ catalysts (except lines corresponding to the Al_2O_3 carrier), nor could evidence for the structure of the active oxide be detected under the electron microscope²⁴.

It is interesting to compare the picture of a chromium oxide-alumina catalyst with the work of Russell and Stokes on molybdenum oxide deposited on alumina²⁵. Russell and Stokes, in comparing the activity of such catalysts of known internal surface, found that the activity increased with increasing molybdenum concentration up to a point where the concentration of active oxide is such that, spread out in a monolayer, it covers approximately the entire surface of the alumina. When this point is reached the activity remains practically constant.

It must be noted that Russell's way of plotting his results differs from that of Selwood. Selwood carried out his experiments in such a way that the same quantity of *active catalytic oxide* was present in every run; that is, in

case a more concentrated catalyst was used this was diluted by mixing it with alumina which had not been impregnated with active oxide. As a result his activities are based on a unit weight of catalytically active oxide, and are comparable with Russell's only if the latter are calculated on the same basis. If this is done the very interesting result emerges that the catalytic activity of Russell's $\text{MoO}_2\text{-Al}_2\text{O}_3$ catalysts is constant until a monolayer is formed, and after that declines in proportion to the increasing concentration.

We then have a contrast between chromium oxide catalysts, which appear to form clusters—the catalytic activity of which declines in proportion to their growth—and the molybdenum oxide catalysts, where the active material spreads out in the form of a monolayer, the catalytic activity of which is constant until the monolayer is approximately complete.

In this connection it is well to review the method of preparing these catalysts. Generally, a concentrated solution of the water-soluble salt of the active substance is absorbed by the alumina, and then heated to some 600 to 800°C. In most cases the salt is in a higher oxidation state. With chromium this is the chromate, with molybdenum, the molybdate.

On calcination chromium trioxide decomposes, leaving Cr_2O_3 , but molybdenum trioxide is stable, and remains in this oxidation state.

Cr_2O_3 has an extremely low vapor pressure at the calcining temperature, while that of molybdenum trioxide is appreciable (0.1 mm Hg at 600°C). Thus it is probable that molybdenum trioxide is able to spread out over the total surface by evaporation and re-adsorption, whereas this is not possible with chromium oxide. It seems reasonable, therefore, that by this mechanism molybdenum trioxide can distribute itself over the entire surface of the support, in contrast to Cr_2O_3 .

TECHNICAL APPLICATIONS

The industrial applications of the cyclization reaction can be found predominantly in the petroleum industry, which quickly saw the possibility of a "catalytic reforming"* process based on the cyclization reaction combined with dehydrogenation of six-ring naphthenes.

The aromatic compounds resulting from cyclization and dehydrogenation of paraffins and naphthenes all show higher octane ratings than the paraffins or naphthenes from which they originated; there is, therefore, a possibility of upgrading "naphthas" of low octane rating to a product of much greater value. The process as developed by the petroleum industry, however, differs in certain respects from the normal method of cyclization as described here, and which is the one carried out in the laboratory²⁶. The great

* A detailed discussion of catalytic reforming and hydroforming as applied in the petroleum industry will be given in Volume VI of this series.

difficulty in applying the reaction industrially was the rapid poisoning of the catalyst and the comparatively small through-puts which are possible if substantial conversion into aromatics is to be achieved. These drawbacks were overcome by working under pressure, and by recycling substantial amounts of the hydrogen split off in the reaction to the reaction chamber. Under these conditions the lifetime of the catalyst before regeneration becomes necessary is considerably prolonged, due to the occurrence of "hydrocracking" reactions, which allow the polymeric surface deposits to be eliminated as methane and ethane. At the same time, the use of pressure has the well-known advantage of longer contact times without reduction in throughput, thus achieving a greater depth of conversion. It is, however, significant that under these conditions the cyclization of paraffins no longer makes a substantial contribution to the yield of aromatics. These yields are based mainly on the dehydrogenation of six-ring naphthenes and on the isomerization and dehydrogenation of appropriate five-ring compounds, such as methyl- or ethylcyclopentanes. The fact that the cyclization of paraffins is suppressed is in agreement with the previously discussed mechanism which assumes that the olefin formed from the corresponding paraffins is the intermediate which undergoes cyclization. While it was shown that small concentrations of hydrogen do not interfere with the dehydrogenation of the paraffins to the olefins, and therefore cyclization was not repressed (see Table 3, p. 537), the much larger partial pressures of hydrogen present in the technical process effectively suppress the first part of the reaction sequence, and therefore stops it altogether.

Another difficulty is the comparatively large heat requirements of the reaction. The original process design involved the use of two adiabatic reactors in series, filled with catalyst and preceded by heaters. Because of the considerable endothermicity of the reaction, the temperature drop would have been too great if only one reactor was used. Because of the catalyst regeneration which is necessary from time to time, two or three reactor trains in parallel are available, and the reaction is switched from one to the other in predetermined cycles. The reactors taken off stream are treated with dilute air and after regeneration put back into circuit.

This plant design is by necessity cumbersome and expensive; it is therefore important that new designs based on the fluidized catalyst technique have become available in the last few years²⁷. In this method, a catalyst in the form of a relatively fine powder is blown into the reactor together with the vapors of the charge. The catalyst powder separates from the reaction vapors in the reactor, and through a separate pipe falls into a second reactor, where it is contacted with air to burn off catalyst deposits. In this way a continuous and economic process can be achieved.

Apart from this application, aiming at an upgrading of low-grade naph-

thas, the use of this process in the synthesis of toluene was already mentioned during World War II. As in World War I, the supply of toluene for explosives from coal-tar sources proved inadequate. The hydroforming process, therefore, became of utmost importance to the war effort of the Allied Powers as a means of supplying practically unlimited amounts of toluene from petroleum. Usually, well-fractionated narrow cuts containing substantial proportions of methylcyclohexane, dimethylcyclopentane, and ethylcyclopentane, were used, all of which were transformed, practically quantitatively, into toluene. The contribution of suitable paraffins, such as *n*-heptane or methylhexane, to the final toluene yield was negligible, most probably for the reasons given previously. The resulting product contained toluene in a concentration of about 60 per cent. From this material the aromatic compound was separated by various methods, using solvent extraction, azeotropic or extractive distillation. The final product was sufficiently pure for nitration.

After the war these plants were put to a variety of uses, including the preparation of special solvents. A more interesting application is the manufacture of *o*-xylene from suitably prepared C₈ fraction. *o*-Xylene can be oxidized in good yields to phthalic anhydride.

Finally, a very important application has been found in the production of benzene. The demand for benzene has exceeded the supply possibilities from coal-tar sources, and production from petroleum is now established.

Some of the plants producing benzene also make use of the "hydroforming process," using charging stocks which contain substantial proportions of cyclohexane and methylcyclopentane. It thus appears that this process continues to be applied on a substantial scale.

It is thus clear that the interest which the discovery of the cyclization reaction aroused in industry, particularly in the petroleum industry, was justified. In the course of the eighteen years which have passed since the discovery of the cyclization reaction, a number of important applications have been found and developed. The field is still being investigated on the industrial side and these investigations may lead to new and valuable applications.

References

1. Moldavski, B. L., and Kamusher, H., *Compt. rend. acad. sci. U.S.S.R.*, 355 (1936).
2. Nenitzescu, C. D., and Cantuniari, I. P., *Ber.*, **66B**, 1097 (1933). Nenitzescu, C. D., and Cioranescu, E., *Ber.*, **69B**, 1040 (1936).
3. Grosse, A. V., and Morrell, J. C., U. S. Patent 2124566, 2123567, 2123583, 2124586, Sept.-Oct. 1936.
4. Kazanski, B. A., and Plate, A. F., *Ber.*, **69**, 1862 (1936).
5. Taylor, H. S., and Turkevich, J., *Trans. Faraday Soc.*, **35**, 921 (1939). Turkevich, J., Fehrer, H., and Taylor, H. S., *J. Am. Chem. Soc.*, **63**, 1129 (1941). Taylor, H. S., and Fehrer, H., *J. Am. Chem. Soc.*, **63**, 1385, 1387 (1941). Taylor, H. S.,

- and Salley, D. J., *J. Am. Chem. Soc.*, **63**, 1131 (1941). Taylor, H. S., and Briggs, R. P., *J. Am. Chem. Soc.*, **63**, 2500 (1941).
6. Hoog, H., Verheus, J., and Zuiderweg, F. J., *Trans. Faraday Soc.*, **35**, 993 (1939).
 7. Herington, E. F. G., and Rideal, E. K., *Proc. Roy. Soc. A.*, **184**, 434; 447 (1945).
 8. Nametkin, S. S., Khotimskaya, M. I., and Rozenberg, L. M., *Bull. acad. sci. U.S.S.R. Classe sci. techn.*, **1947**, 795.
 9. Komarewsky, V. I., Riesz, C. H., and Thodos, G., *J. Am. Chem. Soc.*, **61**, 2525 (1939).
 10. Rossini, F. D., *Selected Values of Properties of Hydrocarbons*, U. S. Govt. Printing Office, 1947.
 11. Pitkethly, R. C., and Steiner, H., *Trans. Faraday Soc.*, **35**, 979 (1939).
 12. Taylor, H. S., and Fehrer, H., *J. Am. Chem. Soc.*, **63**, 1387 (1941).
 13. Plate, A. F., and Tarasova, G. A., *J. Gen. Chem. U.S.S.R.*, **XX**, 1193 (1950).
 14. Twigg, G. H., *Trans. Faraday Soc.*, **35**, 1006 (1939).
 15. Horiuti, I., and Polanyi, M., *Trans. Faraday Soc.*, **30**, 1164 (1934).
 16. Twigg, G. H., and Rideal, E. K., *Proc. Roy. Soc. A.*, **171**, 55 (1939); *Trans. Faraday Soc.*, **35**, 1934 (1939).
 17. Steiner, H., *Trans. Faraday Soc.*, **46**, 264 (1950).
 18. See, for instance, Haensel, V., *Petroleum Processing*, **4**, 356 (1950).
 19. See Chapt. 5. Vol. II of present work.
 20. Weisz, P. B., Prater, C. D., and Ritterhouse, K. D., *J. Chem. Phys.*, **21**, 2236 (1953).
 21. Steiner, H., *J. Am. Chem. Soc.*, **67**, 2052 (1945).
 22. Archibald, R. C., and Greensfelder, B. S., *Ind. Eng. Chem.*, **37**, 356 (1945).
 23. Selwood, P. W., and Eischens, R. P., *J. Am. Chem. Soc.* **69**, 1590, (1947); **69**, 2698 (1947); **70**, 2271 (1948).
 24. Webb, G. M., Smith, M. A., and Ehrhardt, R. P., *Petroleum Processing*, **1**, 835 (1947).
 25. Russell, A. S., and Stokes, J. J., *Ind. Eng. Chem.*, **38**, 1071 (1946); **40**, 520 (1948).
 26. Saegbarth, E. O., *Petroleum Engineer*, **XVII**, No. 8, 95 (1946).
 27. Seebold, J. E., Bertetti, J. W., Snuggs, J. F., and Bock, J. A., *Refiner*, **31**, No. 5, 114 (1952).

AUTHOR INDEX

- Abe, R. 519, 524
 Abelson, M. 144, 158, 318, 319
 Ackermann, P. 193, 198, 289, 290, 292, 316, 373, 408
 Adams, N. G. 110, 114
 Adcock, W. A. 201, 377, 421, 434
 Adler, S. 383
 Aicher, A. 260, 261
 Aikers, W. W. 474, 508
 Al, J. 387
 Alberts, L. 49, 246
 Albrecht, W. H. 409
 Almquist, J. A. 20, 185, 244
 Altshuller, S. B. 396
 Anderson, H. C. 29, 42, 43, 121, 176, 408
 Anderson, J. A. 44
 Anderson, R. B. 1, 7, 29, 34, 36, 42, 43, 44, 45, 46, 58, 59, 60, 61, 69, 70, 71, 72, 73, 74, 75, 76, 77, 85, 86, 87, 94, 95, 96, 98, 103, 107, 108, 109, 110, 111, 112, 118, 121, 123, 124, 125, 127, 134, 143, 149, 150, 151, 153, 166, 167, 168, 169, 170, 171, 172, 173, 174, 175, 176, 183, 184, 186, 187, 188, 189, 190, 191, 196, 197, 201, 202, 203, 204, 205, 206, 210, 211, 213, 215, 216, 218, 219, 220, 222, 227, 229, 230, 231, 238, 243, 259, 262, 263, 265, 266, 267, 268, 269, 270, 271, 274, 275, 276, 277, 278, 279, 280, 283, 285, 286, 287, 288, 289, 295, 296, 297, 300, 304, 320, 330, 335, 336, 341, 345, 346, 347, 348, 350, 352, 353, 354, 357, 359, 362, 366, 373, 374, 375, 377, 378, 379, 383, 392, 394, 406, 408, 409, 411, 415, 421, 429, 431, 432, 433, 434, 435, 444, 468, 483, 490, 498, 509
 Ando, S. 519
 Ando, T. 415
 Andrews, A. 211, 212
 Antheaume, J. 421
 Antia, D. P. 425
 Arata, Y. 425
 Archibald, R. C. 554
 Armstrong, E. F. 474, 482
 Arnold, J. H. 296
 Arnold, J. O. 425
 Asaoka, N. 519
 Atwell, H. V. 138, 153
 Atwood, K. 45
 Averbach, B. L. 415, 425
 Badin, E. J. 319
 Badische Anilin und Soda Fabrik 30
 Bahr, H. A. 335, 383, 384, 387, 388, 389, 391, 394, 395, 396, 397, 400, 411, 412, 416, 420, 426, 427, 482
 Bahr, T. 302, 335, 383, 384, 387, 388, 389, 391, 427, 482, 483
 Bakshi, J. B. 483
 Barbieri-Hermitte, F. 26
 Barnes, D. K. 215, 217
 Basak, N. G. 51, 52, 329
 Bashkirov, A. N. 303, 322
 Batchelder, H. R. 243
 Batuev, M. I. 318
 Baudisch, O. 406
 Baugh, H. M. 45
 Bean, E. H. 304, 394, 396, 400, 401
 Beckett, C. W. 1, 2, 3, 8, 10, 11, 15, 475, 476, 477
 Beebe, R. A. 323
 Beilby, G. T. 389, 390, 405
 Beinlich, A. W. Jr., 140, 141
 Benedicks, G. 377
 Bennett, H. A. Jr., 45
 Benson, H. E. 158, 159, 160, 197, 198, 236, 238, 248, 249, 292
 Benton, A. F. 410
 Berger, A. 383
 Bergius, F. 513
 Berkman, S. 481
 Bernier, R. 377, 383, 384, 386, 391, 426
 Bertetti, J. W. 558
 Bever, M. B. 421
 Bienstock, D. 158, 159, 160, 248, 249
 Billig, R. 51
 Binder, G. G. 508
 Bjurstrom, T. 379, 390, 405, 433
 Black, C. A. 20, 185, 244
 Black, J. F. 159
 Blackburn, W. H. 474, 476, 486, 487, 488, 493, 494, 495, 497, 498, 503, 504, 507, 508, 509
 Bloch, H. S. 443, 471
 Blue, R. W. 332, 333
 Blyudov, A. P. 482
 Bock, J. A. 558
 Bohm, J. 409
 Bokhoven, C. 140
 Booth, N. 247, 474, 475, 485, 494, 495, 496, 498, 499, 500, 502, 503, 505, 507, 509
 Botalsen, E. 482
 Boudouard, O. 387
 Bowles, K. W. 516
 Bowman, N. J. 207, 210, 211, 212, 213, 214, 216, 217, 221, 222, 223, 236, 349, 357, 358, 359
 Bozorth R. M. 379, 382
 Braude, G. 415, 428
 Bredig, G. 386
 Breywisch, 148, 237, 294
 Bridelle, R. 378, 433
 Bridges, G. L. 140, 141
 Briggs, R. P. 529, 539, 549, 550, 551, 552, 553
 Brill, R. 200, 249, 412, 420, 429
 British Fuel Research Board, 483, 484, 485, 489, 494, 500, 507, 514, 515, 516, 519, 520, 526
 British Gas Research Board, 486
 Brock, C. M. 486, 493, 505, 506
 Brötz, W. 263, 264, 270, 271
 Browne, R. Y. 45
 Browning, L. C. 20, 21, 22, 342, 387, 415
 Brunauer, S. 20, 22, 69, 141, 165, 175, 185, 244, 327, 328, 410, 427, 428, 429
 Bruner, F. H. 211, 212, 352, 354
 Bruns, B. 428
 Buelow, H. 474, 482, 483
 Buffeb, H. 9, 238, 240, 241, 242, 297, 298, 299
 Buisson, P. 390
 Cady, W. E. 207, 210, 211, 212, 213, 214, 221, 222, 223, 236, 349, 357, 358, 359, 360
 Cain, D. G. 216, 217
 Cairns, R. W. 382, 383
 Cantuniari, I. P. 529
 Carlson, C. S. 215, 216, 217, 218, 323
 Carrol, K. G. 434
 Cawley, C. M. 519, 525, 527
 Chaffee, C. C. 138, 153
 Chakravorty, K. M. 482, 483, 490
 Charmbury, H. B. 527
 Chaudron, G. 376
 Chesebro, P. R. 483
 Cioranescu, E. 529
 Clark, A. 211, 212
 Clark, E. L. 45, 518, 524, 526
 Clark, J. 376, 377, 404, 405
 Cohen, M. 415, 421, 425
 Cohn, E. M. 188, 201, 202, 374, 377, 381, 382, 387, 388, 389, 399, 415, 418, 419, 421, 422, 423, 425, 430, 434
 Cook, R. S. 19
 Cooperman, J. 486
 Crangle, J. 425
 Craxford, S. R. 31, 49, 50, 61, 70, 78, 82, 83, 85, 89, 91, 92, 96, 97, 98, 99, 108, 118, 120, 127, 139, 153, 157, 161, 164, 181, 243, 245, 273, 303, 313, 314, 335, 337, 338, 339, 340, 341, 346, 427, 509

- Crowell, J. H. 197, 198, 236, 238, 248, 249, 292
- Damick, A. D. 415, 418, 419
- Darkin, L. S. 434
- Davis, H. G. 224
- Davis, J. D. 45
- Davis, J. J. 486
- Davis, W. R. 416
- DeLange, J. J. 78, 383
- Demeter, J. J. 474, 477, 478, 479, 480, 486, 487, 488, 489, 490, 491, 492, 493, 494, 495, 496, 498, 501, 502, 503, 504, 507, 509
- Dent, F. J. 474, 476, 486, 487, 488, 493, 494, 495, 497, 498, 503, 504, 507, 508, 509
- Derrig, M. J. 323
- Dewey, D. R. 443
- DeWitt, T. W. 20, 21, 76, 169, 170, 187, 188, 315, 328, 342, 343, 344, 345, 373, 374, 401, 412, 414, 415, 419, 421, 422, 423, 426
- d'Hont, M. 474
- Dieckmann, T. 412
- Dieter, W. E. 123, 191, 374, 409, 429, 431, 432, 433
- Diltthey, P. 374, 375, 400, 482, 483
- Dingmann, T. 415
- Dokkum, T. 387
- Dolch, P. 1
- Dovani, C. 482
- Dowden, D. A. 374
- Drain, J. 403, 404, 423, 426
- Dressler, R. C. 243
- Dudash, A. P. 42
- Duftscheid, 185
- DuJassoneix, B. 405, 434
- Dunlop, A. K. 40
- Durand, J. F. 421
- Eastwood, A. H. 474, 476, 486, 487, 488, 493, 494, 495, 497, 498, 503, 504, 507, 508, 509
- Ebert, J. P. 1, 2, 3, 8, 10, 11, 15, 475, 476, 477
- Eckstrom, H. C. 201, 377, 421, 434
- Edwards, O. S. 392
- Egleson, G. C. 243, 486, 493, 505, 506
- Egloff, G. 481
- Ehrhardt, R. P. 556
- Eichner, C. 315
- Eidus, Y. T. 318, 319, 341, 342, 396, 414, 426
- Eischens, R. P. 554, 555, 556
- Eisenhut, O. 428
- Eisenstecken, F. 415
- Eisner, A. 526
- Elagina, N. V. 414, 426
- Eliot, T. W. 215, 217
- Elliott, M. A. 125, 127, 143, 150, 151, 196, 197, 220, 222, 227, 229, 230, 231, 238, 283, 285, 286, 287, 288, 289, 295
- Elmore, K. L. 248
- Elvins, O. C. 335, 345
- Emert, O. 420
- Emmctt, P. H. 19, 20, 21, 22, 23, 69, 76, 142, 165, 169, 170, 185, 187, 188, 244, 295, 315, 322, 327, 328, 335, 336, 342, 343, 344, 345, 359, 363, 364, 366, 373, 374, 387, 401, 410, 412, 414, 415, 419, 421, 422, 423, 426, 427, 428, 429, 430
- Ende, U. J. C. 428
- Engelhardt, F. 10, 193, 194, 198, 228, 273, 283, 284, 289, 290, 292, 303, 304, 305, 306, 307, 308, 309, 310, 336, 341, 373
- Epifanskii, P. F. 414, 426
- Ercoli, R. 26
- Erhard, F. 333
- Eroseev, B. V. 266, 268
- Ershov, N. I. 318
- Eru, I. I. 527
- Estes, F. L. 29
- Ewing, F. J. 409
- Fan, S. 319
- Fankuchen, I. 201
- Faragher, W. F. 127, 133, 157
- Fehrer, H. 529, 539, 549, 550, 551, 552, 553
- Feisst, W. 53
- Feitknecht, W. 383
- Feldman, J. 211, 216, 218, 219, 345, 374, 468
- Field, J. H. 158, 159, 160, 197, 198, 236, 238, 248, 249, 292
- Filer, E. W. 434
- Fischer, F. 30, 31, 32, 39, 40, 46, 47, 48, 49, 51, 53, 55, 56, 57, 58, 65, 66, 67, 68, 69, 100, 101, 102, 157, 158, 159, 196, 243, 244, 247, 264, 266, 280, 300, 301, 302, 319, 335, 336, 337, 338, 373, 374, 375, 394, 400, 416, 420, 443, 481, 482, 483
- Fischer, L. E. 319
- Fisher, C. H. 519, 526
- Fitzwilliam, J. W. 404
- Fleming, H. W. 211, 212
- Fletcher, S. G. 425
- Floe, C. F. 421
- Forest, H. O. 482
- Forrer, R. 434
- Franchetti, P. 482
- Frankenburg, W. G. 373
- Franz, H. 415
- Frear, G. L. 244, 248
- Fricke, R. 19, 374, 376, 382, 387, 391, 408, 410
- Friedel, R. A. 42, 109, 110, 111, 112, 118, 210, 266, 267, 268, 269, 274, 275, 276, 277, 278, 279, 280, 300, 341, 347, 350, 352, 353, 354, 357, 362, 367
- Friedman, S. 515, 519, 520, 524
- Frye, C. G. 336
- Fuel Research Board (British) 32
- Fujimura, K. 246, 247, 259, 260, 261
- Fujiwara, K. 519
- Gable, C. M. 40
- Gall, D. 31, 36, 37, 50, 85, 110, 113, 120, 139, 161, 164, 181, 228, 229, 232, 288, 290, 294, 296, 320, 323, 350, 362
- Geiseler, 148, 237, 294
- Gerard, F. W. 483
- Ghosh, J. C. 51, 52, 324, 325, 326, 482, 483
- Gibson, E. J. 110, 113, 266, 280, 281, 282, 320, 321, 322, 323, 350, 362
- Gilfert, W. 312
- Gilkeson, M. M. 488, 508
- Gilmore, R. E. 516
- Glud, W. 412
- Golden, P. L. 316, 319
- Goldschmidt, H. J. 403
- Golumbic, N. I. 7, 29, 34, 36, 42, 43, 46, 59, 85, 121, 123, 149, 153, 176, 186, 213, 215, 243, 259, 266, 270, 296, 335, 336, 346, 348, 354, 359, 366, 373, 408, 444, 468, 498
- Goodeve, C. 430
- Gordon, K. 139, 161, 181, 186
- Graham, J. I. 519, 525
- Grahame, J. H. 443, 471
- Granadam, P. 389
- Greenfield, H. 367
- Greensfelder, B. S. 554
- Gresham, W. F. 240, 242
- Greyson, M. 474, 477, 478, 479, 480, 486, 487, 488, 489, 490, 491, 492, 493, 494, 495, 496, 498, 501, 502, 503, 504, 507, 509
- Griffith, R. H. 341
- Groll, E. 420
- Grosse, A. V. 529
- Grossman, J. P. 243
- Gwathmey, A. T. 388, 401
- Haensel, V. 312, 443, 550
- Hager, G. F. 240
- Hägg, G. 380, 381, 389, 402, 405, 408, 419, 428
- Hahn, F. 409
- Hall, C. C. 31, 36, 37, 39, 49, 50, 61, 82, 83, 85, 89, 91, 92, 93, 96, 98, 99, 100, 103, 104, 105, 106, 107, 108, 110, 113, 120, 127, 139, 153, 157, 161, 164, 181, 228, 229, 232, 243, 266, 280, 281, 282, 288, 290, 294, 296, 320, 323, 350, 362, 527

- Hall, W. K. 42, 44, 45, 58, 59, 61, 69, 70, 71, 72, 73, 74, 75, 76, 77, 87, 94, 95, 96, 98, 103, 107, 108, 166, 167, 168, 169, 170, 172, 173, 174, 175, 176, 187, 188, 189, 191, 203, 262, 263, 271, 295, 304, 373, 374, 377, 383, 392, 429, 431, 432, 433, 434, 435
- Halle, F. 200, 418
- Hamai, S. 362
- Hansford, R. C. 467
- Harkness, R. W. 327
- Haslam, R. T. 482
- Hawk, C. O. 42, 43, 121, 176, 316, 319, 408, 526
- Hebden, D. 474, 476, 486, 487, 488, 493, 494, 495, 497, 498, 503, 504, 507, 508, 509
- Heidenreich, R. D. 418
- Henderson, G. G. 389, 390, 405
- Hendricks, S. B. 23, 392, 407, 418, 427, 428, 429
- Herbert, 138
- Herbst, M. 200, 418
- Heringion, E. F. G. 97, 111, 244, 245, 336, 347, 348, 349, 350, 529, 531, 532, 533, 534, 542, 543, 544, 545, 546, 547, 548, 549, 550, 552, 554
- Hertrich, F. 409
- Hewlett, H. 59, 69, 70, 71, 72
- Hightower, F. W. 482
- Hilberath, F. 112
- Hilditch, T. P. 474, 482
- Hilpert, S. 412
- Hirst, L. L. 519
- Hiteshue, R. W. 518
- Hofer, L. J. E. 42, 43, 58, 59, 61, 70, 73, 74, 75, 77, 78, 86, 96, 121, 123, 124, 125, 176, 188, 191, 201, 202, 271, 304, 330, 373, 374, 375, 377, 380, 381, 382, 383, 387, 388, 389, 392, 393, 394, 395, 396, 399, 400, 401, 402, 403, 406, 408, 409, 415, 416, 418, 419, 421, 422, 423, 425, 429, 430, 431, 432, 433, 434
- Hofmann, U. 412, 420
- Hollings, H. 138, 153
- Holm, V. C. F. 332, 333
- Holmes, J. 410
- Holroyd, R. 141
- Honda, K. 418
- Hoog, H. 418, 529, 531, 536, 540, 542, 543
- Horiuti, I. 541
- Horne, W. A. 157
- Horton, L. 515
- Hougen, O. A. 3, 270, 297
- Howk, B. W. 240
- Hukushima, I. 130, 131
- Hume-Rothery, W. 375, 380, 381, 418, 425
- Hunsmann, W. 323
- Hurota, W. 519
- Hüttig, G. F. 374, 376, 382, 391, 410
- Huzikawa, S. 519
- Igawa, S. 272
- I.G. Farbenindustrie 266, 362
- Ipatieff, V. N. 312, 319
- Irsa, A. P. 311
- Isaichev, I. V. 418
- Ishikawa, S. 118, 261, 262
- Isoda, M. 130, 131
- Iwaizumi, S. 429
- Jack, K. H. 191, 376, 377, 378, 380, 389, 404, 405, 419, 428, 429, 430
- Jacob, K. 482, 483
- Jacobsen, B. 377, 381, 387
- Jaeger, A. 482
- Jefferson, M. E. 23, 392, 428
- Jellinek, M. H. 201
- Jessen, V. 335, 394, 395, 396, 397, 411, 412, 420, 426
- Jochum, P. 481, 482, 483
- Johnson, G. E. 474, 477, 478, 479, 480, 486, 487, 488, 489, 490, 491, 492, 493, 494, 495, 496, 498, 501, 502, 503, 504, 507, 509
- Johnson, M. F. L. 70
- Jolley, L. J. 247, 474, 475, 485, 494, 495, 496, 498, 499, 500, 502, 503, 505, 507, 509
- Jonakin, J. 474, 477, 478, 479, 480, 486, 487, 488, 489, 490, 491, 492, 493, 494, 495, 496, 498, 501, 502, 503, 504, 507, 509
- Jones, I. H. 138, 153
- Joseph, N. 390
- Jungers, J. C. 474
- Juza, R. 373, 378, 389, 390, 392, 393, 404, 405
- Kagan, Y. B. 322
- Kainer, F. 29
- Kakutani, T. 519
- Kallenberger, R. H. 45
- Kamusher, H. 529, 549
- Kamzolkina, E. V. 322
- Kandiner, H. J. 518
- Karn, F. S. 288, 297, 322
- Karzhavin, V. A. 244
- Katayama, I. 54
- Kaupp, E. 428
- Kawamichi, K. 246, 247
- Kazan, Y. B. 303
- Kazanski, B. A. 529, 549, 550
- Kearby, K. L. 59
- Kehrer, V. J. Jr., 388, 401
- Keith, P. C. 296
- Kelley, K. K. 523, 526
- Kelly, R. 125, 127, 143, 150, 151, 196, 197, 220, 222, 227, 229, 230, 231, 238
- Kelly, R. E. 274, 283, 285, 286, 287, 288, 289, 295
- Kemmer, H. 482
- Khotinskaya, M. I. 532
- Kiessling, R. 376, 380
- Kilpatrick, J. E. 1, 2, 3, 8, 10, 11, 15, 475, 476, 477
- Kimura, K. 130, 131
- King, J. G. 138, 153, 515
- Kingman, F. E. T. 519
- Kini, K. A. 324, 325, 326, 329
- Kirkpatrick, W. J. 523
- Kirscht, P. H. 415
- Klas, H. 415
- Klemenc, A. 482
- Klemm, R. 147, 157, 185, 288
- Kleppa, O. J. 19
- Koch, H. 31, 46, 47, 48, 49, 51, 55, 56, 112, 299, 308, 312, 319, 335, 336, 337, 482, 483
- Kodama, S. 128, 129, 130, 131, 220, 324, 415
- Koelbel, H. 10, 130, 132, 133, 134, 139, 140, 193, 194, 198, 228, 248, 273, 283, 284, 289, 290, 292, 303, 304, 305, 306, 307, 308, 309, 310, 316, 317, 335, 336, 341, 373, 415
- Kohlhass, R. 387
- Kölbel, H. See Koelbel, H.
- Koide, H. 54
- Kolthoff, I. M. 123
- Komarewsky, V. I. 29, 334, 533
- Komazawa, S. 130, 131
- Kortengraber, A. 415
- Kosaka, Y. 519
- Koster, W. 379
- Krageloh, F. 415
- Krieg, A. 42, 58, 59, 60, 70, 76, 77, 87, 94, 95, 96, 98, 103, 107, 108, 118, 262, 263, 265, 266, 267, 268, 269, 271, 274, 275, 276, 277, 278, 279, 280, 300, 304, 320, 341, 373, 374
- Kryukov, Y. B. 303, 322
- Kuhn, E. M. 515
- Kummer, J. T. 20, 22, 187, 188, 315, 322, 327, 328, 336, 342, 343, 344, 345, 359, 363, 364, 366, 373, 374, 401, 412, 414, 415, 419, 421, 422, 423, 426
- Kurokawa, M. 519
- Kuss, E. 420
- Kuster, H. 100, 299, 300, 301, 308, 482, 483
- Lahiri, A. 329
- Laidler, K. J. 323
- Lane, J. C. 29
- Langheim, R. 193, 198, 289, 290, 292
- Larson, A. T. 140
- Launer, P. J. 211, 214, 357, 358, 360
- Laymann, A. 415
- Lazier, W. A. 481
- LeBlanc, M. 383

- Lecky, J. A. 203, 204, 205, 206, 270, 330, 374, 421
 LeClerc, G. 374, 377, 383, 384, 386, 387, 391, 408, 410, 420, 426
 LeFebvre, H. 374, 377, 386, 391, 408, 410, 420, 426
 Lehrer, E. 23, 378, 382, 428
 Leidheiser, H. Jr., 388, 401
 Lement, B. S. 415
 Leuna, 111, 116, 117, 141, 149, 198, 266
 Linckh, E. 147, 157, 185, 288
 Lipson, H. 392, 418
 Lister, F. 334
 Little, A. T. 418
 Longuet, J. 410
 Love, K. S. 141, 430
 Luk'yanovich, V. M. 416

Makh, G. M. 518
Mandal, A. K. 527
Manes, M. 349, 350, 351, 415, 418, 419
Marder, H. 39
Mark, H. 412, 420
Markby, R. 367
Marschner, R. F. 45
Martin, F. 109
Mason, L. S. 42, 118, 266, 267, 268, 269, 274, 275, 276, 277, 278, 279, 280, 300, 341
Matsumura, S. 324, 415
Maxwell, L. S. 410
McAteer, J. H. 215, 216, 217, 218, 323
McCartney, J. T. 58, 59, 61, 171, 172, 330, 383, 388, 392, 402, 416, 421
Medsforth, S. 482, 483, 509
Meisinger, E. E. 319
Mentser, M. 415, 418, 419
Merkel, H. 179, 180, 195, 199, 200, 243, 374, 377, 379, 382, 408, 411, 418, 420, 434
Meshcheryakov, A. P. 318
Meusel, A. 302, 483
Meyer, 408
Meyer, G. 387, 389
Meyer, K. 31, 46, 47, 51, 53, 55, 56, 57, 58, 65, 66, 67, 68, 69, 159, 247, 482
Meyer, W. 387
Meyer, W. F. 403
Michael, W. 158, 206
Michel, A. 376, 377, 383, 384, 386, 387, 391, 404, 409, 426, 433
Miller, G. H. 301, 490
Miller, R. W. 40
Milligan, W. O. 123, 391, 409, 410
Milliken, T. H. Jr., 467
Mills, G. A. 467
Mitchell, J. J. 415
Mittasch, A. 142, 420
Mobius, E. 383

Moignard, L. A. 474, 476, 486, 487, 488, 493, 494, 495, 497, 498, 503, 504, 507, 508, 509
Moldavski, B. L. 529, 549
Monroe, G. S. 319
Montgomery, C. W. 26, 323, 346
Morgan, G. T. 482, 483, 515
Morikawa, K. 272, 524
Morrell, C. E. 215, 216, 217, 218, 323
Morrell, J. C. 481, 529
Moskowitz, B. 123
Mulfinger, W. 379
Mulford, R. M. R. 302
Muller, A. 433
Murakami, T. 418
Murata, Y. 54, 118, 128, 129, 130, 132, 133, 261, 262
Myddleton, W. W. 1, 260, 261
Myers, J. W. 474, 477, 478, 479, 480, 486, 487, 488, 489, 490, 491, 492, 493, 494, 495, 496, 498, 501, 502, 503, 504, 507, 509.

Nakai, A. 84, 85
Nametkin, S. S. 532
Nash, A. W. 335, 345
Natta, G. 391
Nenitzescu, C. D. 529
Neumann, B. 482, 483
Newell, A. 29
Nicolai, J. 474
Nielsen, A. 140
Nowotny, H. 392, 393

Oblad, A. G. 467
Ohman, E., 419
Okada, M. 425
Okamura, T. 519, 524
Oketani, S. 415
Olmer, F. 414
O'Neill, W. E. 42, 265, 320
Oppau, 146
Orlov, N. A. 527
Osawa, A. 429
Osswald, E. 385, 387, 388
Ott, E. 382, 383
Otto, H. 412

Pace, P. S. 215, 217
Panning, G. 474, 482, 483
Paranjpe, V. G. 421
Parker, A. M. B. 418
Pascal, P. 482
Passerini, L. 391
Paul, R. 390
Pauling, L. 407, 418
Pearson, J. 428
Pease, R. N. 19, 483
Peebles, W. C. 78, 121, 123, 124, 125, 304, 330, 377, 381, 382, 387, 388, 389, 392, 393, 394, 395, 396, 399, 400, 401, 403, 409, 418, 419, 421, 422

Pelipetz, M. G. 515, 517, 518, 519, 520, 521, 523, 524, 526
Pernoux, E. 61
Perrin, M. 79, 88, 89, 315, 383
Petch, N. J. 418, 421
Petrova, L. V. 414, 426
Phillips, J. R. 45
Phillips, T. R. 383
Phragmen, G. 387, 418
Pichler, H. 9, 25, 32, 39, 40, 51, 69, 96, 100, 101, 102, 114, 115, 118, 119, 120, 121, 122, 123, 126, 127, 128, 132, 133, 135, 161, 163, 164, 176, 177, 178, 179, 180, 181, 193, 195, 196, 198, 199, 200, 220, 225, 229, 232, 234, 237, 238, 239, 240, 241, 242, 243, 246, 264, 266, 280, 284, 285, 288, 289, 297, 298, 299, 300, 301, 303, 345, 346, 374, 375, 377, 379, 382, 408, 411, 418, 420, 434, 443, 458, 463, 464, 468, 469, 482
Pingault, P. 418, 423
Pitkethly, R. C. 537, 538, 553, 558
Pitzer, K. S. 1, 2, 3, 8, 10, 11, 15, 475, 476, 477
Plate, A. F. 529, 540, 542, 550
Podgurski, H. 187, 188, 322, 328, 336, 363, 364, 414, 419, 421, 422, 423
Polanyi, M. 541
Pole, G. R. 140, 141
Postgate, J. R. 243
Powell, A. R. 45
Prater, C. D. 551
Prettre, M. 1, 12, 315
Prokopets, E. I. 527
Puff, H. 378, 404
Puzitski, K. V. 318

Radushkevich, L. V. 416
Randall, M. 483
Raney, M. G. 45
Rapoport, I. B. 482, 519
Raynor, G. V. 418
Read, A. A. 425
Redlich, O. 40
Reichl, E. H. 141
Reisinger, 141, 148, 211, 213, 237, 294
Reitmeier, R. E. 45
Reynolds, D. A. 45
Rheinpreussen, 153, 182
Richardson, C. N. 140
Richardson, F. D. 415, 421
Rideal, E. K. 303, 335, 337, 338, 340, 427, 529, 531, 532, 533, 534, 541, 542, 543, 544, 545, 546, 547, 548, 549, 550, 552
Ries, H. E. 70
Riesz, C. H. 29, 334, 533
Rigby, G. R. 416
Riley, H. L. 379
Ritter, H. 412

- Ritterhouse, K. D. 551
 Roberts, C. S. 415
 Roberts, E. C. 425
 Roberts, J. K. 155
 Robey, R. F. 215, 216, 217, 218, 323
 Roelen, O. 31, 53, 82, 83, 84, 103, 107, 181, 229
 Rossini, F. D. 1, 2, 3, 8, 10, 11, 15, 475, 476, 477, 535, 536
 Royen, P. 333
 Rozenberg, L. M. 532
 Rubin, L. C. 64
 Ruckes, W. L. 486
 Ruhrchemie, 46, 49, 50, 51, 52, 54, 57, 59, 61, 63, 84, 89, 90, 91, 107, 110, 118, 138, 139, 182, 199, 261
 Rundle, R. E. 381
 Runtso, A. P. 266, 268
 Rupp, J. 482
 Ruschenburg, E. 193, 198, 289, 290, 292, 317
 Russell, A. S. 556
 Russell, W. W. 301, 302, 490
 Sabatier, P. 29, 299, 473, 481, 482, 483, 507
 Sachse, W. 378, 389, 390, 404, 405
 Saegbarth, E. O. 557
 Sage, M. 392
 Salley, D. J. 529, 539, 549, 550, 551, 552, 553
 Sand, A. E. 243
 Sarker, J. M. 490
 Sastri, M. V. C. 96, 324, 325, 326, 327
 Sawada, Y. 128, 129, 130, 132, 133
 Schaad, R. E. 443, 471
 Schaarschmidt, A. 39
 Scheffer, F. E. C. 387, 389
 Schellenberg, A. 481, 482
 Schenk, R. 20, 412, 415, 427
 Scheuermann, A. 39, 50, 54, 57, 58, 64, 116, 117, 120, 126, 132, 134, 142, 143, 144, 145, 146, 148, 180, 181, 186, 224, 225, 226, 233, 234, 236, 283, 284, 288, 381, 418
 Schirrmacher, H. 386
 Schlesinger, M. D. 474, 477, 478, 479, 480, 486, 487, 488, 489, 490, 491, 492, 493, 494, 495, 496, 498, 501, 502, 503, 504, 507, 509
 Schmidt, J. 385, 387, 388
 Schneider, I.
 Schuster, P. 474, 482, 483
 Schwartz, F. G. 110, 114
 Schwarz von Bergkamp, E. 386
 Sebastian, J. J. S. 482, 483, 489
 Seebold, J. E. 558
 Seelig, H. S. 45, 141, 142, 155, 156, 201, 207, 210, 211, 212, 213, 214, 221, 222, 223, 236, 349, 357, 358, 359
 Seligman, B. 42, 44, 45, 58, 59, 60, 69, 70, 71, 72, 76, 77, 87, 94, 95, 96, 98, 103, 107, 108, 125, 127, 134, 143, 150, 151, 183, 184, 188, 189, 190, 196, 197, 201, 202, 203, 204, 205, 206, 220, 222, 227, 229, 230, 231, 238, 262, 263, 264, 265, 271, 283, 285, 286, 287, 288, 289, 295, 304, 318, 319, 320, 330, 373, 374, 415, 421, 434
 Sellers, F. B. 443
 Selwood, P. W. 382, 383, 554, 555, 556
 Senderens, J. B. 29, 299, 473, 481, 482, 483, 507
 Sergienko, S. R. 549
 Seyfried, W. C. 44
 Seymour, W. 486
 Shaw, L. 183, 184, 188, 190
 Shimura, S. 418
 Shultz, J. F. 19, 42, 44, 45, 125, 127, 143, 144, 150, 151, 158, 183, 184, 188, 189, 190, 196, 197, 203, 204, 205, 206, 220, 222, 227, 229, 230, 231, 238, 244, 248, 283, 285, 286, 287, 288, 289, 295, 297, 305, 318, 319, 374, 377, 392, 434
 Skinner, D. G. 519, 525
 Slawson, R. J. 416
 Sliepecevic, C. M. 488, 508
 Smart, J. S. 410
 Smith, D. F. 1, 45, 316, 319
 Smith, L. G. 334
 Smith, M. A. 556
 Smith, P. V. 215, 216, 217, 218, 323
 Smith, S. L. 36, 37, 39, 92, 93, 98, 100, 103, 104, 105, 106, 107, 139, 228, 229, 232, 288, 290, 294, 296
 Snuggs, J. F. 558
 Spencer, W. D. 322, 336, 363, 364
 Spengler, H. 271
 Spruit, C. J. P. 243
 Srinivasan, S. R. 96, 326, 327
 Stamme, K. 427
 Stanley, J. K. 415
 Starkey, R. L. 243
 Stein, K. C. 121, 123, 124, 125, 134, 144, 158, 295, 322, 409
 Steinbrecher, 244, 246
 Steiner, H. 537, 538, 549, 553, 558
 Steitz, A. 215, 217
 Stenkhoff, R. 412, 415, 427
 Sterling, E. 388, 402, 416
 Sternberg, H. W. 367
 Stewart, S. G. 382
 Stokes, J. J. 556
 Storch, H. H. 1, 7, 29, 34, 36, 38, 42, 43, 44, 45, 46, 59, 85, 121, 123, 149, 153, 158, 159, 160, 176, 186, 188, 189, 197, 198, 211, 213, 215, 216, 218, 219, 236, 238, 243, 259, 266, 270, 292, 296, 335, 336, 345, 346, 348, 352, 353, 354, 357, 359, 362, 366, 373, 374, 408, 444, 468, 498, 515, 519, 520, 526
 Strada, M. 391
 Strickland-Constable, R. F. 508, 509
 Sturkey, L. 418
 Sucksmith, W. 425
 Sudzilovskaya, M. S. 519
 Suen, T. J. 319
 Synthetic Fuels Report, Secretary of the Interior. 373
 Tahara, H. 130, 131
 Takezaki, Y. 128, 129, 130, 132, 133
 Tanaka, K. 519
 Tarama, K. 324, 415
 Tarasova, G. A. 540, 542
 Tarn, W. H. 58, 59, 60, 166, 167, 168, 169, 170, 172, 173, 174, 175, 176, 187, 295, 435
 Taylor, E. H. 311
 Taylor, H. S. 311, 529, 539, 549, 550, 551, 552, 553
 Taylor, R. 482
 Taylor, W. J. 1, 2, 3, 8, 10, 11, 15, 475, 476, 477.
 Tebbboth, J. A. 247, 386, 387, 474, 475, 485, 494, 495, 496, 498, 499, 500, 502, 503, 505, 507, 509
 Teichner, S. 61, 79, 80, 81
 Teller, E. 69, 165
 Tentschert, H. 373
 Thodos, G. 334, 533
 Thompson, G. P. 374, 377, 434
 Thompson, H. L. 140, 141
 Thompson, J. G. 45
 Thompson, O. F. 138, 153
 Thompson, S. O. 311
 Titzenthaler, E. 312, 443, 463, 464
 Tomlinson, J. R. 26
 Traeger, B. 443, 463, 468
 Trambouze, Y. 79, 383
 Tramm, H. 297
 Trillat, J. J. 415
 Troesch, A. 377, 391
 Tropsch, H. 30, 157, 158, 244, 335, 336, 338, 373, 374, 375, 481, 482, 483
 Tsuneoka, S. 54, 118, 246, 247, 259, 260, 261, 262
 Tsutsumi, S. 46, 54, 65
 Turkevich, J. 311, 529, 539, 549, 550, 551, 552, 553
 Tutiya, H. 385, 386, 414, 420
 Twigg, G. H. 541, 548, 554
 Underwood, A. J. V. 109
 U. S. Bureau of Mines, 523
 Van Heerden, C. 140
 Verheus, J. 529, 531, 536, 540, 542, 543

- Verwey, E. J. W. 408
 Veryard, J. T. 515
 Vignon, L. 481, 482
 Visser, G. H. 78, 383
 Vol'kenshtein, F. F. 324
 Volkowa, A. A. 266, 268
 Volmer, W. 347
 Von Dingen, W. 488
 Von Itterbeek, A. 488
 Von Philippovitch, A. 482
 Von Wangenheim, 400, 416
 Von Weber, U. 112
 Voss, D. J. 141, 142, 155, 156, 201, 221, 222.
 Vournasos, A. C. 404

 Wagner, F. W. 519
 Wainwright, H. W. 243, 486, 493, 505, 506
 Walenda, H. 25
 Walker, J. 260, 261
 Walker, S. W. 155
 Ward, C. C. 110, 114, 350
 Warner, B. R. 323
 Warren, T. E. 516
 Watanabe, S. 54, 55, 56, 61, 64, 237, 272
 Watase, T. 20
 Watson, K. M. 3, 270, 297
 Wauklyn, J. N. 243
 Webb, G. M. 556
 Week, H. I. 141, 142, 155, 156, 201, 221, 222

 Weil, B. H. 29
 Weillbrecht, G. 19
 Weinberger, E. B. 346
 Weingaertner, 244, 246
 Weinrotter, F. 122, 180, 181, 193
 Weiser, H. B. 123, 374, 391, 406, 409
 Weiss, P. 434
 Weisz, P. B. 551
 Weitbrecht, G. 387
 Weitkamp, A. W. 207, 210, 211, 212, 213, 214, 216, 217, 221, 222, 223, 236, 336, 349, 357, 358, 359, 360
 Weller, S. 86, 265, 342, 352, 353, 354, 357, 373, 374, 375, 377, 394, 396, 406, 415, 517, 518, 519, 520, 521, 523, 524, 526
 Welo, L. A. 406
 Wender, I. 367
 Wenner, R. R. 14
 Wenzel, W. 64, 141, 148, 198
 Wenzell, L. P. 243
 Werner, H. G. 1, 2, 3, 8, 10, 11, 15, 475, 476, 477
 Weselcock, H. 415
 Westgren, A. 377, 381, 387, 418, 434
 Westrik, R. 140
 Wever, F. 418, 433
 Wheeler, A. 243, 272, 296
 White, A. H. 482
 White, E. C. 305

 White, R. R. 474, 488, 508
 Wiley, J. L. 29
 Wilkins, E. T. 247, 474, 475, 485, 494, 495, 496, 498, 499, 500, 502, 503, 505, 507, 509
 Willeke, H. 415
 Williams, F. A. 515
 Williams, M. G. 1, 2, 3, 8, 10, 11, 15, 475, 476, 477
 Wilson, A. J. C. 392, 393
 Wilson, T. P. 224
 Winkelmann, H. 400, 416, 482
 Woods, H. L. 418
 Woodward, L. A. 97, 244, 245
 Work, H. K. 519
 Wotiz, J. 367
 Wright, C. C. 527

 Yamanouchi, A. 519
 Yasuda, M. 128, 129, 130, 132, 133
 Yoshimori, K. 415

 Zelinskii, N. D. 318, 396, 414, 426, 549
 Ziesecke, K. H. 443, 449, 458, 463, 464, 468, 469
 Zisson, J. 141, 142, 155, 156, 201, 221, 222
 Zorn, H. 147, 157, 185, 283, 284
 Zuiderweg, F. J. 529, 531, 536, 540, 542, 543
 Zwell, L. 434
 Zwietering, P. 140

SUBJECT INDEX

- Alcohols
 - decomposition on nickel and cobalt catalysts, 319-320
 - incorporation in synthesis, 319-323
 - in Fischer-Tropsch synthesis products, 38, 110, 113, 117, 137, 139, 149, 154, 163, 190, 215-221, 226-238
 - thermodynamics of, 11-14
- Aromatization (see Cyclization and Aromatization)
- Borides
 - of cobalt, 405-406
 - of iron, 433
 - of nickel, 390
- Borocarbides of iron, 434
- Carbide intermediate theory of synthesis
 - carburization and synthesis rates, 341-342
 - Craxford and Rideal hypothesis, 337-341
 - Fischer postulates, 336-337
 - radioactive carbon studies of, 342-345
 - thermodynamics of carbide formation, 20-23
 - thermodynamics of carbide reduction, 342
- Carbon dioxide, hydrogenation of, 299-303
- Carbon filament from carbon monoxide
 - decomposition
 - on cobalt, 402-403
 - on iron, 416-417
 - on nickel, 388-389
- Carbon monoxide, reaction with water vapor, 303-310
- Carbonyls and Fischer-Tropsch synthesis
 - hydrocarbonyl complexes, 367
 - Pichler postulate, 345
- Carriers, 55-64, 133-140
- Catalyst preparation
 - cobalt and nickel catalysts, 46-69, 82-89
 - iron catalysts, 119-160, 176-192
 - ruthenium, 238-239
- Catalysts for methanation
 - British Fuel Research Board, 483-485
 - iron catalysts, 490-493
 - nickel catalysts, 493-506
 - work prior to 1940, 481-483
 - work since 1940, 485-487
- Catalyst testing methods, 36-46, 447-449, 486-492
- Chain growth in synthesis
 - polymerization-depolymerization hypothesis, 346-347
 - stepwise additions, 347-359
- Chemisorption on Fischer-Tropsch catalysts, 76-82, 94-97, 165-174, 323-329
- Coal and tar hydrogenation
 - catalysis and mechanism, 523-527
 - catalyst stability, 522-523
 - catalyst tests, 519-522
 - vehicle and catalyst distribution, 515-519
 - wall effects, 514
- Cobalt
 - thermodynamics of carbides, 20-23
 - thermodynamics of oxides, 19-20
- Cobalt catalysts
 - borides of cobalt, 405-406
 - carbides of, 402-405
 - carbon deposition on, 398-402
 - carburization, 398-402
 - nitrided, 404-405
 - oxides and oxide hydrates, 391-392
 - reduction, 392-394
- Cobalt catalysts and nickel catalysts, 46-118
 - carriers for, 55-64
 - decomposition of salts to oxides, 64-69
 - hydrocarbons and alcohol products-characterization of, 109-114
 - precipitated, 46-47
 - pretreatment of, 86-89
 - products-nature of, 109-118
 - promoters for, 47-55
 - reduction of, 82-86
 - selectivity and operating variables, 114-118
 - skeletal, 64-69
 - surface areas and pore volumes, 69-82

- Cobalt catalysts and nickel catalysts—
cont'd.
synthesis data, one atmosphere, 89-100
synthesis data, medium pressure, 100-108
- Craxford and Rideal hypothesis of Fischer-Tropsch synthesis, 337-341
- Cyclization and aromatization, 529-560
chemistry of, 530-535
cyclization catalysts, 548-557
mechanism, 533-548
technical applications, 557-559
thermodynamics of, 535
- Cyclization catalysts, 548-557
centers for cyclization and isomerization, 553-554
poisoning of, 551-553
structure of supported oxide catalysts, 554-557
- D-band vacancies and catalytic activity, 374-379
- Electron diffraction studies, 330-331
- Fischer's carbide theory, 336-337
- Fischer-Tropsch processes
history of, 29-36
relative yields of, 38
- History of Fischer-Tropsch synthesis, 29-36
- Hydrocracking of paraffins, 311-314
- Incorporation of
alcohols, 319-323
hydrocarbons, 314-319
- Industrial methanation
carbon deposition, 507
catalyst life, 507-509
temperature control, 507
- Interstitial compounds, 379-382
- Iron
thermodynamics of oxide reduction, 19-20
thermodynamics of carbides, 20-23
thermodynamics of nitrides, 23-24
- Iron carbides
composition of, 418-421
formation, 411-416
reaction with acids, 427
reduction of, 426-427
thermal reactions of, 422-426
- Iron catalysts
borides of iron, 423
borocarbides of, 434
carbides, 418-427
carbon deposition on, 416-418
carbonitriles, 429
carburization, 411-416
carriers, 133-140
catalytic activity of, 434-435
electron micrographs of, 171-172
fused, 140-150
hydrocarbons and oxygenated products-characterization, 206-209
nitrides, 427-429
oxides, oxide hydrates, and hydrous oxides, 406-410
precipitated, 119-123, 176-184
pretreatment, 176-192
promoters, 123-133
reduction, 410-411
Schwarzheide tests, 160-164
selectivity, 206-236
and conversion, recycle, and gas flow, 236
and gas composition, 233-236
and operating variables, 225-236
and temperature, 225-229
as a function of pretreatment and composition, 219-225
sintered, cemented, impregnated and miscellaneous, 150-160
surface areas and pore volumes of, 165-176
synthesis data-medium pressure, 193-206
synthesis data-one atmosphere, 193-195
- Iron catalysts for methanation, 490-493
- Kinetics of Fischer-Tropsch Synthesis, 257-298
on cobalt and nickel catalysts, 259-283
on iron catalysts, 283-297
on ruthenium catalysts, 297-298
- Mechanism of the Fischer-Tropsch synthesis
carbide intermediate hypothesis, 336-359
oxygenated intermediate theory, 345-346, 359-367

- Metal carbonyls-thermodynamics of, 24-26
- Methanation, 473-511
catalysts for, 481-506
chemistry of, 474-476
industrial techniques, 506-508
kinetics and mechanism, 508-510
thermodynamics of, 476-480
- Nature of catalyst surface, 323-335
bifunctional catalysts, 334-335
chemisorption, 323-329
electron diffraction studies, 330-331
promoter effects, 331-334
- Nickel
carbides, thermodynamics, 20-23
oxides, thermodynamics, 19-20
- Nickel boride, 390
- Nickel carbides, 386-389
- Nickel catalysts (*see also* Cobalt and Nickel catalysts)
activity of, 391
borides of nickel, 390
carburization, 384-385
nickel carbides, 386-389
nickel oxides and oxide hydrates, 382-385
nitriding, 389-390
reduction, 387
reduction of carbides, 387-388
- Nickel catalysts for methanation
carbon deposition on, 494-500
life of, 501-503
sulfur poisoning, 504-506
thermal stability, 504
- Nickel nitride, 389-390
- Nickel oxide and oxide hydrates, 382-383
- Nitrides
of cobalt, 404-405
of iron, 427-429
of nickel, 389-390
- Oxygenated intermediates-theory
Elvins and Nash, 345
Pichler-carbonyls, 345, 346
radioactive alcohols and, 364-366
Storch, Golumbic, and Anderson hypothesis, 359-366
- Polymerization and depolymerization hypothesis, 346-347
- Pretreatment of catalysts, 81-89, 176-192, 238-239
- Products of synthesis
cobalt and nickel catalysts, 109-118
iron catalysts, 119-164
ruthenium catalysts, 239-242
- Promoters, 47-55, 123-133, 331-334
- Radioactive alcohols in mechanism studies, 364-366
- Radioactive carbon and
carbide intermediate theory, 342-345
oxygenated complex theory, 364-366
- Reactor design, 33-36
- Related reactions in Fischer-Tropsch synthesis
hydrocracking of paraffins, 311-314
incorporation of alcohols, 319-323
incorporation of hydrocarbons, 314-319
- Ruthenium catalysts, 232-242
preparation and pretreatment, 238-239
selectivity and operating conditions, 239-242
- Schwarzheide tests, 160-164
- Selectivity of catalysts
and conversion, recycle and gas flow, 236
and gas composition, 233-236
and operating variables, 114-118, 225-236, 239-242
and pretreatment, 219-225
and temperature, 225-229
hydrocarbons and oxygenated products, and, 109-114, 206-219
- Solid phases in Fischer-Tropsch catalysts, 373-374, 379-435
- Sulfur poisoning
cobalt and nickel catalysts, 244-247
iron catalysts, 248-249
methanation catalysts, 504-506
- Surface areas and pore volumes of catalysts, 69-82, 165-176
- Synthesis data
medium pressure, 100-108, 195-206
one atmosphere, 89-100, 193-195
- Synthin, 30
- Synthol, 30
- Thermodynamics of
carbides of iron, cobalt and nickel, 20-23

Thermodynamics of—cont'd.

carbonyls, 24-26

hydrogenation of carbides, 342

hydrogenation of carbon dioxide, 9

hydrogenation of carbon monoxide, 1-9

of synthesis—a summary, 14-19

oxides of iron, cobalt and nickel, 19-20

reaction of water vapor with carbon monoxide and carbon, 9-11

Variations of the Fischer-Tropsch synthesis

carbon monoxide and water vapor
reaction, 303-310hydrogenation of carbon dioxide, 299-
303

Water gas reaction, 303-310

Water vapor reaction with carbon mon-
oxide

rate of, 303-310

thermodynamics, 9-11



Date Due





0 1163 0135619 6
TRENT UNIVERSITY

QD501 .E65 v.4

Emmett, Paul Hugh ed.

Catalysis.

DATE	ISSUED TO
	44961

44961

QD
501
E65
v.4

Emmett, Paul Hugh (ed.)
Catalysis

Trent
University

